THE SKIDDAW GROUP OF CUMBRIA:
EARLY ORDOVICIAN TURBIDITE SEDIMENTATION AND PROVENANCE ON AN EVOLVING MICROCONTINENTAL MARGIN

Richard Maurice Moore

Submitted in accordance with the requirements
for the degree of Doctor of Philosophy

The University of Leeds
Department of Earth Sciences

January, 1992

The candidate confirms that the work submitted is his own and that appropriate credit has been given where reference has been made to the work of others.

ABSTRACT

During the Early Palaeozoic, the southern British Isles were part of a microcontinent, Eastern Avalonia. In the early Ordovician Eastern Avalonia was close to the continent of Gondwana, in high southern latitudes. Northward drift of Eastern Avalonia during the Ordovician brought it towards Baltica and Laurentia, resulting in continental collision in the Silurian. Three major tectonic events have been postulated in the earlier history of the microcontinent: rifting from Gondwana, onset of subduction and subduction of the mid-ocean ridge. Evidence for such events may be sought in the contemporaneous sedimentary basins; their type and geometry and the depositional environment and composition of their sediment fill.

The Skiddaw Group (Tremadoc to Llanvirn) of Cumbria, comprises turbidites, debrites and a major olistostrome. Sediment was sourced from an orogenic terrain with noncoeval continental volcanic arcs, unroofed plutons, metamorphic basement and sedimentary cover. An additional source of quartzose sediment (e.g. a sandy shelf or delta) was present. Two periods of submarine fan development display the following facies associations: depositional lobe, lobe fringe and inter-lobe, distributary channel, and proximal channel-levee. The first spans the Tremadoc-Arenig boundary and channels distributed sediment to both east and west. Axial flow along a trough orientated approximately east-west is inferred. Contemporaneous depositional lobe facies association in the Isle of Man could represent a more distal portion of this system. The Manx Group displays sediment of similar facies and compositions to the Skiddaw Group. Turbidity current flow on a submarine fan of Arenig age was strongly influenced by sea floor topography. A palaeocurrent interpretation is presented which uses the theory of oblique reflection of turbidity currents (Kneller, Edwards, McCaffrey and Moore, 1991). The angular relationship between sole mark current directions and ripple current directions is used to infer the orientation of intra-basinal topographical features. With additional evidence from thickness variations of sandstone bodies and the orientation of pre-mid Ordovician faults, a tectonic model of syn-depositional extensional faults trending north-northwest, with fault blocks tilted to the northeast is proposed. The controls of fan development are discussed. Gravitational deformation in the Llanvirn is expressed as slump folds in partially lithified sediment, debrites and an olistostrome with sandstone rafts. Slump fold orientations are used to demonstrate the development of a regional westerly palaeoslope which preceded uplift of the depositional basin prior to subaerial volcanism of the Eycott and Borrowdale volcanic groups.

The undated Ingleton Group is described and contrasted with the Skiddaw and Manx Groups. A lithological correlation with Arenig sediments recovered from the Beckermonds Scar borehole is supported, but a continental margin volcanic arc provenance and deposition as a coarse grained lobe of a submarine fan suggests the dispersal system was separate from that of the Skiddaw Group. Lithological comparison is made with contemporaneous strata of southeast Ireland.

With consideration of early Ordovician geology across the southern British Isles, a tectonic model is proposed which incorporates transtensional and transpressional phases of oblique sinistral slip in the overriding plate above a subduction zone of general southerly dip. The present day active margin of Chile is used as an analogue. The long and complex history of Eastern Avalonia's northern margin is analysed to identify the three tectonic events mentioned above.

CONTENTS

List of figures

List of tables

List of plates

List of enclosures

Abbreviations and notes on nomenclature

The use of abbreviations has been avoided as much as possible, but the following do occur:

mm	millimetre	ppm	parts per million
cm	centimetre	wt%	weight per cent
m	metre	g	gram
km	kilometre	LOI	loss on ignition
OIA	oceanic island arc	PAAS	Post-Archaean Australian shale average
CIA	continental island arc	REE	rare earth element
ACM	active continental margin	ICP	inductively coupled plasma
CAAM	continental arc/active continental margin	BGS	British Geological Survey
PM	passive margin	vs	versus

Grainsize intervals used in this study are those of Wentworth (1967), defined below:

	millimetres	grainsize class
	32	
GRAVEL		pebble
	4	
		granule
	2	
		very coarse sand
	1	
		coarse sand
	0.5	
SAND		medium sand
	0.25	
		fine sand
	0.125	
		very fine sand
	0.0625	
		silt
MUD	0.0039	
		clay

Intervals of bed thickness are defined below:

metres	interval
>1.00	very thick beds
0.30 - 1.00	thick beds
0.10 - 0.30	medium beds
0.03 - 0.10	thin beds
0.01 - 0.03	very thin beds
0.003 - 0.01	thick laminae
0.001 - 0.003	thin laminae

The term 'calibre' is used to refer to the maximum grainsize of a sediment.

The term 'greywacke' is used as a textural rock name to describe siliciclastic sedimentary rocks of sand grainsize with >15% matrix (Pettijohn et al, 1972). Almost all samples for petrographical analysis are greywackes. They are referred to as sandstones when a distinction in terms of grainsize is required, e.g. sandstone to mudstone ratio.

The term 'Caledonian' is used to describe the tectonic elements with a northeast-southwest trend in the Lower Palaeozoic of the British Isles, associated with the closure of the Iapetus Ocean. 'Acadian' refers to deformations of the Early Devonian. The northwest-southeast structural trend in the subsurface Lower Palaeozoic of eastern England is referred to as the 'concealed Caledonides of the east Midlands'.

Acknowledgements

I thank the Natural Environment Research Council for funding the project, through a CASE studentship with the British Geological Survey, and my supervisors, Jack Soper, Ben Kneller and Tony Cooper, for initiating and encouraging the research. Derek Cooper kindly provided geochemical data, and Matthew Thirlwall made available results of isotopic analyses. I appreciated the interest in the work shown by Mike Leeder.

I thank my parents for additional financial support and the provision of a word processor and field transport when my own car expired. To my family and friends, who were largely neglected in the latter stages of the work, I apologise; to Jannine, especially.

For technical support I thank Neil Woodhouse, John Mott, Alan Gray for expert tuition in XRF procedures, Frank Buckley for preparation of REE samples, Keith and Mary for preparation of thin sections, and my field assistant, Mark Prior.

John and Sarah Platt and family and members of the West Cumbria canoe club are thanked for the hospitality they showed me while in the field. For accommodation in the Isle of Man, I thank Mark Cooper, Jane Evans and family, and for high-speed transportation I am indebted to Barry McGaw.

I wish to express my appreciation to my fellow students, many of whom should be included in more than one of the following groups: cohabitants of room 9.17a, Bill McCaffrey, Andy Farmer, Tim Salter, Colin Stark, Isaac Njilah, Linda; exhibitors in the 'writing-up' road show, Deb Edwards and Pete Bentham; my lodgers Simon Tempest and Keith Rawnsley for introducing me to existensionalism, big beers and the belief that 'its never too late to give up'; those who provided welcome distractions from work through football, climbing or buying the next round, Simon Welsh, Lochlan Magennis, Neil Evans, Eddie McAllister, the O.U. boys, Pete Bishop, Angela McMahon, Sophie Bowtell, Carolyn Young, Richard Napier, and Alison, who was special; for their mastery of football, the Cameroon boys, and the Celts for their lack of it; the undergraduates at Leeds for their joy of life, especially Heather, Helen and Sue.

View to the southwest from Loweswater Fell showing Crummock Water flanked by Grasmoor and Mellbreak.

Chapter 1

INTRODUCTION

1.1 Regional Geological Setting

During Lower Palaeozoic time it is inferred that an ocean, the Iapetus Ocean, existed in the southern hemisphere (Wilson, 1966; Dewey, 1969) (figure 1.1). In the early Ordovician palaeomagnetic evidence indicates that it had a latitudinal width of 5000 km with its southern margin at about 60° S and its northern margin at about 15° S (Torsvik and Trench, 1991). Northern Britain and much of present-day North America formed part of the northern continent of Laurentia, while southern Britain was marginal to the southern continent of Gondwana comprising much of Europe and Africa (figure 1.1). The micro-continents of Eastern Avalonia (southern Britain and Belgium), Western Avalonia (Newfoundland, New Brunswick and Nova Scotia) and Armorica (Brittany and Iberia) were to rift away from Gondwana during the Ordovician. A third continental plate, Baltica, lay to the east separated from Gondwana by the Tornquist Sea (Cocks and Fortey, 1982). These oceans closed by destruction of oceanic lithosphere at their margins leading to continental collision, deformation, uplift and erosion during the Caledonian orogeny, whose main effects were in the Silurian (Soper and Woodcock, 1990). The history of geological processes at each margin and the timing of collision events is complex and controversial. An extensive summary is provided by Todd et al (1991). Sinistral shear during ocean closure (Soper and Hutton, 1984), continental collision (Caledonian and Acadian orogenies) and later events (Hercynian and Alpine orogenies) have partially obscured the early geological history of the Iapetus Ocean. The opening of the Atlantic Ocean has dissected the trace of the Iapetus suture and has widely separated continental fragments which were once juxtaposed and share common histories; thus the southern margin of the Iapetus Ocean is represented by southern Britain, western and central Europe and parts of Newfoundland, New Brunswick and Nova Scotia (figure 1.1).

Figure 1.1 Palaeocontinental reconstruction for the early Ordovician (from Torsvik and Trench, 1991). 1=southern Britain, 2=western Europe, 3=part of Newfoundland, 4=New Brunswick, EA= Eastern Avalonia, WA=Western Avalonia, A=Armorica.

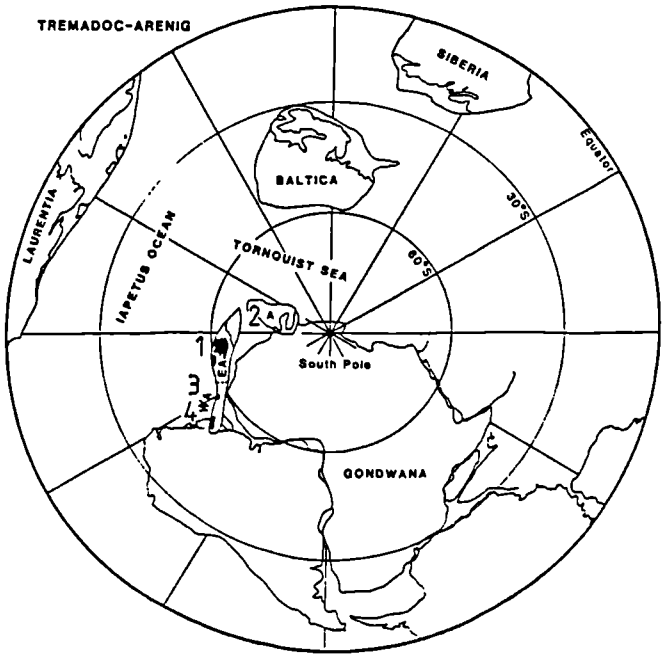

1.2 Evolution of the southern margin of the Iapetus Ocean

From the geological record preserved along the former ocean margin the following types of interpretation can be made: that of the structural style and the timing of deformation events; interaction of sedimentation and tectonics; sedimentary basin type; sediment composition; sedimentary environment and dispersal system geometry; sea level changes; types of volcanism; age of intrusive and extrusive events; the palaeolatitude of continental fragments (using palaeomagnetism) and continental separation (using palaeontology). These enable a sequence of geological events to be postulated for the southern Iapetus margin (e.g. Woodcock, 1990):

evolution of the margin from a passive to active margin with subduction of oceanic crust beneath Gondwana continental crust;

rifting of microcontinental fragments of Avalonia and Armorica away from Gondwana;

collision of microcontinents with Laurentia and closure of the Iapetus ocean.

For the early Ordovician history of the margin some fundamental problems remain, listed in order of decreasing scale:

What was the orientation of the margin?

In which direction was oceanic crust subducted beneath Eastern Avalonia?

When did the microcontinents rift away from the margin of Gondwana?

When was the onset of subduction?

What type of sedimentary basin or basins existed and how were they related to each other and the tectonic regime?

What was the size and geometry of any one basin?

What was the palaeogeography, the distribution of hinterlands around the basin?

What were the sedimentary environments, the size and shape of the sediment dispersal systems into the basin?

Can sedimentary responses to tectonic or eustatic sea level variations be identified?

1.3 Approach

The nature of lower Ordovician outcrops available for study, (i.e. regions of poor exposure, widely dispersed and separated by younger tectonic features), allows the smaller scale problems to be addressed, which can then be used to answer the broader questions. Lower Ordovician sediments of the southern Iapetus margin in the British Isles are exposed in northwest England, the Isle of Man, southeast Ireland and Wales (figure 1.2). For the Skiddaw Group of northwest England, the sedimentary environments and the provenance of sediments are described and interpreted. The evidence for the probable Ordovician age of the Ingleton Group of northern England is discussed, and its sediments are described and contrasted with those of the Skiddaw Group. Comparison is made with the coeval strata of the Isle of Man, southeast Ireland and Wales through field observations and the published work of others. A model of basin development is erected for

the Skiddaw Group, which forms a component of the regional tectonic model for the development of the southern British Isles throughout the early Ordovician. This is compared with a modern analogue: the Andean active continental margin.

1.4 Introduction to the Skiddaw Group

The Skiddaw Group comprises the thick sequence (up to 5 km (Cooper et al, in prep)) of greywackes, siltstones and mudstones of Tremadoc, Arenig and Llanvirn age that crop out in the English Lake District and adjoining areas. It forms the main Skiddaw Inlier and the smaller Ullswater, Bampton, Black Combe and Furness inliers (figure 1.2b). It also occurs to the east in the Cross Fell Inlier (Cooper and Molyneux, 1990) and Teesdale Inlier (Johnson,1961). Rocks of equivalent age have been proved at depth in boreholes through the Carboniferous rocks of the Alston Block (Woolacot, 1923; Burgess, 1971) and the Askrigg Block (Wilson and Cornwell, 1982).

The sediments were largely deposited by turbidity currents in a deep marine environment. They are multiply deformed with complex fold structures, several cleavage orientations and abundant faults. They are unconformably overlain by the Eycott Volcanic Group (Millward and Molyneux, in press) and the Borrowdale Volcanic Group (Moseley, 1975).

1.4.1 Historical review

The Skiddaw Slates were first described in 1820 by Jonathan Otley and designated Skiddaw Group by Sedgwick (1832). The primary mapping for the Geological Survey was undertaken by J. C. Ward in 1872 (Ward, 1876). The Skiddaw Inlier received attention throughout the nineteenth century for its abundant graptolite localities. Large collections were made by early workers, mainly from screes, enabling recognition of species and assemblages and a profusion of papers by the following authors: Sedgwick, Hausmann, Salter, Harkness, Nicholson, Dakyns, Aveline, Ward, Huddleston, Postlethwaite, Goodchild, Marr, Harker, Elles, Wood and Reed. In the early part of this century, wider geological relationships were considered: Green (1917) was concerned with intrusives and the nature of the boundary with the overlying volcanics.

Local stratigraphies were erected on lithological grounds with limited palaeontological control. A four fold subdivision was recognised by Dixon (1925) and Eastwood et al (1931) who correlated occurrences of sandstone (table 1.1). Rose (1955) recognised the Blakefell Mudstones as thermally metamorphosed Kirkstile Slates and simplified the stratigraphy to two formations. Jackson (1961) added the Hope Beck Slates at the base of the group. Palaeontological control was not detailed enough for finer subdivision. Eight formations were described by Simpson (1967), who preferred to define each sandstone occurrence as a separate formation and reinstated the Blake Fell Mudstones.

Progress was made through the use of microfossils, initially in the Cross Fell Inlier (Wadge et al, 1967; Lister et al, 1969), leading to the recognition of Llanvirn age sediments. Sediments of the Skiddaw Inlier (Wadge et al, 1969), Teesdale Inlier (Lister and Holliday, 1970) and Bampton inlier (Skevington, 1970) were correlated with this occurrence.

Figure 1.2 (a) Lower Palaeozoic inliers of the southern British Isles of interest to this study; (b) detail of northwest England showing the distribution of Lower Palaeozoic rocks and early Ordovician inliers.

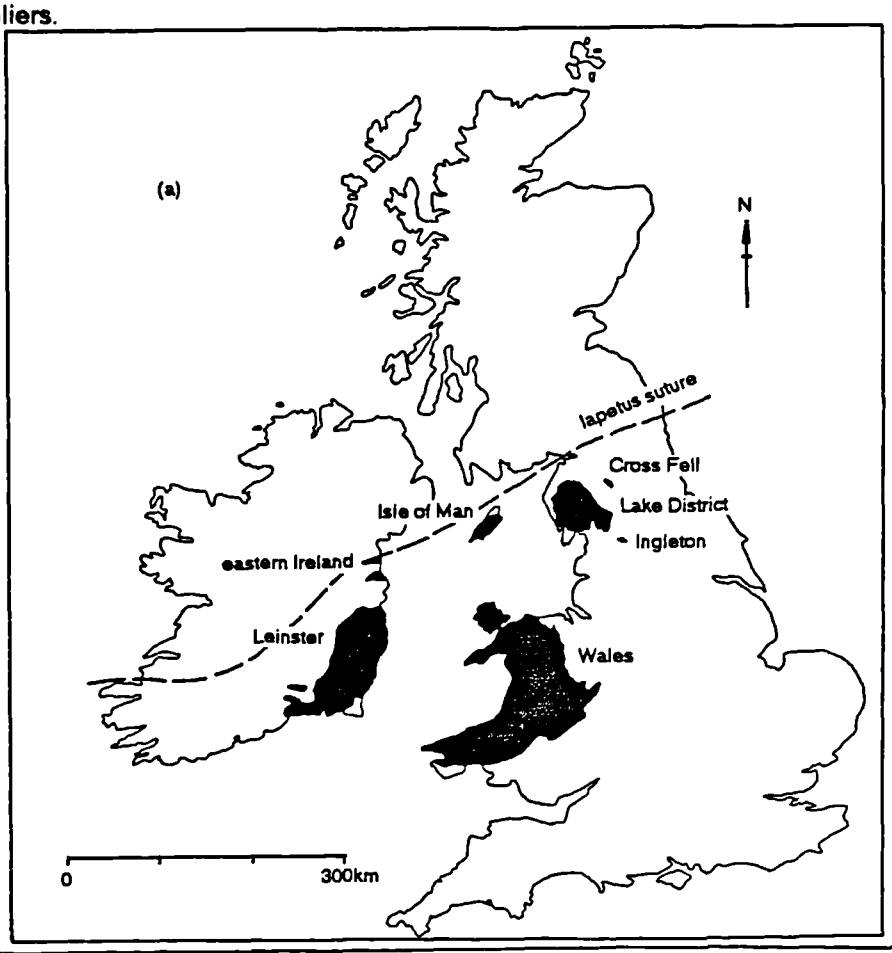

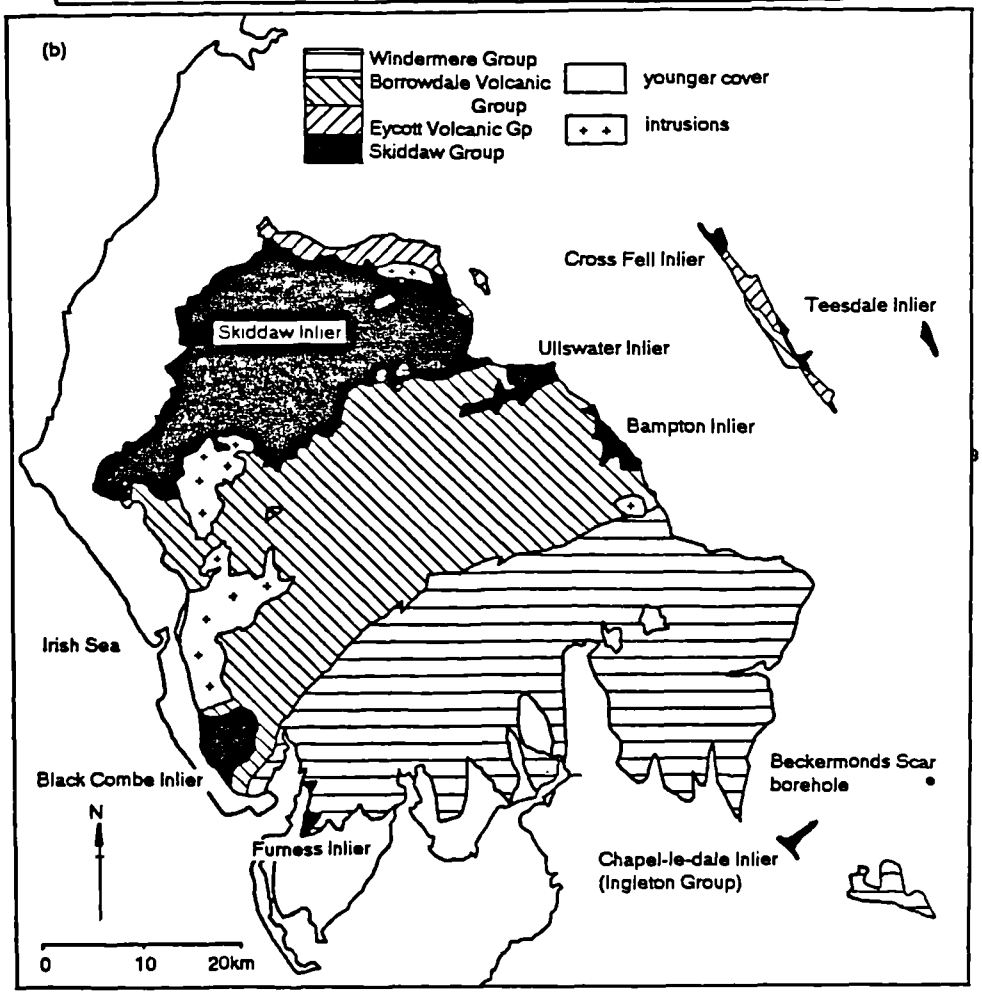

Table 1.1 Comparison of the stratigraphical schemes for the Skiddaw Group (after Cooper et al, in prep).

Ward (1876 p.47)

Skiddaw Slates:
Black Slates of Skiddaw
Gritty beds of Gatesgarth, Latterbarrow, Tongue Beck, Watch Hill and Great Cockup
Dark Slates
Sandstone series of Grasmoor and Whiteside
Dark slates of Kirk Stile

Dixon (1925 p.70)

Skiddaw Slates:
Mosser Striped Slates (including Skiddaw or Watch Hill Grit)
Loweswater Flags
Kirk Stile Slates
Blake Fell Mudstones

Eastwood et al (1931 p.28)

Skiddaw Slates:
Latterbarrow Sandstone
Mosser and Kirkstile Slates, with Watch Hill Grit in upper part
Loweswater Flags and Blakefell Mudstone

Rose (1954)

Skiddaw Slates:
Mosser-Kirkstile Slates
Loweswater Flags (with Watch Hill Grits)

Jackson (1961)

Skiddaw Group:
Latterbarrow Sandstone
Mosser-Kirk Stile Slates
Loweswater Flags (with Watch Hill Grits)
Hope Beck Slates

Simpson (1967)

Latterbarrow Sandstone
--- unconformity ---
Skiddaw Slates:
Sunderland Slates
Watch Hill Grits and Flags
Mosser Slates
Loweswater Flags
Kirkstile Slates
Blakefell Mudstones
Buttermere Flags
Buttermere Slates

Jackson (1978)

Skiddaw Group:
Latterbarrow Sandstone
Tarn Moor and other Llanvirn mudstones
Kirk Stile Slates
Loweswater Flags (with Watch Hill Grits)
Hope Beck Slates

Wadge (1978)

Eycott Group:
Tarn Moor Mudstones (high Ireby and Binsey volcanic formations)
Skiddaw Group:
Latterbarrow Sandstone
Kirkstile Slates
Loweswater Flags
Hope Beck Slates

Moseley (1984)

Skiddaw Group:
Latterbarrow Sandstone Formation
Tarn Moor Mudstone Formation
Kirkstile Slate Formation
Loweswater Flags Formation
Hope Beck Slate Formation

Molyneux and Rushton (1988)

Latterbarrow Sandstone
--- unconformity ---
Skiddaw Group:
Kirk Stile Slates
Loweswater Flags
Hope Beck Slates
Watch Hill Grits
Tremadoc beds of the River Calder

This study (after Cooper et al, in prep)

Skiddaw Group:
Northern Fells Belt
Kirk Stile Formation
Loweswater Formation
Hope Beck Formation
Watch Hill Formation
Bitter Beck Formation

Skiddaw Group:
Central Fells Belt
Tarn Moor Formation
Buttermere Formation

The Tarn Moor Mudstones were defined subsurface in the Tarn Moor tunnel by Wadge et al (1972). They were placed in differing positions in the stratigraphies of Jackson (1978), Wadge (1978) and Moseley (1984), as was the Latterbarrow Sandstone. The Latterbarrow Formation was subsequently shown to rest unconformably on the Skiddaw Group and belong to the Borrowdale Volcanic Group by Allen and Cooper (1986). The boundaries of the Tarn Moor Formation are unclear.

The discovery of a Tremadoc microfossil assemblage (Molyneux and Rushton, 1984) in the Watch Hill Grits, (previously equated with the Loweswater Flags), extended the recognised age range of the group. Molyneux and Rushton (1988) demonstrated that these were separate formations.

Since 1982 the British Geological Survey has been resurveying the Skiddaw Group of the Skiddaw Inlier on the Cockermouth (23), Whitehaven (28) and Keswick (29) 1:50,000 scale geological mapsheets. Reassessments of the Black Combe and Furness inliers (Ulverston sheet 48) and Ullswater Inlier (sheet 30 of 1893) have also been made. A formal definition of Skiddaw Group stratigraphy is being undertaken by Cooper et al (in prep). This paper incorporates the results of mapping and palaeontological study by the British Geological Survey and sedimentological, petrographical and provenance data from this study. It is used as a basis for the following section.

1.4.2 Stratigraphy of the Skiddaw Group

The stratigraphy of the Skiddaw Group is described by reference to two stratigraphical belts: the Northern Fells belt and the Central Fells belt (figure 1.3) appearing in both the Skiddaw and Cross Fell inliers (Cooper and Molyneux, 1990). The two belts are separated by the Causey Pike fault (figure 1.4). The Northern Fells belt consists of alternate mudstone-dominant and sandstone-dominant formations of Tremadoc to Llanvirn age. Rocks of equivalent ages and lithologies occur in the Central Fells belt where they constitute a major olistostrome overlain by mudstone. In the Black Combe and Furness inliers of the Southern Fells, the Skiddaw group consists mainly of undivided mudstone.

1.4.2.1 Stratigraphy of the Northern Fells belt

Five formations are defined (table 1.2) and described below.

Table 1.2 Stratigraphy of the Northern Fells belt.

Formation	Main lithology	Age
Kirk Stile Formation	siltstone & mudstone	Arenig-early Llanvirn
Loweswater Formation	greywacke	Arenig
Hope Beck Formation	siltstone & mudstone	Arenig
Watch Hill Formation	greywacke	Tremadoc-Arenig
Bitter Beck Formation	siltstone & mudstone	Tremadoc

Figure 1.3 Stratigraphy of the Northern Fells belt and Central Fells belt of the Skiddaw Group (after Cooper and Molyneux, 1990).

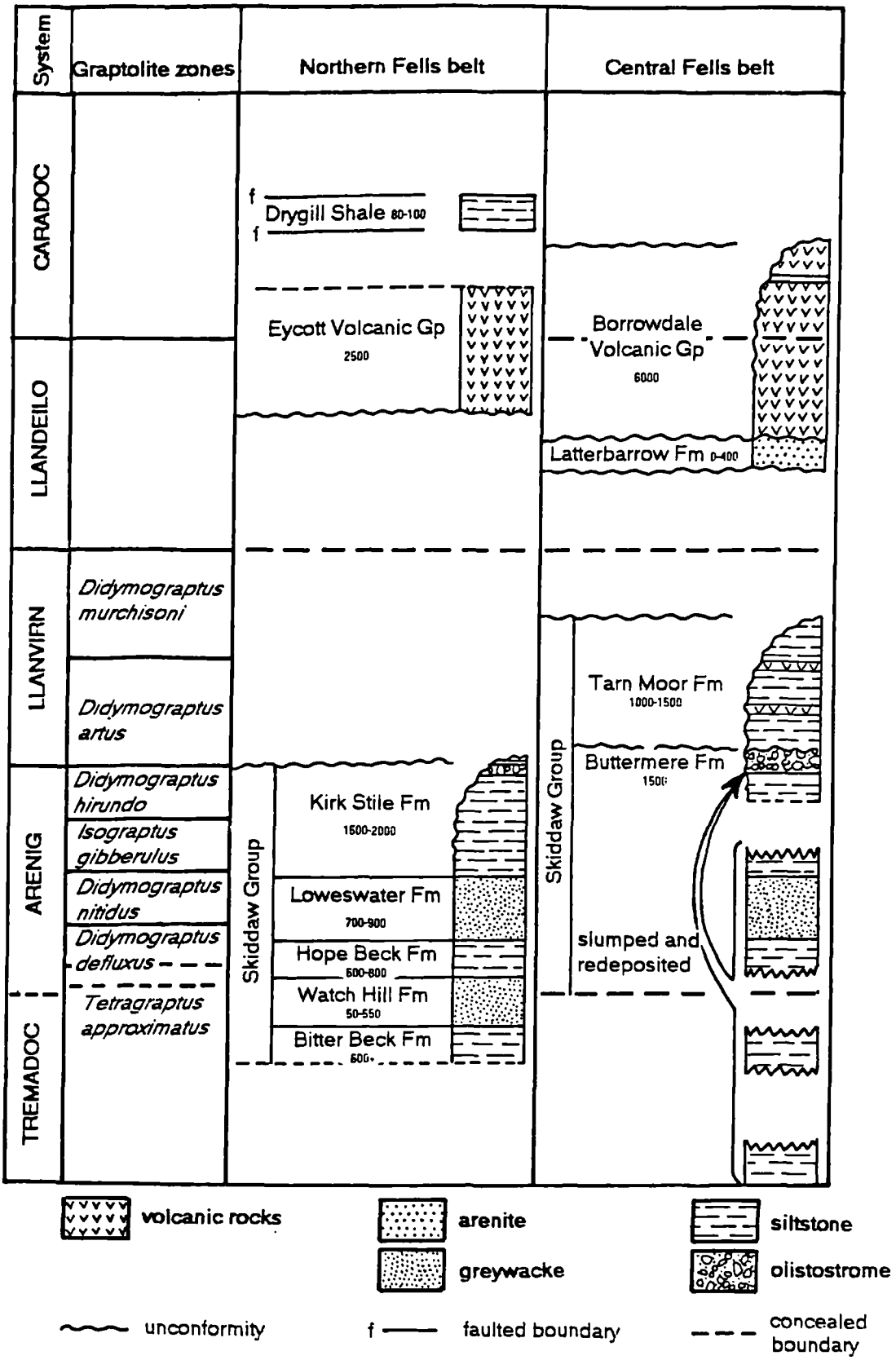

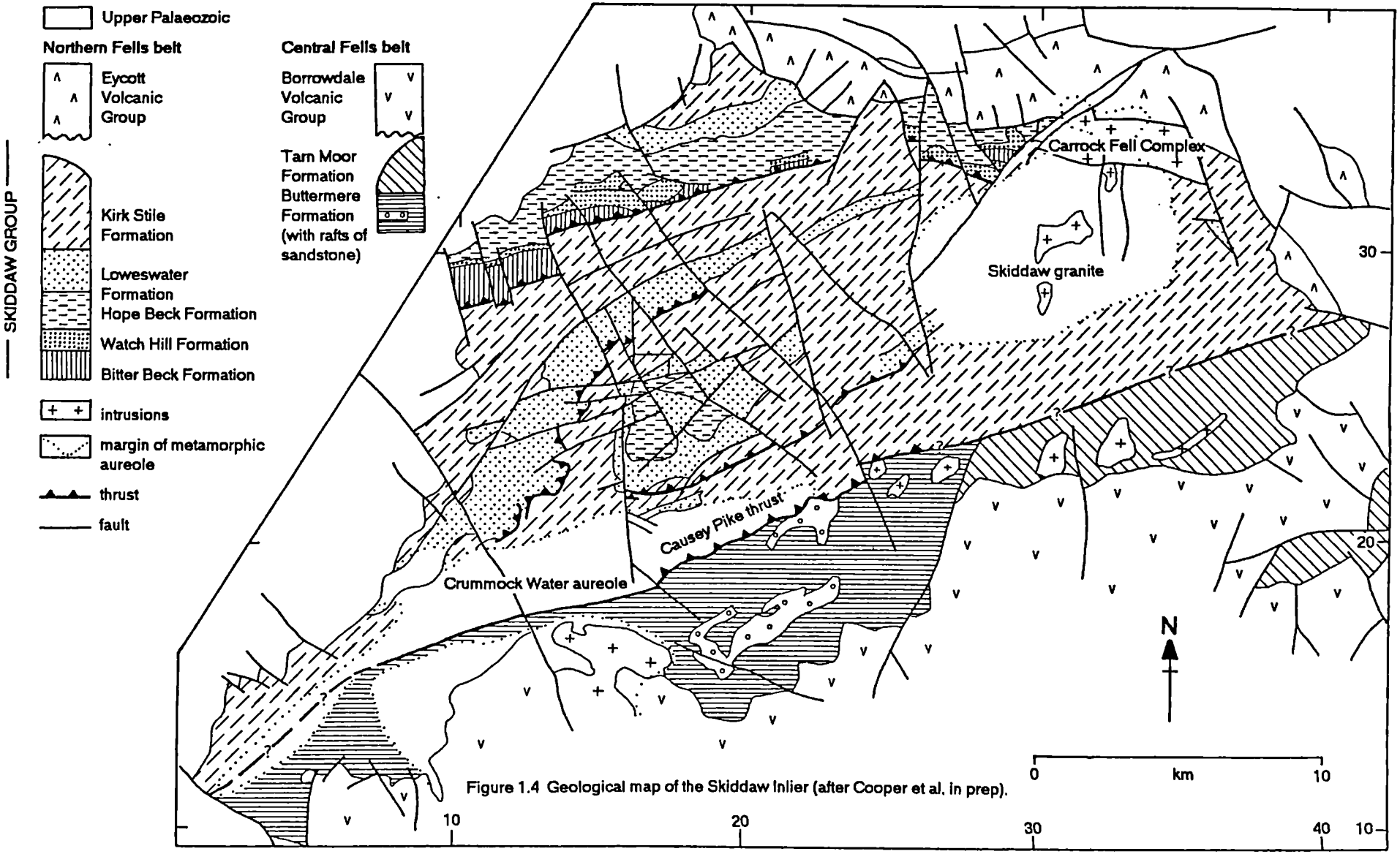

Figure 1.4 Geological map of the Skiddaw Inlier (after Cooper et al. in prep).

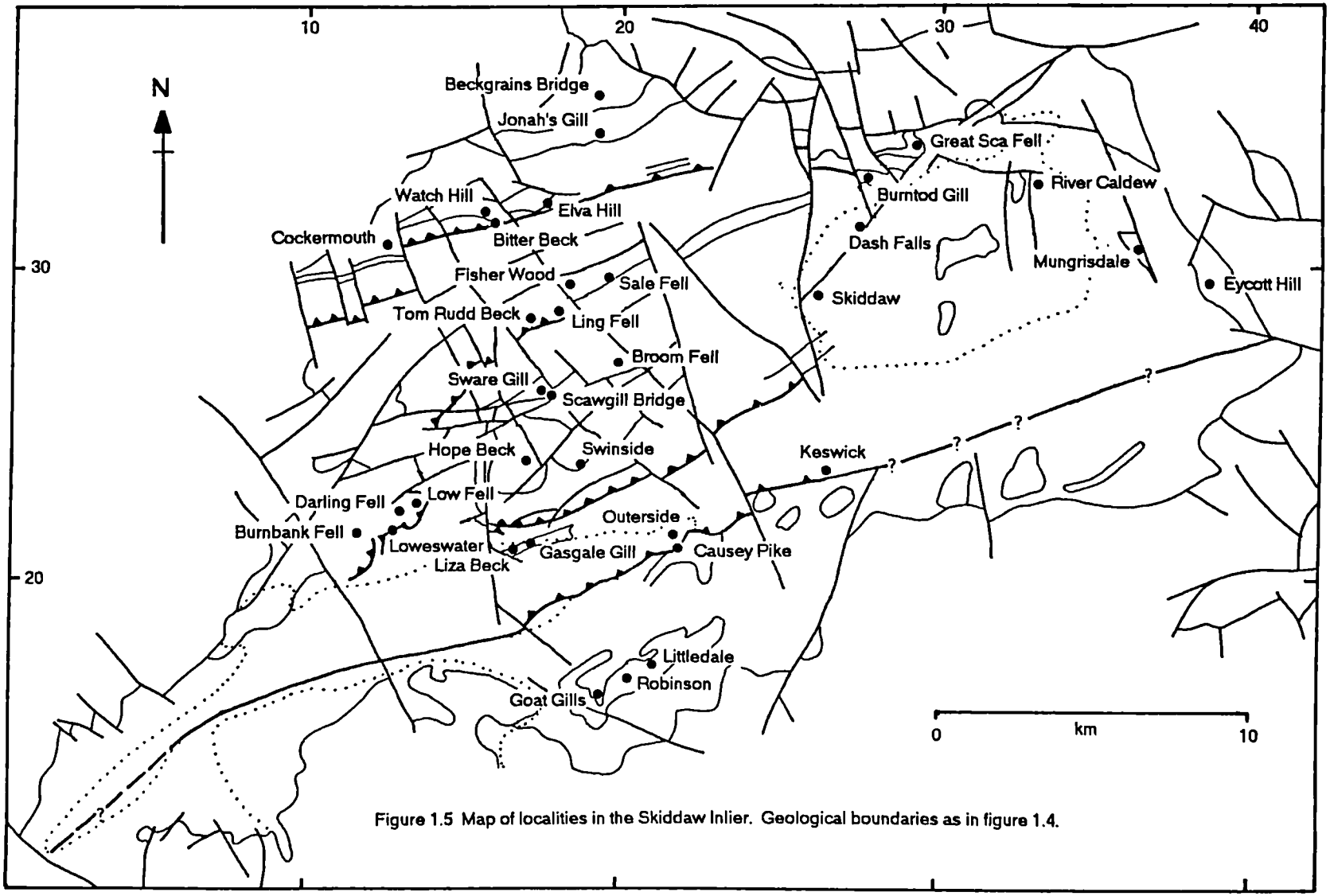

Figure 1.5 Map of localities in the Skiddaw Inlier. Geological boundaries as in figure 1.4.

1.4.2.1.1 Bitter Beck Formation

Up to 500m of Bitter Beck Formation are present in the north of the Skiddaw Inlier (figure 1.4) where it is thrust over the Kirk Stile Formation, so its base is not seen. It is dominated by dark grey mudstones and siltstones. Sequences with up to 20% greywacke occur near Elva Hill [NY 180 316] and at Trusmadoor [NY 2777 3363] (figure 1.5), and are the oldest parts of the formation. The palaeontological age of the formation falls within the *Tetragraptus approximatus* biozone (Molyneux and Rushton, 1988).

Near Eycott Hill [NY 3820 3074] an occurrence of laminated and thinly bedded siltstone and mudstone with tight folds has yielded acritarch assemblages of middle to late Cambrian age (Cooper et al, in prep). Other exposures in the vicinity contain material of Tremadoc and Arenig age. These beds may be part of the Bitter Beck Formation or alternatively may represent an Ordovician olistostrome containing reworked Cambrian acritarchs.

1.4.2.1.2 Watch Hill Formation

There is a rapid interbedded transition from the mudstone-dominant Bitter Beck Formation into the greywacke-dominant Watch Hill Formation. The latter is of latest Tremadoc and earliest Arenig age (Molyneux and Rushton, 1988). At Watch Hill [NY 1495 3189] (figure 1.5) a right way up sequence of between 500m and 800m youngs to the north (figure 1.4). To the west of Watch Hill the formation thins to *c* 200m in the vicinity of Cockermouth. To the east a similar sequence is exposed in the Great Sca Fell area [NY 2900 3387] (figure 1.5). Microfossil evidence suggests a probable equivalence with the sequence at Watch Hill.

1.4.2.1.3 Hope Beck Formation

The dominantly dark grey mudstones and siltstones between the Watch Hill and Loweswater formations are assigned to the Hope Beck Formation. Sandstone-rich units of a few metres thickness are present. No continuous sequence is exposed but the thickness is estimated between 600m and 800m.

1.4.2.1.4 Loweswater Formation

The Loweswater Formation comprises *c* 800m of greywackes with subordinate siltstone and mudstone. In the east of the Skiddaw Inlier it may be substantially thinner. The formation boundaries are interbedded transitions with the argillaceous sequences above and below. Fossils are lacking except where siltstone and mudstone beds dominate in the lower and upper parts of the formation. The upper beds are of *nitidus* biozone age.

Slump folds are present near the top of the formation, e.g. Gasgale Gill [NY 1650 2108] (figure 1.5).

1.4.2.1.5 Kirk Stile Formation

The dark grey siltstones and mudstones above the Loweswater Formation are referred to the Kirk Stile Formation. Its base is a rapid interbedded transition from greywackes. The formation thickness is between 1500m and 2500m and complicated by the stacking of slumped sequences. It is unconformably overlain by the Eycott Volcanic Group (Millward and Molyneux, in press).

About 300m above the base of the formation is a local lenticular body of *c*80m thickness with 20-30% thin greywacke beds.

Associated with slumped sequences in the upper part of the formation are sporadic thick beds of sedimentary breccia, e.g. at Outerside [NY 2132 2140] (figure 1.5) where the 'fluxoturbidite' of Jackson (1978) is hornfelsed by the Crummock Water Aureole, and at Beckgrains Bridge [NY 1904 3552] where a massive unit in excess of 40m thick comprises mudstone, siltstone and sandstone clasts up to 0.5m in diameter supported in a sheared and folded mudstone matrix. Microflora indicate material of Tremadoc age re-worked and slumped in the late Arenig or early Llanvirn. These occurrences of breccia at the Arenig/Llanvirn boundary can be compared with the Buttermere Formation olistostrome in the Central Fells belt (section 1.4.2.2).

Graptolite fauna show the lower half of the Kirk Stile Formation to belong to the *gibberulus* biozone, and the upper part to belong to the *hirundo* biozone.

1.4.2.2 Stratigraphy of the Central Fells belt

Two formations are defined (table 1.3) and described below.

Table 1.3 The stratigraphy of the Central Fells belt.

Formation	Main lithology	Age
Tarn Moor Formation	mudstone with subordinate tuff beds	Llanvirn
Buttermere Formation	olistostrome of siltstone and greywacke	probable early Llanvirn

The Murton and Kirkland formations of the Cross Fell Inlier are equivalent to the Buttermere and Tarn Moor formations respectively (Cooper and Molyneux, 1990), and strata equivalent to the Kirkland Formation are present in the Teesdale Inlier (Johnson, 1961).

1.4.2.2.1 Buttermere Formation

The Buttermere Formation is an olistostrome complex about 1500m thick comprising disrupted, sheared and folded siltstone, mudstone and sandstone turbidites. The formation is not entirely chaotic but retains a relict stratigraphy. Two members are recognised within it: the Goat Gills Member, a sequence of sedimentary breccia, overlain by the Robinson Member, a sequence of sandstone. The Buttermere Formation, Robinson Member and the slump folded nature of the olistostrome deposits were described by Webb and Cooper (1988) and Webb (1990).

The outcrop boundaries of the formation are unclear, faulted or unconformably overlain by the Borrowdale Volcanic Group hence the base and top are not recognised. The Causey Pike thrust places the Kirk Stile Formation of earliest Llanvirn age at Outerside [NY 2142 2162] above the Buttermere Formation. This suggests the olistostrome may be younger than earliest Llanvirn, although possible transcurrent movements on the Causey Pike fault zone may invalidate this inference.

The olistostrome yields macro and microfauna which range in age from Tremadoc to late Arenig and which are only rarely mixed. The close proximity of disparately aged sediments suggests that the bulk of the olistostrome deposit is composed of large clasts, blocks and rafts of siltstone and mudstone with subordinate sandstone set in a silty mudstone matrix. The Robinson Member in Littledale [NY 211 173] (figure 1.5) passes upwards into poorly laminated silty mudstones which have yielded upper Arenig graptolites suggesting that the Robinson Member is of early and middle Arenig age.

1.4.2.2.2 Tarn Moor Formation

The Tarn Moor Formation includes the mudstones and siltstones with subordinate volcanic turbidite and bentonite beds that occur in the eastern part of the Central Fells. It is present in the southeast of the Skiddaw Inlier and forms all of the Ullswater and Bampton inliers (figure 1.2b).

The base of the formation is not seen but age and outcrop relationships suggest it must lie above the highly disrupted Buttermere Formation olistostrome. The formation is unconformably overlain by the Borrowdale Volcanic Group (Wadge, 1972). Its thickness is *c.*1000-1500m.

The lower part of the formation, (not older than early Llanvirn age), is of laminated mudstone with subordinate siltstone. The middle part is typified by mudstone with up to 5% of tuffaceous beds, ranging from very thin bentonites to very thick tuffaceous sandstone turbidites. These belong to the *artus* biozone (Wadge, 1972). The proportion of volcanic beds increases in the Bampton Inlier, also of *artus* biozone age (Skevington, 1970). The youngest part of the formation is very dark grey to black mudstones of the *murchisoni* biozone (Wadge et al, 1969; Wadge et al, 1972) in the Tarn Moor tunnel of the Ullswater Inlier.

1.4.2.3 Occurrences of undivided Skiddaw Group

1.4.2.3.1 Black Combe Inlier

The inlier exhibits a monotonous sequence of laminated mudstones and siltstones with subordinate greywacke, probably in excess of 1000m thick. It was subdivided by Helm (1970) into three units on the basis of colour but this variation has been recognised as secondary alteration due to metasomatism and hornfelsing. The complex structural scheme of Helm (1970) is untenable; the complex structures are related to the development of a shear zone (A. Bell, pers. comm.). A late Arenig age (*hirundo* biozone) is indicated by graptolites and acritarchs (Rushton and Molyneux, 1989).

1.4.2.3.2 Furness Inlier

Medium-dark grey mudstones with thin laminae of siltstone are poorly exposed and graptolites and acritarchs indicate inclusion in the *hirundo* biozone (Rose and Dunham, 1977). These rocks appear to correlate with the Black Combe Inlier.

1.4.2.3.3 Beckermonds Scar borehole

Greywackes of Arenig age have been proved in the Beckermonds Scar borehole [SD 8635 8016] (Wilson and Cornwell, 1982) (figure 1.2b). The lithology has been compared with the Ingleton Group (Berridge, 1982) (section 1.6) of unproven age. This study investigates the lithological and sedimentological attributes of the Arenig greywackes of Beckermonds Scar, the Ingleton Group and Skiddaw Group to reveal any connections in composition, provenance and dispersal system.

1.4.3 Structure of the Skiddaw Group

The complex, polyphase nature of deformation in the Skiddaw Group has been widely recognised, and the timing of deformation events has been the subject of much controversy since the suggestion of an intra-Ordovician orogeny by Simpson (1967). The development of structural models is reviewed in chapter 4.

Table 1.4 Deformation scheme for the Skiddaw Group and correlations of folds (F) and cleavage (S) of the main deformation events with the other Lower Palaeozoic groups of the Lake District. Late minor structures are omitted. Modified after Webb and Cooper (1988).

Tectonics		Skiddaw Group	Borrowdale Volcanic Group	Windermere Group
D_3	Main, early Devonian deformation phase	F3/S3	F_1/S_1	F_1/S_1
D_2	Initiation of Lake District Anticline in late Llanvirn	F_2		
D_1	Major submarine slumps and slides	F_1		

The model in vogue at the inception of this study was that of Webb and Cooper (1988). They described an initial deformation phase related to major submarine slumps and slides emplaced in the Llanvirn (table 1.4).

Figure 1.6 Structural map of part of the Skiddaw Inlier (Webb and Cooper, 1988, figure 2). CPTh = Causey Pike thrust; GA = Grasmoor anticline; GTh = Gasgale thrust; L = Lorton; LA = Loweswater anticline; LBA = Lorton-Barf anticline; LTh = Loweswater thrust; R = Robinson; SLA = Sale Fell-Ling Fell anticline.

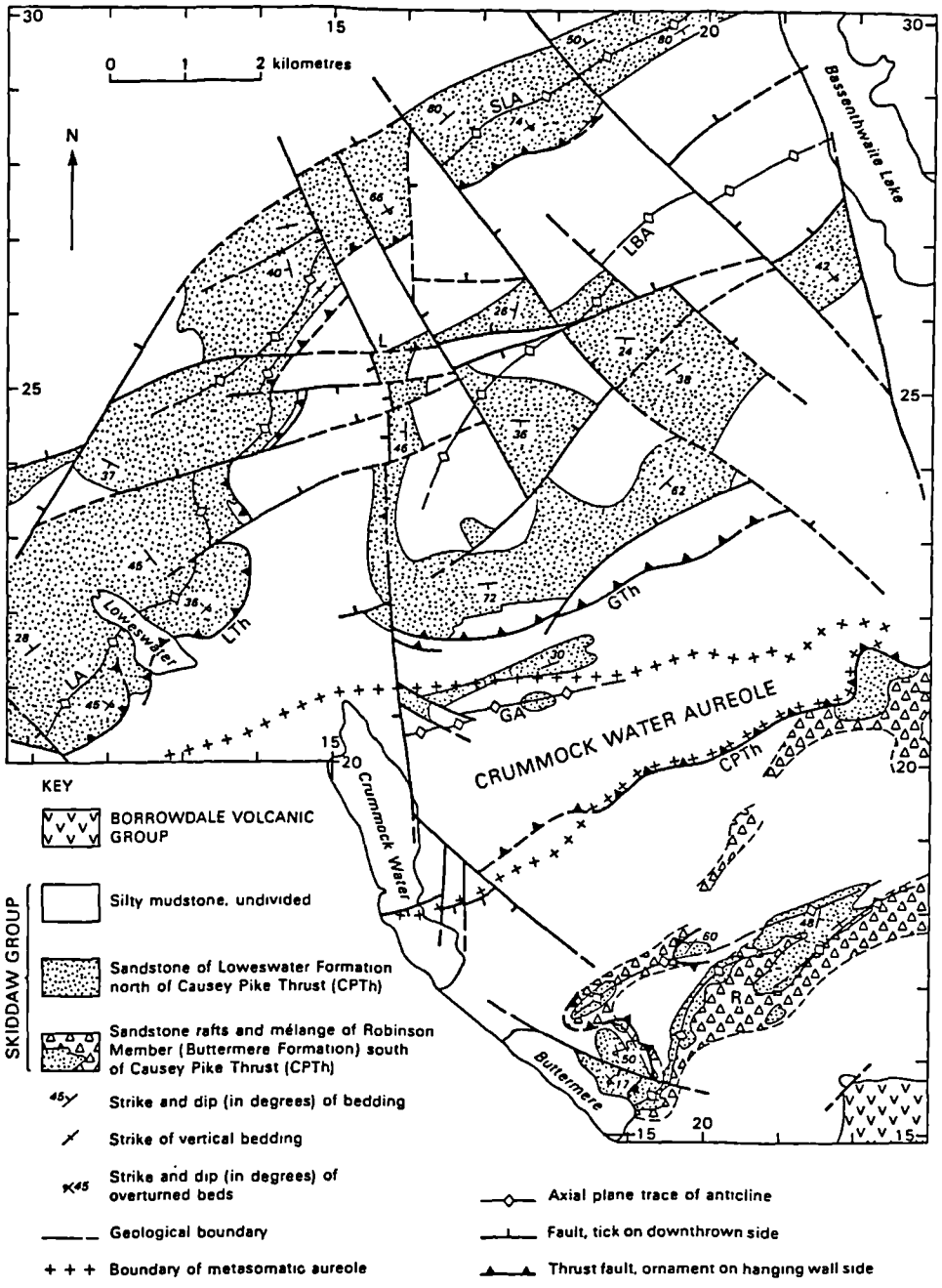

In the Skiddaw Inlier to the north of the Causey Pike thrust there is a series of southeast directed thrusts with associated hanging-wall anticlines (figure 1.6). Minor folds mimic the major structures. The Causey Pike thrust places this sequence above the Buttermere Formation olistostrome. The opposing vergence of structures across the Causey Pike thrust was used to infer the position of the axis of a narrow, fault-controlled depositional basin. The higher strain in the Buttermere Formation implied the north-northwest facing slope was steeper, which was compatible with basin development by extensional normal faulting of basement, throwing down to the north-northwest, away from the continent. The British Geological Survey mapping team now, however, considers the major Loweswater anticline to be a later tectonic structure coaxial to the smaller scale slump folds (Cooper et al, in prep).

At depth along the trace of the Causey Pike thrust, a major strike-slip fault system has been postulated on the evidence of a geophysical lineament and associated elongate intrusion whose aureole is present at the surface: the Crummock Water Aureole (Cooper et al, 1988).

Several later phases of deformation affect the Skiddaw Group:

(a) The largely subaerial Borrowdale Volcanic Group (Branney, 1988) is unconformable on the Skiddaw Group and represents a volcanic arc, accompanied by significant uplift. Structures associated with volcanic doming, partial basin inversion and volcano-tectonic faulting, prevalent in the volcanic group, have not been recognised in the Skiddaw Group.

(b) The Caledonian orogeny caused folding, thrusting and formation of three cleavages in the Skiddaw Group (Webb and Cooper, 1988).

(c) Intrusion of the late-orogenic Skiddaw granite contact metamorphosed the Skiddaw Group country rock, but structures associated with its emplacement have not been recognised.

(d) Faulting occurred in the Carboniferous, with accompanying mineralisation, and in the Permo-Triassic.

Palaeoslope orientations interpreted from slump fold vergence directions are used in this study (chapter 4) to reassess the geometry of the Skiddaw Group depositional basin.

1.5 Other occurrences of Ordovician sediments in the southern British Isles

1.5.1 Isle of Man

The geology of the Isle of Man was studied in the last century and a map and memoir were published by the Geological Survey (Lamplugh, 1903). A thick sequence of mudstones, sandstones and breccias with a complex structural history was recognised.

Simpson (1963) published a stratigraphy and polyphase structural sequence for the 'Manx Slate Series', believed to be of Tremadoc age on the occurrence of a single graptolite. Downie and Ford (1966) recovered a probable early Arenig microfossil assemblage and further micropalaeontological evidence (Molyneux, 1979) has shown Simpson's stratigraphy to be incorrect (table 1.5).

Table 1.5 Stratigraphy of the Lower Palaeozoic rocks of the Isle of Man. (a) after Simpson (1963), (b) after Molyneux (1979).

(a) Simpson (1963)		(b) Molyneux (1979)	
Manx Slate Series		Manx Group	
Glen Dhoo Flags Cronkshamerk Slates Sulby Flags Sulby Slump-breccia Slieau Managh Slates Injebreck Banded Group Barrule Slates Maughold Banded Group Lonan and Niarbyl Flags Ballanayre Slump-Breccia Lady Port Banded Group	Tremadoc	Lady Port Banded 'Group' Maughold Banded 'Group' Glen Dhoo Flags & Lonan Flags Niarbyl Flags	Late Arenig to Early Llanvirn Arenig Late Tremadoc Tremadoc

The Cronkshamerk Slates are of probable Tremadoc age and are overlain by the Lonan, Niarbyl and Glen Dhoo flags, all of Tremadoc age. These units are age equivalent to the Bitter Beck and Watch Hill formations of the Skiddaw Group. The Maughold Banded Group is of probable Arenig age and the Lady Port Banded Group is of probable late Arenig or Llanvirn age (Molyneux, 1979). The relatively young age of the latter is supported by mica-crystallinity studies (Roberts et al, 1990) and it is separated from the Niarbyl Flags by the Ballanayre slump breccia. The faulted junction with the flags (Roberts et al, 1990) may be a faulted unconformity associated with emplacement of the slump breccia. The Sulby slump breccia is possibly equivalent to that at Ballanayre. These resedimented units might equate with the Buttermere Formation olistostrome or the Beckgrains Bridge debris flow of the Kirk Stile Formation.

Close similarity exists between the sediments of the Manx and Skiddaw groups and their structure (Simpson, 1963, 1967). Both groups are intruded by late-orogenic granites (Skiddaw granite and Foxdale-Dhoon granites).

1.5.2 Ireland

Successions of similar age to the Skiddaw Group occur in a number of inliers in eastern and south-eastern Ireland. In Leinster, four lithostratigraphic groups are recognised (Bruck et al, 1979) (table 1.6).

Table 1.6 The four lithostratigraphic groups of Leinster, (Bruck et al, 1979).

northwest	southeast
Kilcullen Group (lower Ordovician to Llandovery)	Duncannon Group (Llandeilo to Ashgill) ~~~~~~~~~~~~~~~~~~~~ Ribband Group (middle Cambrian to Llandeilo) Bray Group (lower to middle Cambrian)

The Bray Group consists of greywackes, quartz arenites and breccias representing turbidites, local deltaic sediments and debris flows. The Ribband Group consists of grey, green and purple mudstone, siltstone and sandstone of distal turbidite and pelagic facies. Minor bentonites, tuffs and debris flows are present. The group is in part time-equivalent to the Bray Group representing deeper or basinal facies starved of clastic sediment. Uplift, westward tilting and differential erosion caused unconformity of the Duncannon Group above the Ribband Group with overstep decreasing to the west leading to a conformable boundary. The Duncannon Group is mainly of Caradoc age and consists of rhyolitic volcanics, limestones and mudstones, of shallow marine and subaerial environments.The Kilcullen Group represents continuous deposition of sandstone turbidites above the Ribband Group in the northwest of the inlier.

Recognition of fault bounded regions with lithological differences led to their interpretation as separate terranes (Murphy, 1987; Max et al, 1990) representing both sediment accretion from subducting ocean crust and amalgamation by strike-slip tectonics of regions previously separated along a northwest-facing continental margin. As lithological variation is diminished in the Silurian sediments, terrane amalgamation is thought to have occurred in the late Ordovician (Murphy, 1987).

1.5.3 Wales

The Ordovician history of Wales is discussed by Kokelaar (1988). Active volcanism, (e.g. the late Tremadoc Robell Volcanic Complex, Aran Volcanic Group of Arenig age and Caradoc volcanism in Snowdonia), was accompanied by dominantly shallow marine sediments, e.g. in the Harlech Dome area (Traynor, 1990) and in southwest Wales (Traynor, 1988). Kokelaar (1988) has suggested that Wales was a marginal basin during the Arenig and Caradoc.

1.6 Introduction to the Ingleton Group

The Ingleton Group crops out in the Chapel-le-dale Inlier (figure 1.2b), near Ingleton, North Yorkshire, and at Horton-in-Ribblesdale. It comprises two lithofacies:

(a) medium to very thick beds of greywacke of very coarse sand to fine sand grainsize, which display large sole marks, rare grading and ripples, with subordinate mudstone interbeds,

(b) mudstone with varying proportions of laminae and very thin beds of silt and very fine sand grainsize, which display small sole marks and ripples.

The argillaceous beds are intensely cleaved and the lithologies are green coloured due to abundant chlorite. A number of isoclinal folds plunge gently to the southeast with axial planes dipping steeply to the southwest (Leedal and Walker, 1950; Sloane,1988). Folds face down on the northwest-southeast trending cleavage implying a major deformation occurred prior to cleavage formation.

The group has proved unfossiliferous, hence age determination is problematical. Dakyns et al (1890) considered the 'Ingletonian Series' to be conformable beneath the 'Coniston Limestone Series', hence of Ordovician age, but Rastall (1906) considered a Precambrian age most likely, with the sediments sourced from a metamorphosed Archaean complex. Leedal and Walker (1950) also

concluded a Precambrian age. O'Nions et al (1973) demonstrated Ashgill mudstones unconformable above the Ingleton Group at Douk Gill, near Horton-in-Ribblesdale. Their interpretation of radiometric ages led them to conclude a Cambrian or early Ordovician age for deposition.

Lithological comparison of the Ingleton Group with greywackes recovered from the Beckermonds Scar borehole was made by Wilson and Cornwell (1982) and Berridge (1982). Acritarchs of probable Arenig age were recovered from a single horizon in the borehole indicating correlation with the Skiddaw Group and implying the Ingleton Group was also equivalent in age.

In this study the sedimentology (chapter 2) and petrography (chapter 3) of the Ingleton Group and greywackes from the Beckermonds Scar borehole are studied in detail and compared with the Skiddaw Group.

Chapter 2
SEDIMENTOLOGY

2.1 Introduction

The aim of this chapter is to describe and characterise the sediments of the Skiddaw Group. Facies are described, including a description and interpretation of previously unrecognised channellised deposits, and application is made of published facies schemes for turbiditic sediments. Current facies models of submarine fan sedimentation and non-fan deep marine deposition are compared with the Skiddaw Group. Interpretation is made of depositional environments, their lateral variations and changes with time. An interpretation of detailed palaeocurrent data is presented to indicate the position and orientation of intra-basin topography. Controls on submarine fan development are discussed.

The sedimentology of the Manx Group is described and comparisons are made with the Skiddaw Group.

Descriptions and environmental interpretation of the undated Ingleton Group and strata from the Beckermonds Scar borehole are presented and compared with the Skiddaw Group.

Thus, the chapter presents the sedimentological evidence upon which, in association with structural data and analysis of sediment composition and provenance, geological models of basin evolution may be postulated.

2.2 Introduction to deep marine clastic sedimentation

This introduction may be omitted by the reader familiar with the subject.

Recent, detailed reviews of the history of study and modern concepts of deep marine sedimentation are given by Pickering et al (1989) and Stow in Reading (1986).

The classic paper 'Turbidity currents as a cause of graded bedding' by Kuenen and Migliorini (1950) initiated an explosion in experimental and field-based research into resedimentation processes and deposits. Geologists had been presented with a mechanism for clastic sediment transport into the deep ocean, leading to the reinterpretation of many shallow marine sequences as the products of resedimentation processes interbedded with sediment derived from pelagic settling and clearwater bottom currents.

2.2.1 Resedimentation Processes

Turbidity currents are one type of *sediment gravity flow* (Middleton and Hampton, 1973), which are mixtures of particles and water that move under the influence of gravity due to their density being greater than that of the ambient fluid, sea water. Gravity acts on the solid particles in the mixture, inducing downslope flow and the admixed water is a passive partner to this process. Conditions for continued flow are:

(a) the shear stress generated by the downslope gravity component acting on the excess density of the mixture exceeds the frictional resistance to flow,

(b) the grains are inhibited from settling by one of several support mechanisms (table 2.1).

Table 2.1 shows four idealized types of sediment gravity flow which are points in a process continuum, each characterised by a different range of particle support mechanisms, e.g. Pickering et al (1989) do not recognise separate categories of grain flow and liquefied flow preferring to show how pore fluid escape, elevated pore pressures and dispersive pressure influence transport and deposition in turbidity currents and debris flows. In a single transport/deposition event, processes may act simultaneously or sequentially. Figure 2.1 summarises the resedimentation processes, their initiation, transport characteristics and deposits.

Flow initiation can be caused by:

1. Sediment failure on a slope in response to (a) increased shear stress due to slope steepening or thickening of the sedimentary pile, or (b) result from decrease in shear strength associated with fluidisation due to earthquake shock or pounding by storm waves. Such triggers produce infrequent flow events.

2. Introduction into the marine environment of suspended sediment from rivers, leading to frequent/continuous resedimentation processes.

Two broad types of sediment gravity flows are important in the Skiddaw Group: turbidity currents and debris flows.

Table 2.1 Types of sediment gravity flow and their characteristics. Data compiled from Pickering et al (1989), Stow (1986).

FLOW TYPE	SLOPE	MAJOR SUPPORT	MINOR SUPPORT
turbidity current *	0-0.5°	turbulence	grain collisions (dispersive pressure) trapped or escaping pore fluids (at high concentrations)
grain flow	>18° (under gravity) 0° (where driven by an overlying flow)	grain collision (dispersive pressure)	
fluidized and liquefied flows	>3° >0.5°	trapped/escaping pore fluids	grain collisions (dispersive pressure) turbulence
debris flow *	>1°	frictional strength buoyancy cohesive strength trapped/escaping pore fluids grain collisions (dispersive pressure)	turbulence (in high velocity, low viscosity flows)

* = flows capable of long-distance sediment transport into the deep sea on relatively gentle slopes (<10°).

Figure 2.1 Probable interrelationship of processes of initiation, long distance transport and deposition of sediment in the deep sea (from Pickering et al, 1989, figure 2.1).

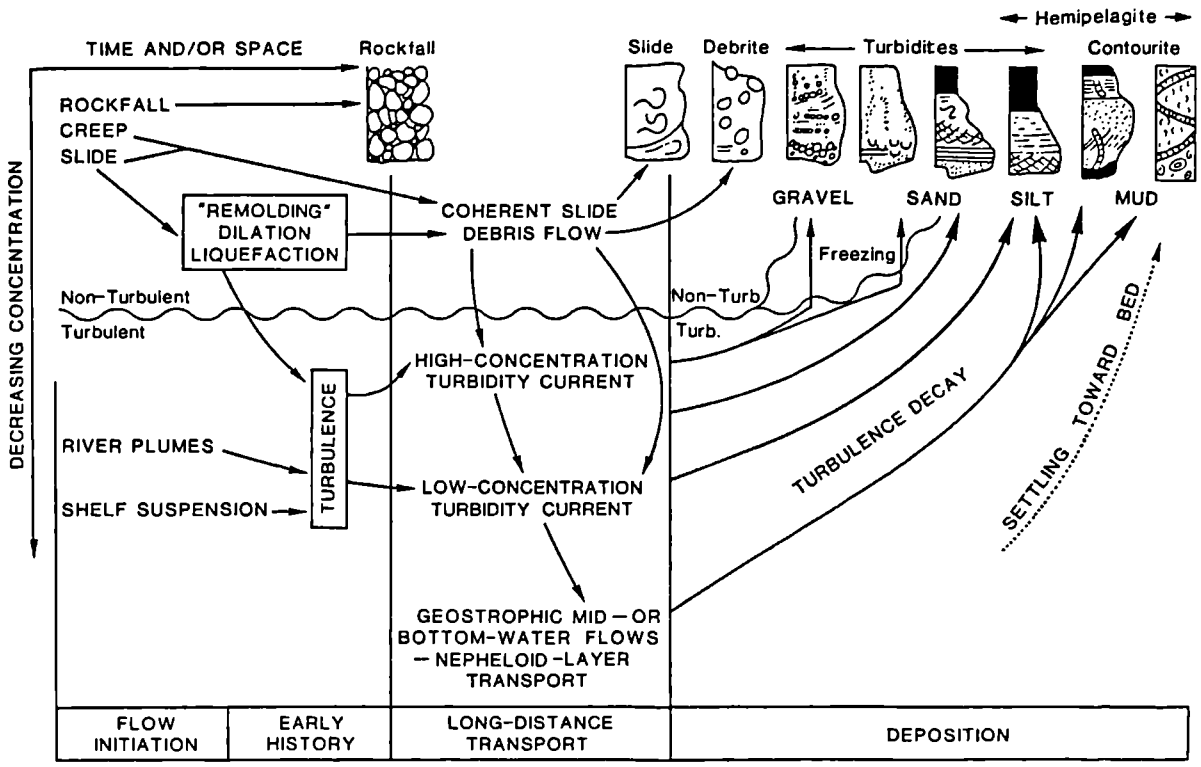

2.2.1.1 Turbidity currents

A turbidity current is a density current (Simpson, 1982), a suspension of sediment grains with particles supported by the upward component of fluid turbulence. High and low density types are commonly described, representing end-members of a continuous spectrum of flow concentrations. They may be relatively short lived surge-type flows, generally with infrequent trigger mechanisms, or long-lived steady or uniform underflows from a prolonged source of input, e.g. river-fed.

Experimental turbidity currents have three components, the head body and tail (figure 2.2).

In the lobate head region flow is forward and upward and the nose can show lobes and clefts which entrain the ambient fluid. The head region, which carries the coarsest grains, is capable of eroding the substrate; the erosional hollows producing sole markings when filled. Deposition may take place from the body while the head still erodes. The tail is relatively thin and dilute. Mixing with sea water in the turbulent region behind the head and loss of sediment by deposition will eventually stop the turbidity current. If unconfined, a turbidity current will spread radially.

Figure 2.2 Simplified section through a turbidity current. Flow direction is from right to left.

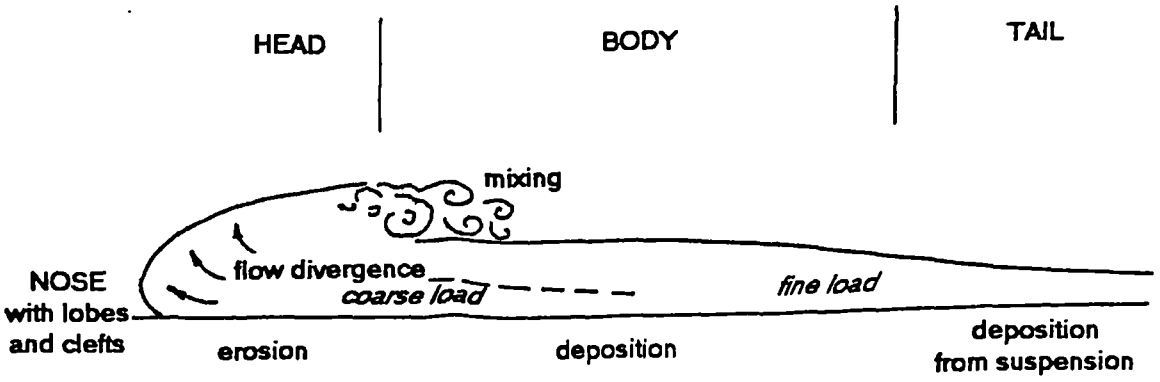

Table 2.2 Estimates of the physical parameters of natural turbidity currents (compiled from data in Stow, 1986, and references therein).

PARAMETER	SOURCE OF ESTIMATE AND LIMITS	ESTIMATED VALUE
velocity	Grand Banks eathquake 1929	70kmh^{-1}
	other documented examples	10's kmh^{-1}
	low density turbidity currents	0.4-1.8kmh^{-1}
distance travelled	length of deep sea channels and size of abyssal plains	up to 4000-5000km
thickness and width	size of levees of submarine channels	100's m thick several km width
	low density turbidity currents	few m to >800m thick
frequency	controls: nature of source area proximity of depositional area to source seismicity in source area sea level (rise lowers frequency)	river fed:1 in 2 years, sand removal in head canyon: 1 in 2 years, deposition in proximal fan: 1 in 10 years, deposition in distal fan/ basin plain: 1 in 1000-3000 years.

It has been argued that turbidity currents can maintain themselves by autosuspension (Bagnold, 1962). This is a state of dynamic equilibrium in which the excess density of the suspended sediment causes motion which generates turbulence which maintains the sediment in suspension. Thus a feedback loop exists if energy loss by friction is compensated by an energy gain from the downslope component of the acceleration due to gravity. Pantin (1979) has shown that a critical flow density exists, below which the flow will decay and deposit its sediment and above which it will achieve autosuspension. In this state it could travel long distances with no net deposition.

In nature, the practical problems of observing infrequent, powerful flows in the deep sea have ensured that most internal characteristics of turbidity currents are determined by indirect evidence. The Grand Banks earthquake of 1929 triggerred a turbidity current which sequentially broke submarine telegraph cables; the current travelled a mimimum distance of 648km with a maximum velocity of 70kmh^{-1} (Heezen and Ewing, 1952). Evidence for turbidity currents travelling large distances is also suggested from the lengths of deep sea channels and abyssal plains, which are up to 5000km. Estimates of other parameters of natural turbidity currents are given in table 2.2.

It has been suggested that flow in turbidity currents will be supercritical (Froude number >1) on slopes >0.5^{0} (Komar, 1971). Transition to subcritical flow will occur when the gradient decreases. Van Andel and Komar (1969) suggested such a change in flow regime would be accompanied by a hydraulic jump involving a transition from a thin, dense, supercritical flow on the basin sides to a thick, less dense, low velocity, subcritical flow on the basin floor. Pantin (pers. comm.) suggests that the change in flow regime with decrease in gradient need not be accompanied by a hydraulic jump if the rate of gradient change is very low. A change from supercritical flow to subritical flow may occur as a turbidity current becomes unconfined at a canyon mouth (Komar,1971).

A decrease in mean flow velocity, with a corresponding decrease in both flow competence (the coarsest particle that can be transported) and flow capacity (sediment discharge), will initiate or increase the rate of deposition. A velocity decrease may be due to:

a decrease in gradient,

flow divergence,

increased bed friction,

increased particle interaction,

decreased flow density due to deposition,

deflection of slow mud-rich flows by contour currents or by the Coriolis effect which constrains flows to move roughly parallel to contours rather than downslope (Hill, 1984).

Flows with a high proportion of suspended mud can flow with less sediment loss, even on gentle slopes, than mud-poor flows, thus travel a greater distance. They are relatively more efficient.

The deposits of turbidity currents are turbidites. Bouma (1962) recognised a sequence of sedimentary structures common in the Gres de Peira-Cava of the southern French Alps. This became known as the Bouma sequence with five divisions (figure 2.3b). The sequence was interpreted hydrodynamically by Walker (1965), (figure 2.3b).

An explanation was required for the lack of dune bedforms expected in the experimental sequence of structures due to waning flow. Walker (1965) suggested that deposition was too rapid for dune bedforms to equilibrate with the decelerating flow. Alternatively, turbidity currents may be too thin for the formation of large bedforms which require a ratio of flow depth to bedform height of about 5:1, (this might be larger for turbidity currents with maximum velocity below the flow top and a strong internal density stratification). Walton (1967) suggested that when flow intensity was sufficient for dune formation then the grainsize of the sediment load was too fine. Clay content suppressed dune formation. Allen (1970) considered sediment fallout rate and suggested a modified sequence of sedimentary structures from a waning flow, where a transition from upper stage plane beds to ripples was possible and dune formation was only expected in coarse grained deposits. Examples of dune bedforms in medium and coarse sand grade turbidites have been reported (Kemp, 1987; Valentine et al, 1984). The occurrence of a hydraulic jump between deposition of Bouma Tb and Tc divisions may replace dune formation (Pickering et al, 1989).

The Bouma sequence adequately describes only medium grained turbidites. The deposits of many high concentration turbidity currents are described by the coarse grained turbidite sequence of structures (Lowe, 1982) (figure 2.3a). Many of the structures result from grain flow, fluidized or liquefied flow mechanisms during the final stages of deposition. Inverse graded laminae have been interpreted as the products of traction carpets, produced by sheared, dense grain dispersions at the base of the flow (Lowe, 1982). In gravels, only one traction carpet is generally developed giving an inversely graded basal division to the deposit. In pebbly sand and coarse to medium sand, traction carpets are thinner and may form a sequence with a decrease in maximum grainsize and thickness between each successive unit.

The products of dilute turbidity currents are largely contained within Bouma Td and Te divisions, so a fine grained turbidite sequence describes their characteristics (figure 2.3a). This is a composite sequence, rarely observed in its entirety, with top-absent or base-absent sequences common.

These idealised turbidites are parts of a continuous spectrum of turbidite facies. A single turbidity current can deposit a range of facies as the flow characteristics change during sediment transport and deposition. An interpretation of the depositional flow conditions reveals the 'proximality' of the deposit (Walker, 1967; Sadler, 1982). This concept was the basis for the first turbidite facies models. The Skiddaw Group displays turbidites from across the range of facies.

Figure 2.3 Idealized sequences of turbidite structures, (a) the fine grained sequence with divisions of Stow and Shanmugam (1980) and Piper (1978), (b) the Bouma sequence and its hydrodynamic interpretation (based on Bouma, 1962, Walker, 1965), (c) the coarse grained sequence of Lowe (1982). Grainsize increases to the right for each column and scalebars give a typical unit thickness. Modified after Stow (1986).

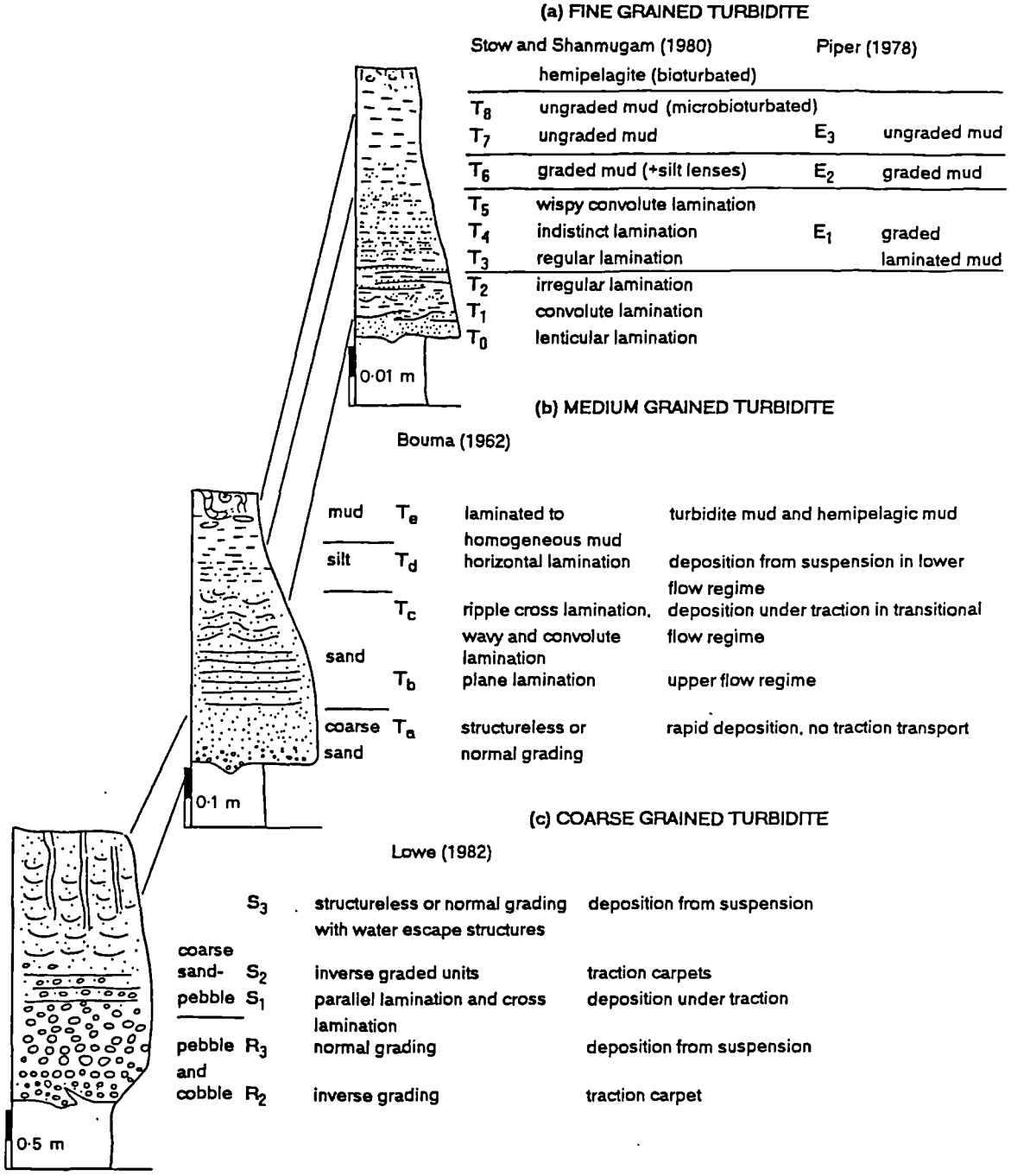

2.2.1.2 Debris flows

Debris flows are highly concentrated, highly viscous, sediment dispersions that possess a yield strength and display plastic flow behaviour (Johnson, 1970; Hampton, 1972). Particle support is from a combination of:

(a) frictional resistance to settling through finer matrix,

(b) matrix cohesion or strength that is not exceeded by the gravitational force acting on dispersed clasts,

(c) buoyancy (partial support only),

(d) elevated pore pressures in the matrix,

(e) dispersive pressure.

Movement is a result of deformation in a basal zone of high shear stress. The upper part of the flow may be rafted as a semi-rigid plug (Johnson, 1970). As shear stress decreases (e.g. by decrease in gradient, or dissipation of excess pore pressure) the plug thickens downwards until movement ceases ('freezing') when shear stress becomes lower than the yield strength. In the submarine environment movement can occur on slopes as low as 0.5^{o}. Debris flows are generally laminar with insignificant basal scour. The front of the flow forms a steep nose which may slump if it becomes oversteepened.

Debris flow deposits (correctly called debrites (Pickering et al, 1989)) are: poorly sorted, lack distinct internal layering but may have a crude stratification, have a poorly developed clast fabric, display irregular mounded tops, show poor normal or inverse grading and may be up to a few tens of metres thick. Examples of debrites occur in the Kirk Stile Formation at Beckgrains Bridge [NY1904 3552] and Outerside [NY 2132 2140] and in the Buttermere Formation at Goat Crags [NY 1887 1633]. The debrites of the Buttermere Formation are part of a major olistostrome comprising folding and shearing of mudstone and sandstone rafts (up to 1km length) as a result of gravitational sliding (Webb and Cooper, 1988) (figure2.1).

2.2.2 Normal marine processes

2.2.2.1 Clear water bottom currents

In addition to resedimentation processes, normal bottom currents are capable of transporting, reworking and depositing sediment in the deep marine envorinment. They are of three principle types:

1) Internal waves and tides, formed between water layers of varying density, have sufficient velocity to suspend and erode sediment at the shelf break and upper parts of basin slopes (Shepard, 1973).

2) Canyon currents, which flow both up and down the axes of submarine canyons with velocities up to $30cms^{-1}$, are caused by tides, internal waves, surface currents, storm surges or cold-water cascading currents. Almost constantly these non-turbid bottom currents can significantly rework sediment and erode canyons and channels. Deposits have fluvial characteristics with features of traction transport, dune bedforms, reworking and coarse lags. Canyon and channel sediments can also be reworked by turbidity currents.

3) Contour currents are deep ocean bottom currents formed by the cooling and sinking of surface water at high latitudes and its circulation throughout ocean basins. The Coriolis force deflects the moving water mass to the right in the northern hemisphere (to the left south of the equator) into a contour-following mode and concentrates flow on the western margins of ocean basins. Common current velocities are 10-20cms^{-1}, but can exceed 100cms^{-1} where flow is restricted. The deposits of bottom currents are contourites, either muddy or sandy, and often thoroughly bioturbated. These are difficult to recognise in ancient sediments and can resemble hemipelagite or mud turbidites and fine grained turbidites respectively.

2.2.2.2 Pelagic settling

Pelagic deposits accumulate from slow settling through the water column of biogenic, siliceous and calcareous skeletons, wind blown dust or ash and ice rafted debris. Pelagic sediments are oozes and red clays. Suspended, terrigenous silt and flocculated clays can contribute a significant proportion of the settling material which forms hemipelagic deposits.

In the Skiddaw Group, deposits of normal marine processes are not easily distinguished from siltstone and mudstone turbidites.

2.2.3 Facies schemes

The classic paper of Mutti and Ricci Lucchi (1972) presented a facies classification which has been widely used for description of deep-water deposits and interpretation of depositional process. It uses grainsize, bed thickness, sandstone to mudstone ratio and sedimentary structures to define facies that can be related spatially to one another.

This classification has been superseded by the facies scheme of Pickering et al (1986), (figure 2.4) which incorporates the research advances and wider understanding of deep marine sediments since the publication of the former scheme. More than forty facies are described, and grouped primarily using grainsize, sand to mud ratio, bed thickness, texture and sedimentary structures. Interpretation of depositional process is made but is not fundamental to the descriptive scheme. The complexity and wide range of deep marine deposits is represented but spatial and temporal facies transitions are not reflected by numerically adjacent facies names. This is because facies, facies class and facies group are each defined using more than one of the six parameters necessary for adequate description, i.e. maximum grainsize, ratio of coarser to finer parts of bed couplets, bed thickness, texture, grading and sedimentary structures. This facies scheme, with minor additions, is used to describe the sediments of the Skiddaw Group.

Figure 2.4 Facies classification scheme for deep marine sediments of Pickering et al (1986). with newly defined facies as follows: B2.3, variably bedded, normally graded sandstones; C2.5, very thin beds and thick laminae of fine and very fine sandstone with up to 60% mudstone interbeds; C2.6, amalgamated thin beds of fine and very fine sandstone with ripple cross lamination; C2.7, very thin beds of medium and coarse sandstone with mudstone interbeds. Detailed descriptions are given in section 2.3.2.

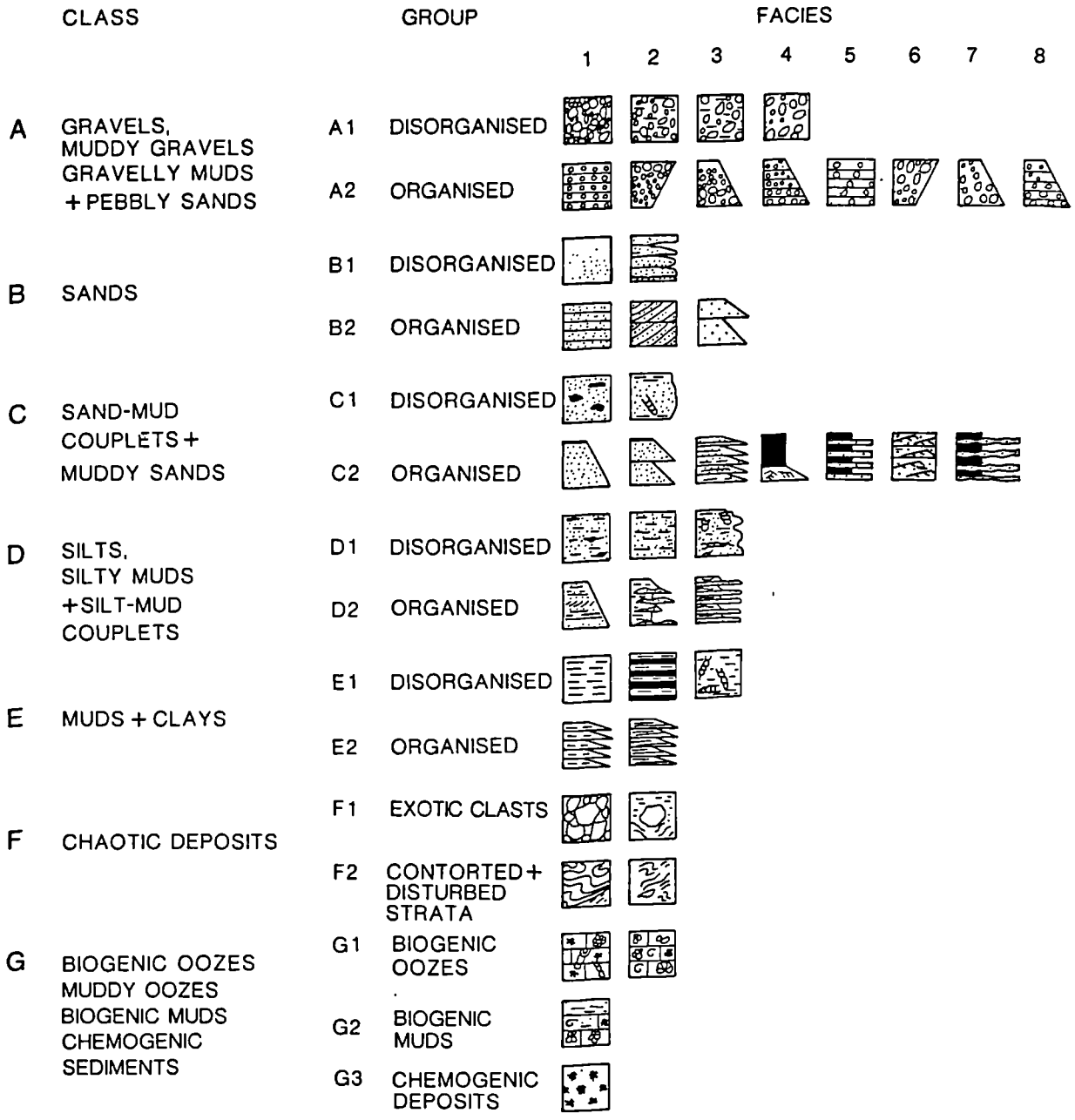

2.2.4 Facies models

Analysis of facies associations in a vertical sequence allows interpretation of the spatial and temporal relationships of ancient environments. Three facies associations defined for deep marine depositional systems are: slope apron, submarine fan, and basin plain (Mutti and Ricci Lucchi, 1972) (figure 2.5a). Construction of a facies model enables visualisation of the sedimentary distributary system and can be used as a descriptive, interpretative and predictive tool. Submarine fan facies models are widely used for deep marine clastic sediments.

A detailed model based on modern fans was introduced by Normark (1970) and for ancient fans by Mutti and Ricci Lucchi (1972). The primary difference between these two models is the position of depositional lobes; lower fan lobes are described for the ancient model, but the modern fan model shows suprafan lobes in a middle fan position. A general submarine fan model was proposed (Walker 1978) (figure 2.5b).

A major problem in comparing modern and ancient fans is the scale of observation. The smallest resolvable features in the modern environment are generally larger then the largest outcrops. Mutti and Normark (1987) proposed a scale with up to five orders for comparison of different fans both ancient and modern:

1st order: basin-fill sequences or complexes,

2nd order: individual fan systems,

3rd order: stages of growth within a system,

4th order: facies associations and component substages, e.g. lobes, channel deposits, overbank deposits,

5th order: outcrop features, e.g. style of bedding, scours, structures within beds.

Ancient thickening-upward cycles, of 3-15m thickness, interpreted as depositional lobes (4th order) are commonly described and compared with modern suprafan lobes an order of magnitude thicker. An alternative explanation for these cycles might be lateral shifts in the site of turbidite deposition resulting in a smoothing of bottom topography and thickening-upwards 'compensation cycles' (Mutti and Sonnino, 1981), or sedimentary response to minor sea level fluctuations (Mutti, 1985).

Since the proposal of the general submarine fan model, observations of modern fans, using sidescan sonar and deep drilling, have highlighted the variability of natural systems and revealed:

fans of differing shape, commonly elongate,

meandering and braided channel fills,

channel fills of silt/mud,

lack of lobe development on large modern fans,

non-fan depositional systems e.g. mid-ocean channel (Hesse, 1989).

Widespread variation from the general fan model was also recorded from ancient systems. A 'submarine ramp model' with multiple sediment sources was proposed for the Eocene Tyee Formation (Heller and Dickinson, 1985). Submarine fan lobes with differing characteristics were recognised. Since they are the principal sites of sandstone deposition, thus hydrocarbon reservoirs, their characteristics (size, texture, vertical and lateral connectivity) must be correctly assessed. Four

Figure 2.5 (a) facies associations of Mutti and Ricci Lucchi (1972), (b) submarine fan facies model of Walker (1978).

(a)

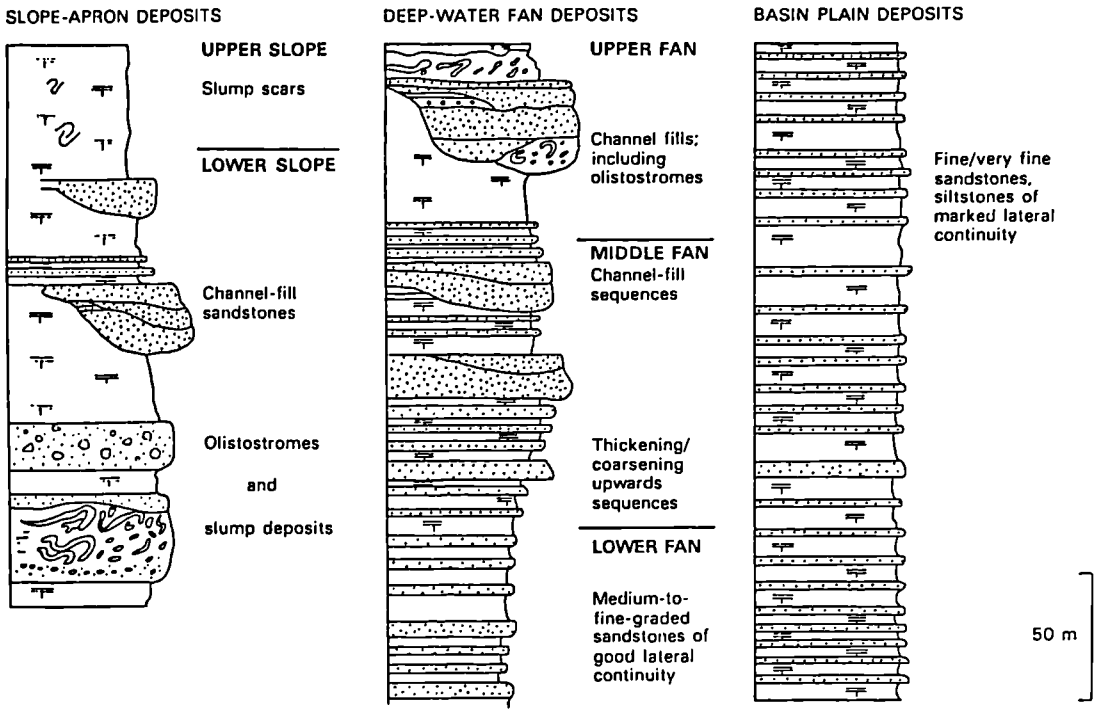

(b)

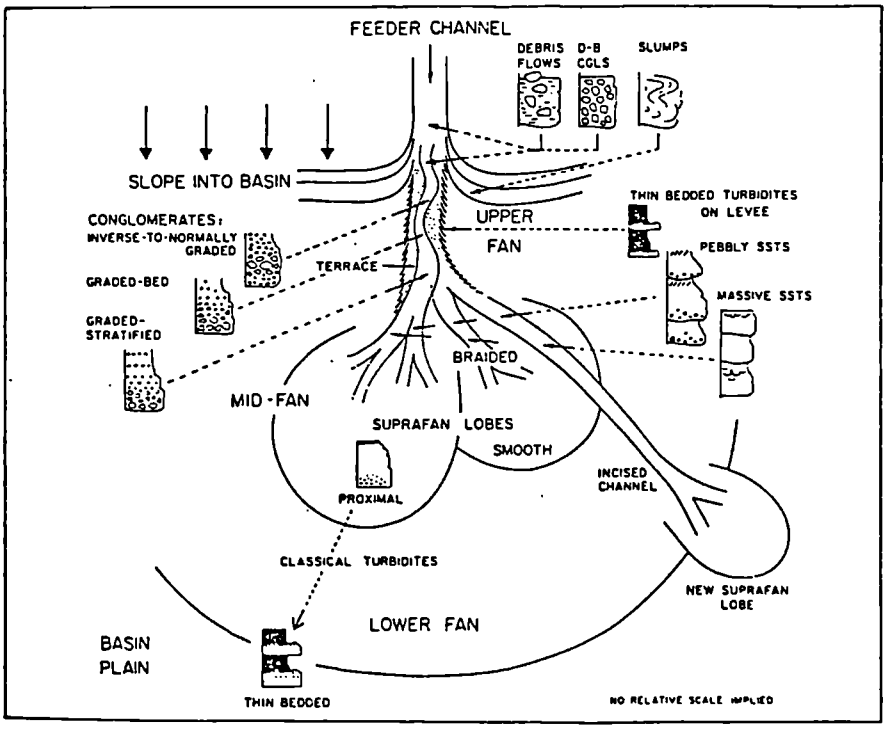

lobe models have been described (Shanmugam and Moiola, 1991): suprafan lobes (stacked channel sand bodies), depositional lobes (sheet sands), fanlobes (channel-levee complexes) and ponded lobes (mud-rich slumps).

Such variability in both modern and ancient depositional systems showed the application of a general facies model to be a gross oversimplification.

In order to understand an ancient system, one must appreciate the factors which control its development.

2.2.5 Controls and classifications of deep sea depositional systems

There are three major controls on submarine fan development: (1) *sediment type and supply,* (2) *tectonic setting and activity,* (3) *sea-level fluctuations.*

(1) *Sediment type and supply.* Classified on grainsize, two end-member fan systems are widely recognised: sand-rich and mud-rich. Sand-rich fans are characteristically small and radial. The lack of suspended mud in turbidity currents ensures rapid deposition of sand hence these are low-efficiency fans (Mutti, 1979), e.g. fans of the California Continental Borderland; the basis for the fan models of Normark (1970) and Walker (1978). Mud-rich fans are characteristically large, elongate, fed by major rivers with high sediment discharge (commonly in a humid or glaciated climate). They are high efficiency fans, with sand transported to the lower fan and basin plain environments. They lack suprafan lobes. Modern examples are the Bengal, Indus, Mississippi, and Amazon fans.

A point source of sediment, e.g. a delta feeding a submarine canyon will generate a radial or elongate submarine fan. A linear sediment supply will lead to development of a slope apron system, common on carbonate shelves.

Reading (1991) proposed qualitative classifications of deep sea depositional systems using sediment calibre and type of feeder system (figure 2.6). This approach promotes an understanding of controlling factors and enables comparison with other systems. Adequate exposure of ancient systems is required to recognise the texture and calibre of the sediment input since different grainsizes are deposited in different parts of the system.

(2) *Tectonic setting and activity.* Tectonic setting controls basin size and geometry, sediment type and supply and syn-sedimentary tectonics control facies distribution and fan geometry. On mature passive margins large, mud-rich fans develop on oceanic crust with sheet sands in lower fan areas e.g. Amazon, Mississippi fans. On active margins (including young rifted margins, convergent and oblique slip margins) small, sand-rich fans with well-developed lobes occur in a variety of types of small basin.

Classifications of submarine fans using the tectonic setting of basins have been proposed (Mutti and Normark, 1987; Shanmugam and Moiola, 1988). For modern fans, difficulty arises in classification of fans influenced by more than one tectonic setting and similar fans are found to occur in different basin types. For ancient fans tectonic setting is not directly observable.

(3) *Sea level fluctuations.* Sea level variations may be (a) eustatic, caused by glaciations (relatively short-term) or change in volume of the world's mid-ocean ridges (relatively long term), or (b) regional/local caused by tectonic activity.

Figure 2.6 Classifications of deep sea depositional systems of Reading (1991).

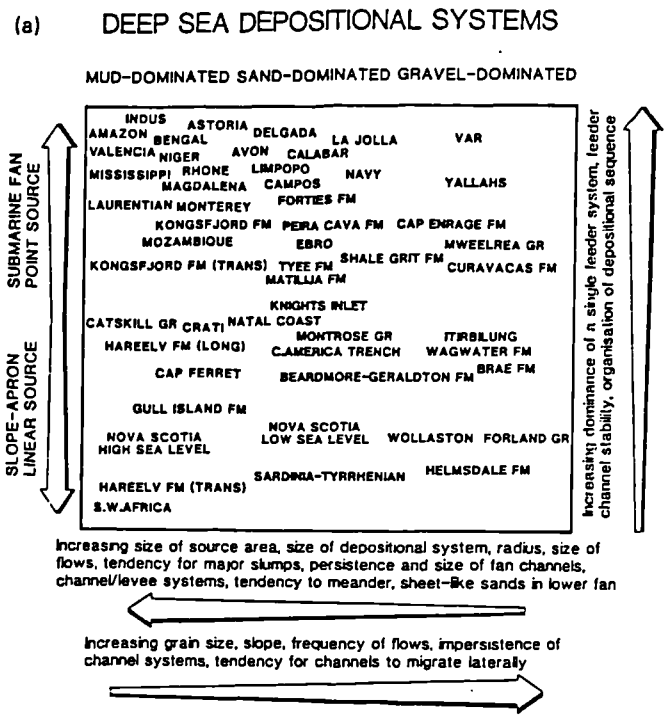

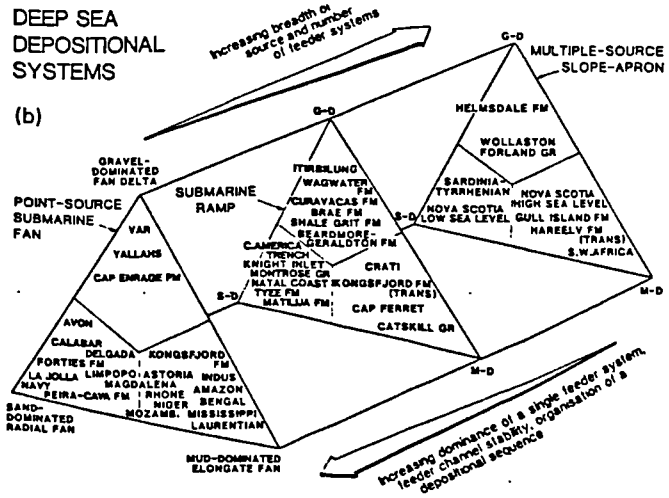

A relative high stand of sea level and accompanying transgression leads to retainment of sediment on the shelf. Sedimentary processes on fans are largely restricted to hemipelagic deposition and reworking by bottom currents.

Relative low stands can be accompanied by emergence of shelves and incision by rivers with discharge directly into deep marine systems. Unconsolidated shelfal sediments which accumulated in the high stand are redeposited in deep marine systems. Fan growth is accelerated. Mutti (1985) related high and low efficiency fans to falls and rises in sea level (figure 2.7). The theory applies to delta-fed systems with high rates of sediment supply in orogenic settings. Type I systems are related to a relative low stand when large volume turbidity currents deposit detached sand lobes in the lower fan region (high-efficiency fans). As sea level rises, turbidity current volume decreases and channelled sand bodies are deposited in the upper fan with channel-attached lobes (suprafan lobes) (Type II system, low-efficiency fan). With continued sea level rise, mud drapes the fan before delta progradation reaches the shelf edge and a mud-rich channel-levee complex is developed in the upper fan (Type III system).

The model suggests that sandstone packets, instead of representing suprafan lobes, represent widespread sand sheets during a sea level low stand. Hence intervening mudstone units do not correspond to lateral equivalents of sandstone facies, but to mud draping the fan during a relative sea level high stand. This model is not applicable to large passive margin fans e.g. Indus fan, where channel-levee complexes persist throughout changes in sea level. This has been attributed to an overriding influence of the other major controls (Kolla and Macurda, 1988).

Fan deposition responds to a complex array of variables with differing proportions and rates of change for each sedimentary system. Hence in nature each fan is different. Interpretation of the characteristics of ancient fan systems must be reviewed in the context of scale of observation, regional tectonic setting, source/basin relationship, sediment supply and sea level fluctuations.

Figure 2.7 The three main types of turbidite system recognised by Mutti (1985).

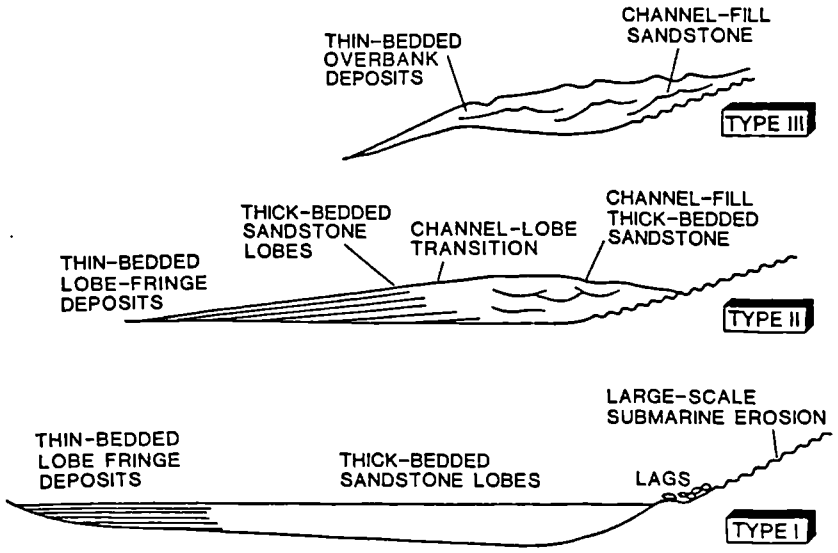

2.2.6 Palaeocurrent analysis in turbidites

In ancient turbidites there are three main types of palaeocurrent indicators: non-directional sole marks (grooves) and directional sole marks (flutes and prods) on bed bases, recording the direction of the erosive current; and ripples within or on top of beds, recording the flow direction of the depositional current or reworking by successive currents.

Current ripples and ripple cross lamination within sandstone turbidites have generally been thought to be less reliable than sole structures as indicators of the principal flow direction of the transporting turbidity current. This is because flow directions indicated by cross lamination are commonly at variance with those indicated by erosional sole structures on the same bed. Ripple directions commonly show quite systematic deviations from sole directions: a near perpendicular relationship has been observed in many elongate turbidite basins e.g. the Lower Palaeozoic of the Welsh basin, (Kelling, 1964), central Ireland (Cope,1959), the Scottish Southern Uplands (Craig and Walton, 1962; Scott, 1967), the Oslo region (Seilacher and Meischner, 1965), the Carboniferous of southwest England (Prentice, 1962), the Windermere Group of northwest England (Norman, 1961; Kneller et al, 1991).

Since Kelling noted this phenomenon more than 25 years ago, no convincing explanation has been presented. The systematic deviation is not adequately explained by flow meandering (Parkash and Middleton, 1970) or inaccurate palaeocurrent measurement. Reworking of bed tops by clear-water bottom currents (Hsu, 1964) is not applicable where ripples are clearly part of a sequence of structures related to waning flow. Erosion of the sole structures by non-depositing currents and subsequent infilling by transverse flows is unlikely and for deposits of high density turbidity currents it is implausible that no erosion was produced. Amalgamation of the deposits of simultaneous lateral and axial flows fails to account for the consistent angular relation between sole and ripple directions. Deflection of downslope currents (sole directions) into a contour following mode (ripple directions) at the base of slope is in contradiction to the palaeocurrent patterns in elongate basins. Deflection by the Coriolis Force would only explain deflections of one sense and cannot account for the lack of intermediate current directions. The latter is also true for banking of flows with progressive change from momentum-driven along slope flow (sole directions) to downslope gravitational flow (ripple directions) (Prentice, 1960; Seilacher and Meischner, 1965).

The phenomenon was addressed during this study in association with other turbidite workers at Leeds University (Pantin and Leeder, 1987; Edwards, 1991) and an explanation was proposed (Kneller et al, 1991). Based on flume tank experiments (Edwards, 1991) it was suggested that the ripples were generated by reflections from topographic features, basin margins and intra-basinal topography, oblique to the incident turbidity current. Thus, a large turbidity current flowing axially along a basin floor would erode sole marks beneath the head of the current. These would be infilled by deposition of much of the sand-grade suspended load from the body of the flow. Where the radially spreading flow was restricted by topography, internal solitary waves would be generated and flow back from the reflection surface, travelling perpendicular to its strike, across the body of the residual turbidity current. Capable of resuspending recently deposited fine sand and reworking it as bedload, the passing wave would produce ripple bedforms. Thus, ripple current directions are likely to be at a high angle to sole

directions. Since ripples are generated by flow normal to the strike of the reflection surface, they may indicate the orientation of basin margins or intra-basinal topography (e.g. associated with normal faulting, thrusting or volcanic edifices).

This model is applied in the interpretation of palaeocurrent patterns for the Skiddaw Group.

2.2.7 Problems of palaeocurrent measurement in ancient turbidites

Sole marks are relatively easily recorded as plunge and plunge directions or pitch with respect to bedding of ancient turbidites. Ripples are more problematic. Within a bed at least two sections through a set of ripple cross lamination are required to envisage its three dimensional orientation and transport direction. On bed surfaces a combination of ripple axis orientation and asymmetrical ripple form can be used to show the ripple migration direction, which can be measured as a lineation. Exposure of foresets within ripple forms of low asymmetry is necessary to prove the transport direction.

The type and dimensions of palaeocurrent indicators and their host beds and facies should be recorded so that only similar types are grouped together.

One requires the palaeocurrent direction with respect to horizontal beds at deposition. Thus folding in ancient sequences must be removed. This is accomplished using a stereographic net and procedures are described by Graham (1988). Where folds are non-plunging, rotation to the horizontal of beds about their strike direction is sufficient, but a two stage process is required for plunging folds to remove both fold plunge and the dip of the fold limbs. In multiply folded sediments or where folds have been rotated due to shear, the uncertainties involved in reorientation renders a palaeocurrent indicator of limited value.

For the Skiddaw Group, rotation to the horizontal about local strike orientation was performed for the majority of cases, except where fold plunge of $> c10^{o}$ could be demonstrated and a two phase reorientation procedure was used. At any one locality, the range of reorientated palaeocurrent directions is low. The range is increased where data were largely collected from overturned beds, e.g. Barf, suggesting these data are less reliable. Data from localities where folding effects are complex have been ignored.

Additional rotation of original palaeocurrent indicators could occur during thrusting. As a thrust propagates, folds in the hanging wall, initiated with axes perpendicular to the thrust transport direction, can be rotated about a vertical axis so that the fold axes approach the thrust transport direction. A horizontal rotation is applied, therefore, to palaeocurent indicators. In the Loweswater fells a lobate thrust sheet has been mapped (British Geological Survey, 1990) with a large-scale reclined hanging-wall anticline with dominantly overturned strata in a 300-700m wide zone adjacent to the thrust (enclosure 3). Axes of minor folds and palaeocurrent indicators were measured within this zone around the thrust lobe. The thrust transport direction was determined by measuring slickensides, slickencrysts and lineations (unrelated to cleavage intersections) on the thrust plane and on minor thrust planes and gently dipping bedding planes within the thrust sheet. The mean direction is to 142^{o}. Figure 2.8a summarises these data which are presented in detail in enclosure 3.

Palaeocurrent data, collected from the gently inclined upper limb of the structure and reorientated by rotation about strike, show a low range of directions for sole structures (figure 2.8b). Two localities were studied within the lower limb of the structure on the east and south sides of the thrust sheet respectively. At the eastern locality [NY 1383 2278] the local fold axis plunged 16° to 018°, an angle of 34° from a direction normal to the thrust transport direction. Thus a clockwise horizontal rotation of 34° should be applied to the sole direction after removal of tectonic tilt. This changes the palaeocurrent direction from towards 285° to 319°.

At the southern locality [NY1304 2186] the local fold axis plunges 15° to 257°, verging southeast, hence is 25° divergent from the normal to the thrust transport direction. An anticlockwise rotation of 25° should be applied to the sole direction changing it from towards 066° to 041°.

The procedure brings the originally widely divergent sole directions at each locality nearer to the mean for directional soles from the relatively less deformed strata of the upper limb (mean direction towards 360°).

An alternative approach is to plot bedding orientations from sub-areas around the thrust lobe on a stereonet to define a mean fold axis orientation for each sub-area (enclosure 3). The deviation of these mean fold axes from the normal to the thrust transport direction will give an indication of the horizontal rotations of each sub-area during thrusting (figure 2.8c).

It is concluded that where horizontal rotations in thrust sheets can be assessed, then they should be included in restoration of palaeocurrent directions. Also, where the degree of rotation is unknown, either through undefined thrust transport directions or local fold axis orientation, then palaeocurrent data should be treated with a full understanding of the limitations. For the Loweswater Fells, there is in excess of 20° difference in the amount of rotation indicated by each of the above methods. Therefore a restoration is not applied and a wider spread of directions is presented than the probable true spread (locality d on enclosures 1 and 2).

In addition to rotations within thrust sheets, rotations between thrust sheets can be significant. In the Skiddaw Inlier, such relative changes in orientation cannot be assessed. Since a workable model for palaeocurrent orientation across the region has been produced, large-scale differential rotations of thrust sheets are assumed to be negligible.

Figure 2.8 Characteristics of thrusting in the Loweswater Fells, (a) summary of lineation data, (b) summary of local fold axis rotations and results of palaeocurrent reorientations, (c) summary of fold axes defined by bedding, their rotations and results of palaeocurrent reorientations.

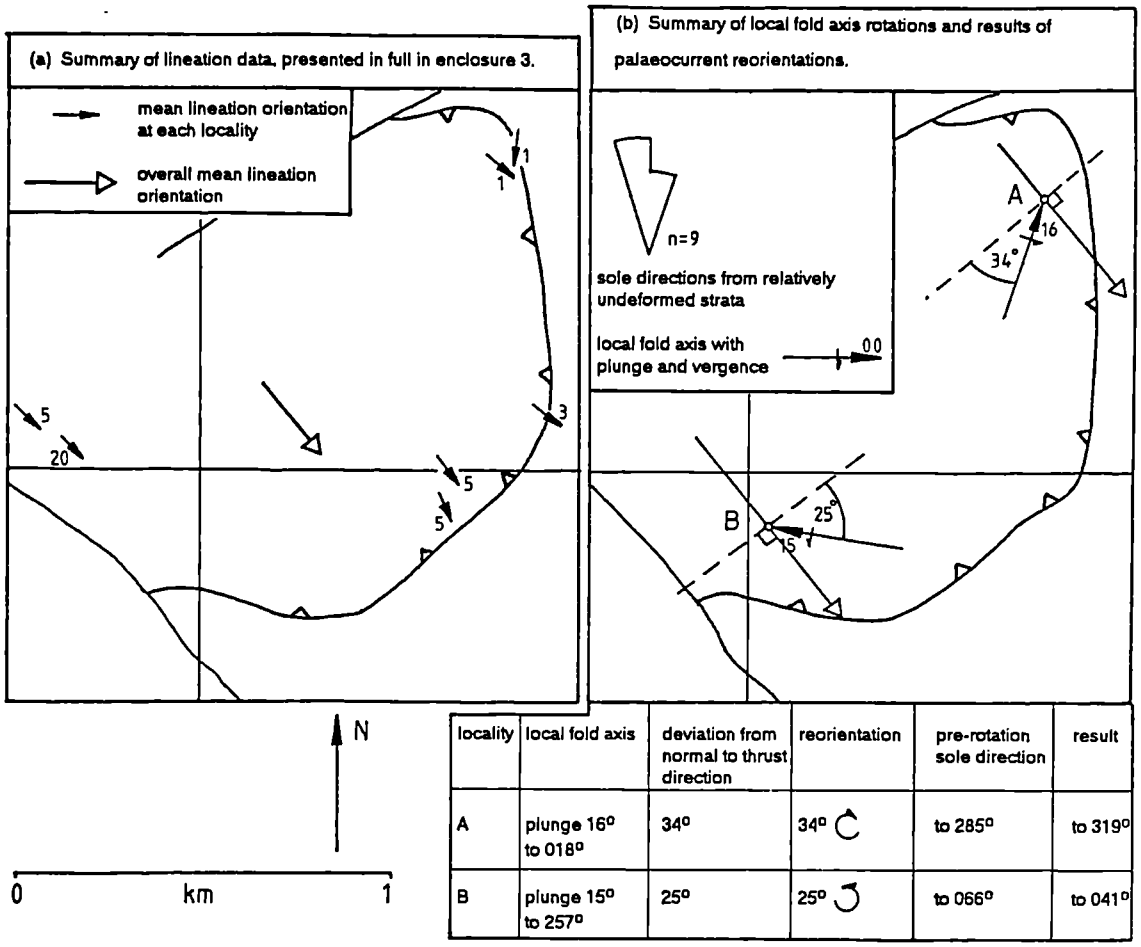

locality	local fold axis	deviation from normal to thrust direction	reorientation	pre-rotation sole direction	result
A	plunge 16° to 018°	34°	34° C	to 285°	to 319°
B	plunge 15° to 257°	25°	25° ↺	to 066°	to 041°

(c) Summary of mean fold axes defined by bedding in sub-areas 1 to 6 (enclosure 3), their rotations and results of palaeocurrent reorientations.

sub-area	mean fold axis	deviation from normal to thrust direction	reorientation	pre-rotation sole direction	result
5	plunge 9° to 166°	66°	66° C	to 307° to 305° to 269° to 285°	to 013° to 011° to 335° to 351°
3	plunge 11° to 238°	4°	4° ↺	to 066°	to 062°

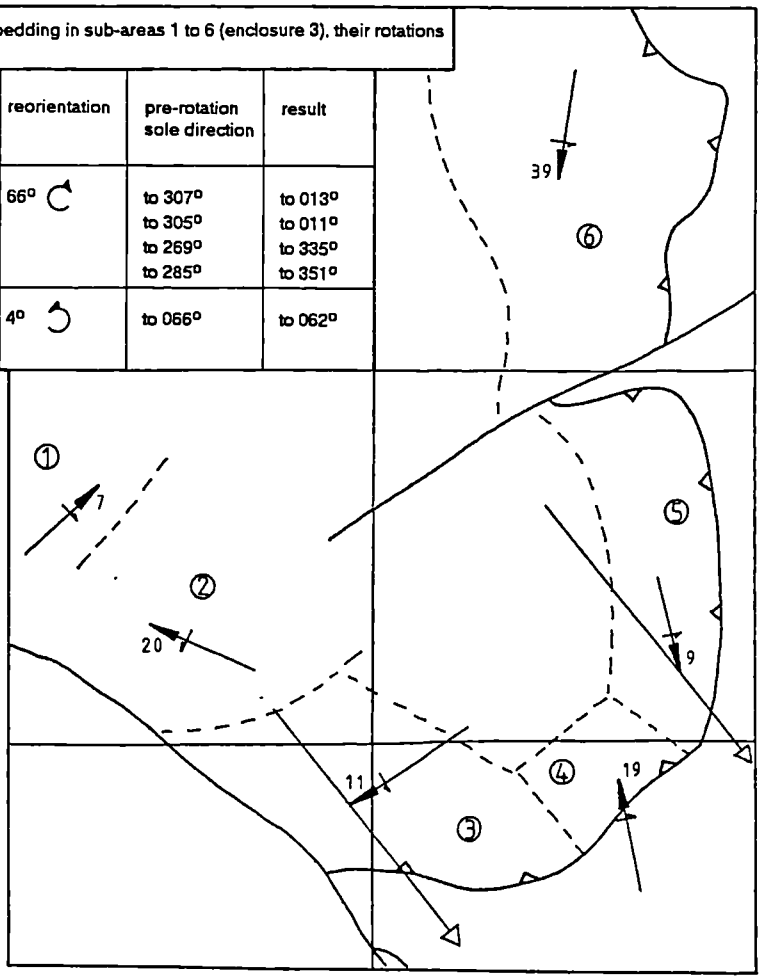

2.3 Sedimentology of the Skiddaw Group

Jackson (1961) described the Skiddaw Group as characteristic of sediments deposited by turbidity currents. It is widely accepted that sedimentation took place in a deep marine environment by a variety of depositional processes: low density and high density turbidity currents, debris flow (fluxoturbidite of Jackson, 1978), slumping and gravity sliding (Webb and Cooper, 1988).

Indicators of water depth are scarce. Wave ripples, indicative of deposition above storm wave base have not been identified. Bioturbation is minimal and confined to sub-horizontal, branched and unbranched, meandering, sub-cylindrical burrows and extremely rare sub-vertical burrows, 0.3-1.5cm in diameter. Trace fossil assemblages have been proposed that correspond to water depth (Seilacher, 1967), and Skiddaw Group examples are best related to the deep water nereites association (plate 2.1.1). Other factors (sediment supply, nutrient availability, grainsize and redox conditions) might significantly modify this depth zonation (Wetzel, 1984). The most abundant fossils are graptolites, common in oceanic sediments, but whose pelagic lifestyle ensures widespread distribution from shelfal to abyssal environments. No shelly fauna, common to shallow marine environments, has been recorded. The restricted occurrence of trilobite genera has been studied by Fortey et al (1989). They show the shallow water *Neseuretus* biofacies is absent but the *Cyclopygid* biofacies is represented, characteristic of sites exterior to the Gondwana platform. A tentative interpretation of water depth of 300m or more (Fortey et al, 1989) was made by comparison with trilobite forms of south Wales.

The sum of the evidence suggests a deep marine setting marginal to the Gondwana craton for the Skiddaw Group in the early Ordovician.

2.3.1 Group characteristics

The Skiddaw Group of the Northern Fells belt (Cooper et al, in prep) comprises two sandstone-dominant formations (the Watch Hill and Loweswater formations) sandwiched between mudstone-dominant formations (the Bitter Beck, Hope Beck and Kirk Stile formations). It corresponds to a first order basin-fill (terminology of Mutti and Normark, 1987). The Watch Hill and Loweswater formations are second or third order turbidite depositional systems which relate to two periods of sand-rich submarine fan activity; one around the Tremadoc-Arenig boundary and one within the Arenig. The sedimentary facies and facies associations (fifth and fourth order respectively) are described and interpreted.

2.3.2 Facies descriptions

Facies displayed by the Skiddaw Group are described below. Newly defined facies C2.5, C2.6, C2.7 and B2.3 are added to the scheme of Pickering et al (1986). Facies class A requires >5% gravel, facies class B requires >80% sandstone and <5% gravel, facies class C contains 20-80% sandstone and <80% mudstone and facies class D has <20% sandstone.

Facies A1.3

Locally, e.g. in the Hope Beck Formation at Swinside [NY 185 240], thin pebbly mudstones occur with matrix supported grains up to pebble grade and represent facies A1.3. They are debris flow deposits resulting from freezing of a cohesive debris flow as shear stress at the base of the flow became less than the cohesive strength (Pickering et al, 1986). Also included in this facies are the debrites of the Kirk Stile Formation at Beckgrains Bridge, and the Buttermere Formation.

Facies A1.4

Facies A1.4 comprises disorganised pebbly sandstones with pebbles and granules dispersed in a matrix of sand, e.g. Watch Hill Formation at Burntod Gill (figure 2.10, 1.3-2.4m, 19.5m) and Watch Hill (figure 2.9e, forest track, 6.1m) where medium and thick beds lack features of internal organization. Pickering et al (1986) suggest deposition of mixed grainsizes was rapid and due to increased inter-granular friction from a high-concentration turbidity current. With decrease in gravel content this facies is transitional into facies B1.1.

Facies A2.5

This facies describes medium beds of pebbly sandstone with horizontal or low-angle cross stratification, e.g. Elva quarry 1, 0-0.9m, 1.3-2.3m (figure 2.9a). Thick horizontal laminae, which sometimes display inverse grading, are interpreted as traction carpets (Lowe, 1982). Additionally laminae are defined by discontinuous strings of pebbles and granules. The facies was deposited from tractional bedload beneath a high-concentrration turbidity currents (Pickering et al, 1986). With decrease in proportion of gravel, this facies is transitional into facies B2.1.

Facies A2.7

Described as normally graded pebbly sands, medium and thick beds of this facies grade upwards from pebbles and granules to very coarse sand, e.g. Burntod Gill 2.6m, 13.7m, 16.7m, 19.0m, 32.0m (figure 2.10). Grain by grain deposition from a high-concentration turbidity current without significant traction transport has been suggested as the depositional mechanism for this facies (Pickering et al, 1986).

Facies B1.1

This facies comprises medium and thick beds of greywacke of fine to medium sand grainsize with sharp, flat bounding surfaces. It is extensively developed in the Watch Hill Formation e.g. Burntod Gill (figure 2.10), and in the Loweswater Formation e.g. Scawgill Bridge Quarry between 42.7m and 59.0m (enclosure 6). Beds are usually structureless, but poorly developed horizontal lamination or laminae cross-cutting at low angles have been observed. Discontinuous siltstone partings are sometimes present and beds of this facies are often amalgamated. Pyrite is a common early diagenetic mineral in these beds and might indicate that reducing conditions existed immediately after rapid deposition of thick sand beds due to separation from the sediment-water interface.

Pickering et al (1986) suggest an origin by rapid deposition from a high-concentration turbidity current, or post-depositional liquefaction to destroy any sedimentary structures. No dewatering structures, e.g. dishes and pillars, were observed.

Facies B1.2

Defined as thin-bedded coarse grained sandstones this facies is occasionally represented, e.g. Elva quarry 1, 4.7m (figure 2.9a). With decrease in bed thickness and increased proportion of mudstone it is transitional to facies C2.7.

Facies B2.1

Facies B2.1 comprises greywacke of dominantly medium to very coarse sand but up to granule grainsize, in dominantly medium beds with subordinate thin and thick beds. Greywackes are generally ungraded with normal grading only developed at the top of beds, suggesting rapid dumping of sediment from high-concentration turbidity currents. They sometimes show horizontal lamination comprising discontinuous thin and thick laminae of very coarse sand to granule grainsize, separated by *c*2cm of medium to coarse sandstone. These, and rare examples of inverse graded intervals of 2cm thickness, are interpreted as products of traction carpets (Lowe, 1982) beneath high density turbidity currents. Examples are Watch Hill forest track 5.6m, Elva quarry 2, 0.5m (figure 2.9e,b).

In the Loweswater Formation, e.g. Darling Fell Unit (enclosure 4), facies B2.1 shows better sorting in medium or coarse sandstone. Horizontal laminae are both thin and thick.

Facies B2.2

In the Loweswater Formation, e.g. Darling Fell Unit (enclosure 4), this facies comprises medium to coarse sandstone in thick and very thick beds, commonly with scoured and channelised bases. Large flute marks are preserved on channel bases and steep channel margins, approaching vertical. Beds are ungraded and display cross stratification, with set size up to 50cm, or horizontal lamination. Beds are amalgamated and sometimes contain elliptical erosional scours (50cm long axis), draped by planar lamination and elliptical depositional mounds (approximate dimensions 100cm x 60cm x 10cm high) with planar lamination thickening into the mounds. Dewatering structures are represented by convolute lamination. The origins of the sedimentary structures and palaeocurrent directions are discussed later. One example of facies B2.2 occurs in the Watch Hill Formation at Elva Quarry 1, 4.0m (figure 2.9a).

Facies B2.3 (new facies)

Facies B2.3 is added to the scheme and defined as variably bedded, normally graded sandstones. Examples are Burntod Gill 25.6m, 31.2m, 48.3m (figure 2.10) and Oval Plantation 1, 0.7m (figure 2.9c). Grain by grain deposition from suspension is inferred, analogous to the Ta division of the medium grained turbidite model.

Figure 2.9 Sedimentary logs and their relative positions in the Watch Hill Formation in the vicinity of Watch Hill. Enclosure 8 is a key for logs.

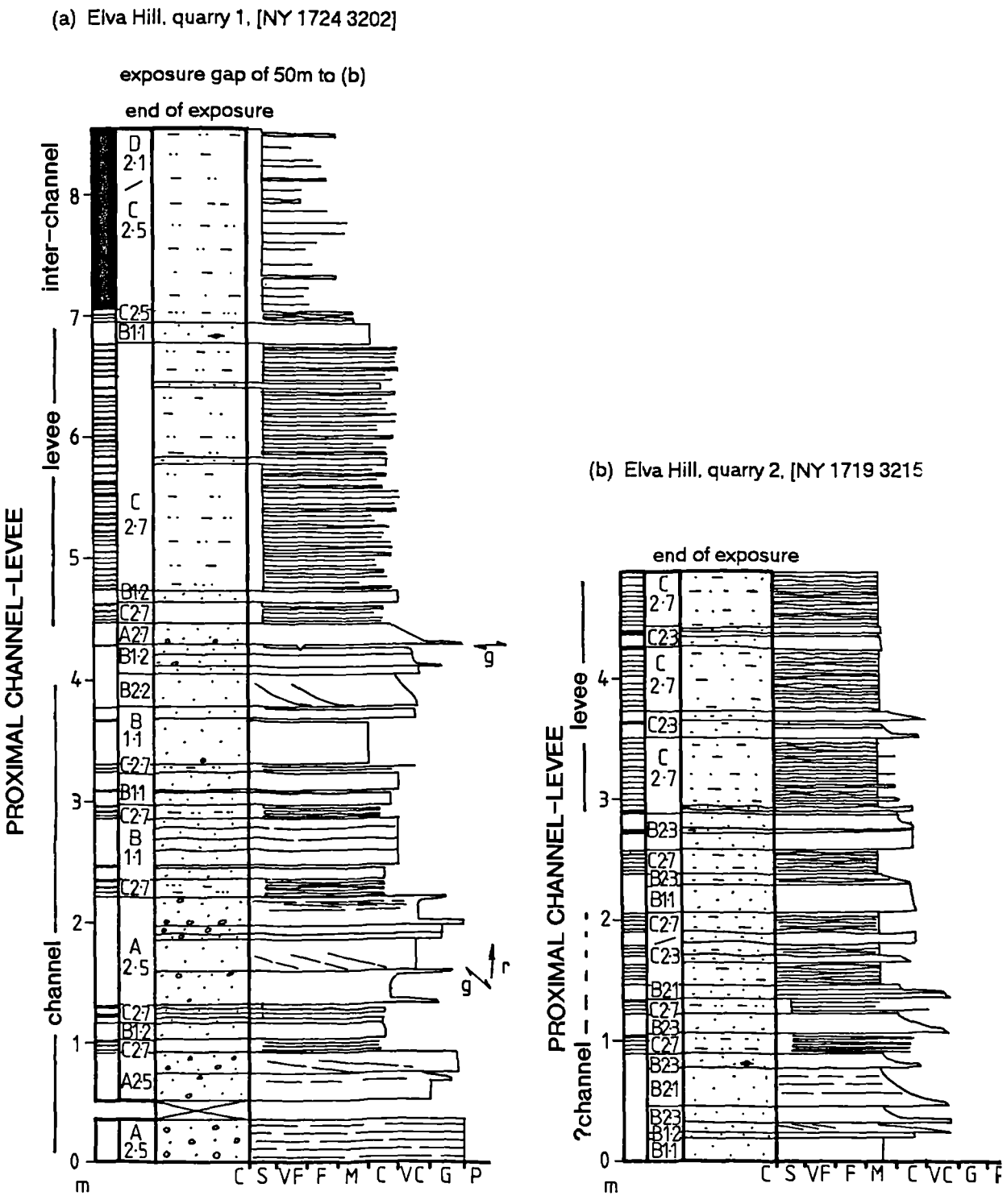

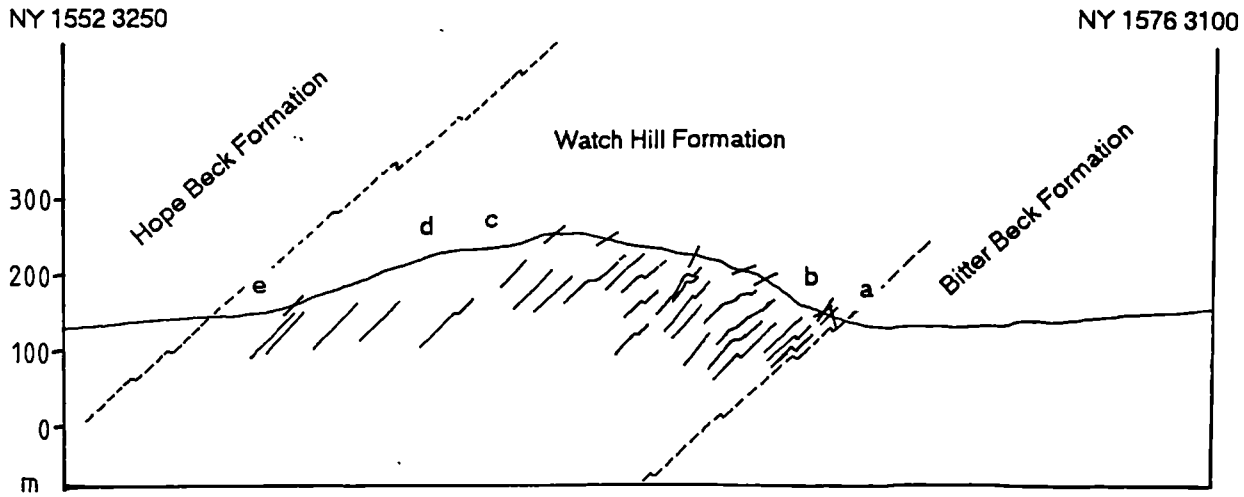

(e) Watch Hill, forest track, [NY 1548 3226]

(d) Watch Hill, Oval plantation, outcrop 2, [NY 1550 3203]

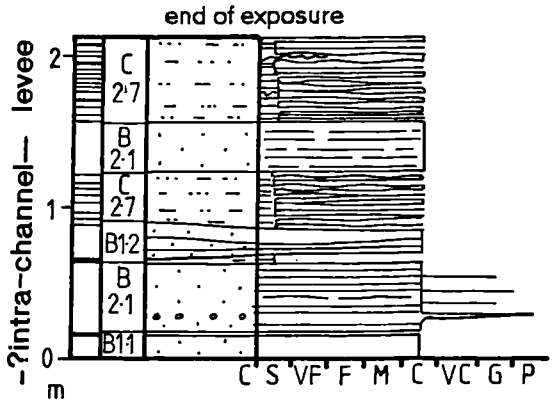

(c) Watch Hill, Oval plantation, outcrop 1, [NY 1570 3199]

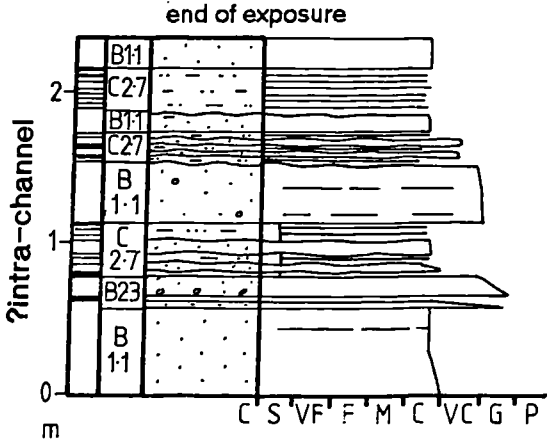

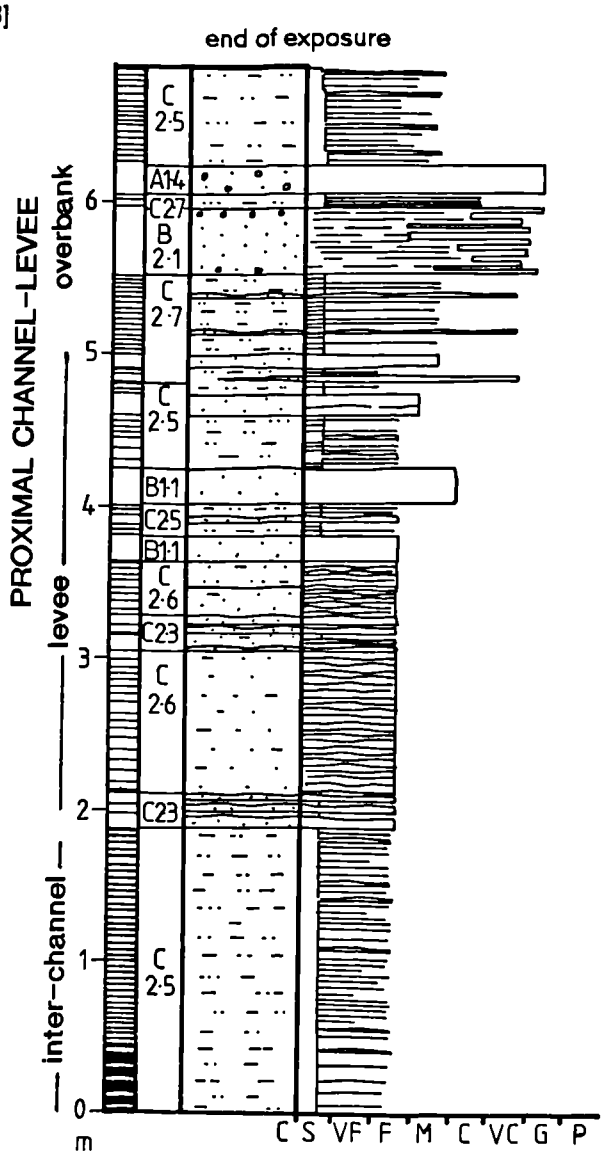

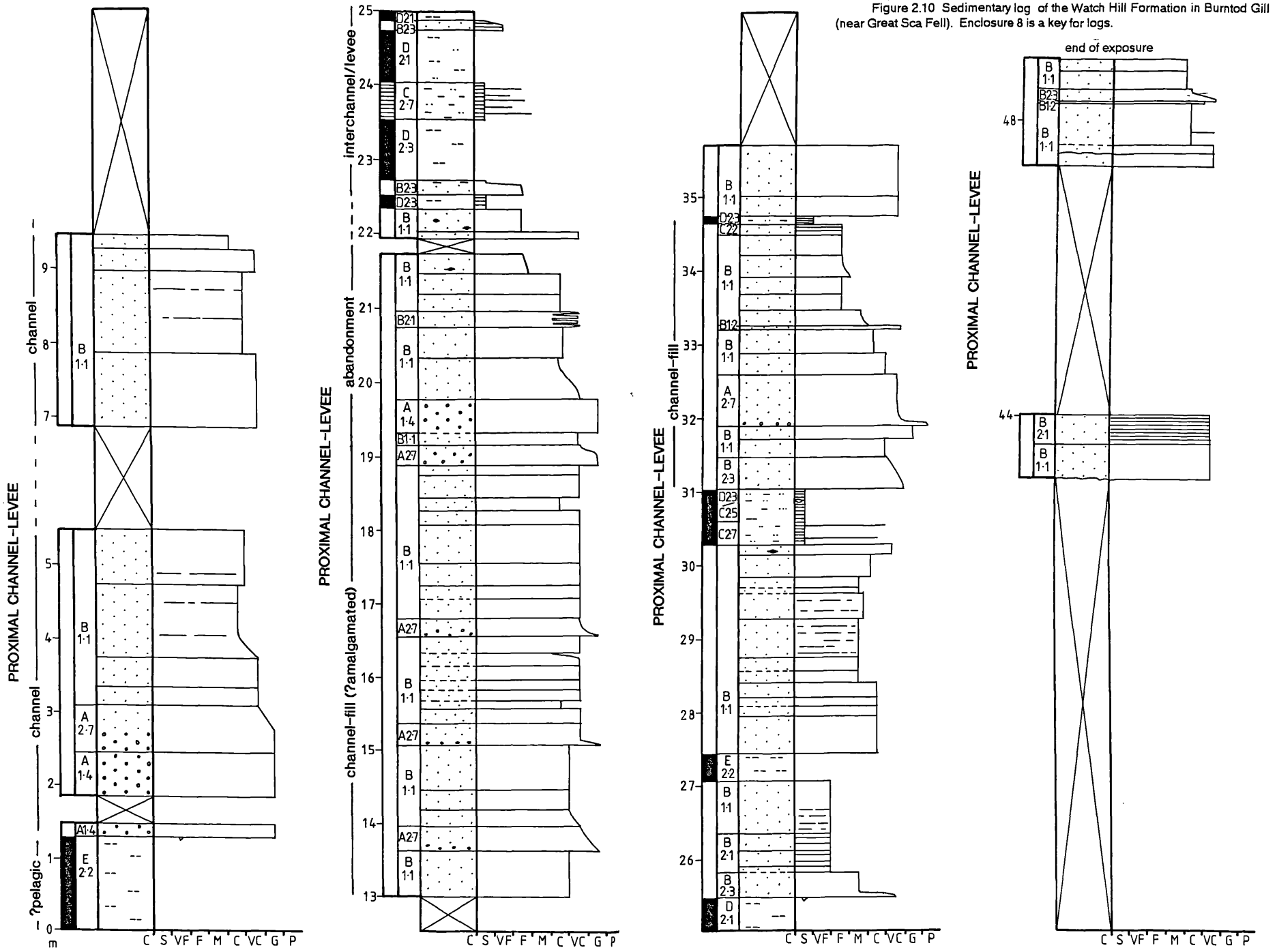

Figure 2.10 Sedimentary log of the Watch Hill Formation in Burntod Gill (near Great Sca Fell). Enclosure 8 is a key for logs.

Facies C1.1

Beds belonging to facies C1.1 have been observed at Fisher Wood between 3.5m and 5.5m and between 22.1m and 26.5m (enclosure 5), and at Mungrisdale [NY 363 208]. They are commonly medium or thick beds, poorly sorted with very coarse to fine sand grains and a few granules in a mudstone matrix, constituting in excess of 50% of the rock. They display a crude normal grading with a rapid transition to mudstone at the tops of beds, but are generally structureless. Convolute lamination is occasionally developed and bed tops may display ripple cross lamination. They can be described as high-matrix greywackes and are strongly cleaved in outcrop displaying cleavage refraction due to the upwards decrease in grainsize. Bases of beds are smooth.

They are interpreted as the products of muddy, high-concentration turbidity currents or fluid sand-mud debris flows (Pickering et al, 1986). These were slow-moving, without erosion of underlying sediment, and deposition was rapid, perhaps an intstantaneous 'freezing' of the flow.

Facies C2.1

This facies is defined as very thick and thick bedded sandstone-mudstone couplets. Beds commonly show normal grading and well developed structures of the medium grained turbidite model (figure 2.3b). The arenaceous component is usually of fine or medium sandstone and commonly displays Tbc divisions. Bed bases may show sole marks. Grooves and flutes are commonly <1cm deep with length to width ratio of c 5 and lengths in the range 5-20cm. Convolution commonly disrupts Tbc divisions. The argillaceous upper part consists of mudstone and siltstone, commonly with thin horizontal laminae (Td), and rarely structureless mudstone (Te). Horizontal feeding trails, present on the upper surface of the argillaceous interval, are sometimes preserved as sole marks on the overlying bed (plate 2.1.1).

Examples of facies C2.1 are Scawgill Bridge Quarry 45.5m, 47.6m, 51.3m and 53.0m (enclosure 6). Decrease in bed thickness accompanies a facies change from C2.1 to C2.2 to C2.3 to C2.5.

Facies C2.2

Facies C2.2 comprises medium bedded sandstone-mudstone couplets with normal grading and Tbcd divisions. Commonly the grainsize is fine sand. The facies is extensive in the Loweswater Formation (enclosures 5, 6, 7; plate 2.1.2).

Facies C2.3

With decreased bed thickness, beds are classified into facies C2.3. It comprises thin bedded sandstone-mudstone couplets, e.g. enclosures 5, 6, 7. Facies C2.3 is interpreted as the products of low concentration turbidity currents.

Facies C2.5 (new facies)

Facies C2.5 comprises thin beds, very thin beds and thick laminae of very fine or fine sandstone with up to 60% mudstone-siltstone interbeds (plate 2.2.1). Sandstone beds and laminae

can be laterally continuous or discontinuous, show variable thickness and can lens out. They are usually ungraded and often display ripple cross lamination throughout the bed or on its top. Sandstone lenses may be starved ripples with internal ripple cross lamination and asymmetrical form, occurring singly or in trains. The facies differs from facies D2.1 or D2.2 in the dominance of sand grade rather than silt grade material in the coarser component of each depositional unit.

This facies is the product of dilute turbidity currents depositing sand from a lower flow regime allowing the generation of tractional bedforms. Mudstone interbeds are the product of settling from suspension of turbidite fines. Lenticular beds, laminae and starved ripples could be due to reworking of sandstone units by currents generating traction bedforms. Such currents may be successive dilute turbidity currents, contour-following bottom currents or the passage of solitary waves generated by turbidity current reflection at topographical features on the sea bed. The high angle of divergence between ripple current directions and sole mark directions (discussed in detail later) suggests that reflected waves alone, or in combination with bottom currents could be responsible.

Examples are extensive in the Loweswater Formation (enclosures 5, 6, 7) and occur in the Watch Hill Formation, e.g. forest track 2.1-3.8m (figure 2.9e).

Facies C2.6 (new facies)

This facies comprises thin and rarely medium beds of dominantly very fine and fine sandstone. Beds are commonly amalgamated and ripple cross lamination is developed extensively throughout (Tc) (plate 2.2.2). Subordinate structureless, horizontally-laminated or convolute-laminated sandstone beds may be present. Siltstone intervals (<3cm thick) sometimes show ripple cross lamination and occasionally horizontal lamination (Td). The facies (e.g. enclosures 6 and 7, and Watch Hill forest track, 2.1-3.8m (figure 2.9e)) occurs in units of up to 2m thickness and is associated with other facies in class C. The extensive ripple cross lamination indicates deposition almost exclusively from a lower flow regime. The low proportion of mudstone can result from turbidity currents transporting exclusively sand or from the suppression of mudstone deposition through high event frequency. The small bed thickness suggests deposition from low volume turbidity currents carrying a small grainsize range of dominantly fine sand.

Facies C2.7 (new facies)

This sandstone-dominant facies comprises very thin and thin beds (and rarely thick laminae) of dominantly medium to coarse sand grainsize (plate 2.3.1). Ripple cross lamination is present and 'pinch and swell' structures related to ripple profiles are common. One example of lunate ripples was recorded. Interbeds are of thin and thick laminae of mudstone and siltstone with thick laminae of very fine to medium sand grainsize. Beds and laminae are laterally continuous over several metres without erosive bases or truncations. Sandstone content is estimated at 60% and the facies constitutes up to 70% of the Watch Hill Formation.

The thin sandstone beds with tractional sedimentary structures were deposited from thin turbidity currents. A levee environment associated with a submarine fan channel is postulated, with sediment derived from overspill of 'within-channel' turbidity currents.

Examples are: Watch Hill Formation, Oval and Elva quarries (figure 2.9b,c,d); Loweswater Formation, Scawgill Bridge, 104.0-106.3m, (enclosure 6).

Facies Group D2

Siltstone turbidites of this facies group are strongly cleaved, obscuring their finer detail. Only the basal division of the sequence of structures of the fine grained turbidite model (Stow and Shanmugam, 1981) (figure 2.3a) was recognised. Examples of this facies group occur in the lower part of Scawgill Bridge Quarry (enclosure 6, 0-22.3m), and Tom Rudd Beck (enclosure 7).

Facies D2.1

Thin and very thin beds and thick laminae of siltstone and very fine sandstone are interbedded with mudstone. Beds vary in thickness laterally and may be continous or discontinous. Ripple cross lamination is common within or on the top surface of beds. This facies was deposited from low concentration turbidity currents in a lower flow regime.

Facies D2.2

This facies comprises lenses and irregular, thick laminae of siltstone or very fine sandstone, commonly displaying ripple cross lamination. Lenses are often isolated (starved) ripples, and represent deposition from low concentration turbidity currents or reworking by bottom currents or reflected currents.

Facies D2.3

Facies D2.3 is closely asociated with other facies of this group. It comprises thin, regular, horizontal laminae of siltstone and mudstone deposited from low concentration turbidity currents by sorting of silt grains and clay flocs in the viscous sublayer of the flow (Pickering et al, 1986). Event boundaries are not recognisable without units of facies D2.1 or D2.2.

Facies class E

Deformation and cleavage obscure the structures within mudstone units such that identification of siltstone and mudstone turbidites and hemipelagite (facies classes D, E and G) is rarely possible. One example of laminated clay (facies E2.2) is recorded, i.e. Burntod Gill 0-1.2m (figure 2.10). This could represent a period devoid of clastic deposition from gravity currents, allowing accumulation of flocculated clay from the water column. Lamination could result from periodic fluctuations in the influx of terrigenous sediment (Pickering et al, 1986).

Facies F2.1

Slump folds in sediment of facies groups D2 and C2 occur locally in the Bitter Beck Formation and extensively in the Kirk Stile Formation and Buttermere Formation. These sediment slides are gravity-induced, possibly in response to a seismic trigger, when sediment shear strength is exceeded and can occur on slopes of $<4^{o}$ (Lewis, 1971). Folds are reclined, asymmetric with overturned middle limbs, mesoscale with half wavelengths up to 2m and display boudinage of thin sandstone beds on the flat limbs. They are associated with compressional and extensional discontinuities. Slump fold orientations reflect palaeoslope orientation (see chapter 4). Slump folds at channel margins are displayed in the Darling Fell Unit, (enclosure 4, log at 146m, height 6.6m).

Plate 2.1

2.1.1 Trace fossils on the base of a turbidite. Sandstone raft of the Buttermere Formation, Causey Pike.

2 1.2 Turbidites of facies C2.2 with interbeds of facies C2.5. Loweswater Formation, Scawgill Bridge Quarry.

Plate 2.2

2.2.1 Boudinaged sandstone beds of facies C2.5 in slump folded strata of the Loweswater Formation, Gasgale Gill.

2 2 2 Ripple cross laminated, very fine sandstone unit of facies C2.6, overlain by a thin bed couplet comprising convoluted ripple cross lamination in very fine sand and horizontal laminated siltstone, Tcd (facies C2.3). Robinson Member, Buttermere Formation, Robinson.

Plate 2.3

2.3.1 A monotonous sequence of very thin beds and lenses of coarse sandstone and siltstone of facies C2.7. Watch Hill Formation, Watch Hill.

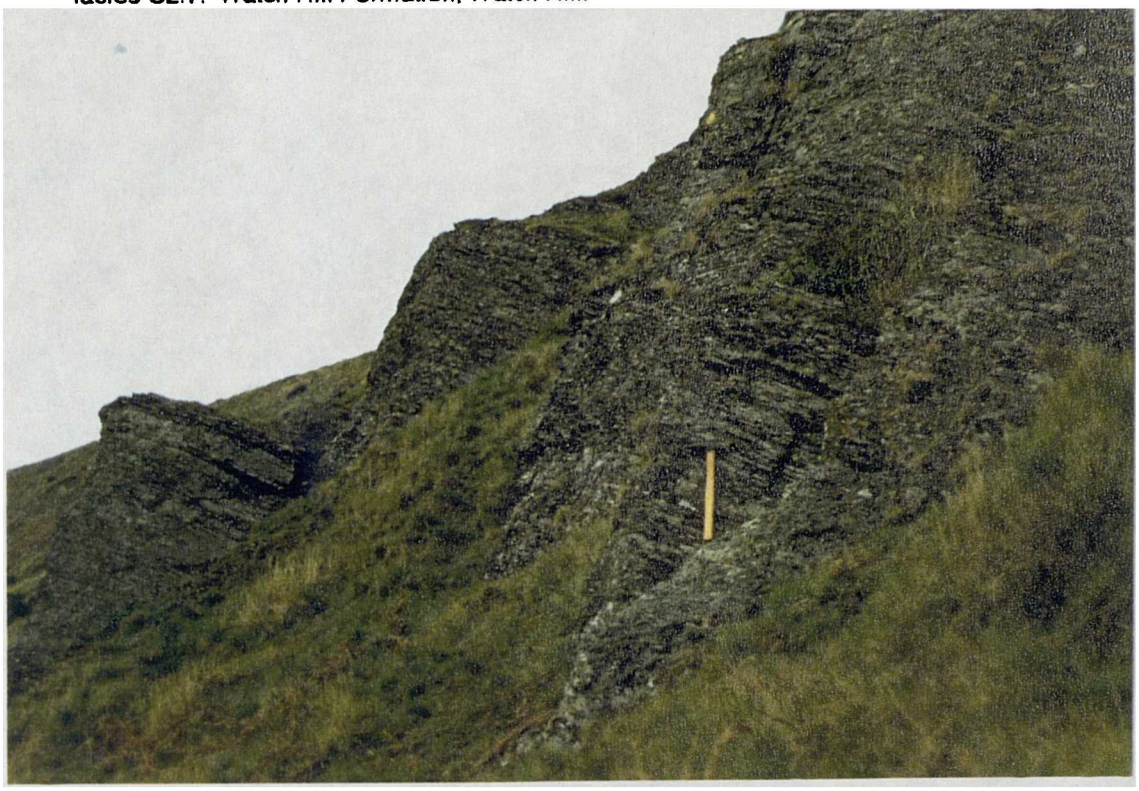

2.3.2 A scour with internal lamination showing an asymmetric fill (concurrent with a flow direction from left to right indicated by flute marks), into medium sand showing a spaced horizontal lamination (facies B2.1). The scour is elliptical in plan view (long axis parallel to flow). Darling Fell unit, Loweswater Formation, Darling Fell.

Plate 2.4

2.4 A mound (elliptical in plan view) flanked by two troughs with a spacing of *c.* 1.5m, and truncated at a planar horizontal surface overlain by sandstone with horizontal laminae. Grainsize is medium-coarse sand Darling Fell unit, Loweswater Formation, Darling Fell. Facies B2.2.

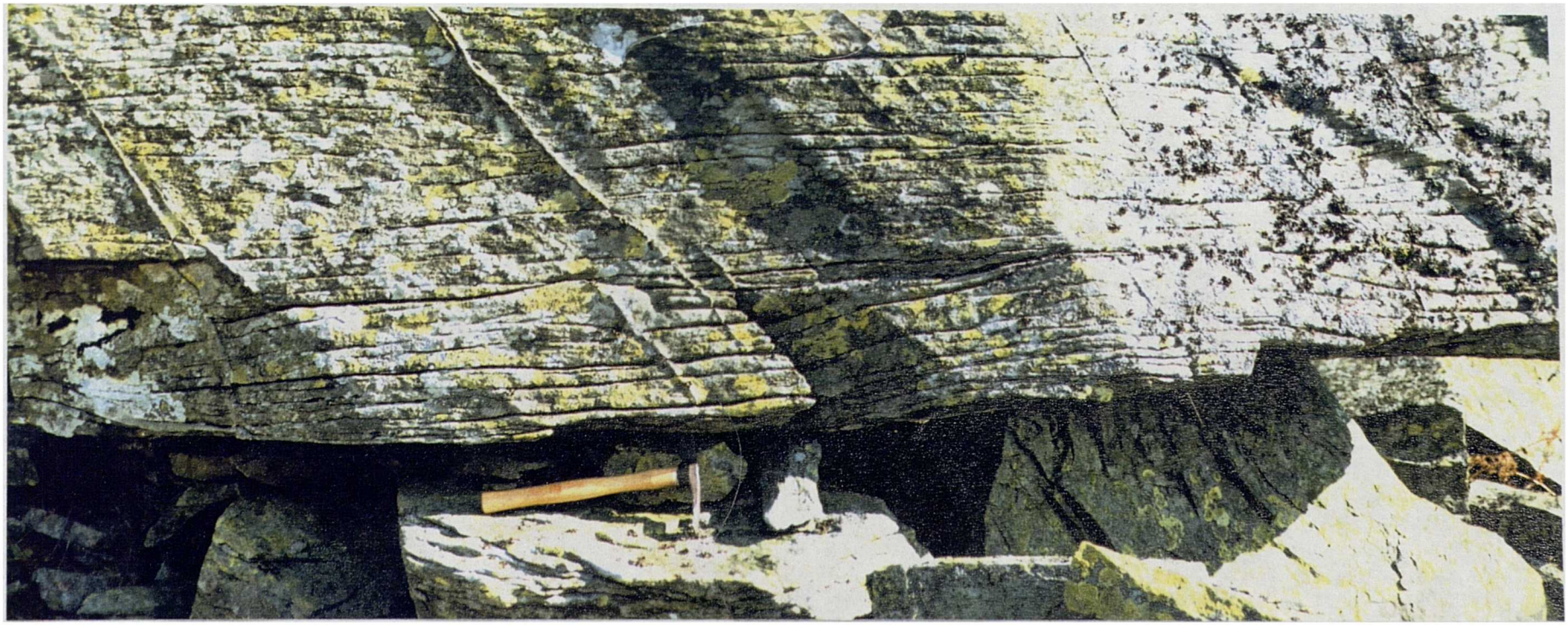

Plate 2.5

2.5.1 A channel margin showing: sole marks on the sides of the channel; medium-coarse sandstone fill with lamination parallel to the margin. Darling Fell unit, Loweswater Formation Darling Fell.

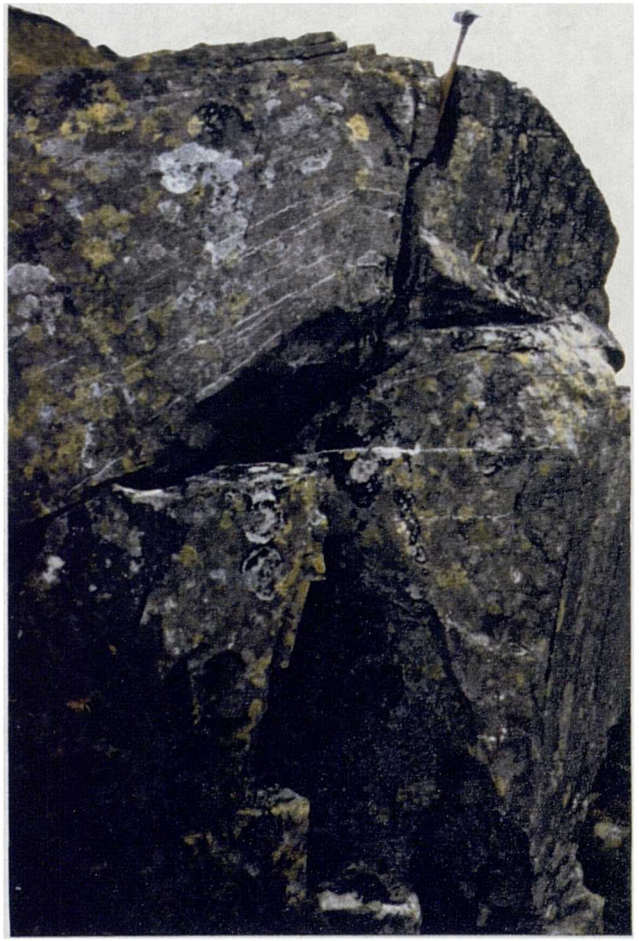

2.5.2 Two examples of convolution of thick fine sandstone turbidites with truncation of convolute laminae by an overlying horizontally laminated turbidite. Sandstone raft of the Buttermere Formation, Causey Pike. Plates are inverted to show an upwards younging direction.

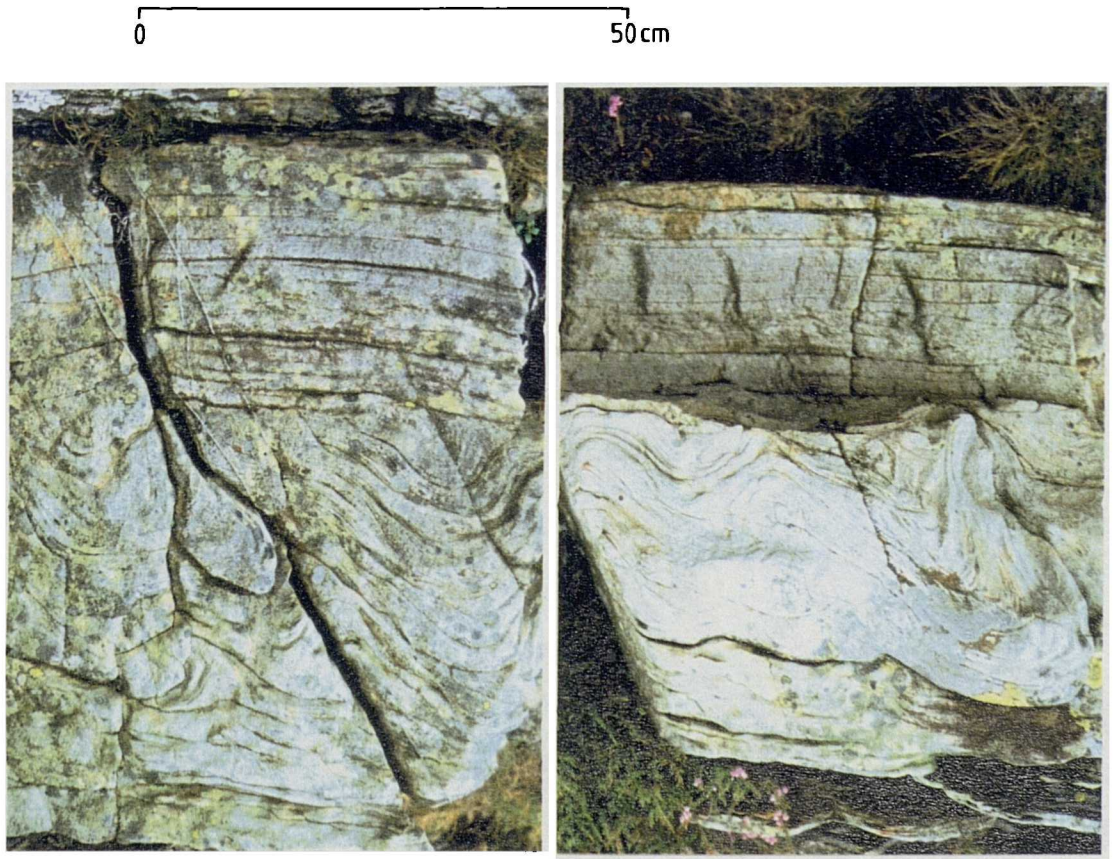

2.3.3 Facies associations, palaeocurrent interpretation and depositional environments

In this section associations of facies and additional information from palaeocurrents and slump folds are used to interpret depositional environments.

2.3.3.1 Proximal channel/levee facies association

This facies association is displayed by the Watch Hill Formation. Facies classes A and B (facies A1.4, A2.5, A2.7, B1.1, B1.2, B2.1, B2.3) occur in fining-upward units e.g. Elva quarry 1, 0-4.5m (figure 2.9a); Burntod Gill, 1.3-4.7m, 19.3-23.0m, 31.8-34.7m (figure 2.10). These units could represent coarse grained turbidites in depositional lobes with gradual abondonment due to lateral lobe migration, but they are interpreted as coarse grained turbidites deposited in channels for the following reasons:

1) individual beds are seen to be highly lenticular and display rapid lateral thickness changes where exposure allows (figure 2.9a);

2) pebble to coarse sand grade beds sometimes display cross stratification, common in channels or scours (Pickering et al, 1986) (figure 2.9a);

3) the occurrence of sharp-based fining-up sequences.

Limited outcrop does not allow determination of the lateral extent of channels. Fining upward intervals are generally *c* 4m thick which might correspond to channel depth. Evidence of basal scour is rare which suggests channel morphology was maintained by deposition on levees, allowing accumulation of thick and medium beds of gravel and coarse sand grainsize. Any mud that accumulated between turbidite events was removed from the channel.

Facies C2.7 with subordinate C2.6, C2.5 and facies class B represent levees to these proximal channels (figure 2.9 a (4.5-8.5m) b, d, e; plate 2.3.1). Variations in channel proximity are recorded by increasing (figure 2.9e, forest track) and decreasing (figure 2.9a, Elva quarry 1) proportions of the coarser and thicker beds (facies class B). Repeated overspill of turbidites carrying coarse sand resulted in alternations of very thin coarse sandstone beds and background mudstone. Straight crested and lunate ripples are commonly developed and cause 'pinch and swell' of the very thin beds. Facies class B represents deposition from larger overbank currents. Extreme lateral thickness changes and lensing are common. Such features are not erosive and are due to rapid dumping of sediment or infilling of topographical lows. Irregular bed surfaces are due to loaded and grooved bases, ripple profiles and convoluted laminae and are possibly accentuated by differences in tectonic strains between greywackes and interbeds.

Facies groups D and E (Burntod Gill, 0-1.2m, 25.5m and 27.5m, figure 2.10) could represent interchannel deposits devoid of coarse clastic sediment and dominated by mudstone deposited from suspension e.g. from dilute turbidity currents or nepheloid layers. Alternatively, a mudstone drape of the submarine fan could result form cessation of coarse clastic sedimentation due to a relative high sea level stand.

2.3.3.1.1 Palaeocurrent interpretation

In the Watch Hill area, non-directional sole marks (grooves) show a distribution not significantly different from random (enclosure 1). This is possibly due to the misidentification and inclusion of linear features relating to loads, ripple profiles in thin greywacke beds and tectonically exaggerated 'pinch and swell' structures. Directional sole marks (flutes and prods) show a spread of orientations directed to an arc between north and southwest (the statistically significant mean direction is to 280°). Ripple current directions show a narrower spread with a mean direction to 023°, which is in excess of 90° divergent from the mean sole direction (enclosure 2).

The large spread in sole directions could result from:

1. Spreading of overbank flows,
2. Topographical control of flow direction due to within-channel bedforms,
3. Meandering of channels.

The divergence of ripple directions from the mean sole direction is likely to result from case 1 above. One example of cross stratificaton (8cm set size) was included in the ripple data set. It comprised units up to 4cm thick, displaying normal grading from very coarse to fine sandstone, dipping at a low angle (16° measured). The set is interpreted as lateral accretion of a small bedform (megaripple) in response to successive turbidity currents. This observation could support case 2 or case 3 above.

The Watch Hill Formation is *c.* 520m thick at Watch Hill (figure 2.9). It thins westwards to *c*200m in the vicinity of Cockermouth and eastwards to *c* 40-100m thickness in the Great Sca Fell area (Cooper et al, in prep.). Since palaeoflow in the Watch Hill area is generally westwards, the westward thinning of the formation could be due to a general downcurrent (distal) thinning or lateral facies change into mudstone-dominant interchannel facies. This would imply the Bitter Beck Formation-Watch Hill Formation boundary is at least in part a lateral facies change. This agrees with observations of bedding orientation on the south side of Watch Hill where the strike direction truncates the boundary, which is not thought to be a tectonic feature.

Sole directions from the Watch Hill Formation in the Great Sca Fell area are directed towards the east-northeast (mean direction to 071°; enclosure 1). This is 150° divergent from soles at Watch Hill and could be interpreted as turbidity current flow in the opposite direction along a linear trough orientated approximately east-west. This would require a source of sediment input into the trough between these two localities; a distance of 10km largely devoid of outcrop of this formation. The reduced thickness of the formation in the Great Sca Fell region suggests the input to the trough was nearer or preferentially directed to Watch Hill. An alternative explanation for the palaeocurrent distribution would be radial spreading of turbidity currents giving widely divergent channel directions on a submarine fan with general flow from south to north and lateral thinning of deposits.

Von der Borch et al (1985) used opposed palaeocurrent directions between outcrops of submarine canyon turbidites to suggest the canyon had a meandering geometry. An interpretation of meandering channels is not substantiated for the Watch Hill Formation but is permitted by the data.

The acquisation of more sole and ripple palaeocurrent data, better understanding of later tectonic structures and higher palaeontological resolution for stratigraphical correlation would lead to a less equivocal interpretation of sediment dispersal, but lack of outcrop thwarts such improvements.

2.3.3.2 Distributary channel facies association

This facies association is displayed in the Loweswater Formation by the Darling Fell Unit [NY 1257 2224 and NY 1173 2151] and is transitional from the depositional lobe facies association (described later). Thin to thick bedded turbidites (facies C2.5, C2.3, C2.2, C2.1), amalgamated thin sandstone beds (facies C2.6) and medium to thick sandstone beds (facies class B) constitute the depositional lobe which is overlain by thick sandstone beds (facies B1.1, B2.1, C2.1) with lobe geometries (e.g. enclosure 4, log at 0m, 8.0m) and incised by channel-fill sandstones (plate 2.5.1). The outcrop at Darling Fell is 150m long and sub-parallel to palaeoflow direction (approximately to the north-northwest), allowing observation of a down-flow change from erosive-based channel facies to non-erosive, lenticular, thick sandstone beds (e.g. enclosure 4, contrast log at 146m, height 6.5-8.0m, with other logs at an equivalent height).

Channels are 0.5-2.0m deep and margins are commonly steep (near vertical e.g. laterally adjacent to log at 86m, height 12.0m, enclosure4; plate 2.5.1) suggesting they were cut and filled by the same depositional event. At height 6.0m on log at 146m (enclosure 4), facies C2.5 is slumped (slump axes are parallel to the channel orientation) at a channel margin suggesting an open channel existed. Channel fill sandstones (facies B2.1, B2.2, B1.1) are of coarse sand and medium sand grainsize. They can be structureless (e.g. log at 0m, 11.2-13.0m), horizontally-laminated (e.g. log at 46m, 16.0-17.2m,) or cross-laminated (e.g. log at 86m, 11.8-12.3m) (enclosure 4). Foreset orientations (set size up to 0.5m) show a wide spread of orientations (figure 2.11) thought to be due to the three dimensional nature of intra-channel dunes. The time required for the generation of such large bedforms in medium and coarse sand could be provided by near-continuous density underflows from a river-fed fan system. Lateral accretion surfaces on channel margins (e.g. log at 146m, 10.8-11.5m, enclosure 4; plate 2.5.1) might reflect meandering of channels.

The channel-fill sandstones are overlain by thick and very thick beds of fine and medium sandstone which commonly display a spaced horizontal lamination (plate 2.4). Additionally present are elliptical scours (long axis of 0.5m parallel to flow direction) draped by sandstone laminae and three dimensional elliptical hummocky bedforms (long axis c 1.5m parallel to flow direction) (plates 2.3.2, 2.4). Such bedforms have previously been described in turbidites (Prave and Duke, 1990) and attributed to antidunes. Such an interpretation is possible for these structures in the Darling Fell Unit. They are thought to have formed at a channel termination (figure 2.12) where rapid flow divergence and deceleration caused a hydraulic jump and sediment dumping. Convolute lamination, developed during dewatering of thick sandstone beds in response to rapid sedimentation, disrupts several units.

Retreat of the channel system caused facies of the depositional lobe facies association to overlie the unit.

Channel dimensions are difficult to determine. Scoured bases generally incise 0.5-2.0m, but channel width cannot be determined. On Burnbank Fell, this facies association occurs at an equivalent horizon where a single channel-fill is 5.5m thick (figure 2.13). Its texture is rich in matrix and as a result it lacks internal structures other than normal grading. Channel facies were developed over a minimum distance of 1km perpendicular to flow direction.

Figure 2.11 Equal area rose diagram and vector statistics for dip directions of cross stratification foresets in the Darling Fell Unit.

Sector interval is 18°
Statistics of circular distribution (Graham, 1988):

θ	= measured direction		
V	= $\Sigma_1^n \cos\theta$	=	8.09
W	= $\Sigma_1^n \sin\theta$	=	2.43
X	= arctan W/V	=	16.72
	= vector mean		
A	= X as azimuth	to	017°
R	= $(V^2 + W^2)^{1/2}$	=	8.45
	= vector magnitude		
L	= (R/n).100 %	=	64.98 (Significant
n	= number of beds	=	13 at 95% level)

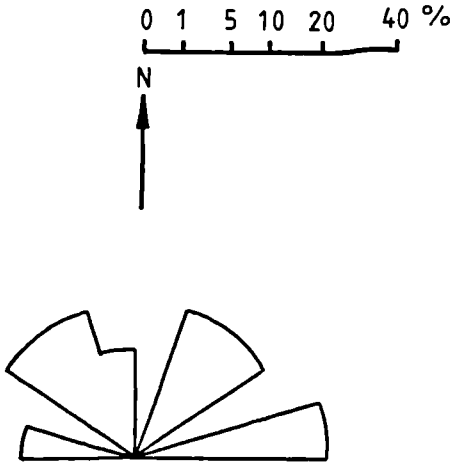

Figure 2.12 Model for the development of the distri butary channel facies association.

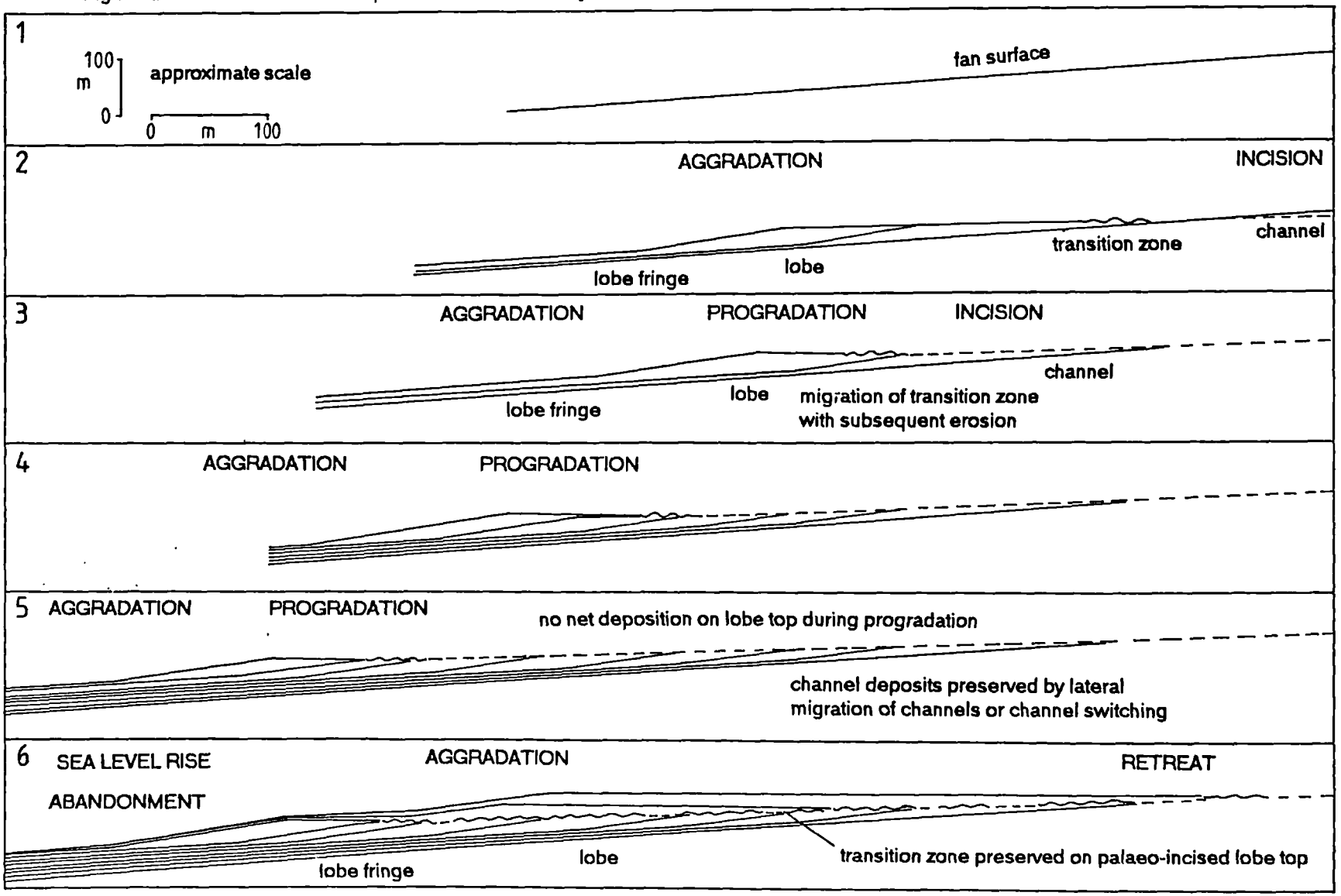

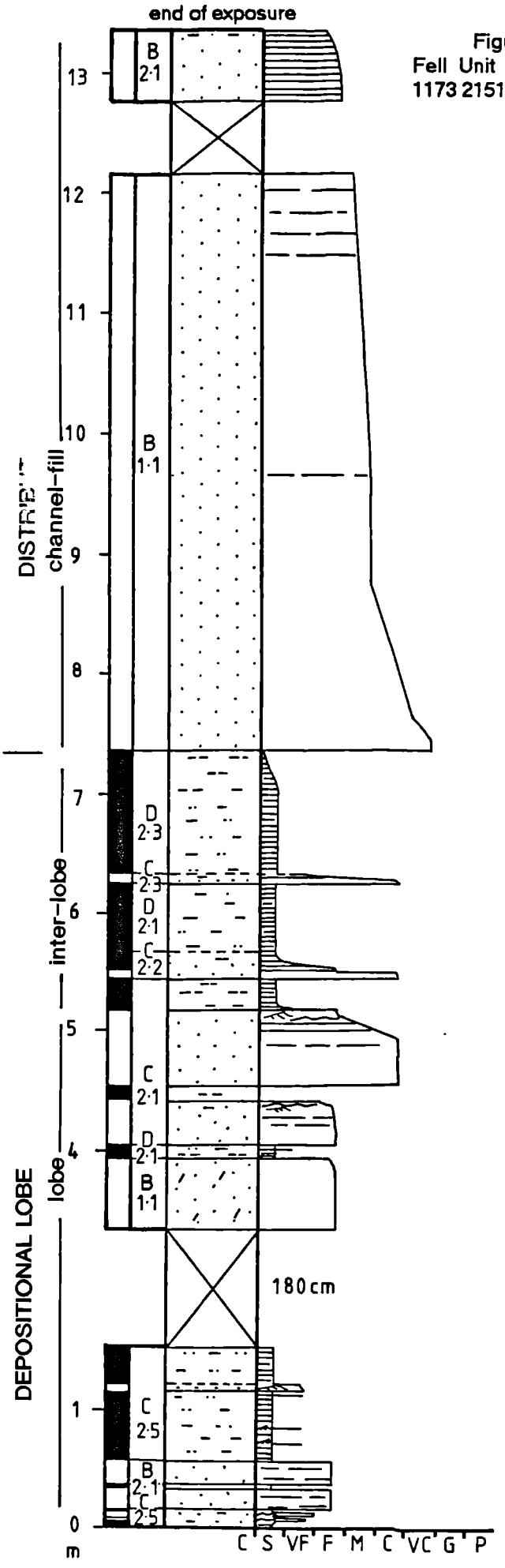

Figure 2.13 Sedimentary log of part of the Darling Fell Unit (Loweswater Formation) at Burnbank Fell [NY 1173 2151]. Enclosure 8 is a key for logs.

Palaeocurrent interpretation

Palaeocurrent directions for the Darling Fell Unit are shown in enclosures 1 and 2. Sole directions are from large flute marks on channel bases. Non-directional soles are from orientations of channel margins and from grooves and elongate scours both within channels and from apparently non-channelised, medium to thick bedded turbidites. Erosive currents flowed to the northwest (mean direction to 322°). Ripple directions are from silty, very fine sandstone of facies C2.6, both beneath and within the channelised unit (e.g. log at 146m, 4.8-5.8m and log at 49m, 13.0m, enclosure 4). Intervals of a few centimetres thickness with ripples of predominantly one direction occur between intervals predominantly showing ripples of opposed direction, giving an oblique bimodal distribution (enclosure 2).

The ripple directions may represent overbank flows or spreading of flows at channel terminations. Rippled intervals of opposed direction could represent overspill events from separate channels in close lateral proximity. The palaeocurrent pattern is thought to reflect the relationship between channel and levee facies.

2.3.3.3 Depositional lobe facies association

Thin and medium beds of dominantly fine sandstone turbidites (facies group C2) are the dominant component of the sandstone-rich depositional lobe facies association. Sandstone-dominant packets of 5-40m thickness, (e.g. Fisher Wood 0.5-15.5m, 19.2-26.5m, 28.8-39.2m, 53.8-87.5m, 94.0-108.2m (enclosure 5); Scawgill Bridge Quarry 43.7-59.0m and Sware Gill 216.0-238.9m (enclosure 6)), are separated by intervals of facies group D2 of *c* 1m thickness.

Beds of facies group C2 are generally laterally continuous over several tens of metres but can show rapid thickness changes and even lens out. Sandstone beds are not amalgamated and are separated by mudstone beds of uniform thickness. Examples are presented from Scawgill Bridge Quarry [NY 1773 2583] (figure 2.14) where observed thickness changes are 30cm to 0cm over a horizontal distance of 3m, and 50cm to 15cm across a 3.5m lateral distance. Two explanations are possible:

1) Erosion of a sand bed by a non-depositing turbidity current, followed by mudstone deposition would create a topographical hollow which would be infilled by a subsequent sand turbidite (figure 2.14a)

2) A single turbidite could show positive relief due to rapid sedimentation (figure 2.14b). Such rapid deposition has been postulated to occur in conjunction with a hydraulic jump associated with spreading and deceleration of a turbidity current as the current becomes unconfined at a channel termination or levee breach. Thus a spatially restricted depositional lobe is formed. A subsequent turbidity current will be deflected around this positive feature, concentrating sediment deposition in adjacent topographical lows, producing overlapping sandstone beds with opposed gradients of diminishing thickness (figure 2.14b). The situation is similar to the mechanism for 'compensation cycles' (Mutti and Sonnino, 1981) as it requires topographical deflection of subsequent turbidity currents, but rapid, spatially restricted sediment deposition is required to give extreme lateral

Figure 2.14 Lateral thickness changes in facies group C2 at Scawgill Bridge Quarry and possible causes : (a) Erosion of a sand turbidite, 1, by a subsequent non-depositing turbidity current, 2, to create topographical relief, which was draped by mud and then infilled by a sand turbidite, 3; (b) Rapid sediment dumping caused positive relief of a sand turbidite, 1, which was draped by turbidite mud and infilled by a subsequent turbidite, 2.

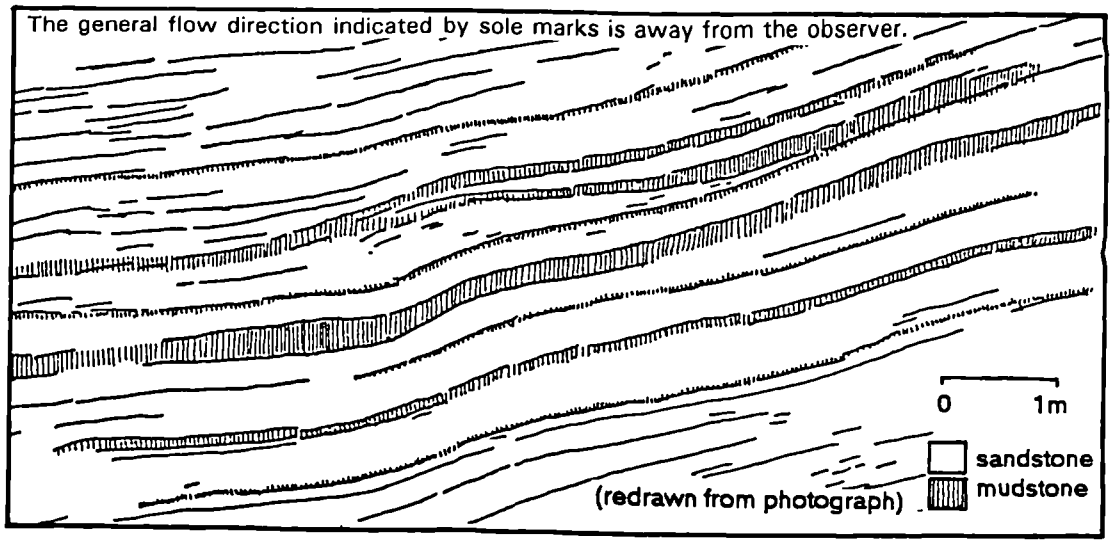

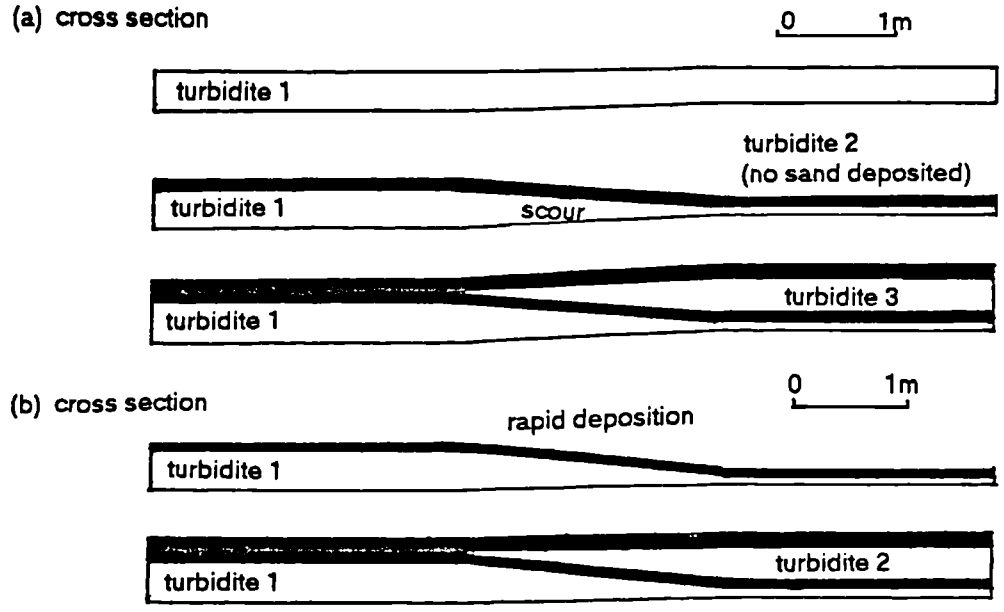

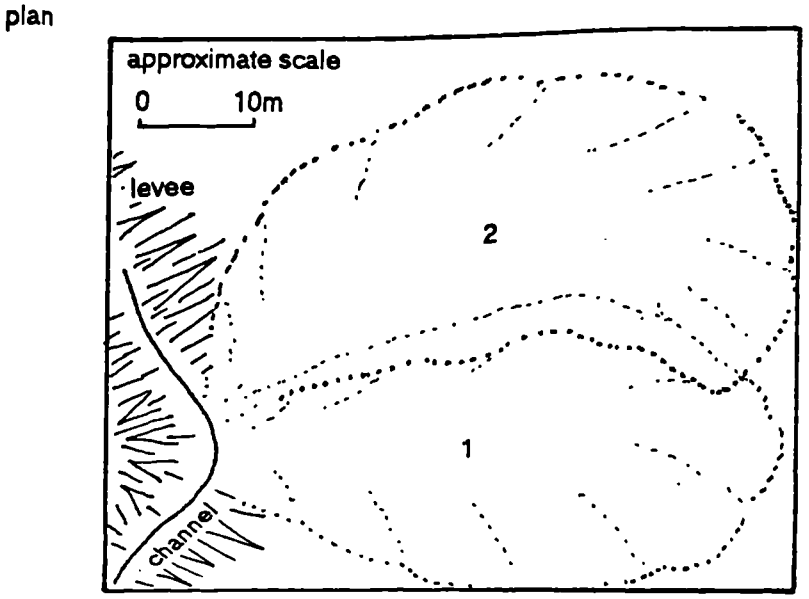

thickness variations in a single bed. Crevasse-splay deposits of a fluvial environment are analogous.

Cyclicity in bed thickness is not apparent. Sandstone packets of 5-10m thickness are probably developed in response to intrinsic causes, e.g. channel switching. Lobe retreat is documented at the top of the Scawgill Bridge-Sware Gill section (enclosure 6) where a general decrease in bed thickness and sandstone to mudstone ratio shows a transitional change to the inter-lobe facies association.

Correlation of depositional lobe development between localities was not possible due to the limited exposure and the lack of a marker horizon.

Progradation and retreat of depositional lobes, estimated between 40m and 100m thick, might be in response to short term sea level variations, either eustatic change due to glaciation or tectonically controlled relative change. Convolute lamination is common. Convolution of the entire thickness of medium and thick beds (e.g. Scawgill Bridge Quarry, 45.5m, enclosure 6) and several beds together (e.g. Scawgill Bridge Quarry, 58.5m) is likely to be in response to dewatering triggerred by seismic shock (Allen, 1977) (plate 2.5.2). Thus a tectonically active environment is inferred.

Palaeocurrent interpretation

Sole mark and ripple current directions for localities across the Skiddaw Inlier are presented as rose diagrams and vector statistics in enclosures 1 and 2. Broadly, the rose diagrams indicate a general palaeoflow towards the north; a conclusion reached by Jackson (1961). In detail, the pattern is more complex. Localities can be grouped as follows:

1) Those localities where sole directions and ripple directions show a large divergence. Sole directions are to the northwest or north-northwest and ripple directions show an oblique bimodal distribution symmetrically disposed about the mean sole direction. Ripple modes are approximately to the north-northeast and west-southwest. Examples are the Darling Fell Unit and Scawgill Bridge Quarry. Low Fell and Hope Gill are also interpreted as this type, although ripple data are limited, as are Barf and Woodend Brow in the absence of ripple data.

2) Those localities where sole directions and ripple directions are similar and directed to the northeast or north-northeast, e.g. Liza Beck and Mungrisdale. Dove Crags, Ling Fell and Sale Fell are interpreted as this type, but lack ripple data.

For an objective interpretation one must consider the sedimentary facies and relationship of palaeocurrent indicators to erosional and depositional events.

Sole marks are flutes and grooves largely from thin and medium bedded turbidites of facies group C2. Ripple directions are from climbing and translational ripple sets within and on top of beds of these facies and from starved ripples in facies C2.5. At Scawgill Bridge Quarry (and other localities in group 1) examples were observed of

(a) soles and ripples in the same bed indicating divergent current directions,

(b) one 15cm thick turbidite of medium to very fine sandstone displaying Tbc divisions with a ripple set within the bed (Tc) with current direction (to 026°) divergent from the sole direction (to 350°) and a ripple set on the top surface with a direction (to 251°) opposing the first ripple set.

The palaeocurrent patterns, therefore, show variation in direction between erosional and depositional current directions of single turbidity currents and possible reworking by subsequent currents (sediment gravity currents or clear water bottom currents). The possible mechanisms for divergent sole and ripple directions in turbidites (section 2.2.6) should be considered in the palaeocurrent interpretation.

These sediments were deposited in the southern hemisphere, hence deflection of turbidity currents and bottom currents by the Coriolis force would have been to the west. It is possible therefore that ripples directed to the west-southwest on top of turbidites are the result of reworking by contour currents. Incident turbidity currents were not deflected in this manner as ripples of the Tc interval are directed to the north-northwest, (e.g. case (b) above).

It has been suggested that ripple current directions produced by solitary waves from oblique reflection of turbidity currents indicate the orientation of slopes responsible for the reflection (Kneller et al, 1991) (section 2.2.6). Applying this principle, two interpretations are possible:

1) Sole marks were eroded beneath turbidity currents travelling north-northwest at a base of slope facing northeast which caused reflection of solitary waves. These travelled to the northeast, normal to the strike of the slope , and generated ripple bedforms. Post-event reworking by bottom currents caused ripple directions to the west-southwest on bed tops.

2) Turbidity currents were confined in troughs trending north-northwest and solitary waves were generated at one or both margins. Reflected waves combined with the incident flow to produce ripple migration in the direction of the sum of the currents. Reflected currents from each margin could alternately sweep across the incident flow to give the bimodal ripple pattern.

Such mechanisms are also alternative explanations for the palaeocurrent pattern of the Darling Fell Unit.

For localities in group 2, sole and ripple directions are similar and one can conclude:

1) flows were unconfined by topography, since there is no evidence of reflected currents, and

2) the low spread of palaeocurrent directions is due to downslope flow with a strong gravitational control on current direction.

These conclusions assume that turbidity currents were large enough to impinge on nearby topographical features (palaeocurrent data include measurements from the thick beds of facies C2.1 which are the products of relatively large turbidity currents). Also assumed is that turbidity currents will normally be reflected by topographical features oblique to flow directions. This is suggested by flume tank experiments (Edwards, 1991) but is not evident in Silurian turbidites of the Welsh basin directed parallel to a fault-controlled basin margin demonstrated by other means (N. H. Woodcock, pers. comm.).

If bottom currents reworked beds at localities of group 2, then, like the turbidity currents, they flowed northeast. This is not expected for currents controlled by the Coriolis force and is in disagreement with a bottom current interpretation of ripples at Scawgill Bridge Quarry.

Figure 2.15 Extensional fault model to explain the observed palaeocurrent patterns of the Loweswater Formation, (a) map of part of the Skiddaw Inlier showing palaeocurrent data and proposed positions of syn-sedimentary faults, (b) three dimensional fault block model with superimposed 5km grid. Vertical exaggeration x10. Localities: c = Darling Fell Unit, d = Low Fell, e = Liza Beck, f = Dove Crag, g = Hope Gill, h = Scawgill Bridge, i = Barf, j = Woodend Brow, k = Ling Fell, l = Sale Fell.

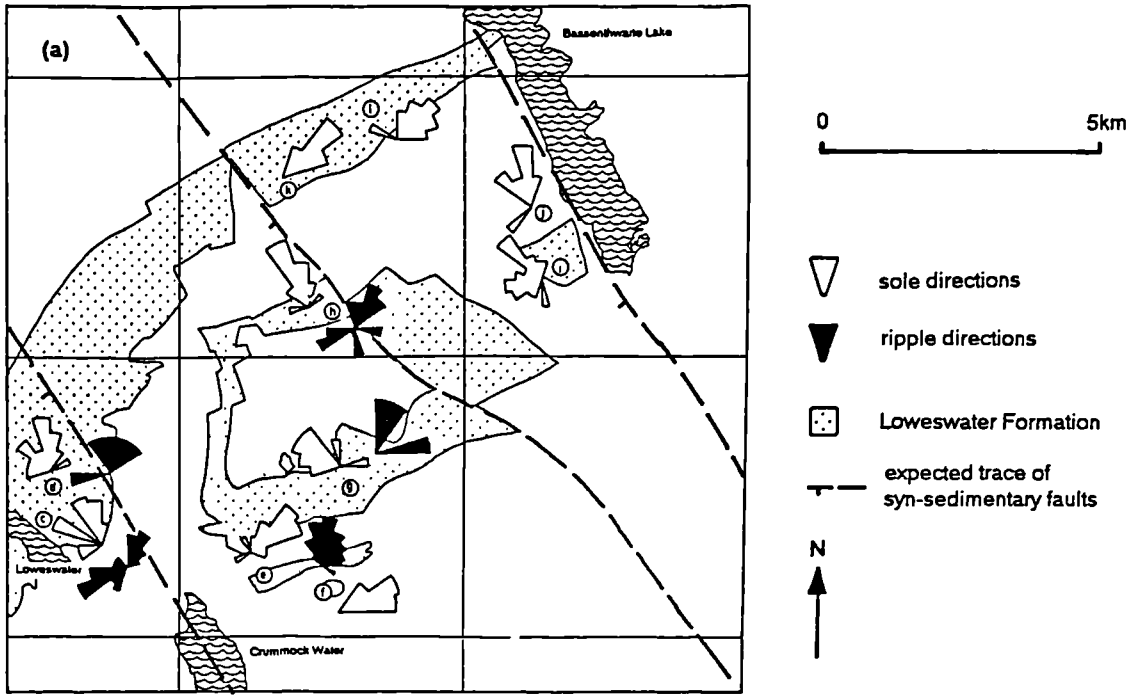

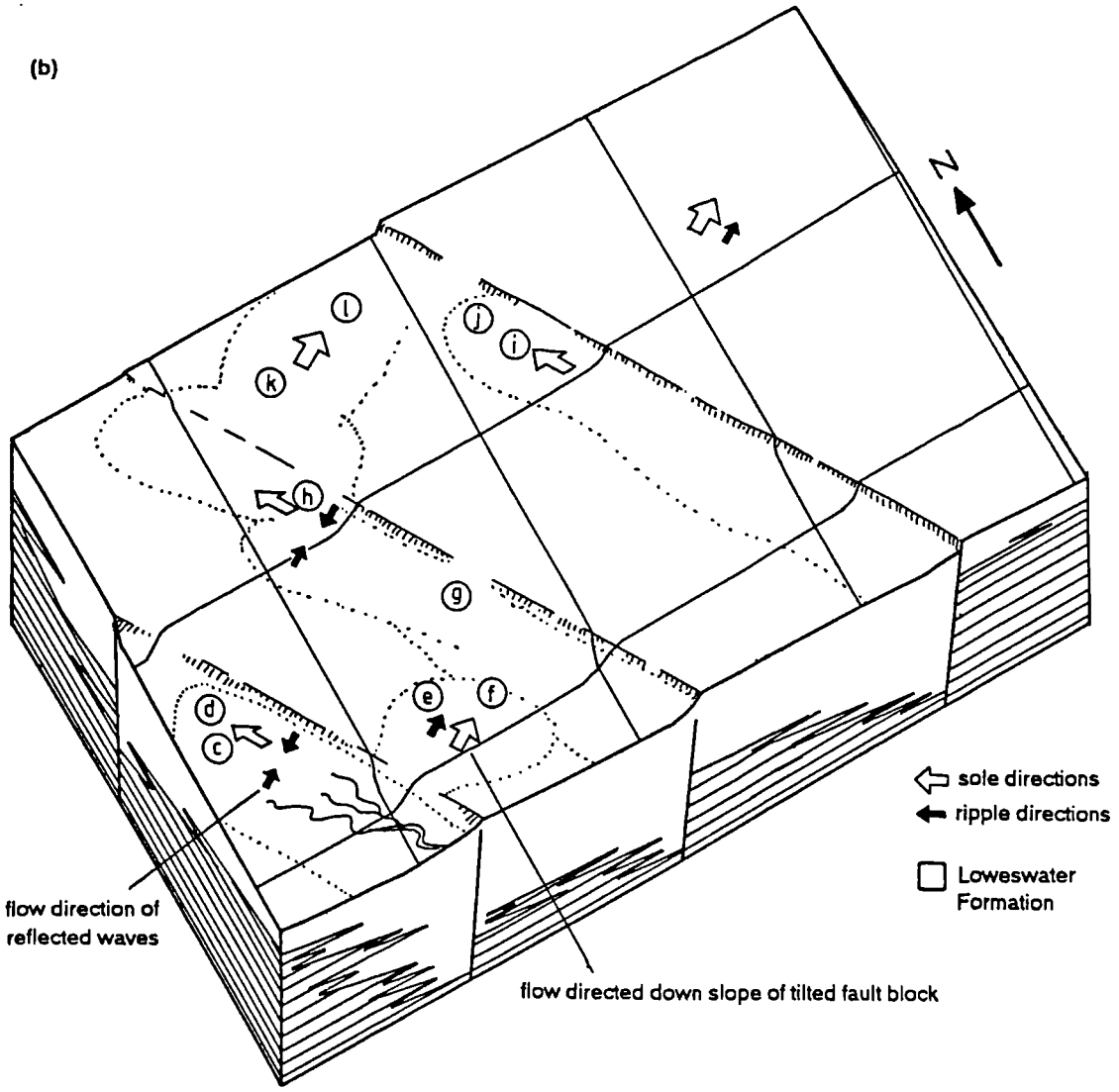

The case for bottom currents sweeping the region and giving southwest directed ripples at group 1 localities is weakened.

The palaeocurrent pattern can be explained by topographical elements controlling turbidity current flow. A possible scenario of north-northwest trending normal faults with fault blocks tilted northeast is presented (figure 2.15). Turbidity current flow and channel orientation were constrained by troughs trending approximately north-northwest adjacent to fault scarps. Distribution of group 1 localities requires at least three parallel troughs with a spacing of *c* 5km. Reflected waves generated at trough margins travelled across the axes. Between the troughs, palaeoslope was approximately to the northeast (demonstrated by group 2 localities).

Additional evidence for syn-sedimentary fault control may be revealed by examples of syn-sedimentary faults or their inferred positions shown by rapid thickness variations. Long-lived faults with a north-northwest orientation have been mapped (e.g. through NY 275 344 and NY 275 337) and while syn-depositional movement cannot be shown it can be demonstrated that movement occurred prior to the Eycott Volcanic Group (A. H. Cooper, pers. comm.). The Loweswater Formation is 800-900m thick in the vicinity of Hope Gill. In the areas of Skiddaw and Mungrisdale, thinner sandstone-dominant sequences are present at an equivalent stratigraphic position, suggesting the formation is significantly reduced in thickness in the east of the Skiddaw Inlier (Cooper et al, in prep). This could result from syn-depositional fault control. The inferred positions of syn-sedimentary faults coincide with known fault lines (figure 2.15).

The interpretation suggests the submarine fan of the Loweswater Formation developed in an extensional tectonic setting with approximately northeast-southwest extension.

2.3.3.4 Inter-lobe facies association

The inter-lobe facies association is dominated by facies group D2 and is displayed by the Loweswater Formation in Tom Rudd Beck (enclosure 7) and the lower part of Scawgill Bridge Quarry (enclosure 6). Siltstone turbidites are predominant, with additional very fine and fine sandstone turbidites in laminae and thin beds. An environment on the lower fan is generally applicable for this facies association but evidence exists for more proximal inter-channel/lobe environments. Development of facies C2.7 at Scawgill Bridge Quarry (enclosure 6, 7.0m and 104.0-106.3m) represents levee deposits to channels controlling distribution of coarse grained sand/gravel. This implies the facies association is not restricted to distal fan regions but occurs in inter-channel areas.

Sharp-based sandstone packets of *c* 5m thickness are dominated by facies group C2 (e.g. Tom Rudd Beck, stream bed 1.6-6.2m, 102.8-106.8m, west bank 37.6-42.8m, enclosure 7). Systematic trends in bed thickness and grainsize are not displayed. Sandstone packets constitute between 15 and 40 depositional events which is similar to the number of events displayed by sandstone packets of 5-40m thickness in the depositional lobe facies association. Thus an origin as lobe fringes, i.e. the distal or lateral equivalents of sand clastic pulses on depositional lobes, is inferred. A vertical transition between inter-lobe facies association and depositional lobe facies association is displayed in Scawgill Bridge Quarry (28.4-42.7m, enclosure 6) where a transition zone

comprises two sandstone packets between mudstone-dominant units of up to 1m thickness. The packets represent sand pulses heralding progradation of the depositional lobe.

2.3.4 Origin of textural variation in greywackes

The different characteristics of facies C2.2, B2.1, B1.1 and C1.1 are largely an effect of primary matrix content and these facies represent a continuum from low to high matrix types. Much of the greywacke matrix is thought to be of secondary origin from the breakdown of lithic fragments and feldspars but the interbedded nature of facies groups C1 and C2 (e.g. Fisher Wood 3.5-6.5m, enclosure 5) implies a variation in primary matrix content. This controls the depositional process and consequently the development of sedimentary structures, e.g. a relatively high proportion of silt and clay size particles is thought to prolong turbidity current flow and suppress the formation of tractional bedforms. Several causes of matrix variation at deposition can be suggested:

a) separate sand-rich and mud-rich sources fed the same deep marine distribution system,

i) mixing of primary sedimentary sources, e.g. volcanic mud flows passed into deep water and fed a dominantly sand-rich submarine fan,

ii) mixing of primary and secondary sediment sources, e.g. a mud-rich delta conveyed sediment to the head of the submarine canyon, largely fed by shelfal sands, or shelf muds occasionally fed a submarine canyon which dominantly conveyed deltaic sand into deeper water,

iii) mixing of secondary sediment sources, e.g. both sand and mud were supplied to a heterolithic shallow water sediment store from which the gravity flows were generated;

b) interdigitation of separate fan systems with sand-rich and mud-rich sources respectively;

c) the texture was acquired during sediment transport, e.g. unconsolidated mud draping the sea floor could have been reworked into an originally sand-rich turbidity current by fluid turbulence thus changing the texture and fluid mechanics of the flow.

For suggestions involving separate sources, especially case (a)i) above, one might expect a difference in composition between deposits derived from different sources. Mineralogical and chemical compositions of high-matrix greywackes (facies C1.1), channel-fill greywackes (facies groups B1 and B2), common greywackes (generally facies C2.1, C2.2) and quartz-wackes (facies C2.1, C2.2) are discussed in chapter 3. For high-matrix types preservation of detrital grains, especially feldspars which appear unaltered and angular, is better than in other greywackes. This is thought to be due to the suppression of diagenetic changes as matrix has acted as a barrier to migrating fluids. A small variation in petrographical composition is observed and either reflects a greater volcanic input in these greywackes or is due to their better preservation. Chemical composition is not significantly different from other greywacke-types, thus a difference in provenance is not apparent.

Sandstone packets of dominantly facies C1.1 are displayed at Fisher Wood, (22.1-26.5m and 73.7-81.2m). Smooth bed bases and lack of sedimentary structures are a characteristic of the facies thus case (b) above cannot be tested with palaeocurrent analysis. Applying the hypothesis of topographical control of turbidity current distribution presented in figure 2.15, this locality is sited on a northeast tilted fault block, largely shielded from turbidity currents. Accumulation of hemipelagic

mudstone would be expected. Overflow from fault-controlled channels by large turbidity currents or infilling of topography by lobe development would cause turbidity currents to travel down the tilted fault block, which could enable reworking of unconsolidated mud (case (c) above). Thus a greater proportion of high-matrix greywackes might be expected at localities in this topographical position (as seen at Fisher Wood, enclosure 5). Facies C1.1 between 73.7m and 81.2m at Fisher Wood (enclosure 5) contains the largest grainsize at this locality. Large, powerful turbidity currents (carrying the coarsest sediment) are most likely to overflow topographical barriers and subsequently rework unconsolidated deposits. Thus case (c) can account for the observed maximum grainsize.

Additionally, variation in matrix content is displayed in channel-fill greywackes of the Darling Fell Unit, e.g. contrast the matrix content of the channel-fills at Burnbank Fell (figure 2.13, 7.4-13.4m) and Darling Fell (enclosure 4, log at 146m, 10.8-12.2m). Accumulation of mud in submarine canyons and upper fan regions prior to reworking by sand-rich turbidity currents (case (c)) could account for such textural variations.

Localities displaying downcurrent facies variations in a single depositional event, in response to changing matrix content, would be required to demonstrate case (c). In the Skiddaw Inlier outcrop is inadequate.

2.3.5 Controls on sedimentation

The components of the Skiddaw Group document the changing environments of a deep marine distributary system. Sea-level fluctuations (either eustatic, or tectonically-controlled, regional fluctuations) will control the supply of sediment to the system (Pickering et al, 1989), and thus cause changes in sedimentary environment. Assuming sea level fall to be the main influence on fan growth, interpretation of sea-level fluctuation can be made from observations of changing facies associations. Figure 2.16 presents a crude curve for variation in relative sea level deduced from the deposits of the Skiddaw Group. In the absence of the shallow marine equivalent of the system, the curve is only a first approximation since environments can change irrespective of sea-level, e.g. intrinsic lobe switching on a relatively small scale (below the resolution of the curve), or in a complex manner, e.g. delivery of sand to a submarine canyon by shelfal currents during a relative high stand of sea level (Reading, 1991), when a reduced sediment supply would be expected. The curve is compared with published eustatic sea level curves and relative sea level curves for the margins of Eastern Avalonia and Gondwana in chapter 5.

The Bitter Beck Formation (500m present, of Tremadoc age), dominated by facies classes D, E with development of facies C2.*7*/C2.*5* and units of *c* 20m thickness of facies C2.3 (e.g. at Trusmadoor [NY 2777 3363]), is interpreted as a mud-dominated fan with limited occurrence of sandstone clastics as channel levees and pulses of sandstone turbidites representing small lobe development. The restricted input of sand clastics suggests a relative high stand of sea level. Alternatively the environment may be largely shielded from coarse clastic detritus by intrabasinal topography (e.g. a starved trench (Underwood and Bachmann, 1982)).

Figure 2.16 Speculative relative sea level curve for the Skiddaw Group. See text for an assessment of its limitations.

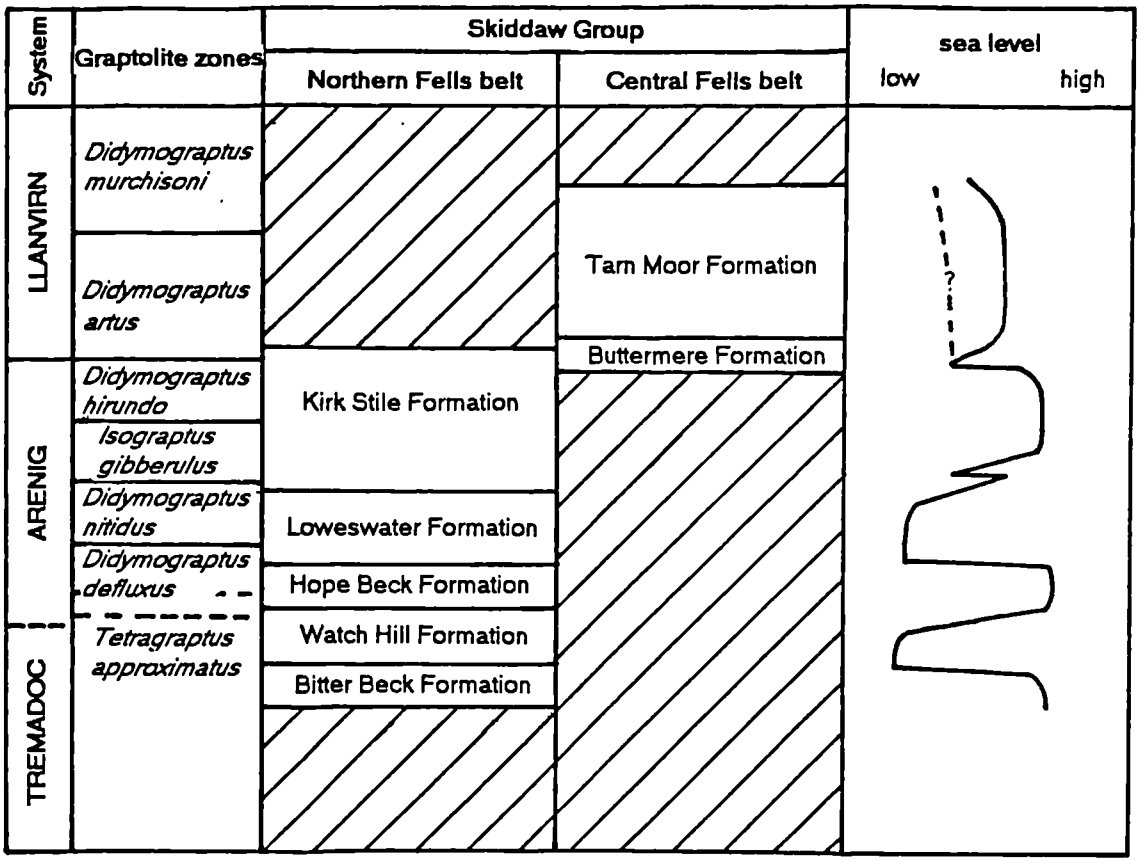

The Watch Hill Formation (Tremadoc-Arenig age and 40-550m thick) is dominated by the proximal channel/levee facies association, representing input of coarse clastic detritus. One might infer a relative lowering of sea level. The transition from the Bitter Beck Formation could largely be a lateral facies change. In the Skiddaw Inlier, sandstone lobes associated with these channels are not observed. Was sedimentation restricted to channels and levees (type III fan of Mutti (1985)), or were these channels sediment pathways to more extensive depositional lobes (type II or type I systems)? The occurrence of very fine and fine sand in overbank deposits to channels bearing dominantly very coarse sand/gravel, suggests fine sand was transported along channels and largely deposited elsewhere. The Manx Group displays depositional lobe facies association (Lonan and Glen Dhoo Flags) of similar age (section 2.4.1) and tempts the suggestion that these units are a distal equivalent to the Watch Hill Formation (discussed further in chapter 5).

The mudstone-dominant (facies classes D,E) Hope Beck Formation (Arenig age and 600-800m thickness) displays limited development of inter-lobe facies association with lobe fringe deposits (facies C2.5, C2.3, C2.2) and rare pebbly mudstones (facies A1.3). Generally a high stand of relative sea level can be inferred. The transition to the Loweswater Formation represents a relative lowering of sea level.

The Loweswater Formation (Arenig age and *c* 800m thick) represents the period of greatest submarine fan development, with inter-lobe, depositional lobe and distributary channel facies associations. Close similarity exists with suprafan lobe development in the general submarine fan facies model of Walker (1978) (figure 2.5b) and the type II system of Mutti (1985) (figure 2.7). Comparison can be made with small, radial, sand-rich fans, commonly in active margin settings, e.g. fans of the California continental borderland. Tectonic activity is implied by the widespread occurrence of convolute lamination interpreted to have a seismic trigger (plate 2.5.2). The palaeocurrent interpretation supports syn-depositional tectonics.

Cessation of sandstone clastic fan sedimentation and transition to the mudstone-dominant Kirk Stile Formation (Arenig-Llanvirn age, 2000m thick) suggests a relative rise in sea level. An exceptional occurrence in the lower part of the formation is a lenticular body of 80m thickness (Cooper et al, in prep.) of facies group C2. It records a final phase of lobe development.

Widespread slump folds (facies F2.1) and debrites (facies A1.3), e.g. at Beckgrains bridge [NY 1904 3552] and Outerside [NY 2132 2140], with intraformational clasts (chapter 3), developed during a slumping event at the Arenig-Llanvirn boundary. The contemporaneous Buttermere Formation olistostrome attests to the development of a regional submarine slope. A tectonic event or widespread lowering of sea level could be responsible. The absence of sandstone turbidites might be due to sandy turbidity currents bypassing the slope region, thus does not necessarily reflect a high relative sea level.

Submarine slope development might be in response to uplift of the Skiddaw Group depositional basin prior to erosion and extrusion of the sub-aerial Borrowdale Volcanic Group (Branney, 1988).

Palaeoslope orientation is investigated in chapter 4 and tectonic models are discussed in chapter 5.

2.4 Sedimentology of the Manx Group

This section aims to describe the range of sedimentary facies displayed by the Manx Group. The relationships of the stratigraphical units of Simpson (1963) are often unclear. A stratigraphical sequence supported by micropalaeontology is incomplete (table 1.5). The structure is little understood beyond the recognition of multi-phase deformation (Simpson, 1963). For these reasons sediments are described from units with palaeontological control. Palaeocurrents are collated from spatially restricted localities displaying a uniform tectonic style. Restoration is by rotation about local strike and plunging fold axes (where applicable). Additionally the origin of 'slump breccias' is discussed.

The Manx Group is situated approximately 100km to the west-southwest of the Skiddaw Group. A comparison of sedimentary environments of the two groups is presented.

2.4.1 Niarbyl Flags and Lonan Flags

The Niarbyl Flags are older than the Lonan Flags (Molyneux, 1979). Both units are of Tremadoc age, and display similar sedimentary facies of siliciclastic turbidites.

The Niarbyl Flags at Niarbyl and Ballanayre Strand (figure 2.17) are of facies C2.5, C2.3, C2.2 and C2.1 (maximum bed thickness is 50cm) and facies group D2. Grainsize is dominantly fine sand with horizontal lamination, ripple cross lamination (sometimes climbing), wavy lamination and convolute lamination common in Tbc turbidites. Sandstone content is 60-80%. Beds commonly display lateral thickness changes, but this is largely due to tectonic deformation.

At Ballanayre Strand, bases of three sandstone turbidites, each of 30cm thickness, display numerous (up to 50) large flutes (maximum dimensions: 50cm longitudinal, 20cm lateral, 10cm depth). The reorientated mean directions for each bed are to 067°, 067° and 130°. The bimodal ripple current pattern shown by the rose diagram for Niarbyl (figure 2.17) confirms field observations of opposed ripple directions in successive thin turbidites.

The Niarbyl Flags show similar characteristics to the sandstone-dominant units within the Bitter Beck Formation (of approximately equivalent age), although bed thickness is generally <15cm in the latter.

The Lonan Flags were studied at Langness, Port Mooar and Maughold Head (figure 2.17). Facies C2.5, C2.3 and C2.2 are present, and sandstone content is 60-80%. Grainsize is dominantly fine sand and Tbc divisions are common. Ripple cross lamination gives abundant palaeocurrent directions (figure 2.17) but sole marks are rarely displayed (partly because beds are right way up at these localities). Small grooves from the outcrops at Maughold Head trend 039°. The lack of sole mark directions and the uncertainties in the structural relationships between localities severely limit palaeocurrent interpretation. Both horizontal and vertical burrows (with strong vertical compression) were observed.

The Lonan Flags are of approximately equivalent age to the Watch Hill Formation. The dominance of facies class C, interpreted as a depositional lobe of a submarine fan, contrasts with the higher calibre, proximal channel-levee facies association of the Watch Hill Formation. These

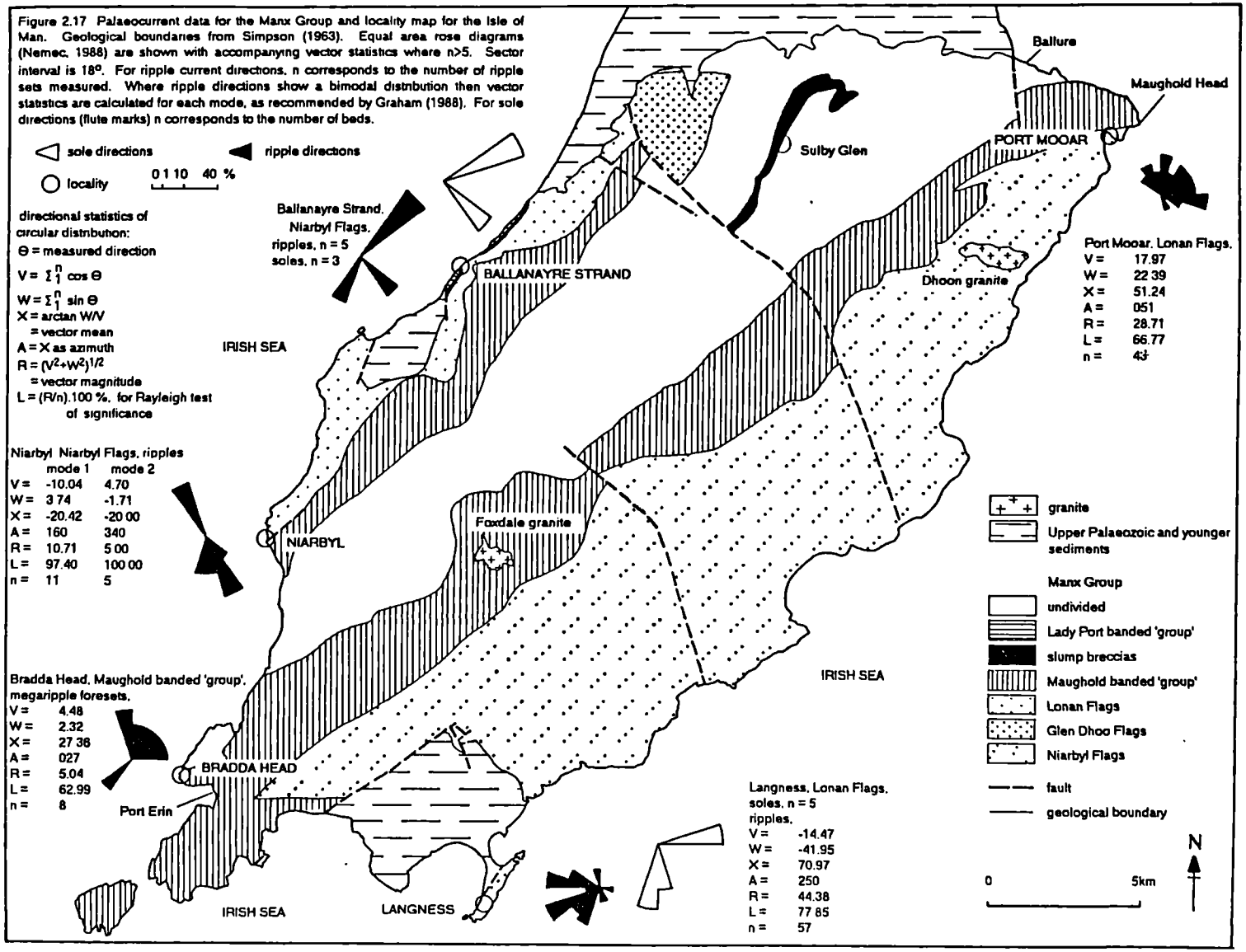
Figure 2.17 Palaeocurrent data for the Manx Group and locality map for the Isle of Man. Geological boundaries from Simpson (1963). Equal area rose diagrams (Nemec, 1988) are shown with accompanying vector statistics where n>5. Sector interval is 18°. For ripple current directions, n corresponds to the number of ripple sets measured. Where ripple directions show a bimodal distribution then vector statistics are calculated for each mode, as recommended by Graham (1988). For sole directions (flute marks) n corresponds to the number of beds.
sole directions
ripple directions
locality
0 1 10 40 %
directional statistics of circular distribution:
Θ = measured direction
V = Σ1n cos Θ
W = Σ1n sin Θ
X = arctan W/V
= vector mean
A = X as azimuth
R = (V2+W2)1/2
= vector magnitude
L = (R/n).100 %, for Rayleigh test of significance
Niarbyl Niarbyl Flags, ripples
mode 1 mode 2
V = -10.04 4.70
W = 3 74 -1.71
X = -20.42 -20 00
A = 160 340
R = 10.71 5 00
L = 97.40 100 00
n = 11 5
Bradda Head, Maughold banded 'group', megaripple foresets,
V = 4.48
W = 2.32
X = 27 36
A = 027
R = 5.04
L = 62.99
n = 8
Ballanayre Strand, Niarbyl Flags, ripples, n = 5 soles, n = 3
Sulby Glen
Ballure
Maughold Head
PORT MOOAR
Port Mooar, Lonan Flags,
V = 17.97
W = 22 39
X = 51.24
A = 051
R = 28.71
L = 66.77
n = 43
BALLANAYRE STRAND
Dhoon granite
IRISH SEA
NIARBYL
Foxdale granite
BRADDA HEAD
Port Erin
IRISH SEA
LANGNESS
IRISH SEA
Langness, Lonan Flags, soles, n = 5 ripples,
V = -14.47
W = -41.95
X = 70.97
A = 250
R = 44.38
L = 77 85
n = 57
granite
Upper Palaeozoic and younger sediments
Manx Group
undivided
Lady Port banded 'group'
slump breccias
Maughold banded 'group'
Lonan Flags
Glen Dhoo Flags
Niarbyl Flags
fault
geological boundary
N
0
5km

Plate 2.6

2.6.1 Thick and thin siltstone laminae (light) in mudstone (dark) (facies D2.1), showing: load balls (top); burrows (bottom right); and strong cleavage. Maughold banded 'group', Manx Group, Port Erin beach, Isle of Man.

2.6.2 Debrite comprising dominantly rounded clasts up to 50cm in size in a mudstone matrix (facies A1.3). Clasts are aligned to a fabric in the mudstone, which is cross-cut by quartz veins. Ballanayre slump breccia, Ballanayre Strand, Isle of Man.

2.6.3 Compressional fold and slide plane in laminated mudstone and siltstone (facies F2.1). Barrule slates, Manx Group, Ballure, Isle of Man.

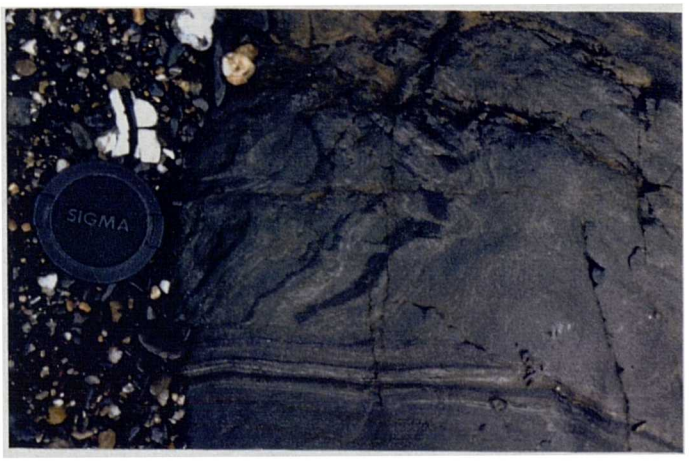

two environments could be related and represent part of a single submarine fan system. Such a scenario is possible if deposition was confined to a trough orientated approximately east-west (one of the alternative explanations for palaeocurrents of the Watch Hill Formation). Points of input to such a trough could have been numerous with development of overlapping axial distributary systems. Comparison of sediment provenance (chapter 3) is used as additional evidence in the discussion of regional models of sediment dispersal (chapter 5).

2.4.2 Maughold Banded Group

The heterolithic Maughold Banded Group is described from Port Erin, Bradda Head and south of Niarbyl. It is dominantly of facies D2.1. Laterally continuous thick laminae (and rarely very thin beds up to 3cm thick) of siltstone (and very fine sand) have ripple profiles which cause lateral bed thickness changes. Horizontal lamination and convolute lamination are also developed. Inter-laminated is an equal proportion of mudstone. Bases of silt/very fine sand units are commonly loaded and load balls may be detached from the overlying bed (plate 2.6.1). Short (<2cm) vertical burrows are common and strongly compressed along their length (plate 2.6.1). At Niarbyl, very dark grey mudstone is the dominant lithology with units of a few metres thickness of thin and thick laminated siltstone and mudstone (facies group D2).

The facies is interpreted as the deposits of dilute turbidity currents. Deposition or reworking by bottom currents is also possible.

Incursions of thin to thick bedded quartz arenite of very coarse to fine sand grainsize into this environment are of several tens of metres thickness (e.g. Port Erin beach, Bradda Head). Facies C2.3, C2.2, C2.1, B2.3 and B2.2 are present. Facies of class C comprise thin to thick beds of fine and medium sand with thin horizontal lamination and rare ripple cross lamination, and mudstone interbeds. Medium and thick beds of facies B2.3 show normal grading from very coarse to medium sand. A slump fold, confined within one bed of 50cm thickness, suggests a downslope direction to 075° (based on fold axis orientation and facing direction). This concurs with foreset dip directions (mean to 027°) in beds of facies B2.2. Cross lamination is often indistinct and defined by thick and thin, light and dark laminae, some of which are asymptotic to bed surfaces. Set size is 10-12cm in medium and thick beds. Petrographical observations show the texture to be largely recrystallised and the lamination is interpreted as relict foresets. At Port Erin beach an exceptional quartzite is 4m thick.

Transport of quartz-rich sediment by turbidity currents or near continuous density underflows could have been in response to relative sea level change (with an eustatic or tectonic control), e.g. progradation of deltaic quartz-arenites to the shelf edge during low stands, or dominance of long-shore shelfal currents during high stands transporting quartz sand into the heads of submarine canyons (Reading, 1991).

The Maughold Banded Group is approximately equivalent in age to the Loweswater Formation. The latter is dominated by the development of depositional lobes of a sand-rich submarine fan. Although the Maughold Banded Group is largely devoid of such lobes, controls of quartz arenite deposition may correspond to controls of lobe development in the Loweswater

Formation. Quartz wackes are present in the Loweswater Formation at Jonah's Gill. Composition and provenance of quartz-rich sediment of the Manx and Skiddaw groups is investigated in chapter 3. Occurrences of quartz arenites in similar facies to the Maughold Banded Group occur in the Ribband Group (Middle Cambrian to Llandeilo) of southeast Ireland (Bruck et al, 1979).

2.4.3 Slump breccias

At Sulby Glen (figure 2.17) there is a mud-supported breccia with both angular and rounded elongate clasts (long axes are generally 5-10cm, and exceptionally 50cm) with a preferred orientation parallel to cleavage. Clasts are dominantly of fine sand with thin parallel lamination, or of mudstone. Some clasts bear quartz veins. Boundaries of the deposit were not observed.

At Ballanayre Strand, 15m thickness of breccia is exposed with clasts (maximum size is 50 x 20 x 20cm) supported in a dark grey mudstone matrix (plate 2.6.2). Clasts are of thin laminated siltstone and mudstone and of very fine sandstone with thin laminae. Some contain quartz veins. Clasts have a preferred long axis orientation in the plane of a strong fabric in the matrix. A raft of 2m x 1m size contains interbedded sandstone and mudstone (facies C2.3). It has brecciated margins.

The slump breccias are debrites. The age of their emplacement is not constrained, but by comparison with debrites of the Skiddaw Group (in the Kirk Stile Formation at Beckgrains Bridge and Outerside, and in the Buttermere Formation), one can crudely infer a similarity of depositional environments for the Manx and Skiddaw regions.

Evidence of slump folding is spectacularly displayed in the Barrule Slates at Ballure (figure 2.17) (plate 2.6.3). These are highly deformed mudstone and siltstone in thin and thick laminae. Graded siltstones are up to 3cm thick and some have loaded bases giving way-up evidence. Younging directions are variable, as would be expected in such complexly deformed sediment. Small (<100cm half wavelength) folds and thrusts are interpreted to have formed in the toe of a slumped unit, but do not show a consistent facing direction.

2.4.4 Summary of comparisons of the Manx and Skiddaw groups

The Manx Group displays a range of deep marine depositional facies, reflecting many of the environments of the Skiddaw Group. These environments cannot be correlated between the groups, but the possibility of a single distributary system connecting the two regions, hence deposition in a single basin, cannot be dismissed on sedimentological grounds.

2.5 Sedimentology of the Ingleton Group

The Ingleton Group was introduced in section 1.6.

A greywacke-dominant unit is exposed in the core of a syncline in the River Twiss, River Doe and Ingleton Quarry (figure 2.18). The unit is at least 120m thick and generally coarsens and thickens upward (facies groups C2 to B2). Its top is not exposed.

2.5.1 Facies description

At Ingleton Quarry (figure 2.19) the greywacke unit is dominated by thick and very thick coarse sandstone beds showing normal grading either throughout beds or in their upper parts (facies B2.3). Ungraded medium and coarse sand beds (facies B1.1) are also present. These are interpreted as deposits of high-concentration turbidity currents. Mudstone caps are sometimes preserved above graded greywackes (coarse and fine sand grainsize) which display rare ripple cross lamination (facies C2.1) (e.g. figure 2.19, 2.0m). Mudstone units vary in colour from greenish-grey to reddish-grey. A single light-green bentonite (2mm thick) was observed. Units of thin bedded sandstone-mudstone couplets (facies C2.3) are occasionally displayed (e.g. figure 2.19, 6.8m). Greywacke beds are generally laterally continuous for several tens of metres. Rare examples of scours and lenticular channel-fills are present.

2.5.2 Palaeocurrent interpretation

Sole marks are common on bed bases. Facies C2.3 displays small flutes and grooves (6cm x 1cm x 0.2cm depth) which contrast with large horse shoe-shaped flute marks (50cm x 25cm x 1cm depth) in facies class B. Sole marks show a consistent direction to the northwest (mean direction to 306°) (figure 2.20). Rare ripple cross lamination (e.g. figure 2.19, 2.1m) indicates a similar flow direction.

This direction for erosional currents mimics that of Loweswater Formation group 1 localities (section 2.3.3.3). Ripple data are insufficient to interpret the presence of constraining topography or down-slope control of current direction. Leedal and Walker (1950) interpret a northwesterly palaeoslope from asymmetric convolutions in thin greywacke beds.

2.5.3 Interpretation of depositional environment

The greywacke-dominant unit is interpreted as a depositional lobe with lobe progradation recorded by the coarsening- and thickening-upward transition from the mudstone-dominant unit below. Thick, laterally continuous beds of coarse sand greywacke represent the maximum progradation of the lobe. Scouring and channel 'cut and fill' sandstones demonstrate incision of the lobe-top. The low proportion of mudstone suggests a high frequency of depositional events, or reworking of turbidite mud and hemipelagic mud. A suprafan lobe (type II system of Mutti (1985)) or depositional lobe of a low-stand fan (type I system) are possible interpretations without more widespread data.

The sandstone lobe of the Ingleton Group contrasts with clastic pulses of the Skiddaw Group in its greater sediment calibre and thickness of beds. Sediment compositions (investigated in chapter 3) are sufficiently different to conclude that the depositional systems of the Skiddaw and Ingleton groups were unconnected.

Figure 2.18 Geological map showing part of the Chapel-le-dale Inlier at Ingleton (redrawn from the unpublished field slip of N. J. Soper).

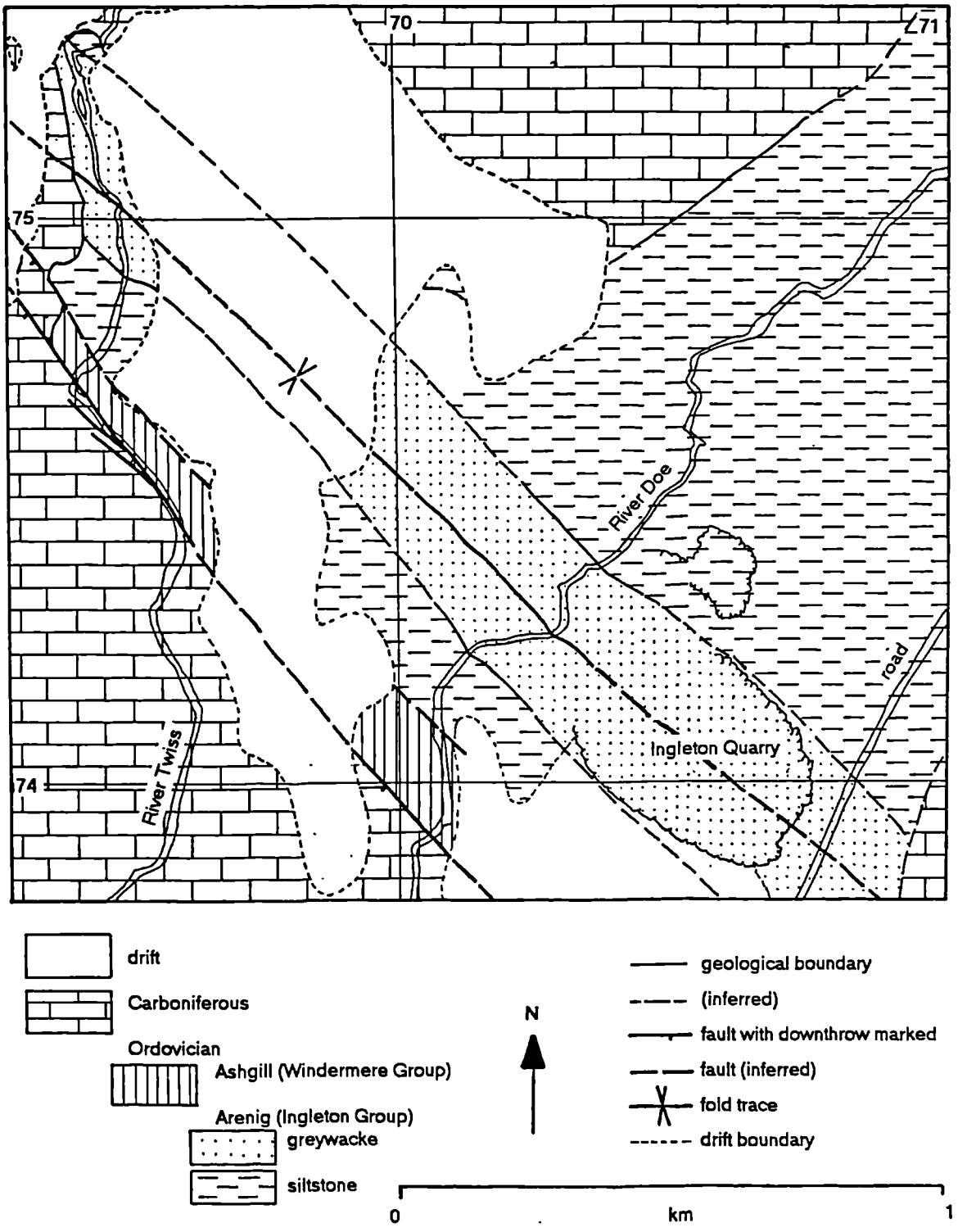

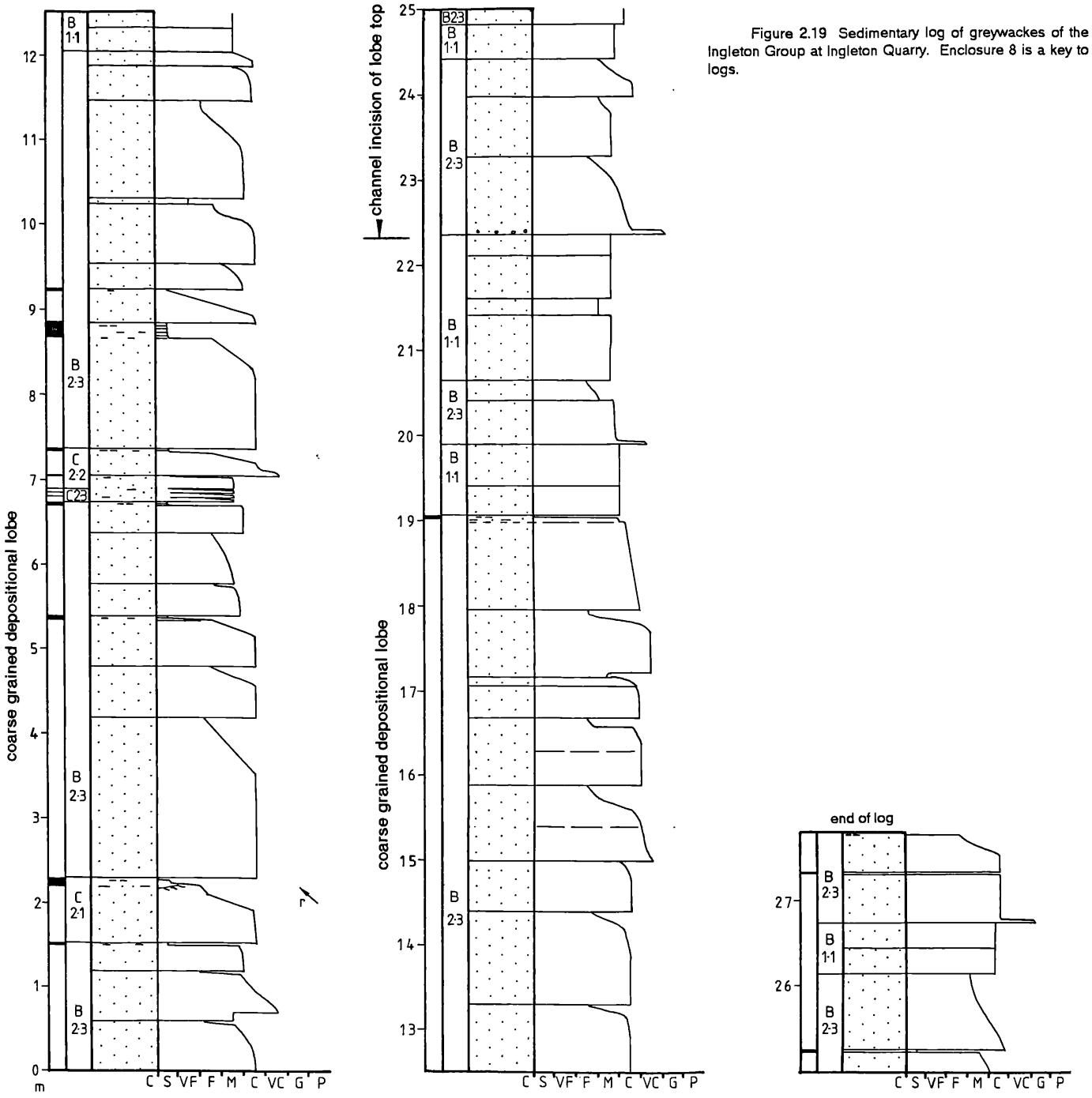

Figure 2.19 Sedimentary log of greywackes of the Ingleton Group at Ingleton Quarry. Enclosure 8 is a key to logs.

Figure 2.20 Equal area rose diagrams and vector statistics for the Ingleton Group; (a) directional sole marks, (b) non-directional sole marks.

Sector interval is 18°

Statistics of circular distribution (Graham, 1988):

(a) directional:			(b) non-directional:		
θ = measured direction			θ = measured direction		
V	$= \Sigma_1^n \cos\theta$	= 9.02	V	$= \Sigma_1^n \cos 2\theta$	= 10.66
W	$= \Sigma_1^n \sin\theta$	= -12.27	W	$= \Sigma_1^n \sin 2\theta$	= -16.03
X	= arctan W/V	= -53.67	X	= 1/2 arctan W/V	= -56.36
	= vector mean			= vector mean	
A	= X as azimuth	to 306°	A	= X as azimuth	trend 304°
R	$= (V^2 + W^2)^{1/2}$	= 15.23	R	= (W2 - V2)1/2	= 19.25
	= vector magnitude			= vector magnitude	
L	= (R/n).100 %	= 95.16	L	= (R/n).100 %	= 96.26
n	= number of beds	= 16	n	= number of beds	= 20

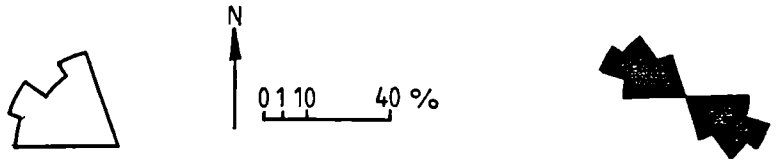

vector magnitudes are significant at a 95% level.

2.5.4 Comparison with the probable Arenig strata of the Beckermonds Scar borehole

The core of probable Arenig strata (Wilson and Cornwell, 1982) from the Beckermonds Scar borehole [SD 8635 8016] is highly fragmented with probable soft-sediment slumps and slides in addition to tectonic folds, faults and mineralization disrupting the core. The true thickness of strata represented in the core cannot be determined due to the folding and discontinuities. Short logs are presented in figure 2.21 to represent the sedimentary facies.

As at Ingleton Quarry, thick beds of facies B2.3, B1.1 and C2.1 are present but the grainsize is reduced from dominantly coarse sand to dominantly medium sand. The proportion of mudstone is greater with facies C2.2, C2.3, C2.5, D2.1 representing a continuum of turbidites of decreasing grainsize and/or bed thickness. Thick units of facies class D (e.g. figure 2.21, log 1, 4.8-6.8m) accumulated during periods devoid of sand clastic input.

The reversal in younging direction in log 3 (2.5m) coincides with a zone of folding and shearing. Boudinage and rotation of brittle sandstone blocks might indicate a slumped origin.

The facies of the Arenig strata of Beckermonds Scar could represent a distal equivalent to the depositional lobe of the Ingleton Group. The compositions of greywackes are compared in chapter 3.

Figure 2.21 Sedimentary logs of Arenig strata of the Beckermonds Scar borehole. True thicknesses are illustrated with accompanying borehole depths. Enclosure 8 is a key to logs.

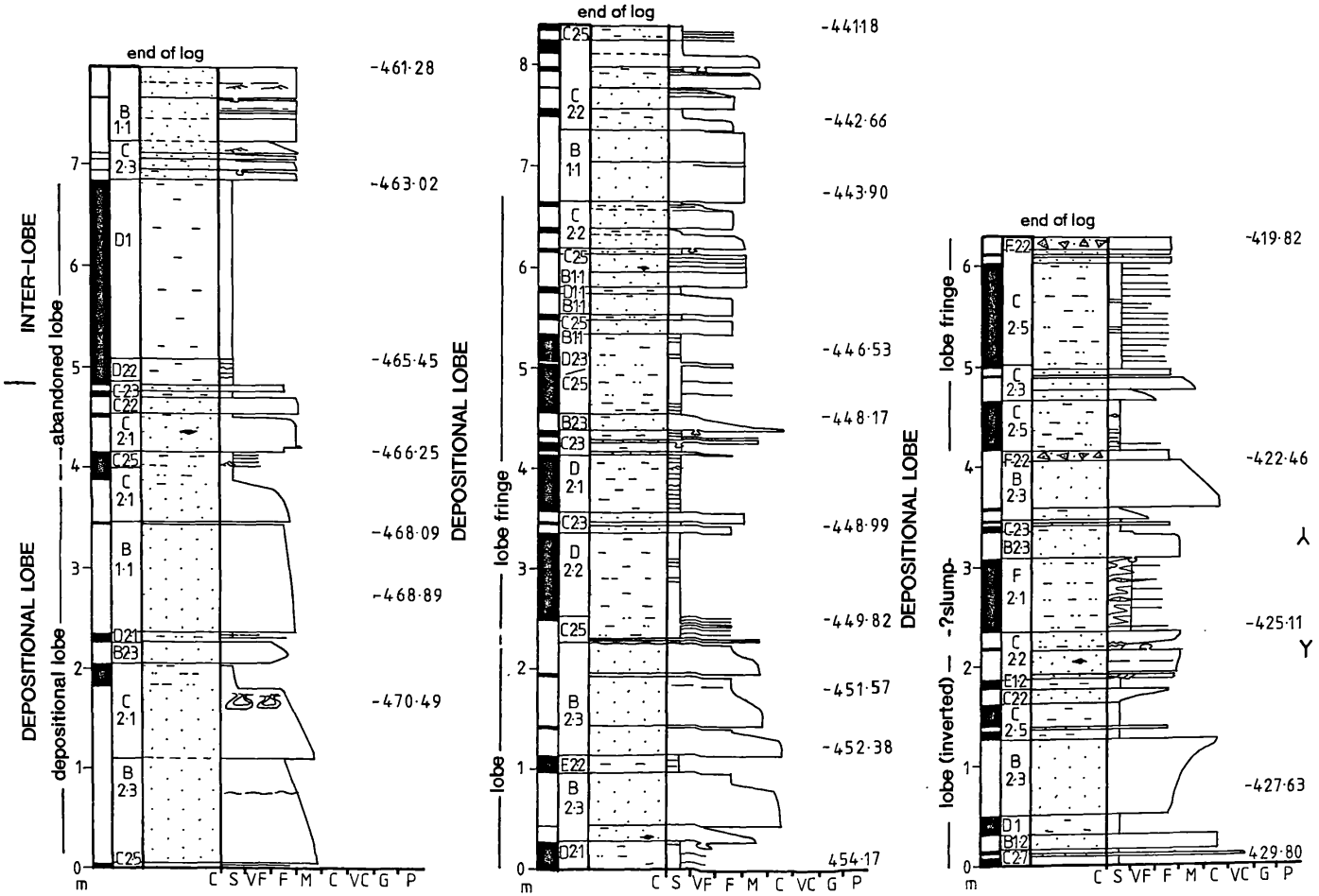

2.6 Summary

Following a review of deep marine clastic sedimentation, this chapter described the theory of oblique reflection of turbidity currents as solitary waves by topographical features (Kneller et al, 1991). Thus the geometry of intra-basinal topography can be interpreted from the relationship of sole and ripple current directions. The importance is stressed of accurate measurement of flow directions, recording of the type of palaeocurrent indicator and an understanding of the deformation history so restoration can be made.

The Skiddaw Group comprises deep marine sediments, deposited marginally to the Gondwana craton. The Group displays two pulses of sand grade siliciclastics: Watch Hill and Loweswater formations. A wide range of sedimentary facies are represented with examples from facies classes A to F of Pickering et al (1986).

The Watch Hill Formation comprises a proximal channel-levee facies association, with deposition in either an east-west trough or on a fan with flow from south to north with divergent or meandering channels.

The Loweswater Formation displays distributary channel, depositional lobe and inter-lobe facies associations. Sediment distribution is interpreted to have been influenced by linear troughs trending approximately north-northwest. A tectonic model of extensional fault blocks tilted to the northeast is proposed to explain palaeocurrent patterns and thickness changes in the Loweswater Formation across the region. The model is supported by observations of faults in favourable orientations which may be of early Ordovician age. Evidence for tectonic activity is provided by convolute lamination, often interpreted to have a seismic trigger.

The proposed origin for high-matrix greywackes involves incorporation into sandy turbidity currents of unconsolidated mud draping both channelled and unchannelled fan regions.

Variations in supply of sand clastics are used to infer changes in relative sea level. The submarine fan system of the Skiddaw Group can be compared with published fan models (Walker, 1978; Mutti, 1985) with an additional tectonic control of sediment distribution.

Sediments of the Manx Group are shown to be of similar depositional environments to the Skiddaw Group. A development of depositional lobe facies association of equivalent age to the proximal channel-levee facies association of the Watch Hill Formation could be a distal portion of the Skiddaw Group fan system, if flow was confined to an approximately east-west trough.

Facies of the Ingleton Group are related to development of a depositional lobe. The Arenig sediments of the Beckermonds Scar borehole represent the lobe-fringe. The higher sediment calibre and differences in composition (investigated in chapter 3) suggest this fan system was not connected with the Skiddaw Group.

Chapter 3

SEDIMENT COMPOSITION AND PROVENANCE

3.1 Introduction

3.1.1 Provenance, tectonic setting and basin type

A provenance study relates the composition of a sediment to the composition of lithologies in its source region through analysis of the sediment's mineralogy and chemistry.

Study of mineralogy with an optical microscope is restricted to sandstones and involves detailed qualitative observations and modal analysis by point-counting. Widespread adoption of the Gazzi-Dickinson technique of point-counting (Dickinson,1970) has enabled comparison of the results of many workers (Zuffa, 1987) and compilation of sandstone compositions, both ancient and modern, from different provenances (e.g. Ingersoll and Suczek, 1979; Dickinson and Suczek, 1979). The important parameters of grain populations have been used in plots that discriminate between sandstones from different sources (e.g. Dickinson and Valloni, 1980; Dickinson et al, 1983). Such diagrams have been widely applied to compare sandstones from related sources (Graham et al, 1976) and to indicate the type of source region for sandstones of unknown provenance (e.g. Floyd and Leveridge, 1987).

Chemical analysis is not grainsize restricted and allows the use of mudstones in provenance studies. Their low permeabilities reduce alteration due to fluid phases so mudrocks may be more reliable indicators of source rock composition than sandstones (Blatt, 1985). Provenance discrimination diagrams have been defined using major element compositions (Middleton, 1960; Bhatia, 1983; Roser and Korsch, 1988) and trace elements (e.g. Bhatia and Crook, 1986) including the rare earth elements (Bhatia, 1985c; Taylor and McLennan, 1985).

Before interpreting the geology of the exposed rocks of the source region, one must consider what the composition of a sedimentary rock sample represents. The source rocks are subject to alteration or breakdown of minerals and mobility of elements upon exposure by the processes of weathering and erosion. The extent is controlled by climate and may result in the detritus not being representative of the hinterland lithologies either in type or proportion (Basu, 1985).

A temperate climate is suggested for southern Britain in the early Ordovician as palaeomagnetic studies (Torsvik and Trench, 1991) suggest a palaeolatitude of 60°S at this time. The degree of weathering is indicated by the chemical index of alteration (CIA) (Nesbitt and Young, 1982):

$$CIA = 100 \times [Al_2O_3 / (Al_2O_3 + CaO^* + Na_2O + K_2O)]$$

where CaO^* is the amount of CaO in the silicate fraction of the rock. An average CIA for Skiddaw Group mudstones with negligible carbonate content is 82, comparable with sediments of the Amazon cone (Pettijohn, 1975). This is higher than the CIA for average shales (70-75) indicating a high degree of weathering. In the absence of a tropical climate this may be due to extensive transport of sediment or recycling of sedimentary formations. The elements used by the index could be mobile after deposition, but the range of CIA values for mudstones of different age and location is narrow (78-85) suggesting either negligible or uniform alteration.

During transport sand grains may be selected according to mechanical durability, grain size, density and shape (Zuffa, 1987) and may pass through several temporary storage environments (e.g. delta, continental shelf) before reaching an ultimate depositional site (e.g. deep marine basin). The final depositional mechanism may induce further sorting by traction e.g. in turbulent mass flows, although high density mass flows will produce massive unsorted deposits (Ricci Lucchi, 1985). Material from within the basin e.g. authigenic or biogenic phases or clasts eroded from the substrate during transport, may be incorporated into the sediment. Most provenance discrimination diagrams were defined using deep marine sediments deposited by turbidity currents, so compositional variation due to different depositional processes is minimal. The changes in flow conditions of the decelerating turbidity current, however, induce significant compositional sorting within the turbidite, which must be considered (section 3.3.2).

Modification of mineralogy and chemistry of sediment may occur during diagenesis, generally resulting in loss of provenance information (e.g. McBride,1985; Milliken, 1988). The diagenetic processes can be related to the tectonic setting of the depositional basin (Siever, 1979) thus aiding interpretation of tectonic setting. The use of modern deep-sea samples in the definition of provenance discrimination diagrams eliminates the effects of post-burial modifications.

Metamorphism (burial, regional, contact or hydrothermal metasomatism) may result in further modification. Fortey (1989) suggests a low-grade metamorphic history for the Skiddaw Group involving anchizonal sub-volcanic metamorphism in the Caradoc, anchizonal burial metamorphism in the Silurian followed by epizonal regional metamorphism in the early Devonian.

Deformation may involve mineral dissolution and element mobility. In the Skiddaw Group this is exemplified by quartz dissolution and subsequent redistribution as numerous quartz veins. Deformation episodes include slumping in partially lithified sediment, a possible volcano-tectonic event, Caledonian and Acadian deformation, and faulting associated with the Hercynian orogeny and later events.

Recent near-surface weathering will cause further mineralogical changes although this effect can be minimised by collecting the freshest samples possible.

In summary, the sample composition could differ significantly from a mean composition of the lithologies exposed in the source region. In order to connect sample to source one must recognise the post-depositional alterations through petrographical observations of relict minerals involved in replacements or alterations. Mineralogical breakdown will result in the redistribution of elements but the bulk chemical compositon of the sample might remain constant if elements do not move in or out of the system. Certain trace elements are relatively immobile and constancy of element ratios within a group of samples would suggest those elements have undergone no systematic alteration (Floyd et al, 1991). One can therefore achieve a good assessment of the sediment composition at deposition and an appreciation of its relation to source rock composition.

How does sediment composition relate to depositional basin type and the tectonic setting of both source and basin? Middleton (1960) showed that sandstones from different geosynclinal settings had different chemical compositions and Crook (1974) demonstrated the three main continental plate margins of Mitchell and Reading (1969) have characteristic greywacke

compositions. Thus a connection was recognised which demanded further investigation and refinement.

Petrographical studies related sample composition to the type of source region and identified three major divisions: *recycled orogen, volcanic arc, craton interior.*

Studies of modern sediments considered the type of depositional basin, classified by its plate tectonic setting (table 3.1). Thus diagrams displayed compositional fields labelled: *backarc, forearc, trailing edge, strike-slip, leading edge.*

Table 3.1 Plate tectonic classification of sedimentary basins (Maynard et al, 1982, after Reading, 1979, Dickinson and Valloni, 1980).

I Spreading-related or passive settings

(a) *Intracratonic rifts* (East Africa), mostly filled by alluvial fans and lakes

(b) *Failed rifts* or aulacogens (Benue Trough), thick sequence of deposits ranging from deep-sea fan to fluvial

(c) *Intercontinental rifts*

1 Early (Red Sea), evaporites and some clastics

2 Late (Atlantic), early stage sediments along margins overlain by continental shelf or deltaic deposits, passing seaward into oceanic crust overlain by turbidites and finally pelagics; often termed *trailing edge*

II Active settings

(A) Continental collision-related

1 *Remnant ocean basins* (Bay of Bengal), thick turbidite fan deposits eventually piled into imbricate thrust sheets

2 *Late orogenic basins* (sub-Himalayas), variety of terrestrial and shallow marine deposits, but dominantly fluvial; termed *peripheral foreland basins* if on the subducting plate

(B) *Strike-slip fault-related settings* (California), thick sequences of deep-marine to fluvial sediments in small basins, mostly derived from adjacent uplifts

(C) Subduction-related settings

1 *Continental margin magmatic arcs* (Andes)

(a) Fore-arc, thin to thick deposits ranging from turbidites to fluvial; termed leading-edge in some classifications

(b) Back-arc, very thick, mostly terrestrial, accumulations; sometimes termed ensialic back-arc or retro-arc

2 *Intra-oceanic arcs* (Japan, Aleutians)

(a) Fore-arc, thin turbidite deposits plus pelagics

(b) Back-arc, thin to thick accumulations of clastics near the arc, passing into pelagics and possibly into terrigeneous clastics again at the continental margin

Studies of the chemical composition of ancient sediments defined provenance fields corresponding to basin type classified by source region, thus they were labelled: *oceanic island arc, continental island arc, active continental margin, passive margin* (Bhatia, 1983). Roser and Korsch (1986) did not consider the arc settings could be separated and Floyd et al (1991) merged the continental settings and introduced a further field: *oceanic within plate*. These differences of opinion were due to the complex interaction of sources feeding basins on active plate margins. This complexity had been recognised by workers considering modern sediments and was reflected in their definition of provenance fields by basin type.

An alternative approach was to define provenance groups by sample composition. Roser and Korsch (1988) studied chemical composition of ancient sediments and defined *mafic, intermediate, felsic* and *recycled* groups and Valloni and Mezzadri (1984) described *quartzofeldspathic, quartzolithic, feldspatholithic* and *volcanolithic* petrographic compositional suites of modern deep-sea sands. These compositional types could be related to a variety of source terrains and occur in more than one basin type.

It is clear, therefore, that provenance fields are not directly comparable between studies based on petrography and chemistry or between modern and ancient data, due to the complexity of the relation between depositional basin, source region and plate tectonic setting (table 3.2).

The suggestion that sediment composition indicates the type of sedimentary basin in terms of its tectonic setting assumes that the composition of the source region is related to the plate tectonic setting of the adjacent basin. Floyd et al (1991) disagree with this assumption in their chemical study of Devonian sandstones. There are several considerations:

> The source terrain will be older, perhaps negligibly or substantially, than its adjacent basin, so the detritus from igneous rocks might reflect contemporaneous volcanics or a palaeo-volcanic signature not related to the tectonic setting of source and basin.
>
> The basin-fill may have been sourced a great distance from its depositional site, e.g. turbidity currents can transport sediment great distances along a deep marine trench or across ocean floor (e.g. Hesse et al, 1987), or littoral drift currents may transport exotic detritus to the head of a submarine canyon (Zuffa, 1987), such that the source region does not reflect the tectonic setting of the basin.
>
> Sedimentary rocks in the source terrain will be recycled. The recognition of recycled material in sediments is a fundamental problem (Blatt, 1967).
>
> A single source may feed more than one type of sedimentary basin, e.g. an uplifted orogen could provide sediment to a foreland basin or deep ocean trench, or a single basin may be fed by more than one source, e.g. a marginal basin with provenance elements of both an active continental margin and oceanic island arc (Rodolfo, 1969).

Table 3.2 A comparison of provenance fields defined by petrographical and chemical studies of modern and ancient sediments. OIA-oceanic island arc, CIA-continental island arc, ACM-active continental margin, PM-passive margin, CAAM-continental arc and active continental margin, OWP-oceanic within plate, RCM-rifted continental margin CM-continental margin, ARC-volcanic arc, SC-subduction complex, LV-lithovolcanic, QF-quartzofeldspathic, FL-feldspatholithic QL-quartzolithic, M-matured.

PROVENANCE FIELDS defined by basin type or *basins fed by a particular source*										basin type and *style of volcanism*	diagrammatical crustal section demonstrating plate tectonic configurations with modern analogues
ancient						modern					
geochemical				petrographical							
Bhatia (1983)	Roser & Korsch (1986)	Roser & Korsch (1988)	Floyd et al (1991)	Dickinson et al (1983) & Suczek (1979)	Ingersoll & Suczek (1979)	Dickinson and Valloni (1980)	Valloni and Maynard (1981)	Maynard et al (1982)	Valloni and Mezzadri (1984)		
			OWP			*intra-plate archipelago*				oceanic abyssal plain *intra-plate oceanic* oceanic abyssal plain	W. PACIFIC
CIA	*ARC*	*P2 intermediate*	*CAAM*	*active margin arc (undissected, transitional, dissected)*	*magmatic arc*	*OIA*	fore-arc	fore-arc	LV	fore-arc *micro-continental arc*	JAPAN
CIA	*ARC*	*P2 intermediate*	*CAAM*	*mixed*	*mixed magmatic arc and RCM*	*RCM (craton & orogenic belt)*	back-arc	back-arc	M, LV, QF	inter-arc and back-arc *marginal sea*	INDIA-ASIA
PM		*P4 recycled*		*recycled orogen (quartzose, transitional, lithic)*	*suture belt*		leading edge	continental margin arc	QL, FL	peripheral foreland *intra-plate continental*	
ACM	*ACM*		*CAAM*	*continental block -basement uplift*		*orogenic CM (transform arc orogen)*		strike-slip	FL, QL	strike-slip fault related *mid-ocean ridge*	SAN ANDREAS
OIA	*ARC*	*P1 mafic*	*OIA*	*active margin arc -undissected*	*magmatic arc*	*OIA*	fore-arc	fore-arc	LV	trench fore-arc *young arc volcanism*	MARIANAS
OIA	*ARC*	*P1 mafic*	*OIA*	*mixed*	*mixed magmatic arc and RCM*	*OIA*	back-arc	back-arc	FL, QF, LV, M	inter-arc and back-arc *marginal sea*	
										intra-cratonic rift *continental rift volcanism*	E. ATLANTIC
PM	*PM*	*P4 recycled*	*PM*	*continental block -basement uplift*	*RCM*	*RCM (craton & rift belt)*	trailing edge	trailing edge	QF, QL, M	passive margin *mid-ocean ridge*	
PM	*PM*	*P4 recycled*	*PM*	*continental block*	*RCM*	*RCM (craton & orogenic belt)*	trailing edge	trailing edge	QF, QL, M, (LV)	passive margin	W. ATLANTIC
ACM	*ACM*	*P4 recycled*		*recycled orogen*					FL, QL	retro-arc (foreland) *continental margin arc*	
ACM	*ACM*	*P3 felsic*	*CAAM*	*active margin arc recycled orogen*	*mixed magmatic arc & SC*	*orogenic CM (CM arc)*	leading edge	CM arc	LV, QL, FL, (QF)	fore-arc	
ACM	*ACM*	*P3 felsic*	*CAAM*	*active margin arc recycled orogen*	*mixed magmatic arc & SC*	*orogenic CM (CM arc)*	leading edge	CM arc	LV, QL, FL, (QF)	trench oceanic abyssal plain *mid-ocean ridge*	E. PACIFIC

The differing volcanic styles in different plate tectonic settings are a major influence on source terrain composition, so an interpretation of plate tectonic setting can be made if coeval volcanism can be proved. The occurrence of pyroclastic beds is a good indicator, or of morphologically immature unaltered crystals (in samples without diagenetic effects) (Zuffa, 1987). Detailed petrographical observations of texture are an essential tool to accompany both mineralogical and chemical analyses, both of which are needed to characterise sediment composition.

The discussion has shown that sediment composition, source terrain, basin type and tectonic setting are connected but in a complex manner. In order to make a correct interpretation of their relationships compositional data must be accompanied by basin analysis (Zuffa, 1987) based on studies of sedimentology and structure (table 3.3). In this chapter provenance diagrams are used to infer source region composition and further interpretation, in conjunction with other evidence, appears later.

3.1.2 Aims

The study set out to determine the composition of early Ordovician sediments in terms of their mineralogy and chemistry. A variety of different techniques, to maximise the information from each sample, were used to investigate the following topics, listed in order of increasing scale:

to analyse the variations in composition within individual turbidites,

to identify the range of greywacke compositions within any formation,

to characterise and compare the composition of each formation of the Skiddaw Group,

to investigate the composition of the sandstone rafts of the Buttermere Formation and sandstone clasts from the Beckgrains Bridge debris flow of the Kirk Stile Formation,

to compare Skiddaw Group sediments with those of the Manx Group and Ingleton Group,

to determine the provenance of each of these formations and identify secular and spatial variations.

Techniques used include modal analysis by optical point-counting, qualitative petrographical observations, geochemical analysis of major and trace elements by x-ray fluorescence spectrometry and rare earth element determination by inductively-coupled plasma spectrometry.

Table 3.3 A flow diagram for interpretation of palaeogeography and tectonic setting of ancient source-area/deep-water basin systems (modified after Zuffa, 1987).

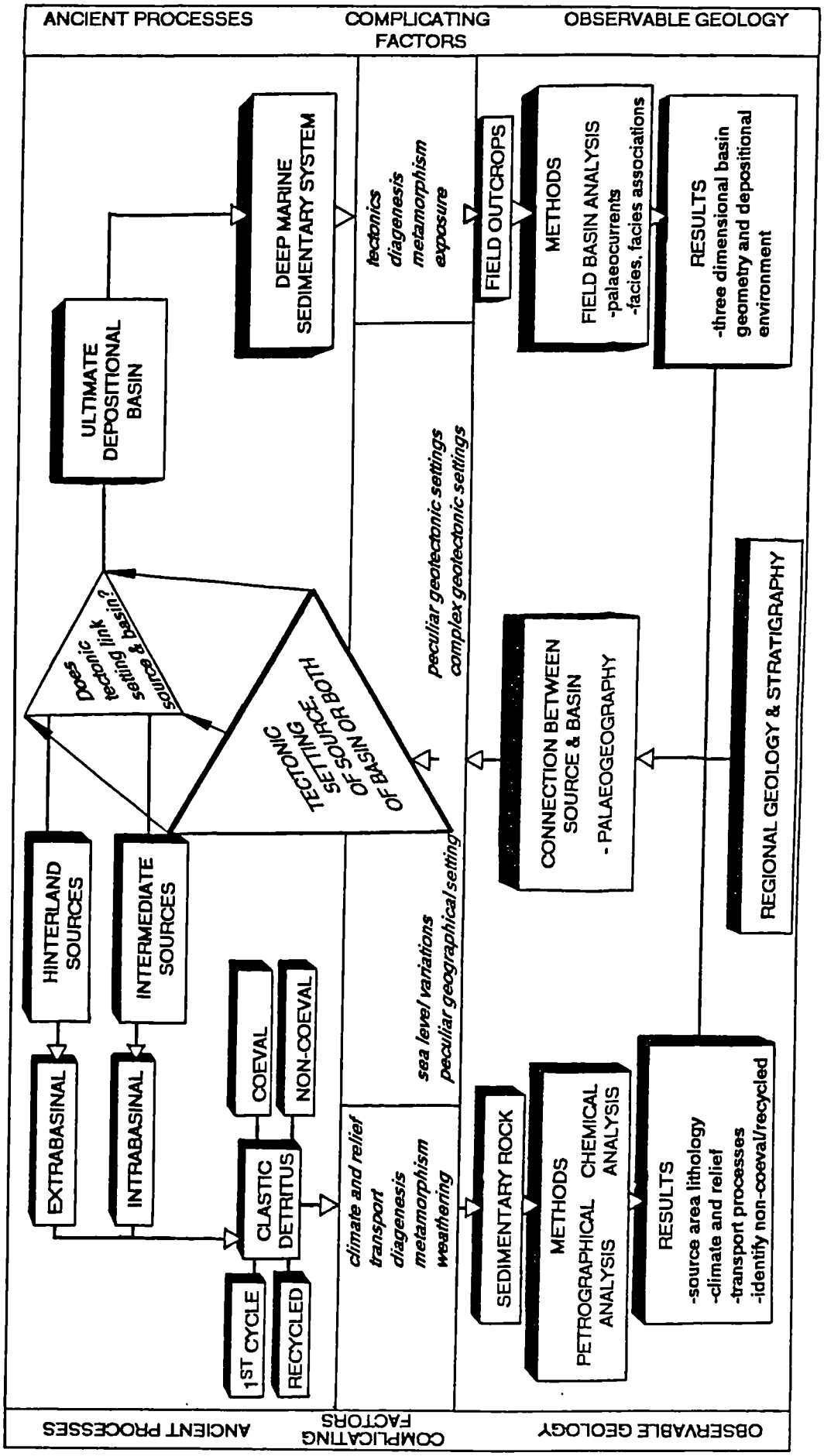

3.2 Petrographical techniques in provenance discrimination

3.2.1 Introduction

The use of petrography and grain populations in provenance studies evolved through the study of ancient sandstones and recognition of the most important discriminating parameters. Dickinson (1970) used three primary parameters displayed as a triangular diagram:

Q - total quartz including polycrystalline quartz

F - total feldspar

L - lithic grains

and three secondary parameters:

C/Q - the ratio of polycrystalline quartz grains to total quartz

P/F - the ratio of plagioclase to total feldspar

V/L - the ratio of volcanic lithics to total lithic fragments.

He recognised three provenance types:

volcanic terrains- feldspathic rocks nearly free of quartz,

plutonic terrains- feldspathic rocks with few lithics,

tectonic terrains- uplifted sedimentary and metasedimentary rocks.

As the number of studies increased so did the refinement of provenance discrimination diagrams. Triangular diagrams with the following parameters were introduced:

Qm - F - Lt - monocrystalline quartz, total feldspar and lithics plus polycrystalline quartz,

Qm - Qp - L - monocrystalline quartz, polycrystalline quartz and lithics,

Qp - Lv - Ls - polycrystalline quartz, volcanic lithics (including metamorphosed volcanic lithics) and sedimentary lithics (including metamorphosed types), (Graham et al, 1976),

Qm - P - K - monocrystalline quartz, plagioclase feldspar and alkali feldspar, (Dickinson and Suczek, 1979),

Lm - Lv - Ls - lithic fragments of metamorphic, volcanic and sedimentary origin respectively (Ingersoll and Suczek, 1979).

The study of ancient rocks of well known provenance culminated in the definition of provenance fields by Dickinson et al (1983) shown in figure 3.1. These fields are compared with data in this study.

Figure 3.1 Ternary provenance discrimination diagrams; (a) Q-F-L, (b) Qm-F-Lt and (c) Qp-Lv-Ls of Dickinson et al (1983), (d) Lm-Lv-Ls and (e) Qp-Lv-Ls of Ingersoll and Suczek (1979). Plotting parameters defined in table 3.5. RCM=rifted continental margin, MA=magmatic arc, SB=suture belt, MA+SC=mixed magmatic arc and subduction complex, MA+RCM=mixed magmatic arc and rifted continental margin.

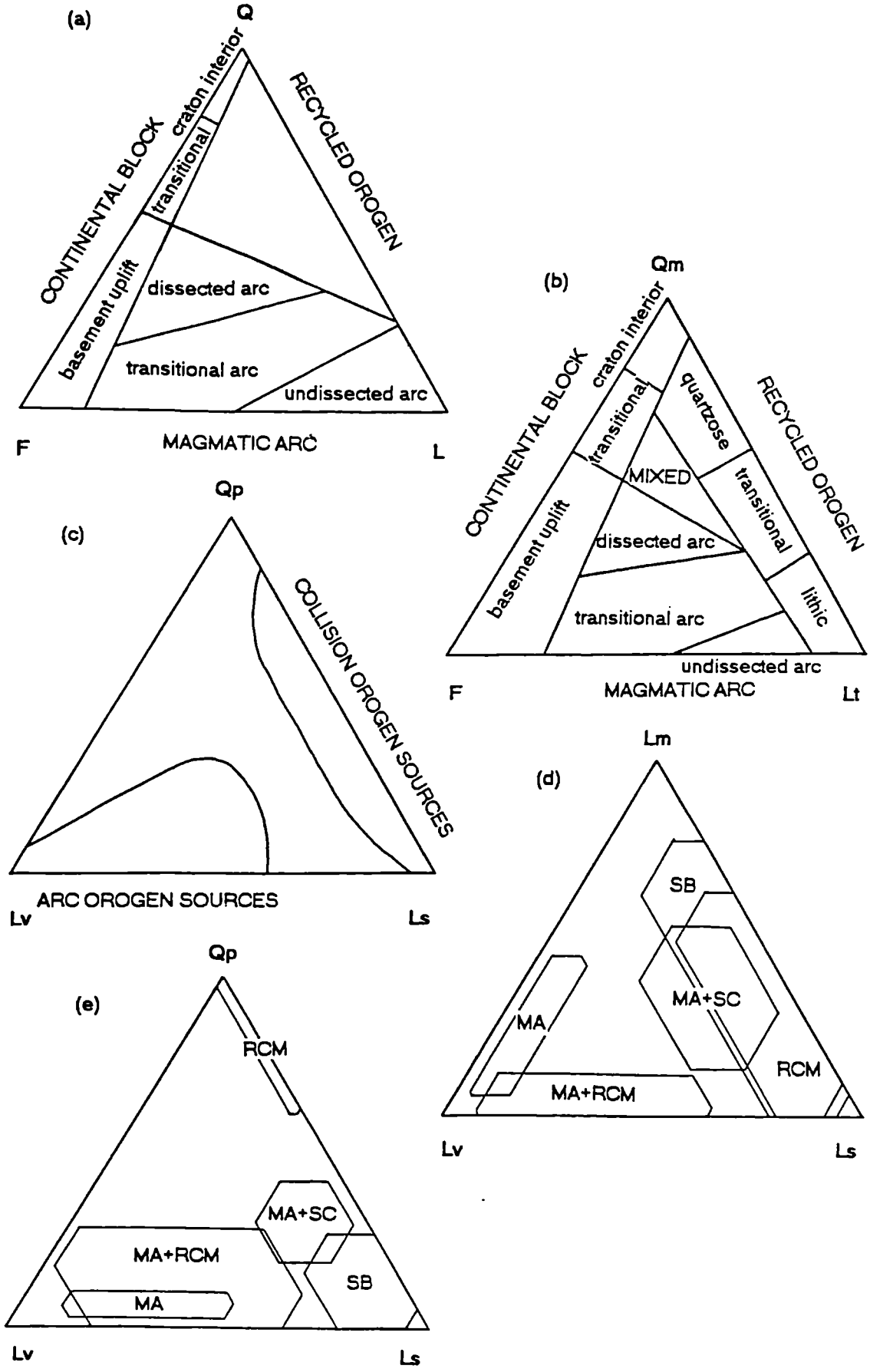

The difficulty in defining the tectonic setting of ancient sedimentary sequences led to parallel studies of the petrography of modern sands. Dickinson and Valloni (1980) used the same primary and secondary parameters of Dickinson (1970) to distinguish successfully sands of different tectonic setting. Similarly, Valloni and Maynard (1981) classified modern samples by tectonic setting of their depositional basin and plotted means and confidence fields on a ternary Q-F-L diagram. The provenance fields defined by Dickinson and Suczek (1979) for ancient samples (figure 3.1d,e) were found to overlap with sands of equivalent modern tectonic setting by Maynard et al (1982). Appreciation of the limitations of assuming a relationship between sandstone composition and tectonic setting is evident in the approach of Valloni and Mezzadri (1984) who applied the standard parameters to define compositional suites of modern sands. They then considered the tectonic setting of basins that may contain each suite (table 3.4). These compositional suites (figure 3.2) are compared with sandstone compositions in this study.

Table 3.4 Source region and depositional basin type for the compositional suites of Valloni and Mezzadri (1984).

suite	principle source area	tectonic setting and basin type
quartzofeldspathic QF	cratonic block	rifted continental margins, plus back-arc/ marginal basins, trenches and basins oceanward of trenches
quartzolithic QL	sedimentary orogenic belt	active and passive margins, rifted continental margins, collision and strike-slip settings, arc-trench systems
feldspatholithic FL	volcanic orogenic belt	strike-slip margins and Andean margins or back-arc and collisional settings
lithovolcanic LV	volcanic arc	fore-arc and back-arc basins adjacent to magmatic arcs in continental margin or intra-oceanic positions plus anomalous occurrences on rifted continental margins
matured (texturally and mineralogically mature types of any suite)		rifted continental margin or less commonly back-arc/marginal basins

Figure 3.2 Compositional suites of Valloni and Mezzadri (1984), defined by primary parameters, Q-F-L (a), and secondary parameters, V/L, P/F, C/Q (b)(c), and Lm-Lv-Ls (d). QF=quartzofeldspathic, QL=quartzolithic, FL=feldspatholithic, LV=lithovolcanic.

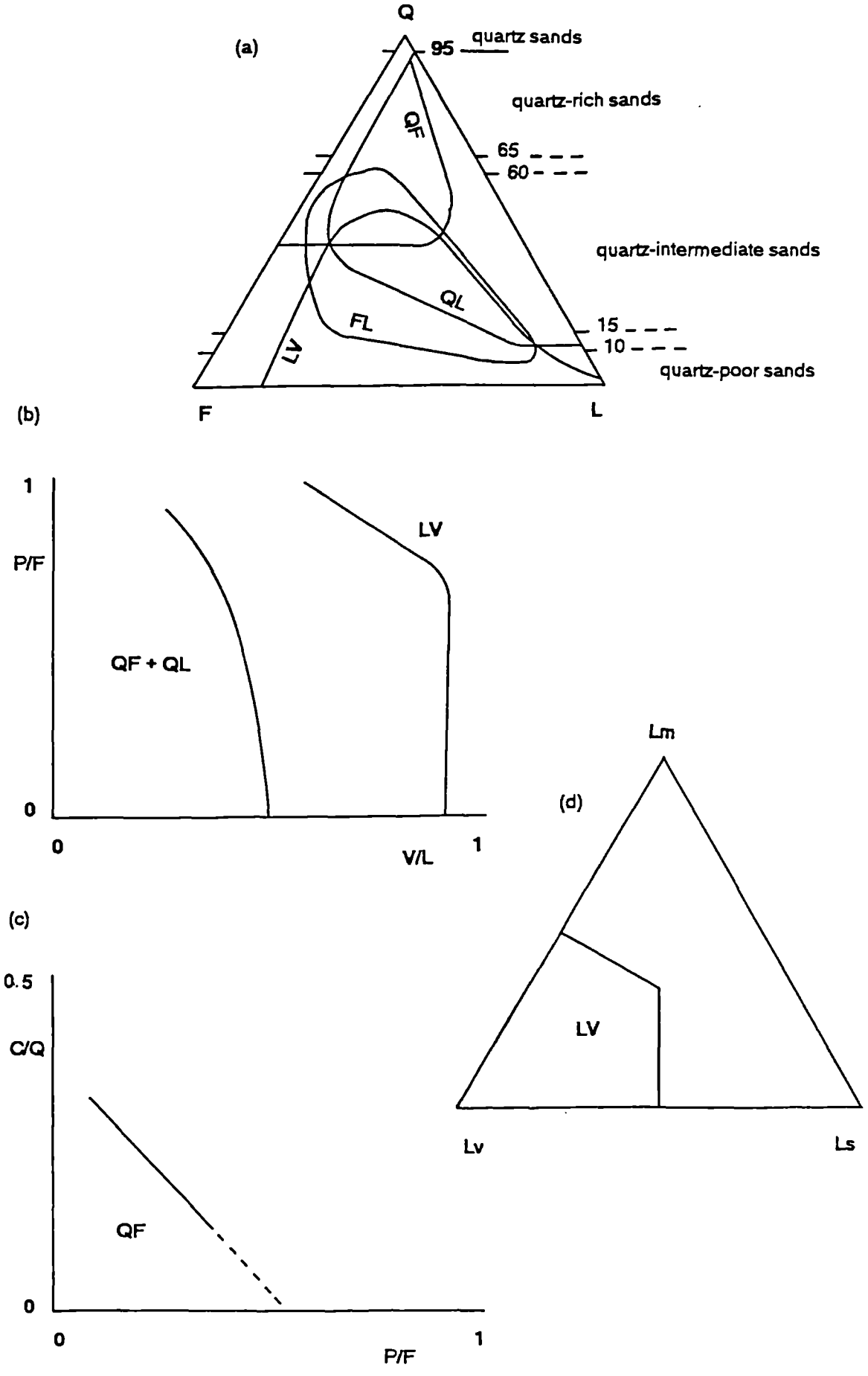

The importance of textural observations in petrographical studies is stressed by Valloni and Mezzadri (1984) and Zuffa (1987). They can indicate mineralogical changes, sediment recycling, coeval volcanism and identification of intrabasinal and extrabasinal sources and are an essential aid to interpretation of grain population data.

3.2.2 Analytical Technique

Thin sections were made available for this study by Dr A. H. Cooper of the British Geological Survey (Newcastle) and thin sections with accompanying chemical analyses by Dr D. C. Cooper (British Geological Survey, Keyworth). Additional samples were collected from horizontally laminated fine to medium grained sandstones, where possible, to reduce the effect of compositional variation due to grainsize and depositional sorting.

Thin sections of sandstone samples were point-counted (100-300 points per slide) using the Gazzi-Dickinson method (Dickinson, 1970) to eliminate variation of modal composition with grainsize due to breakage of lithic fragments into constituent grains (Ingersoll et al, 1984). The method requires that components of lithic clasts >0.0625mm diameter are recorded as separate grains. The method does not account for actual mineralogical variation with grainsize so visual estimates of grainsize were made for consideration with other depositional parameters (e.g. Bouma unit, bed thickness, sedimentary facies) when comparing sandstone samples.

The Badley, Ashton and Associates Ltd. point-counting system with a BBC-Master personal computer, Swift mechanical stage and accompanying software was used for direct data input to computer file and subsequent statistical analysis and graphical data presentation. The phases counted and the provenance discriminatory parameters to which they are assigned are given in table 3.5.

Table 3.5 Phases counted in modal analysis and the constitution of primary and secondary parameters for provenance discrimination.

	primary and secondary parameters					
	Q	Qm	Qm	Qp	Lm	C/Q, P/F,
phases in modal analysis	F L,	F Lt,	P K,	Lv Ls,	Lv Ls,	V/L
unstrained monocrystalline quartz	Q	Qm	Qm			
strained monocrystalline quartz	Q	Qm	Qm			
polycrystalline quartz	Q	Lt		Qp		C
(proportions of chert and metamorphic varieties recorded)						
plagioclase feldspar	F	F	P			P
(estimate of composition recorded separately)						
potassium feldspar	F	F	K			
(including untwinned varieties)						
volcanic lithic fragments	L	Lt		Lv	Lv	V
metavolcanic lithic fragments	L	Lt		Lv	Lm	V
sedimentary lithic fragments	L	Lt		Ls	Ls	
metasedimentary lithic fragments	L	Lt		Ls	Lm	
detrital mica (biotite or muscovite)						MATRIX
pyrite						MATRIX
carbonate cement						MATRIX
clay matrix						MATRIX
chlorite						MATRIX
heavy minerals (identified and recorded separately)						MATRIX

The aim of the analysis was to record the mineralogy at deposition, hence altered grains were counted as the original phase if relict fragments could be identified. Additional notes recorded the nature of alterations, the composition of unstable lithic fragments, the origin of polycrystalline quartz grains (metamorphic, chert or felsite), visual estimates of plagioclase composition using angle between twins at extinction (method in Deer, Howie and Zussman, 1966), types of heavy minerals and varieties of alkali feldspar.

An attempt was made to stain uncovered sections for feldspars using the method of Houghton (1980), but without success. Feldspars could be distinguished from quartz by the presence of one or more of the following:

twinning (multiple, simple or cross-hatch),

perthitic texture,

cleavage,

preferential replacement by carbonate or clay phases,

brown colouration.

The composition of untwinned feldspar could not be determined, although where partial replacement had occurred plagioclase was most commonly replaced by carbonate and alkali feldspar by clay phases. Some errors in feldspar identification must be expected.

The matrix in greywackes is dominantly of secondary origin (Brenchley, 1969; Whetten and Hawkins, 1970) due to the breakdown of lithic fragments and feldspars during diagenesis. On a Q-F-L ternary diagram this has the effect of moving points toward the Q pole (Shail and Floyd, 1988). To minimise the bias of diagenetic changes, the provenance discriminatory diagrams are defined using sandstones with <25% matrix (Dickinson et al, 1983). The sandstones in this study commonly have matrix in excess of this, which must be considered when interpreting diagrams.

In addition to point-counting of grain populations, the range of unstable lithic fragments was studied in the coarser samples (coarse sand to granule grainsize). Lithic compositions remain consistent in different size fractions (Ingersoll et al, 1984) thus comparability with the fine to medium sandstones used for point-counting is valid. Observations of grain texture were used to consider whether volcanic lithic fragments were produced by coeval volcanic sources or recycled palaeo-volcanic sources, although the poor preservation prevented the use of the detailed classification of Zuffa (1987).

3.2.3 Additional techniques

Samples were studied under cathodoluminescence to attempt to distinguish feldspar types. Luminescence colours were inconsistent (ranging from blue to green) and some twinned plagioclase did not luminesce, sharing the same dull brown colour of the quartz.

The technique was not useful and no data are presented.

3.2.4 Petrographical description, classification and provenance of Skiddaw Group greywackes

(Individual modal analyses can be found in appendix 2.)

3.2.4.1 Group characteristics

Skiddaw Group greywackes are quartz-rich and quartz-intermediate (Crook, 1974) and plot in the quartzofeldspathic compositional suite of Valloni and Mezzadri (1984) (figure 3.3). Variability in the secondary parameter ratios is due to the low numbers of these grains encountered in point-counting. Valloni and Mezzadri (1984) used modern sands to define the suites and directly observed the basin type and source terrain of samples. Thus the quartzofeldspathic suite is typical of rifted continental margins but also occurs in back-arc/marginal basins, deep marine trenches and other basin types. Provenance may be from orogenic terrains and/or platform deposits.

Considering textural and mineralogical maturity, many of the samples are quartz-rich with subrounded to rounded grains (especially in coarser samples) and where feldspar dominates over lithic fragments comparison is best made with the *matured* group of the quartzofeldspathic suite. The matured attributes are gained through transport or sediment recycling and matured greywackes are typical of rifted continental margins or back-arc/marginal basins.

Investigations of the use of undularity and polycrystallinity in quartz in provenance studies (Blatt and Christie, 1963; Basu et al, 1975) have been of limited success. Sediment maturity controls the proportions of polycrystalline quartz (least stable), undulose quartz and non-undulose quartz (most stable), and led Blatt and Christie (1963) to conclude the method to be "of very limited usefulness in determining the provenance of sediments". Nevertheless Basu et al (1975) produced a diagram to discriminate 'plutonic' and 'metamorphic' sources using these parameters. For the Skiddaw Group this shows derivation from low rank metamorphic sources, but any interpretation is complicated by the post-depositional strain imposed on the quartz. Evidence of quartz dissolution and crystal-plastic deformation abounds, hence the plot is probably more indicative of the post-depositional history rather than provenance. The occasional occurrence, therefore, of clear unstrained quartz of volcanic origin is all the more significant.

Maturity is reflected in the mineralogical maturity index (MI),

$$MI = 100 \times (Q / [Q + F + L])$$

with an average value of 73 for the group. The index is strongly dependent on the post-depositional breakdown of feldspar and lithics, widely observed in most samples and indicated by a high average matrix content (39%), so unqualified assignment of provenance types would be misleading.

Figure 3.3 Comparison of Skiddaw Group samples with the compositional fields of Valloni and Mezzadri (1984), n=67. QF=quartzofeldspathic, QL=quartzolithic, FL=feldspatholithic, LV=lithovolcanic.

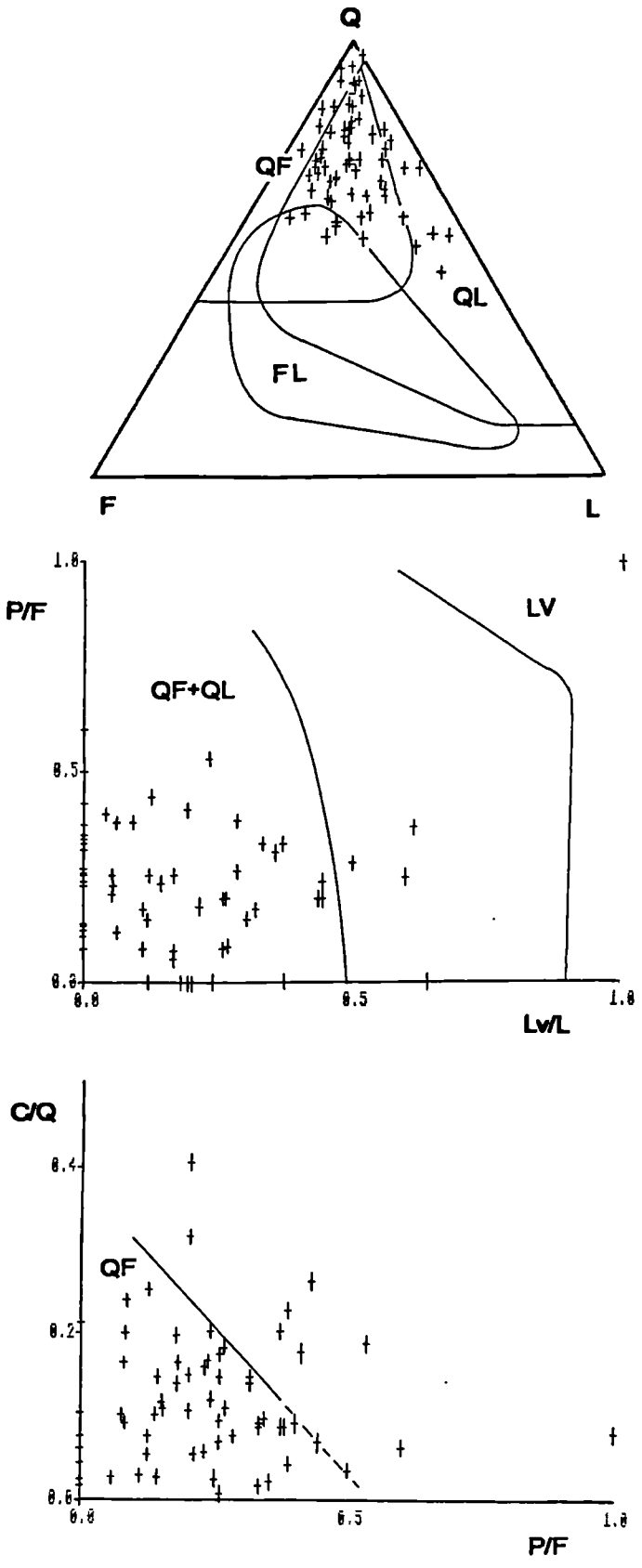

Figure 3.4 Provenance discrimination diagrams for the Bitter Beck Formation, n=1; Q-F-L, Qm-F-Lt., Qp-Lv-Ls with fields after Dickinson et al (1983); Lm-Lv-Ls, Qp-Lv-Ls with fields after Ingersoll and Suczek (1979), RCM=rifted continental margin, MA=magmatic arc, SB=suture belt, MA+SC=mixed magmatic arc and subduction complex, MA+RCM=mixed magmatic arc and rifted continental margin.

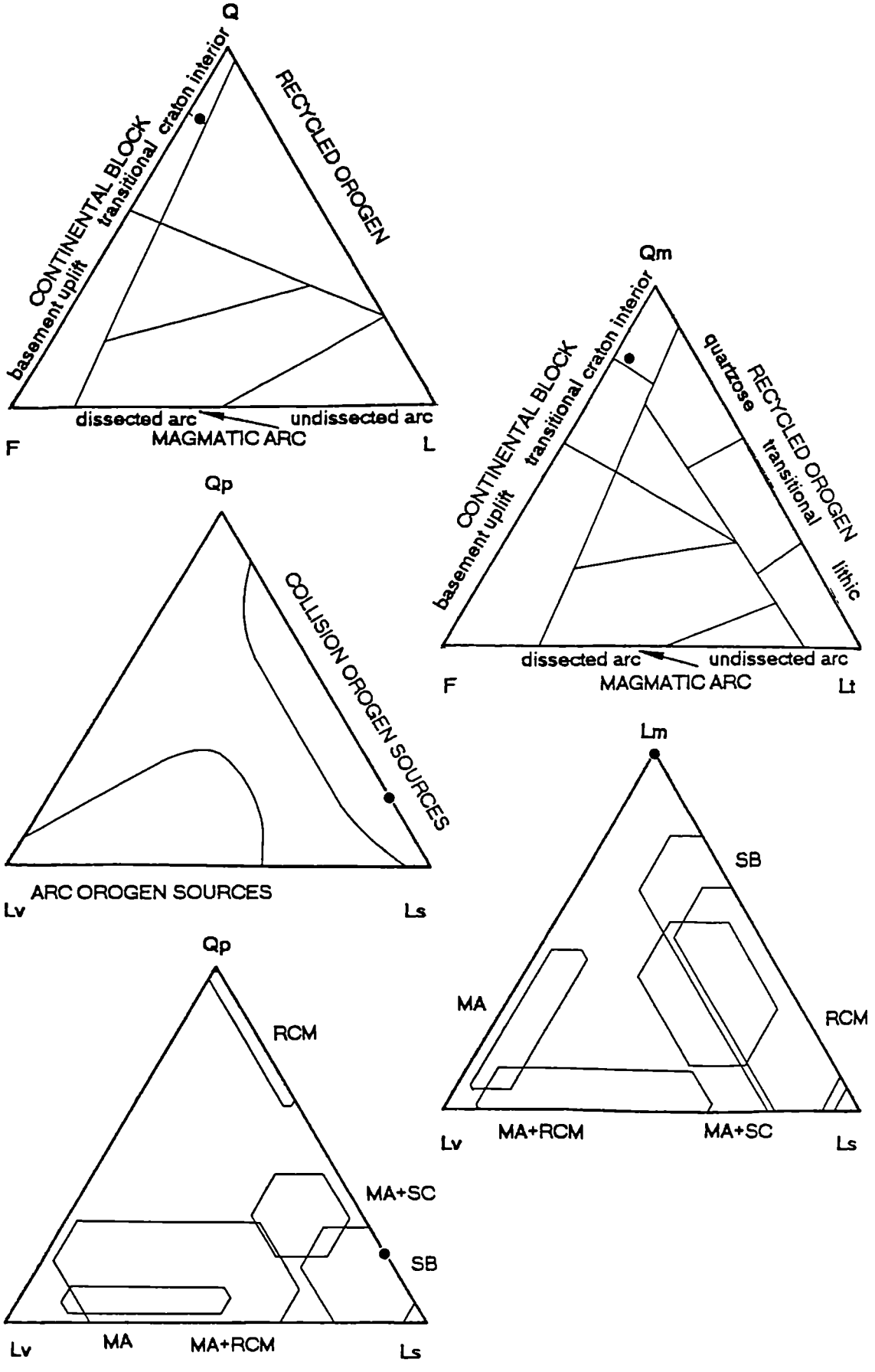

3.2.4.2 Bitter Beck Formation

The petrography is represented by a single sandstone sample from the Bouma Tb unit of a turbidite from Trusmadoor [NY 2777 3363]. It is classified as a feldspathic wacke with feldspar extensively replaced by clay minerals, and untwinned varieties dominant over plagioclase of andesine composition. Quartz is monocrystalline and strained and lithics are of phyllite. Tourmaline, opaques and zircons were recognised in order of decreasing abundance.

On ternary diagrams for provenance interpretation, a *craton interior* source area is indicated (figure 3.4). On Qp-Lv-Lm the sample plots in the field of *collision orogen* sources (Dickinson et al, 1983) and corresponds to occurrence in a remnant ocean basin (Ingersoll and Suczek, 1979).

3.2.4.3 Watch Hill Formation

Greywacke beds of the Watch Hill Formation are commonly of variable grainsize with thick laminae of very coarse sand or granule size grains, in dominantly fine or medium sand grainsize. Samples for pointcounting are from medium thickness beds, with or without horizontal lamination, and the fine-medium sand grainsize fraction was analysed. They are classified as lithic wackes (figure 3.5).

For samples from the Watch Hill area, an early quartz cement is typically present which has inhibited matrix formation and alteration of lithic and feldspar grains (plate 3.1.2). Mean matrix content is 15% (table 3.6). Lithic clasts were further studied in the very coarse sand to granule size range. The range of clast types is illustrated in plates 3.1 to 3.14 at the end of section 3.2.

Quartz is almost exclusively strained and of plutonic origin, but unstrained monocrystalline quartz of volcanic origin is present. Plutonic polycrystalline quartz with a small number of large crystals with undulose extinction, is present, but polycrystalline quartz is dominantly of metamorphic origin. Chert is rare and difficult to distinguish from rhyolite or the groundmass of pyroclastic lithics, especially in the finer grainsizes (plate 3.3.2).

Alkali feldspars (cross-hatched twinned microcline, perthite and untwinned types) are dominant over plagioclase, which is usually in angular grains of andesine composition (plate 3.2.1). Microcline is commonly blocky and unweathered.

Figure 3.5 Classification of greywackes of the Watch Hill Formation (after Dott, 1964, Pettijohn et al, 1972), n=11.

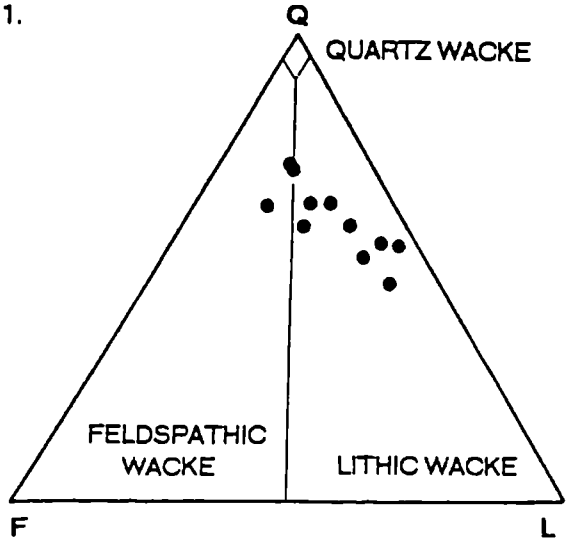

Lithic clasts of volcanic, sedimentary and metamorphic origin are approximately equal in proportion. Well rounded clasts of mudstone, siltstone and very fine sandstone are unlikely to be intraformational (plate 3.3.1), but contorted, intraformational mudstone clasts are present (plate 3.2.2). Volcanic clasts include pyroclastic fragments with relict shards, quartz and feldspar phenocrysts and recrystallised cherty groundmass; volcaniclastic clasts of exclusively angular feldspar fragments in a fine matrix; basalt with relict plagioclase laths; rhyolite; microgranite with strained quartz, potassium feldspar and biotite and sometimes displaying spectacular graphic texture (plates 3.5, 3.4, 3.9, 3.8). Near-isotropic, brown grains with inclusions of feldspar crystals are interpreted as volcanic glass. This range of volcanic lithics is also seen showing strain, cleavage and alteration due to metamorphism. Polycrystalline quartz of metamorphic origin is common (plate 3.11). Phyllite and muscovite schist fragments are present.

Zircon, tourmaline and opaques represent the heavy mineral content (plate 3.14.2). Detrital mica is relatively rare. Secondary opaques are sometimes present as a late-stage alteration following cleavage. Early diagenetic pyrite is common in mudstones.

Volcanic and volcaniclastic clasts with angular components are rounded, which suggests the source of volcanic detritus could have been non-coeval with sedimentation. Large, fresh angular alkali feldspars and graphic granite clasts suggest the presence of first cycle detritus from an unroofed granitic pluton. The hinterland also contained metamorphosed igneous and sedimentary rocks and non-metamorphosed sediments.

On a Q-F-L plot the samples group tightly in the *recycled orogen* field and on Qm-F-Lt fall both in this field and in a *mixed recycled orogen/volcanic arc* field (figure 3.6). Considering lithic proportions alone suggests a mixture of *volcanic arc orogen* and *collision orogen* sources on a Qp-Lv-Ls ternary plot and compares closely with the average for sediment from *mixed magmatic arc and subduction complex* sources, typically deposited in an ocean trench (figure 3.6). Petrographical evidence is inconclusive in demonstrating the presence or absence of coeval arc volcanism. Possible scenarios may be recycling of an older dissected arc with exposure of its underlying pluton and reworking of metamorphic basement, or mixing of an uplifted orogen and coeval arc volcanics.

The Watch Hill Formation at Great Cockup appears more lithic-rich in hand specimen and this is confirmed by petrography. The grainsize of available sections however, was larger, very coarse sand to pebble size, so a greater lithic proportion might be expected, despite the Q-F-L point-counting technique. Also, misidentification of lithic types could have occurred in the smaller grainsizes demonstrated by large igneous lithics with feldspar phenocrysts in a fine quartz groundmass which would appear as grains of polycrystalline quartz with further degradation.

The samples from Great Cockup do not have a quartz cement and clay matrix is more extensive (table 3.6). Polycrystalline quartz is more abundant than at Watch Hill and monocrystalline quartz and feldspars (untwinned types dominant over plagioclase) are less abundant. Lithic types have a similar range but are more abundant in the samples from Great Cockup.

Table 3.6 Means and ranges of petrographical data for the Watch Hill Formation at (a) Watch Hill (n=7) and at (b) Great Cockup (n=4).

(a) Watch Hill (n=7)

	mean	minimum	maximum
strained monocrystalline quartz	45.76	38.00	53.00
unstrained monocrystalline quartz	3.07	0.50	10.00
polycrystalline quartz	7.43	3.00	12.00
plagioclase feldspar	3.14	0.67	5.50
untwinned feldspar	10.07	6.00	15.50
volcanic lithic fragments	2.00	0.00	9.00
metavolcanic lithic fragments	1.17	0.00	5.50
sedimentary lithic fragments	9.36	1.67	12.00
metasedimentary lithic fragments	2.95	0.50	7.00
detrital mica	0.14	0.00	0.50
pyrite	1.50	0.50	3.00
carbonate cement	0.00	0.00	0.00
clay matrix	12.95	4.00	26.00
chlorite	0.38	0.00	1.33
heavy minerals	0.07	0.00	1.50
matrix	15.05	5.50	28.67
mineralogical maturity index	65.16	59.47	72.45

(b) Great Cockup (n=4)

	mean	minimum	maximum
strained monocrystalline quartz	24.75	23.00	26.50
unstrained monocrystalline quartz	4.12	2.50	6.50
polycrystalline quartz	12.00	8.00	18.50
plagioclase feldspar	1.37	0.50	2.50
untwinned feldspar	4.25	2.00	7.00
volcanic lithic fragments	4.62	2.50	7.00
metavolcanic lithic fragments	2.50	0.50	5.50
sedimentary lithic fragments	21.00	12.00	27.50
metasedimentary lithic fragments	0.25	0.00	0.50
detrital mica	0.62	0.50	1.00
pyrite	0.12	0.00	0.50
carbonate cement	0.00	0.00	0.00
clay matrix	23.62	19.00	27.50
chlorite	0.12	0.00	0.50
heavy minerals	0.62	0.00	1.00
matrix	25.12	24.00	38.50
mineralogical maturity index	52.65	46.98	55.83

Figure 3.6 Provenance discrimination diagrams for the Watch Hill Formation. Q-F-L, Qm-F-Lt, Qp-Lv-Ls for greywackes with fields after Dickinson et al (1983), n=11. Samples from Watch Hill are of fine-medium sand grainsize. Samples from Great Cockup are of very coarse sand grainsize which causes points to plot nearer to the lithics pole. Lm-Lv-Ls, Qp-Lv-Ls for lithic range of very coarse sand grainsize greywackes with fields after Ingersoll and Suczek (1979), n=2. RCM=rifted continental margin, MA=magmatic arc, SB=suture belt, MA+SC=mixed magmatic arc and subduction complex, MA+RCM=mixed magmatic arc and rifted continental margin.

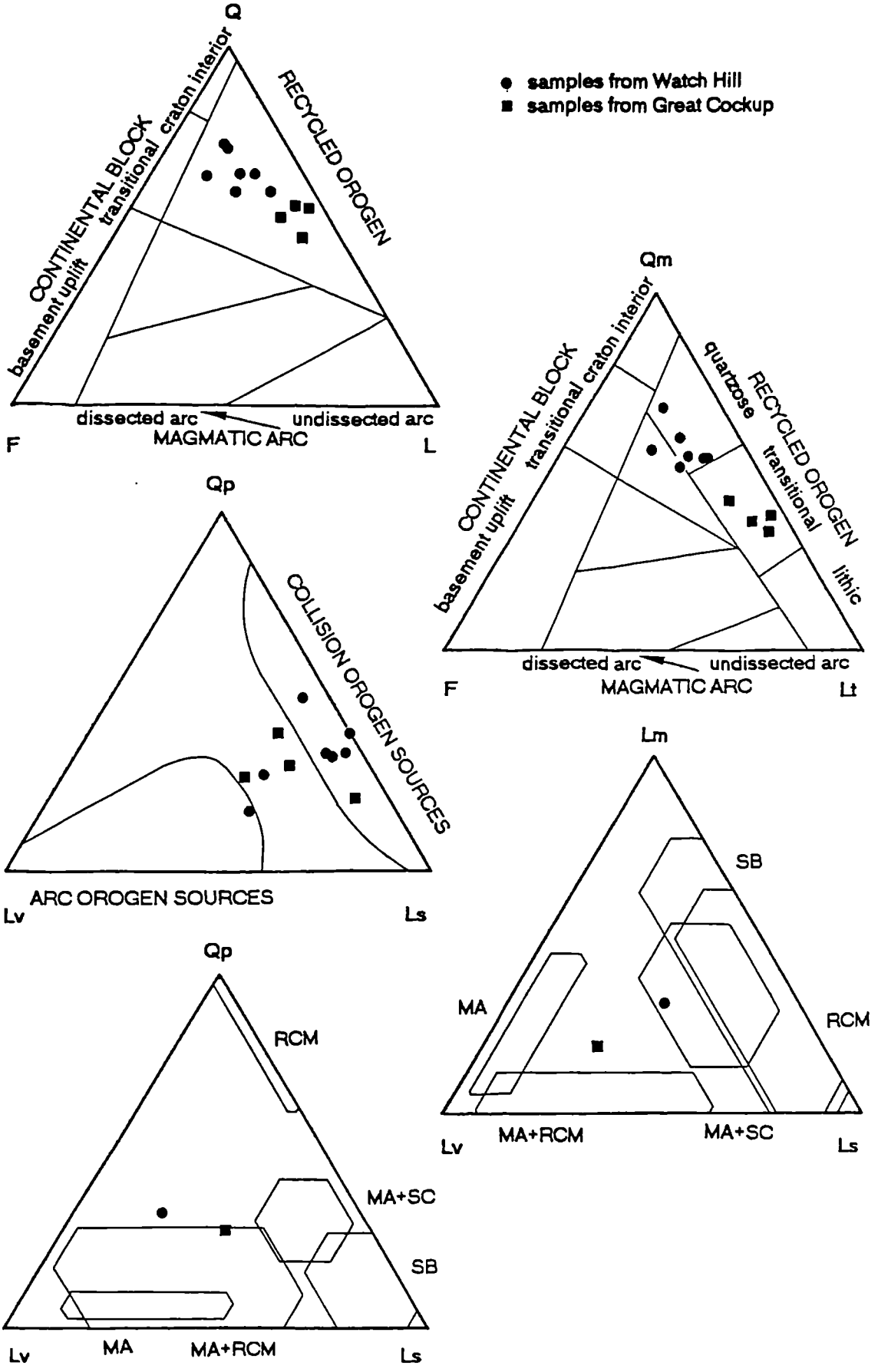

On Q-F-L and Qm-F-Lt (figure 3.6), these lithic wackes plot in a tight group in the compositional field derived from a *recycled orogen* transitional between a quartz-rich and lithic-rich provenance. Qp-Lv-Ls suggests a mixture between *collision orogen* and *arc orogen* sources, but for a count of lithic proportions only, suggests an *arc orogen* source. Comparison of the lithic proportions with data of Ingersoll and Suczek (1979), shows similarity with the *mixed magmatic arc and rifted continental margin* source composition, deposited in a back-arc basin.

The lithic wackes of the Watch Hill Formation of Watch Hill and Great Cockup are from the same hinterland of mixed volcanic, metamorphic and sedimentary lithologies, although proportions of these components differ.

3.2.4.4 Hope Beck Formation

Eight quartz-rich lithic wackes (figure 3.7) with subangular-subrounded grains of generally fine-medium sand and one of coarse sand grainsize were point-counted. Quartz pressure solution and a quartz cement are variably developed and clay commonly replaces feldspar. Monocrystalline quartz (table 3.7) is dominantly strained, of plutonic origin, but some of the largest grains are clear. Polycrystalline quartz is of metamorphic origin. Feldspars are rare and plagioclase of andesine composition is less abundant than untwinned types. Lithic grains include, in order of decreasing abundance, intraformational mudstone, siltstone, crenulated phyllite, quartz-muscovite schist, fine grained quartz-feldspar volcanic lithics and crushed chlorite clasts.

Additionally the lithic contents of two pebbly mudstones with well-rounded clasts (coarse sand to pebble grainsize) were studied. Lithic types include intraformational contorted mudstone, siltstone and very fine sandstone rich in heavy minerals, metamorphic polycrystalline quartz and plutonic monocrystalline and polycrystalline quartz. Rare volcanic lithics include feldsparphyric basalt, rhyolite and volcaniclastic grains.

Figure 3.7 Classification diagram for the Hope Beck Formation (after Dott, 1964, Pettijohn et al, 1972), n=8.

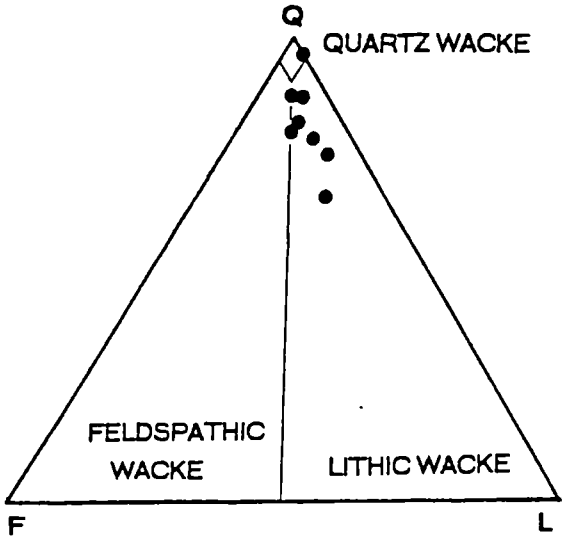

On Q-F-L and Qm-F-Lt the samples plot in an elongate area spanning the *quartzose recycled orogen* and *craton interior* provenance fields. The spread is due to degradation of lithic grains in more altered, generally finer samples. A *collision orogen* source is indicated on Qp-Lv-Ls. This is confirmed when considering lithic proportions in the pebble grainsize which compare with sandstones from a *mixed magmatic arc and subduction complex* provenance (Ingersoll and Suczek, 1979) (figure 3.8).

Table 3.7 Means and ranges of petrographical parameters for the Hope Beck Formation, n=8.

	mean	minimum	maximum
strained monocrystalline quartz	44.71	29.00	56.00
unstrained monocrystalline quartz	2.23	0.00	8.00
polycrystalline quartz	3.77	0.00	7.50
plagioclase feldspar	0.52	0.00	2.00
untwinned feldspar	3.42	0.00	7.00
volcanic lithic fragments	0.52	0.00	2.50
metavolcanic lithic fragments	0.50	0.00	1.50
sedimentary lithic fragments	3.06	0.00	8.00
metasedimentary lithic fragments	1.25	0.00	4.00
detrital mica	0.77	0.00	3.00
pyrite	0.81	0.00	2.00
carbonate cement	0.44	0.00	3.00
clay matrix	37.25	19.00	52.00
chlorite	0.58	0.00	2.00
heavy minerals	0.17	0.00	5.00
matrix	40.02	20.00	52.00
mineralogical maturity index	81.54	65.79	96.30

Figure 3.8 Provenance discrimination diagrams for the Hope Beck Formation; Q-F-L, Qm-F-Lt., Qp-Lv-Ls for greywackes with fields after Dickinson et al (1983), n=8; Lm-Lv-Ls, Qp-Lv-Ls for lithic range of pebbly mudstones with fields after Ingersoll and Suczek (1979), n=2, RCM=rifted continental margin, MA=magmatic arc, SB=suture belt, MA+SC=mixed magmatic arc and subduction complex, MA+RCM=mixed magmatic arc and rifted continental margin.

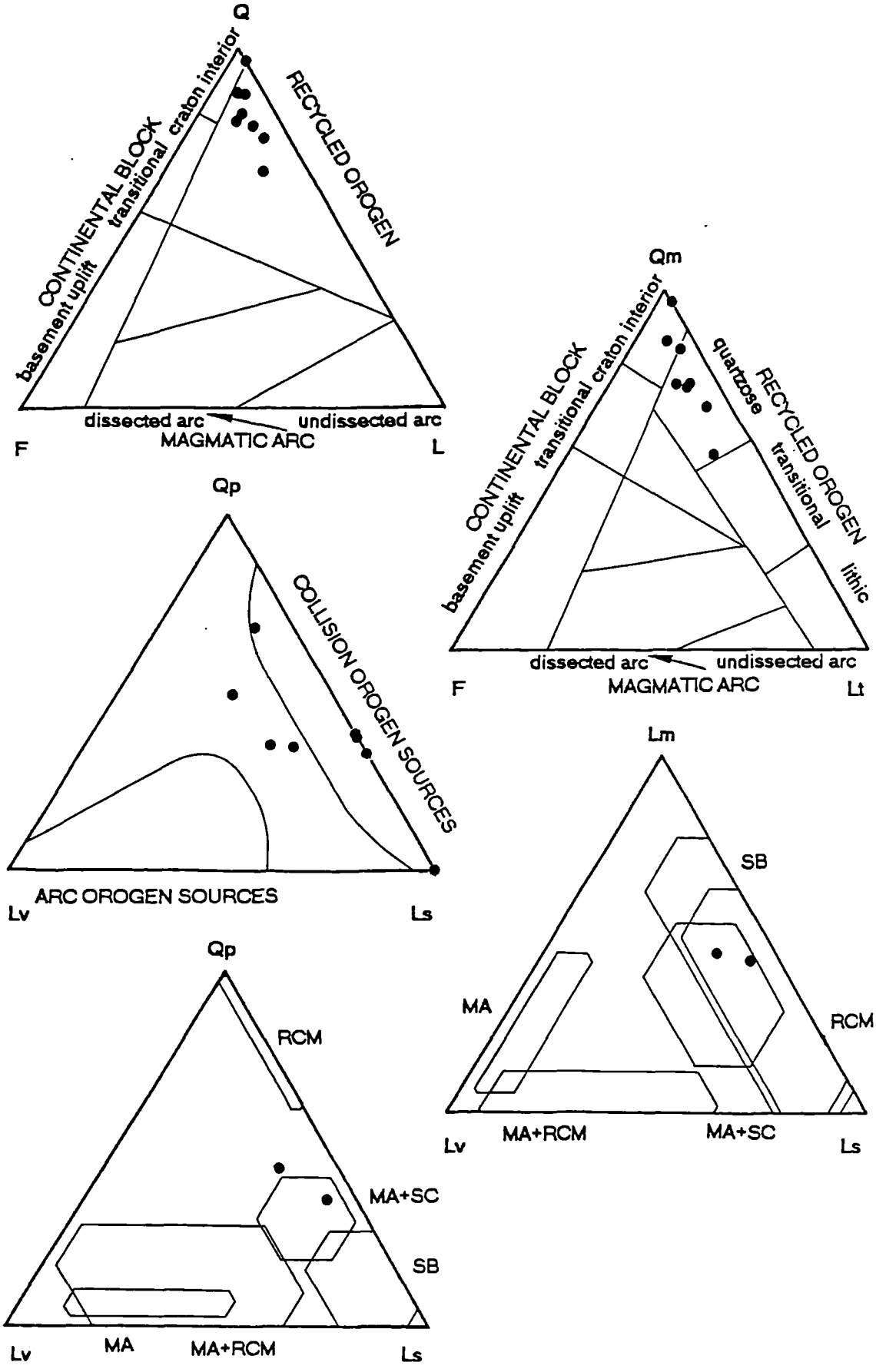

3.2.4.5 Loweswater Formation

Greywackes are dominantly rich in quartz, with feldspar more abundant than lithic fragments, indicating classification as feldspathic wackes (figure 3.9).

Quartz is dominantly monocrystalline (table 3.8) with undulatory extinction, and polycrystalline quartz is strained and of metamorphic origin. Monocrystalline quartz containing books of chlorite is interpreted to be derived from vein quartz (plate 3.6). Larger quartz grains in poorly sorted samples often have non-undulatory extinction. Chert and felsite (microcrystalline quartz with clay replacing feldspar crystallites) are present. Pressure solution, overgrowths and corrosion of quartz margins by clay development are common (plate 3.1.1). Plagioclase feldspars of dominantly andesine composition with rare zoned crystals, untwinned feldspar, microcline and perthite are present but generally show alteration or replacement. Lithic grains are dominantly of sedimentary origin (rounded sandstone, siltstone and mudstone and mudstone intraclasts), but also present are volcaniclastic fragments of angular feldspar grains, siliceous pyroclastic clasts with relict shards, porphyry with quartz and feldspar phenocrysts in felsitic groundmass, fine grained basic volcanic lithics, quartz-feldspar clasts with graphic texture, hornfels, metapelites, quartz-mica schist, strained polycrystalline quartz and mylonite. Detrital muscovite is commonly replaced by chlorite and detrital biotite is rare.

Figure 3.9 Classification diagram for the Loweswater Formation (after Dott, 1964; Pettijohn et al, 1972), n=35.

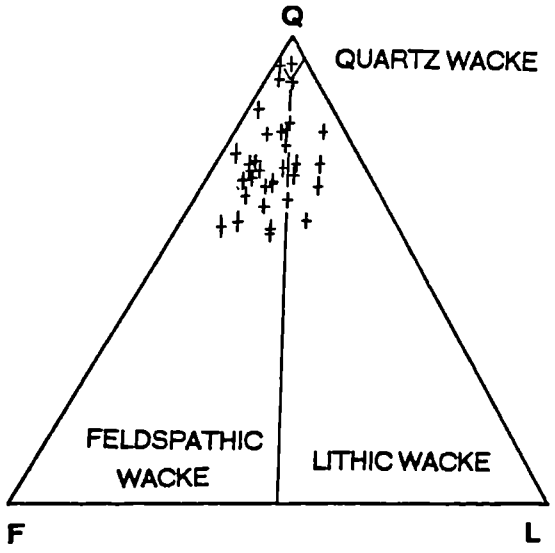

Table 3.8 Means and ranges for petrographical parameters of the Loweswater Formation, excluding high-matrix greywackes and greywackes from Jonah's Gill. (n=26).

	mean	minimum	maximum
strained monocrystalline quartz	36.95	23.50	56.00
unstrained monocrystalline quartz	2.97	0.00	9.50
polycrystalline quartz	5.61	2.00	10.50
plagioclase feldspar	3.03	0.00	6.50
untwinned feldspar	7.33	0.00	14.50
volcanic lithic fragments	0.61	0.00	2.50
metavolcanic lithic fragments	0.72	0.00	4.50
sedimentary lithic fragments	2.29	0.00	5.00
metasedimentary lithic fragments	1.44	0.00	3.67
detrital mica	1.47	0.00	7.00
pyrite	0.79	0.00	4.00
carbonate cement	2.88	0.00	32.50
clay matrix	32.43	11.50	53.67
chlorite	1.06	0.00	8.00
heavy minerals	0.39	0.00	1.50
matrix	39.00	22.00	55.00
mineralogical maturity index	72.30	59.63	93.85

In high-matrix greywackes detrital grains are generally unaltered and are of similar type and abundance to other Loweswater Formation greywackes. Feldspars are more angular and more common relative to quartz, reflected in a lower mineral maturity index than for other samples (table 3.9).

Greywackes from Jonah's Gill [NY 191 342] are more mature (average mineral maturity index = 90, table 3.9) than elsewhere, with less feldspar and a more restricted lithic range. Channel-fill greywackes from the Darling Fell Unit [NY 1265 2218] are no different in composition from other Loweswater Formation samples.

Provenance interpreted from discrimination diagrams (figure 3.10) is a *quartzose recycled orogen* for most samples, although data spread into the *continental block* field. High-matrix greywackes group in the *mixed* provenance field, suggesting a greater contribution from a dissected volcanic arc source. Samples from Jonah's Gill group tightly in the *craton interior* continental block field. The Qp-Lv-Ls plot shows a dominance of *collision orogen sources* over *arc orogen sources* with some mixing. Consideration of lithic types alone, suggests a *collision orogen source* with closest similarity with the *mixed magmatic arc and subduction complex* composition (Ingersoll and Suczek, 1979).

Table 3.9 Means and ranges of petrographical parameters for the Loweswater Formation, (a) high-matrix greywackes, (b) greywackes from Jonah's Gill.

(a) high-matrix greywackes (n=5)

	mean	minimum	maximum
strained monocrystalline quartz	21.47	18.00	29.33
unstrained monocrystalline quartz	4.53	1.67	7.33
polycrystalline quartz	5.53	3.33	7.00
plagioclase feldspar	2.20	1.00	3.00
untwinned feldspar	7.47	3.33	10.67
volcanic lithic fragments	0.87	0.33	2.33
metavolcanic lithic fragments	1.40	0.67	3.00
sedimentary lithic fragments	2.33	1.00	4.67
metasedimentary lithic fragments	1.47	1.00	2.67
detrital mica	2.13	1.33	3.00
pyrite	0.93	0.00	2.00
carbonate cement	0.80	0.00	4.00
clay matrix	46.20	42.00	50.33
chlorite	1.80	0.33	3.00
heavy minerals	0.87	0.00	1.67
matrix	52.73	50.33	56.67
mineralogical maturity index	63.40	57.42	72.66

(b) greywackes from Jonah's Gill (n=4)

	mean	minimum	maximum
strained monocrystalline quartz	45.33	40.67	48.33
unstrained monocrystalline quartz	4.00	1.67	5.00
polycrystalline quartz	3.67	1.33	8.33
plagioclase feldspar	0.75	0.33	1.33
untwinned feldspar	3.83	2.00	7.33
volcanic lithic fragments	0.00	0.00	0.00
metavolcanic lithic fragments	0.00	0.00	0.00
sedimentary lithic fragments	0.67	0.00	1.00
metasedimentary lithic fragments	0.67	0.00	1.33
detrital mica	0.58	0.33	1.33
pyrite	0.50	0.00	1.67
carbonate cement	14.42	4.33	23.33
clay matrix	24.75	10.33	38.33
chlorite	0.42	0.00	0.67
heavy minerals	0.42	0.00	1.00
matrix	41.08	32.33	49.33
mineralogical maturity index	89.67	84.46	93.37

Figure 3.10 Provenance discrimination diagrams for the Loweswater Formation; Q-F-L, Qm-F-Lt, Qp-Lv-Ls for greywackes with fields after Dickinson et al (1983), n=35; Lm-Lv-Ls, Qp-Lv-Ls for lithic range of very coarse sand grainsize greywacke with fields after Ingersoll and Suczek (1979), n=1, RCM=rifted continental margin, MA=magmatic arc, SB=suture belt, MA+SC=mixed magmatic arc and subduction complex, MA+RCM=mixed magmatic arc and rifted continental margin.

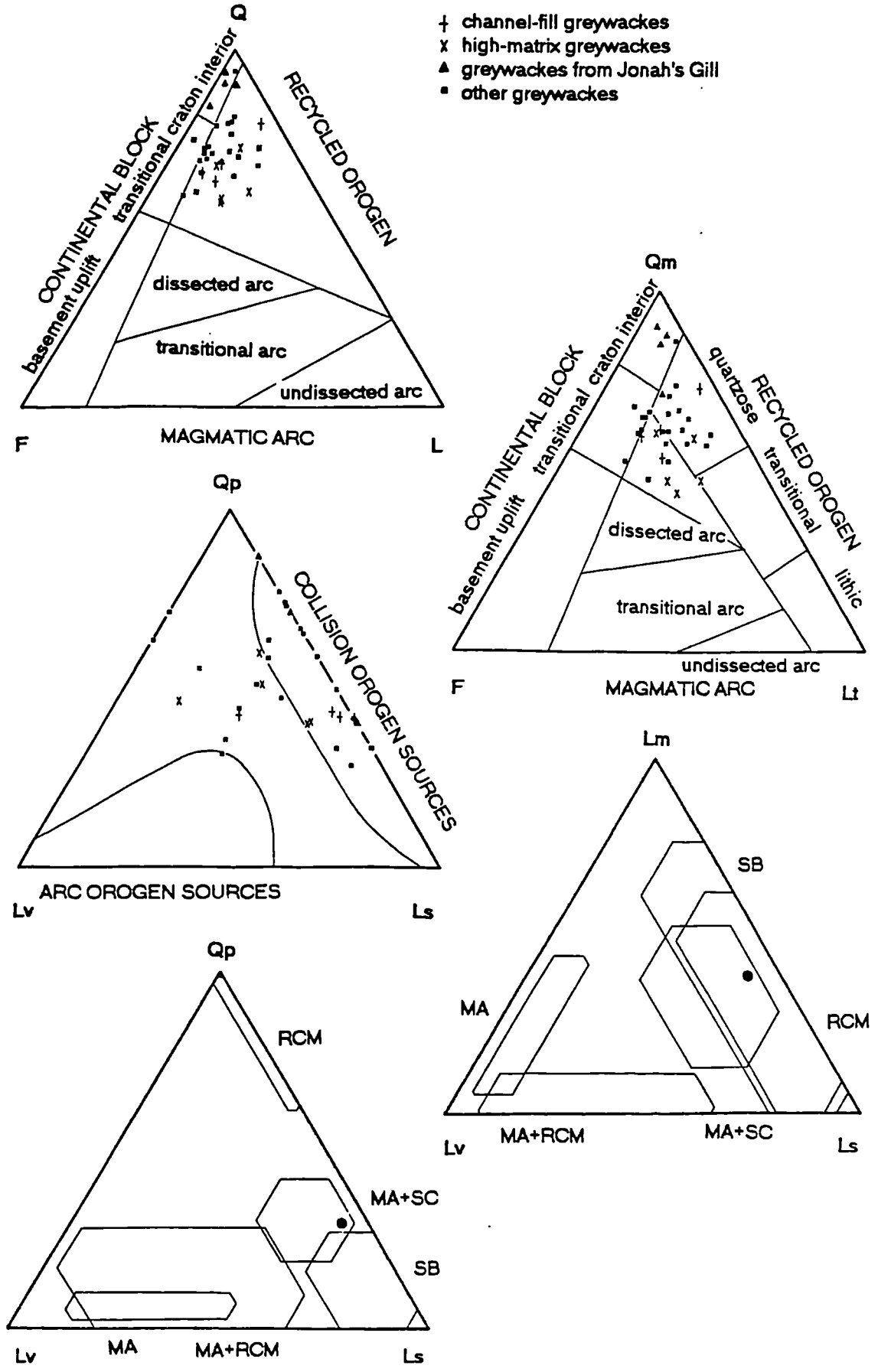

3.2.4.6 Kirk Stile Formation

Four greywackes (figure 3.11) were pointcounted of very fine sand, fine sand and coarse sand grainsize from the thin greywackes above the Loweswater Formation in Hope Gill [NY 1827 2243] and the sandstone body near the base of the formation on Broom Fell [NY 1940 2723]. Strata are commonly deformed and altered thus the samples are not ideal for provenance determination.

The mean composition is presented (table 3.10). Monocrystalline quartz generally shows undulose extinction, although rounded coarser grains in poorly sorted samples are sometimes clear. Polycrystalline quartz, both metamorphic and chert types, is present. Feldspar is rare in the samples from Hope Gill but more abundant in those from Broom Fell, with more untwinned types than twinned plagioclase. Lithic types include phyllite and conspicuous near isotropic mud clasts with angular, siltsize quartz and feldspar grains, thought to represent a volcanic siltstone (plate 3.8.2). Their rounded texture suggests erosion of a volcanogenic sediment, not direct volcanic input. Chlorite is abundant and replaces detrital muscovite, clay and mafic lithic clasts.

Figure 3.11 Classification diagram for the Kirk Stile Formation (after Dott, 1964; Pettijohn et al, 1972), n=4.

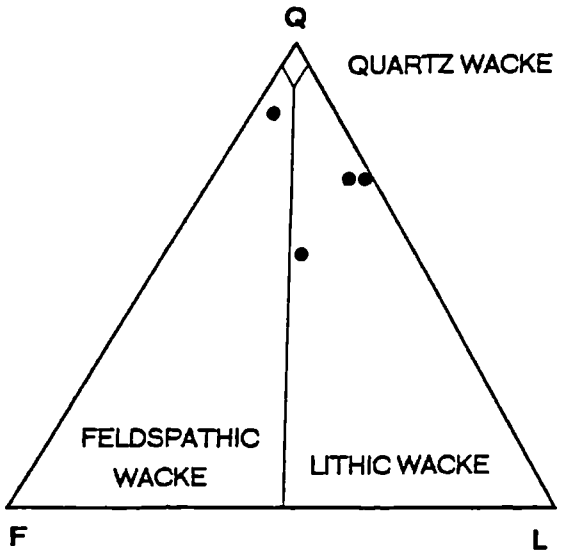

Table 3.10 Means and ranges for petrographical parameters of the Kirk Stile Formation (n=4).

	mean	minimum	maximum
strained monocrystalline quartz	30.12	20.00	42.00
unstrained monocrystalline quartz	1.12	0.00	4.00
polycrystalline quartz	3.00	1.00	6.00
plagioclase feldspar	1.50	0.00	4.00
untwinned feldspar	3.00	0.50	6.00
volcanic lithic fragments	0.37	0.00	1.50
metavolcanic lithic fragments	0.75	0.00	2.00
sedimentary lithic fragments	3.12	0.00	8.50
metasedimentary lithic fragments	2.25	0.00	7.00
detrital mica	1.46	0.00	3.50
pyrite	0.75	0.00	2.50
carbonate cement	11.87	0.00	47.00
clay matrix	35.67	13.50	48.67
chlorite	3.87	0.00	13.00
heavy minerals	1.12	0.00	2.50
matrix	54.75	51.00	61.00
mineralogical maturity index	70.26	54.64	84.96

Ternary provenance discrimination diagrams (figure 3.12) show a spread of samples across *transitional* to *quartzose recycled orogen* sources, *mixed* provenance and *craton interior* fields. The lithic content suggests a volcanic source accompanied a metamorphic basement source. Lithic populations in the coarse sand grainsize range, shown on Qp-Lv-Ls and Lm-Lv-Ls suggest derivation from a *collision orogen* source and comparison with sediment from a *suture belt* (Ingersoll and Suczek, 1979).

Debris flow deposits, in excess of 40m thick, occur within the Kirk Stile Formation at Beckgrains Bridge [NY 1904 3552]. The petrography of two rounded sandstone clasts was studied. A quartz-rich feldspathic wacke of very fine sand grainsize showed strong alteration and development of opaques and carbonate, hence matrix content and maturity index are high (table 3.11). The sample will plot nearer the Q pole on a Q-F-L ternary diagram (figure 3.13) than if it was unaltered. Its composition is comparable to Loweswater Formation samples, especially those from Jonah's Gill.

The second clast was a quartz-intermediate feldspathic wacke of fine sand grainsize, containing abundant opaques and carbonate. Feldspar is common, reflected in a low maturity index (table 3.11). Thus clasts within the debris flow differ in composition but are compatible with the range of compositions within the Loweswater Formation.

Figure 3.12 Provenance discrimination diagrams for the Kirk Stile Formation; Q-F-L, Qm-F-Lt., Qp-Lv-Ls for greywackes with fields after Dickinson et al (1983), n=4; Lm-Lv-Ls, Qp-Lv-Ls for lithic range of a coarse sand grainsize greywacke with fields after Ingersoll and Suczek (1979), n=1, RCM=rifted continental margin, MA=magmatic arc, SB=suture belt, MA+SC=mixed magmatic arc and subduction complex, MA+RCM=mixed magmatic arc and rifted continental margin.

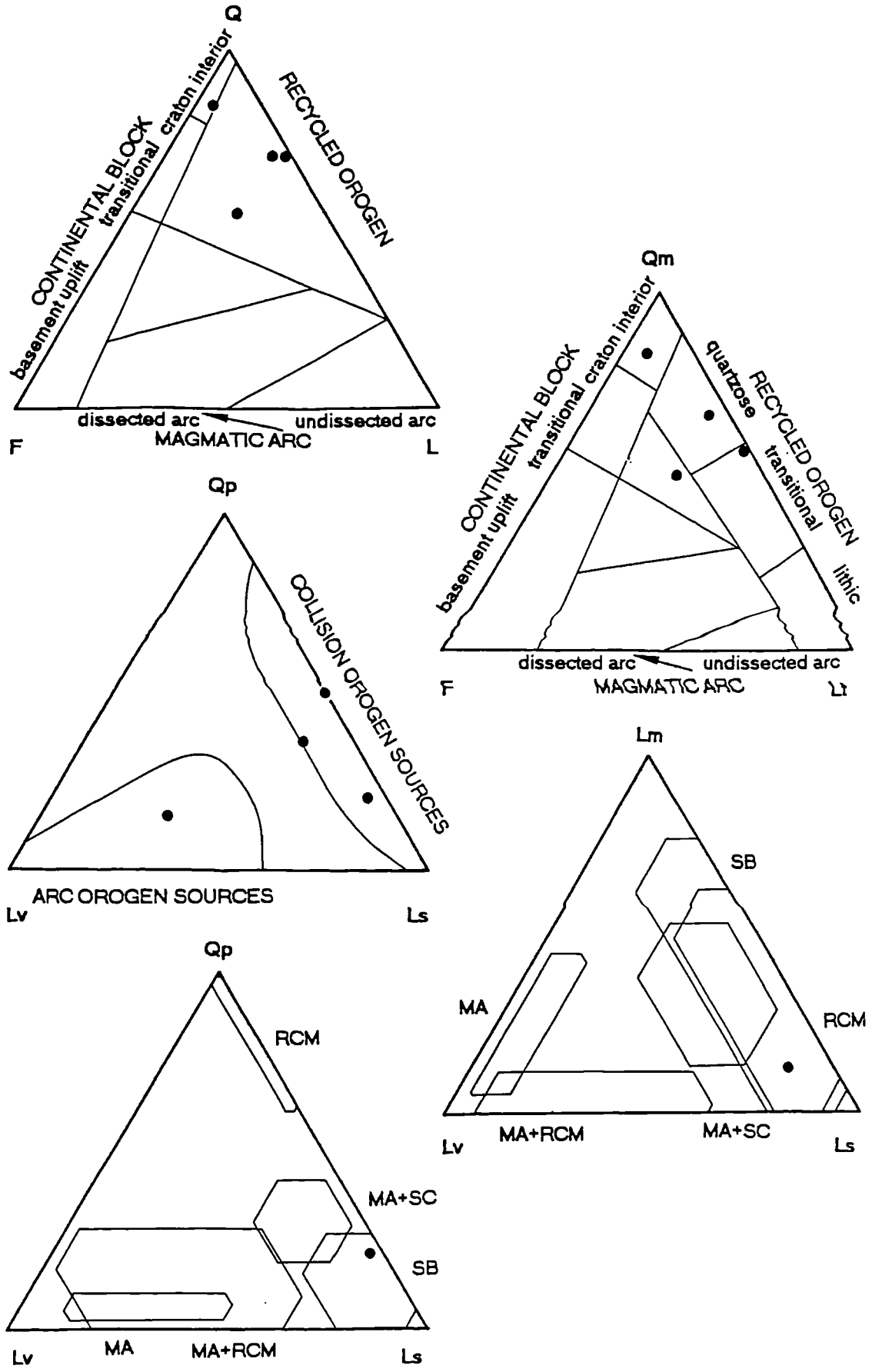

Table 3.11 Compositions of clasts from the Beckgrains Bridge debris flow and sandstone rafts of the Buttermere Formation olistostrome.

unit	Kirk Stile Fm		Buttermere Fm (Robinson Member)					
location	Beckgrains Bridge		Causey Pike			Robinson	Goat Gills	
sample	M907	M908	M901	M902	M903	M906	M904	M905
strained monocrystalline quartz	32.0	20.5	24.0	47.5	52.5	57.5	37.0	49.5
unstrained monocrystalline quartz	0.0	4.0	9.5	2.0	1.5	1.0	1.0	0.5
polycrystalline quartz	0.0	4.0	1.0	1.0	2.5	1.5	1.0	1.0
plagioclase feldspar	0.0	2.5	0.5	0.0	3.5	0.0	0.5	1.5
untwinned feldspar	3.0	11.5	8.0	2.5	5.5	2.0	1.5	3.0
volcanic lithic fragments	0.0	0.5	0.0	1.0	0.0	0.0	1.0	1.0
metavolcanic lithic fragments	0.0	0.5	0.5	0.5	2.0	1.5	0.5	0.5
sedimentary lithic fragments	1.5	5.0	2.5	3.5	4.0	1.0	0.0	0.0
metasedimentary lithic fragments	1.0	0.0	0.0	0.0	0.5	0.0	0.5	1.0
detrital mica	0.5	0.5	0.0	0.0	0.0	0.5	0.0	0.0
pyrite	4.0	11.0	0.0	0.0	1.5	0.0	3.0	0.0
carbonate cement	2.0	12.5	0.0	0.0	0.0	0.0	2.0	2.0
clay matrix	55.0	27.5	53.5	38.5	26.0	33.0	50.5	37.5
chlorite	0.0	0.0	0.0	2.5	0.0	0.0	1.0	0.5
heavy minerals	1.0	0.0	0.5	1.0	0.5	2.0	0.5	2.0
matrix	62.5	51.5	54.0	42.0	28.0	35.5	57.0	42.0
mineralogical maturity index	85.3	55.3	75.0	77.7	77.9	90.9	89.6	85.0

3.2.4.7 Buttermere Formation

Samples were analysed from the sandstone rafts within the olistostrome and represent the Robinson Member at Goat Gills [NY 1910 1625], Robinson [NY 2010 1710] and Causey Pike [NY 2190 2075].

At Goat Gills two quartz-rich lithic wackes were sampled with high maturity indices (table 3.11). Feldspar abundance is low, with untwinned types dominant over plagioclase, and the lithic range includes granite, hornfels, metapelite and chlorite clasts. The composition is comparable with the Hope Beck Formation or the Loweswater Formation of Jonah's Gill.

From Robinson, a quartz-rich lithic wacke with heavy mineral-rich (zircons and opaques), horizontal laminae was analysed. It compares with the *craton interior* provenance field and with other samples from Jonah's Gill or the Hope Beck Formation (figure 3.13).

Three quartz-rich greywackes from Causey Pike display untwinned feldspar dominant over plagioclase and sedimentary lithics dominant over volcanic types. Sample M901 is relatively high in feldspar. The compositions compare with the Loweswater Formation and the Hope Beck Formation.

Figure 3.13 Q-F-L and Qm-F-Lt ternary diagrams for clasts from the Beckgrains Bridge debris flow and sandstone rafts of the Buttermere Formation olistostrome (n=8). Provenance fields after Dickinson et al (1983).

● clasts from the Beckgrains Bridge debris flow
■ Robinson Member

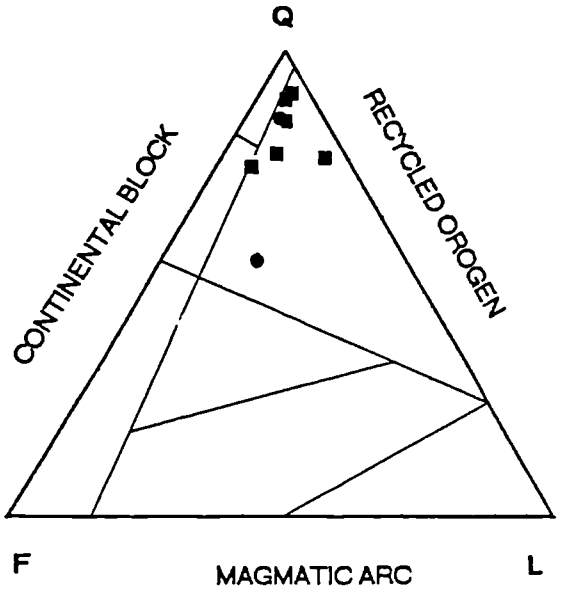

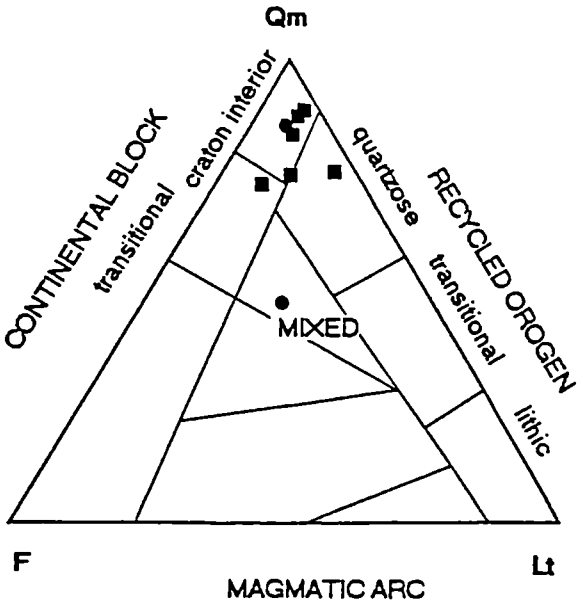

PLATES

Examples from the range of clast types of Skiddaw Group greywackes are illustrated, in the following order: rock texture, feldspars, intraformational lithics, sedimentary lithics, volcanic lithics, metamorphic lithics, heavy minerals.

PLATE 3.1

3.1.1 Quartz grains with subordinate feldspar and lithic fragments in moderately sorted medium sand grainsize greywacke. Quartz grains display pressure solution and quartz is precipitated in strain shadows and in a vein. Thus primary textural attributes of individual grains and the host rock are obscured.
Sample CU35, Loweswater Formation, plane polarized light.
Magnification x25.

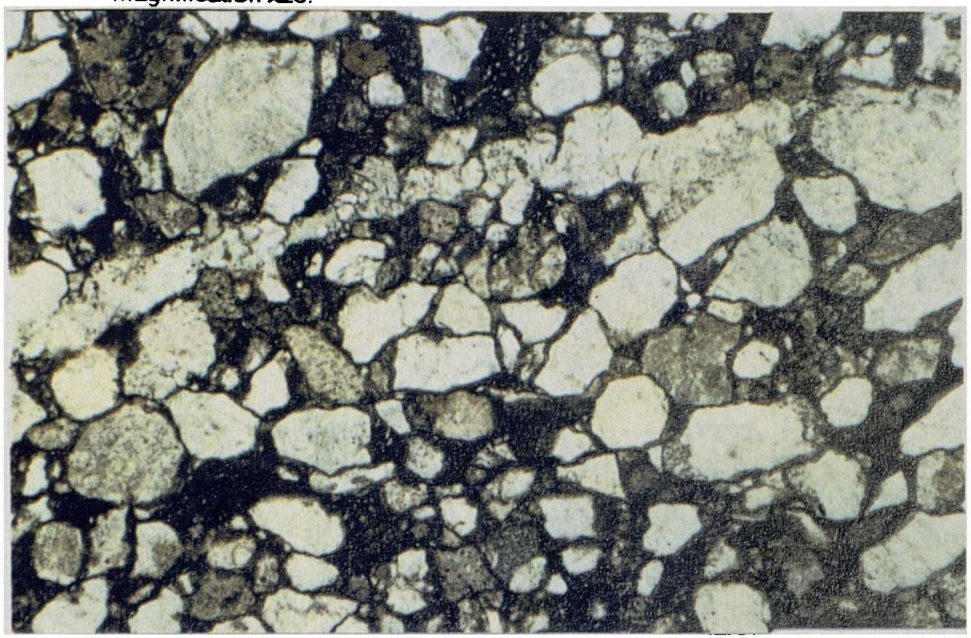

3.1.2 Quartz grains, mudstone lithic fragments and subordinate feldspar grains in a quartz-cemented medium sand.
Sample CU284/1, Watch Hill Formation, plane polarized light.
Magnification x25.

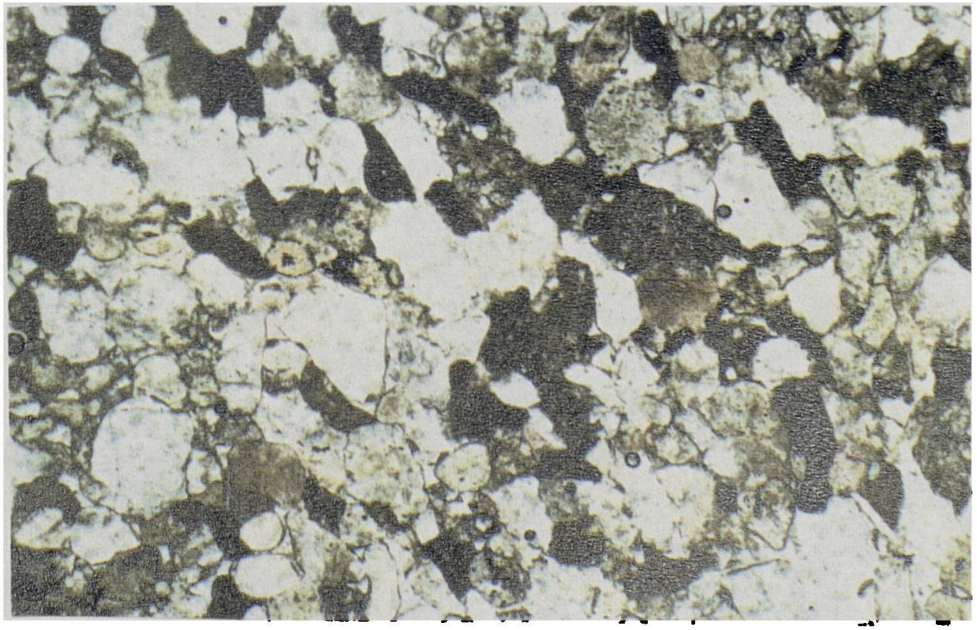

PLATE 3.2

3.2.1 Plagioclase grain with quartz and feldspar grains and contorted detrital mica flake in a matrix of dominantly secondary clay minerals derived from the breakdown of pelitic lithic fragments, one outline of which is discernible in the upper left corner.
Sample CU326, Watch Hill Formation, plane polarized light.
Magnification x40

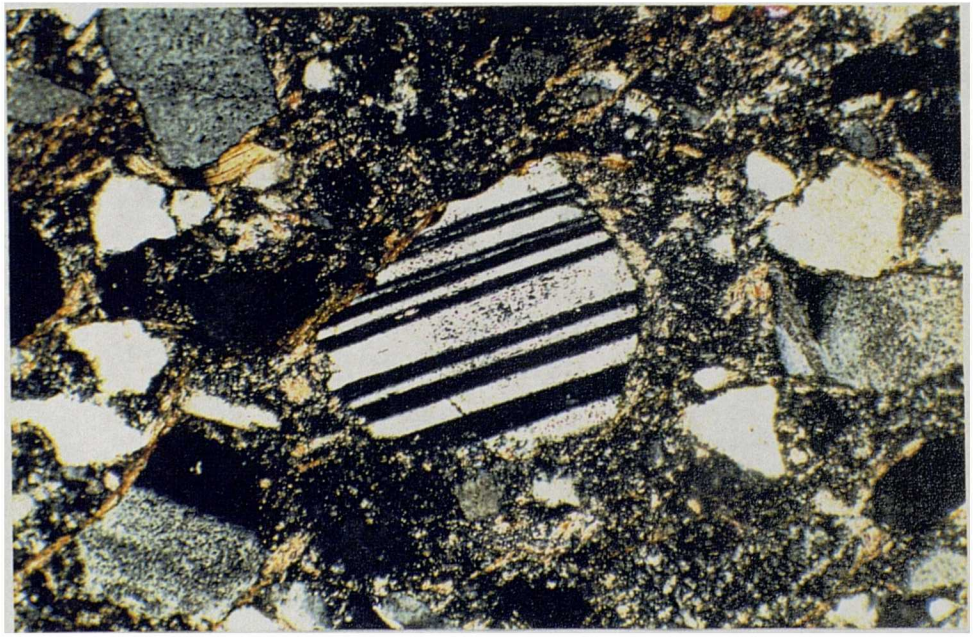

3 2.2 Contorted intraformational mudstone clast with an internal fabric compressed between larger clasts of siltstone (lower right corner), metamorphic polycrystalline quartz, sedimentary quartzite and plutonic monocrystalline quartz.
Sample CU326, Watch Hill Formation, plane polarized light.
Magnification x40.

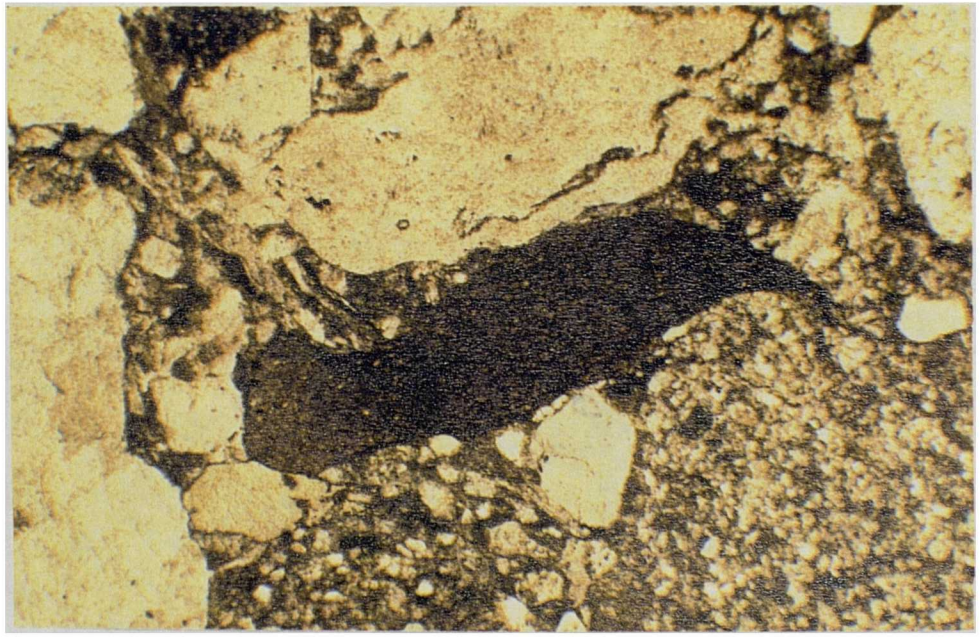

PLATE 3.3

3.3.1 Two competent granule-size clasts of siltstone in a matrix of fine sand grade quartz and feldspar grains.
Sample CU299, Watch Hill Formation, plane polarized light.
Magnification x40.

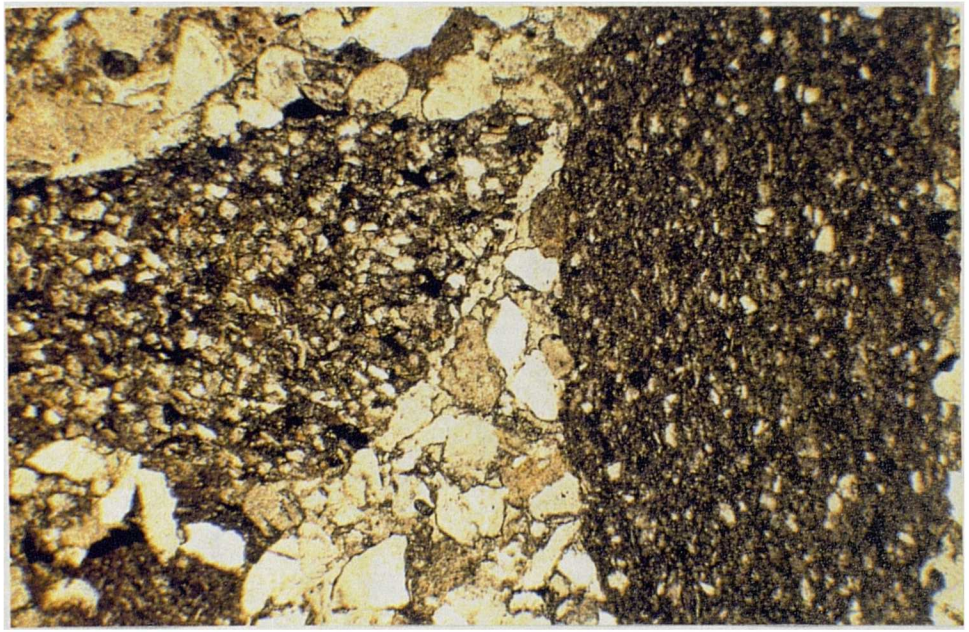

3.3.2 Chert clast with quartz, feldspar (showing alteration to clay), metapelite and contorted detrital mica in a clay matrix.
Sample CU299, Watch Hill Formation, crossed polars.
Magnification x100.

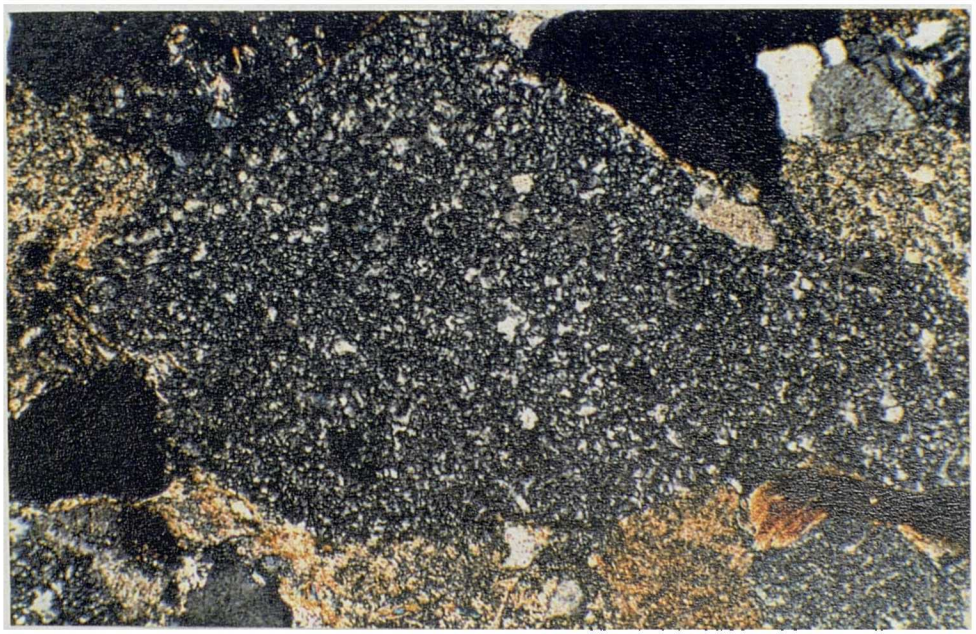

PLATE 3.4

3.4.1 Internal composition of a 4mm diameter rounded pebble of arkose, comprising subangular medium sand size grains in a matrix of microcrystalline quartz.
Sample CU328, Watch Hill Formation, plane polarized light.
Magnification x40.

3.4.2 As 3.4.1, crossed polars.

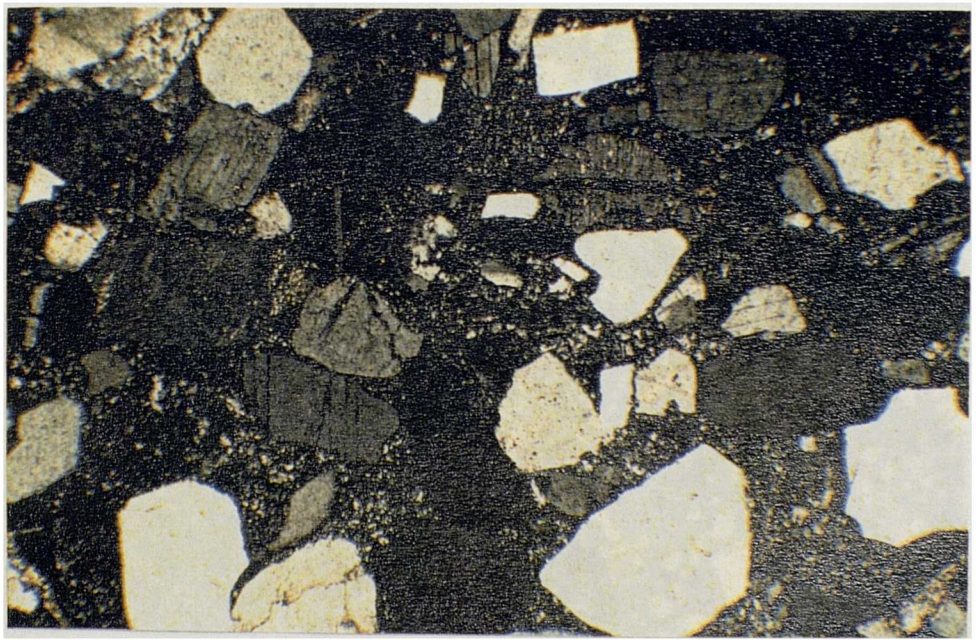

PLATE 3.5

3.5.1 Quartz-clay clast with banded texture and opaque and other euhedral inclusions, interpreted to be a pyroclastic fragment, with large chert (at base) and siltstone (right edge) clasts in a matrix of angular, fine sand grade, quartz and feldspar. Sample CU328, Watch Hill Formation, plane polarized light. Magnification x25.

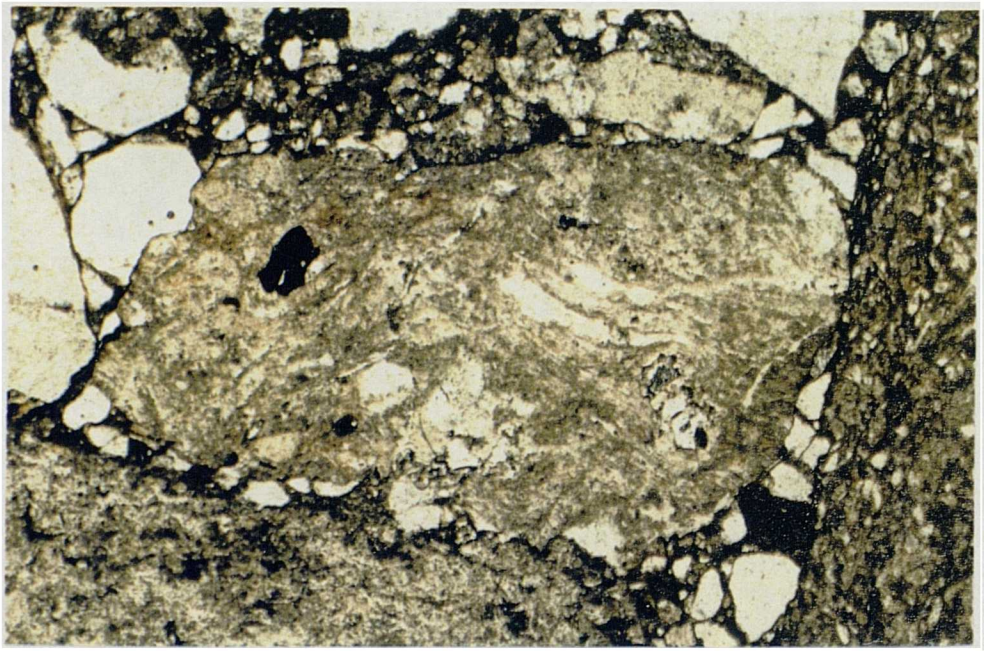

3.5.2 As 3.5.1, crossed polars.

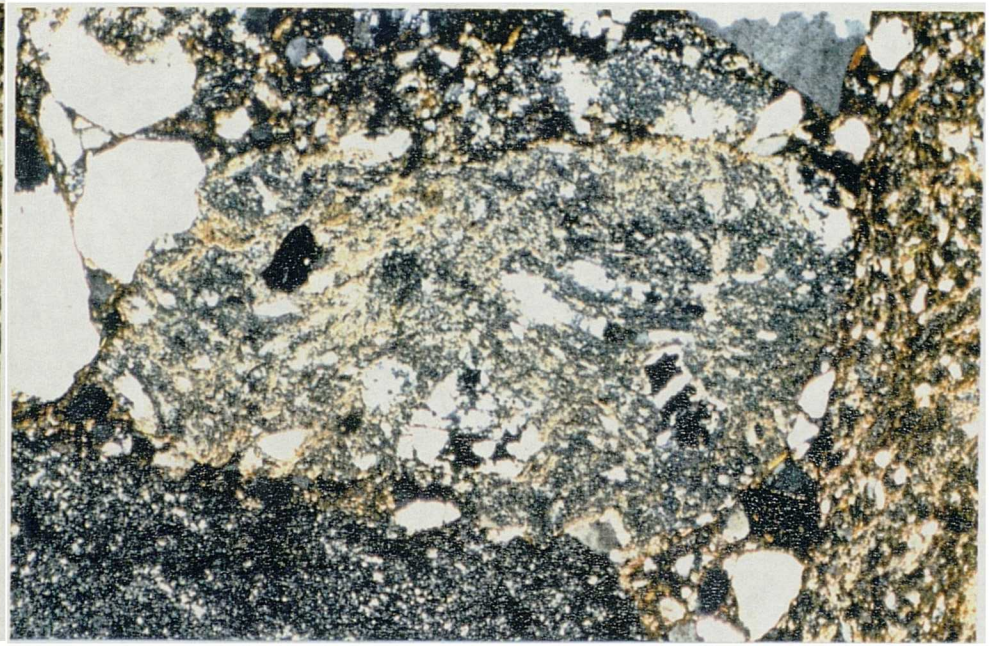

PLATE 3.6

3.6.1 Monocrystalline quartz corroded by clay growth at its margins with inclusions of euhedral crystal stacks of chlorite, interpreted to be derived from vein quartz.
CU30, Loweswater Formation, plane polarized light.
Magnification x100.

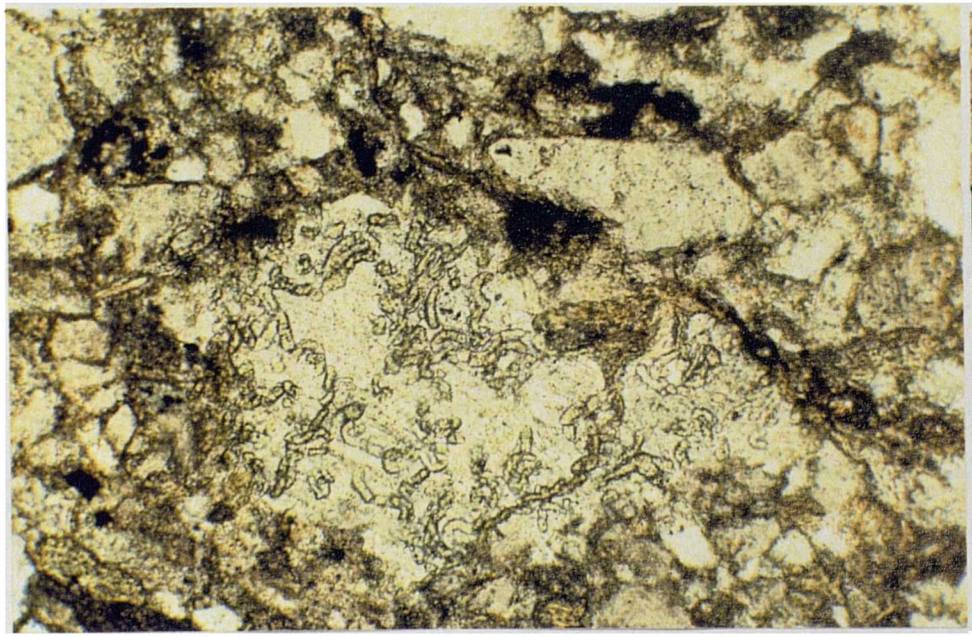

3.6.2 As 3.6.1, crossed polars.

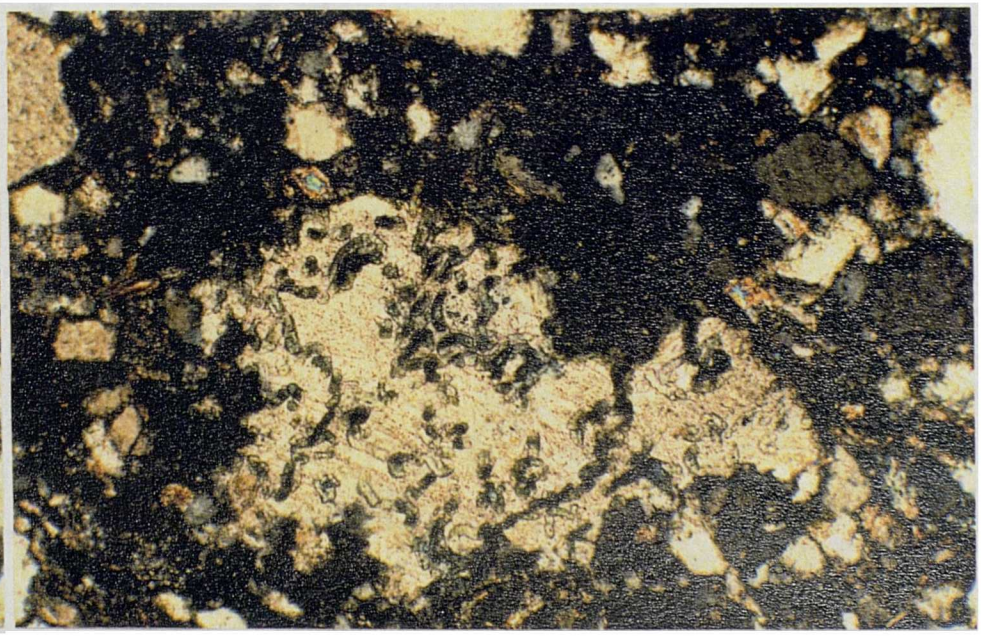

PLATE 3.7

3.7.1 Rounded, brown-coloured, isotropic clast with a few inclusions of randomly orientated phyllosilicate and quartz microcrystals, interpreted to be volcanic glass, in a matrix of very fine sand size quartz and crenulated metapelite lithic (centre base), with a patchy intergranular clay and stained carbonate cement.
Sample CU38, Loweswater Formation, plane polarized light.
Magnification x100.

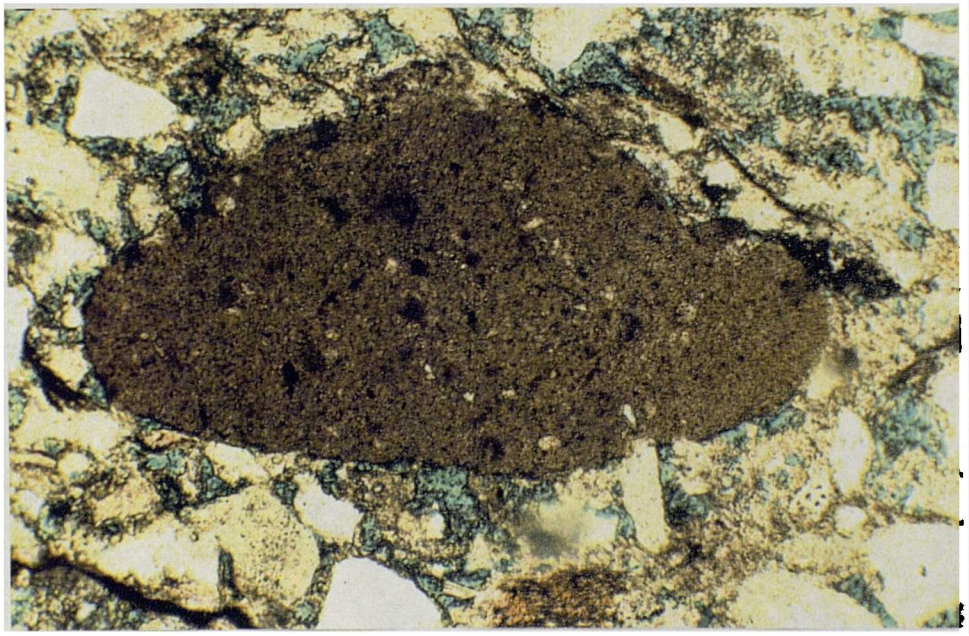

3.7.2 As 3.7.1, crossed polars.

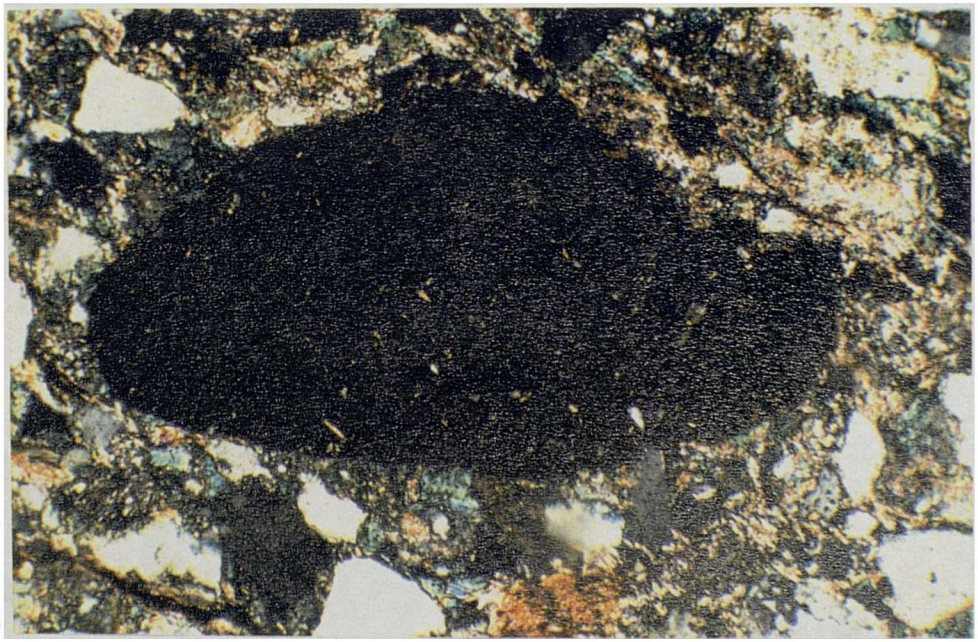

PLATE 3.8

3.8 1 Subrounded clast of quartz and feldspar with graphic texture. Other grains include quartz, chert, subhedral zircon (top, right of centre) with patchy clay matrix and quartz cement.
Sample CU284/3, Watch Hill Formation, crossed polars.
Magnification x100.

3.8.2 Clast of altered microgranite and two near-isotropic mudstone clasts with phyllosilicates, in a carbonate cement.
Sample KDC626, Kirk Stile Formation, crossed polars.
Magnification x100.

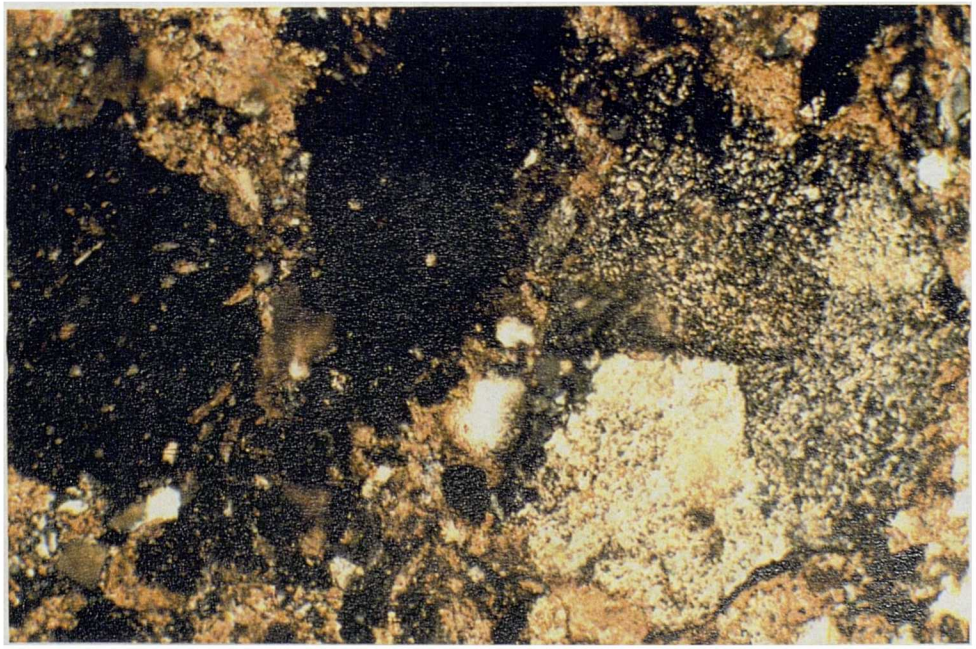

PLATE 3.9

3.9.1 Subrounded clast of basalt with randomly orientated plagioclase laths and traversed by a thin chlorite vein.
Sample CU326, Watch Hill Formation, plane polarized light.
Magnification x40.

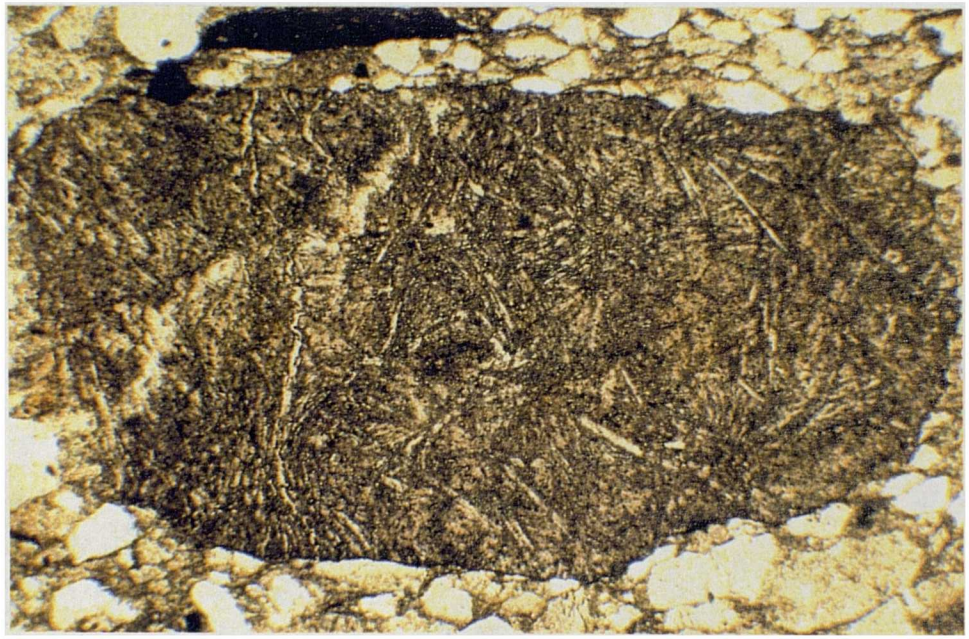

3.9.2 As 3.9.1, with crossed polars.

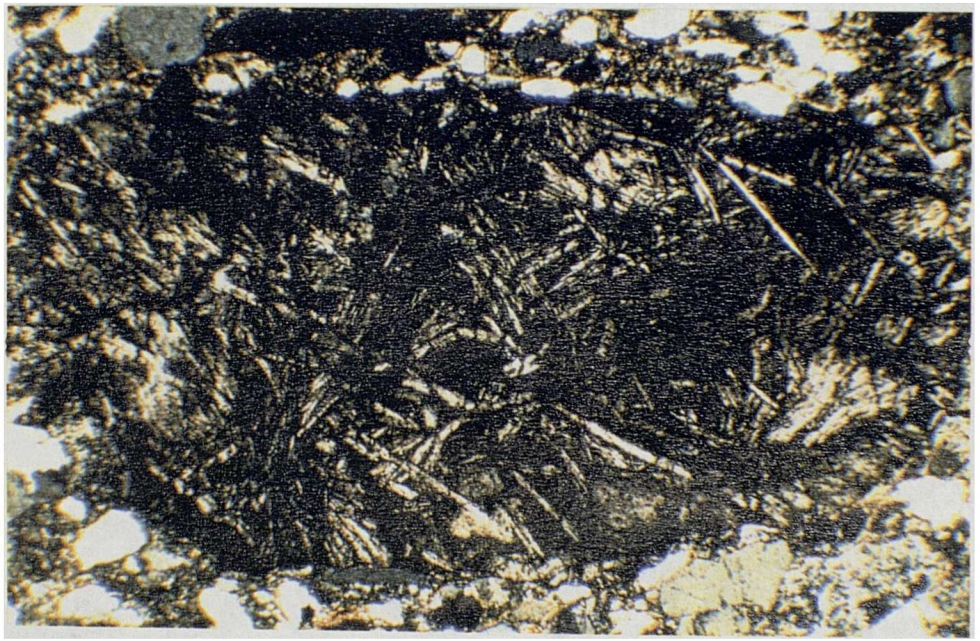

PLATE 3.10

3.10.1 Pale green chlorite clast, terminated against anastamosing cleavage surfaces and associated with subangular quartz and contorted phyllosilicate (bottom right).
Sample M58, Loweswater Formation, plane polarized light.
Magnification x250.

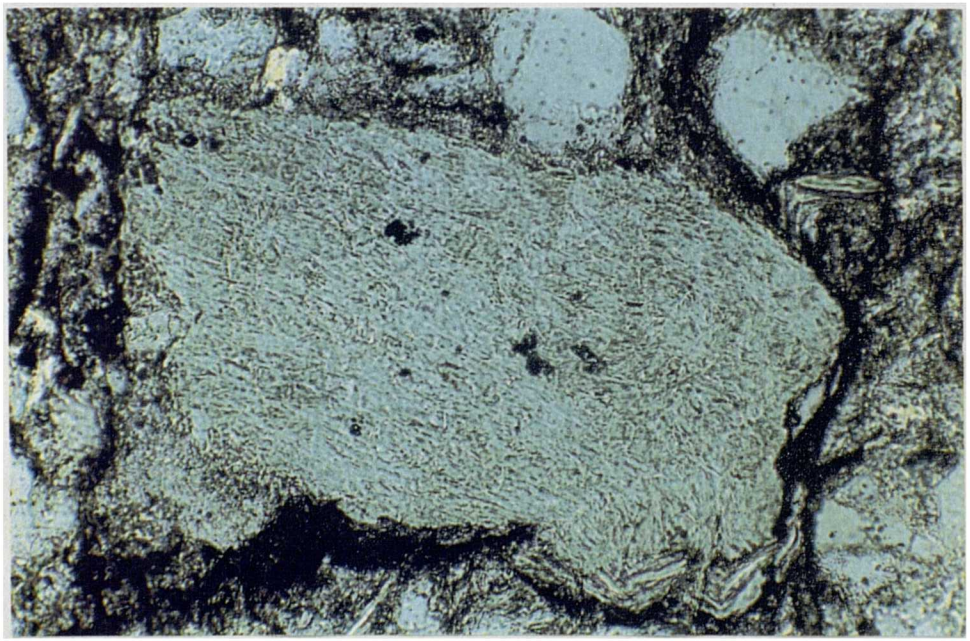

3.10.2 As 3.10.1, with crossed polars and showing blue interference colours and internal structure.

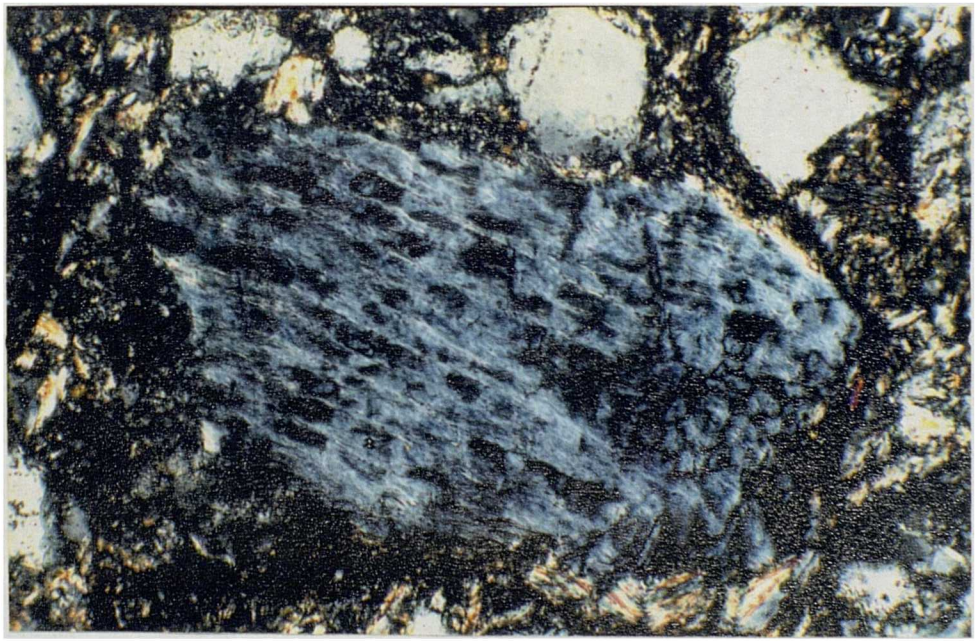

PLATE 3.11

3 11.1 Subrounded clast of metamorphic polycrystalline quartz with strong crystal orientation, undulose extinction in subcrystals and cross-cutting cleavage. Other clasts include rounded mudstone with weathered rim (top left), chert (top right) and very fine sand size quartz grains and clay matrix, almost certainly derived from pelite lithic grains
Sample CU299 Watch Hill Formation, plane polarized light. Magnification x40.

3.11.2 As 3.11 1, with crossed polars.

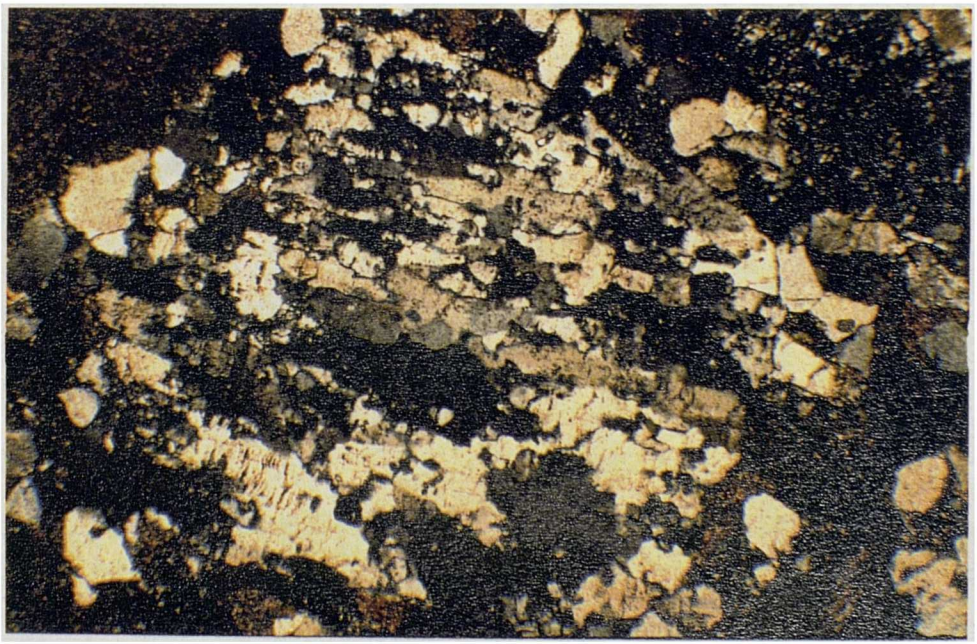

PLATE 3.12

3.12.1 Crenulated metapelite clast in a clay matrix.
Sample CU42, Loweswater Formation, crossed polars.
Magnification x250.

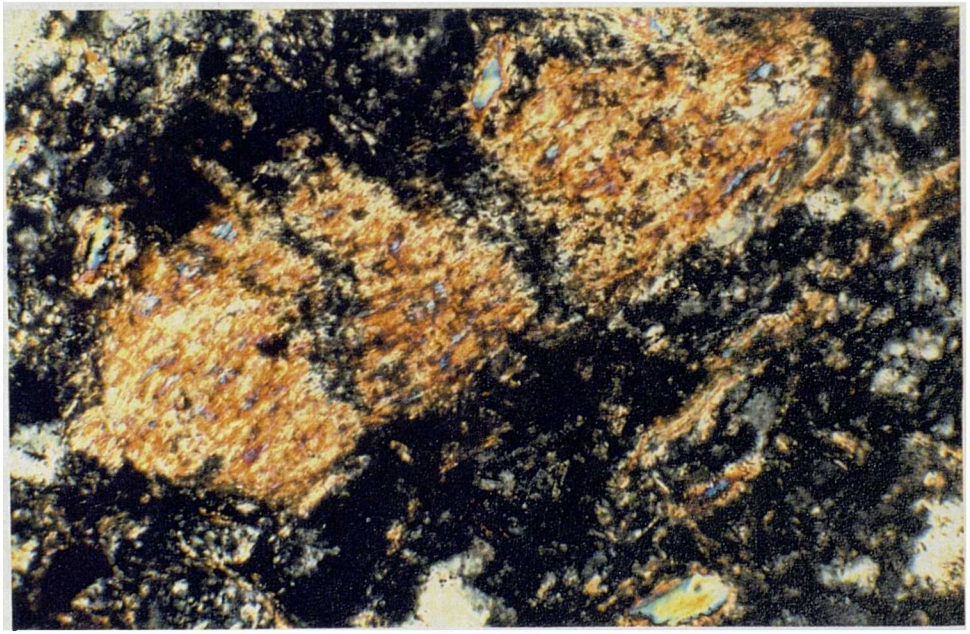

3.12.2 Clast of quartz-muscovite schist with very fine sand size grains of quartz and plagioclase and detrital muscovite in a clay matrix.
Sample M90-19, Loweswater Formation, crossed polars.
Magnification x100.

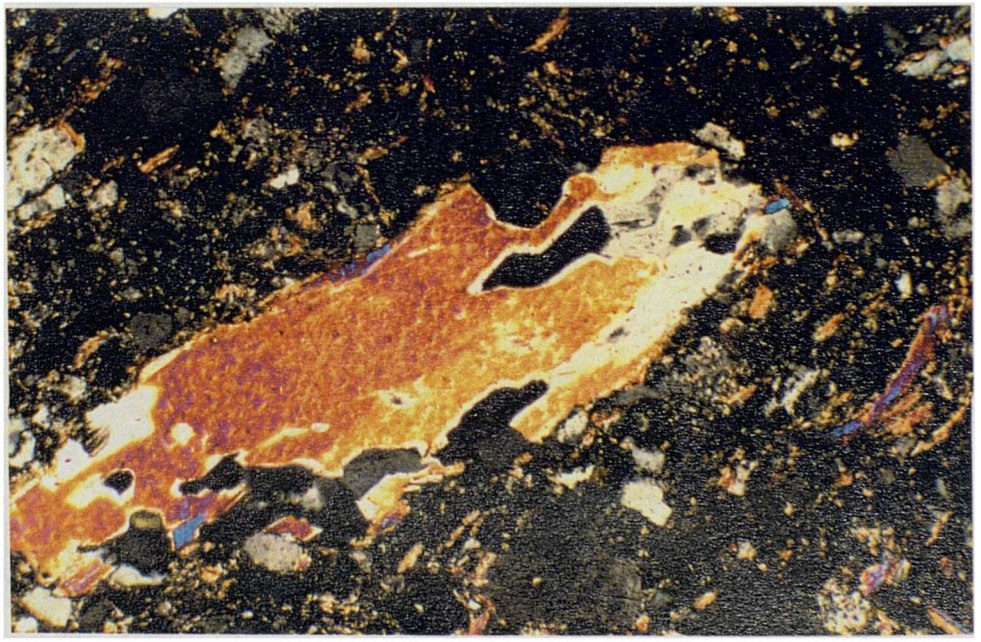

PLATE 3.13

3.13.1 Muscovite pellet partially replaced by chlorite with fine sand size quartz and plagioclase grains.
Sample M18, Loweswater Formation, plane polarized light.
Magnification x 100.

3.13.2 As 3.13.1, with crossed polars.

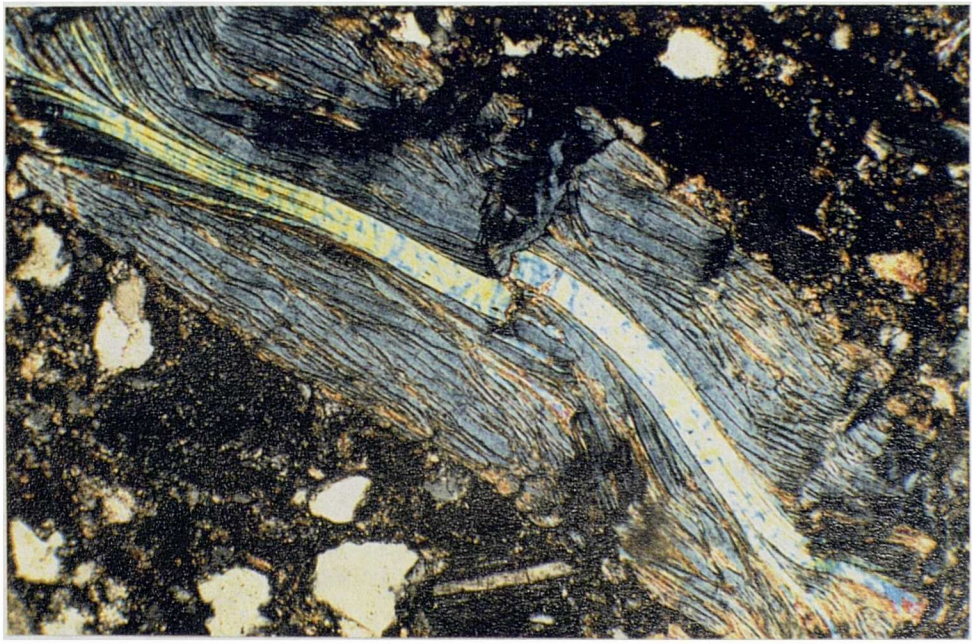

PLATE 3.14

3.14.1 Clast of quartz mylonite with a monocrystalline quartz grain in a matrix of silt grade quartz grains and phyllosilicates and secondary opaque pyrite (top centre).
Sample CU30, Loweswater Formation, crossed polars.
Magnification x100.

3.14.2 Subhedral zircon in a clast of quartzite.
Sample CU326, Watch Hill Formation, crossed polars.
Magnification x 250

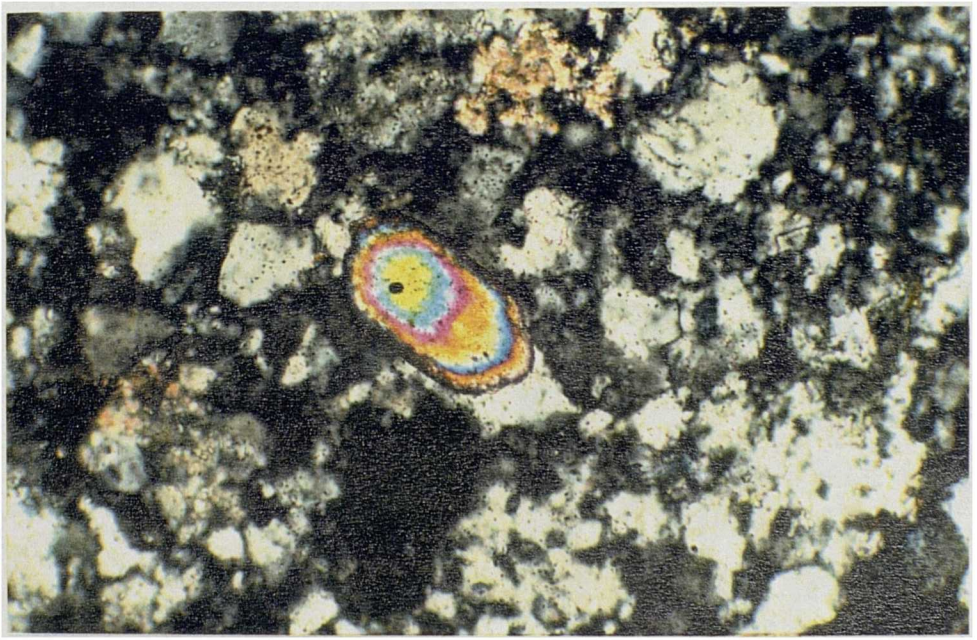

3.3 Geochemical techniques in provenance discrimination

Major element compositions of modern and ancient sediments have been used by several workers (Crook, 1974; Schwab, 1975; Maynard et al, 1982; Bhatia, 1983; Roser and Korsch, 1986) to define provenance discrimination diagrams. Their methods are reviewed and applied to the Skiddaw Group.

The geochemical composition of samples was determined by x-ray fluorescence spectrometry (XRF) giving element abundances as weight % of oxide for majors and in parts per million (ppm) for traces (see appendix 3a for analytical details). Analyses of 71 sandstones and mudstones (appendix 4b) from the Skiddaw Group were supplied by Dr D. C. Cooper, British Geological Survey, Keyworth. An additional 26 samples were analysed at the Earth Sciences Department, Leeds University (appendix 4a). They represent specific greywacke types of the Loweswater Formation, the sandstone rafts of the Buttermere Formation, a sandstone clast from the Beckgrains Bridge debris flow of the Kirk Stile Formation and sediments of the Manx Group and Ingleton Group. Where possible they are of fine or medium sand grainsize from the Tb Bouma unit of turbidites (see section 3.3.2), to reduce any compositional variation due to grainsize or depositional sorting.

XRF analysis gives very accurate results but an appreciation of what the result represents is of vital importance. As described in section 3.1.1, the sample composition might differ markedly from the source rock composition which in turn might not indicate the tectonic setting of the depositional basin. The accuracy of the analytical method, therefore, should not be used to infer a corresponding accuracy in the interpretation.

3.3.1 Geochemical classification of analyses

Figure 3.14a shows a geochemical classification of Blatt et al (1972) applied to Skiddaw Group samples. Analyses plot as lithic sandstones or greywackes, and tend towards the K_2O pole with decrease in grainsize. Figure 3.14b shows the classification of Crook (1974) (diagram after Floyd and Leveridge, 1987). Samples of the Hope Beck and Kirk Stile formations show an affinity with the 'quartz-rich' group of Crook (Kirk Stile samples are devoid of Na_2O). Watch Hill Formation analyses compare with the 'quartz- intermediate' group with finer samples plotting with the 'quartz-rich' group. For the Loweswater Formation, samples plot with both the 'quartz-intermediate' and 'quartz-rich' groups.

Figure 3.14 Geochemical classification for sandstones of the Skiddaw Group after (a) Blatt et al (1972) and (b) Crook (1974) (diagram after Floyd and Leveridge, 1987). *Fe_2O_3=total iron as Fe_2O_3.

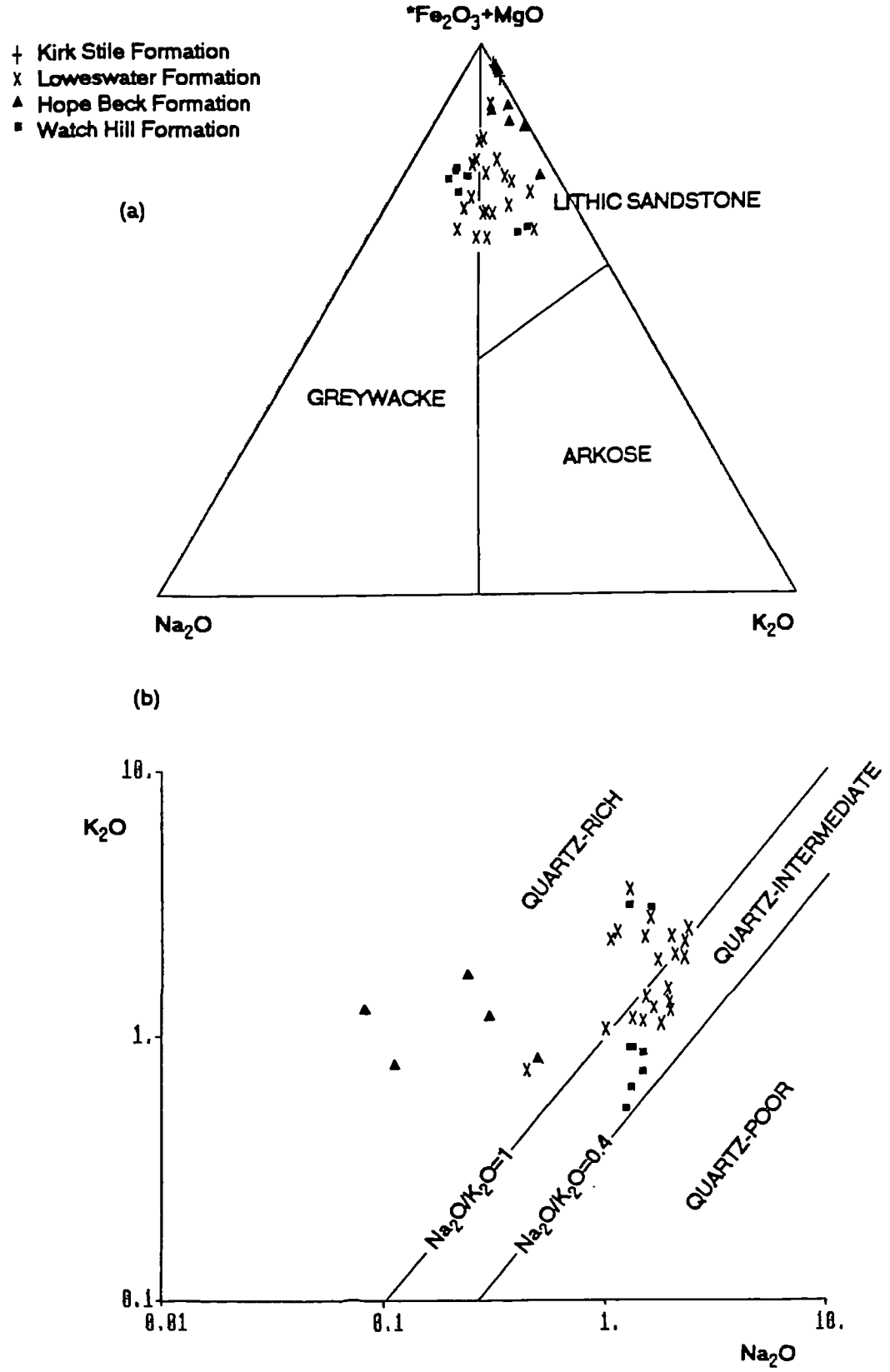

3.3.2 Investigation of compositional variation within a turbidite

From the base to the top of a turbidite there is generally a grainsize decrease from sandstone to mudstone with a corresponding change in composition due to the increase in matrix and decrease in silica. This is demonstrated by variation diagrams with major elements plotted against silica for Skiddaw Group samples from different Bouma divisions (figure 3.15). Thus high silica contents correspond to the coarsest sands, and decrease with grainsize. Silica content also varies for different source regions of sediment (figure 3.16). This causes problems in interpretation of provenance discrimination diagrams which use elements whose abundance is related to grainsize: samples of similar provenance may plot in different fields due to grainsize variations (Roser and Korsch, 1985). The variation can be reduced by using samples of a restricted size range (Bhatia, 1983). An alternative approach is to define a provenance discrimination plot where grainsize variations do not cross field boundaries, e.g. the SiO_2 vs K_2O/Na_2O plot of Roser and Korsch (1986) (section 3.3.5).

Figure 3.17 shows for each of four formations of the Skiddaw Group, average values of the relative elements from each Bouma unit, Ta, Tb, Tc and mudstone, linked by a line. The lines for each formation are not straight, (as would be expected for systematic grainsize variation), due to the following:

The presence of mudclasts in the Ta unit significantly alters the composition.

The mudstone composition is similar for each formation, though the sandstone compositions show significant differences. This might indicate (a) a single provenance throughout the group and either post-depositional alteration of sandstone compositions, or differing proportions of components from a heterolithic source; (b) variations in provenance and a single dominantly hemipelagic mudstone composition unrelated to turbidite source (see below).

Bouma units are defined by sedimentary structures and only loosely correspond to grainsize. The flow parameters that control bedforms are responsible for transporting or depositing grains depending on size and density, in turn related to composition. Thus specific grain types might be concentrated in a particular Bouma unit, e.g. mafic lithic grains in the Tc units of the Kirk Stile Formation (figure 3.17).

To make comparisons between turbidite samples, therefore, one must not only consider uniform grainsize but also the depositional flow regime indicated by the sedimentary structures. Fine-medium sandstones displaying horizontal lamination of the Tb unit are recommended. Alternatively, one could consider each Bouma unit of a turbidite and study the compositional variation from base to mudstone top. Sediment of different provenance classes containing differing clast types may be sorted by a decelerating turbidity current in such a way that each defines a characteristic variation in composition. This will appear as a characteristic curve on a variation diagram. Thereby turbidites of unknown provenance could be studied in a similar manner to interpret the nature of their source region by comparison with such curves. Unfortunately the carefully sampled data required to produce definitive discrimination diagrams cannot be collated from the literature and such a widespread and detailed sampling program was beyond the scope of the project.

Figure 3.15 Silica variation diagrams for the Skiddaw Group. Analyses recalculated to 100% free of volatiles, excluding samples with carbonate cement (n=69). *Fe_2O_3 is total iron as Fe_2O_3.

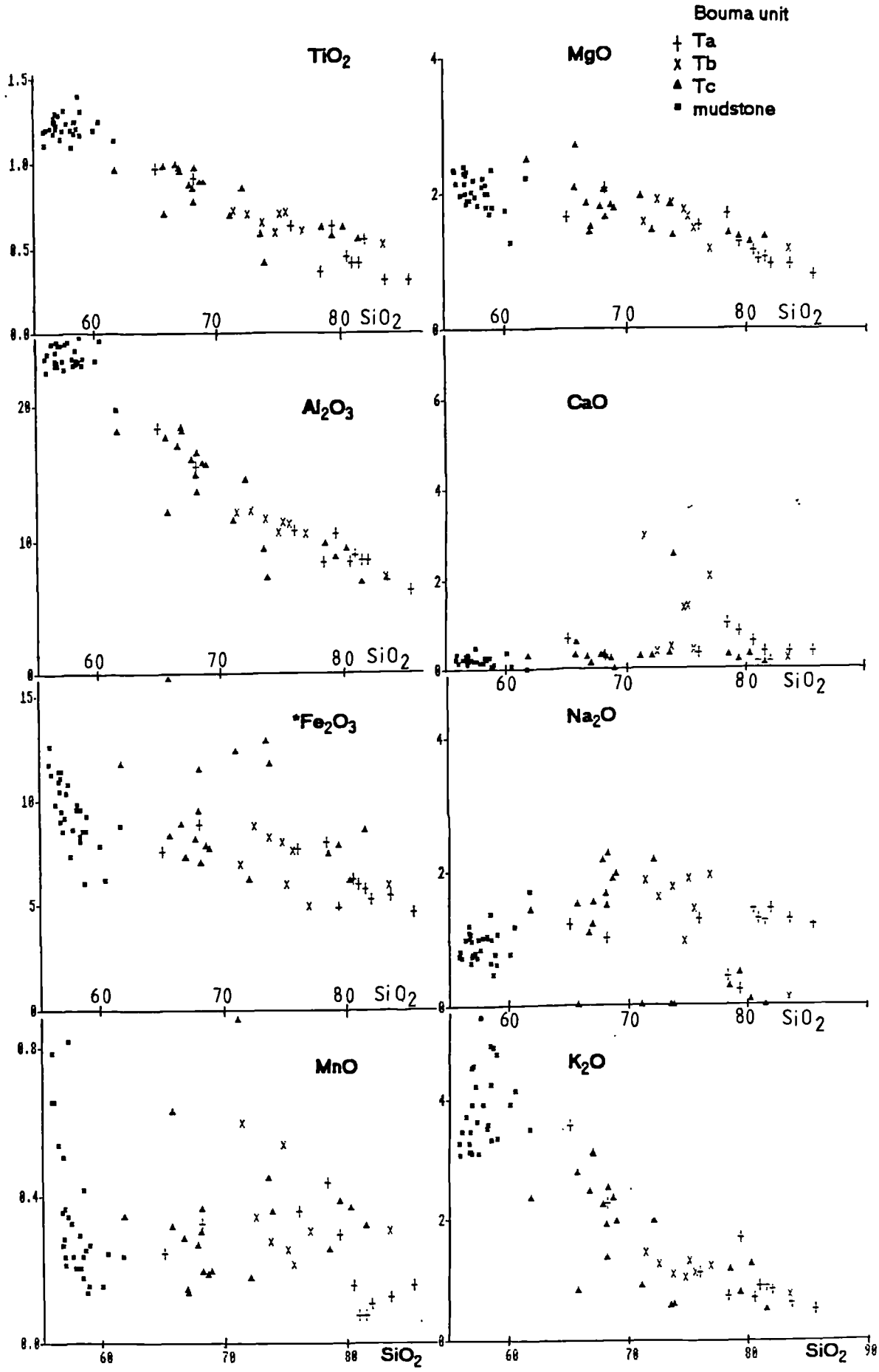

Figure 3.16 Silica variation diagrams for samples of different provenances. Analyses recalculated to 100% free of volatiles. *Fe_2O_3 is total iron as Fe_2O_3. (n=115).

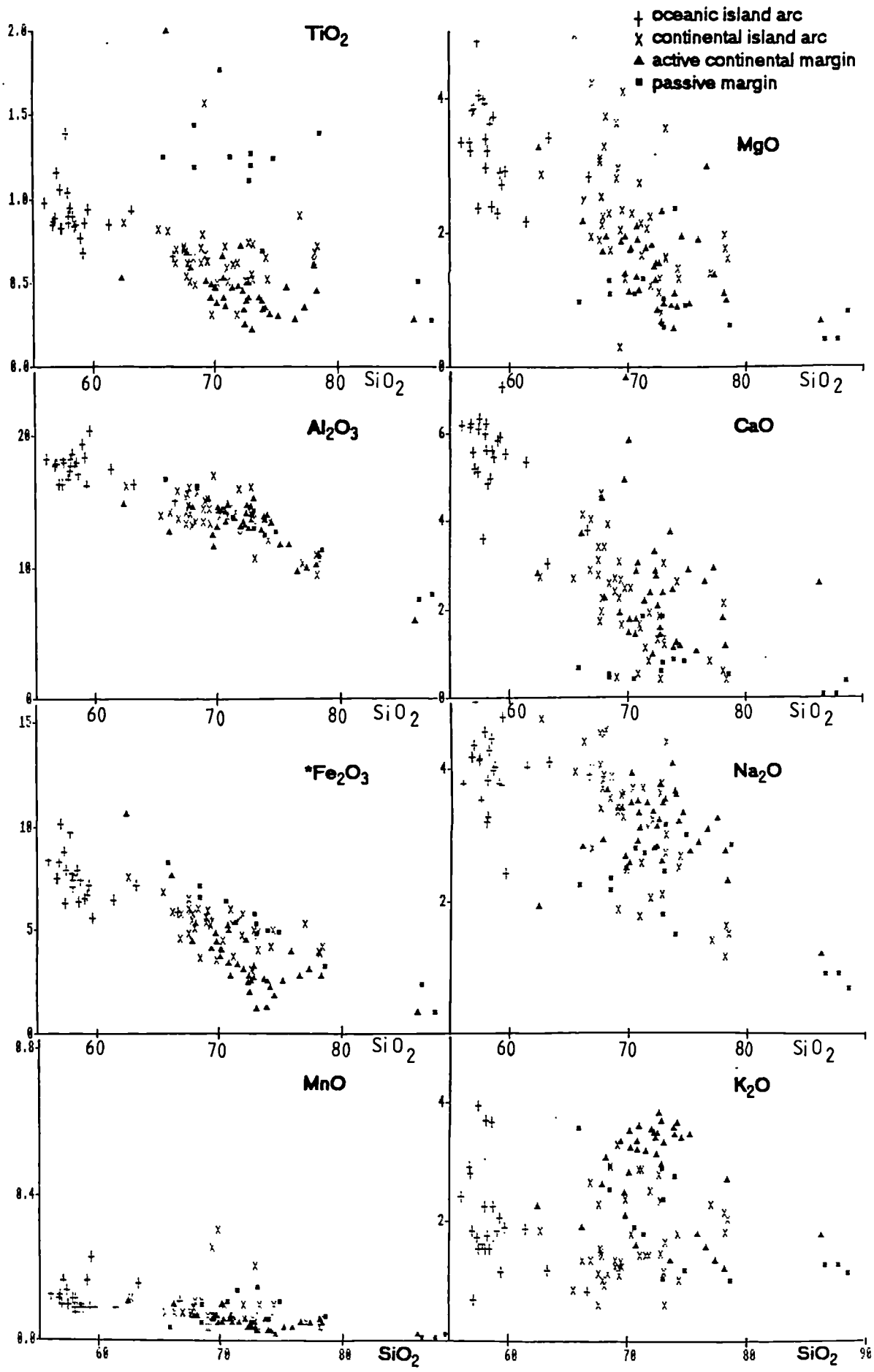

Figure 3.17 *Fe_2O_3+MgO vs TiO_2 and *Fe_2O_3+MgO vs Al_2O_3/SiO_2 for the Skiddaw Group formations showing average values for each Bouma unit (A, B, C) and mudstone (M). *Fe_2O_3 is total iron as Fe_2O_3. Compositional variation within turbidites is large compared with provenance fields of Bhatia (1983). OIA=oceanic island arc, CIA=continental island arc, ACM=active continental margin, PM=passive margin.

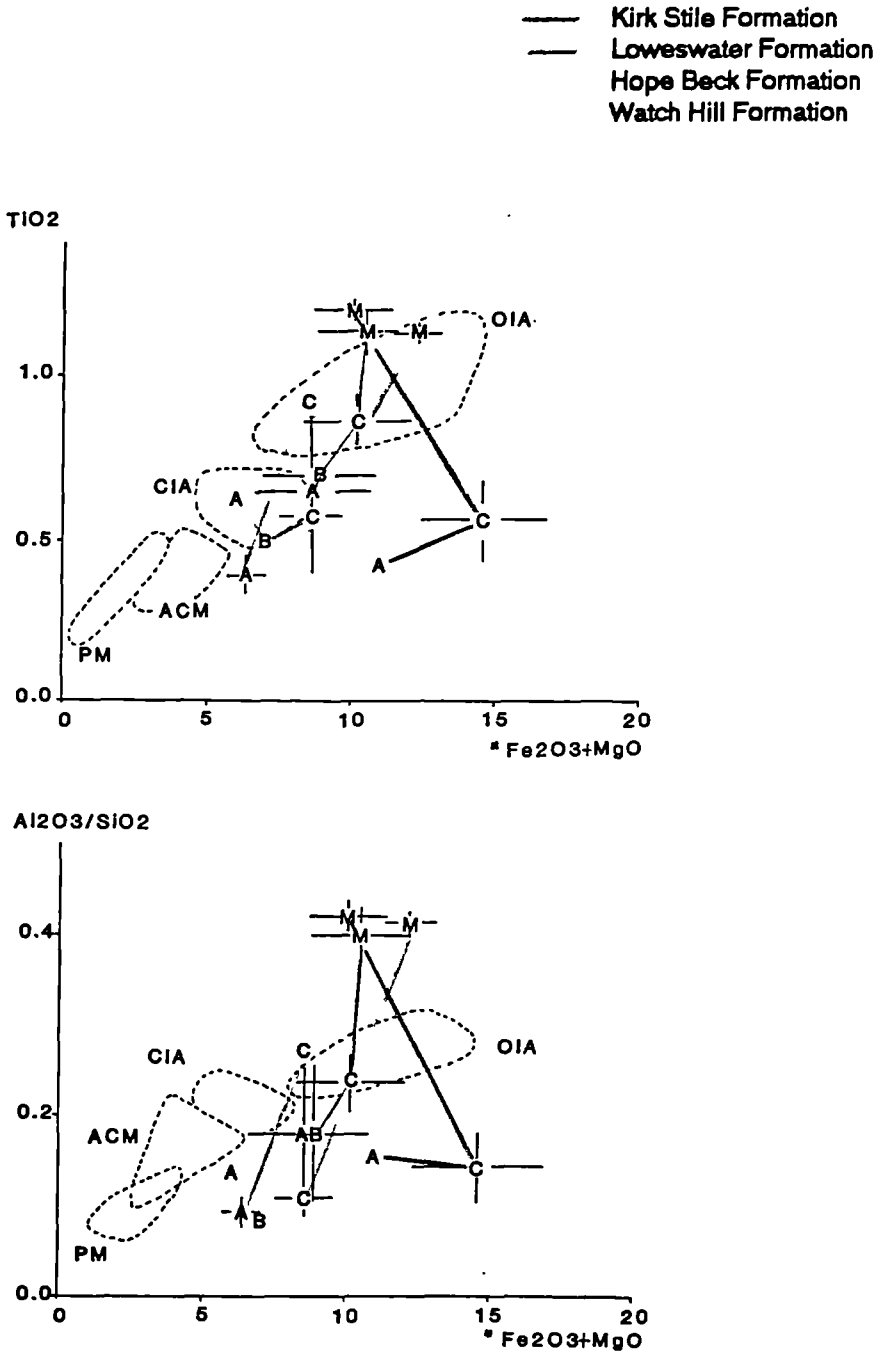

Mudstone compositions contrast with the range of sandstone compositions in that they are remarkably uniform throughout the group (figures 3.15 and 3.17). The reason for this could be:

(1) an origin as turbidite mud of uniform composition from a single source region. Variation in sandstone compositions could result from differing proportions of components from a heterolithic source. This effect would be largely eliminated from mud grade material due to better mixing during transport;

(2) A hemipelagic origin for much of the mudstone, unrelated in composition to turbidite sources;

(3) Homogenisation of mudstone compositions since deposition.

The relationship between composition of matrix in turbidites and that of mudstone interbeds can be investigated by considering ratios of element pairs. Al_2O_3 and TiO_2 are two dominantly clay-associated elements with relative immobility in low temperature environments (Spears and Amin, 1981). A variation diagram (figure 3.18a) for Skiddaw Group sediments displays a straight line through both sandstone and mudstone analyses, suggesting a constant composition for the matrix within sandstones (Shail and Floyd, 1988), which is equivalent to the mudstone composition. This supports case (1) above. If the mudstones had displayed a different ratio of Al_2O_3 / TiO_2 then a hemipelagic origin might have been indicated.

A good correlation of K_2O and Al_2O_3 (figure 3.18b) is displayed by sandstones from each formation. For all sandstones, the correlation is diminished. The range of Al_2O_3 in mudstones is small but for K_2O is large, probably due to post-depositional mobility.

Evidence of chemical mobility is provided by trace elements. Floyd and Leveridge (1987) showed for Devonian sandstones constant inter-element ratios for the large-ion-lithophile (LIL) elements and transition elements but variability in the high field strength (HFS) elements. The same parameters are considered for the Skiddaw Group.

The LIL elements (e.g. K, Rb, Cs, Sr, La, Th, U) show a range of abundances but K and Rb show an approximately constant inter-element ratio (figure 3.19) within each formation. Thus some LIL elements have been mobile but important compositional differences exist between the formations.

The transition elements (Ni, Cr, V) are similar. Cr/Ni is approximately constant for sandstones in each formation (figure 3.20a) especially if one considers individual beds (figure 3.20b). The Kirk Stile Formation displays a low Cr/Ni for sandstones contrasting with a Cr/Ni for mudstones similar to other Skiddaw Group mudstones. The presence of mafic lithic clasts in sandstone samples (observed in thin sections) could be responsible.

The high field strength elements (Ti, Zr, Y, Nb, Hf) are related to the presence of heavy mineral phases so constant ratios of element pairs are not always displayed. This is not the case for the Watch Hill Formation sandstones which show strong correlation coefficients for these elements (table 3.12). The abundances in mudstones show similar ranges for each formation.

Figure 3.18 Skiddaw Group sediments plotted by formation on (a) TiO_2 vs Al_2O_3 and (b) K_2O vs Al_2O_3.

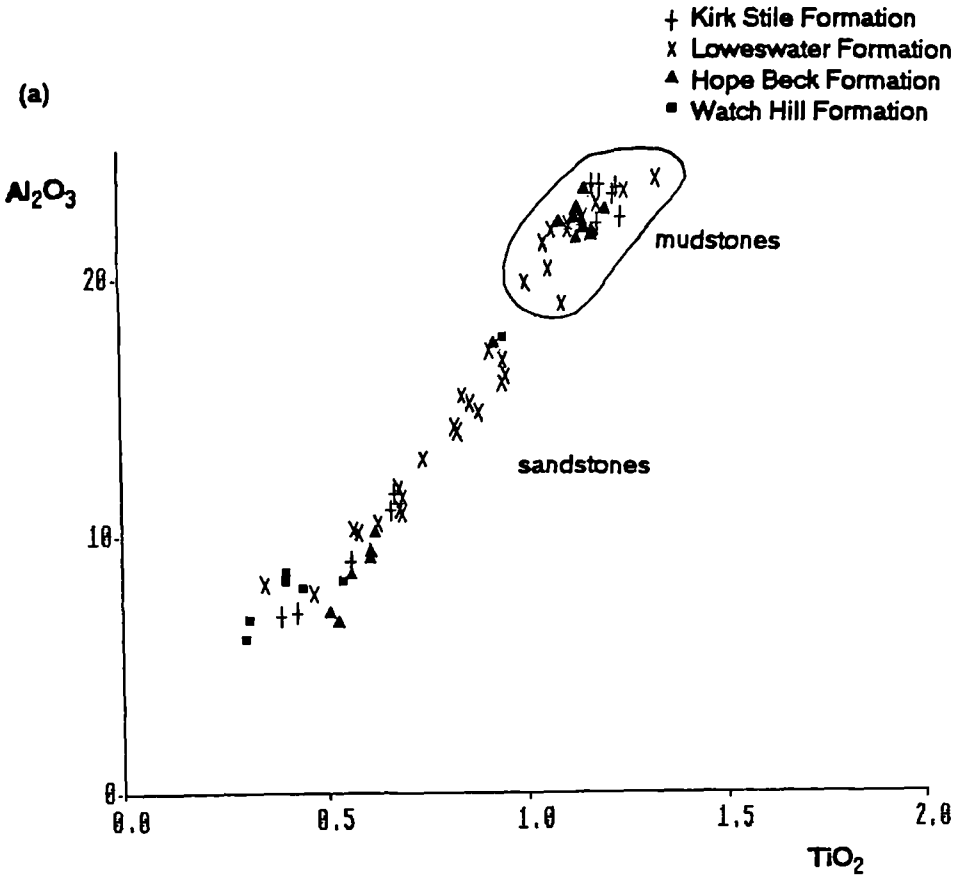

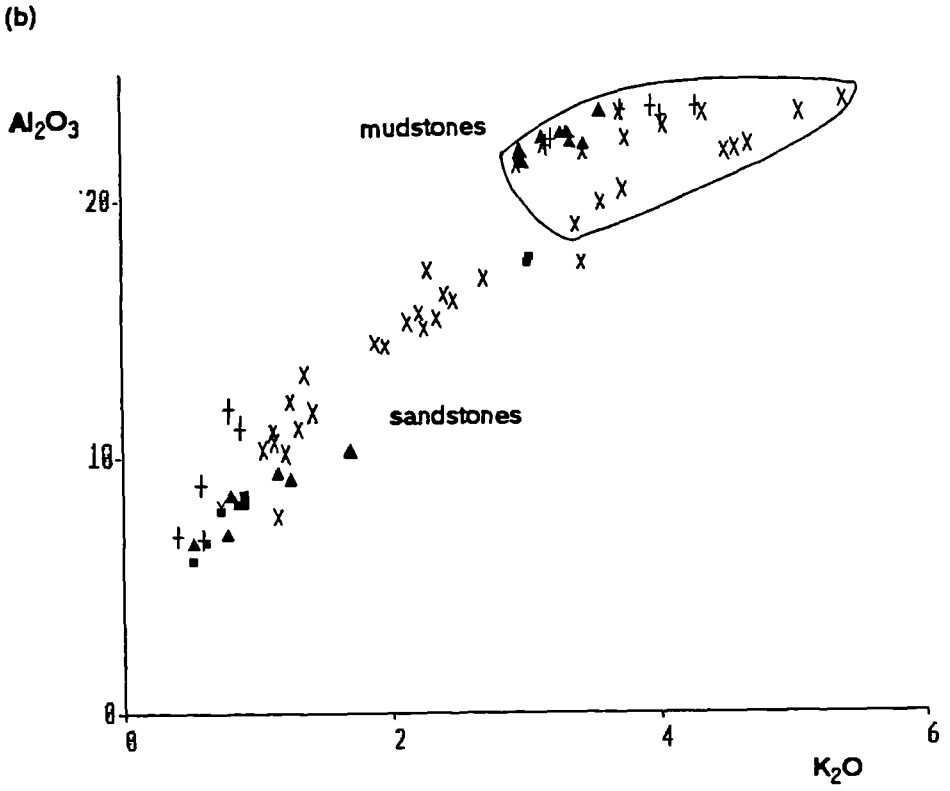

In summary, important differences in composition exist between sandstones of each formation since element pairs with poor correlation for all Skiddaw Group sandstones are strongly correlated for each formation (compare tables 3.12a to e). Although some major and trace elements have undoubtedly been mobile since deposition, constant ratios of some LIL, transition and HFS elements suggest widespread homogenisation of mudstone composition has not occurred. In the absence of evidence for hemipelagic mudstone, an origin as turbidite mud (case 1 above) is considered most likely.

Figure 3.19 Rb vs K_2O for the Skiddaw Group.

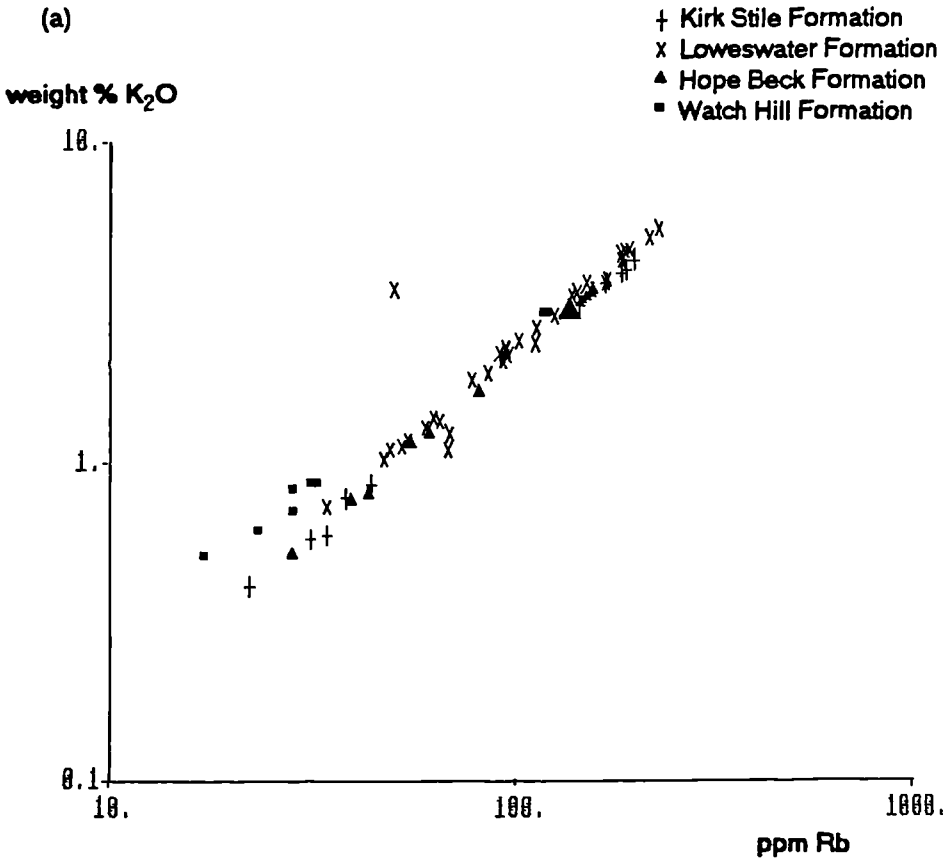

Figure 3.20 Cr vs Ni for (a) formations of the Skiddaw Group and (b) channel-fill greywackes of the Darling Fell Unit.

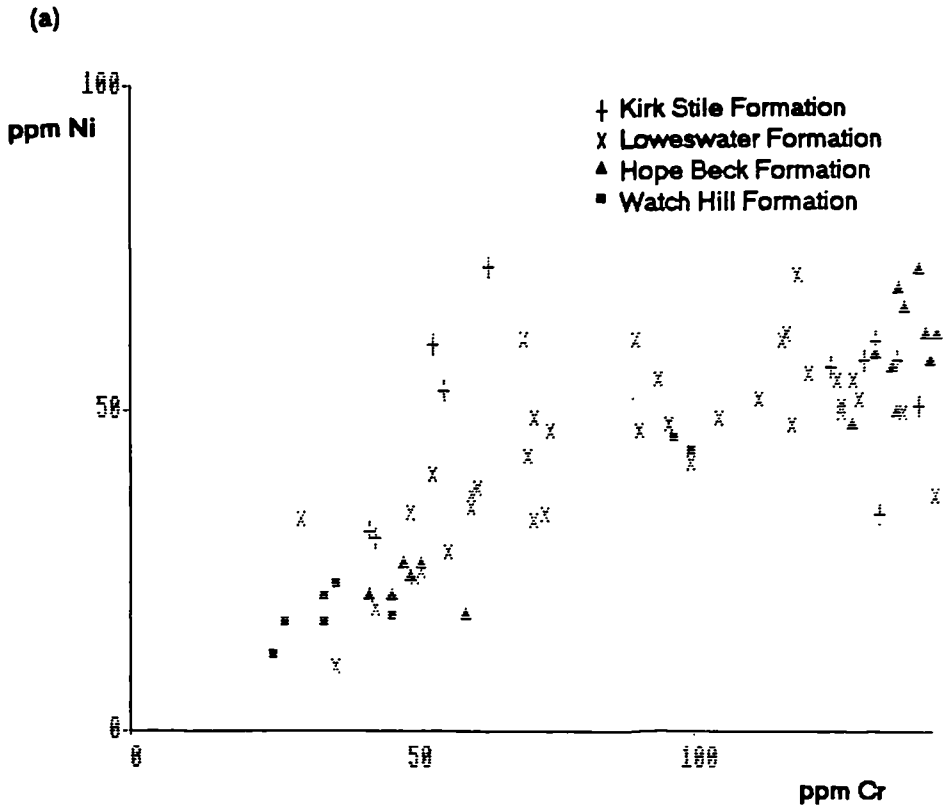

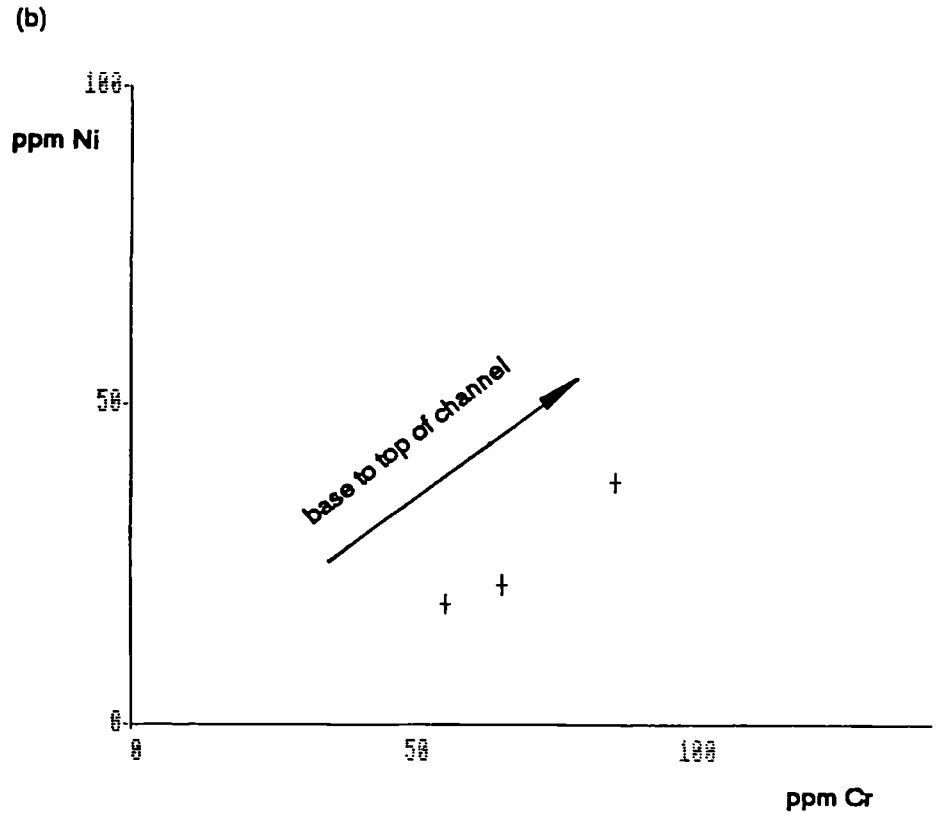

Table 3.12 Correlation coefficients for large ion lithophile (LIL), transition and high field strength (HFS) elements for sandstones from (a) the Skiddaw Group, (b) Watch Hill Formation, (c) Hope Beck Formation, (d) Loweswater Formation and (e) Kirk Stile Formation.
Values at a 95% level of significance are indicated in square brackets.

(a) Skiddaw Group (n=39) [0.32]

	K	Rb	Sr	La	Th	U	Ba	Ni	Cr	Ti	Zr	Y	
Rb	0.98												
Sr	0.78	0.79											
La	0.70	0.73	0.41										
Th	0.65	0.63	0.52	0.38									LIL elements
U	0.40	0.46	0.36	0.50	0.28								
Ba	0.98	0.97	0.78	0.66	0.65	0.40							
Ce	0.61	0.60	0.30	0.66	0.42	0.45	0.60						
Cr								0.67					transition
V								0.64	0.97				elements
Zr										0.59			
Y										0.36	-0.08		HFS elements
Nb										0.96	0.56	0.27	

(b) Watch Hill Formation (n=8) [0.71]

	K	Rb	Sr	La	Th	U	Ba	Ni	Cr	Ti	Zr	Y	
Rb	1.00												
Sr	0.96	0.97											
La	0.90	0.91	0.90										
Th	0.97	0.96	0.92	0.85									LIL elements
U	0.95	0.95	0.93	0.76	0.98								
Ba	1.00	1.00	0.97	0.89	0.96	0.95							
Ce	0.91	0.91	0.93	0.75	0.93	0.96	0.91						
Cr								0.97					transition
V								0.99	0.99				elements
Zr										0.70			
Y										0.94	0.55		HFS elements
Nb										0.99	0.69	0.94	

(c) Hope Beck Formation (n=6) [0.88]

	K	Rb	Sr	La	Th	U	Ba	Ni	Cr	Ti	Zr	Y	
Rb	1.00												
Sr	0.98	0.99											
La	0.96	0.95	0.92										
Th	-0.52	-0.51	-0.53	-0.31									LIL elements
U	0.46	0.43	0.36	0.33	-0.57								
Ba	0.98	0.99	0.98	0.92	-0.50	0.48							
Ce	0.68	0.64	0.53	0.72	-0.11	0.64	0.63						
Cr								-0.29					transition
V								-0.31	0.92				elements
Zr										-0.62			
Y										0.79	-0.80		HFS elements
Nb										0.62	-0.56	0.90	

(Table 3.12 continued)

(d) Loweswater Formation (n=21) [0.43]

	K	Rb	Sr	La	Th	U	Ba	Ni	Cr	Ti	Zr	Y	
Rb	0.98												
Sr	0.62	0.57											
La	0.77	0.80	0.33										
Th	0.47	0.49	0.45	0.29									LIL elements
U	0.14	0.18	-0.05	0.33	0.07								
Ba	0.97	0.95	0.62	0.67	0.57	0.09							
Ce	0.85	0.82	0.39	0.63	0.22	0.11	0.81						
Cr								0.69					transition
V								0.62	0.95				elements
Zr										0.49			
Y										0.56	-0.16		HFS elements
Nb										0.95	0.52	0.42	

(e) Kirk Stile Formation (n=4) [0.95]

	K	Rb	Sr	La	Th	U	Ba	Ni	Cr	Ti	Zr	Y	
Rb	0.95												
Sr	-0.43	-0.20											
La	-0.43	-0.68	-0.50										
Th	0.69	0.70	0.22	-0.52									LIL elements
U	-0.59	-0.68	-0.44	0.71	-0.96								
Ba	0.77	0.54	-0.85	0.24	0.33	-0.08							
Ce	-0.28	-0.35	0.50	0.22	0.42	-0.37	-0.22						
Cr								0.96					transition
V								0.92	0.99				elements
Zr										0.94			
Y										-0.76	-0.92		HFS elements
Nb										0.92	1.00	-0.93	

3.3.3 Discriminant function analysis

3.3.3.1 Description

Bhatia (1983) used two data sets of major element composition of sandstone samples:

1. 65 analyses from five Lower Palaeozoic Australian basins of four tectonic settings (*oceanic island arc, active continental margin, continental island arc* and *passive margin*).

2. 34 averages of analyses from widespread Phanerozoic basins of known tectonic setting.

He applied a powerful statistical technique, discriminant function analysis, to the first data set, to show that the four tectonic settings could be successfully discriminated. The computer based analysis considers the major element content of the samples, each of which has been assigned to a group; in this case basin type classified on the tectonic setting of the source region. It defines a mathematical function along which groups are separated to a maximum extent, while samples within each group are tightly clustered.

The number of discriminant functions that exist is one less than the number of groups. The percentage of variation in the data accounted for by each function is, however, greatest for the first function and diminishes rapidly for later functions. The first two functions account for almost all the variation in the data set.

The function takes the form

$D_i = a_i x_1 + b_i x_2 + c_i x_3 + \ldots + n_i x_n + C$

where x_1, x_2 etc. are coefficients, a_i, b_i etc. are variables, in this case values for each major element in sample i, and C is a constant. D_i is the discriminant score for the sample. A plot of discriminant scores for the first function against discriminant scores for the second function is a graphical representation of the ability of the analysis to discriminate samples of each group. Further details of discriminant function analysis and its geological applications can be found in Davis (1986). On his plot for data set 1, Bhatia constructed straight line boundaries between provenance fields (shown on figure 3.21) from loci equidistant from the points representing the average of scores from each group.

If the program is instructed to use unstandardised variables, then the functions defined can be used to classify other data sets. Bhatia did this to the second data set to test the analysis and showed that all but three averages were correctly assigned to their expected tectonic setting. Discriminant scores were calculated for the Skiddaw Group (Figure 3.21). Missing FeO values were problematical but were calculated following the practice of Bhatia (discussed below) by splitting the total iron in the same ratio as the average for the continental island arc setting, thus introducing an unavoidable bias to the analysis. The result shows separation of the Hope Beck Formation, but is inconclusive in assigning tectonic setting. Most samples are clustered along the boundaries of the *continental island arc* field with either the *passive margin* or *active continental margin* fields.

3.3.3.2 Problems

Roser and Korsch (1985) were unable to repeat the results of Bhatia (1983) and Haughton (1988) attempted to use this diagram without success. This was due to a number of reasons (see discussion by Roser and Korsch (1985) and reply). The method can be criticised as follows:

Actual analyses not recalculated on a volatile-free basis were used to define the functions.

The procedure for using incomplete analyses including those with total iron as Fe_2O_3 was unclear; the group average for the missing element had been used, thus introducing a bias into the analysis, though this was considered small (Bhatia in reply to Roser and Korsch,1985).

Grainsize has a strong effect on the discriminant function diagram, though it was stressed that the diagram was only applicable to fine and medium grained sandstones.

Use of averages of analyses in the second data set overlooked variations in compositions, some of which were due to grainsize, but important information may have been lost.

Some of the averages, e.g. Pettijohn's average sandstone, were based on many analyses from diverse tectonic settings, thus, assigning a tectonic setting to the average was invalid.

In addition, Lower Palaeozoic sediments, especially mudstones, have anomalously high primary K_2O contents (Maynard et al, 1982; Taylor and McLennan, 1985), (figure 3.22), such that comparison with other Phanerozoic samples is dubious. It is not feasible, however, to compile a data set of solely Lower Palaeozic basins on which to perform the statistical analysis.

In summary, the discriminant function analysis technique is most elegant but the discrimination diagram of Bhatia (1983) is flawed.

Figure 3.21 Plot of discriminant score 1 against discriminant score 2 for the Skiddaw Group using the discriminant functions of Bhatia (1983), who defined the fields. OIA=oceanic island arc, CIA=continental island arc, ACM=active continental margin, PM=passive margin.

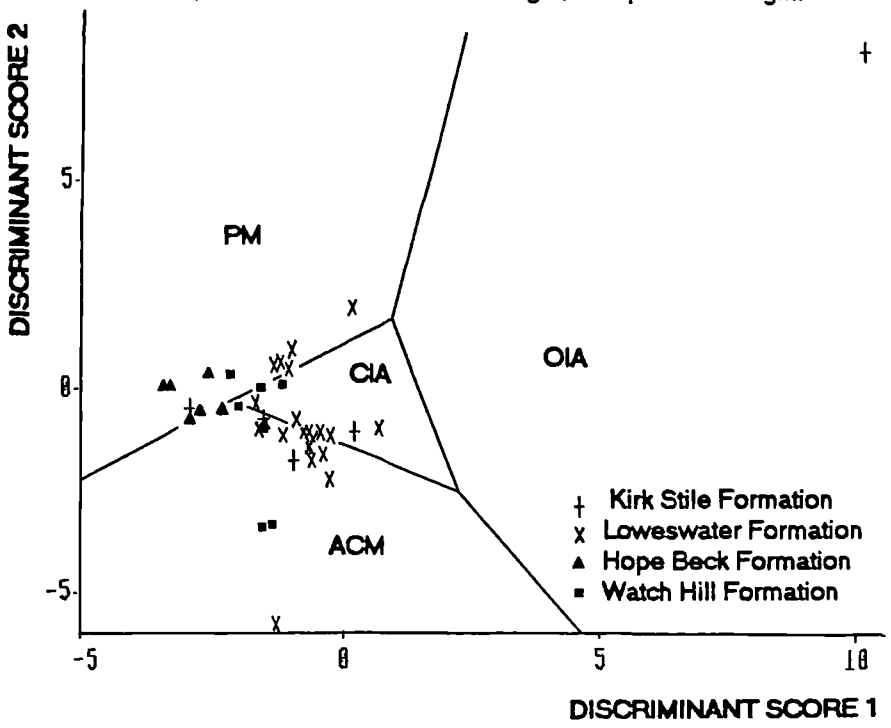

Figure 3.22 Plots showing sandstone-mudstone pairs with tie lines for Phanerozoic sediments (data from Maynard et al.1982).

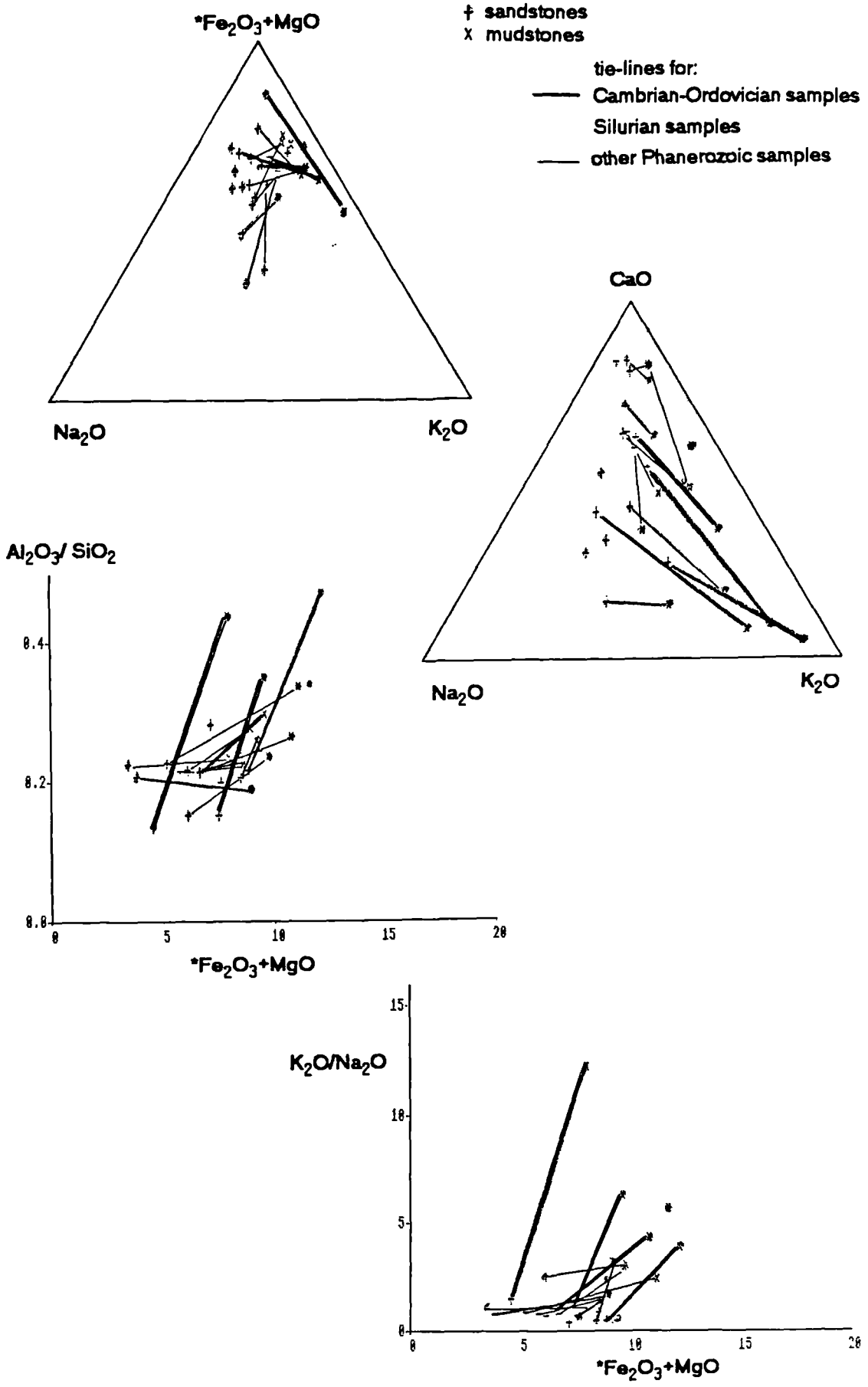

3.3.3.3 A reappraisal of the technique

An analysis of major elements is a closed data set, i.e. since it sums to 100% the abundance of each element is affected by the others. This creates variations on plots of individual elements or element ratios that are inherent in the data. Since discriminant function analysis considers all major elements in the analysis, this problem is minimised.

The method could be useful if a procedure was adopted as follows:

The data set should include samples from a large number of sedimentary basins whose tectonic settings have been constrained by other means where possible.

Individual analyses and not averages of formations should be used, so significant compositional variations are not overlooked. One of the strengths of discriminant function analysis is its ability to consider large data sets.

Samples should be sandstones of a restricted grainsize range (fine to medium sand), deposited in a similar sedimentary environment by a single mechanism, i.e. from a turbidity current.

Only reliable analyses should be used, i.e. those whose totals sum to 100% +/- 1.5%, and these should be analysed for all major elements.

Since many published analyses do not separate FeO and Fe_2O_3, total iron should always be expressed as Fe_2O_3.

All analyses should be recalculated to 100% volatile-free.

The above criteria were applied to data from sources used by Bhatia (1983). 115 analyses were compiled (appendix 4d).

Bhatia (1983) classified sedimentary basins by the nature of their source terrain and recognised four types:

Oceanic island arc- sedimentary basins (fore-arc, oceanic back-arc) adjacent to island arcs on oceanic (e.g. Marianas) or thinned continental crust (e.g. Aleutians) with sediment mainly derived from the calc-alkaline or tholeiitic arc.

Continental island arc- sedimentary basins adjacent to island arcs of detached continental fragments on well developed continental crust (e.g. Lau Basin, Japan Sea) or on thin continental margins (e.g. Cascades, western U.S.A.). Sediments are mainly derived from felsic volcanic rocks.

Active continental margins - sedimentary basins on Andean-type continental margins and strike-slip basins with sediments dominantly sourced from granite gneisses and siliceous volcanics of uplifted older fold belts.

Passive margins - basins on Atlantic-type rifted continental margins, remnant ocean basins adjacent to collision orogens and basins on inactive or extinct convergent margins. Sediment is highly matured from recycled platform sedimentary and metamorphic rocks or a recycled orogen.

An interpretation of a basin's tectonic setting can only be made if one assumes that the sediment source was related to the basin and any volcanism was contemporaneous with basin formation. The style of volcanism or its absence is a major influence on sediment composition which has been exploited in the above classification. Van de Kamp and Leake (1985) and Floyd et al (1991) questioned whether the *continental island arc* type could be adequately distinguished

from the *active continental margin* type. Also Maynard et al (1982) considered that bulk chemistry would not distinguish between arc related settings. Despite these reservations such subdivisions would be useful in interpreting sources for Skiddaw Group sediment, hence it was decided to retain the four-fold classification. One should consider the four types to refer to the style of sediment source terrain and not to a particular basin type or necessarily the tectonic setting of source and basin.

3.3.3.4 A new discriminant function

A discriminant function analysis was performed on these data using the Statistical Analysis System program 'DISCRIM' on an Amdahl mainframe computer. This program generates a single discriminant function and analyses are assigned to the tectonic setting from which they have the shortest generalised squared distance. Table 3.13 shows the percentage of correctly classified analyses in each setting.

The function was extremely successful in distinguishing source type with even the poorest results, for *continental island arc* provenance, showing 86% correctly classified. Functions were also defined excluding alkalies, and alkalies and silica in an attempt to remove the more mobile elements from the analysis. These were less successful in discriminating basin type so were discarded. The cause might have been that only part of a closed data set was being considered. Alternatively, even these mobile element abundances may hold important provenance information.

Table 3.13 Results of sample classification by provenance type for the new discriminant function. ACM = active continental margin, CIA = continental island arc, OIA = oceanic island arc, PM = passive margin.

	number of observations and percents classified into provenance type:				
from type:	ACM	CIA	OIA	PM	TOTAL
ACM	35 97.22	1 2.78	0 0.00	0 0.00	36 100.00
CIA	4 9.52	36 85.71	0 0.00	2 4.76	42 100.00
OIA	0 0.00	0 0.00	23 100.00	0 0.00	23 100.00
PM	0 0.00	0 0.00	0 0.00	14 100.00	14 100.00
TOTAL PERCENT	39 33.91	37 32.17	23 20.00	16 13.91	115 100.00

3.3.3.5 Results

The calibration data are retained by the program so application to other data sets is possible. A classification of the Skiddaw Group sandstone analyses was performed. All but two samples were classified as belonging to basins fed by a *continental island arc* source. Two analyses, one from the Watch Hill Formation and one from the Kirk Stile Formation, indicate an *active continental margin* source. To test if the Skiddaw Group formations could be discriminated, a discriminant function analysis was performed on 39 sandstone analyses (appendix 4c). All were classified to their correct formation.

The calibration data were applied to four analyses of clasts in redeposited sediment; three from sandstone rafts in the Buttermere Formation and one from a sandstone clast in the Beckgrains Bridge debris flow of the Kirk Stile Formation [NY 1904 3552] (all of which were classified by discriminant function analysis as having *continental island arc* provenance). Samples from sandstone rafts (Webb and Cooper, 1987) on Causey Pike [NY 2195 2075] and at Goat Gills [NY 1910 1625] were classified as most similar to the Watch Hill Formation. A second sample from the latter locality was classified as Hope Beck Formation. These sandstone rafts are thought to be of early to middle Arenig age from palaeontological evidence (Cooper et al, in prep) hence contemporaneous with the Loweswater Formation. This new evidence suggests the composition of turbidite sandstones in the Skiddaw Group basin throughout the Arenig was not uniform, but was derived from a single type of source region: a continental island arc. The clast from the debris flow was classified as belonging to the Loweswater Formation, suggesting reworking of this older sandstone-rich formation during deposition of the Kirk Stile Formation. This result was also suggested by petrographical analysis.

3.3.3.6 An alternative discriminant function analysis

Roser and Korsch (1988) defined a provenance discrimination diagram by discriminant function analysis of selected sandstone and mudstone analyses from New Zealand. Analyses were recalculated to 100% volatile- and LOI-free after total iron had been expressed as Fe_2O_3. Seven major elements were used in defining the functions: Al_2O_3, TiO_2, Fe_2O_3, MgO, CaO, Na_2O, K_2O. They defined four provenance groups (table 3.14).

Table 3.14 Provenance groups of Roser and Korsch (1988).

Provenance group	sediment description	source
P1 (mafic)	first cycle volcanogenic basaltic and lesser andesitic detritus	primitive oceanic island arc
P2 (intermediate)	dominantly volcanogenic andesitic detritus	volcanic island arc
P3 (felsic)	acid plutonic and volcanic detritus	active continental margin arc
P4 (recycled)	mature polycyclic quartzose detritus	granitic-gneissic or sedimentary terrain

The inclusion of a *recycled* provenance field allows comparison with petrographical provenance diagrams (table 3.2).

These discriminant functions were applied to the data set used in the previous section and the resulting plot with the provenance fields is shown in figure 3.23. There is some overlap of samples from the predefined provenance types, but both the *oceanic* and *continental island arc* types are dominantly placed in the P2 field (andesitic volcanic island arc). The *active continental margin* samples are correctly assigned to the P3 field. The *passive margin* samples are scattered across the P2, P3 and P4 (recycled) fields with less than 50% in the expected P4 field. This might suggest a failure of the plot to distinguish quartz-rich sandstones in the absence of silica, or the *recycled* and *passive* margin fields are not compatible, or the *passive margin* provenance type is inadequately represented by these data.

A plot of results for the Skiddaw Group is shown in figure 3.24a. The samples from the Watch Hill and Hope Beck formations plot in field P4, with the finest samples just in the P2 field. The Loweswater Fomation sandstones plot ambiguously around the apex of fields P1, P2 and P4 with high matrix varieties not separated. The analyses from the Kirk Stile Formation are separate in the P1 field due to their content of mafic clasts. Samples from the sandstone rafts of the Buttermere Formation plot with Hope Beck Formation sandstones, but the sandstone clast from the Beckgrains Bridge debris flow plots in the P2 field near to Loweswater Formation sandstones (figure 3.24b). The effect of grainsize is displayed by the Watch Hill Formation rocks and the channel-fill of the Loweswater Formation such that finer samples are moved towards the top right of the diagram (figure 3.24b). The analysis successfully separated each formation indicating variations in provenance throughout the Skiddaw Group.

Figure 3.23 Discriminant score 1 vs discriminant score 2 for sandstones of different provenance using the discriminant function of Roser and Korsch (1988). P1=mafic, P2=intermediate, P3=felsic, P4=recycled.

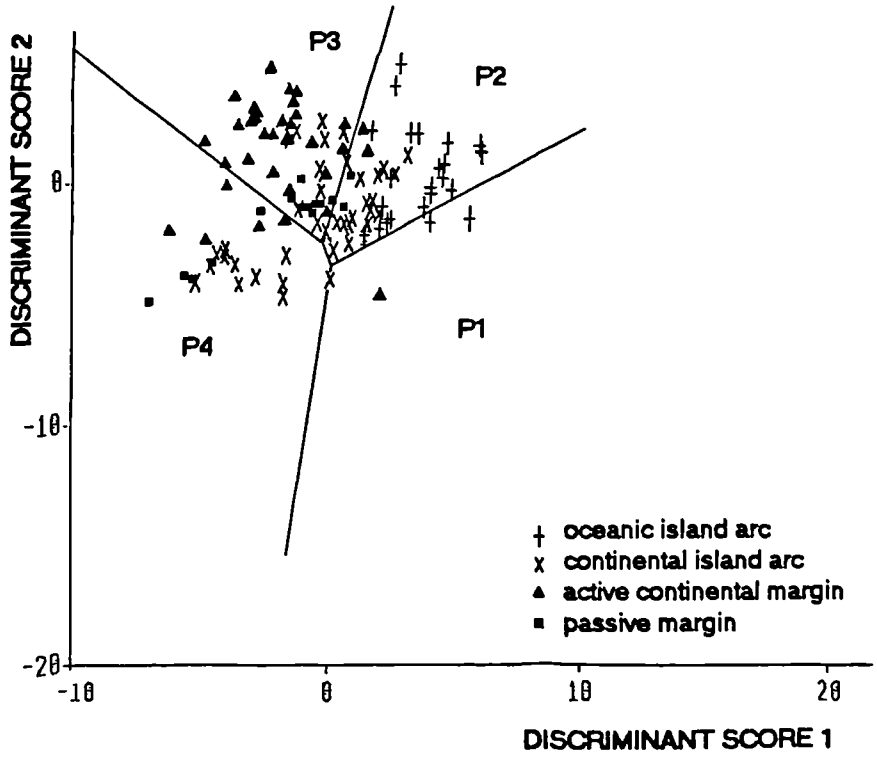

Figure 3.24 Discriminant score 1 vs discriminant score 2 using the discriminant function of Roser and Korsch (1988) for Skiddaw Group sandstones (a) by formation, (b) by location. P1=mafic, P2=intermediate, P3=felsic, P4=recycled.

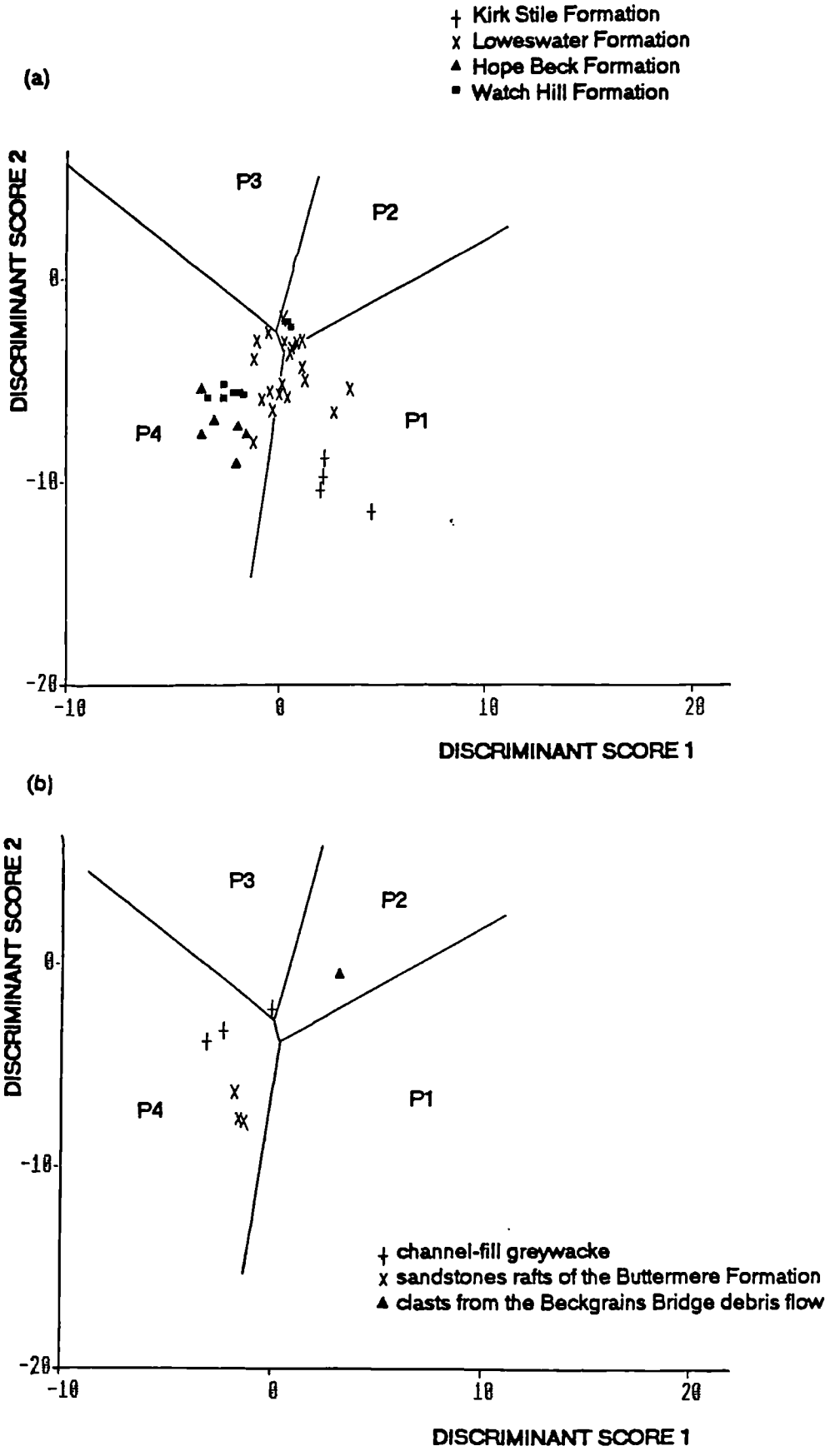

3.3.4 Bivariate plots

Bhatia (1983) considered which elements discriminated the basin types most strongly and produced a set of plots as follows:

($^*Fe_2O_3$ + MgO) vs TiO_2

($^*Fe_2O_3$ + MgO) vs Al_2O_3/SiO_2

($^*Fe_2O_3$ + MgO) vs K_2O/Na_2O

($^*Fe_2O_3$ + MgO) vs $Al_2O_3/(CaO + Na_2O)$

triangular plot CaO - Na_2O - K_2O

$^*Fe_2O_3$ is total iron as Fe_2O_3. He used his second data set with each analysis recalculated to 100% free of volatiles and qualitatively drew fields for each tectonic setting (figure 3.25).

These discrimination plots have been used to assign tectonic settings to ancient sandstones (Haughton, 1988; McCann, 1991) largely without success. Inspection of the diagrams shows the fields for each basin type to be idealised. They do not include all data points, which show considerable overlap, and the *passive margin* field does not correspond to the data. The triangular plot is unlikely to be reliable due to the mobility of the alkalies. It was felt necessary to redefine these diagrams using the improved data set (appendix 4d).

The new diagrams show considerable overlap of *active continental margin* and *continental island arc* samples since they are not adequately distinguished by $^*Fe_2O_3$ + MgO (figure 3.26). The *passive margin* samples generally shows a wide spread of points, but *oceanic island arc* samples are tightly grouped with little overlap with other fields. The plot $^*Fe_2O_3$ + MgO vs TiO_2 discriminates with some success since the *passive margin* samples have a high TiO_2 content due to the heavy mineral content of mature sediments. An attempt has been made to designate field boundaries.

These new field boundaries have been applied to the Skiddaw Group data (Figure 3.27a). Most samples plot in the *continental island arc* field, with Watch Hill Formation sandstones near the boundary with the *active continental margin* field and Loweswater Formation sandstones straddling the boundary with the *oceanic island arc* field. It should be remembered that these field boundaries are diffuse bands. In addition the variation due to grainsize causes spread of points across field borders; e.g. figure 3.27b shows three samples from increasingly higher positions within a channel-fill defining a line with positive gradient. High-matrix greywackes are not distinct from other Loweswater Formation greywackes, although the quartz-rich types from Jonah's Gill are lower in TiO_2. The latter consistently plot with Watch Hill Formation or Hope Beck Formation sandstones, as do sandstone clasts from the Buttermere Formation and Beckgrains Bridge debris flow (figure 3.27b). The Kirk Stile Formation analyses plot in an undefined region, high in $^*Fe_2O_3$+MgO. This could be due to the presence of mafic volcanic clasts. There is a systematic variation for sandstones from the Watch Hill to Hope Beck to Loweswater formations, which might indicate a secular change in provenance.

Figure 3.25 Bivariate plots of Bhatia (1983) for sandstones, with provenance fields.

Samples are from basins from the following tectonic settings:

- ● oceanic island arc
- continental island arc
- active continental margin
- passive margin

Provenance fields are:

A	oceanic island arc
B	continental island arc
C	active continental margin
D	passive margin

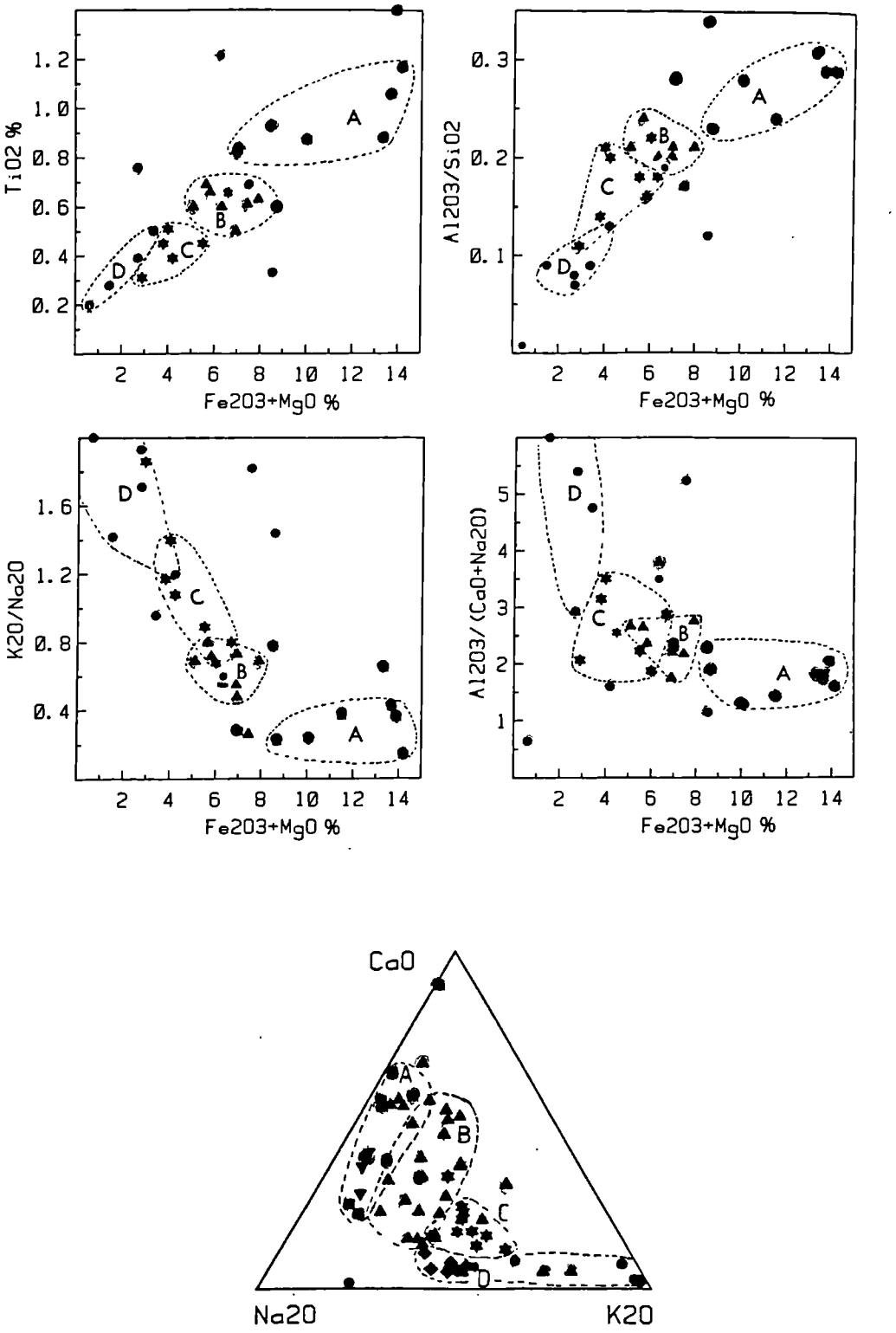

Figure 3.26 Bivariate plots for sandstones from different provenances with redefined provenance fields.

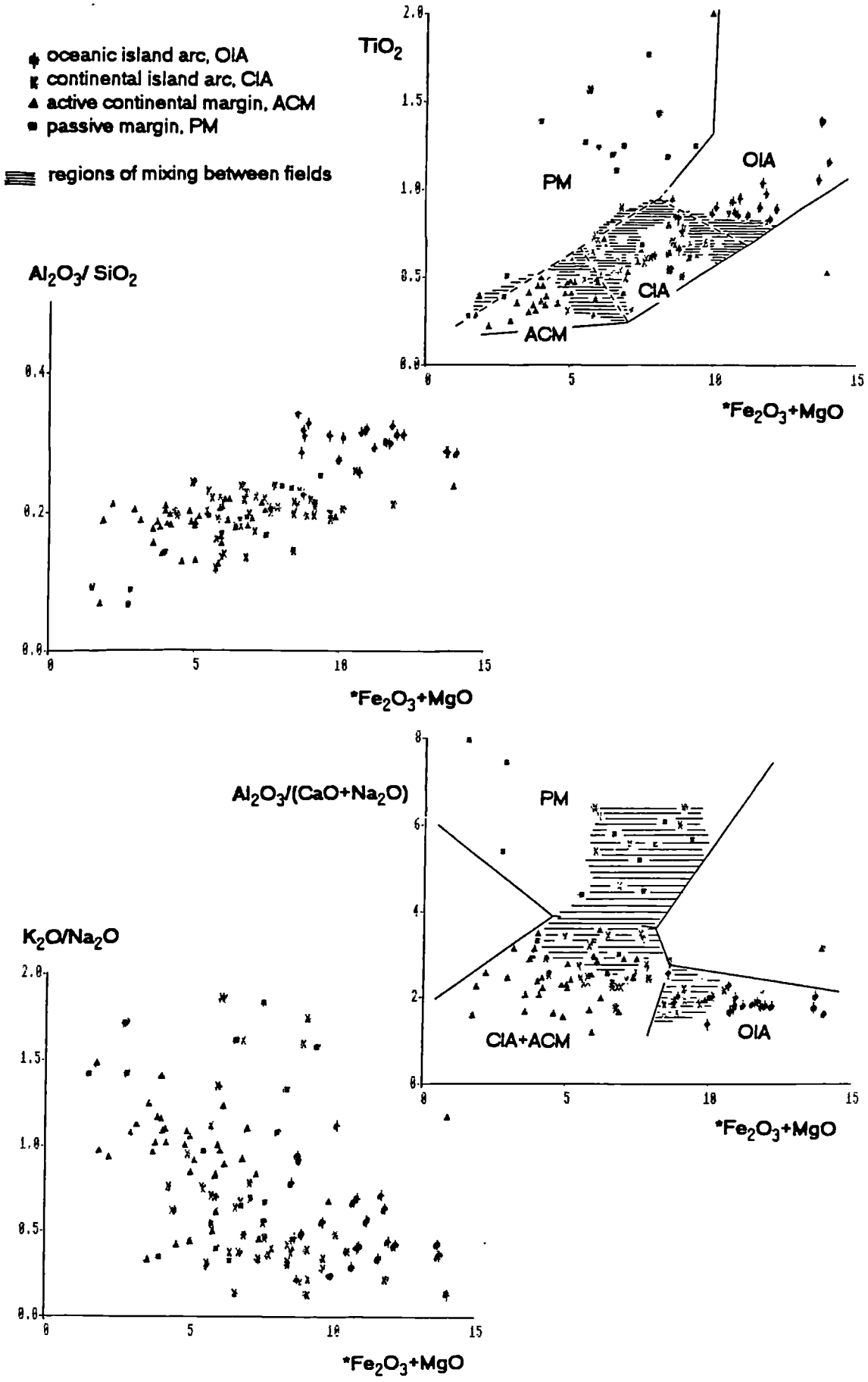

Figure 3.27 $*Fe_2O_3$+MgO vs TiO_2 for Skiddaw Group sandstones (a) by formation and (b) by location. $*Fe_2O_3$ is total iron as Fe_2O_3. OIA=oceanic island arc, CIA=continental island arc, ACM=active continental margin, PM=passive margin.

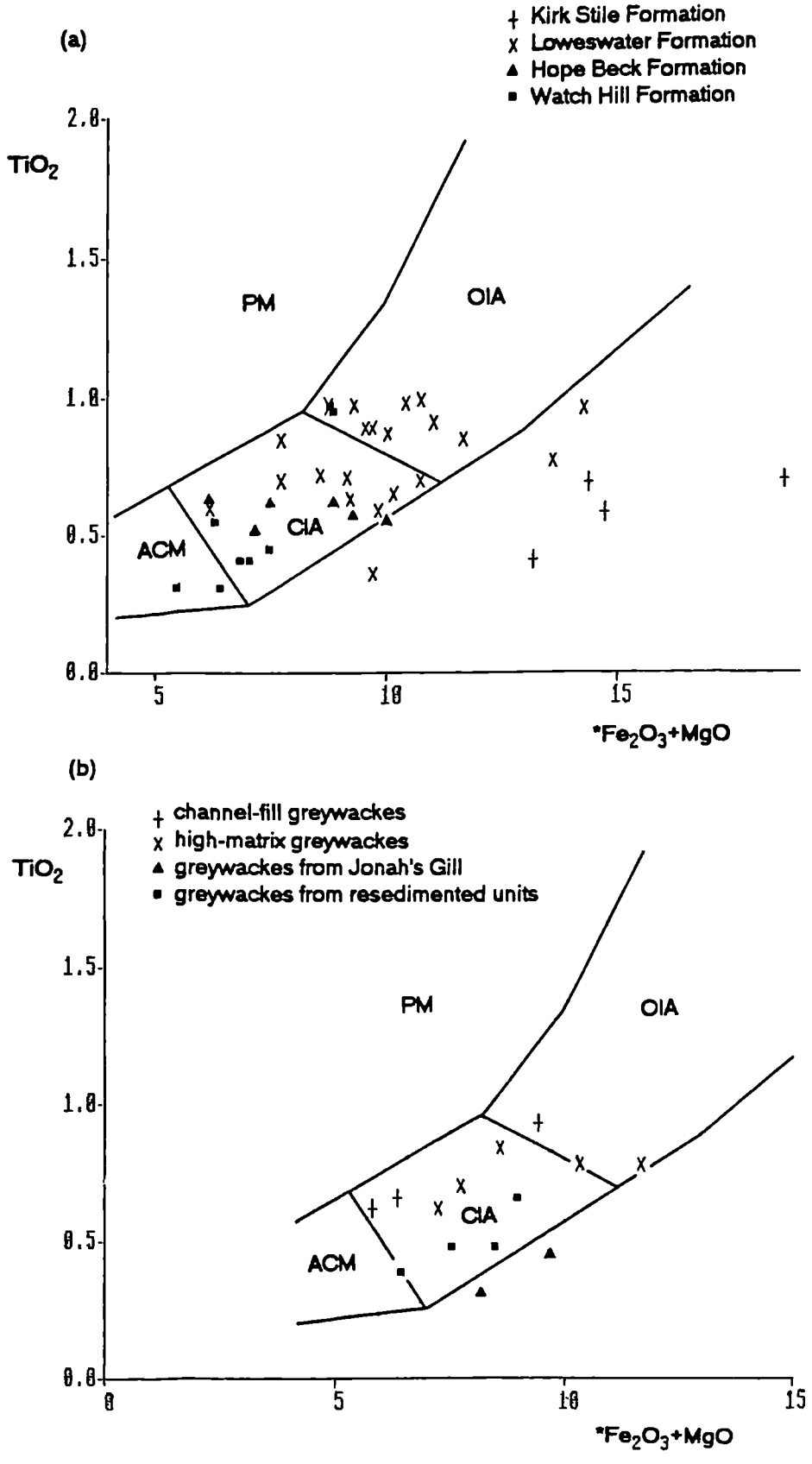

3.3.5 The SiO_2 vs K_2O/Na_2O discriminant plot

3.3.5.1 Background

Crook (1974) showed that the greywackes associated with the three distinct types of continental margins of Mitchell and Reading (1969) have characteristic compositions (table 3.15).

Table 3.15 Characteristic compositions of different types of continental margin (after Crook, 1974).

greywacke type	% quartz	% silica	K_2O/N_2O	continental margin
quartz-rich	> 65 %	89 %	> 1	Atlantic type
quartz-intermediate	15 - 65 %	68 - 74 %	< 1	Andean type
quartz-poor	<15 %	58%	<<1	magmatic arc

The concept was supported by Schwab (1975) who considered the same parameters in a wide data set of greywackes and sandstones, including modern sands, but called for more modern sand analyses to confirm the classification. Modern deep-sea sand compositions were studied by Maynard et al (1982) who doubted whether bulk chemistry would distinguish between arc related settings in ancient rocks.

The investigation of silica content and K_2O/Na_2O ratio was extended to include mudstones by Roser and Korsch (1986). They presented a discriminant plot for analyses recalculated to 100% volatile-free with three fields:

> *Passive continental margin* (PM) - quartz-rich sediment derived from stable continental areas deposited in sites away from active plate boundaries. It is equivalent to the modern trailing edge of Maynard et al (1982).
>
> *Active continental margin* (ACM) - quartz-intermediate sediment derived from tectonically active continental margins on or adjacent to active plate boundaries. It may include continental margin magmatic arcs, uplifted areas in strike-slip settings, or deeply dissected magmatic island arcs.
>
> *Oceanic island arc* (ARC) - quartz-poor volcanogenic sediments derived from oceanic island arcs.

Figure 3.28 for the refined data set (appendix 4d) shows many of the *passive margin* samples to plot in the *active continental margin* field. This suggests the *passive margin* field is not adequately represented by these data (which include only 14 analyses compared with 32 of Roser and Korsch (1986)), which should be considered when interpreting other discriminant diagrams.

Figure 3.28 SiO_2 vs K_2O/Na_2O plot for greywackes of differing provenances with provenance fields from Roser and Korsch (1986). ARC=island arc, ACM=active continental margin, PM=passive margin.

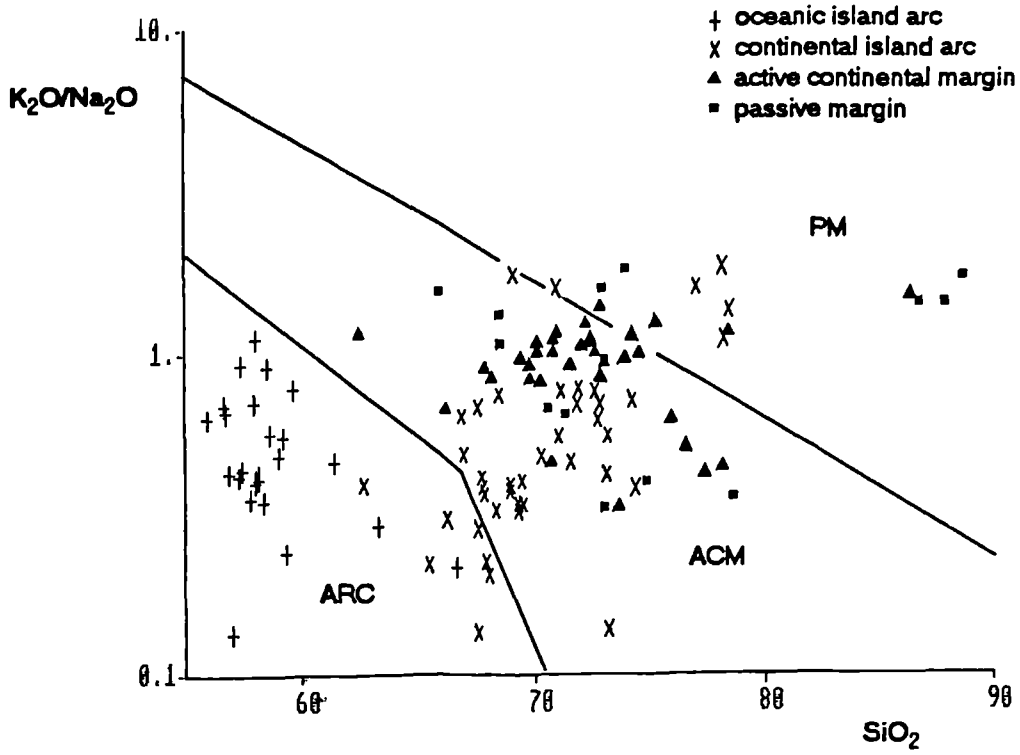

Figure 3.29 SiO_2 vs K_2O/Na_2O plot for Skiddaw Group samples, with provenance fields after Roser and Korsch (1986). ARC=island arc, ACM=active continental margin, PM=passive margin.

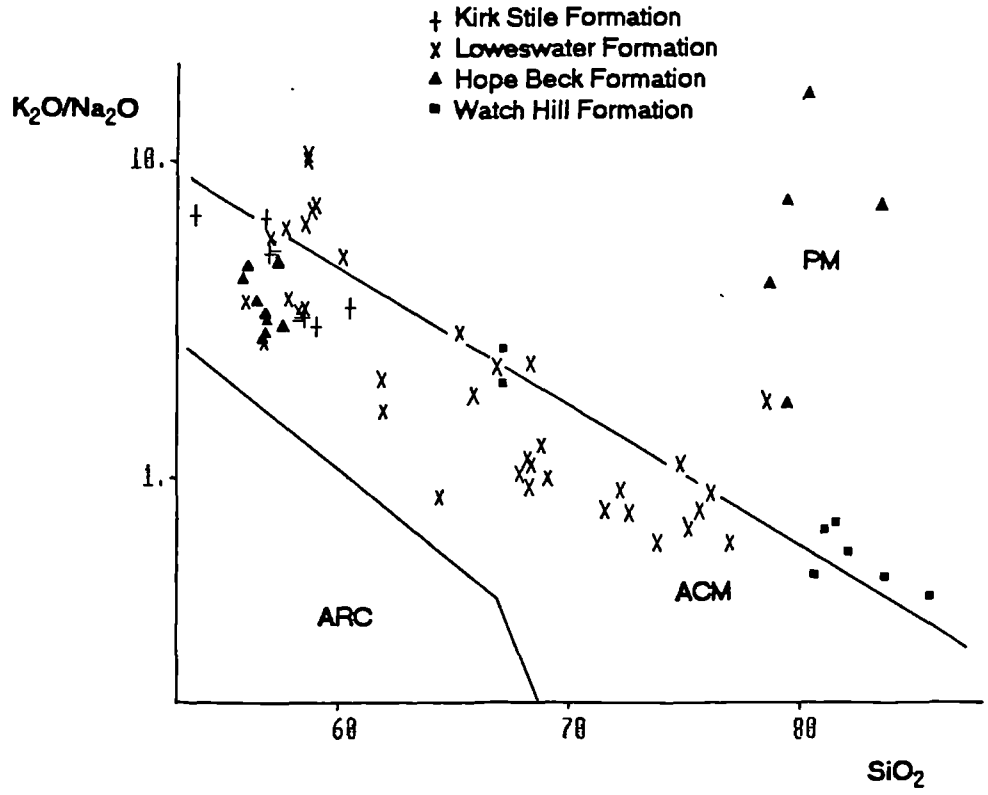

3.3.5.2 Problems

The ratio K_2O/Na_2O in ancient sediments will not remain constant from deposition due to the mobility of these elements. In addition the K_2O content of Lower Palaeozoic sediments, especially mudstones, is anomalously high (see section 3.3.3.2) hence comparison with younger sediments should be treated with caution.

Despite these reservations, the discriminant diagram was defined using many Lower Palaeozoic samples and has been shown to be successful (Roser and Korsch, 1986).

3.3.5.3 Application to the Skiddaw Group

Figure 3.29 shows Watch Hill Formation samples plotting along the boundary between *active continental margin* and *passive margin* thus the systematic variation due to grainsize parallels the boundary. Most Loweswater Formation sandstones fall in the *active continental margin* field along with most mudstone analyses. The high-matrix types do not plot distinctively. Hope Beck Formation sandstones plot in the *passive margin* field, due to their low Na_2O contents, as would Kirk Stile Formation sandstones (not shown since their Na_2O content is zero). This could be caused by removal of Na_2O since deposition. Petrographical observations (section 3.2.4.6) indicate very little plagioclase present which might suggest the Na_2O content was controlled by provenance.

The mudstones from each formation plot in a tight group mainly in the *active continental margin* field. This could indicate there is no secular variation in provenance or alternatively that major element contents of mudstones have been homogenized. The latter is favoured (see discussion in section 3.3.2).

Figure 3.30 SiO_2 vs K_2O/Na_2O plot for specific greywacke types of the Loweswater Formation and from resedimented units, with provenance fields after Roser and Korsch (1986). ARC=island arc, ACM=active continental margin, PM=passive margin.

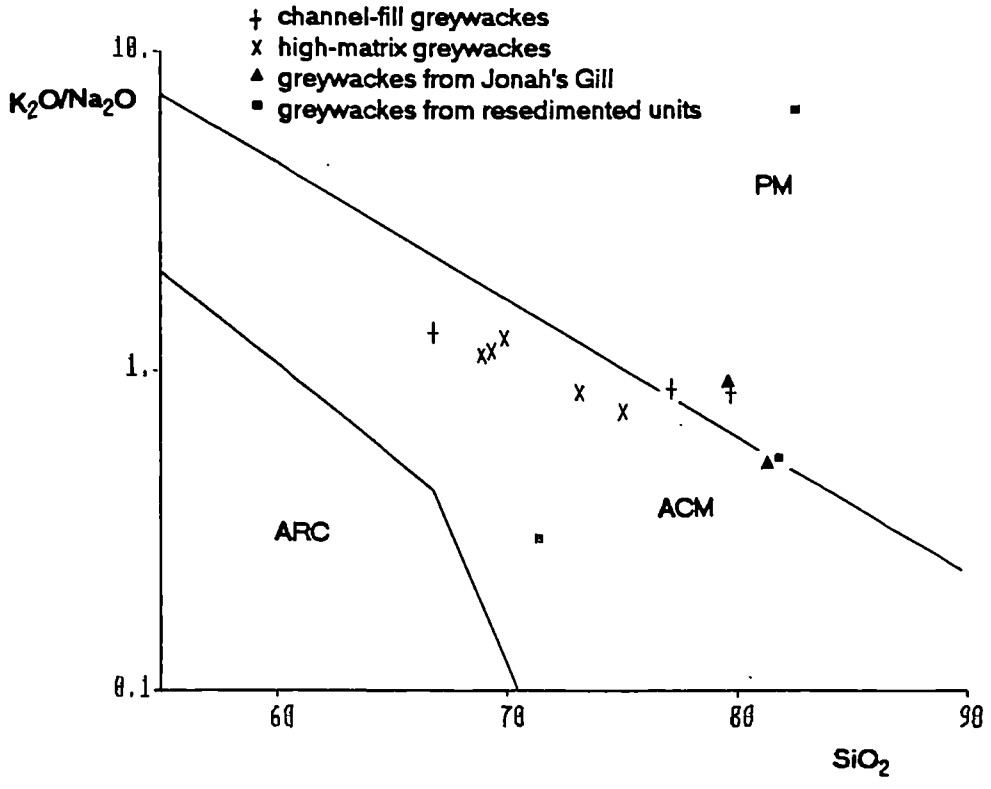

Samples from the sandstone rafts of the Buttermere Formation at Goat Gills [NY 1910 1645] and Causey Pike [NY 2195 2075], classified by the discriminant function (section 3.3.3.5) as belonging to the Hope Beck and Watch Hill formations respectively, plot in the *passive margin* field adjacent to other sandstones of the Hope Beck Formation (figure 3.30). A *second* sample from Goat Gills, indicated by discriminant function analysis to be most similar to the Watch Hill Formation, plots with the Watch Hill Formation sandstones. The clast from the Beckgrains Bridge debris flow plots in the *active continental margin* field, consistent with Loweswater Formation sandstones.

3.3.6 Trace elements in provenance discrimination

3.3.6.1 Introduction

Specific trace elements have been used successfully in provenance determination of sedimentary rocks due to their relative immobility compared to the major elements. They are fractionated by igneous processes enabling different source regions to be distinguished on variation diagrams. Elements with low ocean residence times can be considered immobile in the sedimentary environment so their abundances in sedimentary rocks will accurately reflect their source. An appreciation of trace element mobility in diagenesis and metamorphism and behaviour of the host minerals should be maintained when considering provenance of ancient sediments. The more stable trace elements are Ti, Hf, Th, Sc, Ta, Y, Zr, Nb and the rare earth elements (Bhatia and Taylor, 1981; Bhatia and Crook, 1986). The rare earth elements are largely dealt with separately (see section 3.3.7). Mobility of large ion lithophile elements, transition elements and high field strength elements in the Skiddaw Group was discussed in section 3.3.2, considering constancy of inter-element ratios.

3.3.6.2 Variation diagrams

A set of provenance discrimination diagrams for greywackes was developed by Bhatia and Taylor (1981) and Bhatia and Crook (1986) using the elements La, Ce, Nd, K, U, Th, Sr, Ba, Co, Ni, Cr, V, Sc, Ti, Zr, Y, Nb, Hf. They were defined using data from Australian greywackes of four provenance types, described in section 3.3.3.3.

The plot Th-Zr (figure 3.31) is most useful in distinguishing the *active continental margin* provenance setting, with a low Zr/Th ratio (average Zr/Th= 9.5). Skiddaw Group sandstones have higher ratios and greater abundance of Th and Zr than the *oceanic island arc* setting, hence a *continental island arc* or *passive margin* source is implicated. V and Sc are successful in separating the *passive margin* setting since they are ferromagnesian trace elements with high abundances in mafic sources. The channel-fill and high matrix greywackes of the Loweswater Formation correspond to an arc provenance but the Jonah's Gill sandstones have lower abundances suggesting more than one source for the Loweswater Formation (figure 3.32).

The triangular plots Th-Sc-Zr and Th-Co-Zr indicate *continental island arc* provenance for all Skiddaw Group greywackes (figure 3.33).

Figure 3.31 Th vs Zr for Skiddaw Group sandstones.

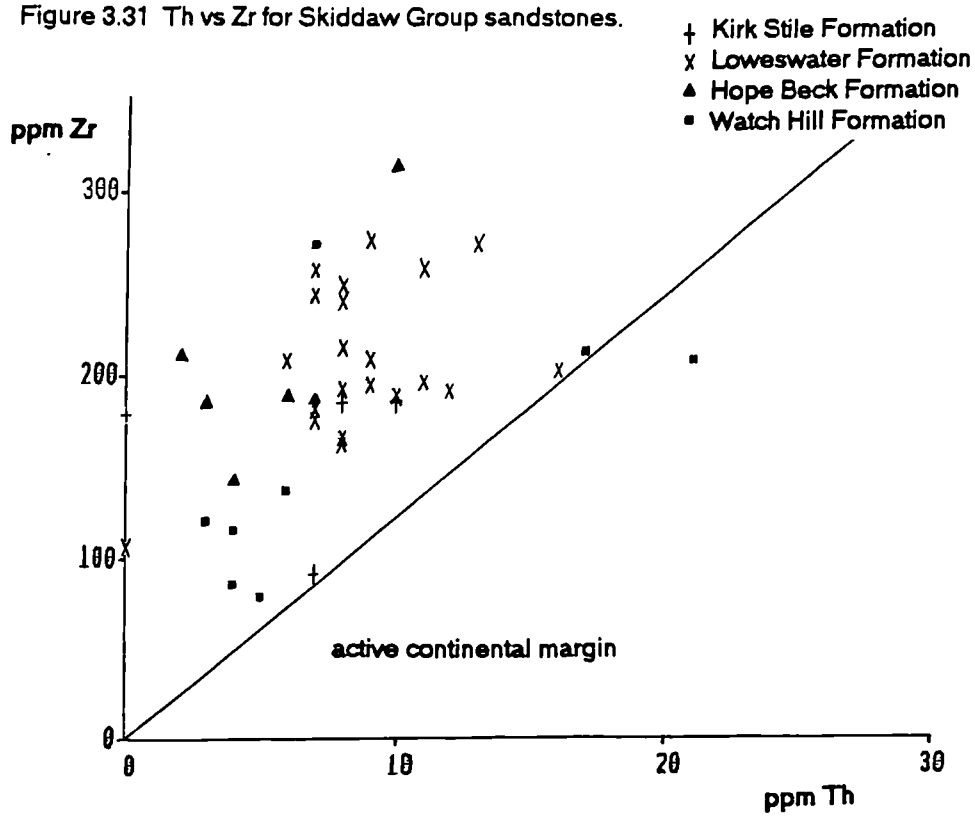

Figure 3.32 Sc vs V for Loweswater Formation sandstones. Fields are interpreted from the data of Bhatia and Crook (1986); AM = active margin, PM = passive margin.

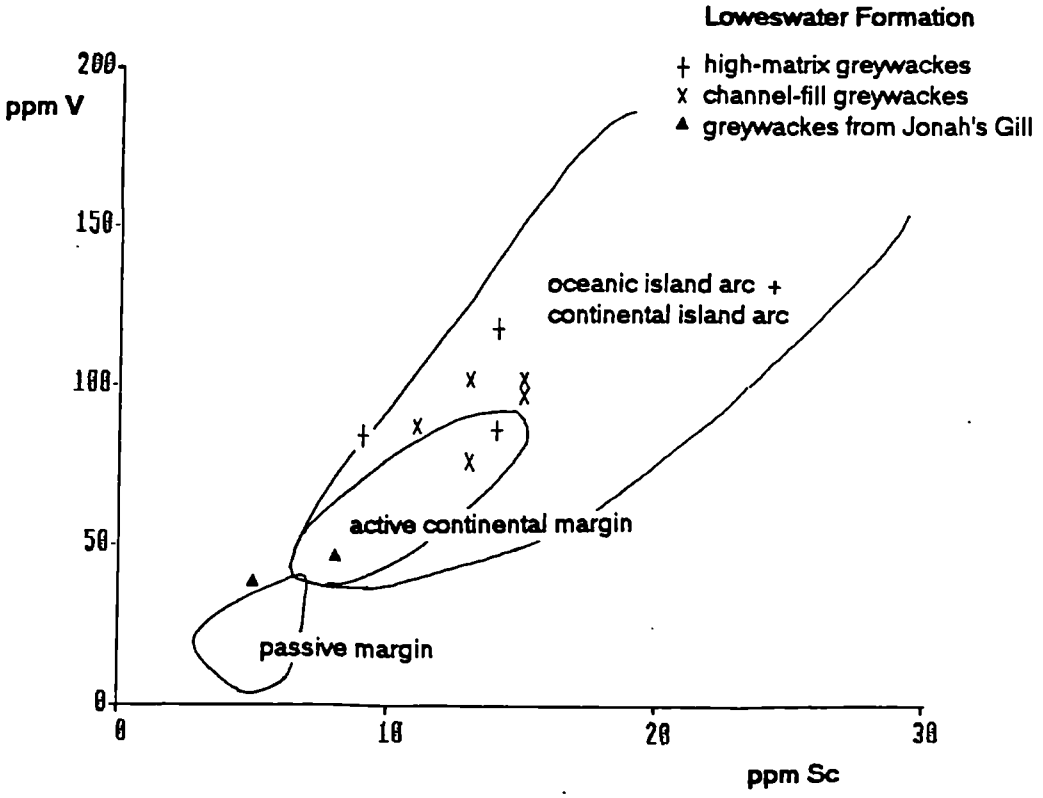

Figure 3.33 (a) Th-Sc-Zr for Loweswater Formation sandstones and (b) Th-Co-Zr for Skiddaw Group sandstones with provenance fields redrawn from the data of Bhatia and Crook (1986). OIA=oceanic island arc, CIA=continental island arc, ACM=active continental margin, PM=passive margin.

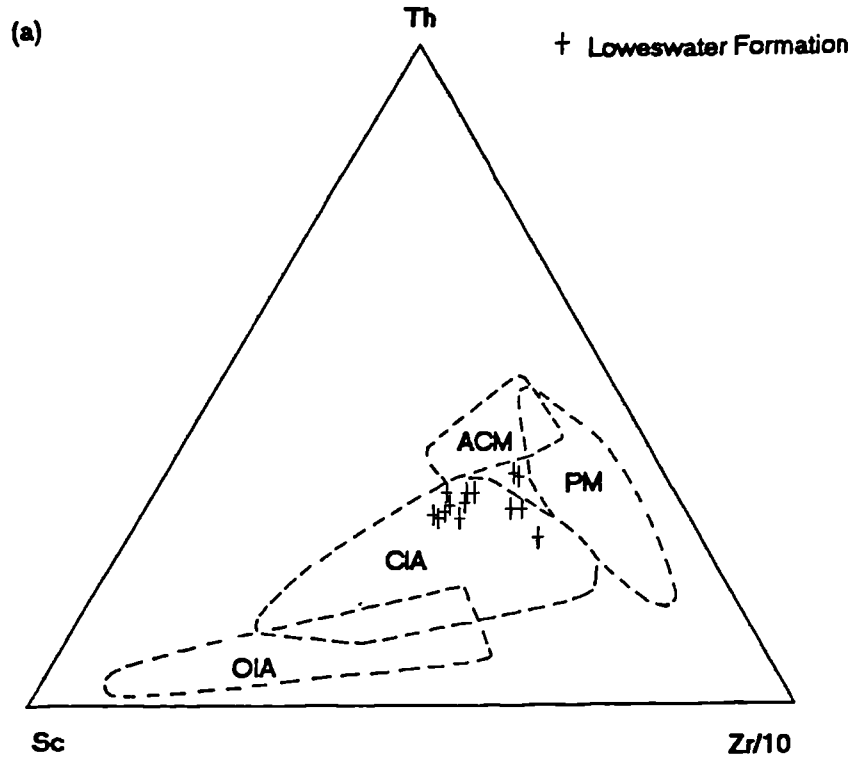

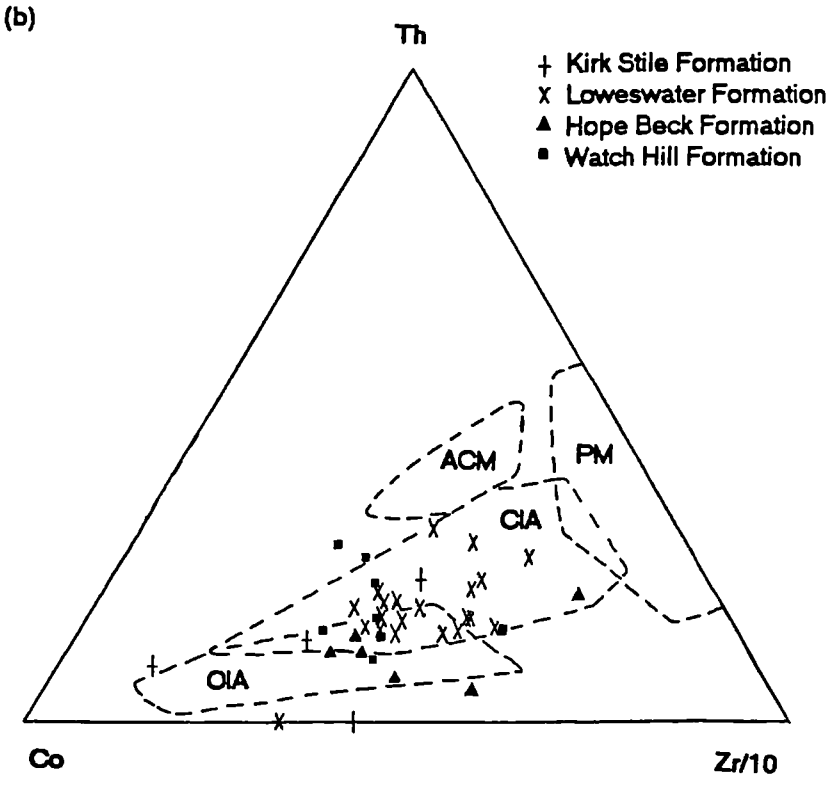

La and Th show low correlation coefficients (table 3.12), suggesting element mobility, for each formation except the Watch Hill Formation which may have experienced less alteration. The ratio La/Th generally lies between 2 and 5, indicating volcanic arc influence. U and Th do not show a strong positive correlation (table 3.12) so are not considered reliable provenance indicators.

Source rock composition can be interpreted from a plot of Rb versus K (Floyd and Leveridge, 1987) (figure 3.34). These elements are strongly correlated in all formations in both sandstones and mudstones. The Watch Hill Formation has a different K/Rb ratio from other formations, but all have a ratio near to K/Rb=230, which is typical for a differentiated magmatic suite (Shaw, 1968), implying a source of eroded basic to acidic magmatic rocks. Alternatively, the coherence of K and Rb could be a result of redistribution of these elements by hydrothermal fluids, which must be considered a possibility as the volcanic arc of the Borrowdale Volcanic Group was sited adjacent to or above these sediments in Caradoc times. Considering the sandstones, acidic and intermediate sources are indicated for most samples (figure 3.34b). The coarsest Watch Hill Formation sandstones imply a basic source component, but this may be a grainsize effect, demonstrated by the channel-fill sandstones which have lower K and Rb abundances in coarser samples but maintain a constant K/Rb ratio. This is not the case for the Kirk Stile Formation samples which are of fine and very fine sand. Their position indicates a source component of basic composition mixed with an acidic type.

Similar provenance fields were defined on a Ni versus TiO_2 plot for greywackes by Floyd et al (1989,1991) (figure 3.35). The Skiddaw Group is from an acidic source. The diagram is successful in separating each formation, reflecting compositional differences. The Loweswater Formation is again shown to have more than one sandstone composition with Jonah's Gill samples plotting with the Watch Hill Formation, but high-matrix types are not distinct from other Loweswater Formation samples.

Figure 3.34 Rb vs K for the Skiddaw Group with K/Rb=230 representing a differentiated magmatic suite (Shaw, 1968). (a) for sandstones and mudstones, (b) for sandstones.

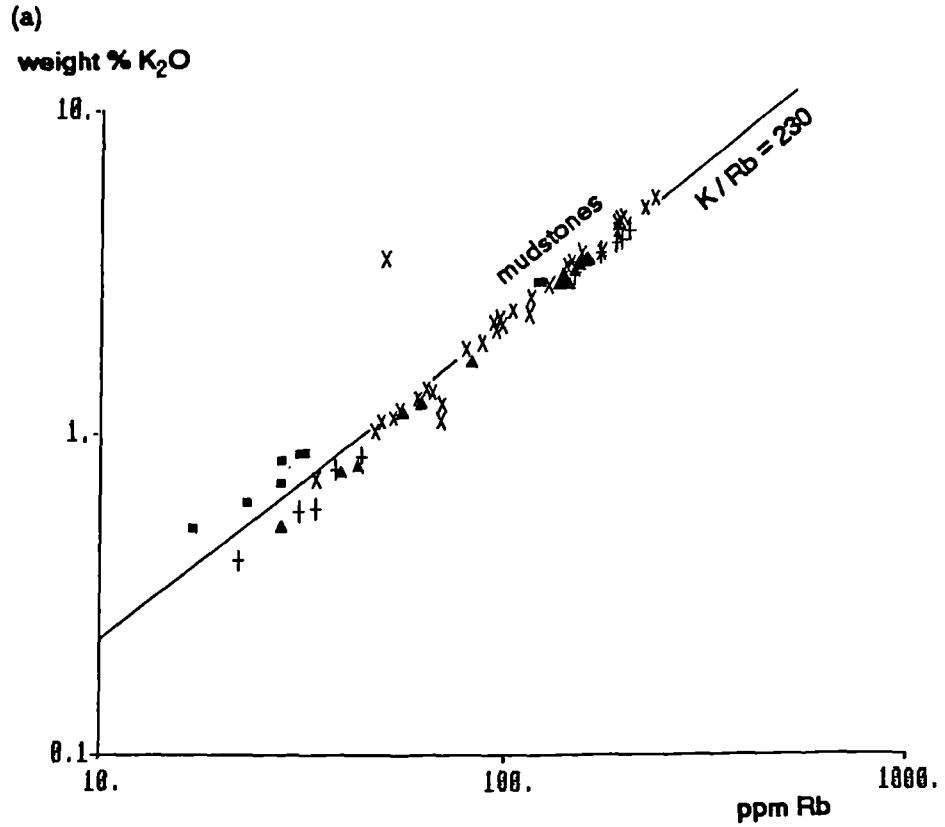

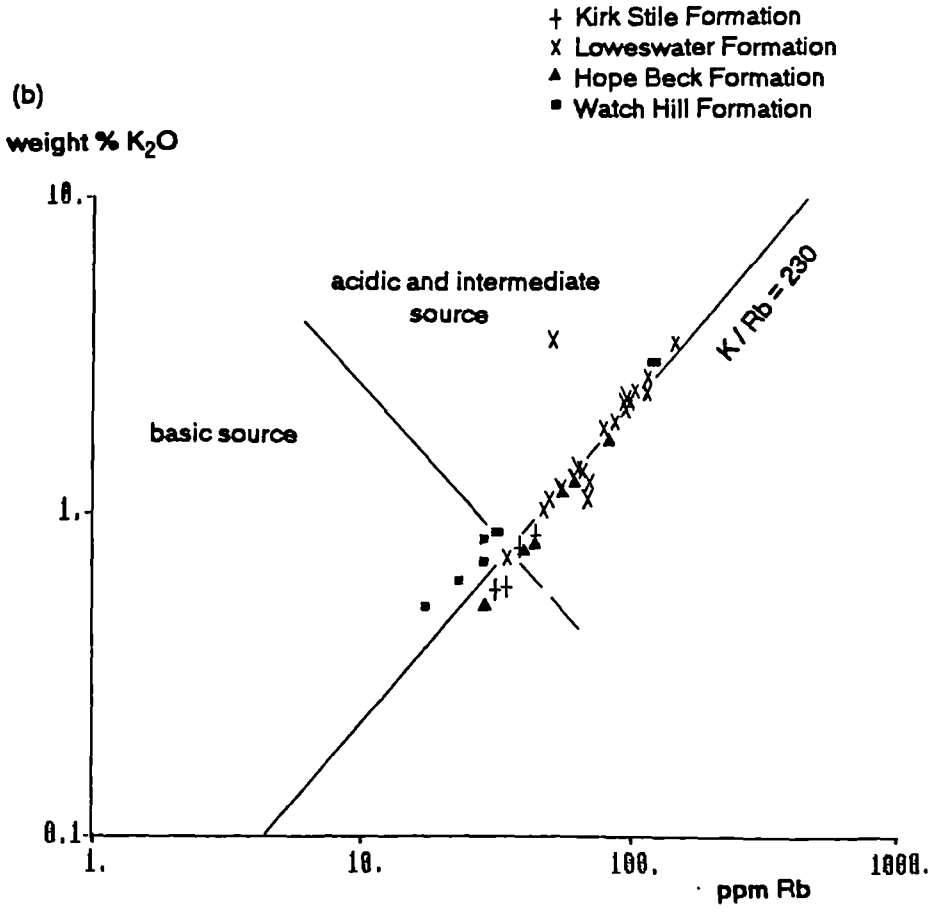

Figure 3.35 Ni vs TiO_2 for (a) Skiddaw Group sandstones, (b) components of the Loweswater Formation.

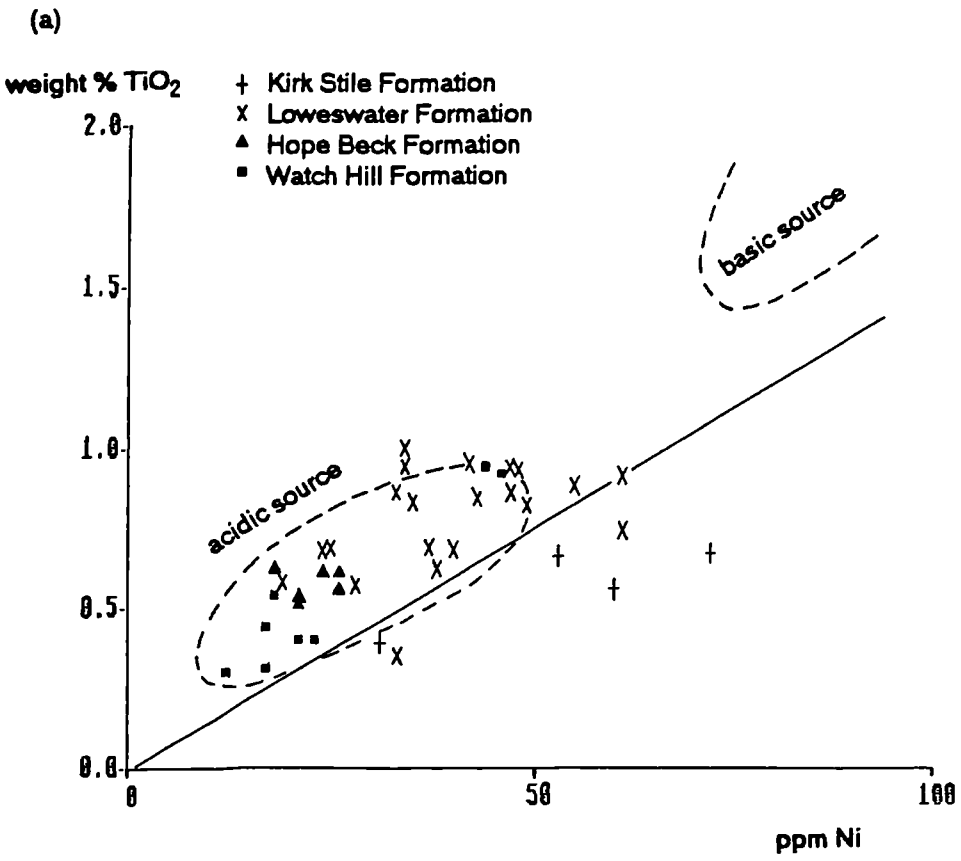

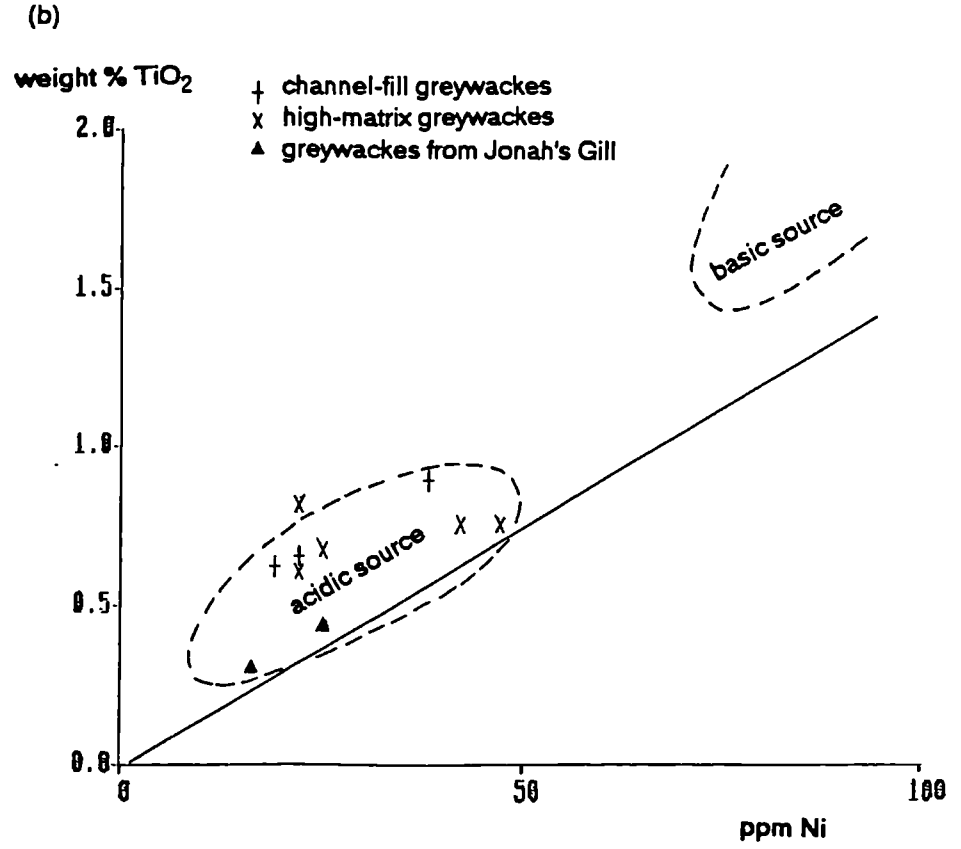

3.3.6.3 Trace elements in mudstones

The provenance and tectonic setting of ancient mudrocks was investigated by Bhatia (1985b). He suggested the immobile trace elements (e.g. La, Th, Nb, Y, Zr, Sc) faithfully preserved source rock signatures and he presented average values of the most discriminating trace element parameters for four tectonic settings (table 3.16). The same parameters were considered for the Skiddaw Group and no significant variation existed between the formations, hence averaged values for the whole group are given in table 3.16.

Table 3.16 Trace element characteristics of mudrocks from various tectonic settings (after Bhatia, 1985b, table VI) and average for Skiddaw Group mudstones (n=30).

	Oceanic island arc	Continental island arc	Active continental margin	Passive margin	Skiddaw Group
Th	5.5	16.2	28.0	22.0	12.7
U	2.4	3.2	6.0	3.6	3.6
Nb	3.7	9.0	16.5	15.8	20.0
Th/U	2.8	5.2	5.0	6.7	4.0
Zr/Th	28	12	7	7	15
Zr/Nb	38	21	11	10	9
Nb/Y	0.17	0.35	0.50	0.54	0.50
La	18	24	42	34	50
La/Sc	1.0	1.8	2.5	1.9	-
Cr	39	55	58	100	129
Ni	15	18	26	36	56
Sc/Ni	1.70	0.96	0.75	0.45	-
Rb/Sr	0.29	1.31	2.90	5.80	1.19
Ba/Sr	2.5	6.3	8.7	17.6	5.7

The abundances and ratios compare with *continental island arc* (Th, Zr/Th, Rb/Sr, Ba/Sr), *active continental margin* (Nb, Th/U, Nb/Y, La) and *passive margin* (U, Zr/Nb, Cr, Ni) provenance. The average Nb abundance for the Skiddaw Group is high which influences the ratios Zr/Nb and Nb/Y and these parameters correspond to an *active continental margin* or *passive margin* source. The high La and Cr values indicate *active continental margin* and *passive margin* provenances respectively. La abundance is governed by adsorption onto phyllosilicates, with high values resulting from prolonged weathering, transportation or recycling; typical for a passive margin source.

McCann (1991) expressed reservations in using the model of Bhatia (1985b) on the grounds that the data set was restricted to Australian basins and was too small (n=23) to define provenance fields, the geochemical history of the sediments had not been appreciated and certain elements (Rb, Sr, Ba) are not reliable indicators of provenance. Despite these reservations the discriminatory parameters are consistent throughout the Skiddaw Group samples. In addition the technique was defined using data from Lower Palaeozoic basins and thus may have more validity for samples of that age than methods that utilise younger Phanerozoic or modern data.

In conclusion the Skiddaw Group mudstones indicate a volcanic arc provenance with a *passive margin* influence. Such a scenario may occur through mixing of juvenile arc detritus and mature sediment in a back-arc basin or erosion and recycling of a 'palaeo' volcanic arc on a non-volcanic continental margin.

3.3.6.4 Multi-element variation diagrams

Upper continental crust-normalised multi-element patterns were defined by Floyd et al (1991) for four tectonic environments using trace element data from Proterozoic and Phanerozoic greywackes worldwide. The tectonic environments are: *oceanic island arc, continental arc and active continental margin, passive margin* and *oceanic within-plate* (ocean islands and seamounts). Substantial overlap between the separate *continental arc* and *active continental margin* fields of other authors (e.g.Bhatia, 1983) and recognition of the complex tectonics on convergent margins (Van de Kamp and Leake, 1985) prompted amalgamation of these two settings. The elements are arranged from right to left in order of increasing ocean residence times and comprise a relatively stable group, Th to Ta, and a more mobile group, Ni to K. The averaged patterns for each setting are shown in figure 3.36. Floyd et al (1991) describe four important features of the patterns:

a) all patterns show negative Nb-Ta anomalies, which can be quantified by the Nb/Nb* ratio (normalized Nb abundance divided by the normalized Nb abundance calculated by extrapolation between Ni and Ti). Sediment from sources with subduction-related magmatic rocks show an anomaly of *c* 0.15-0.30, contrasting with passive margin sources with low mafic input (Nb/Nb*= *c.* 0.5);

b) positive V-Cr-Ni-Ti-Sc anomalies indicate mafic input, with only the passive margin source showing depletion;

c) only the passive margin source shows a positive Ti-Hf-Zr-Y anomaly reflecting a heavy mineral input (mainly zircon);

d) the soluble elements (Ba-K) with normalised values <1 become less abundant with increasing ocean residence time, although Sr and P peaks indicate mafic input.

The shape of the patterns from the oceanic sources are similar, as are the patterns from the continental sources. It is the size of the anomalies described above that distinguish the settings. It is therefore important to appreciate the variation that can exist within a single bed. Figure 3.37 shows normalised plots for each Bouma unit, Tabc, and the mudstone of a single turbidite of the Loweswater Formation. Significant variation in total abundance and size of anomaly exists between the sandstone units (of fine to very fine sand grainsize) and between these and the mudstone. Thus it is imperative to compare only samples of the same grainsize deposited under similar flow conditions.

In addition, use of averages in this type of diagram can be very misleading if more than one compositional type exists in a group, as the resulting shape of the curve will not correspond to the sample composition. A plot was constructed, therefore, for each sandstone analysis to determine the range of compositions before samples in any particular group were averaged. Patterns for both individual analyses and formation averages are presented (figure 3.38).

Within each formation the greatest variation occurs in the mobile group of elements, commonly large ion lithophile elements, whose mobility was discussed in the previous section. Other variability can be attributed to grainsize and sorting. There is a general similarity between the patterns for each formation, particularly the Watch Hill and Hope Beck formations. They share a similar Nb anomaly (*c.*0.35) which corresponds to a *passive margin* source. This parameter is

Figure 3.36 Multi-element variation diagram with characteristic patterns for different tectonic settings (Floyd et al,1991).

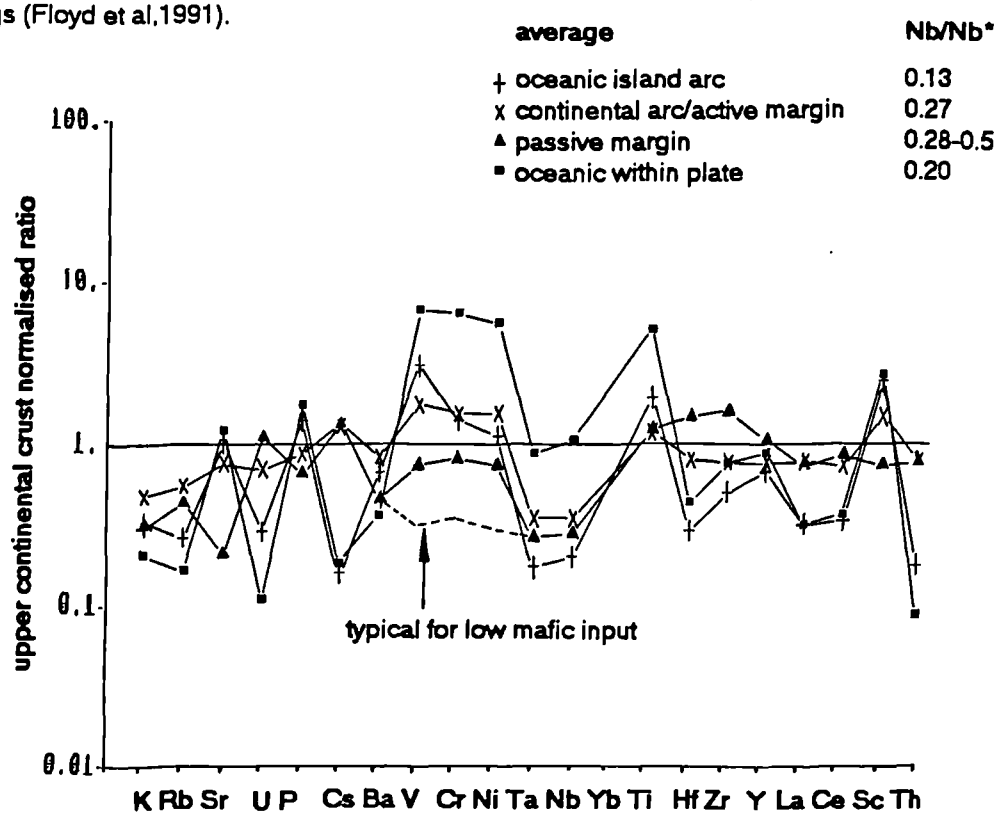

Figure 3.37 Multi-element variation diagram for Bouma units Ta, Tb, Tc and mudstone of a single turbidite of the Loweswater Formation.

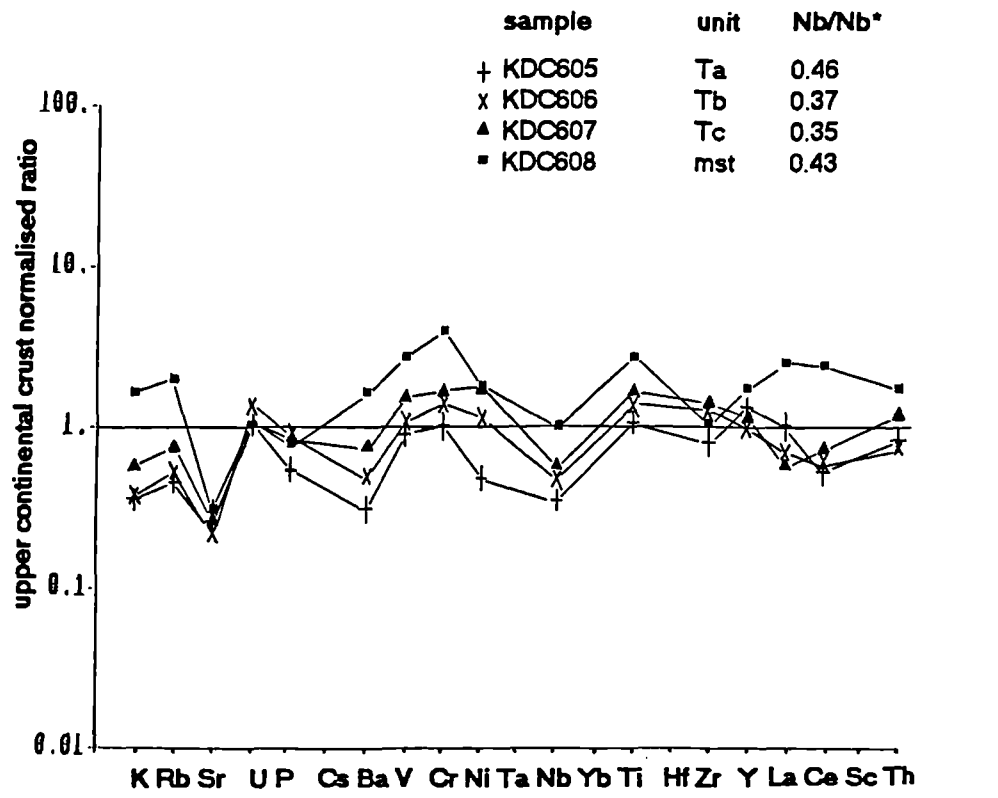

Figure 3.38 Multi-element variation diagrams for Skiddaw Group samples. (a) Sandstone averages for each formation, and representative samples from (b) the Kirk Stile Formation, (c) Loweswater Formation, (d) Hope Beck Formation, and (e) Watch Hill Formation.

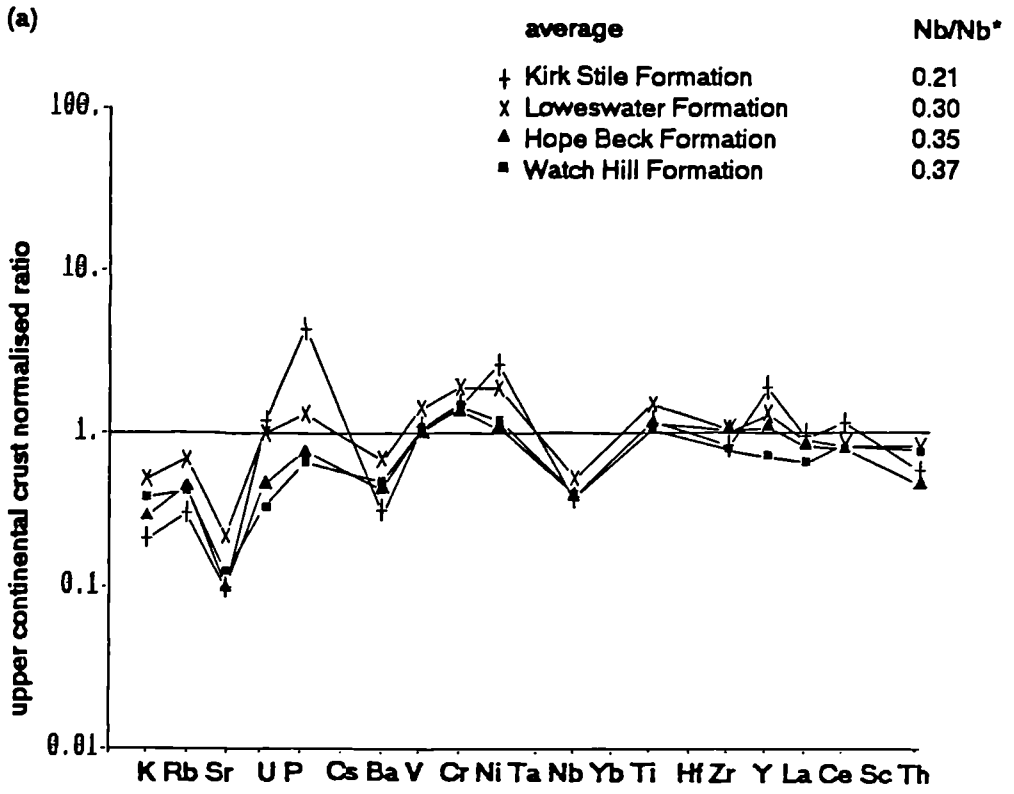

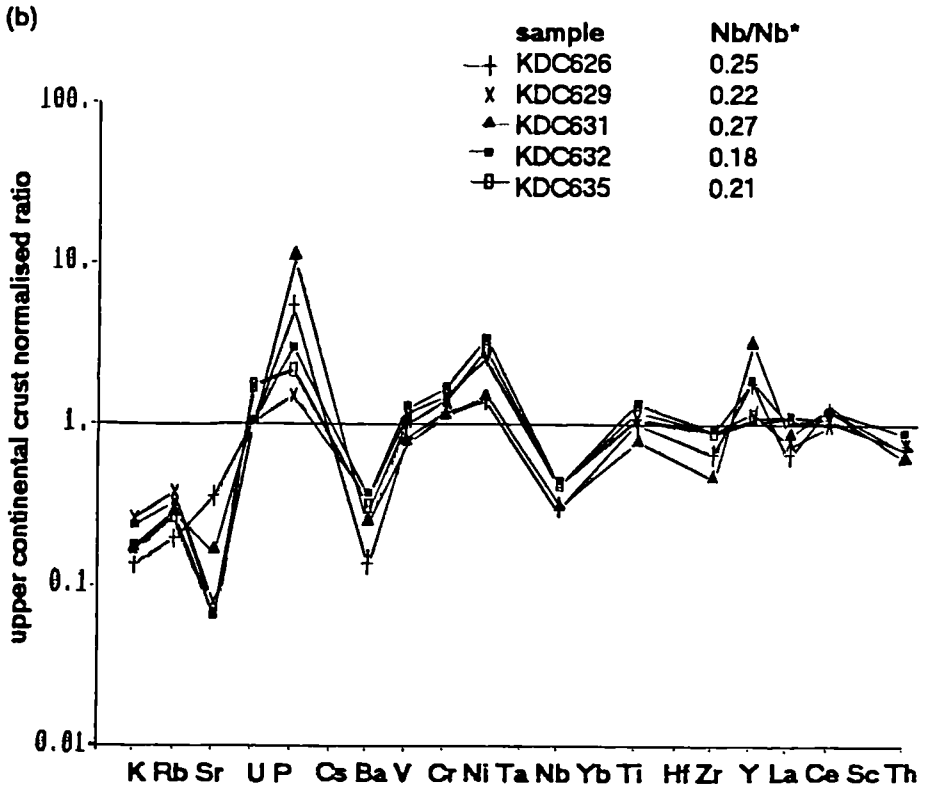

Figure 3.38 (continued) (c) Loweswater Formation, (d) Hope Beck Formation

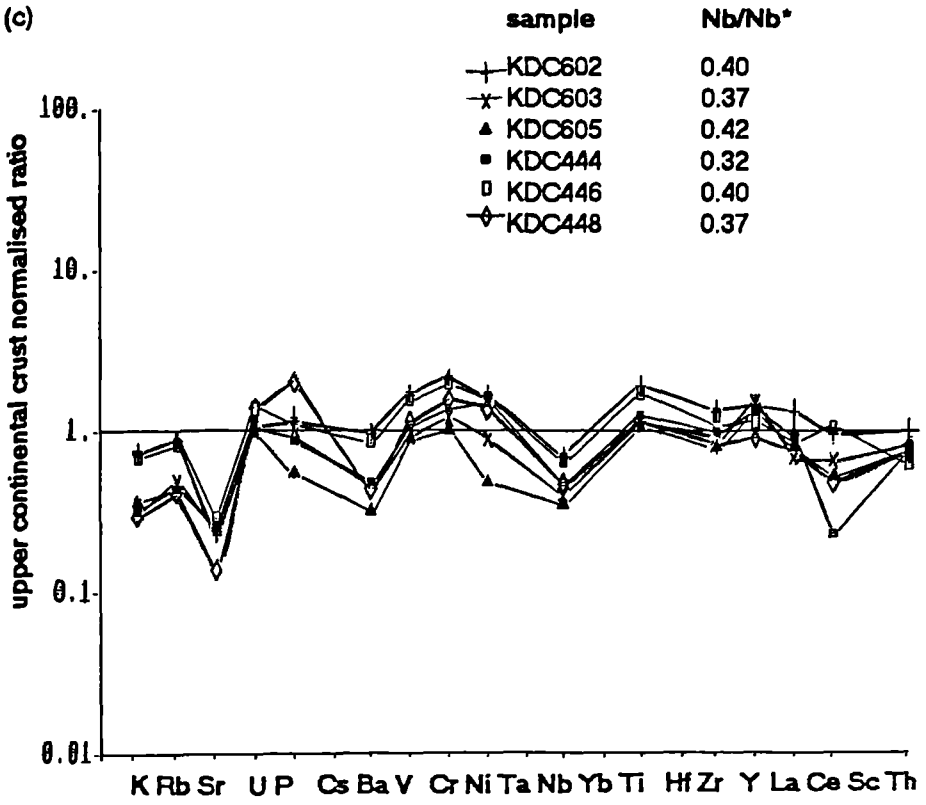

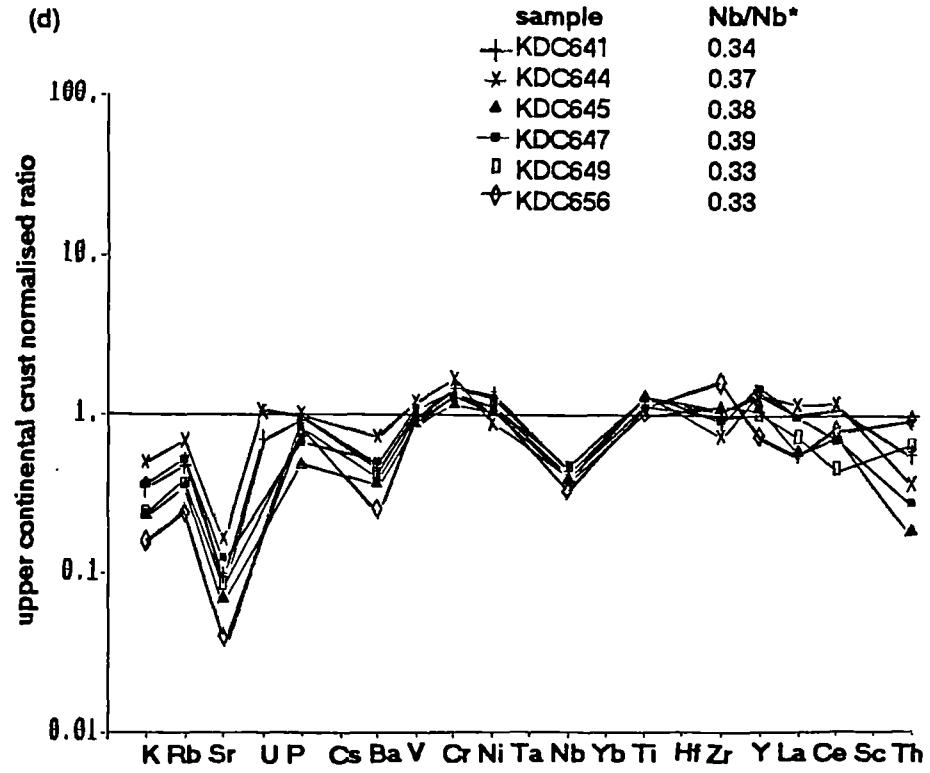

Figure 3.38 (continued) (e) Watch Hill Formation.

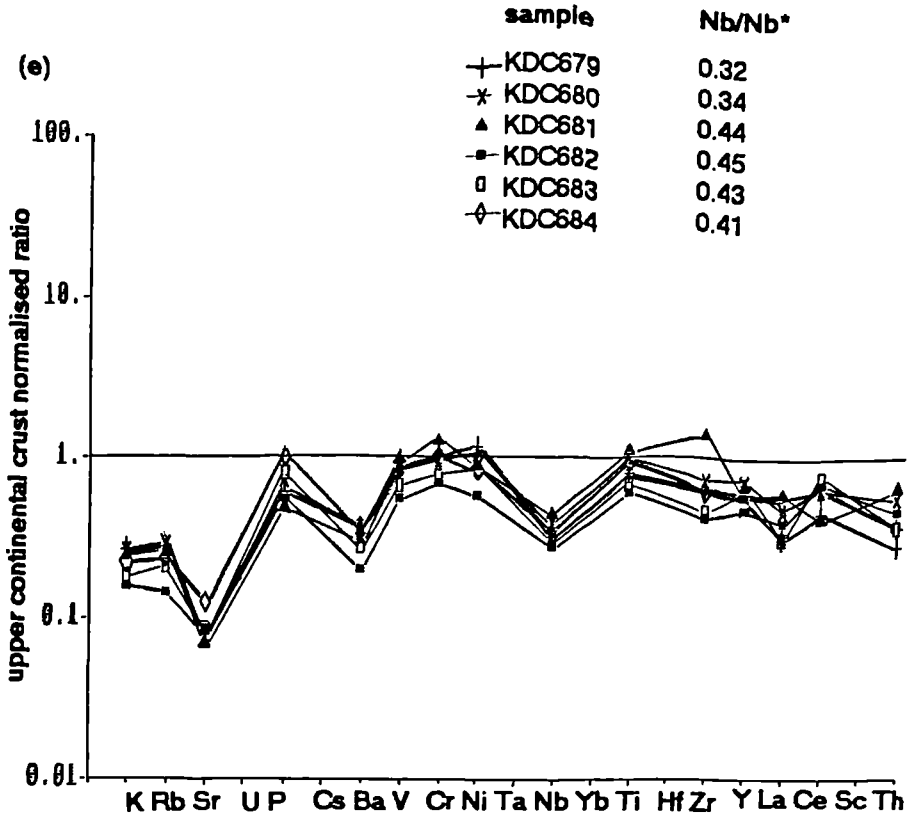

reduced in the Loweswater Formation (average Nb/Nb*=0.30) and is much smaller in the Kirk Stile Formation (average Nb/Nb*=0.21) implying inclusion of a significant amount of mafic detritus. This is supported by the V-Cr-Ni values which are highest in these formations, but correspond to a *continental arc/active margin* source for all formations. The Kirk Stile Formation average displays a P peak, which might indicate mafic input (Floyd et al, 1991).

Within the Loweswater Formation the channel-fill and high-matrix greywackes are similar to other types (figure 3.39). The samples from Jonah's Gill are depleted in almost all elements relative to the formation average due to their high quartz content, but the shape of the pattern is not significantly altered. A small P peak is displayed.

Comparison with the characteristic patterns for each source type is aided if the formation averages are normalised with respect to each source type. A horizontal line on such a diagram would indicate close correspondence. Figure 3.40 shows the average for each formation normalised to the *continental arc/active margin* values and the *passive margin* values respectively. Considering the mobile group of elements, the Skiddaw Group formations are more similar to the *passive margin* setting but correspondence with the *continental arc/active margin* is best in the stable elements. In conclusion, influence from both these source types is inferred and important secular variation is indicated by the introduction of mafic detritus into the Kirk Stile Formation.

Figure 3.39 Multi-element variation diagram for different greywacke types of the Loweswater Formation, (a) high-matrix greywackes, (b) channel-fill greywackes and greywackes from Jonah's Gill.

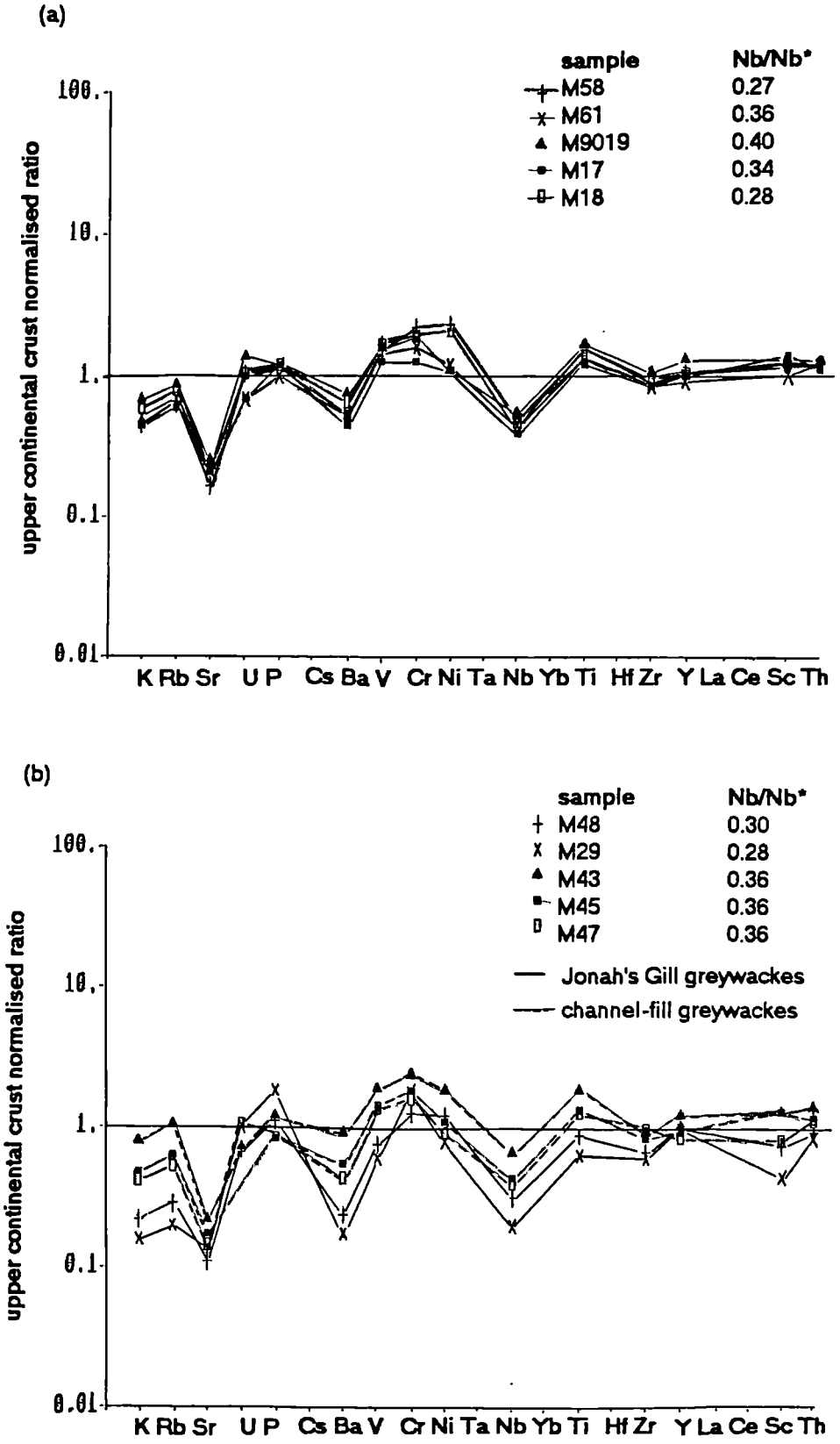

Figure 3.40 Multi-element variation diagram for Skiddaw Group samples normalised with respect to (a) average *continental arc/active margin* values and (b) average *passive margin* values.

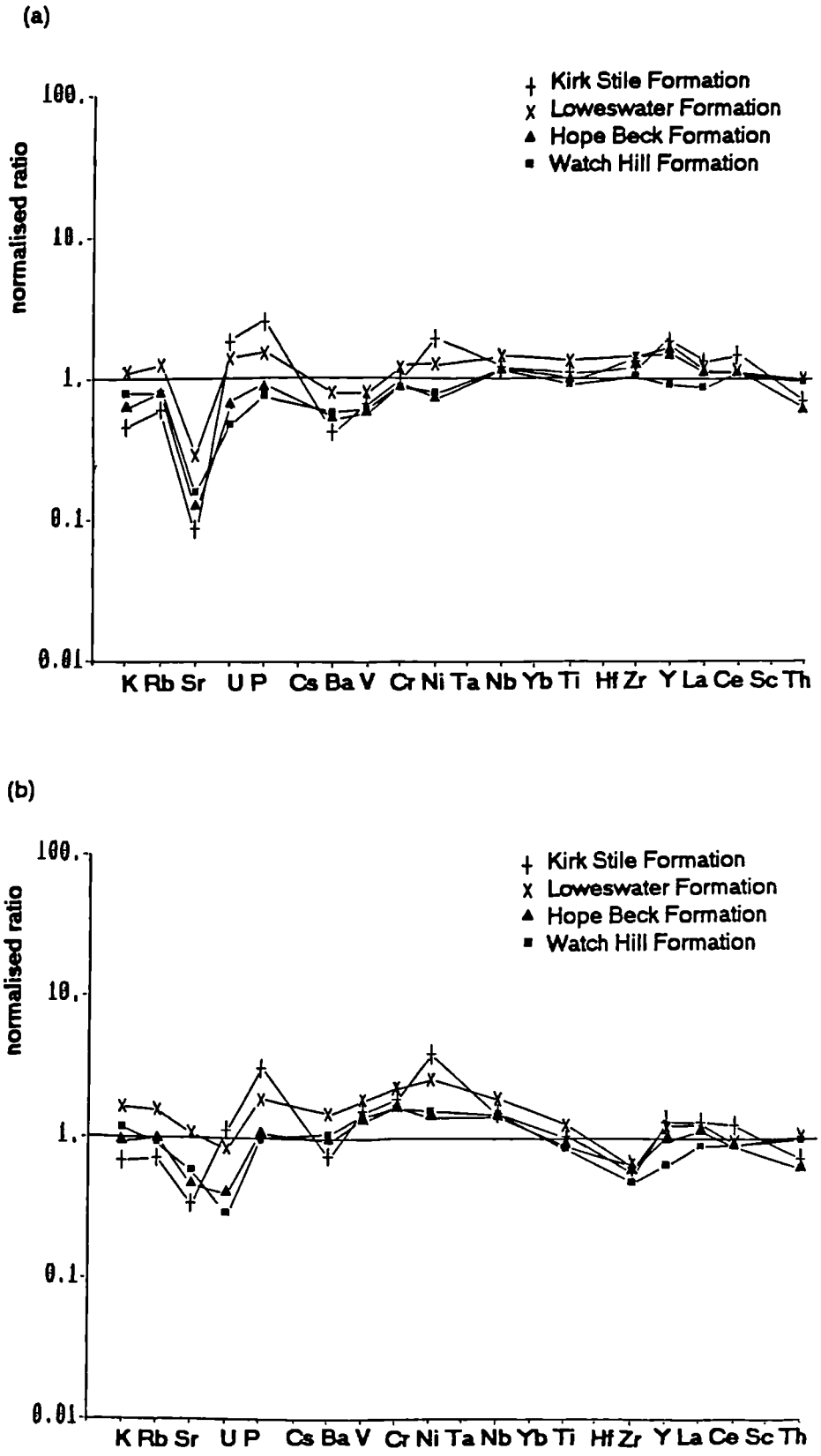

3.3.7 Rare earth elements

3.3.7.1 Introduction

The rare earth elements (atomic numbers 57 - 71) lie in group IIIA of the periodic table and display similar chemical and physical properties. They are:

lanthanum	La
cerium	Ce
praseodymium	Pr
neodymium	Nd
promethium	Pm
samarium	Sm
europium	Eu
gadolinium	Gd
terbium	Tb
dysprosium	Dy
holmium	Ho
erbium	Er
thulium	Tm
ytterbium	Yb
lutetium	Lu

There is a small but steady decrease in ionic radius with increase in atomic number. Elements La to Sm, with lower atomic numbers and masses, are called the light rare earth elements (LREE). Those from Gd to Lu, with higher atomic numbers and masses, are the heavy rare earth elements (HREE). The ratio of LREE to HREE is expressed by the ratio La/Yb such that this value is high when LREE are enriched. Due to their electronic configurations, the REE tend to occur as a group rather than singly. They are lithophile, occurring predominantly in silicate rather than metal or sulphide phases, and dispersed elements, being present in trace amounts in many minerals.

REE abundances of carbonaceous chondrites are used to estimate relative abundances in the solar system and they reveal a rhythmic alternation in abundances of elements of odd and even atomic number. This is due to elements being most stable when both atomic number and mass number are even. This effect is eliminated when presenting data by normalising against a standard. In this study REE abundances in each sample are normalised with respect to type 1 carbonaceous chondrites (Taylor and McLennan, 1985) (appendix 6b). All plots show the REE distribution of the average post-Archaean Australian shale (PAAS) to enable comparisons to be made. This average has been used by Taylor as an approximation to REE abundance in the upper continental crust. It shows LREE to be enriched with respect to HREE.

The REE are particularly useful in petrogenetic studies since they can be fractionated during igneous processes: partial melting, fractional crystallisation and magma mixing. This is due to the variety of types and sizes of cation co-ordination polyhedra in the rock-forming minerals. The variability of their ionic radii allows partitioning of the REE between minerals. The REE substitute for cations of similar radii and charge or of different charge if associated charge-compensating substitutions can occur. Eu and Ce exhibit variable valency, thus commonly have anomalous abundance compared to their neighbours. Eu* is the value indicated by extrapolation between Sm and Gd and the europium anomaly (Eu/Eu*) is an important indicator of petrogenesis.

3.3.7.2 Rare earth elements in rocks

In igneous rocks REE are concentrated in accessory minerals. Sphene, apatite and monazite are LREE enriched. The rock forming minerals contain very small amounts of REE which are most abundant in minerals crystallising early in Bowen's reaction series. Hence abundance in plagioclase > in alkali feldspar > in biotite. There is a large increase in mineral/melt distribution coefficients as melts become more silicic, so late-stage differentiates have high REE abundances.

In sedimentary rocks the bulk of REE are held in the clay fraction. Shales have the most abundant REE, therefore, and the abundance is less in sandstones with more framework minerals and less matrix. Sandstones may have significant REE abundances from heavy minerals, commonly recycled in sediments due to their resistance to weathering.

The REE are among the most stable of the trace elements. Their behaviour in the sedimentary cycle is described in Henderson (1984). During weathering there is a tendency to homogenise the REE fractionation of igneous processes. The weathering product holds most of the REE of the original rock with very minor amounts going into solution. They pass from the weathered product to deposition without significant fractionation. REE held in solution may be incorporated in authigenic minerals (Piper, 1974). In diagenesis they are relatively unaffected but in metamorphic reactions and alteration the behaviour of REE depends on the presence of a fluid phase, partitioning between fluid and solid phases and the ability of any new phase to accommodate released REE. In the Skiddaw Group with its complex tectonic history and low grade metamorphism the REE are perhaps the least overprinted chemical group.

3.3.7.3 Sample selection

To investigate secular variations in REE abundance patterns within the Skiddaw Group and to draw comparisons with the Ingleton Group, eight samples were selected for analysis. Since REE abundance is greater in mudstones than sandstones, turbidite mudstone was sampled. Mudstones tend to have very similar patterns, hence small variations in shape may signify an important change in provenance. Clays may have distinct REE patterns due to localised inputs of volcanic material (Fleet et al, 1976; Dypvik and Brunfelt, 1979).

Details of sample preparation and analytical method are given in appendix 3b.

3.3.7.4 Analysis of results

Figure 3.41 shows REE patterns normalised to chondritic abundances and showing PAAS to aid comparison. The shape of the patterns from each of the Skiddaw Group formations closely mimic PAAS, with LREE enrichment and small europium anomalies. The total REE are greater than PAAS in each formation except the Bitter Beck Formation, where abundant thin sandstone laminae in the sample reduce the REE abundance.

Figure 3.41 Rare earth element patterns normalised to type 1 carbonaceous chondrites for Skiddaw Group mudstones. PAAS=post-Archaean Australian shale. (a) Bitter Beck Formation, (b) Watch Hill, Hope Beck and Kirk Stile formations, (c) Loweswater Formation.

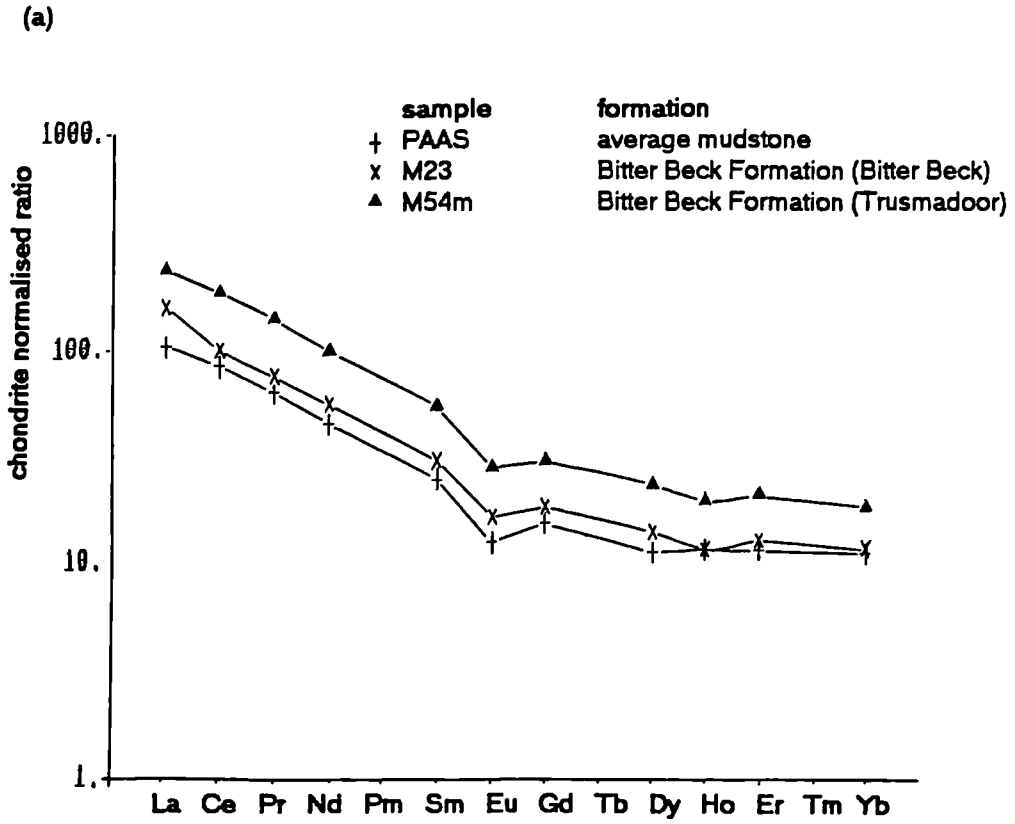

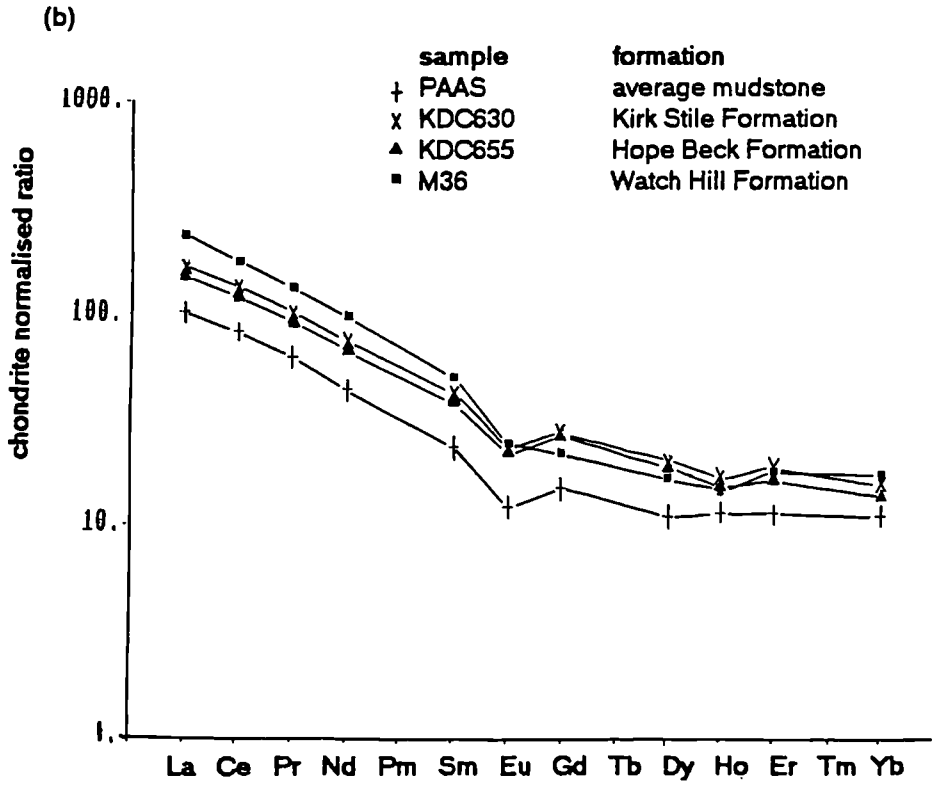

Figure 3.41 (continued) (c) Loweswater Formation.

(c)

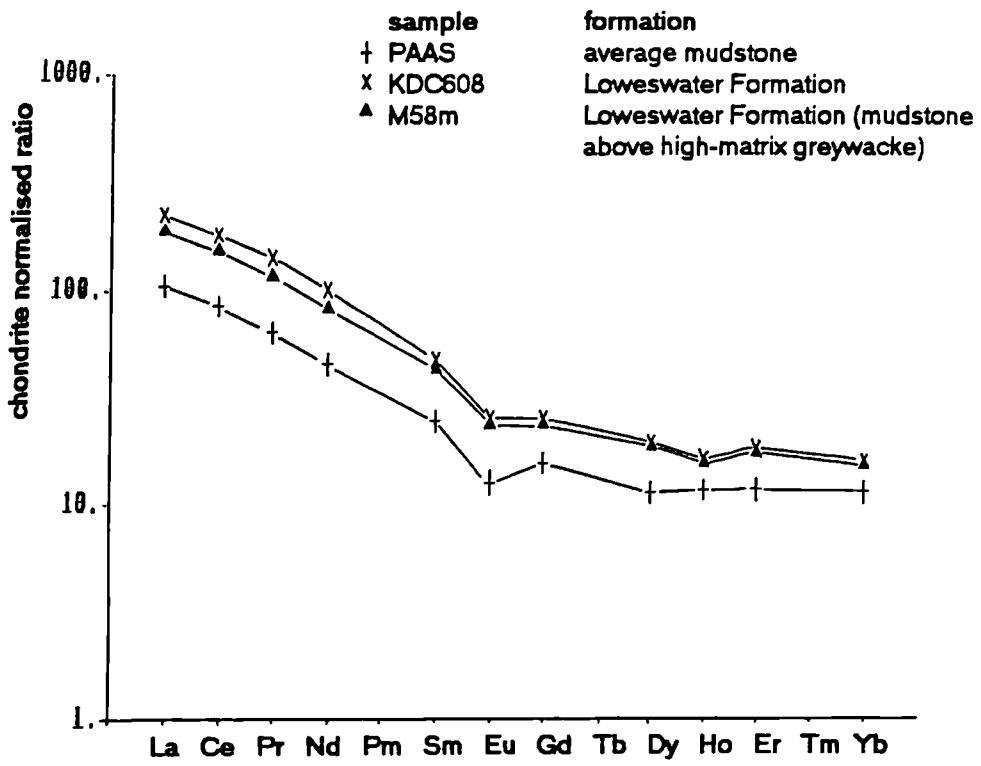

Table 3.17 Rare earth element criteria for provenance determination (after Bhatia, 1985c).

Tectonic Setting		
oceanic island arc	continental arc	active continental margin, passive margin and cratonic basin
lower total REE, slight enrichment of LREE over HREE (La/Yb), no negative europium anomaly	higher total REE, higher La/Yb, small negative europium anomaly, enrichment in europium with respect to PAAS	indistinguishable by REE pattern alone, high La/Yb, pronounced negative europium anomaly

The general similarity with PAAS suggests the source area exposed rocks of average upper continental crust composition and was not strongly influenced by a single characteristic rock type, e.g. a metamorphic source with HREE enriched garnets, or volcanics with a very small europium anomaly. Furthermore the source was post-Archaean. Archaean patterns show no europium anomaly (Taylor and McLennan, 1985).

The lack of variation between the formations might indicate no secular variation in source for the turbidite mudstones. Alternatively, if the mudstones are predominantly pelagic then a uniformity in composition would be expected. This is not thought to be the case as samples were collected from immediately above the underlying turbidite sandstone and do not show rhythmic banding commonly associated with pelagic sediments. Some variation is apparent. Comparing the patterns (figure 3.41) for Loweswater Formation mudstones associated with high matrix greywacke and common greywacke, the former shows less LREE enrichment reflecting a greater volcanic component.

Bhatia (1985c) demonstrated that the REE characteristics of terrigenous sedimentary rocks reflect the tectonic setting of their depositional basin (table 3.17).

Figure 3.42 shows REE patterns for modern muds in trailing edge, leading edge and forearc basin settings (Taylor & McLennan, 1985). Plots for the Skiddaw Group are unlike the modern forearc mud with its low total REE, low La/Yb, and negligible europium anomaly (table 3.18). The modern active margin mud has a lower La/Yb ratio but similar total REE to PAAS, i.e. lower than the Skiddaw Group, with which it shares a similar europium anomaly. This last point is also true of the modern passive margin mud which is similar to PAAS but whose La/Yb ratio is not as great as Skiddaw Group samples. Nevertheless it is this of the modern muds which is most similar to the Skiddaw Group samples.

Figure 3.43 shows REE patterns for ancient sandstones derived from a variety of sources. Sandstones have lower REE abundances than mudstones but the shapes of the patterns are comparable. The Skiddaw Group plots are unlike those for quartz-poor sandstones from ancient forearc basins and the ancient passive margin sandstone has a greater europium anomaly. The plot for sandstone from a recycled plutonic provenance is similar to PAAS, but has a lower La/Yb ratio than the Skiddaw Group and a greater europium anomaly. The Skiddaw Group patterns are very similar with those of ancient quartz-intermediate sandstones: the ranges of La/Yb ratios overlap and the europium anomalies are equivalent.

Of the ancient sandstone samples the Skiddaw Group REE patterns are most comparable with those of quartz-intermediate sandstones from continental arc provenance. Their La/Yb ratios (10-14) and negative europium anomalies ($Eu/Eu^{*}=0.7$) are comparable to active continental margin rhyolites (Floyd et al, 1991; Taylor et al, 1968; Ewart et al, 1968) which may be considered a source.

Figure 3.42 Chondrite-normalised rare earth element patterns for modern muds of different tectonic settings (from Taylor and McLennan, 1985). PAAS=average post-Archaean Australian shale.

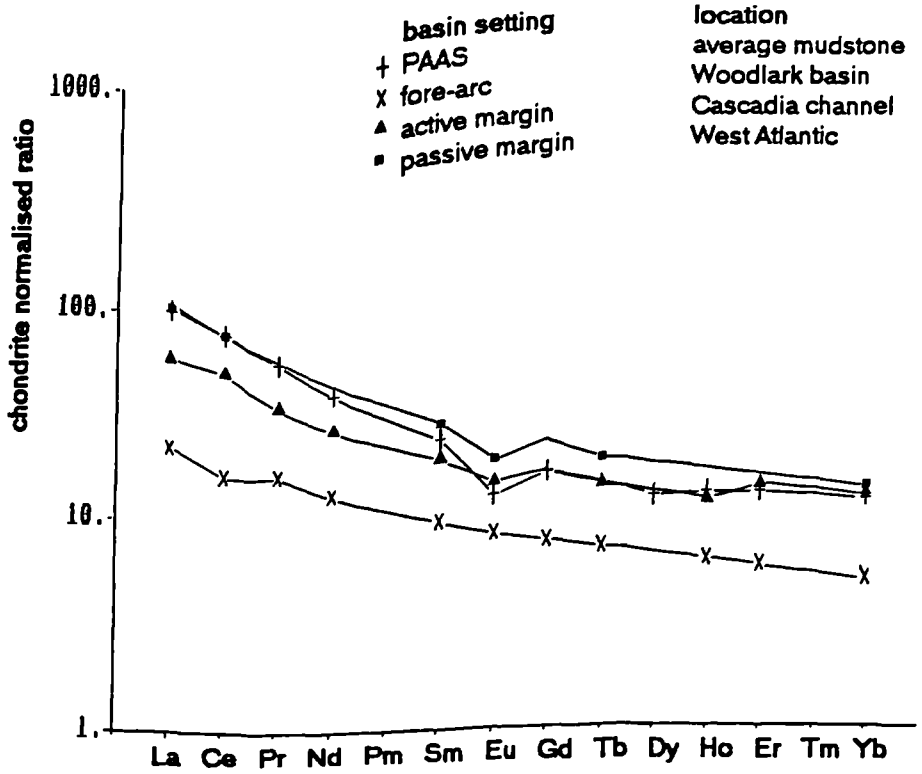

Figure 3.43 Chondrite-normalised rare earth element patterns for ancient sandstones of different tectonic settings (from Taylor and McLennan, 1985). (a) fore-arc, (b) continental arc, (c) passive margin and recycled sandstone. PAAS=average post-Archaean Australian shale.

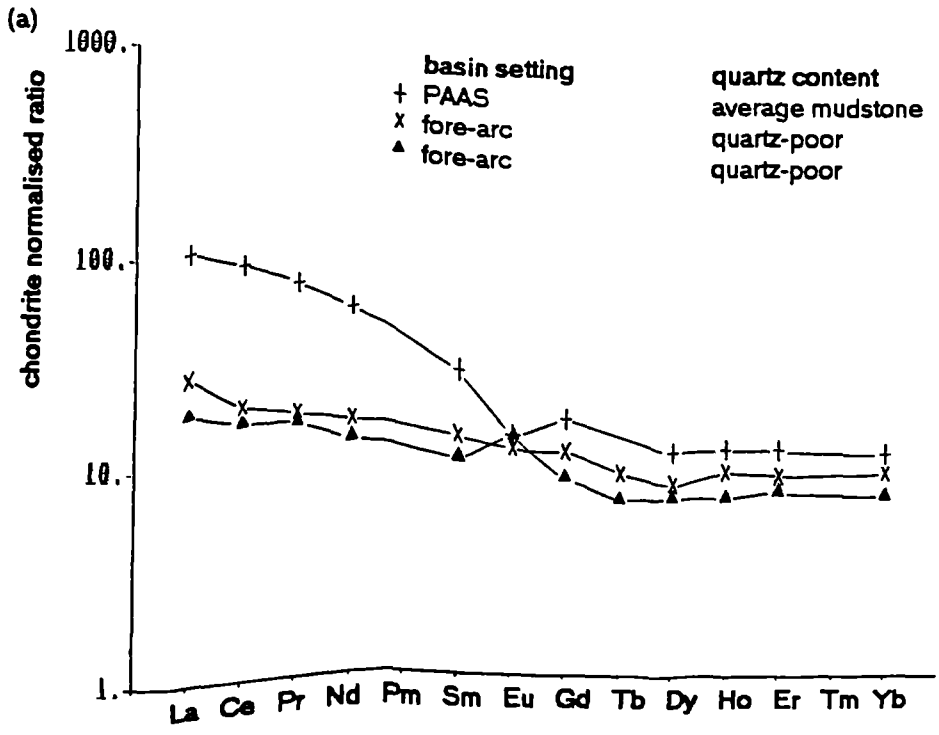

Figure 3.43 (continued)

(b)

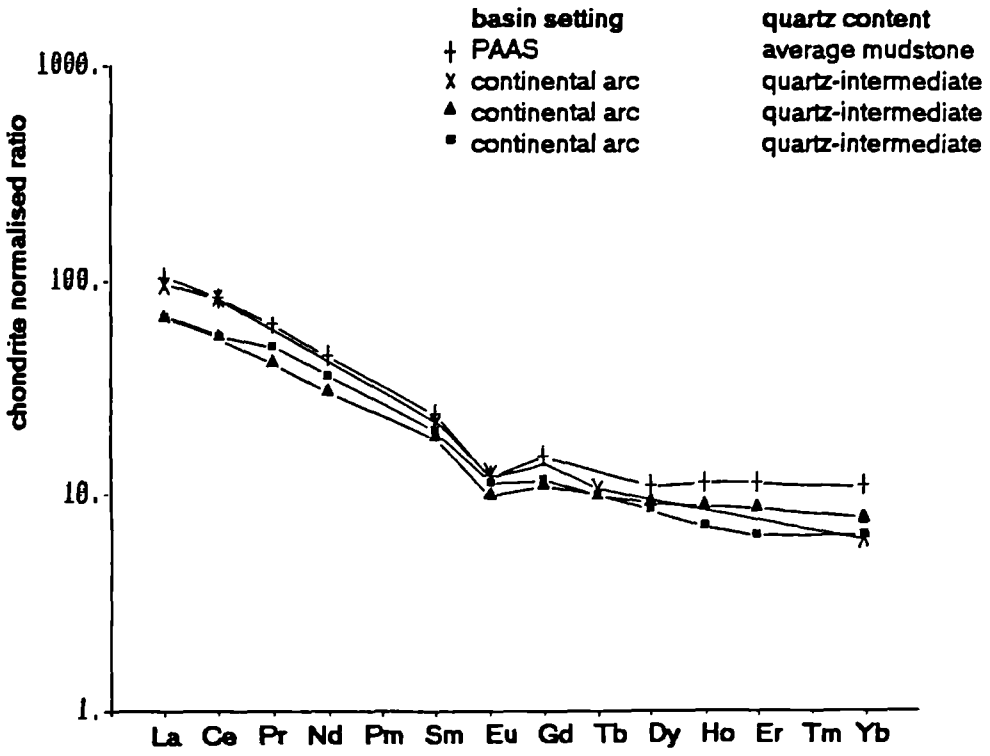

(c)

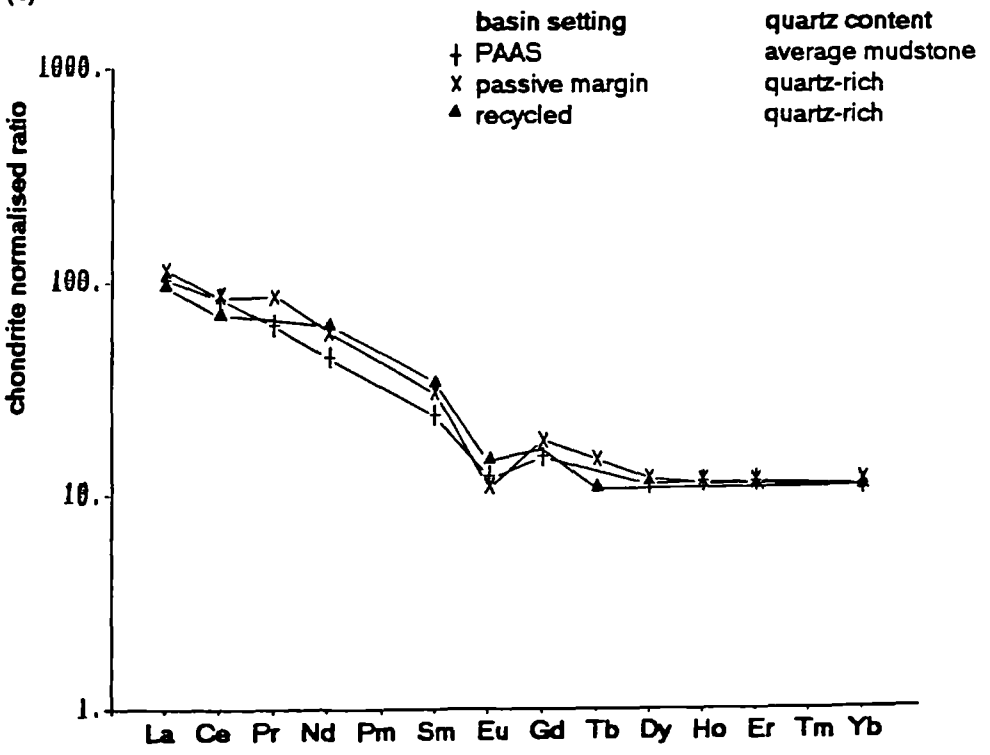

Table 3.18 Distinctive rare earth element parameters for the Skiddaw Group and for modern and ancient sediments of different tectonic settings (compiled from Taylor and McLennan, 1985). PAAS=post-Archaean Australian shale average.

Skiddaw Group

sample	formation	La_N/Yb_N	Eu/Eu*
M54m	Bitter Beck Formation	12.77	0.69
M23	Bitter Beck Formation	13.29	0.70
M36	Watch Hill Formation	13.09	0.73
KDC655	Hope Beck Formation	10.90	0.68
KDC608	Loweswater Formation	14.30	0.72
M58m	Loweswater Formation	12.48	0.73
KDC630	Kirk Stile Formation	10.53	0.70
PAAS		9.17	0.65

Modern muds

basin setting	location	La_N/Yb_N	Eu/Eu*
fore-arc	Woodlark basin	4.9	0.96
active margin	Cascadia channel	5.4	0.76
passive margin	West Atlantic (average of 3)	8.5	0.75

Ancient sandstones

basin setting	quartz content	La_N/Yb_N	Eu/Eu*
fore-arc	quartz-poor	2.9	0.96
fore-arc	quartz-poor	2.5	1.41
continental arc	quartz-intermediate	14.8	0.70
continental arc	quartz-intermediate	8.4	0.96
continental arc	quartz-intermediate	10.1	0.75
recycled	quartz-rich	8.5	0.63
passive margin	quartz-rich	10.0	0.48

3.4 Summary of provenance classifications for the Skiddaw Group

Table 3.19 summarises the provenance groupings of the Skiddaw Group and its components by both petrographical and chemical techniques. Consistently, a continental arc is indicated as a sediment source by geochemical techniques. This might be on a microcontinental fragment, *continental island arc* or on a continental plate margin, *active continental margin*. In addition sediment derivation from a passive margin is implied. Both geochemical and petrographical techniques suggest a recycled terrain as a sediment source. The latter consistently imply a recycled collision orogen source, and mixing with a craton interior/passive margin source.

There is evidence of secular variation in composition e.g. dominantly acidic sources with an increasing contribution from mafic sources with time. This variation does not signify a change in provenance type or tectonic setting within the Skiddaw Group, but rather a compositional variation from a single provenance type: a recycled arc terrain. This is reflected in the range of lithic fragments which is similar in all formations but in differing proportions (figure 3.44).

There is evidence of more than one sediment source feeding the depositional system, exemplified by the contrasting compositions of greywacke types within the Loweswater Formation. A possible origin for the mature, quartz wackes of Jonah's Gill may be as shelf sands moved by longshore currents and captured by submarine canyons feeding the deep marine distribution system. The origin of the high-matrix greywackes is discussed in chapter 2. Grains are more angular than in other greywackes and feldspars are more abundant, hinting at an origin from volcanic mud flows. These attributes, however, could result from suppression of post-depositional alteration by a high primary matrix content. This textural characteristic could have been assimilated during transport (chapter 2). Thus a difference in provenance for high-matrix greywackes is unclear.

Specific sources can be identified from petrographical observations. Lithic fragments of granite, the abundance of plutonic quartz, the dominance of untwinned and potassium feldspar over plagioclase, and the common occurrence of tourmaline, suggest an unroofed acid pluton in the source region. Pyroclastic and volcaniclastic fragments suggest erosion of arc-related deposits. Fragments of cleaved granite and shale and quartz-mica schist suggest a recycled orogenic source.

The texture of the sediment is generally mature with quartz-rich greywackes displaying dominantly subrounded grains. Well rounded grains in pebbly mudstones of the Hope Beck Formation suggest recycling or substantial abrasion of grains during transport. First cycle angular grains are rare, though represented in high-matrix greywackes of the Loweswater Formation. There is no direct evidence of coeval volcanism until the Tarn Moor Formation, which contains tuffs and volcaniclastic turbidites. Thus the strong continental arc geochemical signature could relate to erosion of a non-coeval arc.

The question of coeval versus non-coeval arc source can be addressed using the samarium-neodymium isotopic decay scheme. Samarium and neodymium, both rare earth elements, are thought to behave coherently in the continental crust and to resist fractionation by weathering, erosion, transport, deposition and diagenesis, and low grade metamorphism (Thorogood, 1990). The neodymium model age records the time of separation of the sample material from the mantle.

Table 3.19 Summary of provenance classifications and compositional comparisons for the Skiddaw Group, WHG-Watch Hill Formation, HBE-Hope Beck Formation, LWF-Loweswater Formation,OIA-oceanic island arc, CIA-CIA-continental island arc, ACM-active continental margin, PM-passive margin, CAAM-continental arc/active continental margin.

technique (with section number in text)	provenance of the Skiddaw Group (undifferentiated)	provenance and/or similarity with another group: formations								
		Bitter Beck	Watch Hill	Hope Beck	Loweswater	(Jonah's Gill,	high-matrix type)	Kirk Stile	(debris flow)	Buttermere Formation rafts
compositional suites (3241) (Valloni and Mezzadri, 1984)	quartzofeldspathic, matured source: orogenic terranes/ platform deposits setting: rifted continental margin, back-arc/marginal basin									
provenance diagrams (324) (Dickinson et al, 1983)		craton interior	recycled orogen and mixed;	quartzose recycled	quartzose recycled orogen (and continental block); collision orogen> arc orogen sources; mixed magmatic arc and subduction complex (trench)	craton interior	mixed	transitional to quartzose recycled orogen, mixed and craton interior; collision orogen sources; suture belt	LWF (Jonah's Gill)	craton interior HBE or LWF (Jonah's Gill)
(Ingersoll and Suczek, 1979)		collision orogen sources; remnant ocean basin	volcanic arc & collision orogen sources; mixed magmatic arc with subduction complex (trench), or rifted continental margin (back-arc)	orogen and craton interior; collision orogen sources; mixed magmatic arc and subduction complex (trench)						
discriminant function analysis (3335) (this study)	CIA								LWF	WHG/HBE
discriminant function analysis (3336) (Roser and Korsch, 1988)			recycled	recycled	recycled, mafic & intermediate			mafic	LWF intermediate	HBE
major element bivariate plots (334)	CIA		CIA	CIA	CIA/OIA	WHG/HBE		not defined	WHG/HBE	WHG/HBE
			>>>>>>>>>>>> secular variation >>>>>>>>>>>							
SiO_2 vs K_2O/Na_2O (3353)										
sandstones:			ACM/PM	PM	ACM			PM	ACM, LWF	PM, WHG/HBE
mudstones:				ACM	ACM			ACM		
trace element plots (3362)										
Th-Zr	CIA/PM									
Sc-V						PM/ACM	arc		ACM	ACM
Th-Sc-Zr	CIA									
Th-Co-Zr	CIA									
La/Th			arc influence							
Rb-K	differentiated magmatic suite		----------acidic/intermediate sources ----					basic component		
Ni-TiO_2	acidic source		----------distinct formations ----------			WHG				
trace elements in mudstones (3363)	CIA, ACM & PM all indicated Nb indicates ACM/PM influence La indicates ACM influence Cr indicates PM influence									
multi-element variation diagrams (3364)	Nb anomaly indicates: mobile group: PM stable group:CAAM		PM	PM	mafic input			significant mafic input		
rare earth elements (337)	average shale compostion, similar to modern PM mud, ancient continental arc and ACM rhyolite									

Figure 3.44 Proportions and range of lithic fragments in coarse sand to pebble grainsize samples of the Skiddaw Group.

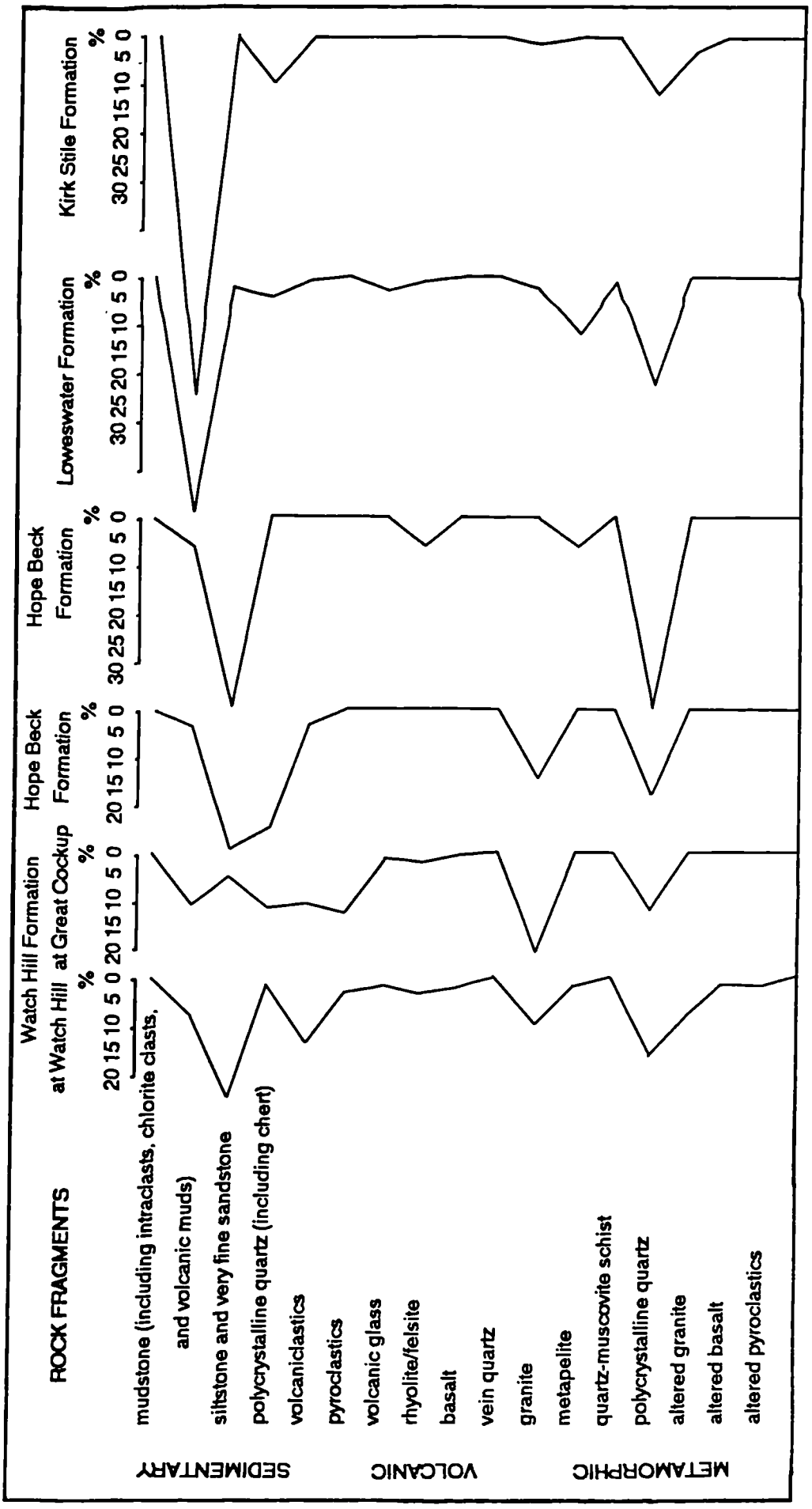

For mantle-derived igneous rocks, Nd model age records the age of intrusion or extrusion, given an appropriate mantle model. For a sedimentary rock, inheriting the Sm-Nd compositions of its protoliths, Nd model age represents a weighted average of the amount of time that its component neodymium has resided in the crust (O'Nions et al, 1983) and may be called its 'crustal residence age'. Thus sedimentary rocks from long established continents have relatively old Nd model ages compared to detritus from coeval volcanic sources. Juvenile detritus from contemporaneous volcanism might only contribute to a sedimentary rock during and shortly after active volcanism (Thorogood, 1990).

Table 3.20 shows Nd model ages for sedimentary rocks of the Welsh Basin. The interpretation of Thorogood (1990) suggests sedimentary rocks of ages 473-462Ma and 450-449Ma incorporated detritus from active volcanism, which lowered their Nd model age relative to other samples derived from long established continental crust. Considering Nd model ages for the Skiddaw Group, the unpublished range (Thirlwall,1990, pers. comm.) corresponds to derivation from the latter source. The model age calculated by Davies et al (1985) is lower and may result from juvenile volcanic input. The stratigraphic position of this sample is unknown. It may herald the volcanogenic detritus in the Tarn Moor Formation, or indicate limited input from an active volcanic source at any time in the early Ordovician. It is possible that the immature matrix-rich greywackes of the Loweswater Formation contain juvenile volcanogenic detritus. Sm-Nd isotope analysis of each greywacke-type could be used to investigate the presence of coeval volcanism in the Skiddaw Group.

It is suggested, therefore, that the Skiddaw Group was derived from a terrain with largely non-coeval volcanogenic rocks.

In summary, sediment was sourced from an old, inactive continental arc terrain comprising volcanic deposits, unroofed plutons, cleaved and metamorphosed rocks and sedimentary strata from recycling of an orogen. Active volcanism fed detritus to the basin in Llanvirn times when tuffs and volcanogenic deposits are included in the Tarn Moor Formation. Mature quartzose sediments fed the depositional system from shelfal (?) sediment storage areas. These heterolithic source regions existed throughout deposition of the Skiddaw Group, contributing more mafic detritus into the Kirk Stile Formation. The tectonic setting of source and basin is discussed in chapter 5.

Table 3.20 Nd model ages for early-mid Ordovician samples from the Lake District and Wales, Welsh borders and English midlands. Nd model age calculated using the depleted mantle parameters of DePaolo (1981). Stratigraphic ages from the timescale of McKerrow et al (1985).

Skiddaw Group			Wales, Welsh borders and English midlands			
source	sample	Nd model age (Ga)	source	sample	stratigraphic age (Ma)	Nd model age (Ga)
O'Nions et al (1983)	81-16c	1.52	Thorogood (1991)		Caradoc	
	81-81	1.53		EJT33'	443	1.50
				EJT32	444	1.60
Davies et al (1985)	81/14	1.44		EJT5b	447	2.08
				EJT5b	447	2.02
				EJT5a	447	1.40
Thirlwall, pers comm.	minimum	1.59		EJT10b	449	1.49
	maximum	2.52		EJT10a	449	1.42
				EJT18a	449	1.46
				EJT19	450	1.51
				EJT23	450	1.26
				EJT8	450	1.45
				EJT8	450	1.44
				EJT92	451	1.59
				EJT97b	451	1.85
				EJT13	451	1.62
				EJT9	452	1.71
				EJT11a	452	1.70
				EJT12	452	1.49
				EJT22	452	1.46
				EJT15	454	1.60
					Llandeilo	
				EJT41	456	1.62
					Llanvirn	
				EJT40b	462	1.34
				EJT7b	469	1.43
				EJT17	470	1.65
					Arenig	
				EJT39	473	1.38
					Tremadoc	
				EJT14	493	1.63
				EJT105	500	1.55
				EJT50	505	1.57
				EJT3b	507	1.66

3.4.1 Origin of clasts in the Beckgrains Bridge debris flow

Clasts are most similar in composition to the Loweswater Formation, especially the mature greywackes of Jonah's Gill. Since the chemical composition of the latter is similar to the Watch Hill Formation or Hope Beck Formation, derivation through reworking of these units is also possible.

An origin for the debris flow through oversteepening of a submarine slope would result in cannibalisation of Skiddaw Group sediment. Microfossil evidence suggests mixed Tremadoc-Arenig floras within the debris flow (Cooper et al, in prep), which supports compositional evidence for an intrabasinal origin for the unit.

The well-rounded clasts suggest substantial degradation occurred during transportation. If this could not occur during matrix-supported downslope movement in the submarine environment then either significant uplift and exposure of deep marine Skiddaw Group sediments must have occurred in the earliest Llanvirn, or the clasts could have been derived from lithified shelf sands which had acted as a sediment source for turbidites in the Arenig.

3.4.2 Origin of sandstone rafts of the Buttermere Formation

Samples from sandstone rafts are comparable with the Hope Beck and Watch Hill formations in composition. The rafts are thought to be age equivalent to the Loweswater Formation from palaeontology (Cooper et al, in prep) and sedimentary facies and are compositionally similar to the Loweswater Formation of Jonah's Gill. Since compositional variation has been demonstrated within and between Skiddaw Group formations, all derived from similar heterolithic sources, direct age and compositional equivalence of the Robinson and Goat Gills members with one of the formations of the Northern Fells belt is not expected. Gravitational reworking of large thicknesses of Skiddaw Group strata within the Buttermere Formation is important however, since it implies development of submarine slopes in the earliest Llanvirn.

3.5 Provenance of the Manx Group

The Manx Group comprises turbidite greywackes, quartz wackes and mudstones with a similar age range to the Skiddaw Group: Tremadoc to early Llanvirn (table 3.21).

Table 3.21 Comparison of dated Manx Group units (Molyneux, 1979) with the Skiddaw Group, and Manx group samples used for petrographical and chemical analysis (location details appear in appendix 1).

age	unit of the Manx Group	sample analysed by: petrography,	geochemistry	equivalent unit of the Skiddaw Group
late Arenig-early Llanvirn	Lady Port banded 'group'			Kirk Stile Formation
Arenig	Maughold banded 'group'	IOM 22	IOM 22	Loweswater Formation
late Tremadoc	Glen Dhoo Flags & Lonan Flags	IOM 10, 12, 13, 14, 20, 21	IOM 10, 12, 13	Watch Hill Formation
Tremadoc	Niarbyl Flags	IOM 9	IOM 7, 9	Bitter Beck Formation

3.5.1 Petrographical techniques

The samples are mainly of fine-medium sand grainsize and are classified as quartz wackes, quartz-rich greywackes and a quartz-intermediate feldspathic wacke, and plot in the quartzofeldspathic suite of Valloni and Mezzadri (1984) (figure 3.45).

The Lonan Flags samples from Port Mooar show the highest metamorphic grade with a strong fabric, extensive recrystallisation and development of secondary tourmaline. Reliable provenance interpretation is not possible.

The Niarbyl Flags samples from Langness are similar in appearance to samples from the Watch Hill Formation with a quartz cement. Untwinned, simple twinned and perthitic feldspar types are more common than plagioclase. Lithic grains are dominantly of sedimentary origin and include: mudstone, siltstone, granitic plutonic clasts, clasts with graphic texture, hornfels, metapelite, quartz-mica schist and metamorphic polycrystalline quartz. Muscovite, biotite, tourmaline and rounded zircons were all recorded. The sample from the Maughold banded 'group' at Bradda Head is a poorly sorted quartzite with recrystallised quartz-chlorite matrix and grey chert lithics.

Figure 3.45 Classification diagrams for sandstone samples from the Manx Group (a) after Dott (1964), Pettijohn et al (1972), and (b) from Valloni and Mezzadri (1984). QF=quartzofeldspathic suite, QL=quartzolithic suite. n=8.

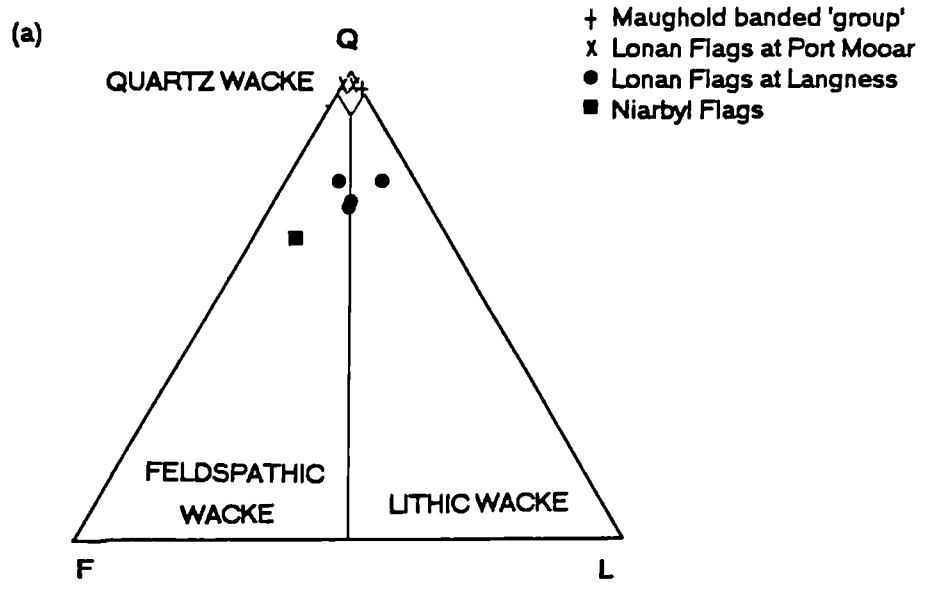

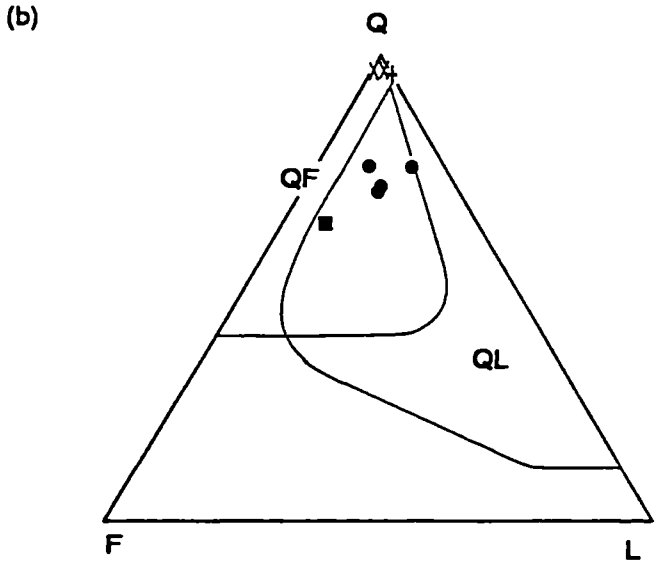

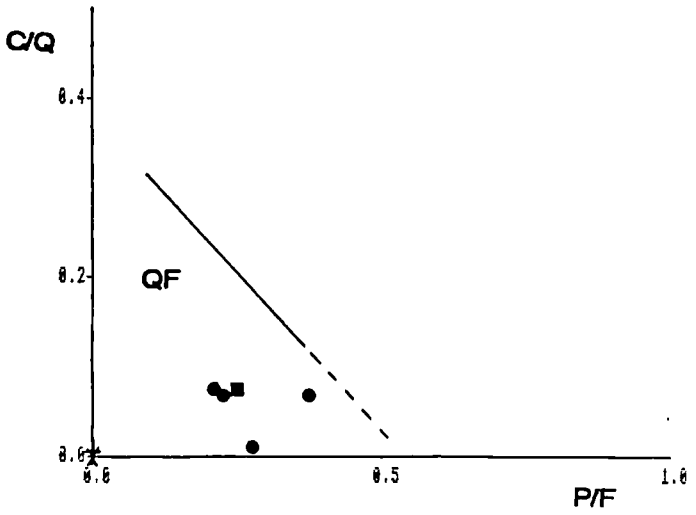

On provenance discrimination diagrams (figure 3.46) the feldspathic nature of the sample from the Niarbyl Flags compares with the sample from the Bitter Beck Formation and they share a *continental block* source.

The Lonan Flags samples plot in the *quartzose recycled orogen* field, and nearer the quartz pole than the samples from the Watch Hill Formation at Watch Hill, with which they share a similar range of lithic and feldspar types. Since the sedimentary facies represent more distal turbidite deposits than at Watch Hill and sediment grainsize is finer, then derivation from a single source is possible.

The quartzite from Bradda Head plots in the *craton interior* provenance field. The age-equivalent Loweswater Formation at Jonah's Gill shares a similar provenance type, but lithologies and sedimentary facies do not compare directly. The occurrence of quartzwackes in both the Lake District and the Isle of Man during the Arenig (also reported in the Ribband Group of southeast Ireland) is significant.

Figure 3.46 Provenance discrimination diagrams for Manx Group sandstones, n = 8; Q-F-L, Qm-F-Lt, with fields after Dickinson et al (1983).

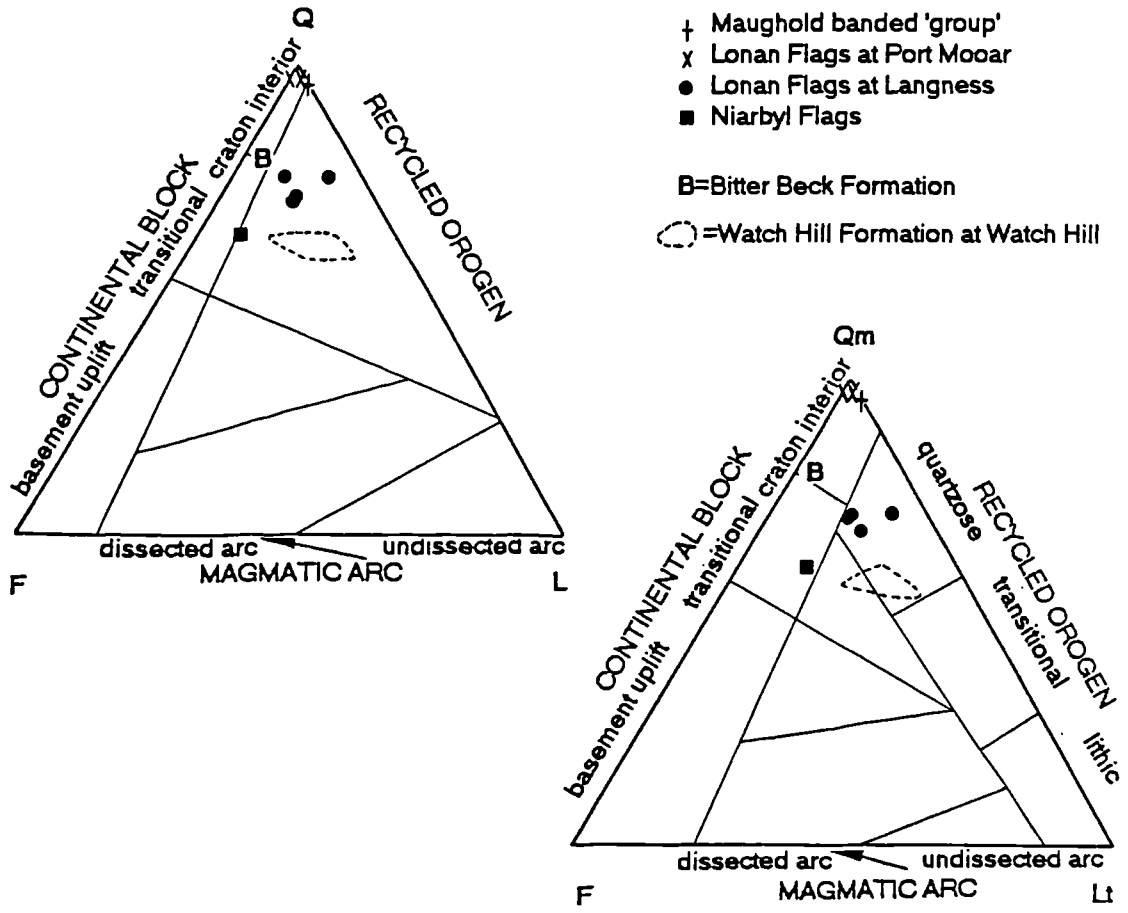

3.5.2 Geochemical techniques

Six samples (table 3.21) were analysed for major and trace elements by x-ray fluorescence spectrography.

Results of classification by the discriminant function defined in section 3.3.3.4 are given in table 3.22.

Table 3.22 Results of discriminant function classification by provenance type for Manx Group sandstones. CIA=continental island arc, ACM=active continental margin.

sample	unit	provenance setting
IOM7	Niarbyl Flags	CIA
IOM9	Niarbyl Flags	ACM
IOM10	Lonan Flags	CIA
IOM12	Lonan Flags	CIA
IOM13	Lonan Flags	ACM
IOM22	Maughold banded 'group'	ACM

Derivation from a continental arc is indicated.

The discriminant functions of Roser and Korsch (1988) suggest a *recycled* provenance with the Niarbyl Flags plotting near the boundary with the *felsic* volcanic provenance field (figure 3.47a).

On a Fe_2O_3+MgO vs TiO_2 plot (figure 3.47b) with provenance fields as defined in section 3.3.4. Niarbyl Flags samples indicate provenance from an island arc. Lonan Flags samples plot in the *active continental margin* field with one in the *passive margin* field.

On SiO_2 vs K_2O/Na_2O (figure 3.48a), the Niarbyl Flags samples plot in the *active continental margin* field whereas others plot in the *passive margin* field.

The trace elements V and Sc are associated with mafic sources. Their low abundance in the quartz-wacke of the Maughold 'banded' group shows it to be of passive margin provenance (figure 3.48b). Their abundance is also low in the Lonan Flags samples but higher in the samples from the Niarbyl Flags.

Ternary trace element plots (figure 3.49) suggest a mixture of provenance fields. A *continental island arc* provenance is most commonly indicated, but samples spread into *passive margin* and *active continental margin* fields.

Rb versus K shows the Manx Group samples plotting closely to a ratio K/Rb=230 corresponding to a differentiated magmatic suite (Shaw, 1968) (Figure 3.50a). The low abundance of these elements in sample IOM22 is due to its extremely quartzose nature and not due to mafic components. Samples from the Lonan Flags may contain a mafic component as volcanic clasts were observed amongst a range of lithic fragments in petrographical analysis.

Ni versus TiO_2 shows an acidic source for most samples but a high Ni content is exhibited by IOM7 of the Niarbyl Flags suggesting a mafic component is present (figure 3.50b).

Figure 3.51 shows the multi-element variation diagram for the Manx Group samples compared with the average patterns for different provenance settings defined by Floyd et al (1991). The total abundance of elements differs markedly between samples although relative abundances

Figure 3.47 (a) Plot of discriminant score 1 versus discriminant score 2 for Manx Group sandstones using the discriminant function of Roser and Korsch (1988). Provenance fields, P1=mafic, P2=intermediate, P3=felsic, P4=recycled. (b) $*Fe_2O_3+MgO$ versus TiO_2 plot with provenance fields defined in section 3.3.4, OIA=oceanic island arc, CIA=continental island arc, ACM=active continental margin, PM=passive margin. $*Fe_2O_3$ is total iron as Fe_2O_3.

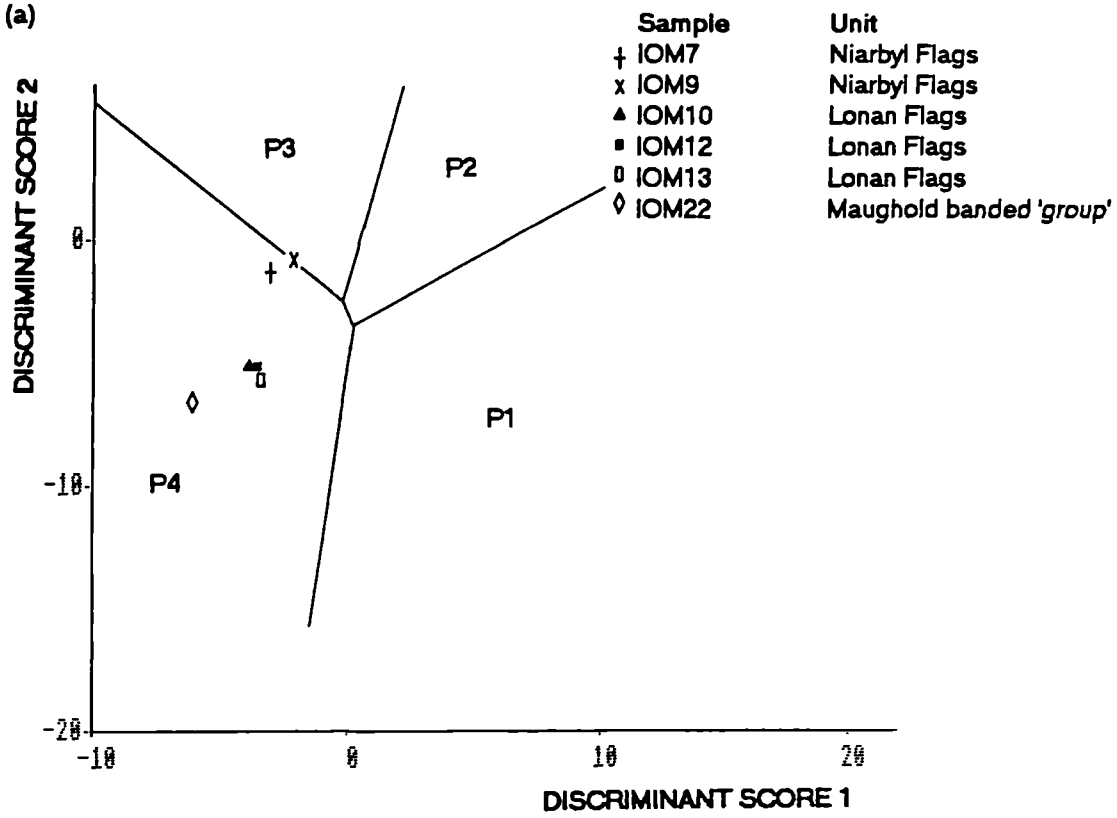

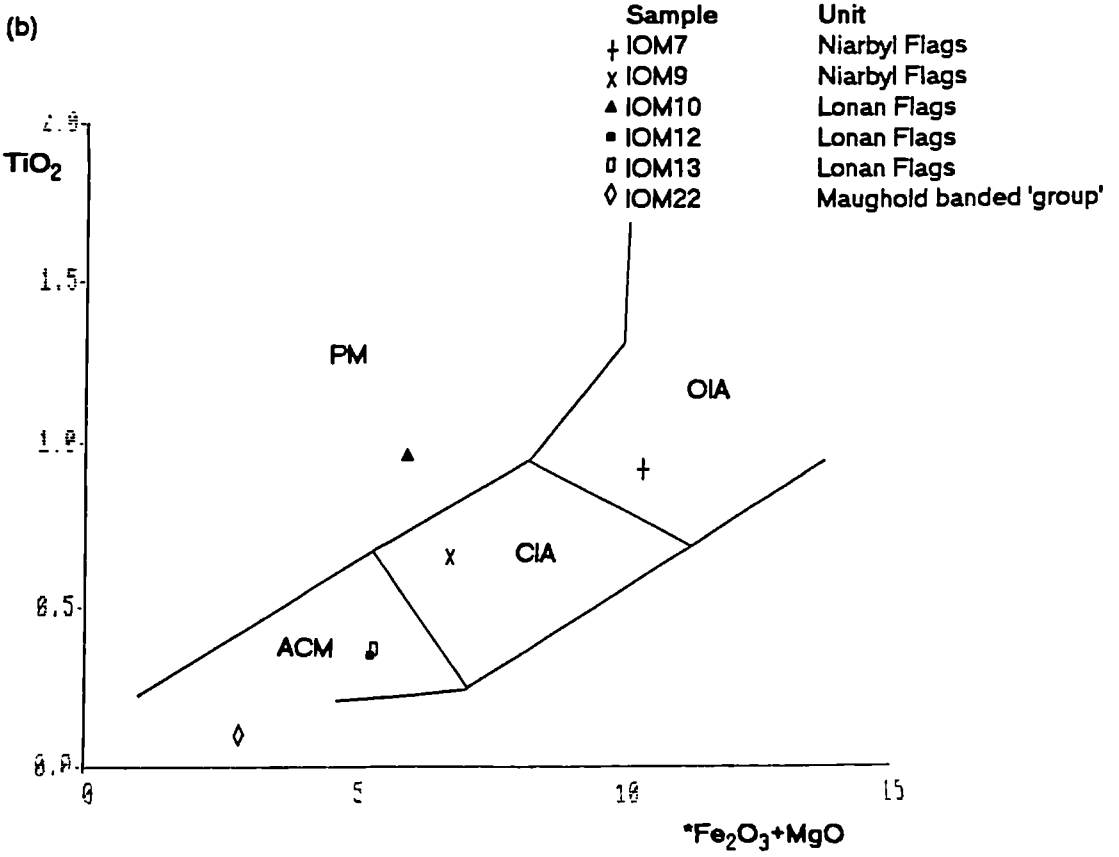

Figure 3.48 (a) SiO_2 versus K_2O/Na_2O plot for the Manx Group with fields after Roser and Korsch (1986). ARC=island arc, ACM=active continental margin, PM=passive margin; (b) Sc versus V for the Manx Group samples.

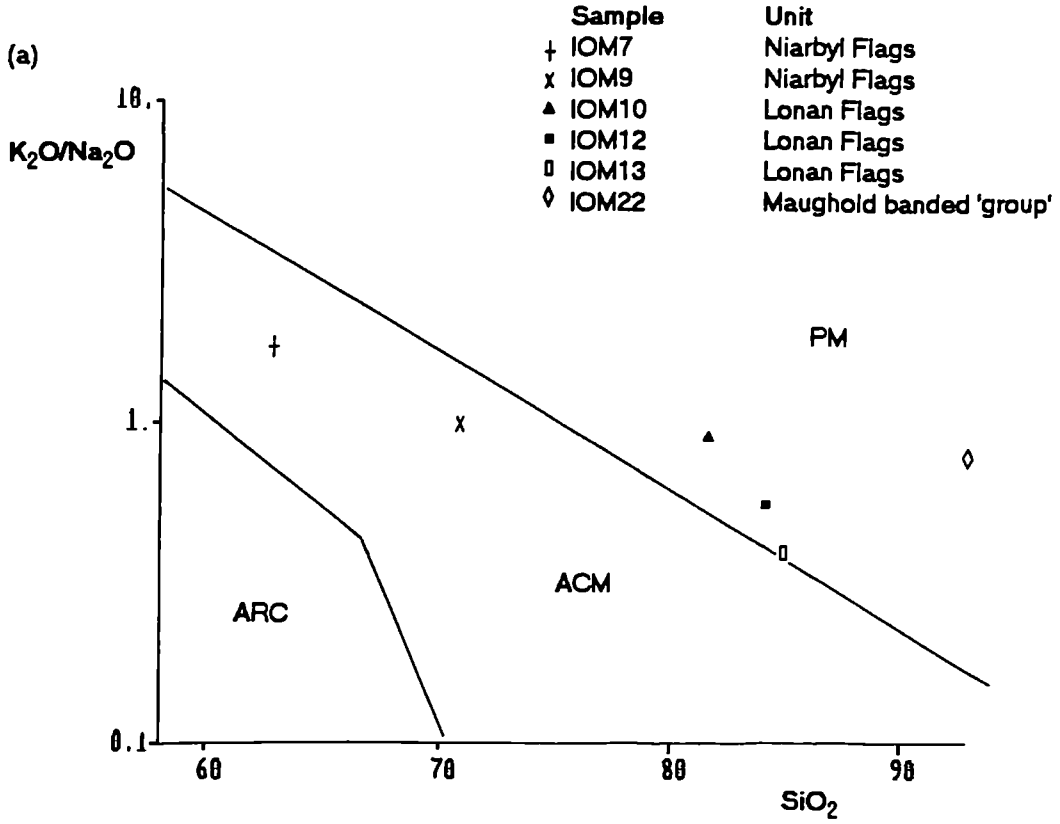

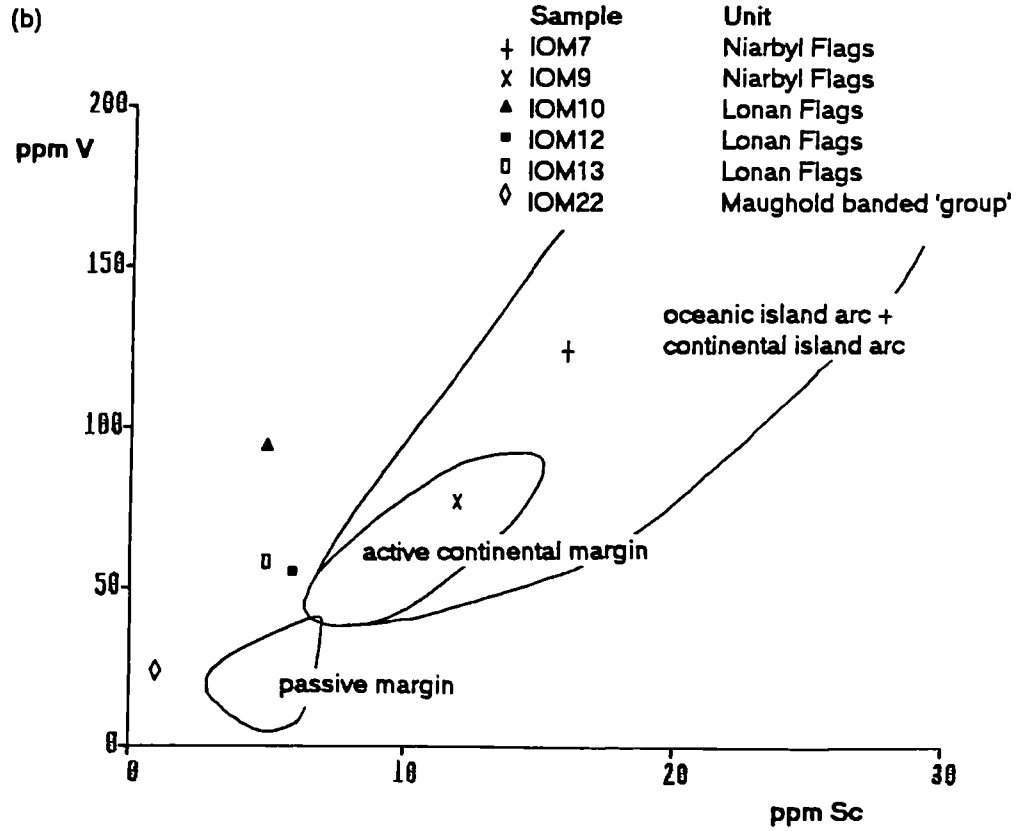

Figure 3.49 (a) Th-Sc-Zr and (b) Th-Co-Zr for Manx Group sandstones with provenance fields redrawn from the data of Bhatia and Crook (1986). OIA=oceanic island arc, CIA=continental island arc, ACM=active continental margin, PM=passive margin.

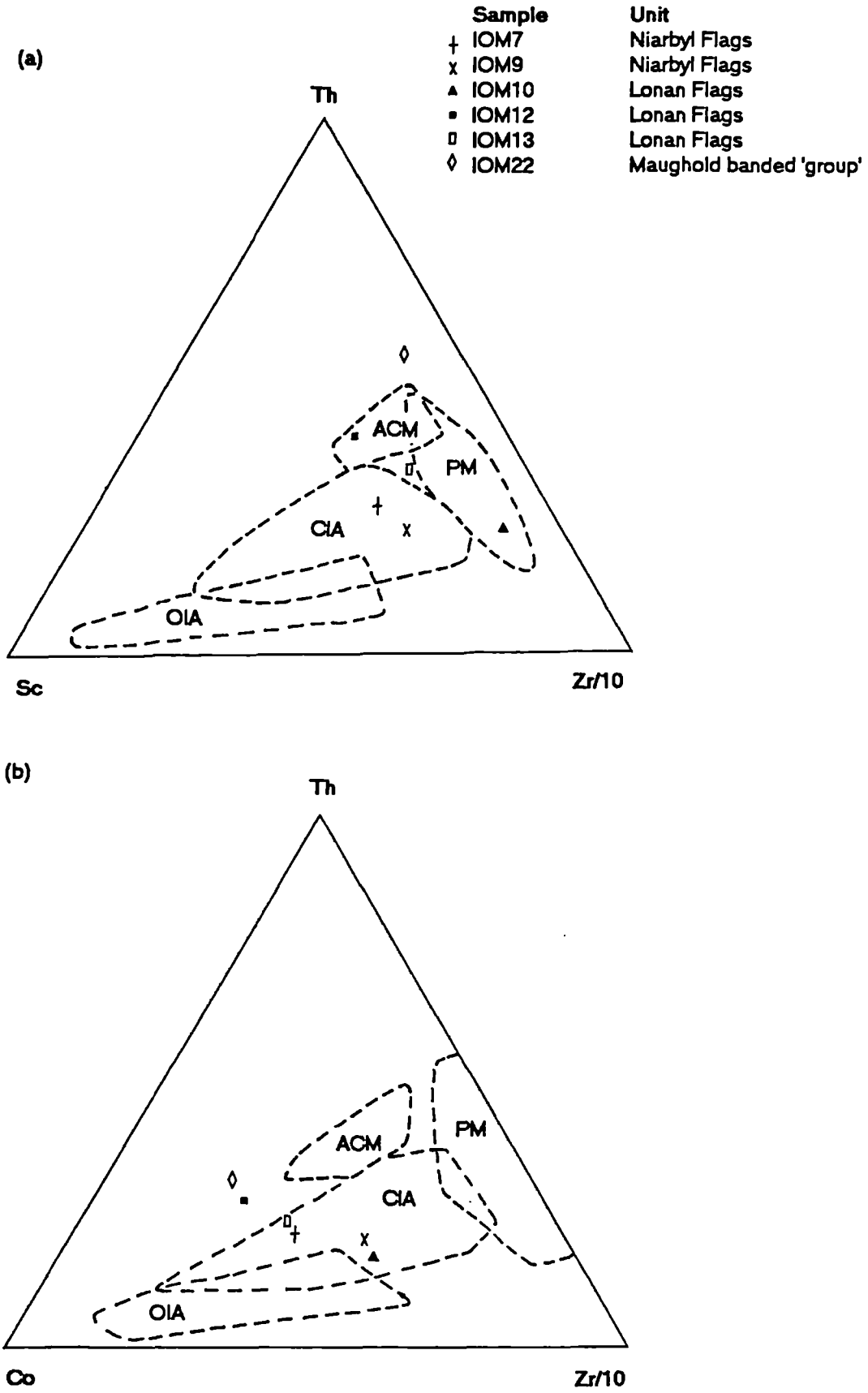

Figure 3.50 (a) Rb vs K for the Manx Group with K/Rb=230 representing a differentiated magmatic suite (Shaw, 1968), (b) Ni versus TiO_2 for Manx Group sandstones with provenance fields after Floyd et al (1991).

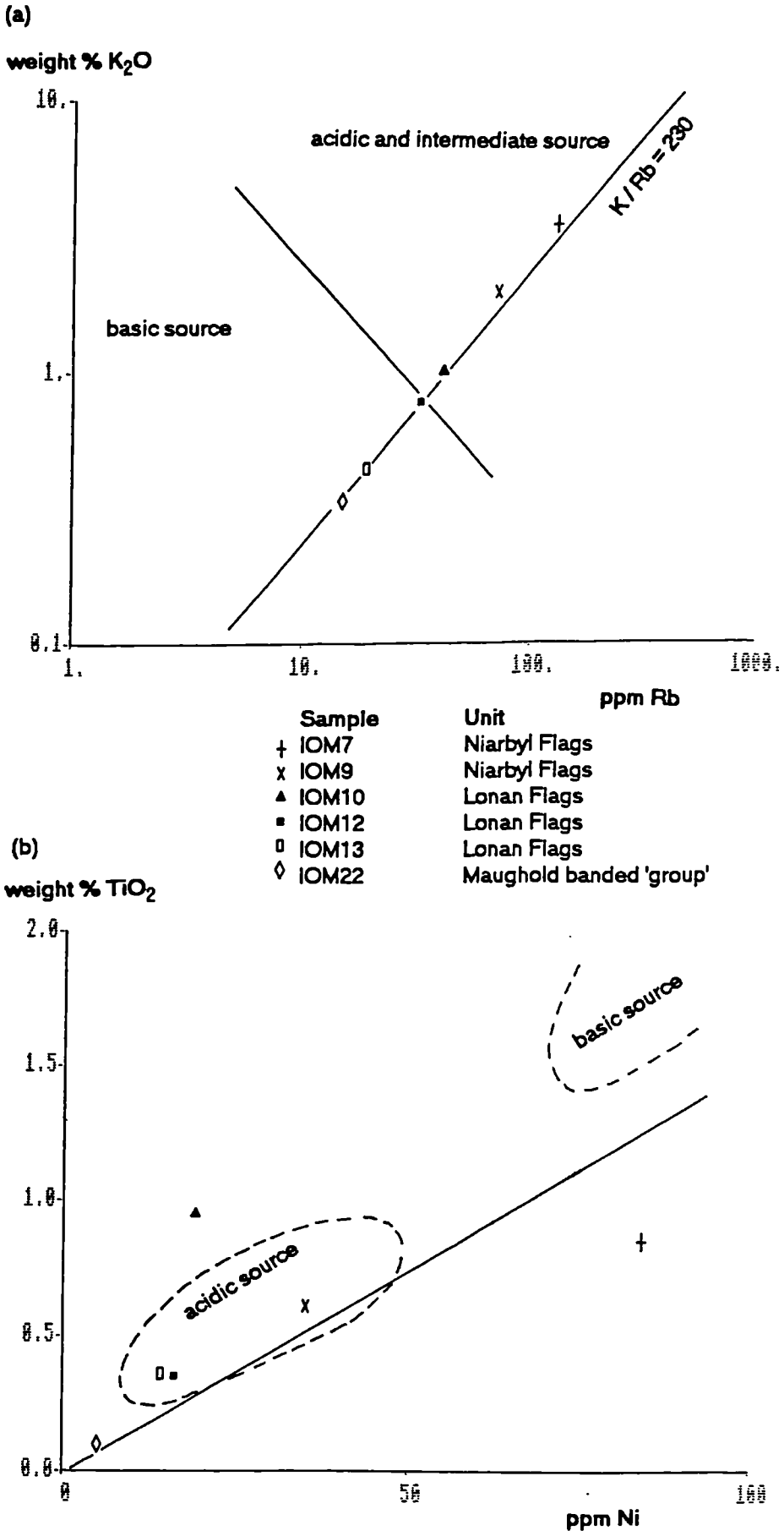

Figure 3.51 Multi-element variation diagrams (a) with characteristic patterns for different tectonic settings (Floyd et al. 1991), (b) for samples from the Manx Group.

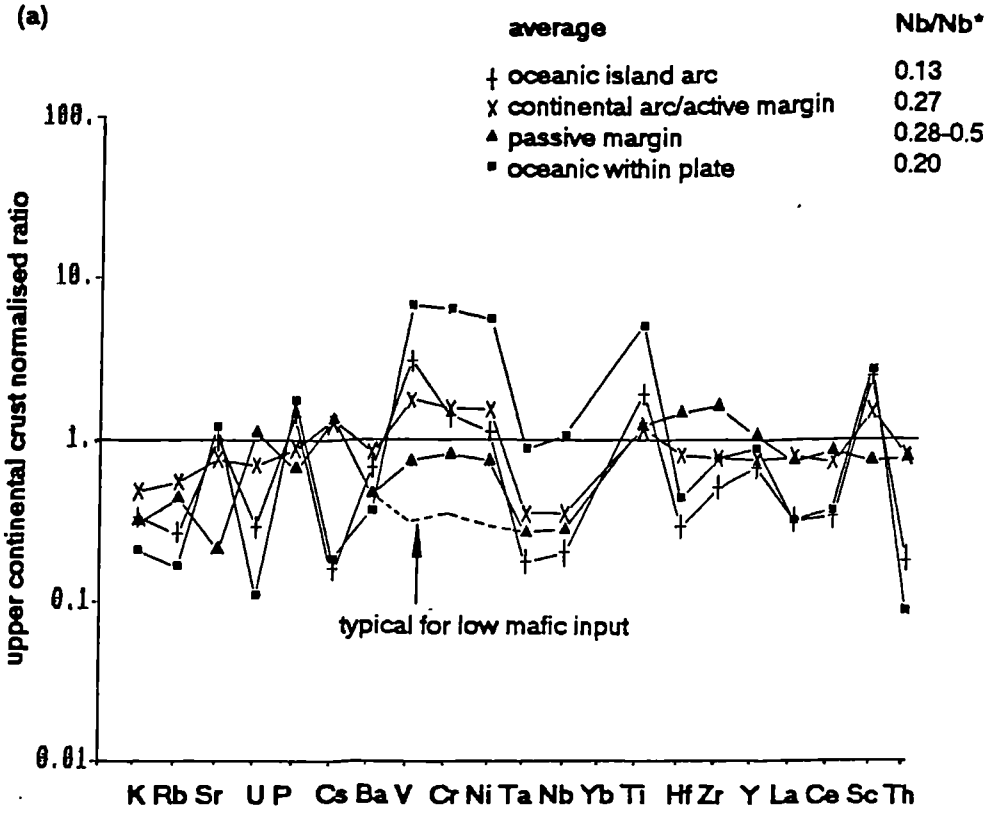

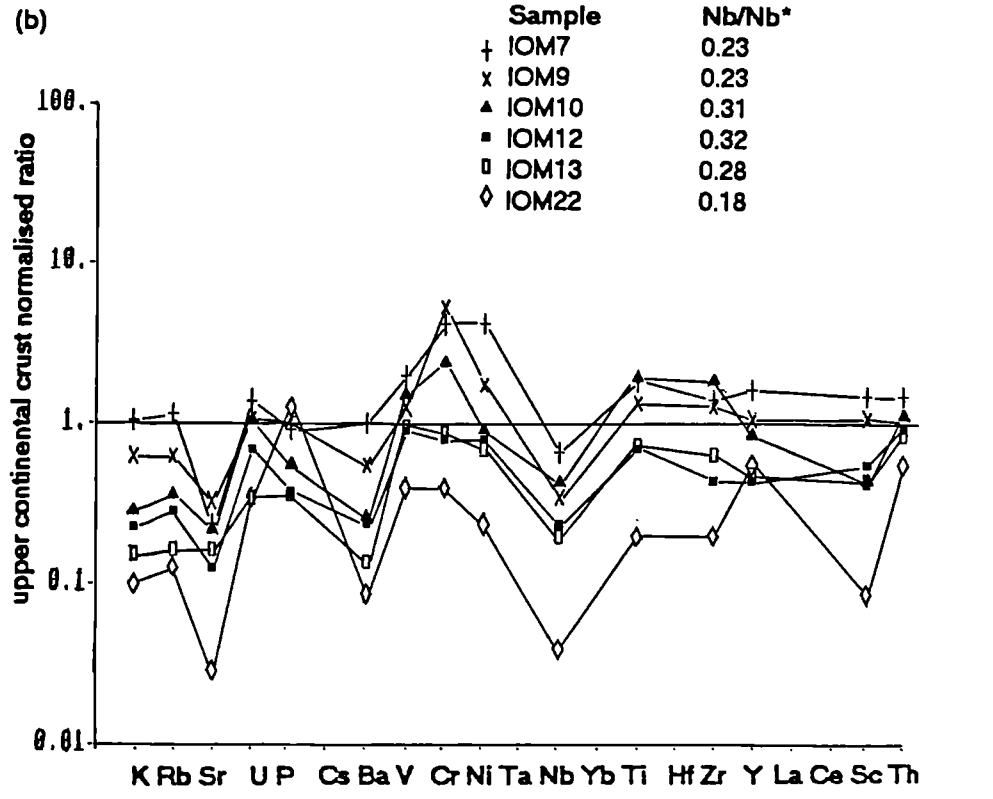

are similar within each unit resulting in similar pattern shapes. Samples from the Niarbyl Flags (IOM7,9) correspond generally to the *continental arc/active margin* pattern. High Ni and Cr values suggest a significant mafic input and positive Ti-Zr-Y values reflect a *passive margin* source. The Nb anomaly of 0.23 is slightly lower than the average for the *continental arc/active margin* average (0.27) due to the mafic content. The Lonan Flags (IOM10,12,13) samples show components of average *passive margin* and *continental arc/active margin* patterns: the Nb anomaly corresponds to a *passive margin* Sample IOM22 from the Maughold banded 'group' shows very low total abundances due to its high Si content. Some sections of the pattern reflect oceanic provenance (U-P, Y content, Nb anomaly), but this analysis is unreliable since elemental depletion may not be uniform.

3.5.3 Summary

The results of provenance discrimination techniques are shown in table 3.23. As with the Skiddaw Group, Manx Group samples do not fall into a single predefined provenance field but reflect a mixture of components. Compositions vary within and between stratigraphic units. Geochemical techniques indicate continental arc sources, with a mafic component, particularly in the Niarbyl Flags, mixed with passive margin sources. Recycled provenance is indicated by petrography and the discriminant function of Roser and Korsch (1988), and quartz wackes are exhibited by the Lonan Flags and Maughold banded 'group'.

Comparisons can be made with age equivalent Skiddaw Group formations. Petrography of the Tremadoc age Niarbyl Flags sample indicates *continental block* provenance, similar to the Bitter Beck Formation. Geochemistry of the Niarbyl Flags shows the greatest arc influence in this unit. The Lonan Flags samples (latest Tremadoc age) plot in equivalent positions to the Watch Hill Formation samples in nearly all geochemical discrimination plots. On petrographical ternary plots displacement of Lonan Flags samples away from the Watch Hill Formation towards the Q pole is due to their finer grainsize. The Maughold banded 'group' and Loweswater Formation share an Arenig age and both exhibit quartz wackes.

Thus the Skiddaw and Manx groups may share a common provenance interpreted to be a heterolithic recycled terrain containing a non-active volcanic arc, metamorphic and sedimentary strata augmented by a mature, possibly shelfal, intermediate source of quartz sands. Lithological comparisons of age-equivalent units suggest the Manx and Skiddaw groups shared a common depositional basin.

Table 3.23 Summary of provenance classifications for the Manx Group and compositional comparisons with the Skiddaw Group. BBE=Bitter Beck Formation, WHG=Watch Hill Formation, LWF-JG=Loweswater Formation of Jonah's Gill, OIA=oceanic island arc, CIA=continental island arc, ACM=active continental margin, PM=passive margin, ARC=volcanic island arc, CAAM=continental arc/active continental margin.

technique	provenance field and comparison with the Skiddaw Group unit of the Manx Group			
	Niarbyl Flags	Lonan Flags		Maughold band
		Langness	Port Mooar	-ed 'group'
compositional suites of Valloni and Mezzadri (1984)	quartzofeldspathic suite for all units source: orogenic terranes/platform deposits setting: rifted continental margin, back-arc/marginal basin			
provenance discrimination diagrams of Dickinson et al (1983)	transitional continental block BBE/WHG	quartzose recycled orogen WHG	craton interior LWF-JG	craton interior LWF-JG
discriminant function analysis (this study)	CIA/ACM	CIA/ACM		ACM
discriminant function analysis (Roser and Korsch, 1988)	recycled/felsic	recycled WHG		recycled
Fe_2O_3+MgO vs TiO_2 plot (fields of this study)	OIA/CIA	ACM/PM WHG		ACM
SiO_2 vs K_2O/Na_2O (Roser and Korsch, 1986)	ACM	PM WHG		PM
trace element plots				
Sc-V	mafic component	PM		PM
Th-Sc-Zr	CIA	ACM/PM		ACM?
Th-Co-Zr	CIA	CIA+ACM? WHG		ACM?
Rb-K	acidic and intermediate source	mixed acidic and basic source		
Ni-TiO_2	mafic component	acidic source		
multi-element variation diagram (Floyd et al, 1991)	CAAM/(PM) significant mafic input	PM/CAAM		
Nb/Nb*	CAAM	PM		

3.6 Provenance of the Ingleton Group

This section aims to describe the composition of Ingleton Group sediments, identify their provenance, and compare and contrast these with the Arenig greywackes of the Beckermonds Scar borehole and the Skiddaw Group.

Samples used in the study are shown in table 3.24.

Table 3.24 Samples used in petrographical and geochemical analysis of (a) Ingleton Group, and (b) Arenig greywackes of the Beckermonds Scar borehole.

sample	description	petrographical analysis	geochemical analysis
(a) Ingleton Group			
M90-9	very fine-fine sand grainsize	/	/
M90-10	medium-coarse sand grainsize	/	/
M90-11	coarse silt-very fine sand grainsize	/	/
M90-12	medium sand grainsize	/	/
ING-L	very coarse sand grainsize	lithic proportions only	
ING-C	composite sample of medium sand grainsize greywackes		/
ING-M	mudstone		/
(b) Beckermonds Scar borehole			
E50441	coarse-very coarse sand grainsize	/ (modal analysis & lithic proportions)	
E50449	fine-medium sand grainsize	/	
E50445	fine-medium sand grainsize	/	
E50448	medium sand grainsize	/	
E50442	very coarse sand grainsize	/	

3.6.1 Petrographical techniques

Samples from both Ingleton Quarry and Beckermonds Scar borehole are classified as quartz-intermediate feldspathic wackes (figure 3.52), but plot ambiguously using primary parameters to determine compositional suites (figure 3.53). Secondary parameters show both quartzofeldspathic and feldspatholithic suites to be represented. These correspond to *cratonic block* and *volcanic orogenic belt* sources respectively. A basin setting common to both suites is a back-arc basin.

Application of provenance discrimination diagrams (figure 3.54) indicates a *dissected volcanic arc* source for samples from Ingleton quarry. Greywackes from the Beckermonds Scar borehole plot further away from the lithic pole on Q-F-L, but largely within the field for *dissected volcanic arc* provenance on a Qm-F-Lt plot. Their lower lithic content, compared to Ingleton quarry samples, probably reflects the difference in sedimentary facies association of the two localities, i.e. coarse grained depositional lobe for the quarry and lobe fringe deposits for the borehole (chapter 2). Thus lithic disaggregation during transport would have been more pronounced in the latter.

Proportions of lithic fragment types in the coarsest grainsize samples show a dominance of volcanic types, suggesting a magmatic arc source, but the samples do not plot in any of the fields of Ingersoll and Suczek (1979) (figure 3.54).

The mineral maturity indi ces are low for the Ingleton quarry greywackes (average MI=39), but higher for greywackes from Beckermonds Scar borehole (average MI=52). This relationship could result from lithic disaggregation during transport. It could not result from post-depositional lithic replacement by matrix, since matrix content is higher in the lithic-rich quarry samples (41% in very coarse sand grade, to 76% in siltstone/very fine sand grade) compared with the relatively lithic-poor borehole samples (13.5% in very coarse sand grade, to 34% in fine sand grade).

At both localities, potassium and untwinned feldspars dominate over plagioclase feldspar of andesine composition. The range of lithic fragments (plates 3.15 to 3.18) includes:

mudstone and siltstone,
red chert, with a dusting of red pigment (haematite) on microcrystalline quartz containing spheroids with opaque rims, possibly radiolaria. Clasts are commonly cut by quartz veins (plate 3.15),
quartz-mica schist (plate 3.18.1),
quartz-chlorite schist (plate 3.18.2),
quartz mylonite,
abundant strained polycrystalline quartz of metamorphic origin (plate 3.17.2),
hornfels,
meta-carbonate,
phyllite,
acid plutonic clasts of quartz and feldspar, sometimes with graphic texture,
rhyolite,
basalt,
gabbro with zoned plagioclase,
pyroclastic clasts with relict glass shards (plate 3.17.1),
chlorite clasts (plate 3.16).

Matrix is dominantly of secondary chlorite and epidote.

Figure 3.52 Classification diagram for greywackes of the Ingleton Group (n=4) and the Beckermonds Scar borehole (n=5), with fields of Dott (1964), Pettijohn et al (1972).

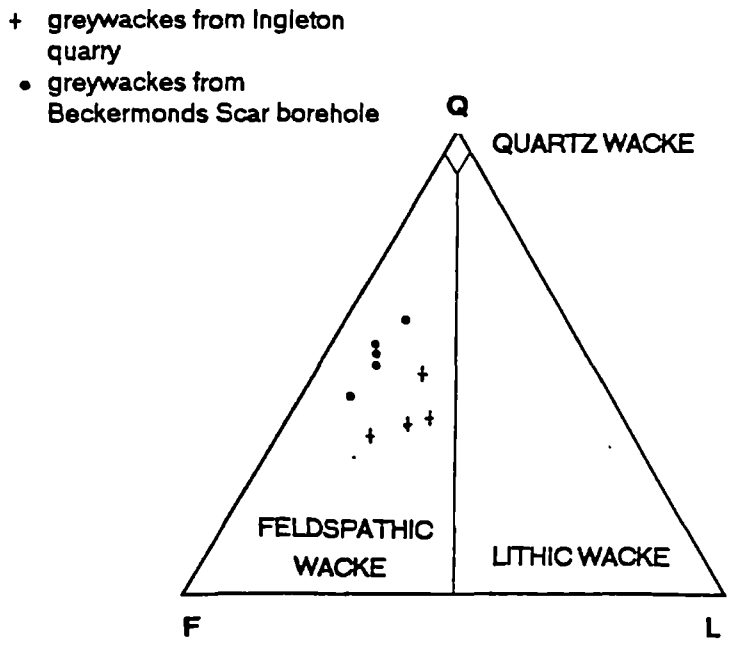

Figure 3.53 Comparison of Ingleton Group greywackes (n=4) and greywackes from the Beckermonds borehole (n=5) with the compositional suites of Valloni and Mezzadri (1984): QF=quartzofeldspathic, QL=quartzolithic, FL=feldspatholithic, LV=lithovolcanic.

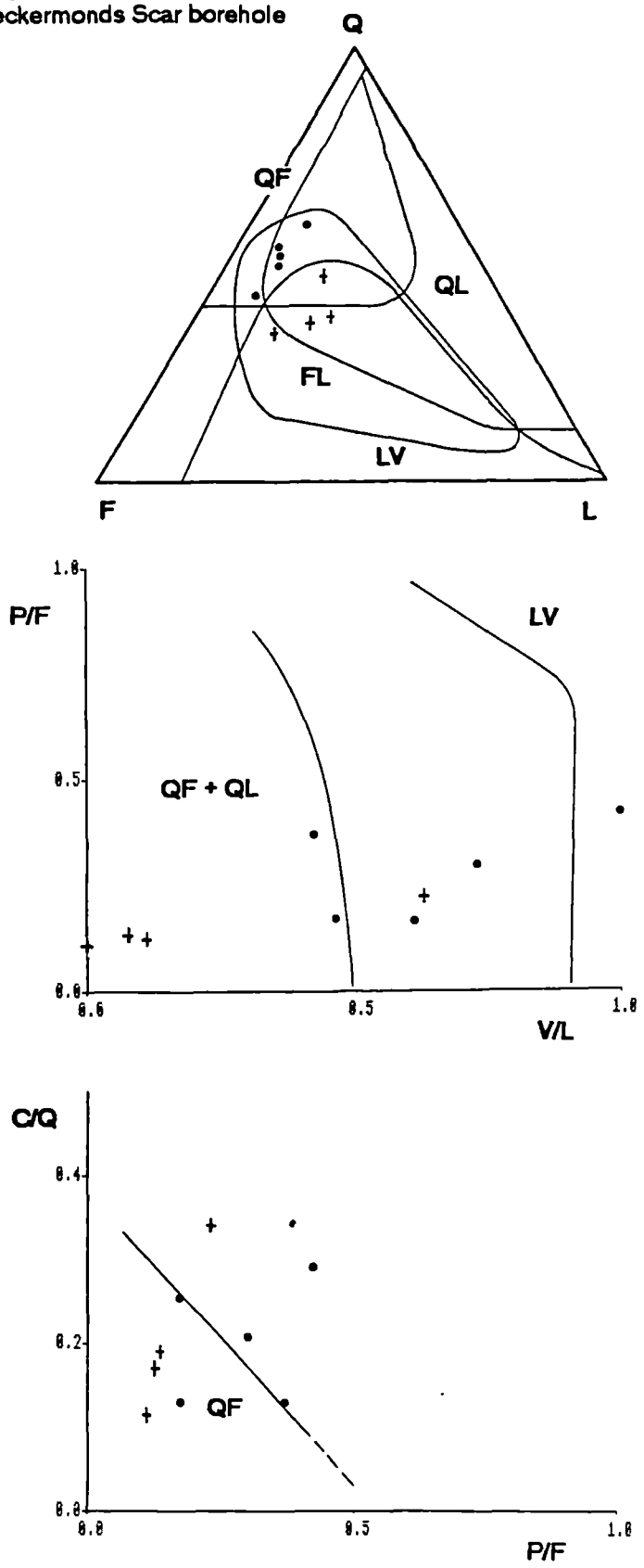

Figure 3.54 Provenance discrimination diagrams for the Ingleton Group (n=4) and Beckermonds Scar borehole (n=5): Q-F-L, Qm-F-Lt., Qp-Lv-Ls for greywackes with fields after Dickinson et al (1983). Lm-Lv-Ls, Qp-Lv-Ls for lithic range of very coarse sand grainsize greywackes with fields after Ingersoll and Suczek (1979) (n=2). RCM=rifted continental margin, MA=magmatic arc, SB=suture belt, MA+SC=mixed magmatic arc and subduction complex, MA+RCM=mixed magmatic arc and rifted continental margin.

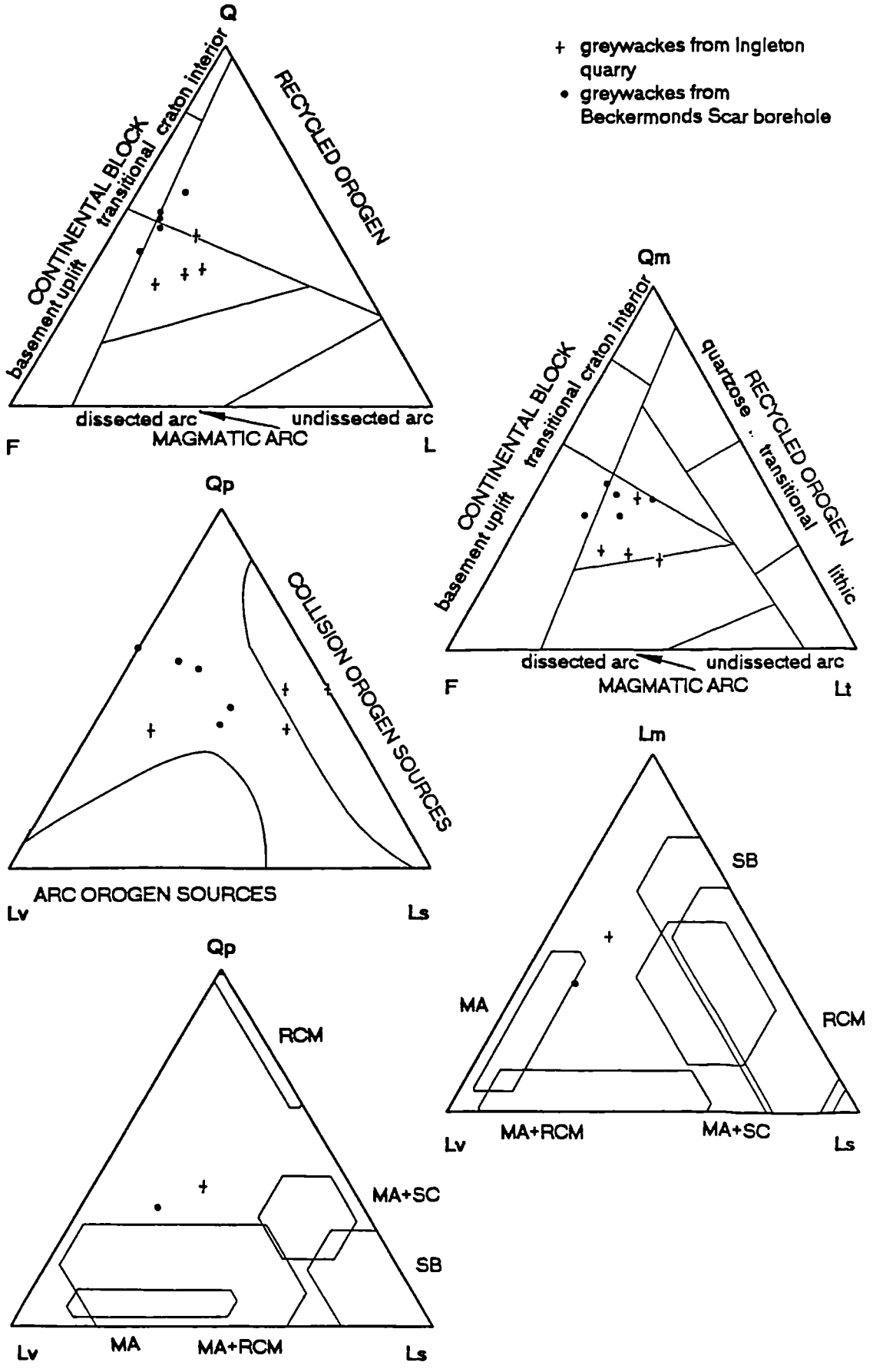

PLATE 3.15

3.15.1 Subangular clast of red chert with fine-coarse sand size grains of quartz and feldspar in a chlorite matrix.
Sample ING-L Ingleton Group, plane polarized light.
Magnification x25.

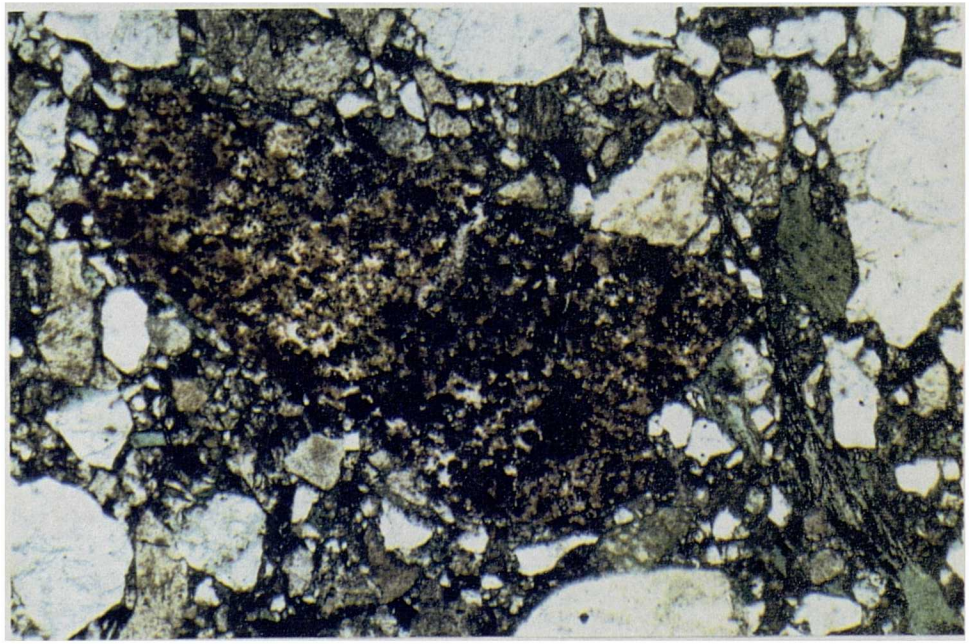

3.15.2 Detail of chert of 3.15.1 showing partially opaque spheres, possibly radiolaria, patches of red pigment and cross-cutting micro vein of quartz.
Sample ING-L, Ingleton Group, plane polarized light.
Magnification x250.

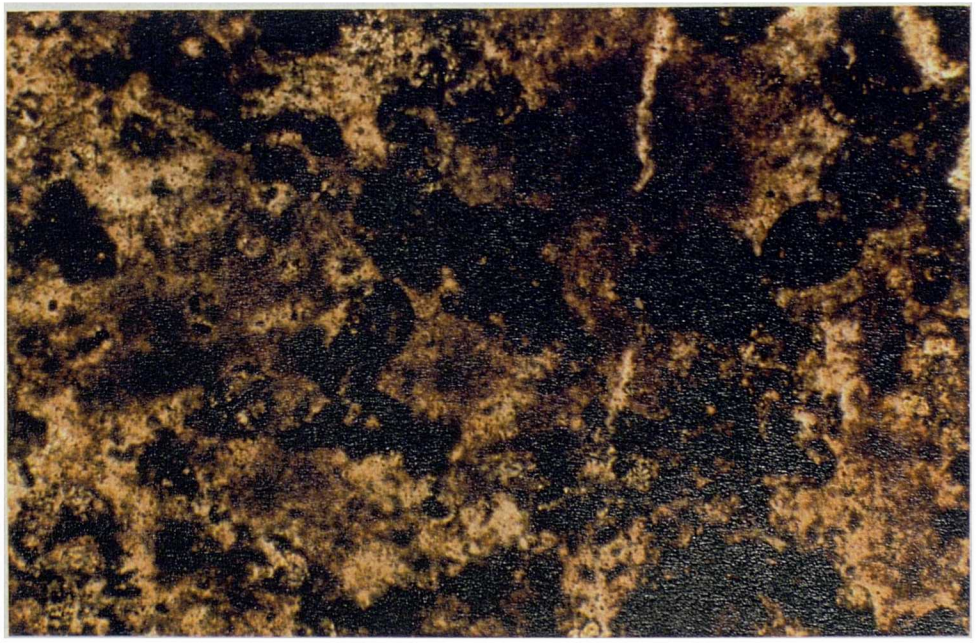

PLATE 3.16

3.16.1 Clast of chlorite with relict plagioclase laths and phyllosilicates interpreted as a basic volcanic lithic, with subrounded fine sand size grains of plagioclase, monocrystalline quartz and metamorphic polycrystalline quartz and chlorite matrix. Sample ING-L, Ingleton Group, plane polarized light. Magnification x100

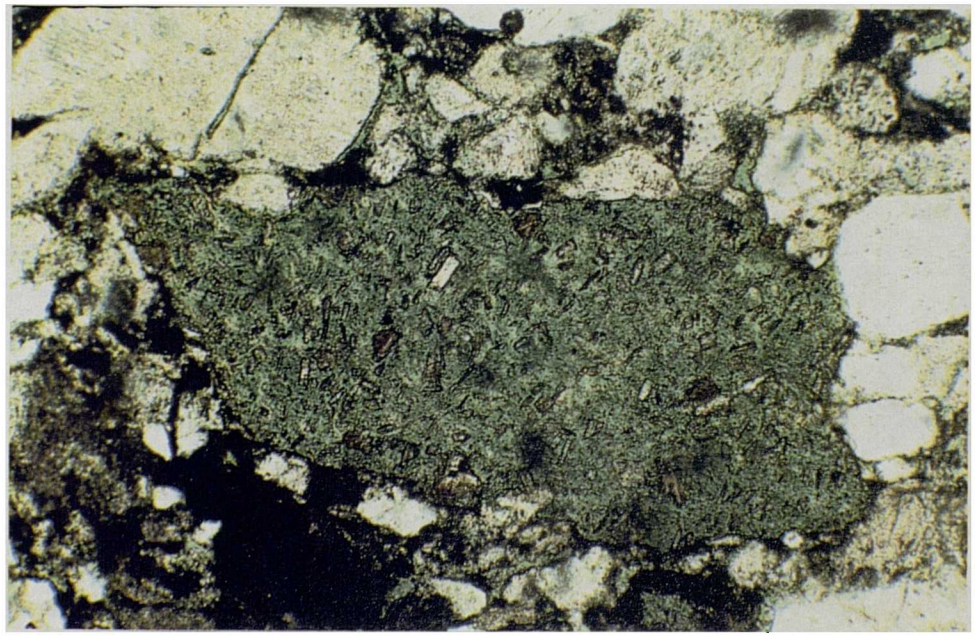

3.16.2 As 3.16.1, with crossed polars.

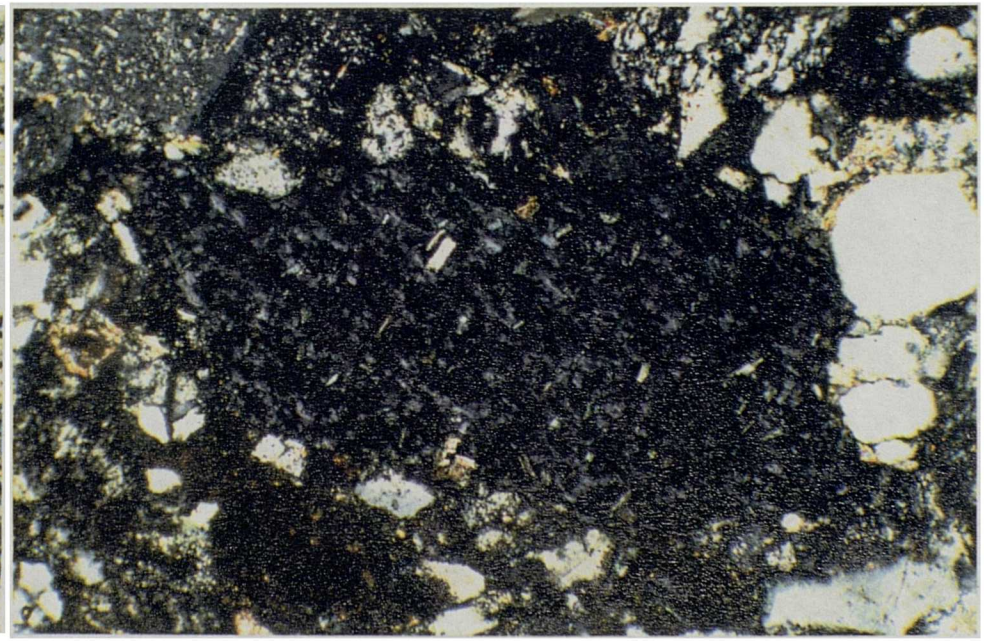

PLATE 3.17

3.17.1 Pyroclastic fragment with glass shards and angular crystal fragments, partially replaced by clay and carbonate. Sample ING-L, Ingleton Group, plane polarized light. Magnification x100.

3.17.2 Clast of metamorphic polycrystalline quartz with grains of quartz and feldspar, a pelitic lithic fragment and detrital muscovite. Sample ING-L, Ingleton Group, crossed polars Magnification x25.

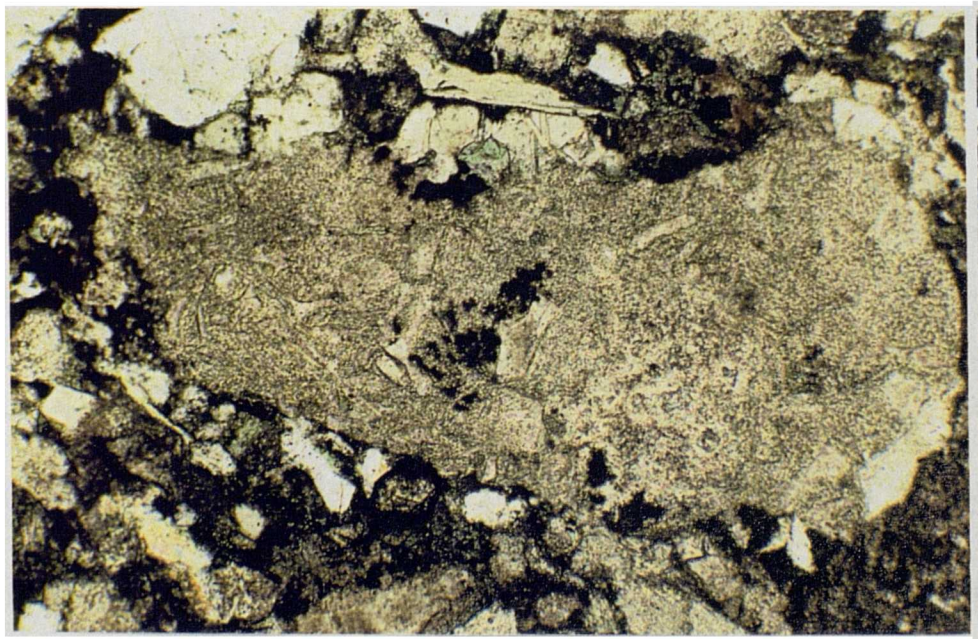

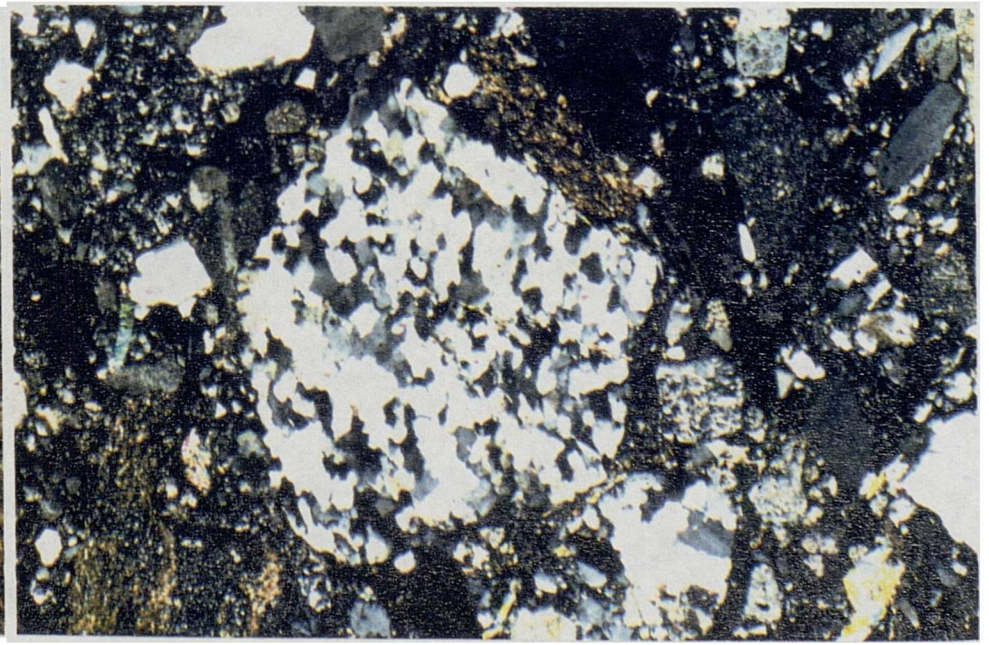

PLATE 3.18

3.18.1 Subrounded clast of quartz-muscovite schist with rounded grain of monocrystalline quartz and subangular feldspar grains, phyllite and detrital muscovite.
Sample ING-L, Ingleton Group, crossed polars.
Magnification x40.

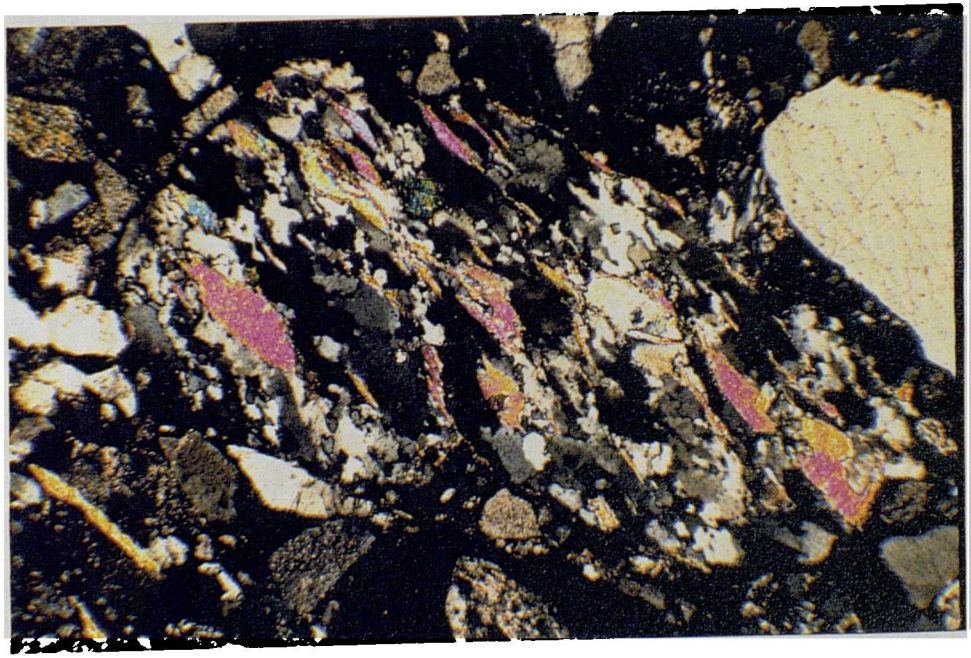

3.18.2 Metamorphic clast of schist comprising bands of quartz-chlorite and rotated blocky feldspars
Sample ING-L, Ingleton Group, plane polarized light.
Magnification x40.

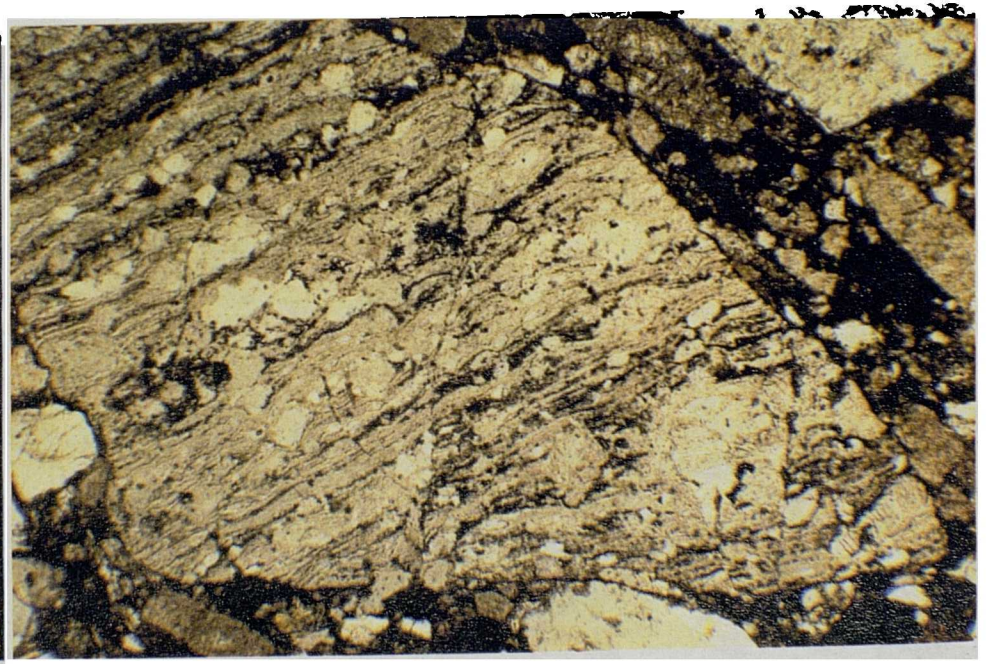

3.6.2 Geochemical techniques

On geochemical classifications, Ingleton Group greywackes plot in the fields of greywacke and lithic sandstone, and show affinities with the quartz-intermediate and quartz-rich groups of Crook (1974) (figure 3.55).

The discriminant function defined in section 3.3.3.4 classifies the sandstones into a range of provenance fields (table 3.25). Sample M90-11 is of coarse silt to very fine sand grainsize hence classification is unreliable. A continental arc source is indicated for other samples.

Table 3.25 Results of discriminant function classification by provenance type for Ingleton Group greywackes. CIA=continental island arc, ACM=active continental margin, PM=passive margin.

sample	provenance setting
M90-9	ACM
M90-10	CIA
M90-11	PM
M90-12	ACM
ING-C	CIA

The discriminant functions of Roser and Korsch (1988) classify Ingleton Group samples exclusively to the *felsic* provenance field indicating a source of acid plutonic and volcanic detritus from an active continental margin (figure 3.56).

The $^{*}Fe_2O_3$+MgO versus TiO_2 plot with provenance fields as defined in section 3.3.4, indicates provenance from an island arc (figure 3.57a).

On a diagram of SiO_2 versus K_2O/Na_2O (figure 3.57b) Ingletonian samples plot in the *active continental margin* field of Roser and Korsch (1986).

Trace element plots also indicate a continental arc source. The Zr/Th ratio (figure 3.58a) of *c*15 for Ingletonian greywackes is above the maximum of 12 for active continental margin sandstones and relates to a *continental island arc* provenance (Bhatia and Crook, 1986). The high V and Sc values (figure 3.58b) correspond to an island arc provenance. Ternary trace element plots Th-Sc-Zr and Th-Co-Zr (figure 3.59) both indicate *continental island arc* provenance. Acidic sources are indicated by both Rb versus K and Ni versus TiO_2 plots (figure 3.60a,b).

Table 3.26 shows trace element characteristics of mudstones of different tectonic settings and values for Ingletonian mudstone. The parameters indicate a *continental island arc* source is dominant and the values are generally similar to those for average Skiddaw Group mudstone. Cr and Ni values are higher in the Skiddaw Group suggesting it contains a greater mafic component than the Ingleton Group.

A multi-element variation diagram for Ingletonian sediments (figure 3.61) shows little variation between samples. The pattern shape and Nb anomaly correspond most closely to the average for sandstones from *continental arc/active continental margin* provenance.

Figure 3.55 Geochemical classification for sandstones of the Ingleton Group after (a) Blatt et al (1972) and (b) Crook (1974) (diagram after Floyd and Leveridge, 1987). *Fe_2O_3=total iron as Fe_2O_3.

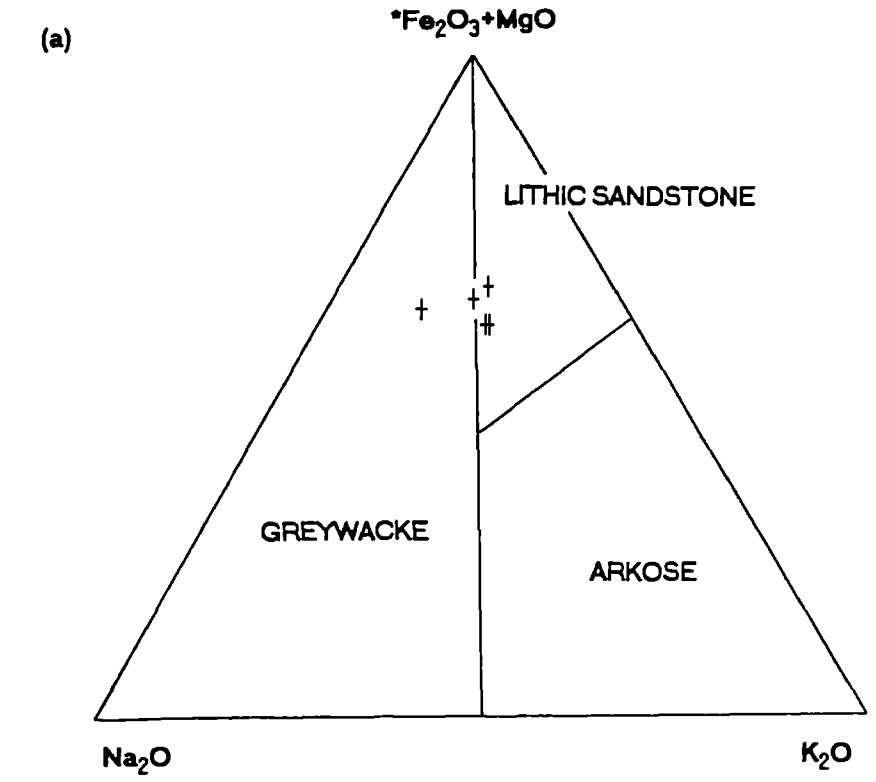

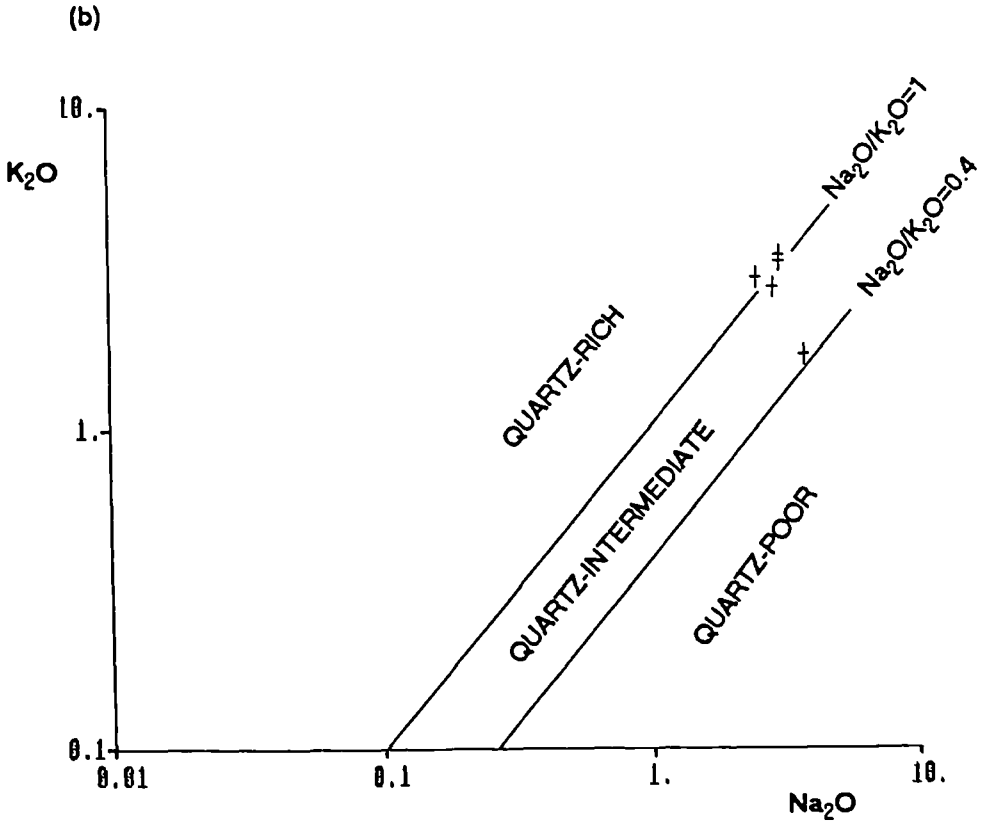

Figure 3.56 Discriminant score 1 versus discriminant score 2 using the discriminant functions of Roser and Korsch (1988) for Ingleton Group sediments. P1=mafic, P2=intermediate, P3=felsic, P4=recycled.

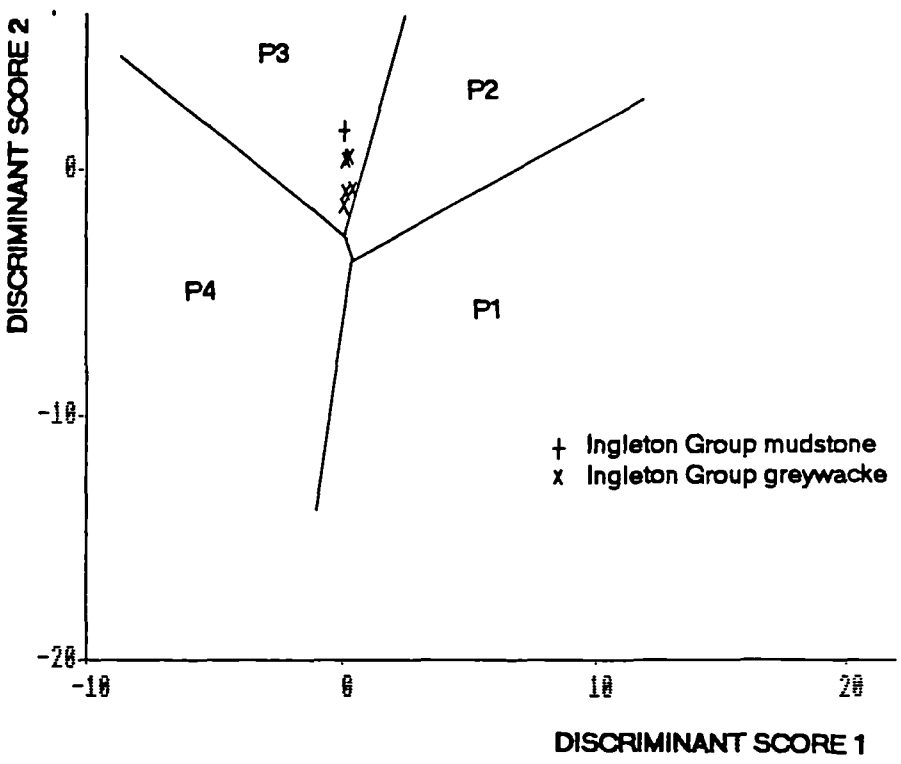

Figure 3.57 (a) $*Fe_2O_3+MgO$ versus TiO_2 plot for Ingleton Group greywackes with provenance fields defined in section 3.3.4, OIA=oceanic island arc, CIA=continental island arc, ACM=active continental margin, PM=passive margin, $*Fe_2O_3$ is total iron as Fe_2O_3; (b) SiO_2 versus K_2O/Na_2O plot for the Ingleton Group with fields after Roser and Korsch (1986), ARC=island arc, ACM=active continental margin, PM=passive margin.

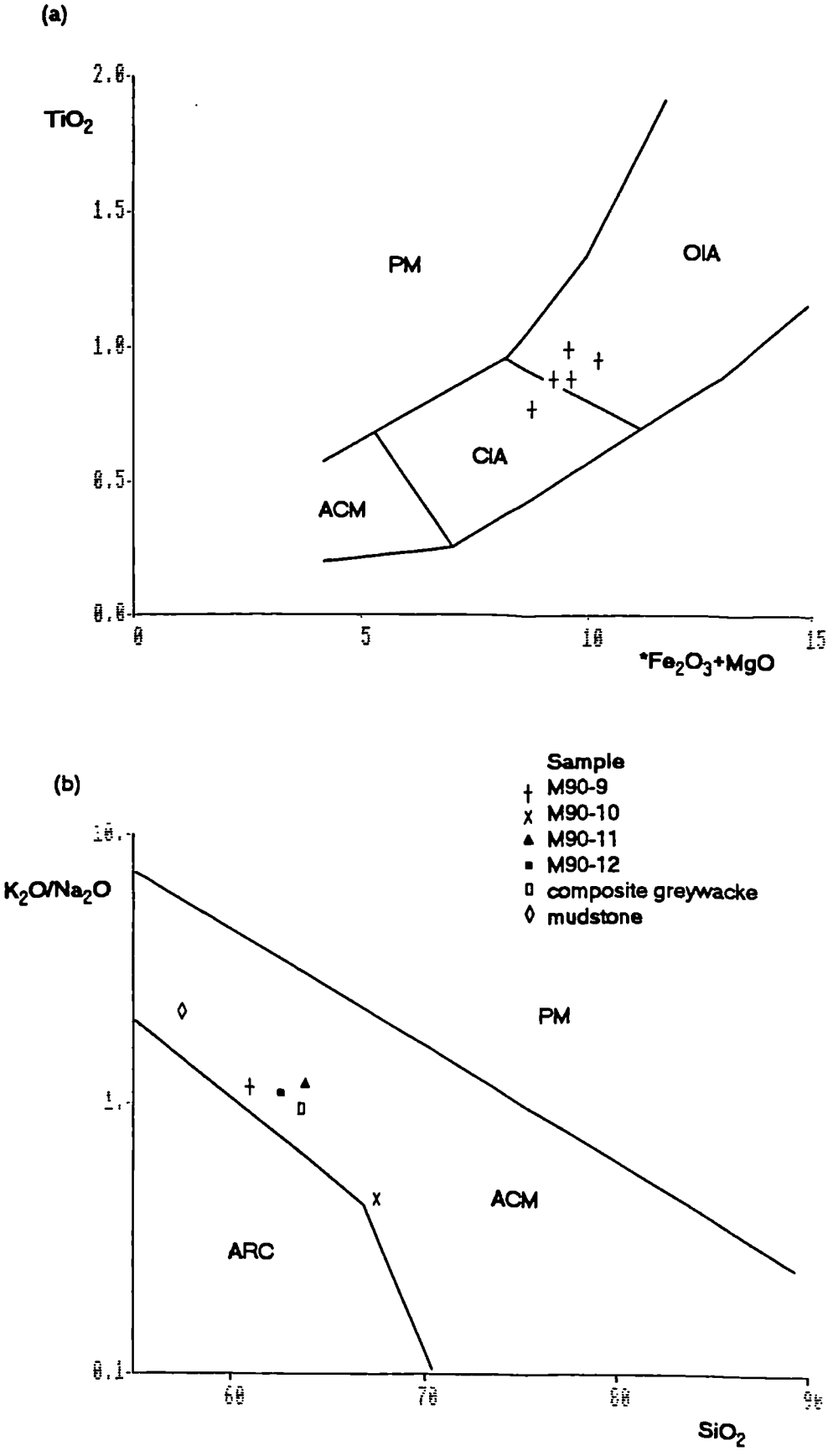

Figure 3.58 (a) Th versus Zr with active continental margin field from Bhatia and Crook (1986) and (b) Sc versus V for Ingleton Group greywackes.

(a)

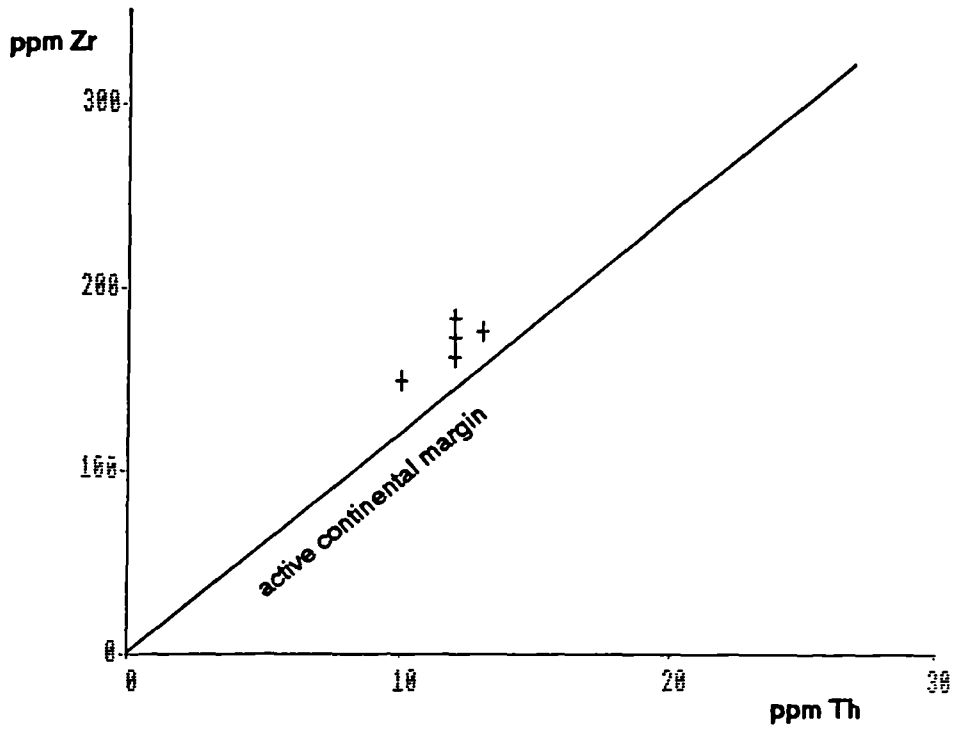

(b)

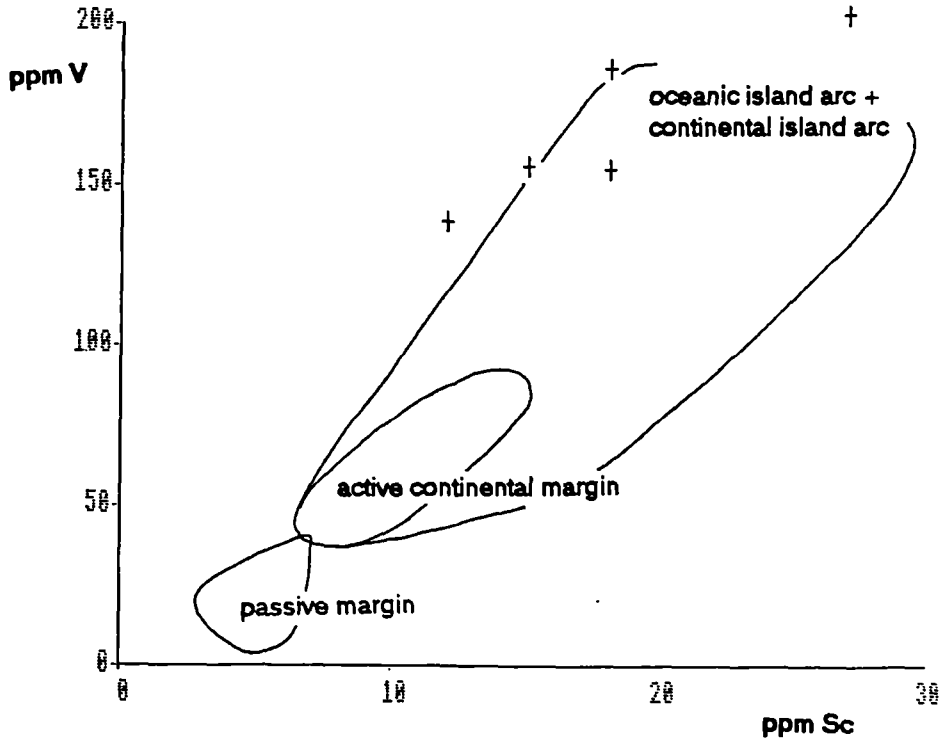

Figure 3.59 (a) Th-Sc-Zr and (b) Th-Co-Zr for Ingleton Group greywackes with provenance fields redrawn from the data of Bhatia and Crook (1986). OIA=oceanic island arc, CIA=continental island arc, ACM=active continental margin, PM=passive margin.

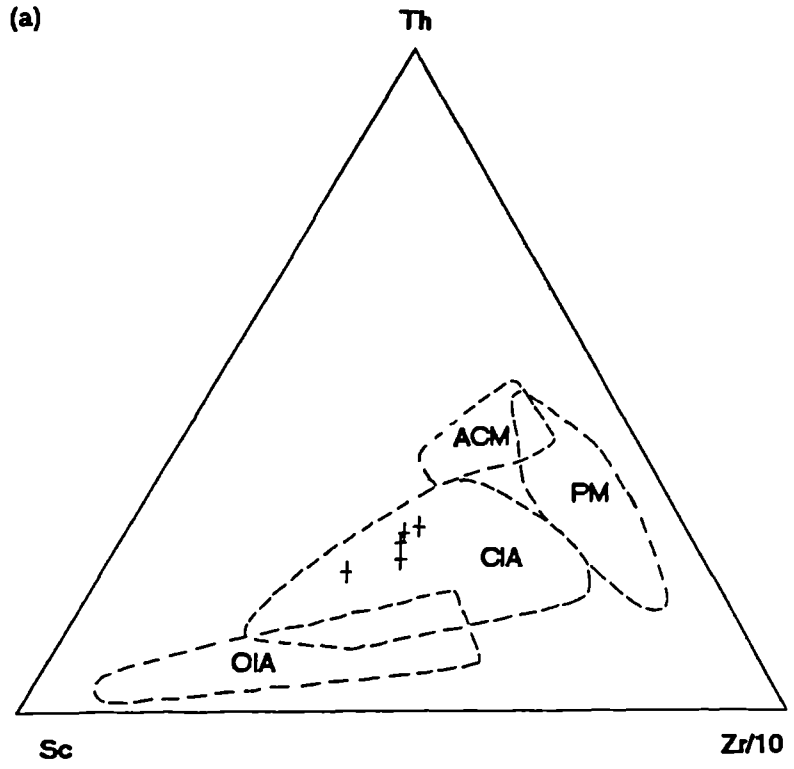

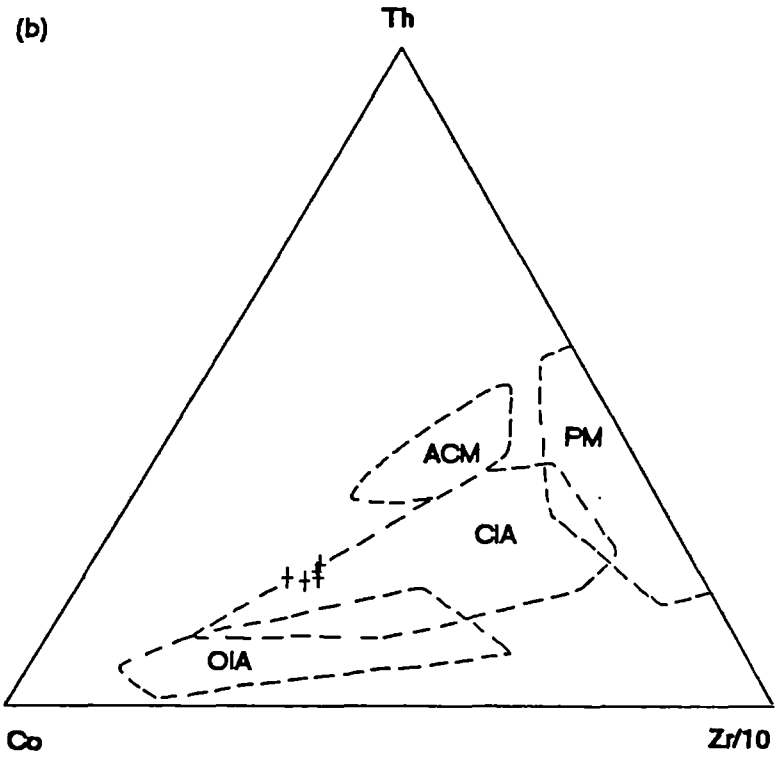

Figure 3.60 (a) Rb vs K for the Ingleton Group with K/Rb=230 representing a differentiated magmatic suite (Shaw, 1968); (b) Ni versus TiO_2 for Ingleton Group greywackes with provenance fields after Floyd et al (1991).

(a)

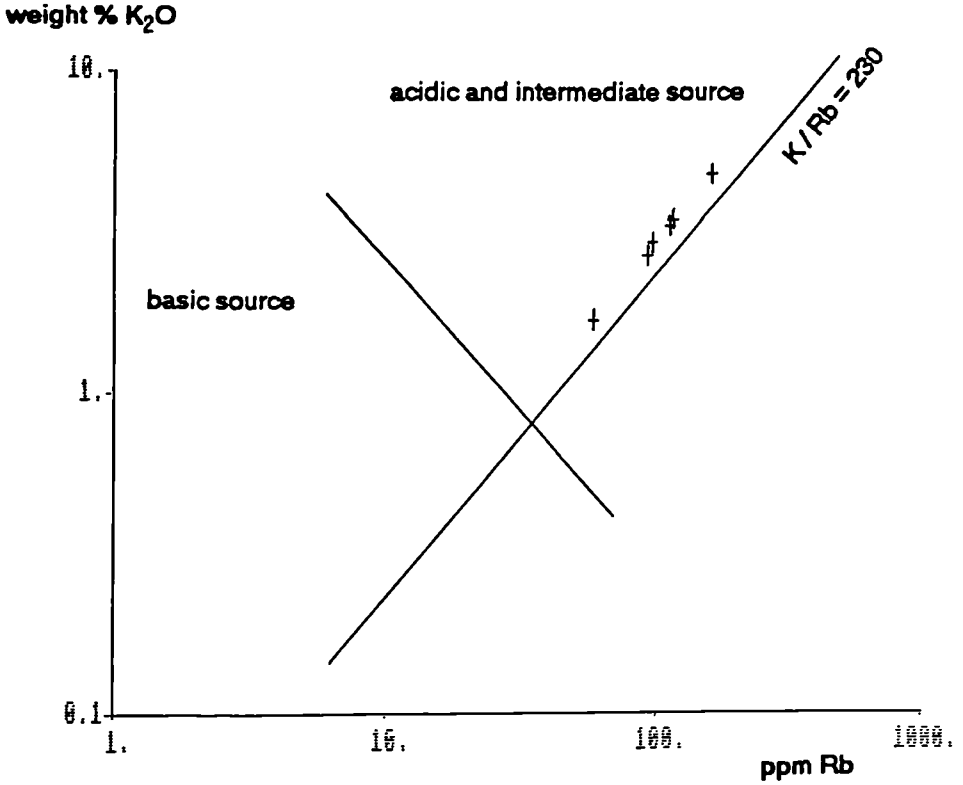

(b)

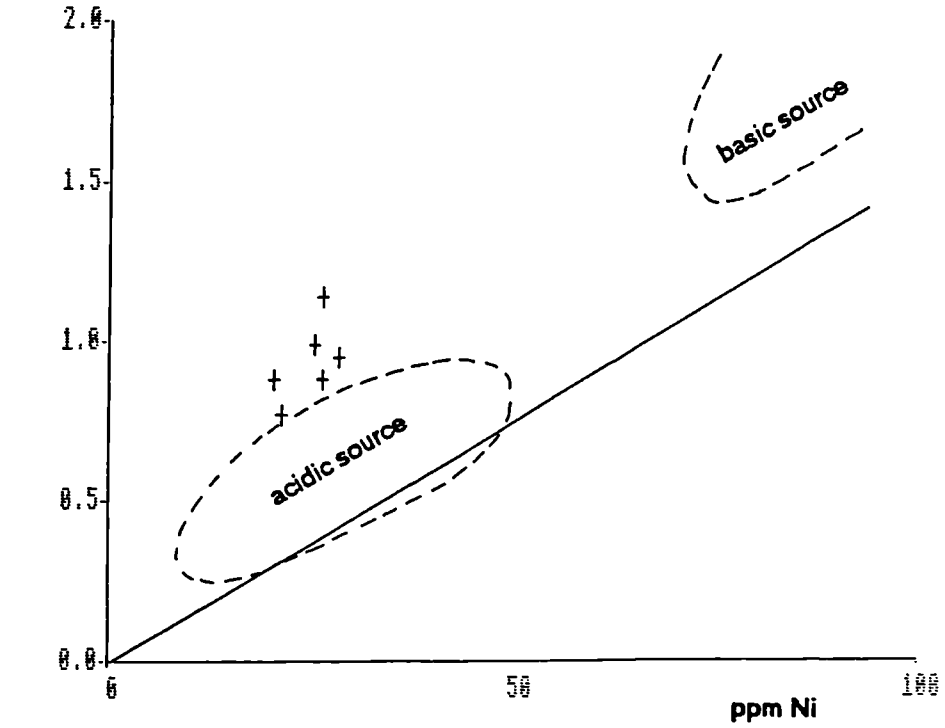

Figure 3.61 Multi-element variation diagrams (a) with characteristic patterns for different tectonic settings (Floyd et al, 1991); (b) for samples from the Ingleton Group.

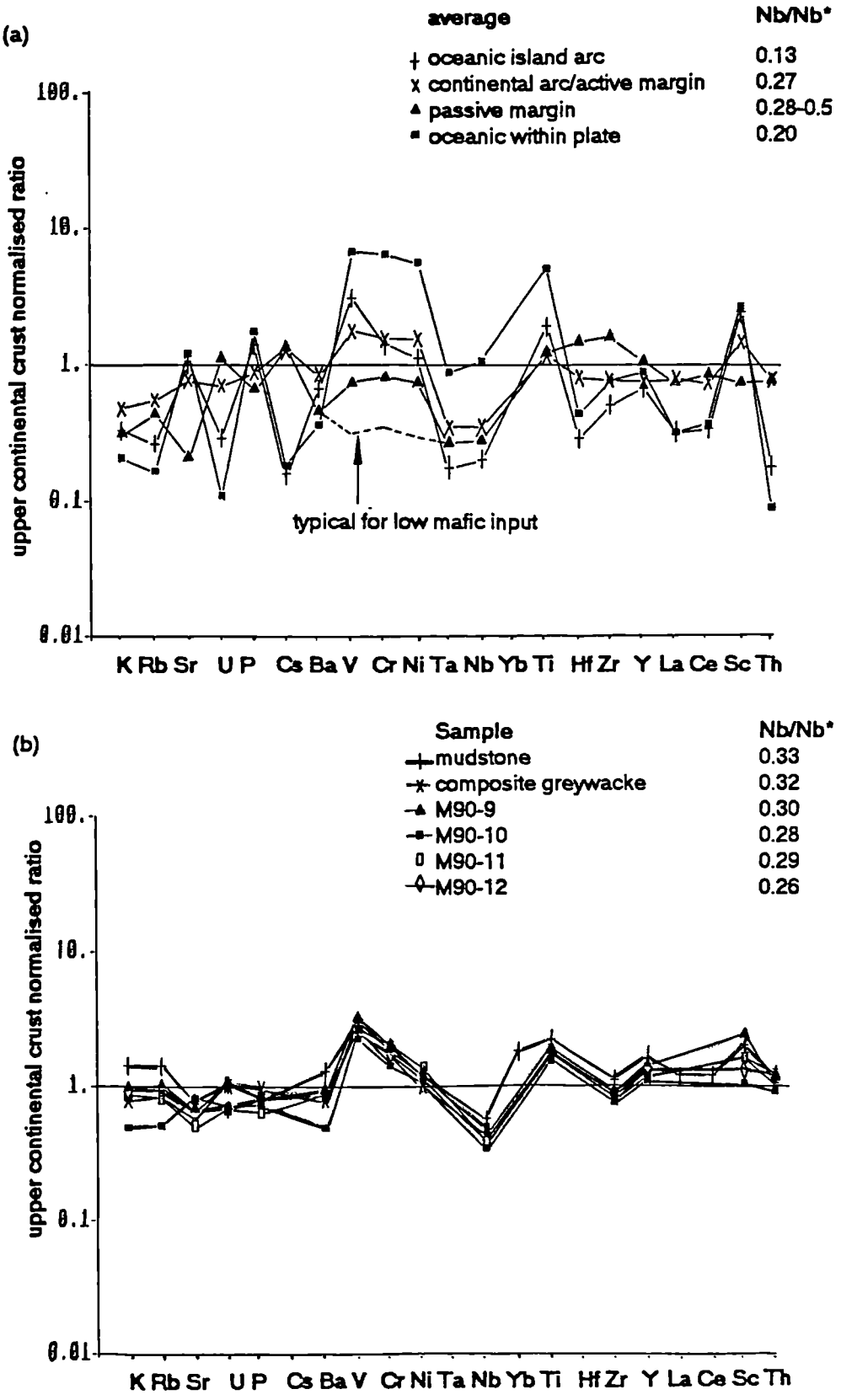

The rare earth element pattern for the Ingleton Group mudstone is flatter than PAAS and Skiddaw Group patterns, and has a smaller Eu anomaly (La_N/Yb_N=5.97, Eu/Eu*=0.79) (figure 3.62). These parameters agree closely with the modern mud sample from an active continental margin (figure 3.42, table 3.18) although this has slightly lower total rare earth element content. Of the ancient sandstone samples whose rare earth element patterns are depicted in figure 3.43, the Ingletonian mudstone pattern (as for the Skiddaw Group mudstones) is most similar to quartz-intermediate sandstones of continental arc provenance.

Table 3.26 Trace element characteristics of mudrocks from various tectonic settings (after Bhatia, 1985, tableVI), average for Skiddaw Group mudstones (n=30) and Ingleton Group mudstone (n=1).

	Oceanic island arc	Continental island arc	Active continental margin	Passive margin	Skiddaw Group	Ingleton Group
Th	5.5	16.2	28.0	22.0	12.7	13.0
U	2.4	3.2	6.0	3.6	3.6	3.0
Nb	3.7	9.0	16.5	15.8	20.0	15
Th/U	2.8	5.2	5.0	6.7	4.0	4.3
Zr/Th	28	12	7	7	15	16
Zr/Nb	38	21	11	10	9	14
Nb/Y	0.17	0.35	0.50	0.54	0.50	0.42
La	18	24	42	34	50	36
La/Sc	1.0	1.8	2.5	1.9	-	1.6
Cr	39	55	58	100	129	72
Ni	15	18	26	36	56	26
Sc/Ni	1.70	0.96	0.75	0.45	-	0.85
Rb/Sr	0.29	1.31	2.90	5.80	1.19	0.70
Ba/Sr	2.5	6.3	8.7	17.6	5.7	3.1

Figure 3.62 Rare earth element patterns normalised to type 1 carbonaceous chondrites for Ingleton Group mudstone, PAAS and Watch Hill Formation mudstone. PAAS=post Archaean Australian shale average.

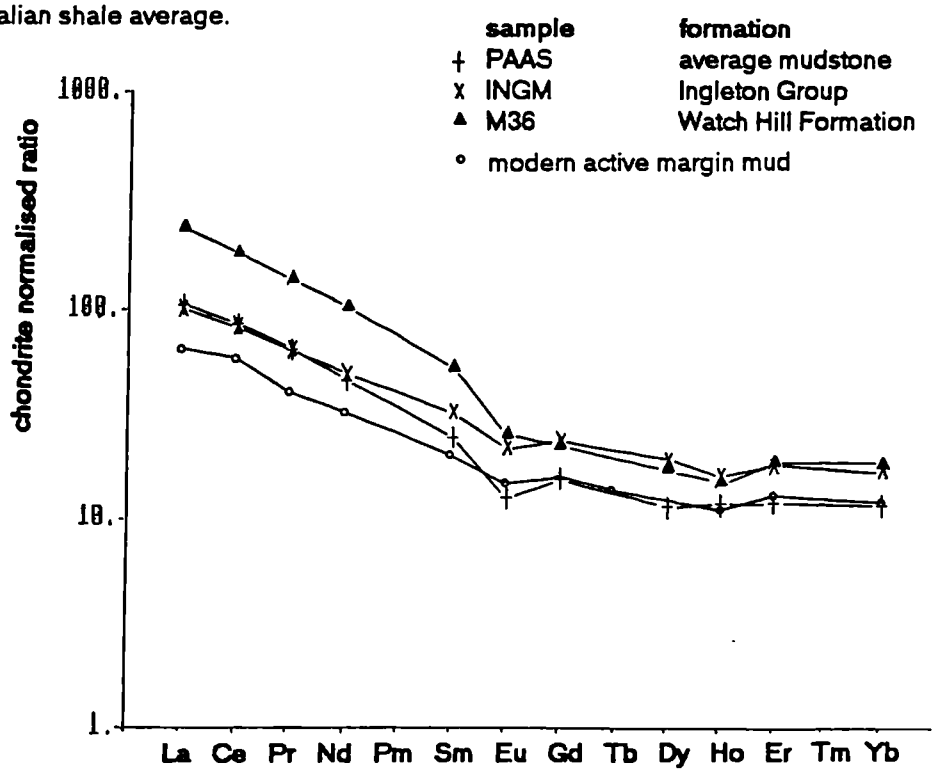

3.6.3 Summary

Greywacke samples from Ingleton quarry and Beckermonds Scar borehole have been compared petrographically and grain populations, the range of lithic fragments and the occurrence of distinctive red cherts at both localities suggests a similarity in composition and provenance. Variation in plotting position on Q-F-L and Qm-F-Lt diagrams (figure 3.54) could reflect the difference in dominant depositional environment at each locality. This conclusion supports the lithological correlation of Arenig strata of the Beckermonds Scar borehole with the Ingleton Group, which implies a depositional age for the latter (Wilson and Cornwell, 1982; Berridge, 1982).

Both petrographical and geochemical provenance discrimination techniques consistently indicate a continental arc provenance for the Ingleton Group (table 3.28). The position of the arc on an active continental margin or microcontinental arc, and sediment deposition in a trench, fore-arc or back-arc basin is unclear from sediment composition alone.

Since the greywackes are immature with abundant volcanic lithics then sediment is probably first cycle from this eroding arc orogen. The observation of a bentonite ash band at Ingleton Quarry suggests that volcanism was active during sedimentation, but this volcanic centre may have been distant from the sediment source region. The contemporaneity of volcanism and sedimentation, can be assessed from neodymium model age data. Table 3.27 shows published neodymium model ages for the Ingleton Group to be lower than the Skiddaw Group, due to abundant volcanic detritus in the former. The Nd model ages for the Ingleton Group are lower than for Ordovician sediments coeval with volcanism in Wales (minimum 1.26Ga), but fall within the range for Precambrian sediments derived from the Uriconian volcanics (1.04-1.48Ga) (Thorogood, 1990). Since the abundance of non-volcanic lithic fragments observed in Ingletonian greywackes is likely to increase the Nd model age of the samples, and assuming that contemporaneous volcanism in northwest England and Wales would have similar isotopic characteristics, it is unlikely that the Ingleton Group was sourced from an Ordovician volcanic arc. A source of Precambrian arc rocks could explain the Nd model age data.

Table 3.27 Neodymium model ages for the Ingleton Group and Skiddaw Group, calculated using the depleted mantle parameters of DePaolo (1981).

Ingleton Group			Skiddaw Group		
source	sample	Nd model age (Ga)	source	sample	Nd model age (Ga)
O'Nions et al (1983)	16	1.18	O'Nions et al (1983)	81-16c 81-81	1.52 1.53
Davies et al (1985)	ARC1 ARC2	1.23 1.20	Davies et al (1985)	81/14	1.44
			Thirlwall (pers comm)	minimum maximum	1.59 2.52

Table 3.28 Summary of provenance classifications for the Ingleton Group. OIA=oceanic island arc, CIA=continental island arc, ACM=active continental margin, PM=passive margin, ARC=volcanic island arc, CAAM=continental arc/active continental margin.

technique	provenance field for the Ingleton Group
compositional suites of Valloni and Mezzadri (1984)	quartzofeldspathic suite source: orogenic terranes/platform deposits setting: rifted continental margin, back-arc/marginal basin feldspatholithic suite; source: volcanic orogen setting: strike-slip or Andean margins, back-arc basins
provenance discrimination diagrams of Dickinson et al (1983)	dissected volcanic arc volcanic arc orogen
discriminant function analysis (this study)	CIA/ACM
discriminant function analysis (Roser and Korsch, 1988)	felsic; acid plutonic and volcanic detritus from an active continental margin
Fe_2O_3+MgO vs TiO_2 plot (fields of this study)	OIA/CIA
SiO_2 vs K_2O/Na_2O (Roser and Korsch, 1986)	ACM
trace element plots	
Th-Zr	continental arc
Sc-V	volcanic island arc
Th-Sc-Zr	CIA
Th-Co-Zr	CIA
Rb-K	acidic and intermediate sources
Ni-TiO_2	acidic source
trace elements in mudstones	CIA, (ACM)
multi-element variation diagram (Floyd et al, 1991)	CAAM
Nb/Nb*	CAAM
rare earth elements	similarity with modern active continental margin mud and ancient sandstone of continental arc provenance

In addition to conflicting Nd model ages for the Ingleton and Skiddaw groups, other compositional differences are apparent. Table 3.29 compares the mean modal analyses for the two groups. The Skiddaw Group is more mature (mean MI=73), with less feldspar but the large range of lithic fragments is similar for both groups. The characteristic red cherts of the Ingleton Group are not present in the Skiddaw Group.

Similar red cherts are observed in greywackes of the Cambrian Bray Group of southeast Ireland, which displays similar sedimentary facies to the Ingleton Group. The composition of the greywackes of the two groups is distinct, however, shown by a Q-F-L ternary plot (figure 3.63). The quartz-rich Bray Group greywackes have a small lithic range of acid plutonic clasts, rhyolite, quartz-mica schist and chert and correspond to a *craton interior* provenance.

McArdle (1981) correlated the greywackes of the Ballbeg Pelite Formation (Ribband Group, Cambrian to Llandeilo age) with the Bray Group. Max et al (1990) argue against this lithological correlation since the former contains a dominance of volcaniclastic lithics. This observation prompts comparison with the Ingleton Group. It is probable, therefore, that early Ordovician sediment distributary systems of southeast Ireland and Ingleton shared common provenance elements. Distinctive red cherts, derived from recycled marine sediments, are absent from the Skiddaw Group, which suggests the group represents a separate dispersal system which was unconnected to the source of red cherts, either directly or through recycling of Ingletonian sediment.

In summary, the Ingleton Group was derived from first cycle detritus from an eroding arc orogen. Volcanism was active during the Arenig (assuming an Arenig depositional age, inferred from lithological comparison with Arenig strata from the Beckermonds Scar borehole) and provided wind-blown ash, but not necessarily surface-transported detritus. Sediment could have been derived from a provenance of Precambrian volcanic arcs, as could the Skiddaw Group. The Skiddaw and Ingleton groups, however, are of different compositions. It is suggested that the two groups were sourced from different regions and deposited in different distributary systems.

Figure 3.63 Q-F-L diagram for Bray Group greywackes. Modal analysis of this study, n=1; data of Shannon (1978), n=16. Compositional field for Ingleton Group greywackes, n=4, and for greywackes of the Beckermonds Scar borehole, n=5.

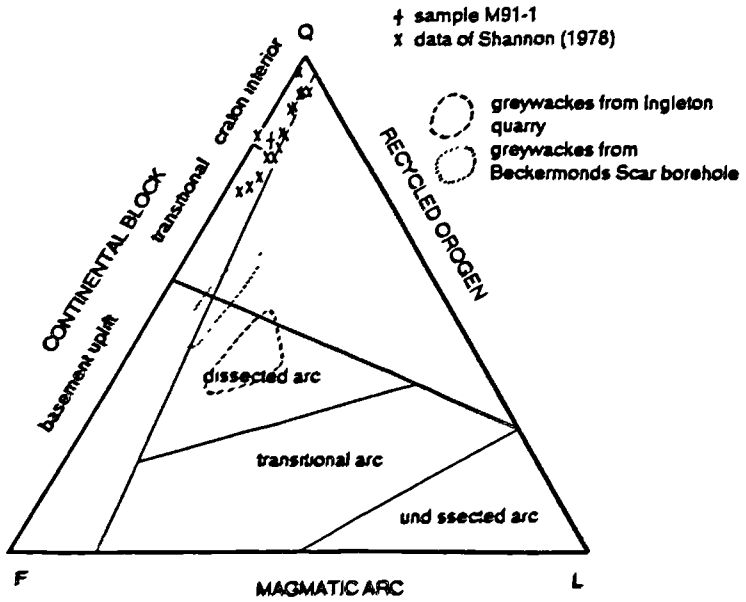

Table 3.29 Statistics for petrographical phases of greywackes of (a) the Ingleton Group (n=4), (b) Beckermonds Scar borehole (n=5), and (c) Skiddaw Group (n=67).

	(a) Ingleton Group greywackes (n=4)			(b) Beckermonds Scar borehole (n=5)			(c) Skiddaw Group (n=67)		
	mean	minimum	maximum	mean	minimum	maximum	mean	minimum	maximum
strained monocrystalline quartz	10.87	9.50	11.50	23.00	18.50	30.00	37.40	18.00	57.50
unstrained monocrystalline quartz	1.50	0.00	4.50	7.20	2.00	11.50	2.92	0.00	10.00
polycrystalline quartz	3.62	1.50	8.00	8.20	4.00	14.00	5.11	0.00	18.50
plagioclase feldspar	2.62	1.00	5.00	7.80	6.00	10.00	2.10	0.00	6.50
untwinned feldspar	13.75	8.00	17.00	20.60	13.50	28.50	6.15	0.00	15.50
volcanic lithic fragments	2.00	0.00	7.00	3.60	1.00	7.00	0.92	0.00	9.00
metavolcanic lithic fragments	0.87	0.00	3.00	1.20	0.00	2.00	0.85	0.00	5.50
sedimentary lithic fragments	0.50	0.00	1.00	1.10	0.00	3.00	4.15	0.00	27.50
metasedimentary lithic fragments	1.87	1.50	2.50	1.10	0.00	2.50	1.38	0.00	7.00
detrital mica	2.37	1.50	3.50	0.10	0.00	0.50	1.05	0.00	7.00
pyrite	0.00	0.00	0.00	0.00	0.00	0.00	1.03	0.00	11.00
carbonate cement	0.37	0.00	1.00	0.70	0.00	2.00	3.07	0.00	47.00
clay matrix	57.00	37.00	70.00	22.30	10.00	30.00	32.37	4.00	55.00
chlorite	1.50	0.00	2.50	1.30	0.00	3.50	0.98	0.00	13.00
heavy minerals	1.12	0.00	2.00	1.80	0.50	4.00	0.50	0.00	2.50
matrix	62.37	41.50	76.50	25.90	13.50	34.00	39.00	5.50	62.50
mineralogical maturity index	39.10	34.21	47.27	51.74	42.96	59.63	72.73	46.98	96.30

Chapter 4

ANALYSIS OF PALAEOSLOPE ORIENTATIONS OF THE SKIDDAW GROUP

4.1 Introduction to the structure of the Skiddaw Group

The structure of the Skiddaw Group is complex. This has led to controversial interpretations of deformation episodes, their timing and the nature of the boundary with the overlying volcanic rocks. Difficulty in erecting a workable stratigraphy has compounded the problems and led to erroneous structural interpretations.

The development of stratigraphical ideas has been reviewed (see section 1.4.1). With the advent of modern structural analysis, several workers described detailed fold and cleavage relationships from restricted areas in the late 1960's and early 1970's. The structural interpretation of Simpson (1967) was the catalyst for a multitude of papers. He suggested that two fold phases were developed in the Skiddaw Group during an intra-Ordovician (end-Llanvirn) orogeny. The younger Borrowdale Volcanic Group was thought to overlie with angular unconformity, which may have acted as a decollement during 'end-Silurian' deformation; this deformation was to thought to have had little effect on the Skiddaw Group (Simpson, 1967). An intra-Ordovician orogeny was also favoured by Helm (1969) based on the deformation sequence of the Skiddaw Group in the Black Combe Inlier. He recognised six deformation episodes (D_1 to D_6) of which three were persistent: the first and second, related to intra-Ordovician tectonics, and the fourth, due to 'end-Silurian' deformation. He believed regional uplift and erosion occurred prior to subaerial extrusion of the Borrowdale Volcanic Group (Helm 1970).

Soper (1970) demonstrated that the hypothesis of pre-volcanic orogeny could be tested at the Skiddaw Group-Borrowdale Volcanic Group boundary. He described 'three critical localities' showing:

(a) the earliest cleavage in the Skiddaw Group passing into the Borrowdale Volcanic Group,

(b) a volcanic breccia, with 'end-Silurian' cleavage, bearing previously uncleaved mudstone clasts,

(c) conformity with a gradational or interbedded junction or minor unconformity at the boundary.

He concluded no major tectonic episode occurred in the mid-Ordovician and an unconformity of orogenic proportions did not exist at the boundary. The cleavages were dated by consideration of their relationships with the aureole of the Skiddaw granite (Soper and Roberts, 1971) of known radiometric age (Miller, 1961). Thus the earliest two deformation episodes of Simpson were shown to be 'end-Silurian' age.

The presence of cleavage passing from Skiddaw Group to Borrowdale Volcanic Group could be explained if the slates in question were part of the Borrowdale Volcanic Group, hence above the major unconformity (Helm and Roberts, 1971). Such arguments could not be substantiated in the field (Jeans, 1971) where rock relationships were often unclear leading to conflicting interpretations within field parties (Moseley, 1975).

The widespread occurrence in the Skiddaw Group of early folds with north-south axes (Helm, 1970; Roberts, 1971; Wadge,1971; Helm and Roberts in Moseley, 1972; Webb, 1972) not present in the younger volcanics was presented in support of intra-Ordovician orogeny (Helm and Roberts, 1971). These folds, however, commonly had no associated cleavage and could be explained by folding of unconsolidated Skiddaw Group sediments on north-south axes (Moseley, 1972, 1975) and syn-volcanic deformation producing folds with similar axes and locally developed cleavage (Helm, 1970).

Burgess (in discussion of Helm, 1970) stated that a great thickness of Llanvirn sediments exposed in the Cross Fell Inlier was missing in the Lake District to the west, suggesting the presence of a regional unconformity. Unconformity could be demonstrated in the field (Jeans, 1972; Wadge, 1972) but its significance, whether orogenic or local, was much debated. The volcanic rocks to the north of the Skiddaw Group outcrop were shown to overlie conformably since lavas were interbedded with mudstones (Downie and Soper,1972). Microfossils collected from the mudstone interbeds showed a Llanvirn age, older than the Borrowdale Volcanic Group, hence a new name (the Eycott Volcanic Group) was required for this sequence (Downie and Soper,1972). Recently these lavas have been interpreted as intrusive sills and an unconformable contact has been demonstrated using palaeontology (Molyneux and Millward, in press) thus invalidating this argument. Moseley (1975) described 21 localities exposing the nature of the junction above the Skiddaw Group and concluded the presence of an unconformity of non-orogenic proportions.

Roberts (1977) suggested a structural sequence for the Skiddaw Group, reappraising and correlating previous authors schemes, and presenting the culmination of a decade of scientific debate (table 4.1).

Further advances in understanding of Skiddaw Group geology have been made since 1980 through the mapping program of the British Geological Survey (BGS). Extensive micro- and macro-palaeontological work has led to a revision of the stratigraphy (see chapter 1) and hence provided a sound foundation for new structural interpretation.

The recognition of deformation of unconsolidated sediments (Moseley,1972) was fundamental to the BGS structural model. Webb and Cooper (1988) described major slumping of Skiddaw Group sediments towards the central east-west axis of a local depositional basin. The coherent stratigraphy (see figure 1.3) to the north of the Causey Pike fault is affected by south vergent folds (1-100m scale) with associated thrust planes: Loweswater thrust, Gasgale thrust and Causey Pike thrust (figure 1.4). The less coherent stratigraphy to the south of the Causey Pike thrust was interpreted as an olistostrome which involves the formations of the northern stratigraphy in a disrupted, folded and sheared complex constituting the Buttermere Formation (Webb and Cooper, 1988). Vergence of folds with curvilinear axes implied northward movement of the slumped mass down a submarine slope. The line of the Causey Pike thrust (figure 1.4) was thought to correspond to the axis of a narrow fault-controlled marginal basin. Deformations due to volcanic doming associated with the overlying volcanic groups and Silurian deformations have overprinted the gravitational folds and reactivated some of the thrusts (Gasgale and Causey Pike thrusts). Early Devonian deformation was dominantly along southeast directed thrusts with reclined hanging wall

Table 4.1 A correlation of structural interpretations of the Skiddaw Group by Roberts (1977) and previous authors (after Roberts, 1977).

	Various authors pre-1963	Simpson (1967) reinterpreted by Roberts (1977)	Helm (1970) reinterpreted by Roberts (1977)	Soper (1970)	Webb (1972) Jeans (1972)	Roberts (1977)
end-Silurian		Minor N-S flexures in slates with steep fracture cleavage, (F3)	Minor sporadic N-S folds and cleavage, (D6)	Minor N-S flexures and weak steeply inclined cleavage, (D3)		Formation of minor N-S flexures and fracture cleavage - the result of axial shortening, (D4)
		Reclined E-W folds; crenulation cleavage, (F2)	Reclined folds and gently inclined cleavage, sporadically developed, (D5)	Reclined E-W structures, (D2)		Formation of reclined folds and crenulation cleavage as a result of the intrusion of the Lake District Batholith, (D3)
	Upright E-W folds and steep, slaty cleavage	Upright E-W folds; strong cleavage in slates, (F1)	Upright E-W and steeply inclined cleavage, (D4)	Upright E-W structures and main slaty cleavage, (D1)	Upright E-W folds and steeply inclined cleavage, (D2)	Upright E-W folds and main cleavage, formed by the principal Caledonian movements, (D2)
pre-Late Ordovician	Folds and monoclines recognised in volcanics only		Minor N-S folds and cleavage, (D3)			Probably present, but not readily recognisable in the slates of the Blencathra-*Mungrisedale area*
			Reclined folds and gently inclined cleavage, (D2)	Intra-Lower Palaeozoic structures; no cleavage production		
pre-volcanic			Tight to isoclinal N-S folds, (D1)		Reclined N-S folds; no cleavage production, (D1)	N-S recumbent folds in largely unconsolidated Skiddaw Group; no cleavage production; gravity collapse structure; (D1)

anticlines. The supposed north directed Gilbrae Nappe (Banham et al, 1981) is not supported by field evidence.

At the inception of this study the BGS structural sequence (table 1.4) was to be used as a template for models of sediment dispersal systems and basin geometry.

Results are presented of study of palaeoslope indicators in both the Northern Fells and Central Fells stratigraphical belts, in which soft-sediment deformation occurred simultaneously in earliest Llanvirn times (Webb and Cooper, 1988).

4.2 Slump folds of the River Caldew section

The River Caldew [NY 332 326] in the east of the Skiddaw Inlier exposes hornfelsed Skiddaw Group of the Northern Fells belt, equivalent to the Kirk Stile Formation. Spectacular folds are displayed in laminated mudstone and siltstone with siltstone lenses (<1cm thick) showing ripple cross lamination. The section was mapped and described by Roberts (1971). The folds are tight, trend north-south with near vertical axial planes and fold axes plunge steeply to the north. No cleavage is associated. They were interpreted as slump folds by Roberts (1977).

Fold axis orientations, vergence and younging data were collected to determine the palaeoslope direction. Both compressional and extensional discontinuities were observed with accompanying folds (figure 4.1), typical of slumped deposits (Woodcock,1976). Younging evidence from ripple cross lamination was often ambiguous but a uniform direction was indicated from several southward younging observations consistent with the assumption that thrust faults cut up section and extensional faults cut down section. Assuming that the long limbs of folds and the bedding parallel thrusts were originally horizontal, vergence directions were rotated about strike to remove the effects of later folding. The results showed a consistent westward vergence direction for both compressional and extensional structures (figure 4.2).

Roberts (1971) removed a 70° northerly dip from fold orientation data to compensate the effects of later folding. This is inconsistent with the younging evidence observed and would reorientate beds to a near-horizontal but inverted attitude. Jackson (1956) showed an east-west major fold axis to the north of the River Caldew separating it from the Eycott Volcanic Group, which Roberts (1971) did not consider. The observed southward younging direction is consistent with its position on the southern limb of this anticline. The structural data of Roberts (1971) should be reorientated about a *c.* 70° southerly dip to return the slump folds to a horizontal attitude. Figure 4.3 shows this result with a north-south distribution of fold axes with easterly dipping axial planes. In conjunction with the observations of vergence, these data support the interpretation of a westerly palaeoslope.

Figure 4.1 Sketches of structures in the Caldew River valley [NY 332 326].

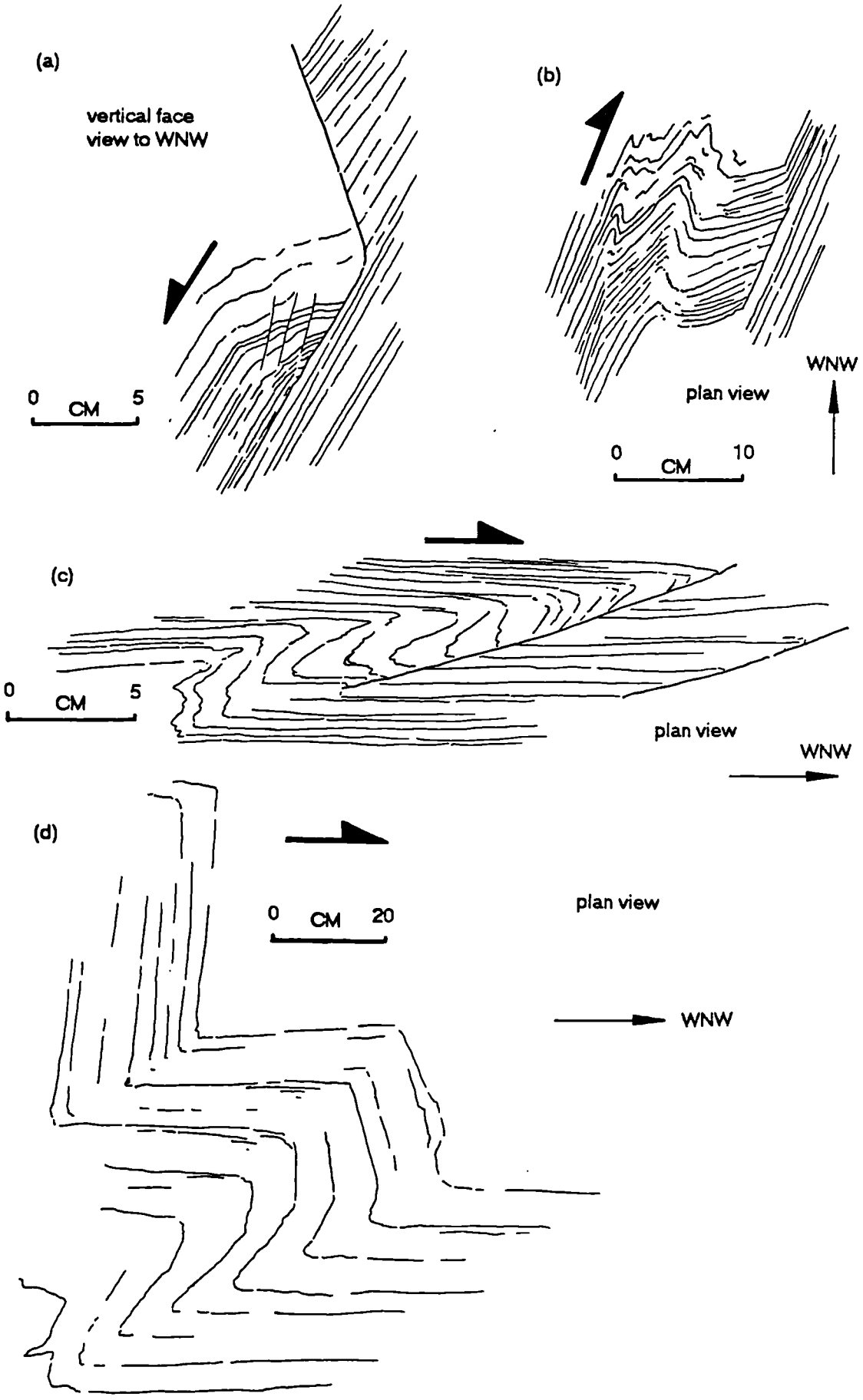

Figure 4.2 Equal-area lower hemisphere stereographic projections showing vergence directions indicated by soft sediment deformation structures from the Caldew River valley (a) before and (b) after removal of later folding. Vergence defined by the direction perpendicular to:
◁— the slump fold axis measured in the fold axial plane,
◁|— the intersection of bedding and soft-sediment fault measured in the bedding plane,
◀— the intersection of bedding and soft-sediment fault measured in the thrust plane.
a-d refer to examples in figure 4.1.
● mean pole to local bedding.

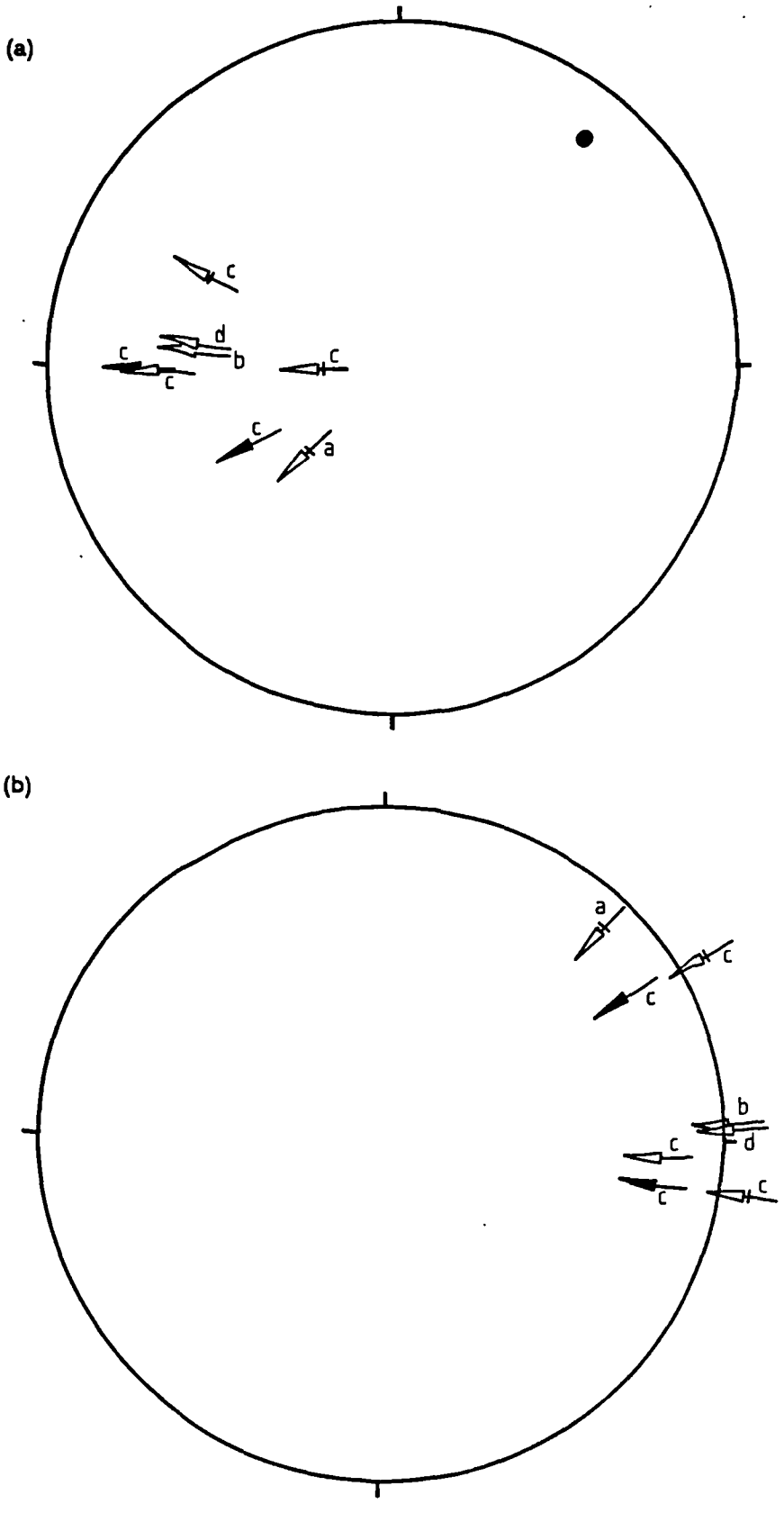

Figure 4.3 Equal-area lower hemisphere stereographic projections showing fold orientation data from the Caldew River valley; (a), (b) field measurements of Roberts (1977), (c), (d) after removal of a regional dip of 70° south.

(a) plunge of fold axes, n=112

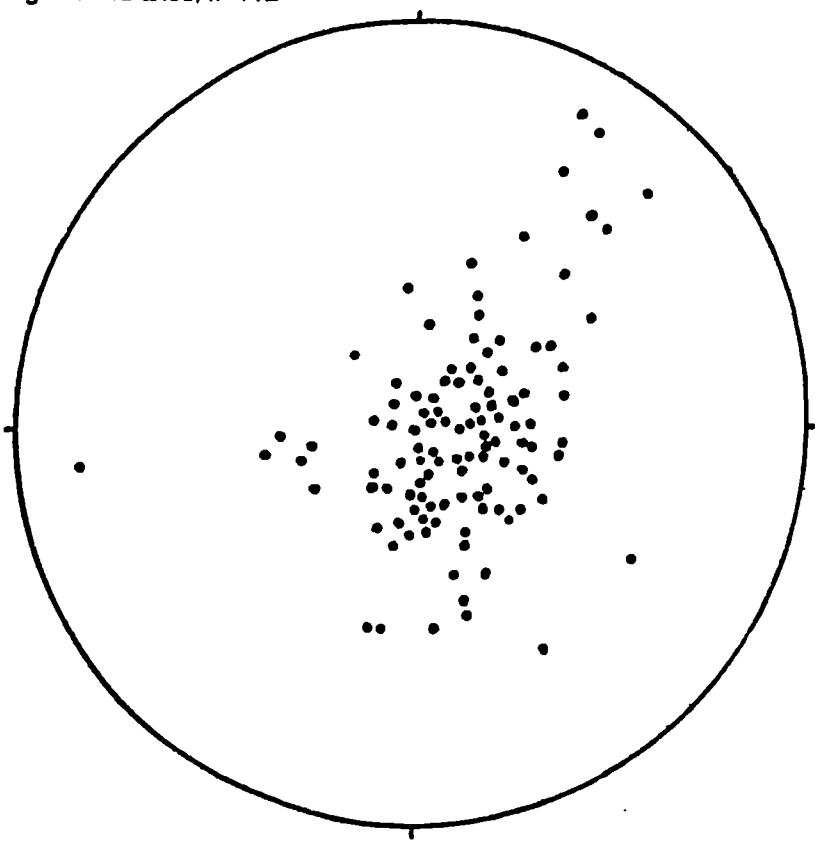

(b) poles to fold axial planes, n=48

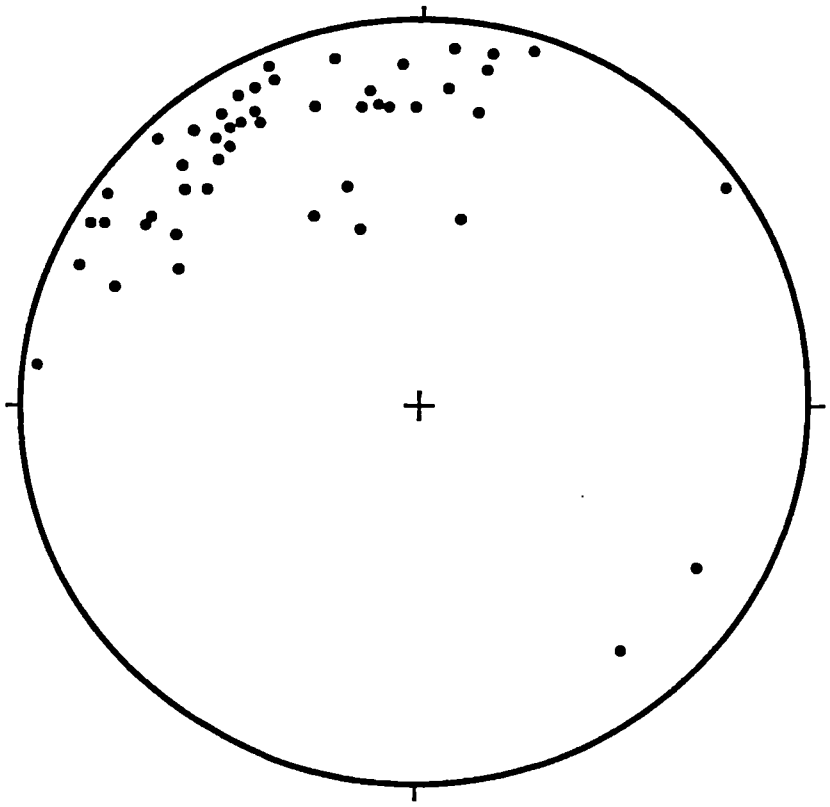

Figure 4.3 (continued)

(c) fold axes after removal of dip 70°S
■ = mean

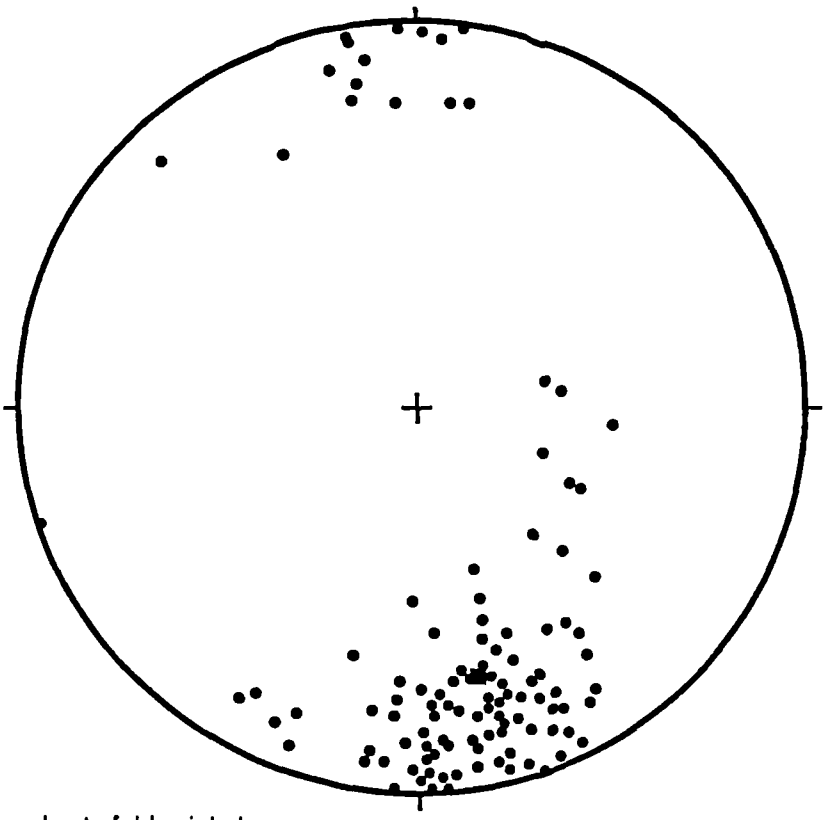

(d) poles to fold axial planes
after removal of dip 70°S.
■ = mean

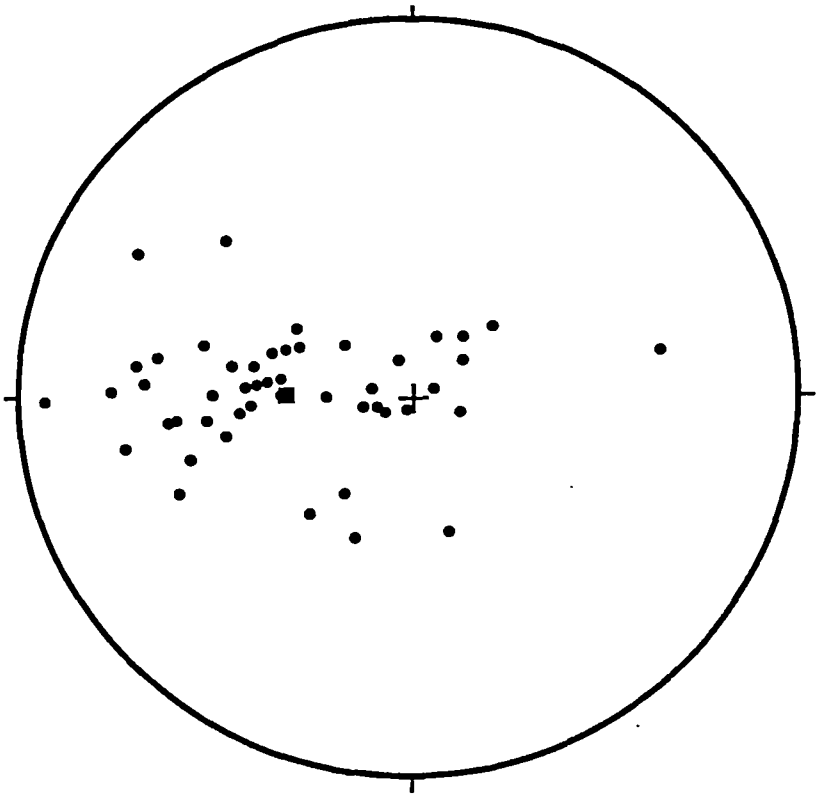

4.3 Slump folds of Gasgale Gill

At the top of the Loweswater Formation in Gasgale Gill [NY 1646 2095] asymmetric folds are displayed with low-angled axial planes and short limbs overturned to the southeast (figure 4.4). They are associated with thrusts, boudinage and extensional discontinuities on the long limbs. Folds disappear up and down section (plate 4.1). They are of possible slump origin but are sub-parallel to southeast directed folds of tectonic origin associated with the Gasgale thrust (figure 1.6). The rocks display a steep northwest-southeast cleavage and a low-angle cleavage cutting the folds.

A slump origin would suggest a southeasterly palaeoslope. The folds affect *c.* 50m thickness of sediment, but no truncated folds are seen, suggesting syn-depositional slumping did not occur, but a slumping event affecting a large thickness of partially consolidated sediment occurred after deposition of the Loweswater Formation. This concurs with the interpretation of palaeocurrent directions (chapter 2). At this locality (locality e, enclosure 2) sole marks and ripple marks show a consistent current direction to the northeast. This relationship suggests downslope movement of topographically unconfined turbidity currents. Thus the palaeoslope responsible for the slump folds probably developed after deposition of the Loweswater Formation.

4.4 Clast orientation in the Beckgrains Bridge debris flow

At Beckgrains Bridge, debris flow deposits in excess of 40m total thickness occur within the Kirk Stile Formation. They comprise rounded clasts of mudstone, siltstone and sandstone, supported in a cleaved mudstone matrix. The long axes of the clasts range in length from *c.* 3-10cm, and show a preferred orientation (in a north-south vertical plane) parallel to the fabric in the matrix, which refracts around clasts. A small vertical shear plane cuts and folds the fabric. The clast orientation may be a depositional characteristic or may reflect rotation of clasts in the matrix during tectonic deformation. Without detailed knowledge of local, subsequent fold orientations, no conclusions could be drawn.

4.5 Slump folds of the Buttermere Formation

The Buttermere Formation olistostrome of the Central Fells belt displays large and small-scale slump folds. Webb and Cooper (1988) present fold axis and vergence data (figure 4.5) from which they deduce a north-facing palaeoslope. The data clearly indicate vergence of arcuate fold axes to the west-northwest. The data are reinterpreted here to indicate a westerly palaeoslope, consistent with palaeoslope orientations in probable synchronous deposits in the Caldew valley of the Northern Fells belt.

Figure 4.4 Equal-area lower hemisphere stereographic projections showing structural data of folds in Gasgale Gill.

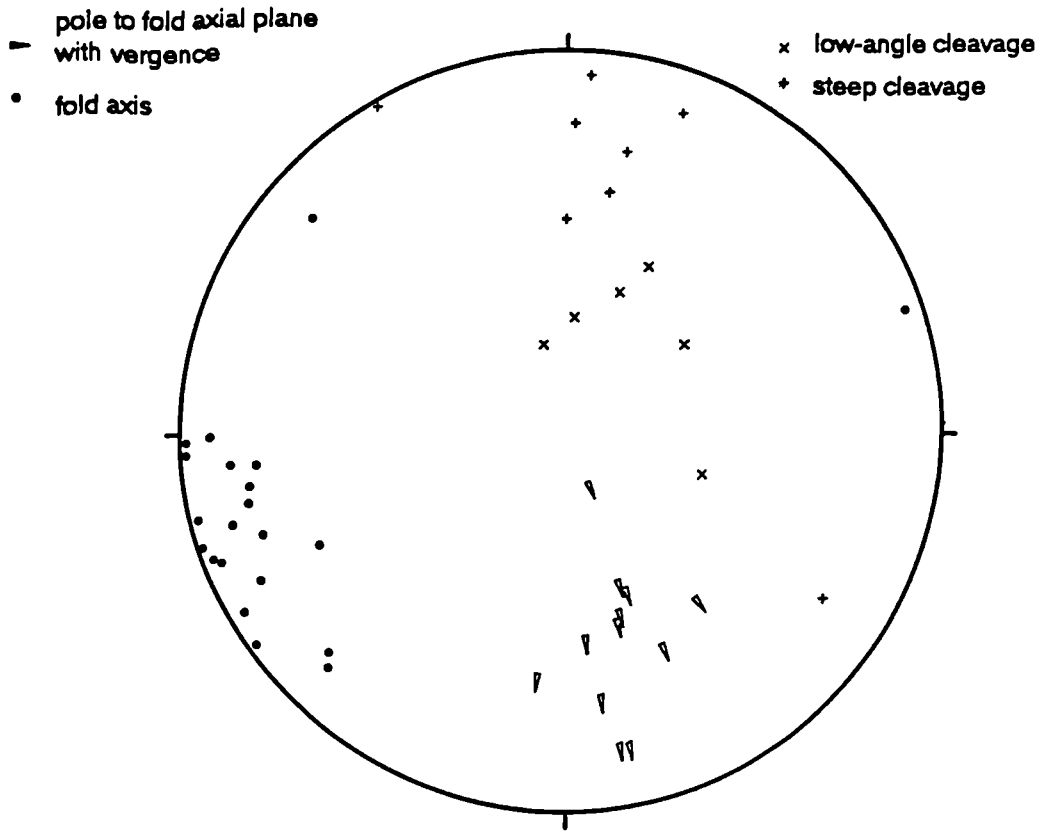

Figure 4.5 Equal-area lower hemisphere stereographic projection for the Buttermere Formation showing slump fold axes and plan-view diagram showing axial curvature and westerly vergence (figure 6(b) of Webb and Cooper, 1988).

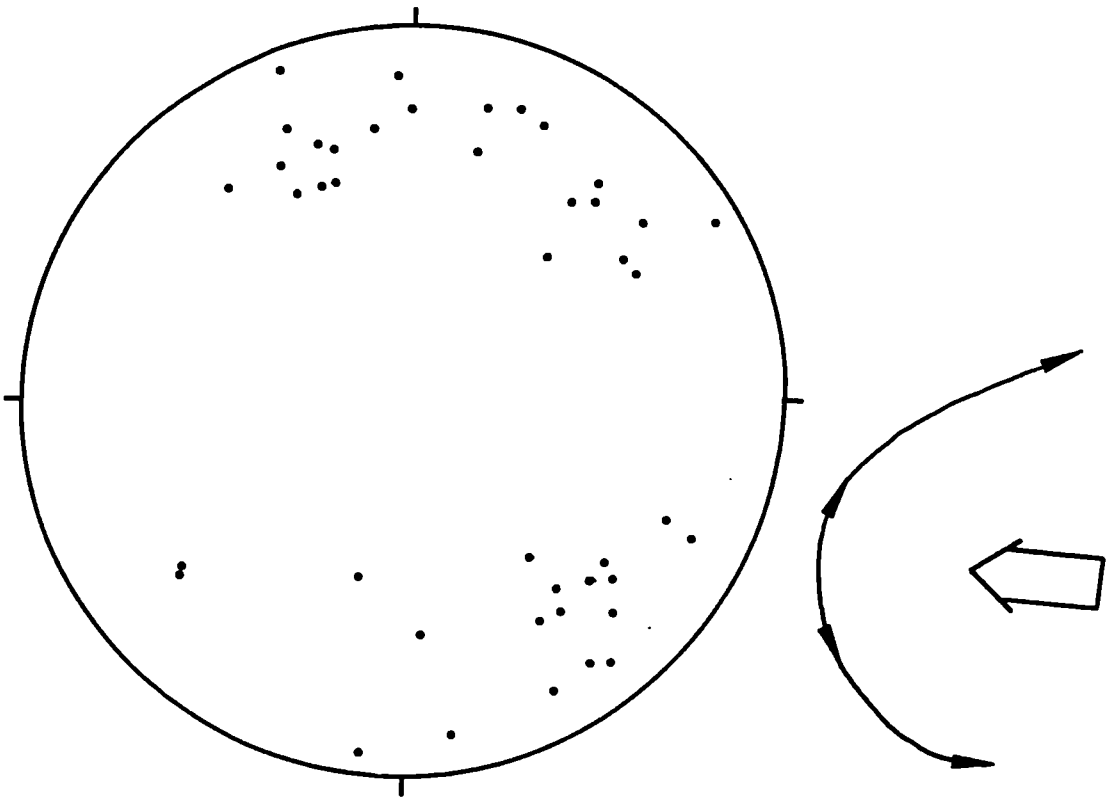

PLATE 4.1

4.1.1 Fold with an overturned upper limb, interpreted to be of slump origin in beds of facies C2.3, Loweswater Formation, Gasgale Gill.

4.1.2 The overturned middle of a slump fold pair, showing disrupted beds of facies C2.3, Loweswater Formation, Gasgale Gill. Top of the picture is to the left.

4.6 Discussion

The structural interpretation by the British Geological Survey mapping team has progressed with further mapping. North vergent folds and thrusts to the north of the Causey Pike thrust in the east of the Skiddaw Inlier show that the Causey Pike thrust does not always correspond to a change in vergence direction across the region, previously interpreted as the axis to the depositional basin (Webb and Cooper, 1988). The Loweswater anticline and underlying thrust are associated with a strong fabric, minor thrusts and slickensides on thrust and low-angle bedding surfaces (enclosure 3). It is now considered to be related to deformation during early Devonian compression, rather than induced during gravitational sliding in partially consolidated sediment.

The east-northeast trending structures of the Silurian and early Devonian overprint the structural regime of the early Ordovician, which need not bear any relation to them. Only structures that can be shown to predate the volcanic groups can be considered.

Cooper and Molyneux (1990) suggest that the Causey Pike fault, a major lineament imaged by geophysical methods (Cooper et al, 1988), was active during the early Ordovician, because of the stratigraphical differences between the Northern and Central Fells belts, which were juxtaposed by sinistral strike-slip movements. Sinistral strike-slip displacements during the early Devonian have been postulated from the bending of cleavages across the fault zone (A. H. Cooper, pers. comm.). Intrusion into the zone of the elongate body responsible for the Crummock Water Aureole (Cooper et al, 1988) shows that the lineament predates the early Devonian. It is considered here that the Ordovician lithologies differ remarkably little across the fault, although the gravitational deformation is more intense in the Central Fells belt. No evidence for early Ordovician movement on this lineament exists (although the slump folds of Gasgale Gill may be related to a structure in this orientation).

Slump fold data suggest a westerly palaeoslope is common to both the Northern and Central Fells belts in earliest Llanvirn times and that slumping to the southeast occurred locally, (e.g. at Gasgale Gill). The recognition, across the Skiddaw and Black Combe inliers, of reclined to recumbent first phase folds with north-south axes and no cleavage has been made by many authors (Helm, 1970; Roberts, 1971; Wadge,1971; Helm and Roberts in Moseley, 1972; Webb, 1972) . Since the mid-1970's they have generally been interpreted as slump related (Moseley, 1975; Roberts, 1977).

The development of a palaeoslope facing west appears to be a regional feature.

The palaeoslope which controlled earliest Llanvirn slumping did not correspond directly to the palaeoslope which affected Arenig deposition (chapter 2), e.g. Loweswater Formation turbidites in Gasgale Gill show no evidence of a southeast facing slope, which was, however, in existence before sediment was entirely consolidated. The occurrence of north-south trending basin floor topography controlling Arenig turbidite deposition, deduced from palaeocurrent evidence, might relate to north-south faults which controlled the west facing palaeoslope during the earliest Llanvirn. Discussion of the evidence for syn-sedimentary faulting inferred from thickness changes in the Loweswater Formation and fault movement pre-dating the Eycott Volcanic Group, on north-south trending faults, was presented in chapter 2.

4.7 Summary

A west facing submarine slope was developed throughout the Skiddaw Group in the early Llanvirn, with associated soft-sediment deformation. Gravitational deformation is expressed as slump folds in the Kirk Stile Formation of the Northern Fells belt and as a major olistostrome, the Buttermere Formation, affecting a greater thickness of sediment in the Central Fells belt. Local variations in slumping direction are apparent in Gasgale Gill where a southeast facing slope developed after deposition and prior to lithification. Such a slope could be related to the east-northeast trending lineament along the Causey Pike Fault, but no evidence exists for Ordovician movement on this fault.

The north-south strike of the early Llanvirn submarine slope could be related to the syn-depositional structure of the Arenig Loweswater Formation where north-south trending topographical features caused reflection of turbidity currents (chapter 2). The stress regimes controlling the syn-depositional structures and syn-soft sediment deformational structures are considered in chapter 5.

Chapter 5

A TECTONIC MODEL FOR THE SOUTHERN BRITISH ISLES IN THE EARLY ORDOVICIAN

This chapter presents a tectonic framework, within which the geological features of the early Ordovician rocks of the southern British Isles can be explained. It begins with a summary of the findings of chapters 2, 3 and 4: the sedimentology, compositions and initial deformations of the Skiddaw, Manx and Ingleton groups. There follows a review of contemporaneous sedimentation and volcanism in Wales, Ireland and eastern England, which, combined with a discussion of tectonic control of sedimentation, is used to propose an active continental margin tectonic setting.

Features of neotectonism, sedimentation and the long and complex history of the modern active continental margin of Chile are used to illustrate the model. The orientation and dominant tectonic elements of the Ordovician margin are discussed. The sedimentological and tectonic processes identified in the Skiddaw Group are explained within the context of the model. The history of the active continental margin prior and subsequent to the early Ordovician is reviewed in order to address the broad questions posed in chapter 1, i.e.:

When was the onset of subduction?

When did Eastern Avalonia rift away from Gondwana?

When was the mid-ocean ridge subducted?

The concluding remarks appraise the strengths and weaknesses of the model and propose improvements through future work. The achievements of this study are highlighted in terms of the advancement of knowledge of early Ordovician geology of northern England and the Isle of Man (Skiddaw, Ingleton and Manx groups), and improvements in the application of techniques (provenance discrimination; turbidite facies analysis and palaeocurrent interpretation).

5.1 Summary of the sedimentology and tectonics of northern England and the Isle of Man

The deep marine siliciclastic sediments of the Skiddaw and Manx groups compare closely in age, composition and depositional environments. Sediments were sourced from an orogenic terrain with inactive continental volcanic arcs. Provenance elements are mixed and include *continental arc*, *passive margin* and *recycled orogen* types.

Two periods of submarine fan development occur in the Skiddaw Group. The first, spanning the Tremadoc-Arenig boundary, is represented by the Watch Hill Formation. Channels distributed sediment to east and west, possibly along a trough of this orientation. The occurrence of sediment of similar composition in depositional lobes of the Lonan Flags of the Manx Group, presently sited 100km to the west-southwest, might correspond to the distal portions of this distributary system. It is probable, however, that there were several points of sediment input to the trough.

The Loweswater Formation of Arenig age represents depositional lobe development with a tectonic control of sediment distribution. Troughs, trending approximately north-northwest, controlled turbidity current flow. A tectonic model of syn-depositional extensional faults in this orientation, with fault blocks tilted to the northeast, has been erected. Tectonic activity is indicated by convolute lamination, interpreted to have a seismic trigger.

The Ingleton Group, of probable Arenig age, has a different composition to the Skiddaw Group and represents submarine fan lobes of higher sediment calibre. The distributary systems of the two groups were not connected.

During the early Llanvirn, a west-facing submarine slope developed across the Skiddaw Inlier which caused slumping in the Kirk Stile Formation and major gravitational reworking to form the olistostrome deposits of the Buttermere Formation. Locally, slumping was directed to the southeast, e.g. in Gasgale Gill.

Volcanism was active in the Llanvirn and supplied tuffs and volcaniclastic turbidites to the Tarn Moor Formation.

The deep marine basin experienced substantial uplift prior to the unconformable deposition of the sub-aerial Borrowdale and Eycott volcanic groups (Branney, 1988; Millward and Molyneux, in press).

5.2 Regional geological setting

The Ordovician history of Wales is discussed by Kokelaar (1988). In north Wales, Cambrian to mid-Tremadoc marine sedimentation in a rift basin was succeeded in the late Tremadoc by folding, faulting, uplift and erosion accompanied by arc volcanism, represented by the Robell Volcanic Complex (Kokelaar, 1988). The Robell Volcanic Complex is the first indication of ensialic destructive plate margin volcanism in the southern British Isles in the Palaeozoic.

In the Arenig, subsidence caused a diachronous transgression; shallow seas surrounded a subaerial Harlech Dome before total submergence in the mid-Arenig; marine sedimentation and submarine volcanism, represented by the Aran Volcanic Group, continued until the early Caradoc (Kokelaar, 1988). The eroding arc and contemporaneous volcanism contributed to shallow marine sandstones and conglomerates with mudstones in deeper water; shallower water deltaic and tidal sediments represent the arc-apron (Traynor, 1990). Sedimentation kept pace with subsidence in north-south troughs and syn-sedimentary north-south and northeast-southwest faults were active in the Harlech Dome area; an olistostrome is present with rafts of Upper Cambrian and lower Ordovician sedimentary rocks transported from the south (Traynor, 1990).

In southwest Wales the transgressive Arenig sediments are represented by conglomerates, sandstones and mudstones of deltaic to turbiditic facies deposited in a wave-storm/tidal influenced shallow sea; sediment was derived from varying proportions of coeval marginal basin volcanism and Precambrian and Cambrian basement rocks, and ponded in small interconnected sub-basins; active tectonism controlled clastic influxes, overriding the influence of a eustatic sea level rise (Traynor, 1988). Intra-Caradoc volcanism continued in central and north Snowdonia and the Lleyn peninsular (Kokelaar, 1988).

The Lower Palaeozoic rocks of east and southeast Ireland have been interpreted as an assemblage of fault-bounded terranes (Murphy, 1987, Max et al, 1990). Bruck et al (1979) describe the Cambrian and Ordovician sequences:

> In the Cambrian, source areas of Precambrian igneous and metamorphic rocks provided sediment which laterally infilled tectonically active marine basins with northeast-southwest axes.

Early Ordovician sedimentation was dominantly of mudstone and siltstone of deep marine turbidite and pelagic facies. Thin to medium bedded silt-grade quartz wackes and arenites represent turbidites and contourites respectively. Basin axes trended northeast, with sediment transport from the northeast and south.

Caradocian rhyolitic volcanics, limestones and mudstones of shallow marine and subaerial environments are unconformable on earlier sediments. Deposition was in small fault-controlled basins with variable current directions.

In eastern England, Lower Palaeozoic rocks are concealed beneath younger cover. Arc-related volcanics and volcaniclastics are of probable mid to late Ordovician age (Pharaoh et al, 1987, 1991).

In the Lake District, the Skiddaw Group is unconformably overlain by the tholeiitic volcanics of the Eycott Volcanic Group (Millward and Molyneux, in press) and the subaerial calc-alkaline volcanics of the Borrowdale Volcanic Group (Branney, 1988), both of mid-Ordovician age.

Thus the southern British Isles were sited on an active continental margin in the early Ordovician with onset of subduction-related volcanism in the late Tremadoc in Wales. Volcanism was widespread in the mid-Ordovician. Sedimentation was in fault-controlled marine basins. Deep marine environments existed away from volcanic centres where shallow marine and sub-aerial environments were dominant.

5.3 Controls of sedimentation

Identification of sedimentary response to eustatic sea level change or local relative sea level change due to tectonism can be made by comparing curves of relative sea level for different regions. For the Ordovician, curves of eustatic sea level (Vail et al, 1977; Hallam, 1984; Ross and Ross, 1988; Leggett et al, 1981; Fortey and Cocks, 1986) are compared with relative sea level curves for the margin of Eastern Avalonia (north and south Wales (Fortey and Cocks, 1986); northwest England (chapter 2)) and for the margin of Gondwana (Nova Scotia (Schenk, 1991); northwest Africa (Combaz, 1967)) (figure 5.1). The eustatic sea level curves represent sea level changes that are recognised on more than one continent. Similarity of a regional relative sea level curve with a eustatic curve would suggest sedimentation was controlled by eustacy. Variation from the eustatic curve would suggest an overriding influence of tectonic processes. These could affect several regions of a single continental margin (e.g. due to a change in the tectonic setting of the plate margin) or could be restricted to a single region (e.g. due to a local tectonic event).

The principle has limitations in its application. The accuracy of a relative sea level curve depends on the precision of determination of chronostratigraphy. Hence accuracy is limited to the resolution of the stratigraphic markers that can be recognised in any particular sequence. This must be considered when comparing curves of different regions. Additionally, the shapes of curves reflect the authors' interpretations of rates of sea level change, e.g. equal rates of sea level rise and fall (Hallam, 1984; Fortey and Cocks, 1986) or rapid falls and prolonged rises of sea level (Vail et al, 1977).

Despite these reservations, several important points can be interpreted from comparison of early to mid-Ordovician sea level curves (figure 5.1).

Figure 5.1 Comparison of Ordovician eustatic sea level curves with relative sea level curves for the margins of Eastern Avalonia and Gondwana. Eustatic sea level: 1 = Vail et al (1977); 2 = Hallam (1984); 3 = Ross and Ross (1988); 4 = Leggett et al (1981); 5 = Fortey and Cocks (1986). Eastern Avalonia: 6 = south Wales (Fortey and Cocks, 1986); 7 = north Wales (Fortey and Cocks, 1986); 8 = northwest England (this study). Gondwana: 9 = Nova Scotia (Schenk, 1991); 10 = Sahara (Combaz, 1967). Timescale from McKerrow et al (1985).

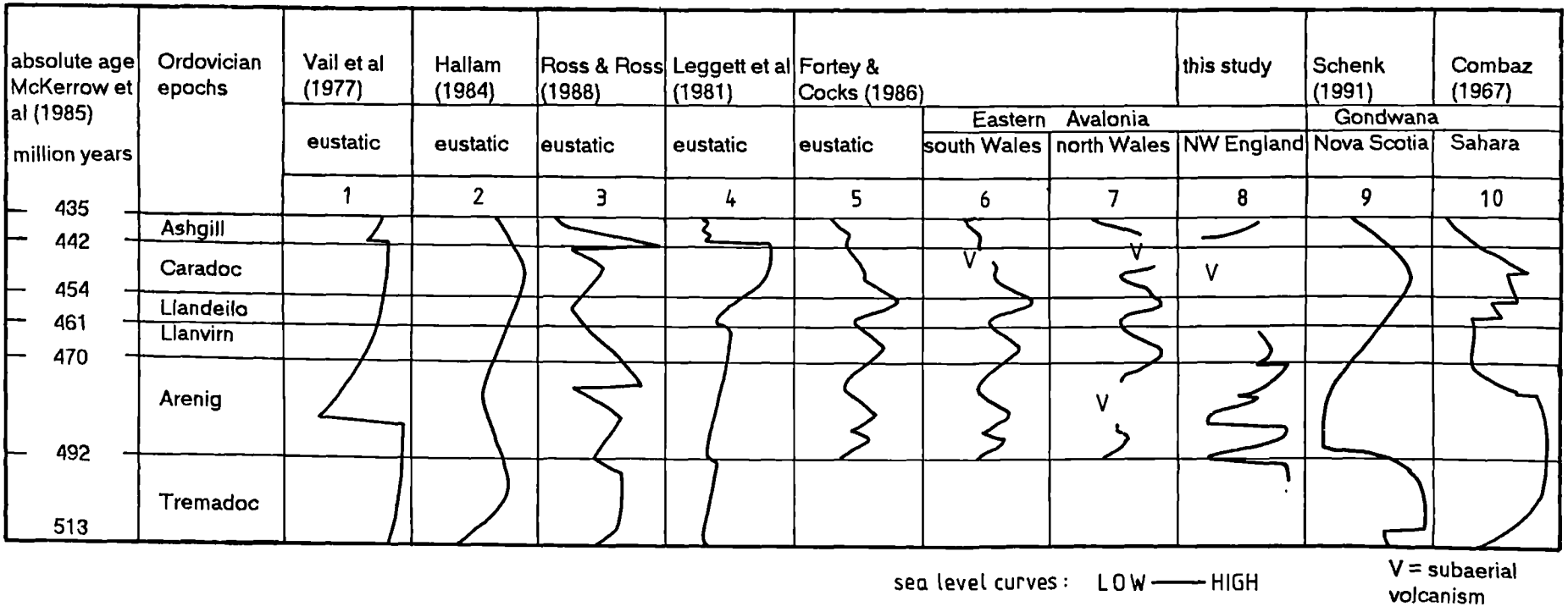

1. *Eustatic low stands.* A low stand of sea level in the Arenig is shown by the curves of Vail et al (1977) and Hallam (1984). The sea level curves of Ross and Ross (1988) and Fortey and Cocks (1986) show more than one Arenig low stand and an additional low stand at the end Tremadoc. In Wales, Woodcock (1990) attributes this event to a probable eustatic effect with a definite tectonic effect. Therefore sand-grade clastic pulses of the Watch Hill Formation (Tremadoc-Arenig) and Loweswater Formation (Arenig) could be in response to eustatic sea level low stands.

2. *Regional sea level changes affecting the margin of Eastern Avalonia.* The curves for Wales and northwest England show numerous sea level changes which indicate the effect of tectonic processes additional to eustatic changes. The 'eustatic' sea level curves of Leggett et al (1981) and Fortey and Cocks (1986) (curves 4 and 5, figure 5.1) include data from the tectonically active margins of the Iapetus Ocean, thus probably do not reflect purely eustatic sea level change, hence their differences from the curves of Vail et al (1977) and Hallam (1984) (curves 1 and 2, figure 5.1). The similarity of these curves (4 and 5) with those for north Wales and northwest England (curves 7 and 8) is probably due to regional tectonic controls on sea level.

Events common to curves for Eastern Avalonia are: a sea level low stand at the Tremadoc-Arenig boundary and a sea level low stand in the Llandeilo. Therefore the submarine fan of the Watch Hill Formation (Tremadoc-Arenig) could have developed in response to tectonic uplift of the margin of Eastern Avalonia, as could uplift prior to the subaerial volcanism of the Borrowdale and Eycott volcanic groups.

Sea level changes on the margin of Eastern Avalonia differ from those of Gondwana (curves 9 and 10, figure 5.1). The latter reflect the eustatic curves (curves 1 and 2) suggesting Gondwana had a passive margin. Prominent characteristics include a Tremadoc high stand of sea level, an Arenig low stand (late Arenig for west Africa) and a generally rising sea level throughout Llanvirn to Caradoc times.

3. *Local sea level changes.* In Wales in the Arenig and Caradoc, and in northwest England during the Caradoc, uplift and emergence accompanied volcanism. Therefore local volcanic centres associated with active subduction caused uplift and regression.

A fall in sea level is interpreted at the start of the Llanvirn in northwest England since large-scale sediment slumping and sliding could be associated with a fall in sea level. No similar event is observed on other parts of Eastern Avalonia, hence a local tectonic control is inferred. This might correspond to the shallowing event in the early Llandeilo in north and south Wales and represent a progressive tectonic uplift along the continental margin. Alternatively, slumping might not have been directly related to sea level change and could have occurred on a deep marine submarine slope (e.g. in response to seismicity associated with the onset of the volcanism which contributed detritus to the Tarn Moor Formation).

5.4 Introducing a modern analogue

The active continental margin of the Andes has been considered as the type example of a continental-oceanic destructive plate margin (e.g. Dewey and Bird, 1970). Recent study has identified many features (presented below) which differ from the classic model of volcaniclastic sedimentation in trench and fore-arc basins. The margin between the oceanic Nazca plate and continental South America plate trends approximately north-south (figure 5.2a). The ocean trench is separated from the active volcanic chain of the Andean cordillera by a 200km wide fore-arc region. This zone comprises the 'Coastal Cordillera', of accreted Jurassic marginal basin deposits, and the 'central depression' of enclosed, tectonically controlled, subaerial sedimentary basins (figure 5.2b).

The active continental margin of South America has previously been used as an analogue for the Lower Palaeozoic of southern Britain: Jeans (1973) considered the distribution of Ordovician volcanics to be due to variation in the steepness of subduction by comparison with the position of Andean volcanism through time; McCann (1991) cited the southern tip of South America as an example of active and passive geotectonic settings in close proximity and of similar dimensions to the Eastern Avalonia microcontinent.

The analogies of interest to this study concern tectonic elements: fault orientations and their changes with time, block rotations, controls and sediment responses. The subaerial setting of the Andean fore-arc region contrasts markedly with the shallow and deep marine, early Ordovician sediments of the southern British Isles. This fundamental difference could result from greater extension and subsidence of the Avalonian fore-arc region, or from differences in continental freeboard related to global eustacy (i.e. sea level today is relatively low). It is not thought to invalidate comparison of tectonic features.

The Coastal Cordillera comprises andesites, shallow marine limestones and sandstones of a Jurassic to Middle Cretaceous back-arc basin (Scanlan et al, in press). These rocks are intruded by the dioritic to granodioritic plutons of the coastal batholith. Thus the margin has been active for at least 180 million years and has had a complex history involving marginal basin volcanism and sedimentation, basin inversion and terrane accretion.

Study of palaeomagnetism (Scanlan and Turner, 1992; Scanlan et al, in press) has shown rotations of crustal blocks by up to 40° since the Middle Cretaceous. These observations have important implications for the relative orientations of the Ordovician inliers of the southern British Isles. Oblique convergence between the Nazca and South America plates is thought to have controlled block rotations. Scanlan et al (in press) propose a model of domino-block rotation through dextral transpression on trench-parallel faults, e.g. the Atacama fault system. Such faults are long-lived since they are in a favourable orientation for reactivation during periods of oblique plate convergence. Basins were formed as pull-apart basins at releasing bends on strike-slip faults or extensional basins created by block rotations. A change in plate convergence direction from oblique convergence (with trench-parallel dextral shear) to increased normal convergence at 26 Ma was recognised by Pilger (1984). Intense deformation events coincide with periods of rapid plate convergence of the order of <10 million years duration (Scanlan et al, in press, and references therein). These time periods correspond to the duration of Ordovician epochs (McKerrow et al,

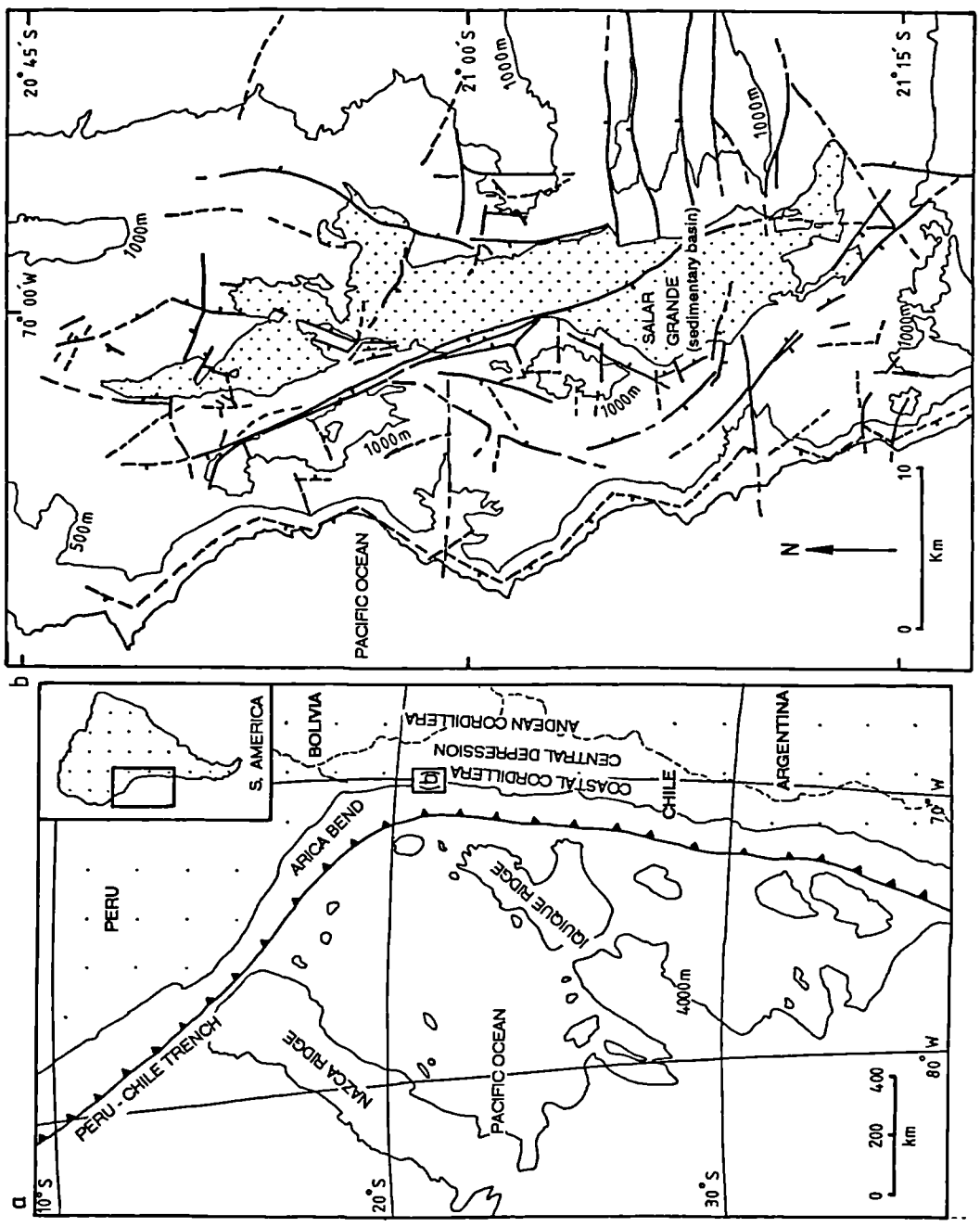

Figure 5.2 (a) The plate tectonic setting of the Andean margin; (b) Tectonic elements of the fore-arc region, displayed by part of the Atacama fault system. Redrawn from Scanlan et al (in press).

1985), thus more than one change in tectonic regime could have acted on the Avalonian active margin during the early Ordovician.

Neotectonic trench-normal extensional faults have been described in the Coastal Cordillera (Mortimer and Sarie, 1972; Scanlan et al, in press). Scanlan et al (in press) propose a strain ellipse model controlled by trench-normal compression to explain trench-parallel extensional faults, with accompanying synthetic dextral strike-slip faults and antithetic sinistral strike-slip faults (similar to figure 5.7a).

An additional cause of east-west normal faulting, block rotations and local uplift ot the fore-arc region is subduction of the aseismic Iquique Ridge (Flint et al, 1991), and other topographical features of the oceanic plate.

5.5 An active continental margin tectonic model

5.5.1 Orientation of the margin

The configuration of plates and orientation of plate margins in the Ordovician is difficult to determine except on the crudest scale. This is because the deformation of continental collision of Eastern Avalonia, Baltica and Laurentia overprints earlier structures which record tectonic processes during ocean closure. For example the Midlands microcraton is thought to have acted as a rigid indenter (Turner, 1949) which caused a change in the cleavage strike orientation across southern Britain (Soper et al, 1987).

Several authors have proposed plate tectonic models which define a direction for subduction (figure 5.3). Fitton and Hughes (1970, 1977) considered the Ordovician igneous rocks of the Lake District and Wales to be a contemporaneous volcanic belt of 300km width. The most northerly occurrence, the Eycott Volcanic Group, is of transitional tholeiitic to calc-alkaline affinity. The Borrowdale Volcanic Group is broadly calc-alkaline. Volcanics of the Harlech Dome and Snowdonia are both bimodal (dominantly rhyolitic, with tholeiitic and alkaline basalts). Thus a southward trend from tholeiitic to calc-alkaline to alkaline volcanism was recognised and related to a south-dipping subduction zone (figure 5.3a, c). For the earlier volcanic phases (Tremadoc to early Llanvirn) of the Harlech Dome a separate subduction zone could have been responsible.

The distribution, type and timing of volcanism has been related to the steepness of the subduction zone, by comparison with the active continental margin of Chile (Jeans, 1973). A shallow subduction zone could have been responsible for the Welsh volcanics and a steepened subduction zone could have caused volcanism in the Lake District with a plume causing crustal melting beneath Wales (Jeans, 1973).

The age of the volcanic groups in the Lake District remains poorly defined: the Eycott Volcanic Group is post-early Llanvirn (Millward and Molyneux, in press; Downie and Soper, 1972) and the Borrowdale Volcanic Group is probably largely of Caradoc age (Branney and Soper, 1988). The possibility of contemporaneity cannot be dismissed and the model of Fitton and Hughes (1970) remains credible. The possible occurrence of strike-slip faults separating the Lake District and Wales was not considered in the model.

Figure 5.3 Possible plate tectonic configurations for Eastern Avalonia in the early Ordovician: (a) southeast directed subduction, as suggested by Fitton and Hughes (1970, 1977), Jeans (1973), Phillips et al (1976), Stillman and Williams (1978) and Max et al (1990); (b) southwest directed subduction, as suggested by Pharaoh et al (1987, 1991); (c) combination of models assuming minimal displacement and/or rotation of component regions; (d) generalised model with a loosely defined plate margin orientation and allowing for local variations in plate margin trend, tectonic regime and unspecified deformation, displacement and rotation of component regions. The outline of the southern British Isles is shown for scale only; in all models, deformation would make this shape unrecognisable in the Ordovician.

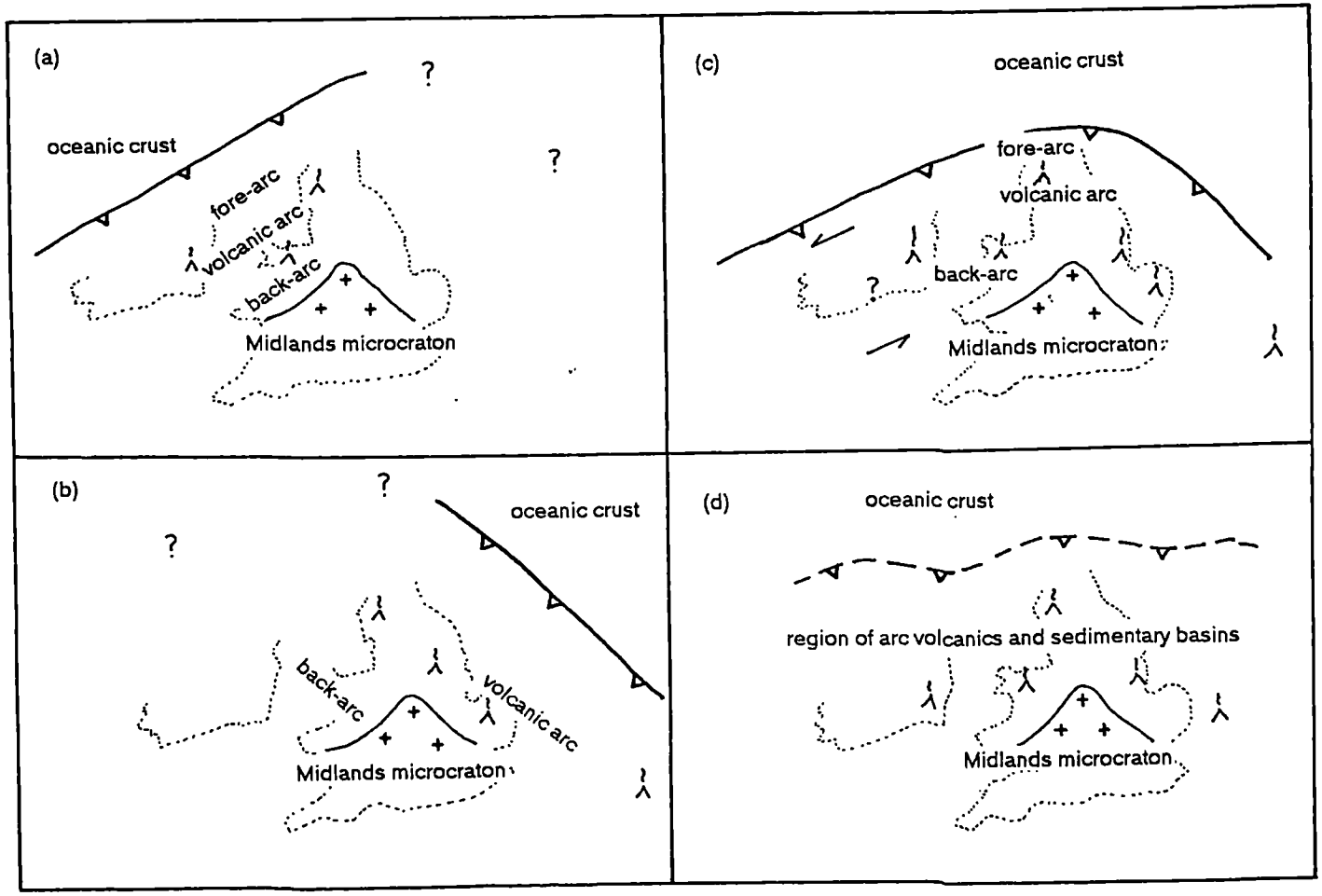

The Cambrian to lower Ordovician rocks of the Leinster Massif of southeast Ireland record deep marine sedimentation in a northeast-southwest aligned basin bounded both north and south by Precambrian basement (Todd et al, 1991; Bruck et al, 1979). Llandeilo to Caradoc volcanic rocks have been attributed to southeast subduction of Iapetus ocean crust (Phillips et al, 1976; Stillman and Williams, 1978) (figure 5.3a, c). The Leinster Massif has been interpreted as a series of northeast-southwest trending tectonostratigraphic terranes (figure 5.4) amalgamated along major sinistral transcurrent faults in the late Ordovician and early Silurian (Max et al, 1990). Generally the age of the terranes decreases from southeast to northwest. Their geometries are likely to reflect the orientation of the continental margin. The Ribband Group of the Waterford-Wicklow and Dublin terranes was considered by Max et al (1990) to represent accreted ocean floor sediments at a southeast dipping subduction zone (figure 5.3a, c).

In the Lake District, there is no structural or stratigraphical evidence consistent with an origin for Ordovician rocks as accreted ocean floor sediments. They are currently sited on continental crust (Bamford et al, 1978) and were probably deposited on extended continental crust of the edge of the microcontinent of Eastern Avalonia. The Ordovician rocks of the Lake District lack evidence for plate margin orientation and the direction of subduction (e.g. Branney and Soper, 1988).

The concealed Caledonides of eastern England contain a northwest-southeast trending belt of arc-related volcanics of probable mid to late Ordovician age (Pharaoh et al, 1987, 1991). Pharaoh et al (1991) describe the geochemistry and isotopic ages of volcanic strata recovered from boreholes of eastern England. They propose a subaerial, calc-alkaline volcanic arc extended from the Brabant Massif in Belgium to the Lake District during the Ordovician. It would have developed in response to southwest directed subduction of ocean crust of the Tornquist Sea (figure 5.3b). Wales and Ireland would represent back-arc basins in this scenario.

In summary, evidence for the plate margin orientation and direction of subduction is inconsistent for the Ordovician rocks across the southern British Isles. One must consider two important points. Firstly, the relative positions and orientations of localities across the region may have been different in the Ordovician from those of the present-day. Block rotations and juxtaposition along strike-slip faults or thrusts could have occurred during ocean closure and continental collision. Secondly, modern active margins are very complex. They can combine elements of transcurrent and extensional motion with collision in close spatial and temporal proximity (e.g. Japan, Indonesia and Chile). The orientation of plate margin, sedimentary basins and tectonic grain can vary significantly on a local scale.

In conclusion, only the large-scale tectonic configuration can be interpreted with confidence: ocean crust existed to the 'north' of a microcontinent, beneath which it was subducted. A wide zone of subduction-related volcanism and sedimentation in a fore-arc, inter-arc or back-arc setting is represented (figure 5.3d).

Figure 5.4 The Lower Palaeozoic tectonostratigraphic terranes of Leinster (in *italic* type),and possible correlations of early Ordovician sediments across the southern British Isles (shown by similarity of ornament). Data from Max et al (1990), Tietzsch-Tyler and Phillips (1989), Todd et al (1990), Cooper et al (in prep) and this study.

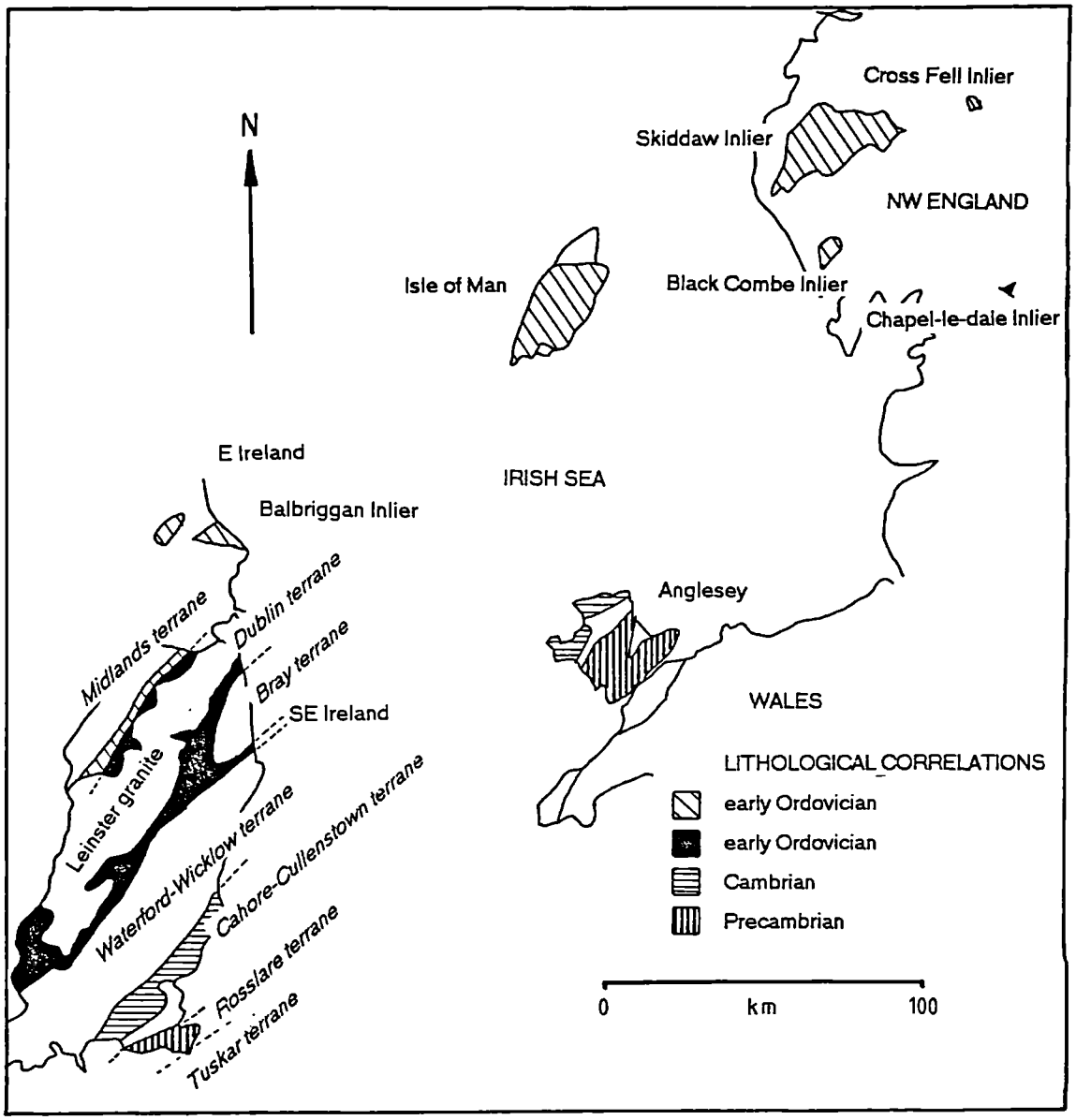

5.5.2 Plate convergence vector

Palaentological evidence shows that Eastern Avalonia, Baltica and Laurentia were widely separated in the early Ordovician but faunal provinciality diminished first between Eastern Avalonia and Baltica (by the late Ordovician), and then with Laurentia during the Silurian (Cocks and Fortey, 1982).

Palaeomagnetism shows a latitudinal width of 5000km for the Iapetus Ocean in the early Ordovician, which had diminished to 3300km by the mid-Ordovician (Torsvik and Trench, 1991).

Palaeontological and palaeomagnetic evidence are consistent with a northward drift of Eastern Avalonia in the Ordovician, bringing it into proximity with Baltica and diminishing its distance from Laurentia. This is consistent with a north-south plate convergence vector between Eastern Avalonia and oceanic crust. The evidence does not, however, preclude plate convergence in virtually any orientation.

5.5.3 Evidence of strike-slip tectonics

5.5.3.1 Wales

The Ordovician of Wales displays the following features of volcanism, tectonism and sedimentation:

> Tremadoc and Arenig volcanism was centred on deep, steep crustal discontinuities with surface expressions as grabens and fractures of approximately north-south trend; these were interpreted as splay faults of a deep-crustal, sinistral, strike-slip duplex (Kokelaar, 1988).
>
> Arenig sedimentation was inanorth-south trending graben, e.g. the Robell graben of 40km length and 13km width and divided into several narrow north-south graben and half-graben (Kokelaar, 1988). Arenig syn-sedimentary north-south and northeast-southwest faults were active in the Harlech Dome area (Traynor, 1990).
>
> Intra-Caradoc volcanism of Snowdonia was controlled by northeast trending fractures (Kokelaar, 1988).

Kokelaar (1988) related these features to a sinistral strike-slip tectonic regime in the early Ordovician (figure 5.5). This stress regime would have been induced in the microcontinental plate overriding a south directed subduction zone at a northeast trending plate margin. Transtension would cause east-west extension.

This model implies the present day positions of Ordovician outcrops of southern Britain differ from their relative positions at deposition.

5.5.3.2 Ireland

Late Ordovician to Silurian sinistral strike-slip motion is thought to have been responsible for amalgamation of the fault-bounded terranes of eastern and southeastern Ireland (Murphy, 1987; Max et al, 1990) (figure 5.4). These Lower Palaeozoic sediments can be compared lithologically with contemporaneous strata of Wales and England.

Figure 5.5 A plate tectonic model to explain early Ordovician tectonism in Wales. Half arrows indicate possible shear sense, small arrows the local extension and topped triangles the location of arc volcanoes (figure 6 of Kokelaar, 1988).

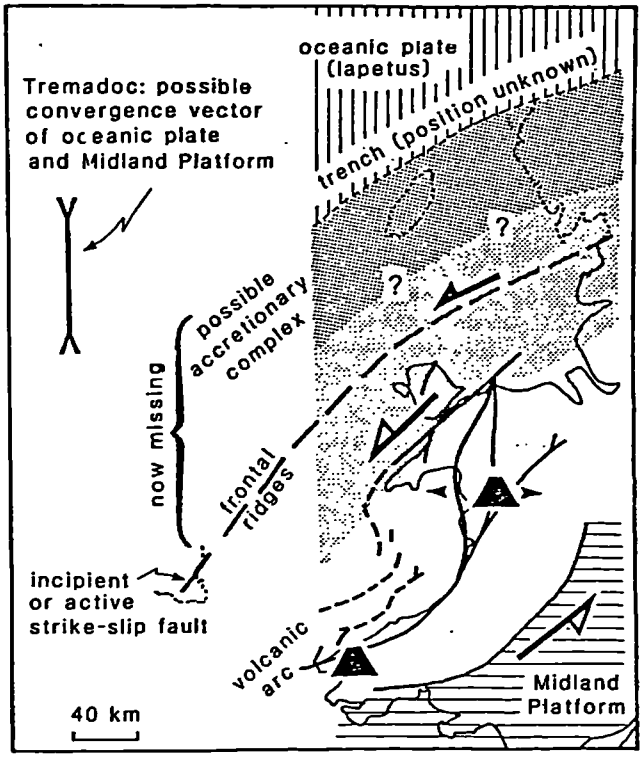

5.5.3.3 Linear stratigraphical belts

Tietzsch-Tyler and Phillips (1989) correlated the Monian Supergroup in northwest Anglesey with the Cambrian Cahore Group in southeast Ireland, which defined a linear stratigraphical belt of northeast-southwest trend (figure 5.4).

The Ingleton Group (probable Arenig) is lithologically distinct from the Skiddaw Group (Tremadoc to Llanvirn) (chapters 2 and 3). It displays similar sedimentary facies to the Bray Group (Cambrian) of Leinster (chapter 2) but differs in age and composition (chapter 3) and displays a volcanic arc provenance. McArdle (1981) correlated the greywackes of the Ballbeg Pelite Formation (Ribband Group (Cambrian to Llandeilo)) of the Dublin terrane of Leinster with the Bray Group. A dominance of volcaniclastic lithics in the former cannot be matched with the Bray Group (Max et al, 1990), but prompts comparison with the Ingleton Group. Thus it is likely that the Ingleton Group correlates with strata of the Dublin terrane of Leinster (figure 5.4).

The lithologies of the Skiddaw Group compare closely with the Balbriggan Inlier of eastern Ireland and the Midlands terrane of Leinster (Cooper et al, in prep.).

These lithological comparisons along strike define stratigraphical belts of at least 300km length (figure 5.4). Juxtaposed belts of equivalent age, common transverse sediment dispersal direction (south to north), but different sediment compositions require different relative positions during deposition (e.g. the Dublin and Midlands terranes of Leinster, traced into northwest England, could not have been juxtaposed in the Arenig). Three scenarios are considered (figure 5.6).

Figure 5.6 Three scenarios to explain the development of contemporaneous, but lithologically distinct sediments of similar dispersal direction of the stratigraphical belts of Ireland, Anglesey and northern England: (a) sinistral strike-slip amalgamation of longitudinally adjacent terranes; (b) amalgamation of laterally adjacent sedimentary basins by compression orthogonal to the plate margin; (c) tectonic control of sediment distribution and subsequent deformation.

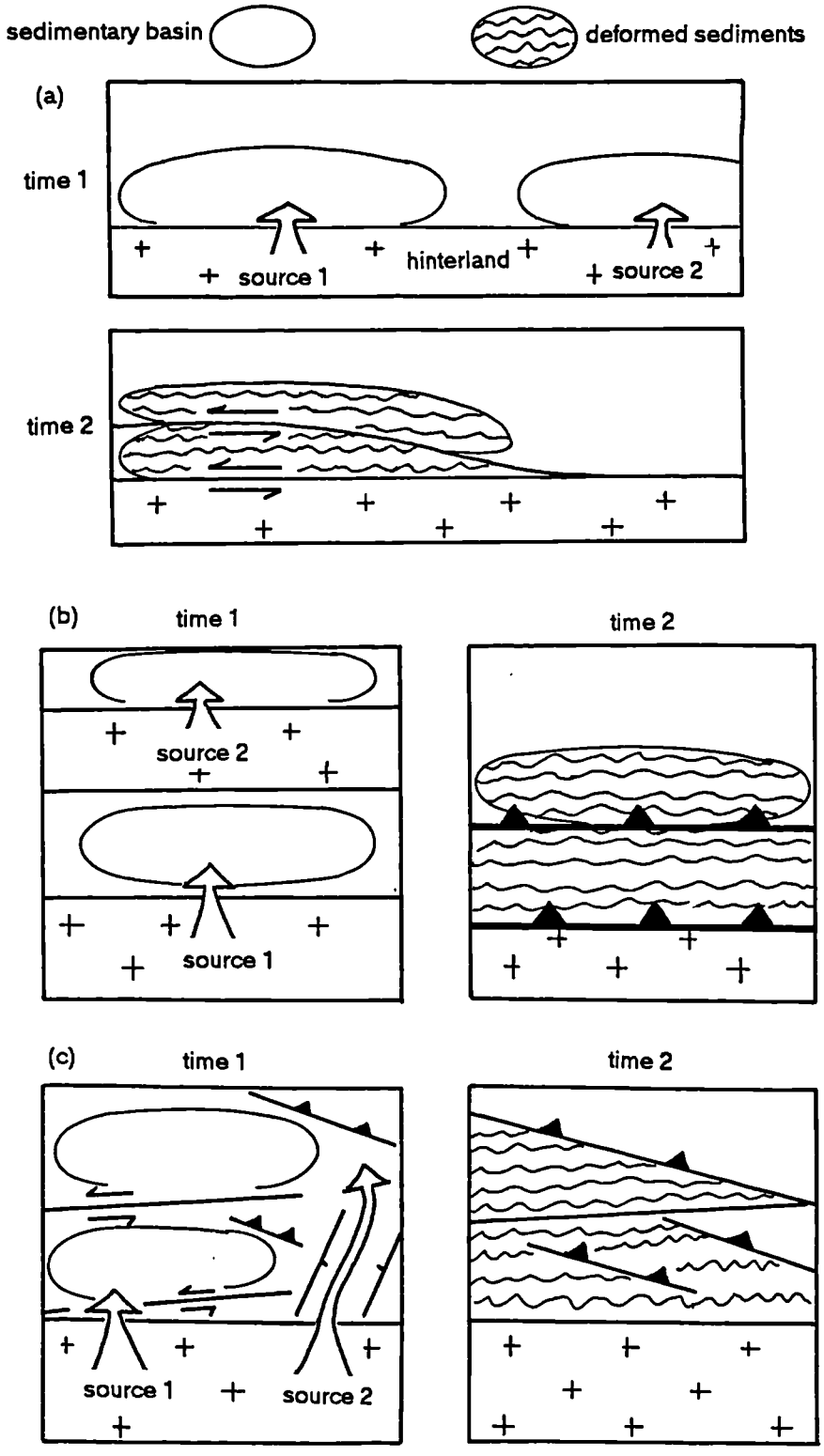

(a) The stratigraphical belts were longitudinally adjacent in the Arenig with sediment sourced from Eastern Avalonia (figure 5.6a). Variations in sediment composition would reflect heterogeneity of the hinterland (chapter 3). Amalgamation would have been largely by sinistral strike-slip displacement in the late Ordovician (Murphy, 1987; Max et al, 1990). An indication for the magnitude of strike-slip displacement is the length of the stratigraphical belts (i.e. 300km). This theory suffers from geometrical problems: Baltica was in close proximity to the 'east' of Eastern Avalonia in the late Ordovician (McKerrow and Cocks, 1986), thus the origin for terranes of Avalonian affinity is limited by the position of the Tornquist convergence zone. Large-scale strike-slip amalgamation is not feasible.

(b) The stratigraphical belts were separated by continental fragments which were overthrust during basin inversion due largely to compression orthogonal to the plate margin (figure 5.6b). Basin inversion and thrusting onto adjacent basement blocks has been described from southeast Ireland (prior to the upper Arenig (Tietzsch-Tyler and Phillips, 1989) and in the Llanvirn (Bennett et al, 1989)). There is no evidence of basement sediment sources between the Dublin and Midland terranes or between the Skiddaw and Ingleton groups. This is implausible since the size of such sediment hinterlands must have been substantial to provide large volumes of sand grade clastics.

(c) The stratigraphical belts represent a complex region of sedimentary basins with strong tectonic control (figure 5.6c). Sediment was sourced from various parts of the heterogeneous Eastern Avalonia microcontinent and dispersed within the system of variously connected or isolated marine basins depending on the tectonic elements active during sedimentation. Tectonic features with northeast-southwest orientation acted largely as barriers to sediment dispersal. Thus dispersal systems of differing composition and calibre constitute distinct stratigraphical belts. Basin inversion and juxtaposition by both northwest-southeast compression and northeast-southwest strike-slip is in evidence, but need not be of the large magnitudes required by scenarios (a) and (b).

5.5.4 Tectonic control of sedimentation in the Skiddaw Group

At the Tremadoc-Arenig boundary, submarine fan channels distributed sand-grade clastics in the Skiddaw Group depositional basin. Fan development could have been in response to eustatic sea level fall (section 5.3) or local tectonic uplift of the hinterland. From studies of sedimentation in the back-arc basins of the west Pacific, Klein (1985) suggested that lithologies were controlled by tectonism and volcanism; large uplift rates of source terrains were necessary for fan sedimentation. It is suggested that sediment distribution was controlled by a trough orientated approximately east-west, which could have acted as a conduit for sediment transport to contemporaneous depositional lobes of the Manx Group (chapter 2). This topographical feature reflects the orientation of tectonic elements contemporaneous with sedimentation.

In the early part of the Arenig, represented by the Hope Beck Formation, high relative sea level restricted sand-grade submarine fan development to small depositional lobes, each of which may have been a response to tectonic uplift of the hinterland. Extensive fan sedimentation was resumed during the Arenig (Loweswater Formation), probably in response to a combination of eustatic sea level fall and regional tectonic uplift (section 5.3). To explain sediment distribution and

palaeocurrents, a model of extensional fault blocks trending north-northwest and dipping northeast has been presented (chapter 2).

Given the uncertainties in the determination of plate margin orientation (which might be irregular), and plate convergence vector (which could have changed through time), strain ellipse models can be applied tentatively to explain the inferred fault geometries. Two possible settings are presented (figure 5.7).

Setting 1 assumes an approximately east-west orientated plate margin with convergence normal to the trench (north-south) and associated extension parallel to the trench (east-west) (figure 5.7a). This would have given thrusts in an approximately east-west orientation and normal faults trending approximately north-south. Evidence of intra-Arenig basin inversion, and thrusting of sediments onto adjacent basement blocks exists in Leinster (Tietzsch-Tyler and Phillips, 1987; Bennett et al, 1989). This could result from 'trench-normal' compression of the overriding microcontinental plate in setting 1 (or setting 2 below). Additionally, it provides evidence of tectonic uplift and erosion in both pre-late Arenig and Llanvirn times, which would have provided sediment to adjacent depositional basins. Therefore Loweswater Formation fan development could have been in response to tectonic uplift, although this is not meant to imply that southeast Ireland was an immediate source.

Setting 2 assumes a northeast-southwest trend for the plate margin, with a north-south plate convergence vector, which would induce sinistral strike-slip deformation in the overriding microcontinental plate (figure 5.7b). In the late Tremadoc and early Arenig, east-northeast trending thrust faults would have developed during transpression. These could have been responsible for the topographical feature of this approximate orientation which controlled distribution of sediment of the Watch Hill Formation. North-northwest trending normal faults would have resulted from transtension during the Arenig. Setting 2 was used by Kokelaar (1988) to explain Tremadoc to Caradoc faulting and volcanism of north Wales (section 5.5.3.1; figure 5.5).

Setting 1 explains features of the Skiddaw Group, but not the strike-slip features observed regionally. Thus setting 2 is the preferred interpretation.

Slump folds of Gasgale Gill were generated after deposition and partial lithification of the Loweswater Formation (chapter 4). They show that a topographical feature (fault scarp, strike of submarine slope) trended northeast and sloping down to the southeast. A synthetic strike-slip fault of setting 2 would be in a favourable orientation. The tectonic process responsible for producing the palaeoslope cannot be identified with any certainty.

At the end Arenig and early Llanvirn, slump folds were developed in the Kirk Stile Formation and major gravitational sliding produced the Buttermere Formation. Palaeoslope was to the west (chapter 4). Sediments are dominantly of siltstone and mudstone turbidites of submarine slope facies. Apart from a sandstone lobe near its base, the formation is devoid of sand-grade clastics. This might be due to a relative sea level high stand reducing input from hinterlands, or bypassing of sandy turbidity currents onto the basin floor (not exposed). Initiation of the westerly palaeoslope preceded uplift and emergence of the Skiddaw Group basin with development of the overlying

Figure 5.7 Strain ellipse models to explain proposed syn-sedimentary fault geometries in the Skiddaw Group: (a) trench-normal compression; (b) trench-parallel sinistral strike-slip (after Harding, 1974).

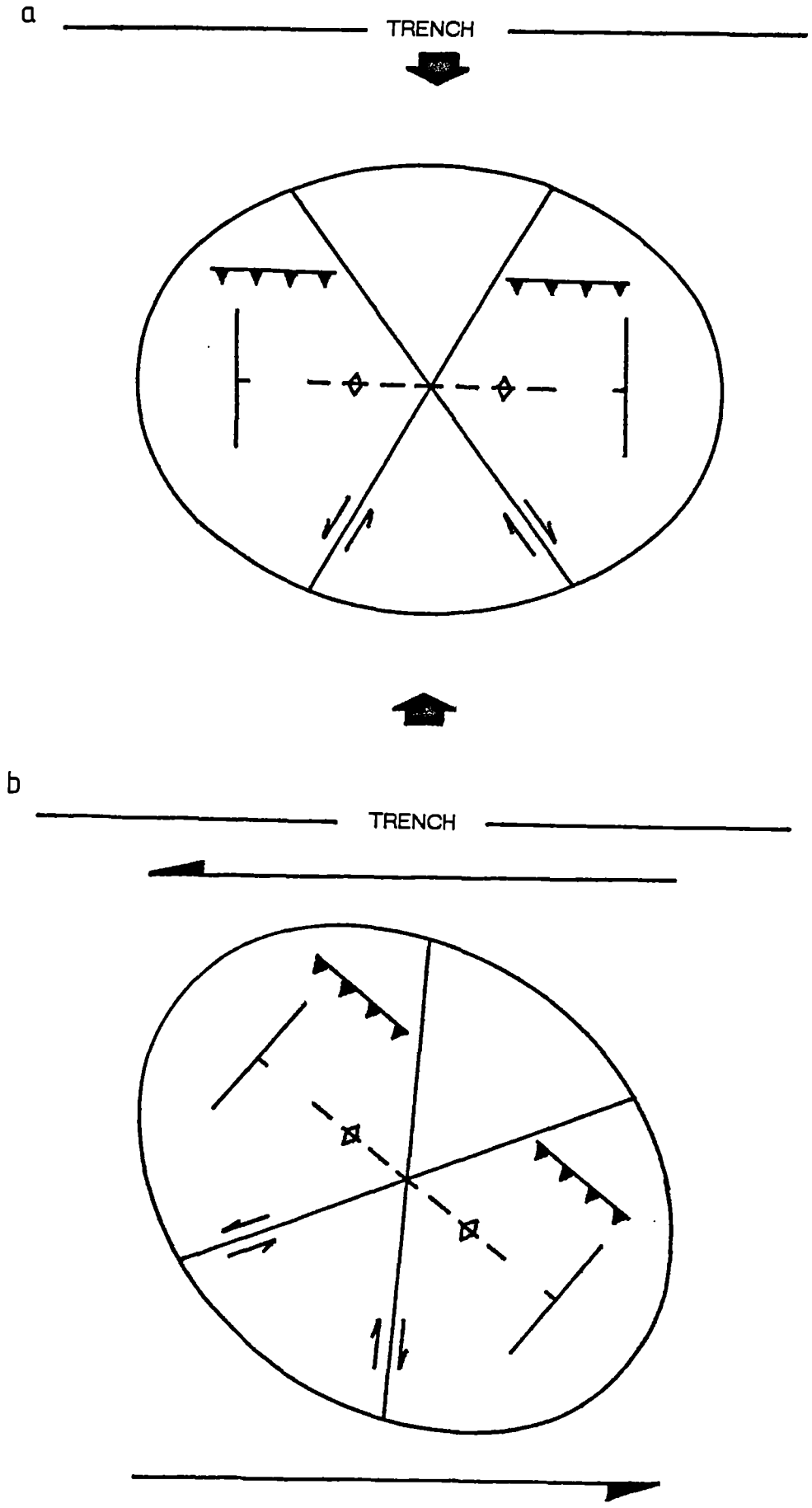

subaerial volcanic groups. The palaeoslope might be part of this major tectonic eposide and three possible causes relating palaeoslope and uplift are explored:

(a) Compression normal to the Tornquist convergence zone may have caused inversion of the Skiddaw Group basin. The age of the northwest-southeast structural trend of the Tornquist convergence zone of eastern England can be constrained by the age of the youngest rocks it deforms and the oldest undeformed rocks which overlie. Mid-Ordovician volcanics have been recovered from boreholes into rocks with this structural trend (Pharaoh, 1987, 1991). The Ingleton Group, of probable Arenig age, displays pre-cleavage folds with northwest-southeast trend and might be the most northern extension of this structural province. It is unconformably overlain by relatively less deformed mudstones of Ashgill age (O'Nions et al, 1973). Thus a mid-Ordovician deformation is implied.

(b) Uplift could be in response to volcanic doming and intrusion of the Ordovician batholith, which fed the volcanic effusion of the Eycott and Borrowdale volcanic groups (Firman and Lee, 1986; Soper et al, 1987). Precursors of the volcanic groups are represented by the volcaniclastic turbidites and tuffs of the Tarn Moor Formation, suggesting volcanism was active in the Lake District in the Llanvirn. Development of a palaeoslope is explained by this model, but its orientation is incidental.

(c) By analogy with the active margin of Chile, uplift of the fore-arc region could result from subduction of topographical features of the oceanic plate, e.g. aseismic ridges, mid-ocean ridge or seamounts (Flint et al, 1991). Plate convergence oblique to the plate margin would cause any uplift effect due to ridge subduction to migrate along the margin (figure 5.8). For setting 2 above, involving sinistral strike-slip motion, migration would be to the west.

As for (a) and (b) above, unequivocal proof for this cause of uplift is not possible. It is attractive since the observed direction of palaeoslope is inherent to the model.

Figure 5.8 Illustration of uplift in the overriding plate due to the subduction of an oceanic topographical feature, and its migration due to oblique plate collision.

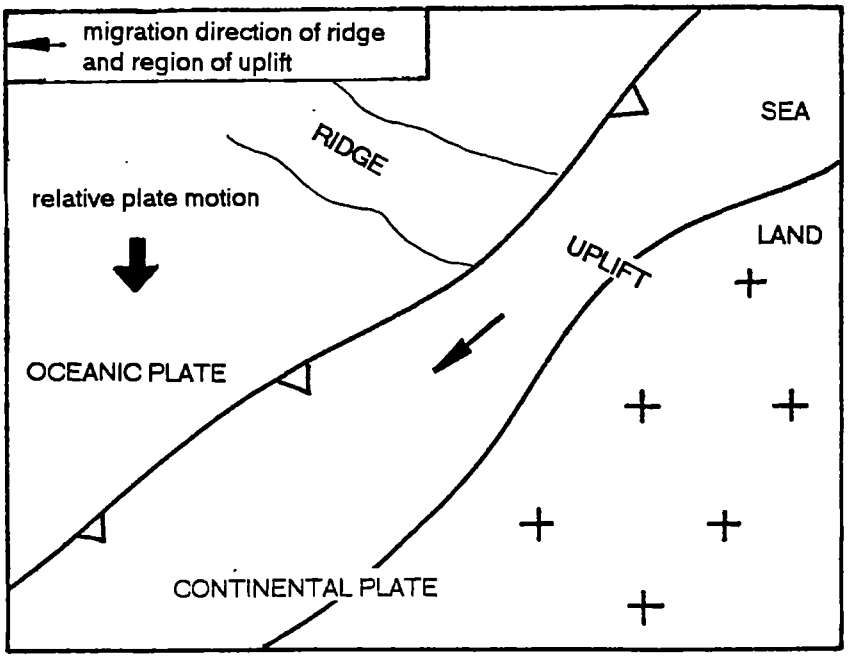

5.5.5 Implications for the structure in the Skiddaw Group

Much literature has been written in response to the suggestion by Simpson (1967) of a mid-Ordovician orogenic event in the Lake District (see review in chapter 4). After a decade of scientific debate, a widely held view was that the Borrowdale Volcanic Group rested with unconformity on the Skiddaw Group, but that this relationship did not represent an orogenic event (e.g. Moseley, 1975). The recognition of volcano-tectonic faulting in the Borrowdale Volcanic Group was used to illustrate the nature of the unconformity (Branney and Soper, 1988). Causes of uplift and inversion of the Skiddaw Group basin have been discussed above and structures of either gravitational (Moseley, 1972, 1975; Webb and Cooper, 1988) or tectonic origin in the Skiddaw Group could be truncated by the unconformity.

In the context of the regional active continental margin tectonic setting, it is possible that:

1. the stress regime changed its orientation through time with compression-, extension- and strike-slip-dominant phases acting across the 'fore-arc' region, e.g. transtensional and transpressional phases;

2. the Skiddaw Group depositional basin could have been rotated relative to the plate margin during the early Ordovician.

Thus faults and folds (and possibly cleavage) could have occurred in numerous orientations prior to the Borrowdale Volcanic Group. Orogeny by continental collision or accretion of an exotic terrane did not occur, but deformation as part of the strike-slip orogenic cycle (Mitchell and Reading, 1978) could be present. Structures related to such deformation episodes have not been recognised in the Skiddaw Inlier, but could be coaxial to later structures. Helm (1969), studying the Skiddaw Group of the Black Combe Inlier, recognised three deformation phases which preceded deformation of younger rocks. His structural scheme has not been supported by subsequent workers (A. Bell, pers. comm.).

In conclusion, any pre-mid-Ordovician deformations of the Skiddaw Group are likely to be inconsistent in their styles and geometries across the available outcrop. Coaxial structures could have formed at different times, complicating widespread correlation of deformation events. Thus one cannot assume that all coaxial structures are synchronous (e.g. coaxial soft-sediment and Acadian deformation events distinguished by Webb and Cooper (1988)). Only through detailed field mapping and observation of cross-cutting structures can the geometries and relative ages of structural elements be determined. Even if this is successful at outcrop scale it is probably unreasonable to expect that pre-ocean closure deformation events for the Skiddaw Group could be widely correlated.

5.6 History of the active continental margin

Late Precambrian to Early Palaeozoic tectono-thermal activity of the Cadomian orogeny records active plate margin processes, analogous to Andean-type orogeny, sited possibly at the southern margin of the Iapetus Ocean (D' Lemos et al, 1990). Coeval rocks include: the 'Cadomian' of northwest France, Spain and Czechoslovakia; the 'Avalonian' of southern Britain, Newfoundland, the Maritime Provinces of Canada, and New England, USA; and the 'Monian' of northwest Wales and

southeast Ireland (D'Lemos et al, 1990). Treloar and Strachan (1990) propose that the Cadomian belt of northern Brittany represents terranes amalgamated by sinistrally transpressive strike-slip motion in the hanging wall of an oblique subduction zone located to the north. There is no evidence for continent-continent collision (D' Lemos et al, 1990).

There was a pause in subduction in the Cambrian, and marine rift basins developed in Wales (Kokelaar, 1988; Woodcock, 1990) and Ireland (Bruck et al, 1979). During this period it has been suggested that the Eastern Avalonia microcontinent began to rift away from Gondwana (Woodcock, 1990). There is no record of this event in northern England since sediments generally post-date the late Tremadoc[1], and Ordovician evidence of rifting (e.g. extensional volcanism, sedimentation in rift basins) is absent. Continental separation could have either preceded the late Tremadoc or sedimentation on the northern margin of Eastern Avalonia could have been unaffected by rifting at the southern margin (presently obscured by the Hercynian front). The rifting event occurred prior to mid-Ordovician times since ostracod faunas of Avalonia and Armorica show a decreasing similarity after the Llanvirn (Vannier et al, 1989). Thus the event remains poorly constrained.

In the early Ordovician (late Tremadoc) subduction resumed with arc volcanism in Wales. Many variously connected or isolated marine basins were formed in response to changing tectonic regimes across the 'fore-arc' region of the active continental margin. Both eustatic sea level and local tectonic events (e.g. periods of transtension/transpression related to sinistral strike-slip motion) controlled sedimentation.

In the Llanvirn, uplift of the Skiddaw Group basin could have been related to subduction of an ocean ridge. Uplift could have been diachronous along the active continental margin and might correspond to relative sea level fall in Wales in the Llandeilo. Alternatively, Llanvirn uplift of the Skiddaw Group might have been in response to deformation due to convergence along a plate margin parallel to the Tornquist line, or due to volcanic doming preceding Caradoc volcanism of the Borrowdale Volcanic Group. Volcanism was widespread across the margin (Lake District, Wales and Ireland) at this time, but ceased at the end-Caradoc. This has been variously attributed to: the closure of the Tornquist Sea (and collision of Eastern Avalonia and Baltica in the early Ashgill (McKerrow and Cocks, 1986)); closure of the Iapetus Ocean (Pickering et al, 1988); or ridge subduction (Fitches and Campbell, 1987). Despite proximity of Eastern Avalonia to both Baltica and Laurentia, contintental collision did not occur until the Silurian (Soper and Woodcock, 1990). Evidence from Ireland (Murphy, 1987) suggests northeast-southwest sinistral strike-slip motion largely replaced northwest-southeast convergence by the late Ordovician.

Cooling and contraction of the sub-volcanic batholith of the Lake District allowed transgression in the Ashgill (Firman and Lee, 1986). The tectonic setting had changed in the Lake District in the Silurian with a foreland basin developing in response to loading by Laurentian continental crust (Kneller, 1991).

---

[1] A single occurrence of Cambrian microfossils has been found in the Skiddaw Group, but it is unclear whether this represents Cambrian deposits or a large clast of Cambrian mudstone in an olistostrome (Cooper et al, in prep.).

5.7 Concluding remarks

The findings of each chapter have been interpreted in terms of the regional tectonic model presented here. This section assesses the strengths and weaknesses of the model. There follows an account of the conclusions of the main body of the thesis in terms of the advances in understanding of each of the Skiddaw, Manx and Ingleton groups. Finally, conclusions are drawn on the application of the techniques used in the study. Throughout, suggestions for future work are made where it would be particularly beneficial.

5.7.1 The tectonic model

The strength of the model lies in its ability to explain the varied geological character of Eastern Avalonia in the Ordovician. It describes a complex array of interacting tectonic, volcanic and sedimentary proceses, which are applicable to the observed, complicated geological relationships. It is relevant through its flexibility: it draws a broad, general picture of low resolution. Details of plate margin orientation, subduction direction and plate convergence vectors are beyond the scope of the data. This is the main limitation of the model: its inability to predict details. It acknowledges the possibility of block rotations and strike-slip faults which might complicate or obscure stratigraphical and structural relationships between the Ordovician inliers, but it cannot assess their magnitude. Refinements could come through detailed palaeomagnetic studies of contemporaneous strata of each inlier. Problems of post-depositional deformation and remagnetization would have to be overcome for an assessment to be made of their relative positions at deposition and subsequent rotations. Revisions, improvements and additions to the model are expected through mapping programs in England, Wales and Ireland. Greater refinement of local chronostratigraphy will enable detailed correlation of 'events' across the region. A better understanding of Ordovician and subsequent deformations will enable more accurate reconstructions of Ordovician sedimentary systems. Development of the model would benefit from improved communication between workers in different inliers.

5.7.2 Early Ordovician sediments of northern England

5.7.2.1 The Skiddaw Group

The study has improved the understanding of the sedimentary environments, sediment distribution and the extent, calibre and controls of the depositional system.

Tectonic uplift probably caused sea level fall and submarine fan development along Eastern Avalonia's active margin at the end Tremadoc and earliest Arenig, represented by the Watch Hill Formation. The proximal channel-levee facies association represents widely divergent channel orientations which could be interpreted as flow in opposite directions away from a point of input into an east-west trough. Depositional lobes of the Manx Group could be the westerly extension of the same distribution system. Relative sea level rise curtailed sand-grade fan sedimentation and allowed accumulation of the mudstone-dominant Hope Beck Formation, with limited development of sandstone lobes related to local tectonic uplift of the hinterland.

Relative sea level fall in the Arenig (in response to either eustacy or tectonic uplift, or both) caused renewed fan progradation with distributary channel, depositional lobe and inter-lobe facies associations. Sediment distribution is interpreted to have been influenced by linear troughs trending approximately north-northwest. A tectonic model of extensional fault blocks tilted to the northeast, could explain the observations. Detailed mapping of thickness changes in the Loweswater Formation might confirm the existence of proposed syn-sedimentary faults.

Local sandstone depositional lobe development near the base of the Kirk Stile Formation could have been in response to local tectonic uplift and relative sea level fall during a dominantly high stand of sea level with dominantly mudstone/siltstone deposition.

Increased resolution of biostratigraphy through the continuing BGS mapping program could enable better appreciation of the duration of periods of sandy submarine fan development. It is expected that evidence from areas of the Skiddaw Inlier yet to be mapped within the current program will prompt revision of the proposed hypotheses.

Sediment that fed the Skiddaw Group basin was largely sourced from a *recycled orogenic terrain* with inactive continental margin volcanic arcs. In addition was a source of mature quartzose sediments of *craton interior* or *passive margin* provenance. This could have been an intermediate source of shelf/deltaic sands.

The *recyled orogenic terrain* was heterogeneous with unroofed acid plutons, volcaniclastic and pyroclastic deposits, metamorphosed and cleaved sedimentary, volcanic and plutonic clasts and intraformational sediments. Different proportions of clast types are reflected in variations in greywacke composition within the Skiddaw Group. The hinterland was probably equivalent to the terrain of accreted Precambrian volcanic arcs of the Midlands microcraton. Greywackes with a high matrix content were probably generated by mixing during transport of sandy turbidity currents with unconsolidated mud on the surface of the submarine fan. An origin as volcaniclastic mud flows cannot be dismissed. Further work studying neodymium model ages of different greywacke types might answer the question of intrinsic or extrinsic genesis of matrix-rich greywackes.

Coeval volcanism occurred in the Llanvirn and provided volcaniclastic turbidites and tuffs to the Tarn Moor Formation. Evidence for coeval volcanism in Tremadoc and Arenig greywackes might be found from a study of samarium-neodymium, and other, isotopic systems of greywackes, combined with a knowledge of their petrographical and geochemical composition, their sedimentary environment and direction of their depositional current.

Analysis of palaeoslope indicators by consideration of the distribution of slump fold axes, axial planes, and vergence directions has revealed a westerly palaeoslope across the Skiddaw Inlier in the early Llanvirn. In the Northern Fells belt, gravitational deformation is restricted to slump folds and occasional debrites. The sandstone clasts of the Beckgrains Bridge debris flow are of similar composition to the Loweswater Formation, suggesting reworking of this older formation or of its shallow water equivalent. In the Central Fells belt the major olistostrome of the Buttermere Formation (Webb and Cooper, 1988) contains rafts of turbidite sandstones. These turbidites are of similar composition to those of the Hope Beck and Watch Hill formations or the Loweswater Formation of Jonah's Gill, and suggest gravitational reworking of Skiddaw Group sediments.

Controls of submarine slope formation were discussed in the context of the tectonic model (section 5.5.4). Slope formation might correspond to uplift of the depositional basin prior to subaerial extrusion of the volcanic arcs in the Caradoc.

Variation from west directed slumping is found in Gasgale Gill where slump folds verging southeast were formed after deposition and partial lithification of *c.* 50m of Arenig turbidites. This could be related to local fault control. Further analysis of slump fold orientations throughout the Skiddaw Group might reveal: syn-sedimentary topography; post-depositional topography responsible for gravitational deformation; changes in slope orientations with time, which might reflect the influence of different tectonic elements.

5.7.2.2 The Manx Group

Turbidites and debrites of the Manx Group are of similar depositional environments to the Skiddaw Group. The depositional lobe facies association of end-Tremadoc age could be a distal extension of the distributary system displaying proximal channel-levee facies association in the Watch Hill Formation. A better understanding of deformations of the Manx Group would enable accurate restoration of palaeocurrent data. Collection and interpretation of such data would enable an interpretation of palaeoslope and sea floor topography.

Sediment was derived from *continental arc, passive margin* and *recycled* provenances and compositions of turbidites of the Niarbyl Flags, Lonan Flags and Maughold Banded Group are comparable with those of the Bitter Beck, Watch Hill and Loweswater Formations respectively. An intermediate source of mature quartz sands is present (e.g. shelf sands). The Manx and Skiddaw groups share a common hinterland and probably a common depositional basin.

A mapping program for the Isle of Man with integrated structural, sedimentological and provenance analysis would provide an invaluable link between the early Ordovician geology of northwest England and southeast Ireland.

5.7.2.3 The Ingleton Group

Development of a depositional lobe is represented by the greywackes of the Ingleton Group. Lithological comparison with the Arenig strata of the Beckermonds Scar borehole is confirmed and these represent the lobe fringe. Detritus is first cycle from a *continental arc, but volcanism coeval* with sedimentation cannot be proven. The location of active volcanism indicated by a bentonite is unknown and does not prove an active volcanic source for surface transported sediment. Published neodymium model ages could be explained by a Precambrian volcanic arc source.

Sediment composition, neodymium model ages and sediment calibre of depositional lobe facies contrast markedly with the Skiddaw Group. Separate distributary systems in unconnected sedimentary basins are proposed. Red chert clasts, characteristic of the Ingleton and Beckermonds Scar borehole greywackes are present in the Bray Group of southeast Ireland. Further comparison of composition does not support a lithological correlation, but the Ingleton Group may correlate with sediments of the Dublin terrane of Leinster.

Further isotopic analysis of the Ingleton Group might answer the question of coeval versus non-coeval volcanism. Additional useful work includes comparing compositions and isotopic systems of the Ingleton Group with the concealed Caledonides of the east Midlands.

5.7.3 Techniques

5.7.3.1 Sedimentology

The interpretation of ripple and sole palaeocurrent directions of turbidites due to the oblique reflection of turbidity currents at topographical features (Kneller et al, 1991) has been extended in this study to include turbidity currents confined within troughs. Additional data, e.g. thickness changes of sandstone lobe deposits, enabled an interpretation of extensional tectonic elements responsible for the intra-basinal topography. Comparison with other turbidite systems in extensional tectonic settings, e.g. the late Jurassic to early Cretaceous of the North Sea (Boote and Gustav, 1987), would be a useful test of the model.

Turbidite reflection theories are supported by studies of deformed ancient sequences. Further study is required of relatively less deformed turbidite sequences known to have a topographical control of sediment distribution, (e.g. the Carboniferous of northern England, or modern environments), to assess the widespread applicability of 'reflection theory'. Experimental modelling of turbidity current interaction with the sides of topographical troughs is required to test the theoretical palaeocurrent interpretation of chapter 2.

The theory has potential for predicting the distribution of turbidites, sand bodies and, therefore, the geometries and extents of hydrocarbon reservoirs.

The combination of palaeocurrent data, thickness changes of units of depositional lobe facies associations, syn-depositional palaeoslope orientations from slump folds, and the geometry of syn-sedimentary faults are all required for a robust model of tectonic control of turbidity current flow.

5.7.3.2 Provenance

The successful identification of sedimentary provenance requires the application of numerous petrographical (QFL grain populations; identification of lithic range) and geochemical (whole rock major and trace elements; rare earth elements and isotopes) techniques (McCann, 1991; McCaffrey, 1991). Since the pioneering work of Crook (1974), most provenance studies have used greywackes deposited from turbidity currents. Compositional variation with grainsize has been recognised (Dickinson, 1970; Ingersoll et al, 1984), prompting comparison of samples of similar grainsize (generally fine and medium sand) (e.g. Bhatia, 1983). It is shown in chapter 3 that the ranges of variation in composition due to grainsize and depositional flow regime respectively, are as great as the compositional variation between sediments of different provenance. It is recommended therefore, that comparison is valid only for samples of both the same grainsize and depositional flow regime.

The use of averages of sample compositions can be misleading. An 'average' of samples of mixed provenance will not relate to any true sample composition. Workers should appreciate the

range of sample compositions and the causes of variation (e.g. grainsize and depositional sorting, different provenance elements, poorly mixed sediment of heterogeneous provenance).

The study of a range of grainsizes of turbidites is to be encouraged. Different grainsize fractions might have different diagenetic histories with better or worse preservation of the sample composition at deposition. Identification of lithic fragments by petrography is best in samples of gravel or very coarse sand grainsize. Characteristic lithic fragments are of invaluable use in lithological correlation and provenance identification. The degree of disaggregation of lithic fragments can be assessed by comparison with sediment of finer calibre. The QFL pointcounting technique (Dickinson, 1970) and petrographical provenance discrimination diagrams require samples of fine and medium sand grainsize. Use of these diagrams alone ignores important information regarding distinct sediment sources that can be identified from lithic fragments. Comparison of turbidites of different facies is best made with an appreciation of the displacement on a QFL diagram due to lithic disaggregation, decrease in grainsize and decreasing flow power at deposition.

Application of published provenance discrimination diagrams must be made with an understanding of the meaning of different provenance fields, how they were defined and the margins of error inherent in the diagram. It has been shown that Cambro-Ordovician turbidites differ in composition from younger turbidites (e.g. elevated K_2O values in Lower Palaeozoic mudstones), so comparison of the former with provenance fields defined from the latter, is suspect. Comparison of sample compositions with published provenance discrimination diagrams without a discussion of the applicability of the approach is probably flawed.

The statistical approach of Bhatia (1983), who used discriminant function analysis of whole rock major element geochemical data of fine and medium sandstones, was repeated in this study using a refined data set without the errors of the previous work. The resulting discriminant function was used to classify by provenance type the samples of this study. Amendments to the provenance fields of the geochemical bivariate diagrams of Bhatia (1983) were also made.

Useful further work would be the compilation of petrographical and geochemical data of turbidite samples of known age, facies, grainsize, sedimentary structures and relatively well constrained provenance to produce new provenance discrimination diagrams. The statistical approach of discriminant function analysis is recommended.

In order to assess the tectonic setting, provenance identification must be accompanied by analysis of sedimentary facies (to promote an understanding of the distributary system, its size, shape, controls, depositional basin, and changes with time) and studies of syn- and post-depositional deformations (to reveal the geometry of the basin, its internal topography, tectonic regimes and to enable the restoration of subsequent deformations).

REFERENCES

ALLEN, J. R. L. 1970. The sequence of sedimentary structures in turbidites, with special reference to dunes. *Scottish Journal of Geology,* **6**, 146-161.

ALLEN, J. R. L. 1977. The possible mechanics of convolute lamination in graded sand beds. *Journal of the Geological Society, London,* **134**, 19-31.

ALLEN, P.M. & COOPER, D. C. 1986. The stratigraphy and composition of the Latterbarrow and Redmain sandstones, Lake District, England. *Geological Journal,* **21**, 59-76.

BAGNOLD, R. A. 1962. Auto-suspension of transported sediment: turbidity currents. *Proceedings of the Royal Society, London (A),* **265**, 315-319.

BAILEY, E. H., IRWIN, W. P. & JONES, D. L. 1964. Franciscan and related rocks and their significance in the geology of western California. *Bulletin of the California Division of Mines and Geology,* **183**, 177 p.

BAMFORD, D., NUNN, K., PRODEHL, C. & JACOB, B. 1978. LISPB-IV. Crustal structure of Northern Britain. *Geophysical Journal of the Royal Astronomical Society,* **54**, 43-60.

BANHAM, P. H., HOPPER, F. M. W. & JACKSON, J. B. 1981. The Gillbrea Nappe in the Skiddaw Group, Cockermouth, Cumbria, England. *Geological Magazine,* **118**, 509-516.

BASU, A. 1985. Influence of climate and relief on compositions of sands released at source areas. *In:* ZUFFA, G. G. (ed), *Provenance of Arenites,* NATO-ASI Series, Dordrecht, D. Reidel, 1-18.

BASU, A., YOUNG, S. W., SUTTNER, L. J., JAMES, W. C. & MACK, G. H. 1975. Re-evaluation of the use of undulatory extinction and polycrystallinity in detrital quartz for provenance interpretation. *Journal of Sedimentary Petrology,* **45**, 873-882.

BENNETT, M. C., DUNNE, W. M. & TODD, S. P. 1989. Reappraisal of the 'Cullenstown Formation': Implications for the Lower Palaeozoic tectonic history of SE Ireland. *Geological Journal,* **24**, 317-329.

BERRIDGE, N. G. 1982. Petrography of the pre-Carboniferous rocks of the Beckermonds Scar Borehole in the context of the magnetic anomaly at the site. *Proceedings of the Yorkshire Geological Society,* **44**, 89-98.

BHATIA, M. R. 1983. Plate tectonics and geochemical composition of sandstones. *Journal of Geology,* **91**, 611-627.

BHATIA, M. R. 1985a. Plate tectonics and geochemical composition of sandstones: a reply. *Journal of Geology,* **93**, 85-87.

BHATIA, M. R. 1985b. Composition and classification of Paleozoic flysch mudrocks of eastern Australia: implications in provenance and tectonic setting interpretation. *Sedimentary Geology,* **41**, 249-268.

BHATIA, M. R. 1985c. Rare earth element geochemistry of Australian Palaeozoic greywackes and mudrocks: provenance and tectonic control. *Sedimentary Geology,* **45**, 97-113.

BHATIA, M. R. & CROOK, K. A. W. 1986. Trace element characteristics of greywackes and tectonic setting discrimination of sedimentary basins. *Contributiions to Mineralogy and Petrology,* **92**, 181-193.

BHATIA, M. R. & TAYLOR, S. R. 1981. Trace element geochemistry and sedimentary provinces: a study from the Tasman Geosyncline, Australia. *Chemical Geology*, **33**, 115-125.

BLATT, H. 1967. Provenance determinations and recycling of sediments. *Journal of Sedimentary Petrology*, **37**, 1031-1044.

BLATT, H. 1985. Provenance studies and mudrocks. *Journal of Sedimentary Petrology*, **55**, 69-75.

BLATT, H., & CHRISTIE, J. M. 1963. Undulatory extinction in quartz of igneous and metamorphic rocks and its significance in provenance studies of sedimentary rocks. *Journal of Sedimentary Petrology*, **33**, 559-579.

BLATT, H., MIDDLETON, G. V. & MURRAY, R. 1972. *Origin of sedimentary rocks.* Prentice-Hall, New Jersey, 634p.

BOOTE, B. R. D. & GUSTAV, S. H. 1987. Evolving depositional systems within an active rift, Witch Ground Graben, North Sea. *In:* BROOKES, J. & GLENNIE, K. (eds), *Petroleum Geology of NW Europe*, Graham & Trotman, London, 819-833.

BOUMA, A. H. 1962. *Sedimentology of some Flysch Deposits: A graphic approach to facies interpretation.* Elsevier, Amsterdam, 168p.

BRANNEY, M. J. 1988. The subaerial setting of the Borrowdale Volcanic Group, English Lake District. *Journal of the Geological Society, London*, **145**, 887-890.

BRANNEY, M. J. & SOPER, N. J. 1988. Ordovician volcano-tectonics in the English Lake District. *Journal of the Geological Society, London*, **145**, 367-376.

BRENCHLEY, P. J. 1969. Origin of matrix in Ordovician greywackes, Berwyn Hills, North Wales. *Journal of Sedimentary Petrology*, **39**, 1297-1301.

BRITISH GEOLOGICAL SURVEY, 1990. Lorton and Loweswater, sheet NY 12, solid and drift, 1:25000.

BRUCK, P. M., COLTHURST, J. R. J., FEELY, M., GARDINER, P. R. R., PENNEY, S. R., REEVES, T. J., SHANNON, P. M., SMITH, D. G. & VANGUESTAINE, M. 1979. South-east Ireland: Lower Palaeozoic stratigraphy and depositional history. *In:* HARRIS, A. L., HOLLAND, C. H. & LEAKE, B. E. (eds) *The Caledonides of the British Isles - reviewed.* Geological Society, London, Special Publication, **8**, 533-544.

BURGESS, I. C. 1971. Synopses of logs of Allenheads No.1 borehole ([8604 4539]; OD 406.76m) and No. 2 borehole ([8715 4505]; OD 536.45m). *Annual Report of the Institute of Geological Sciences for 1970*, **33**.

CHAPPELL, B. W. 1968. Volcanic graywackes from the Upper Devonian Baldwin Formation, Tamworth-Barraba district, N.S.W. *Journal of the Geological Society of Australia*, **15**, 87-102.

COCKS, L. R. M. & FORTEY, R. A. 1982. Faunal evidence for oceanic separations in the Palaeozoic of Britain. *Journal of the Geological Society, London*, **139**, 467-480.

COLEMAN, R. G. 1972. The Colebrook Schist of Southwestern Oregon and its relation to the tectonic evolution of the region. *Bulletin of the United States Geological Survey*, **1339**, 61p.

COMBAZ, A. 1967. Un microbios du Tremadocien dans un sondage d'Hassi-Messaoud. *Actes de la Societe Linneene de Bordeaux*, **104**, 26.

CONNELLY, W. 1978. Uyak complex, Kodiak Island, Alaska: a Cretaceous subduction complex. *Geological Society of America, Bulletin,* **89**, 755-769.

COOMBS, D. S. 1954. The nature and alteration of some Triassic sediments from Southland, New Zealand. *Transactions of the Royal Society of New Zealand,* **82**, 65-109.

COOPER, A. H. 1990. The Skiddaw Group of Causey Pike. *Proceedings of the Cumberland Geological Society,* **5**, 222-230.

COOPER, A. H. & MOLYNEUX, S. G. 1990. The age and correlation of Skiddaw Group (early Ordovician) sediments in the Cross Fell inlier (northern England). *Geological Magazine,* **127**, 147-157.

COOPER, A. H., WEBB, B. C., RUSHTON, A. W. A., MOLYNEUX, S. G., HUGHES, R. A. & MOORE, R. M. in prep. The stratigraphy and correlation of the Skiddaw Group (Ordovician) of the English Lake District.

COOPER, D. C., LEE, M. K., FORTEY, N. J., COOPER, A. H., RUNDLE, C. C., WEBB, B. C. & ALLEN, P. M. 1988. The Crummock Water aureole: a zone of metasomatiam and source of ore metals in the English Lake District. *Journal of the Geological Society, London,* **145**, 523-540.

COPE, R. N. 1959. The Silurian rocks of the Devilsbit Mountain district, County Tipperary. *Royal Irish Academy Proceedings, section B,* **60**, 217-242.

CRAIG, G. Y. & WALTON, E. K. 1962. Sedimentary structures and palaeocurrent directions form the Silurian rocks of Kirkcudbrightshire. *Transactions of the Geological Society, Edinburgh,* **19**, 100-119.

CROOK, K. A. 1974. Lithogenesis and geotectonics: the significance of compositional variation in flysch arenties (greywackes). *In:* DOTT, R. H. Jr. & SHAVER, R. H. (eds) *Modern and Ancient Geosynclinal Sedimentation.* Society of Economic Palaeontologists and Mineralogists, Special Publication, **19**, 304-310.

DAKYNS, J. R., TIDDEMAN, R. H., GUNN, & STRAHAN, 1890. *Geology of Ingleborough,* Memoir of the Geological Survey.

DAVIES, G., GLEDHILL, A. & HAWKESWORTH, C. 1985. Upper crustal recycling in southern Britain: evidence from Nd and Sr isotopes. *Earth and Planetary Science Letters,* **75**, 1-12.

DAVIS, J. C. 1986. *Statistics and data analysis in geology.* Second edition. John Wiley and Sons Inc.

DEER, W. A., HOWIE, R. A. & ZUSSMAN, J. 1966. *An introduction to the rock forming minerals.* Longman. 528p.

DEPAOLO, D. J. 1981. Neodymium isotopes in the Colorado Front Range and crust-mantle evolution in the Proterozoic. *Nature,* **291**, 193-196.

DEWEY, J. F. 1969. Evolution of the Caledonian/Appalachian orogen. *Nature,* **222**, 124-129.

DEWEY, J. F. & BIRD, J. M. 1970. Mountain belts and the new global tectonics. *Journal of Geophysical Research,* **75**, 2625-2647.

DICKINSON, W. R. 1962. Petrology and diagenesis of Jurassic andesitic strata in central Oregon. *American Journal of Science,* **260**, 481-500.

DICKINSON, W. R. 1970. Interpreting detrital modes of graywacke and arkose. *Journal of Sedimentary Petrology*, **40**, 695-707.

DICKINSON, W. R., BEARD, L. S., BRAKENRIDGE, G. R., ERJAVEC, J. L., FERGUSON, R. C., INMAN,K. F., KNEPP, R. A., LINDBERG, F. A. & RYBERG, P. T. 1983. Provenance of North American Phanerozoic sandstones in relation to tectonic setting. *Geological Society of America, Bulletin*, **94**, 222-235.

DICKINSON, W. R. & SUCZEK, C. A. 1979. Plate tectonics and sandstone compositions. *American Association of Petroleum Geologists, Bulletin*, **63**, 2164-2182.

DICKINSON, W. R. & VALLONI, R. 1980. Plate settings and provenance of sands in modern ocean basins. *Geology*, **8**, 82-86.

DIXON, E. E. L. 1925. *Summary of progress*, Geological Survey of Great Britain, for 1924, 70-71.

D'LEMOS, R. S., STRACHAN, R. A. & TOPLEY, C. G. 1990. The Cadomian Orogeny in the North Armorican Massif; a brief review. *In:* D'LEMOS, R. S., STRACHAN, R. A. & TOPLEY, C. G. (eds) *The Cadomian Orogeny*, The Geological Society, London, Special Publication, **51**, 3-12.

DOTT, R. L. 1964. Wacke, greywacke and matrix - what approach to immature sandstone classification. *Journal of Sedimentary Petrology*, **34**, 625-632.

DOWNIE, C. & FORD, T. D. 1966. Microfossils from the Manx Slate Series. *Proceedings of the Yorkshire Geological Society*, **35**, 307-322.

DOWNIE, C. & SOPER, N. J. 1972. Age of the Eycott Volcanic Group and its conformable relationship to the Skiddaw Slates in the English Lake District. *Geological Magazine*, **109**, 259-268.

DYPVIK, H. & BRUNFELT, A. O. 1979. Distribution of rare earth elements in some North Atlantic Kimmeridgian black shales. *Nature*, **278**, 339-341.

EASTWOOD, T., DIXON, E. E. L., HOLLINGWORTH, S. E. & SMITH, B. 1931. The geology of the Whitehaven and Workington District. *Memoir of the Geological Survey of Great Britain*, 304p.

EDWARDS, A. B. 1950. The petrology of the Miocene sediments of the Aure Trough, Papua. *Proceedings of the Royal Society of Victoria*, **60**, 123-148.

EDWARDS, D. A. 1991. *Turbidity currents: dynamics, deposits and reversals*. PhD Thesis, Leeds University.

FIRMAN, R. J. & LEE, M. K. 1986. The age and structure of the concealed English Lake district batholith and its probable influence on subsequent sedimentation, tectonics and mineralisation. *In:* NESBITT, R. W. & NICHOL, I., *Geology in the real world - the Kingsley Dunham volume*, Institution of Mining and Metallurgy, London, 117-127.

FITCHES, W. R. & CAMPBELL, S. D. G. 1987. Tectonic evolution of the Bala Lineament in the Welsh Basin. *Geological Journal*, **22**, 131-153.

FITTON, J. G. & HUGHES, D. J. 1970. Volcanism and plate tectonics in the British Ordovician. *Earth and Planetary Science Letters*, **8**, 223-228.

FITTON, J. G. & HUGHES, D. J. 1977. Ordovician volcanism in England and Wales - a review. *In:* STILLMAN, C. J., *Conference Report - Palaeozoic volcanism in Great Britain and Ireland*, Journal of the Geological Society, London, **133**, 404-405.

FLEET, A. J., HENDERSON, P., KEMPE, D. R. C. 1976. Rare earth element and related chemistry of some drilled southern Indian Ocean basalts and volcanogenic sediments. *Journal of Geophysical Research*, **81**, 4257-4268.

FLINT, S., TURNER, P. & JOLLEY, E. J. 1991. High frequency cyclicity in Quaternary fan-delta deposits of the Andean forearc: Relative sea level changes as a response to aseismic ridge subduction. *In:* MACDONALD, D. (ed), *Sea level changes at active plate margins.* International Association of Sedimentologists, Special Publication.

FLOYD, P. A. & LEVERIDGE, B. E. 1987. Tectonic environment of the Devonian Gramscatho basin, south Cornwall: framework mode and geochemical evidence from turbiditic sandstones. *Journal of the Geological Society, London*, **144**, 531-542.

FLOYD, P. A., SHAIL, R., LEVERIDGE, B. E. & FRANKE, W. 1991. Geochemistry and provenance of Rhenohercynian synorogenic sandstones: implications for tectonic environment discrimination. *In:* MORTON, A. C., TODD, S. P. & HAUGHTON, P. D. W. (eds) *Developments in Sedimentary Provenance Studies.* Geological Society, London, Special Publication, **57**, 173-188.

FLOYD, P. A., WINCHESTER, J. A. & PARK, R. G. 1989. Geochemistry and tectonic setting of Lewisian clastic metasediments from the early Proterozoic Loch Maree Group of Gairloch, N. W. Scotland. *Precambrian Research*, **45**, 203-214.

FORTEY, N. J. 1989. Low grade metamorphism in the Lower Ordovician Skiddaw Group of the Lake District, England. *Proceedings of the Yorkshire Geological Society*, **47**, 325-337.

FORTEY, R. A. & COCKS, L. R. M. 1986. Marginal faunal belts and their structural implications, with examples from the Lower Palaeozoic. *Journal of the Geological Society, London*, **143**, 151-160.

FORTEY, R. A., OWENS, R. M. & RUSHTON, A. W. A. 1989. The palaeogeographic position of the Lake District in the early Ordovician. *Geological Magazine*, **126**, 9-17.

GRAHAM, J. 1988. Collection and analysis of field data. *In:* Tucker, M. E. (ed.), *Techniques in Sedimentology*, Blackwell Scientific Publications, Oxford, 5-62.

GRAHAM, S. A., INGERSOLL, R. V. & DICKINSON, W. R. 1976. Common provenance for lithic grains in Carboniferous sandstones from Ouachita Mountains and Black Warrior Basin. *Journal of Sedimentary Petrology*, **46**, 620-632.

GREEN, J. F. N. 1917. The age of the chief intrusions of the Lake District. *Proceedings of the Geological Association*, **28**, 1-31.

HALLAM, A. 1984. Pre-Quaternary sea-level changes. *Annual Review of Earth and Planetary Sciences*, **12**, 205-243.

HAMPTON, M. A. 1972. The role of subaqueous debris flow in generating turbidity currents. *Journal of Sedimentary Petrology*, **42**, 775-793.

HARDING, T. P. 1974. Petroleum traps associated with wrench faults. *Bulletin of the American Association of Petroleum Geologists*, **58**, 1290-1304.

HAUGHTON, P. W. D. 1988. A cryptic Caledonian flysch terrane in Scotland. *Journal of the Geological Society, London*, **145**, 685-703.

HEEZEN, B. C. & EWING, M. 1952. Turbidity currents and submarine slumps and the 1929 Grand Banks earthquake. *American Journal of Science*, **250**, 849-873.

HELLER, P. L. & DICKINSON, W. R. 1985. Submarine ramp facies model for delta-fed, sand-rich turbidite systems. *Bulletin of the American Association of Petroleum Geologists*, **69**, 960-976.

HELM, D. G. 1969. Microscopic and megascopic fabrics in the Skiddaw Group, Black Combe Inlier, English Lake District. *Geological Magazine*, **106**, 587-594.

HELM, D. G. 1970. Stratigraphy and structure in the Black Combe Inlier, English Lake District. *Proceedings of the Yorkshire Geological Society*, **38**, 105-148.

HELM, D. G. & ROBERTS, B. 1971. The relationship between the Skiddaw Slates and the Borrowdale Volcanic Groups in the English Lake District. *Nature*, **232**, 181-183.

HELM, D. G. & ROBERTS, B. 1971. Reply on Skiddaw Slates and Borrowdale Volcanics. *Nature*, **234**, 59-60.

HENDERSON, P. (ed) 1984. *Rare earth element geochemistry*. Elsevier Science Publishers.

HESSE, R. 1989. "Drainage systems" associated with mid-ocean channels and submarine yazoos: Alternative to submarine fan depositional systems. *Geology*, **17**, 1148-1151.

HESSE, R., SUNG, K. C., & RAKOFSKY, A. 1987. The Northwest Atlantic Mid-Ocean Channel of the Labrador Sea. V. Sedimentology of a giant deep-sea channel. *Canadian Journal of Earth Sciences*, **24**, 1595-1624.

HILL, P. R. 1984. Sedimentary facies of the Nova Scotian upper and middle continental slope, offshore eastern Canada. *Sedimentology*, **31**, 293-309.

HOUGHTON, H. F. 1980. Refined techniques for staining plagioclase and alkali feldspars in thin section. *Journal of Sedimentary Petrology*, **50**, 629-631.

HSU, K. J. 1964. Cross-laminations in graded bed sequences. *Journal of Sedimentary Petrology*, **34**, 379-388.

HUCKENHOLZ, H. G. 1963. Mineral composition and texture in graywackes from the Harz Mountains (Germany) and in arkoses from the Auvergne (France). *Journal of Sedimentary Petrology*, **33**, 914-918.

INGERSOLL, R. V. & SUCZEK, C. A. 1979. Petrology and provenance of Neogene sand from Nicobar and Bengal Fans, DSDP sites 211 and 218. *Journal of Sedimentary Petrology*, **49**, 1217-1228.

INGERSOLL, R. V., BULLARD, T. F., FORD, R. L., GRIMM, J. P., PICKLE, J. D. & SARES, S. W. 1984. The effect of grainsize on detrital modes: a test of the Gazzi-Dickinson point-counting method. *Journal of Sedimentary Petrology*, **54**, 103-116.

JACKSON, D. E. 1956. *Geology of the Skiddaw slates between the Lorton-Buttermere Valley and Troutbeck, Cumberland*. PhD Thesis, Kings College, University of Durham.

JACKSON, D. E. 1961. Stratigraphy of the Skiddaw Group between Buttermere and Mungrisdale, Cumberland. *Geological Magazine*, **98**, 515-528.

JACKSON, D. E. 1978. The Skiddaw Group. *In:* MOSELEY, F. (ed) *The geology of the Lake District*. Yorkshire Geological Society, Occasional Publication, **3**, 79-98.

JEANS, P. J. F. 1971. Relationship between the Skiddaw Slates and Borrowdale Volcanics. *Nature*, **234**, 59.

JEANS, P. J. F. 1972. The junction between the Skiddaw Slates and the Borrowdale Volcanics in Newlands Beck, Cumberland. *Geological Magazine*, **109**, 25-28.

JEANS, P. J. F. 1973. Plate tectonic reconstruction of the southern Caledonides of Great Britain. *Nature*, **245**, 120-122.

JOHNSON, A. M. 1970. *Physical processes in geology*. Freeman, Cooper and Company, San Francisco, 577p.

JOHNSON, G. A. L. 1961. Skiddaw Slates proved in the Teesdale inlier. *Nature*, **190**, 996.

KELLING, G. 1964. The turbidite concept in Britain. *In:* BOUMA, A. H. & BROUWER, A. (eds.), *Turbidites*. Developments in Sedimentology, 3, Elsevier, Amsterdam, 75-92.

KEMP, A. E. S. 1987. Evolution of Silurian depositional systems in the Southern Uplands, Scotland. *In:* LEGGETT, J. K. & ZUFFA, G. G. *Marine Clastic Sedimentology*. Graham & Trotman, 125-155.

KLEIN, G. D. 1985. The control of depositional depth, tectonic uplift, and volcanism on sedimentation processes in the back-arc basins of the western Pacific Ocean. *Journal of Geology*, **93**, 1-25.

KNELLER, B. C. 1991. A foreland basin on the southern margin of Iapetus. *Journal of the Geological Society, London*, **148**, 207-210.

KNELLER, B. C., EDWARDS, D. A., McCAFFREY, W. D. & MOORE, R. M. 1991. Oblique reflection of turbidity currents. *Geology*, **14**, 250-252.

KOKELAAR, P. 1988. Tectonic controls of Ordovician arc and marginal basin volcanism in Wales. *Journal of the Geological Society, London*, **145**, 759-775.

KOLLA, V. & MACURDA, D. B. Jr. 1988. Sea level changes and timing of turbidity current events in deep-sea fan systems. *In:* Sea level changes: an integrated approach. *Society of Economic Palaeontologists and Mineralogists, Special Publication* **42**, 381-392.

KOMAR, P. D. 1971. Hydraulic jumps in turbidity currents. *Bulletin of the Geological Society of America* **82**, 1477-1488.

KUENEN, PH. H. & MIGLIORINI, C. I. 1950. Turbidity currents as a cause of graded bedding. *Journal of Geology* **58**, 91-127.

LAMPLUGH, G. W. 1903. The geology of the Isle of Man. *Memoir of the Geological Survey of Great Britain*.

LEEDAL, G. P. & WALKER, G. P. L. 1950. A restudy of the Ingletonian Series of Yorkshire. *Geological Magazine*, **87**, 57-66.

LEGGETT, J. K., McKERROW, W. S., COCKS, L. R. M. & RICKARDS, R. B. 1981. Periodicity in the early Palaeozoic marine realm. *Journal of the Geological Society, London*, **138**, 167-176.

LEWIS, K. B. 1971. Slumping on a continental slope inclined at 1°-4°. *Sedimentology*, **16**, 97-110.

LISTER, T. R. & HOLLIDAY, D. W. 1970. Phytoplankton (acritarchs) from a small Ordovician inlier in Teesdale (County Durham) England. *Proceedings of the Yorkshire Geological Society*, **37**, 449-460.

LISTER, T. R., BURGESS, I. C. & WADGE, A. J. 1969. Microfossils from cleaved Skiddaw Slates of Murton Pike and Brownber (Cross Fell Inlier). *Geological Magazine*, **106**, 97-99.

LOWE, D. R. 1982. Sediment gravity flows: II. Depositional models with special reference to the deposits of high-density turbidity currents. *Journal of Sedimentary Petrology*, **52**, 279-297.

MAX, M. D., BARBER, A. J. & MARTINEZ, J. 1990. Terrane assemblage of the Leinster Massif, SE Ireland, during the Lower Palaeozoic. *Journal of the Geological Society, London*, **147**, 1035-1050.

MAYNARD, J.B., VALLONI, R. & YU, H-S. 1982. Composition of modern deep-sea sands from arc-related basins. *In:* LEGGETT, J. K. (ed) *Trench-Forearc Geology*. Geological Society, London, Special Publication, **10**, 551-561.

McARDLE, P. 1981. The country rocks flanking the Leinster Granite between Aughrim and Ballymurphy. *Bulletin of the Geological Survey of Ireland*, **3**, 237-255.

McBRIDE, E. F. 1985. Diagenetic processes that affect provenance determinations in sandstone. *In:* ZUFFA, G. G. (ed) *Provenance of arenites*. NATO-ASI Series, Dordrecht, D. Riedel, 95-113.

McCAFFREY, W. D. 1991. *Silurian turbidite provenance in NW England*. PhD thesis, Leeds University.

McCANN, T. 1991. Petrological and geochemical determination of provenance in the southern Welsh Basin. *In:* MORTON, A. C., TODD, S. P. & HAUGHTON, P. D. W. (eds) *Developments in Sedimentary Provenance Studies*. Geological Society, London, Special Publication, **57**, 215-230.

McKERROW, W. S. & COCKS, L. R. M. 1986. Oceans, island arcs and olistostromes: the use of fossils in distinguishing sutures, terranes and environments around the Iapetus Ocean. *Journal of the Geological Society, London*, **143**, 185-191.

McKERROW, W. S., LAMBERT, R. St. J. & COCKS, L. R. M. 1985. The Ordovician, Silurian and Devonian periods. *In:* SNELLING, N. J. (ed) *The Chronology of the Geological Record*, Geological Society, London, Memoir, **10**, 73-80.

MIDDLETON, G. V. 1960. Chemical composition of sandstones. *Geological Society of America, Bulletin*, **71**, 1011-1026.

MIDDLETON, G. V. 1972. Albite of secondary origin in Charny sandstones, Quebec. *Journal of Sedimentary Petrology*, **42**, 341-349.

MIDDLETON, G. V. & HAMPTON, M. A. 1973. Sediment gravity flows: mechanics of flow and deposition. *In:* MIDDLETON, G. V. & BOUMA, A. H. (eds) *Turbidites and deep water sedimentation* Short course notes, Pacific Section, Society of Economic Palaeontologists and Mineralogists, 1-38.

MILLER, J. A. 1961. The potassium-argon ages of the Skiddaw and Eskdale Granites. *Geophysical Journal*, **6**, 391-393.

MILLIKEN, K. L. 1988. Loss of provenance information through subsurface diagenesis in Plio-Pleistocene sandstones, Northern Gulf of Mexico. *Journal of Sedimentary Petrology*, **58**, 992-1002.

MILLWARD, D. & MOLYNEUX, S. G. in press. Field and biostratigraphic evidence for an unconformity at the base of the Eycott Volcanic Group in the English Lake District. *Geological Magazine*.

MITCHELL, A. H. & READING, H. G. 1969. Continental margins, geosynclines, and ocean floor spreading. *Journal of Geology*, **77**, 629-646.

MITCHELL, A. H. & READING, H. G. 1971. Evolution of island arcs. *Journal of Geology*, **79**, 253-284.

MITCHELL, A. H. & READING, H. G. 1978. Sedimentation and tectonics. *In:* READING, H. G. (ed), *Sedimentary Environments and Facies*, Blackwell Scientific Publications, Oxford, 439-476.

MOLYNEUX, S. G. 1979. New evidence for the age of the Manx Group, Isle of Man. *In:* HARRIS, A. L., HOLLAND, C. H. & LEAKE, B. E. (eds) *The Caledonides of the British Isles - reviewed*. Geological Society, London, Special Publication, **8**, 415-421.

MOLYNEUX, S. G. & RUSHTON, A. W. A. 1984. Discovery of Tremadoc rocks in the Lake District. *Proceedings of the Yorkshire Geological Society*, **45**, 123-127.

MOLYNEUX, S. G. & RUSHTON, A. W. A. 1988. The age of the Watch Hill Grits (Ordovician), English Lake District: structural and palaeogeographical implications. *Transactions of the Royal Society of Edinburgh: Earth Sciences*, **79**, 43-69.

MORTIMER, C. & SARIE, N. 1972. Landform evolution in the Coastal Region of Tarapaca Province, Chile. *Revue de Geomorphologie Dynamique*, **21**, 162-170.

MOSELEY, F. 1972. A tectonic history of NW England. *Journal of the Geological Society, London*, **128**, 561-598.

MOSELEY, F. 1975. Structural relations between the Skiddaw Slates and the Borrowdale volcanics. *Proceedings of the Cumberland Geological Society*, **3**, 127-145.

MOSELEY, F. 1984. Lower Palaeozoic lithostratigraphical classification in the English Lake District. *Geological Journal*, **19**, 239-247.

MURPHY, F. C. 1987. Evidence for late Ordovician amalgamation of volcanogenic terranes in the Iapetus suture zone, eastern Ireland. *Transactions of the Royal Society of Edinburgh: Earth Sciences*, **78**, 153-167.

MUTTI, E. 1979. Turbidites et cones sous-marins profonds. *In:* HOMEWOOD, P. (ed) *Sedimentation detritique (fluviatile, littorale et marine)*. Institut Geologique University Fribourg, Switzerland, 353-419.

MUTTI, E. 1985. Turbidite systems and their relations to depositional sequences. *In:* ZUFFA, G. G. (ed) *Provenance of Arenites*, NATO-ASI Series, Dordrecht, D.Reidel, 65-93.

MUTTI, E. & NORMARK, W. R. 1987. Comparing examples of modern and ancient turbidite systems: problems and concepts. *In:* LEGGETT, J. K. & ZUFFA, G. G. *Marine Clastic Sedimentology*, Graham & Trotman, 1-38.

MUTTI, E. & RICCI LUCCHI, F. 1972. Le torbiditi dell'Appennino settentrionale: introduzione all'analisi di facies. *Mem. Soc. Geol. Italy*, **11**, 161-199 (English translation, NILSEN, T. H. 1978. Turbidites of the northern Appenines: introduction to facies analysis. *International Geological Review*, **20**, 125-166.

MUTTI, E. & SONNINO, M. 1981. Compensation cycles: a diagnostic feature of turbidite sandstone lobes. *In:* International Association of Sedimentologists, Second European Regional Meeting, Bologna, Italy, *Abstracts*, 120-123.

NATHAN, S. 1977. Geochemistry of the Greenland Group (Early Ordovician), New Zealand. *New Zealand Journal of Geophysics*, **19**, 683-706.

NEMEC, W. 1988. The shape of the rose. *Sedimentary Geology*, **59**, 149-152.

NESBITT, H. W. & YOUNG, G. M. 1982. Early Proterozoic climates and plate motions inferred from major element chemistry of lutites. *Nature*, **299**, 715-717.

NORMAN, T. N. 1961. The geology of the Silurian strata in the Blawith area, Furness. *PhD Thesis, University of Birmingham*, 294p.

NORMARK, W. R. 1970. Growth patterns of deep-sea fans. *Bulletin of the American Association of Petroleum Geologists*, **54**, 2170-2195.

NORMARK, W. R. 1978. Fan valleys, channels and depositional lobes on modern submarine fans: characters for recognition of sandy turbidite environments. *Bulletin of the American Association of Petroleum Geologists*, **62**, 912-931.

O'NIONS, R. K., HAMILTON, P. J. & HOOKER, P. J. 1983. A Nd isotope investigation of sediments related to crustal development in the British Isles. *Earth and Planetary Science Letters*, **63**, 229-240.

O'NIONS, R. K., OXBURGH, E. R., HAWKESWORTH, C. J. & MACINTYRE, R. M. 1973. New isotopic and stratigraphical evidence on the age of the Ingletonian. *Journal of the Geological Society, London*, **129**, 445-452.

OTLEY, J. 1820. Succession of rocks in the District of the Lakes. *Philosophical Magazine*, **1**, 527.

PANTIN, H. M. 1979. Interaction between velocity and effective density in turbidite flow: phase plane analysis, with criteria for autosuspension. *Marine Geology*, **31**, 59-99.

PARKASH, B. & MIDDLETON, G. V. 1970. Downcurrent textural changes in Ordovician turbidite greywackes. *Sedimentology*, **14**, 259-293.

PETTIJOHN, F. J. 1975. *Sedimentary Rocks*. Harper and Row, New York, 628p.

PETTIJOHN, F. J., POTTER, P.E. & SIEVER, R. 1972. *Sand and sandstone*. Springer, New York.

PHARAOH, T. C., MERRIMAN, R. J., WEBB, P. C. & BECKINSALE, R. D. 1987. The concealed Caledonides of eastern England: preliminary results of a multidisciplinary study. *Proceedings of the Yorkshire Geological Society*, **46**, 355-369.

PHARAOH, T. C., MERRIMAN, R. J., EVANS, J. A., BREWER, T. S., WEBB, P. C. & SMITH, N. J. P. 1991. Early Palaeozoic arc-related volcanism in the concealed Caledonides of southern Britain. *Annales de la Societe Geologique de Belgique*, **114**, 63-91.

PHILLIPS, W. E. A., STILLMAN, C. J. & MURPHY, T. 1976. A Caledonian plate tectonic model. *Journal of the Geological Society, London*, **132**, 579-609.

PICKERING, K. T., BASSETT, M. G. & SIVETER, D. J. 1988. Late Ordovician-early Silurian destruction of the Iapetus Ocean: Newfoundland, British Isles and Scandinavia - a discussion. *Transactions of the Royal Society of Edinburgh: Earth Sciences*, **79**, 361-382.

PICKERING, K. T., HISCOTT, R. N. & HEIN, F. J. 1989. *Deep marine environments: clastic sedimentation and tectonics*, Unwin Hyman, London, 416p.

PICKERING, K. T., STOW, D. A. V., WATSON, M. P. & HISCOTT, R. N., 1986. Deep-water facies, processes and models: a review and classification scheme for modern and ancient sediments. *Earth-Science Reviews*, **23**, 75-174.

PILGER, R. H. 1984. Cenozoic plate kinematics, subduction and magmatism: South American Andes. *Journal of the Geological Society, London*, **141**, 793-802.

PIPER, D. Z. 1974. Rare earth elements in the sedimentary cycle: a summary. *Chemical Geology*, **14**, 285-304.

PIPER, D. J. W. 1978. Turbidite muds and silts on deep-sea fans and abyssal plains. *In:* STANLEY, D. J. & KELLING, G. (eds) *Sedimentation in submarine canyons, fans and trenches*. Stroudsburg, PA: Dowden, Hutchinson and Ross, 163-176.

PRAVE, A. R. & DUKE, W. L. 1990. Small-scale hummocky cross-stratification in turbidites: a form of antidune stratification? *Sedimentology*, **37**, 531-539.

PRENTICE, J. E. 1960. Flow structures in sedimentary rocks. *Journal of Geology*, **68**, 217-225.

PRENTICE, J. E. 1962. The sedimentation history of the Carboniferous in Devon. *In:* COE, K. (ed.) *Some Aspects of the Variscan fold belt*, Manchester University Press, 93-108.

RASTALL, R. H. 1906. The Ingletonian Series of West Yorkshire. *Proceedings of the Yorkshire Geological Society*, **16**, 87-100.

READING, H. G. 1986. *Sedimentary environments and facies*, Second edition, Blackwell Scientific Publications, 615p.

READING, H. G. 1991. The classification of deep-sea depositional systems by sediment calibre and feeder system. *Journal of the Geological Society, London*, **148**, 427-430.

REED, J. J. 1957. Petrology of the Lower Mesozoic rocks of the Wellington District. *Bulletin of the Geological Survey of New Zealand*, **57**, 9-60.

RICCI, C. A. & SABATINI, G. 1976. An example of sedimentary differentiation in volcano-sedimentary series; the high chromium metagraywackes of Central sardinia (Italy). *Neues Jahrbuch fuer Mineralogie Mh.*, **7**, 307-319.

RICCI LUCCHI, F. 1985. Influence of transport processes and basin geometry on sand composition. *In:* G. G. ZUFFA (ed.), *Provenance of Arenites*, NATO-ASI Series, Dordrecht, D.Reidel, 19-45.

RODOLFO, K. S. 1969. Bathymetry and marine geology of the Andaman Basin, and tectonic implications for southeast Asia. *Geological Society of America, Bulletin*, **80**, 1203-1230.

ROBERTS, D. E. 1971. Structures of the Skiddaw Slates in the Caldew Valley. *Geological Journal*, **7**, 225-238.

ROBERTS, D. E. 1977. The structure of the Skiddaw Slates in the Blencathra-Mungrisedale area, Cumbria. *Geological Journal*, **12**, 33-58.

ROBERTS, B., MORRISON, C. & HIRONS, S. 1990. Low grade metamorphism of the Manx Group, Isle of Man: a comparative study of white mica 'crystallinity' techniques. *Journal of the Geological Society, London*, **147**, 271-277.

ROSE, W. C. C. 1955. The sequence and structure of the Skiddaw Slates in the Keswick and Buttermere area. *Proceedings of the Geological Association*, **65**, 403-406.

ROSE, W. C. C. & DUNHAM, K. C. D. 1977. Geology and haematite deposits of south Cumbria. *Economic Memoir of the Geological Survey of Great Britain Sheets 58, part 48,* 170p.

ROSER, B. P. & KORSCH, R. J. 1985. Plate tectonics and geochemical composition of sandstones: a discussion. *Journal of Geology,* **93**, 81-84.

ROSER, B. P. & KORSCH, R. J. 1986. Determination of tectonic setting of sandstone-mudstone suites using SiO_2 content and K_2O/Na_2O ratio. *Journal of Geology,* **94**, 635-650.

ROSER, B. P. & KORSCH, R. J. 1988. Provenance signatures of sandstone-mudstone suites determined using discriminant function analysis of major element data. *Chemical Geology,* **67**, 119-139.

ROSS, C.A. & ROSS, J. R. P. 1988. Late Paleozoic transgressive-regressive deposits. *In:* WILGUS, C. K., HASTINGS, B. S., KENDALL, C. G. St., POSAMENTIER, H. W., ROSS, C. A., & VAN WAGONER, F. C. (eds), *Sea-level change - An integrated approach.* Society of Economic Paleontologists and Mineralogists Special Publication, **42**, 227-247.

RUSHTON, A. W. A. & MOLYNEUX, S. G. 1989. The biostratigraphic age of the Skiddaw Group in the Black Combe Inlier, English Lake District. *Proceedings of the Yorkshire Geological Society,* **47**, 267-276.

SADLER, P. M. 1982. Bed-thickness and grain size of turbidites. *Sedimentology,* **29**, 37-51.

SCANLAN, P. M. & TURNER, P. 1992. Structural constraints on palaeomagnetic rotations south of the Arica Bend, northern Chile: implications for the Bolivian Orocline. *Tectonophysics,* in press.

SCANLAN, P. M., TURNER, P. & CHONG DIAZ, G. 1992. The role of tectonic rotations in Tertiary-Recent basin evolution and forearc mobility, the Salar Grande, northern Chile. *Journal of the Geological Society, London,* in press.

SCHENK, P. E. 1991. Events and sea-level changes on Gondwana's margin: The Meguma Zone (Cambrian to Devonian) of Nova Scotia, Canada. *Bulletin of the Geological Society of America,* **103**, 512-521.

SCHWAB, F. L. 1975. Framework mineralogy and chemical composition of continental margin-type sandstone. *Geology,* **3**, 487-490.

SCOTT, K. M. 1967. Intra-bed palaeocurrent variations in a Silurian flysch sequence, Kirkcudbrightshire, Southern uplands, Scotland. *Scottish Journal of Geology,* **3**, 268-281.

SEDGWICK, A. 1832. On the geological relations of the stratified and unstratified groups of rocks composing the Cumbrian mountains. *Proceedings of the Geological Society of London,* **1**, 399-401.

SEILACHER, A. 1967. Bathymetry of trace fossils. *Marine Geology,* **5**, 413-428.

SEILACHER, A. & MEISCHNER, D. 1965. Fazies-analyse im palaozoikum des Oslo-Gebietes. *Geologische Rundschau,* **54**, 596-619.

SHAIL, R. & FLOYD, P. A. 1988. An evaluation of flysch provenance - example from the Gramscatho Group of southern Cornwall. *Proceedings of the Ussher Society,* **7**, 62-66.

SHANMUGAM, G. & MOIOLA, R. J. 1988. Submarine fans: characteristics, models, classification and reservoir potential. *Earth Science Reviews,* **24**, 383-428.

SHANMUGAM, G. & MOIOLA, R. J. 1991. Types of submarine fan lobes: models and implications. *Bulletin of the American Association of Petroleum Geologists*, **75**, 156-179.

SHANNON, P. M. 1978. Petrology of some Lower Palaeozoic greywackes from south-east Ireland: a clue to the origin of the matrix. *Journal of Sedimentary Petrology*, **48**, 1185-1192.

SHAW, D. M. 1968. A review of K-Rb fractionation trends by covariance analysis. *Geochimica et Cosmochimica Acta*, **32**, 573-602.

SIEVER, R. 1979. Plate tectonic controls on diagenesis. *Journal of Geology*, **87**, 127-155.

SIMPSON, A. 1963. The stratigraphy and tectonics of the Manx Slate Series, Isle of Man. *Quarterly Journal of the Geological Society of London*, **119**, 367-400.

SIMPSON, A. 1967. The stratigraphy and tectonics of the Skiddaw Slates and the relationship of the overlying Borrowdale Volcanic Series in part of the Lake District. *Geological Journal*, **5**, 391-418.

SIMPSON, J. E. 1982. Gravity currents in the laboratory, atmosphere and ocean. *Ann. Rev. Fluid Mechanics*, **14**, 213-234.

SKEVINGTON, D. 1970. A Lower Llanvirn graptolite fauna from the Skiddaw Slates, Westmorland. *Proceedings of the Yorkshire Geological Society*, **37**, 395-444.

SLOANE, A. 1988. *Analysis of slope stability in Ingleton Quarry*. MSc Thesis, University of Leeds.

SOPER, N. J. 1970. Three critical localities on the junction of the Borrowdale volcanic rocks with the Skiddaw Slates in the Lake District. *Proceedings of the Yorkshire Geological Society*, **37**,461-493.

SOPER, N. J., BRANNEY, M. J., MATHIESON, N. A. & DAVIS, N. C. 1987a. The Ordovician batholith of the English Lake District - reply. *Geological Magazine*, **124**, 483-484.

SOPER, N. J. & HUTTON, D. H. W. 1984. Late Caledonian sinistral displacements in Britain: implications for a three-plate collision model. *Tectonics*, **3**, 781-794.

SOPER, N. J. & ROBERTS, D. E. 1971. Age of cleavage in the Skiddaw Slates in relation to the Skiddaw aureole. *Geological Magazine*, **108**, 293-302.

SOPER, N. J., WEBB, B. C. & WOODCOCK, N. H. 1987b. Late Caledonian (Acadian) transpression in north-west England: timing, geometry and geotectonic significance. *Proceedings of the Yorkshire Geological Society*, **46**, 175-192.

SOPER, N. J. & WOODCOCK, N. H. 1990. Silurian collision and sediment dispersal patterns in southern Britain. *Geological Magazine*, **127**, 527-542.

STILLMAN, C. J. & WILLIAMS, C. T. 1978. Geochemistry and setting of some Upper Ordovician volcanic rocks in east and southeast Ireland. *Earth and Planetary Science Letters*, **41**, 288-310.

STOW, D. A. V. 1986. Deep clastic seas. *In:* READING, H. G. (ed), *Sedimentary environments and facies*, second edition, Blackwell Scientific Publications, Oxford, 614p.

STOW, D. A. V. & SHANMUGAM, G. 1980. Sequence of structures in fine grained turbidites: comparison of recent deep sea and ancient flysch sediments. *Sedimentary Geology*, **25**, 23-42.

TAYLOR, S. R. & McLENNAN, S. M. 1985. *The continental crust: its composition and evolution*. Blackwell Scientific Publications, Oxford, 312p.

THOMPSON, M. & WALSH, J. N. 1989. *Handbook of inductively coupled plasma spectroscopy,* second edition. Blackie, 316p.

THOROGOOD, E. J. 1990. Provenance of the pre-Devonian sediments of England and Wales: Sm-Nd isotopic evidence. *Journal of the Geological Society, London,* **147**, 591-594.

TIETZSCH-TYLER, D. & PHILLIPS, E. 1989. Extended abstract: Correlation of the Monian Supergroup in NW Anglesey with the Cahore Group in SE Ireland. *Journal of the Geological Society, London,* **146**, 417-418.

TRAYNOR, J-J. 1988. The Arenig in south Wales: sedimentary and volcanic processes during the initiation of a marginal basin. *Geological Journal,* **23**, 275-292.

TRAYNOR, J-J. 1990. Arenig sedimentation and basin tectonics in the Harlech Dome area (Dolgellau Basin), North Wales. *Geological Magazine,* **127**, 13-30.

TRELOAR, P. J. & STRACHAN, R. A. 1990. Cadomian strike-slip tectonics in NE Brittany. *In:* D'LEMOS, R. S., STRACHAN, R. A. & TOPLEY, C. G. (eds) *The Cadomian Orogeny.* The Geological Society, London, Special Publication, **51**, 151-168.

TODD, S. P., MURPHY, F. C. & KENNAN, P. S. 1991. On the trace of the Iapetus suture in Ireland and Britain. *Journal of the Geological Society, London,* **148**, 869-880.

TORSVIK, T. H. & TRENCH, A. 1991. Short paper: The Ordovician history of the Iapetus ocean in Britain: new palaeomagnetic constraints. *Journal of the Geological Society, London,* **148** 423-426.

TURNER, J. S. 1949. The deeper structure of central and northern England. *Proceedings of the Yorkshire Geological Society,* **27**, 280-297.

UNDERWOOD, M. B. & BACHMAN, S. B. 1982. Sedimentary facies associations within subduction complexes. *In:* LEGGETT, J. K. (ed.) *Trench-forearc geology.* Geological Society of London Special Publication, **10**, 537-550.

VAIL, P. R., MITCHUM, R. M., TODD, R. G., WIDMIER, J. M., *etal,* 1977. Seismic stratigraphy and global changes of sea level. *In:* PAYTON, C. E. (ed), *Stratigraphic interpretation of seismic data.* American Association of Petroleum Geologists Memoir, **26**, 49-212.

VALENTINE, P. C., COOPER, R. A. & UZMANN, J. R. 1984. Submarine sand dunes and sedimentary environments in Oceanographer Canyon. *Journal of Sedimentary Petrology,* **54**, 704-715.

VALLONI, R. & MAYNARD, J. B. 1981. Detrital modes of recent deep-sea sands and their relation to tectonic setting: a first approximation. *Sedimentology,* **28**, 75-83.

VALLONI, R. & MEZZADRI, G. 1984. Compositional suites of terrigenous deep-sea sands of the present continental margin. *Sedimentology,* **31**, 353-364.

VAN ANDEL, T. H. & KOMAR, P. D. 1969. Ponded sediments of the Mid-Atlantic Ridge between 22° and 23° north latitude. *Bulletin of the Geological Society of America,* **80**, 1163-1190.

VAN DE KAMP, P. C. & LEAKE, B. E. 1985. Petrography and geochemistry of feldspathic and mafic sediments of the northeastern Pacific margin. *Transactions of the Royal Society of Edinburgh Earth Sciences,* **76**, 411-419.

VAN DE KAMP, P. C., LEAKE, B. E. & SENIOR, A. 1976. The petrography and geochemistry of some Californian arkoses with application to identifying gneisses of metasedimentary origin. *Journal of Geology*, **84**, 195-212.

VANNIER, J. M. C., SIVETER, D. J. & SCHALLREUTER, R. E. L. 1989. The composition, affinity and palaeoenvironmental significance of the Ordovician ostracode faunas of Britain, Baltoscandia and Ibero-Armorica. *Palaeontology*, **32**, 163-222.

VON DER BORCH, C. C., GRADY, A. E., ALDAM, R., MILLER, D., NEUMANN, R., ROVIRA, A. & EICKHOFF,K. 1985. A large-scale meandering submarine canyon: outcrop example from the late Proterozoic Adelaide Geosyncline, South Australia. *Sedimentology*, **32**, 507-518.

WADGE, A. J. 1971. Skiddaw Slates and the Borrowdale Volcanics. *Nature, Physical Science*, **234**, 58-59.

WADGE, A. J. 1972. Sections through the Skiddaw-Borrowdale unconformity in Eastern Lakeland. *Proceedings of the Yorkshire Geological Society*, **39**, 179-198.

WADGE, A.J. 1978. Classification and stratigraphical relationships of the Lower Ordovician rocks. *In:* MOSELEY, F. (ed) *The geology of the Lake District*. Yorkshire Geological Society, Occasional Publication, **3**, 164-167.

WADGE, A. J., NUTT, M. J. C., LISTER, T. R. & SKEVINGTON, D. 1969. A probable *Didymograptus murchisoni*Zone fauna from the Lake District. *Geological Magazine*, **106**, 595-598.

WADGE, A. J., NUTT, M. J. C. & SKEVINGTON, D. 1972. Geology of the Tarn Moor Tunnel in the Lake District. *Bulletin of the Geological Survey of Great Britain*, **41**, 55-73.

WADGE, A. J., OWENS, B. & DOWNIE, C. 1967. Microfossils from the Skiddaw Group. *Geological Magazine*, **104**, 506-507.

WALKER, R. G. 1965. The origin and significance of the internal sedimentary structures of turbidites. *Proceedings of the Yorkshire Geological Society*, **35**, 1-32.

WALKER, R. G. 1978. Deep water sandstone facies and ancient submarine fans: models for exploration for stratigraphic traps. *Bulletin of the American Association of Petroleum Geologists*, **62**, 932-966.

WALTON, E. K. 1967. The sequence of internal structures in turbidites. *Scottish Journal of Geology*, **3**, 306-317.

WARD, J. C. 1876. The geology of the northern part of the English Lake District. *Memoir of the Geological Survey of Great Britain*, 132p.

WEBB, B. C. 1972. North-south trending pre-cleavage folds in the Skiddaw Slate Group of the English Lake District. *Nature, Physical Science*, **235**, 138-140.

WEBB, B. C. 1990. The Buttermere Formation (Skiddaw Group) in the Robinson area. *In:* MOSELEY, F., *Geology of the Lake District*, Geologists Association, 213p.

WEBB, B. C. & COOPER, A. H. 1988. Slump folds and gravity slide structures in a Lower Palaeozoic marginal basin sequence (the Skiddaw Group), NW England. *Journal of Structural Geology*, **10**, 463-472.

WEBB, W. M. & POTTER, P. E. 1969. Petrology and chemical composition of modern detritus derived from rhyolitic terrain, western Chihuahua. *Soc. Geol. Mexicana Bol.*, **32**, 45-61.

WETZEL, A. 1984. Bioturbation in deep-sea fine-grained sediments: influence of sediment texture, turbidite frequency and rates of environmental change. *In:* STOW, D. A. V. & PIPER, D. J. W. (eds) *Fine-grained sediments: Deep water Processes and Facies,* Geological Society, London, Special Publication, **15**, 595-609.

WHETTEN, J. T. & HAWKINS, J. W. 1970. Diagenetic origin of greywacke matrix minerals. *Sedimentology,* **15**, 347-361.

WILSON, J. T. 1966. Did the Atlantic close and then re-open? *Nature,* **211**, 676-681.

WILSON, A. A. & CORNWELL, J. D. 1982. The Institute of Geological Sciences borehole at Beckermonds Scar, North Yorkshire. *Proceedings of the Yorkshire Geological Society,* **44**, 59-88.

WOODCOCK, N. H. 1976. Structural style in slump sheets: Ludlow Series, Powys, Wales. *Journal of the Geological Society, London,* **132**, 399-415.

WOODCOCK, N. H. 1990. Sequence stratigraphy of the Palaeozoic Welsh Basin. *Journal of the Geological Society, London,* **147**, 537-547.

WOOLACOT, D. 1923. On a boring at Roddymoor Colliery, near Crook, County Durham. *Geological Magazine,* **60**, 50-62.

ZUFFA, G. G. 1987. Unravelling hinterland and offshore palaeogeography from deep-water arenites. *In:* LEGGETT, J. K. & ZUFFA, G. G., *Marine clastic sedimentology: concepts and case studies,* Graham & Trotman, 39-61.

PANTIN, H. & LEEDER, M.R. 1987. Reverse flow in turbidity currents: the role of internal solitons. *Sedimentology,* **34**, 1143-1155.

Appendix 1

LIST OF SAMPLES

Samples, rock powders and slides will be stored in the Department of Earth Sciences, Leeds University.

KEY

formation: Skiddaw Group: BBE = Bitter Beck Fm; BUF = Buttermere Fm; HBE = Hope Beck Fm; KST = Kirk Stile Fm; LWF = Loweswater Fm; WHG = Watch Hill Fm;
Manx Group: LBG = Lady Port banded group; LF = Lonan Flags; MBG = Maughold banded group; NF = Niarbyl Flags; SMS = Slieau Monagh slates; SSB = Sulby slump breccia;
Ingleton Group (ING);
Bray Group (BRAY).

description: gwk = greywacke; mst = mudstone; VF = very fine; F = fine; M = medium; C = coarse; VC = very coarse; G = granule; P = pebble
hand specimen (HS).
powder prepared (P).
thin section type: C = covered; P = polished; ST = stained; U = uncovered.
modal analysis (MA); L = count of lithic types.
major and trace element composition by x-ray fluorescence spectrometry (XRF).
rare earth element (REE) composition determined by inductively-coupled plasma spectrometry.
proportions of heavy minerals (HM).

number	formation	locality and grid reference	description	hand specimen	powder	thin section number	modal analysis	XRF	REE	HM
M1	LWF	Scawgill Bridge Quarry, NY 1770 2560	M sand grade greywacke; base of bed 6.1	HS		50536 U				
M2	LWF	Scawgill Bridge Quarry, NY 1770 2560	greywacke; middle of bed 6.1	HS						
M3	LWF	Scawgill Bridge Quarry, NY 1770 2560	greywacke; top of bed 6.1	HS						
M4	LWF	Scawgill Bridge Quarry, NY 1770 2560	bed 7.0. 32cm thick, M sand grade greywacke	HS		50537 U				
M5	LWF	Scawgill Bridge Quarry, NY 1770 2560	bed 7.0. M-C sand grey-wacke with lamination	HS						
M6	LWF	Scawgill Bridge Quarry	12cm, C-VC sand grade	HS		50538 U				
M7	LWF	Scawgill Bridge Quarry	7cm, granule grade fining-up to F sand	HS		50539 U 50540 U				
M8	LWF	Scawgill Bridge Quarry	bed 3.1, 21.5cm M sand grade gwk and mst	HS		50541 U				
M9	LWF	Scawgill Bridge Quarry	bed 3.2, gwk and mst	HS						
M10	LWF	NY 1753 2575	C sand, fining-up gwk	HS						
M11	LWF	NY 1753 2575	inverse graded base C-VC sand	HS		50542 U				
M12	LWF	Sware Gill	F sand gwk, Tb, convolute lam	HS						
M13	WHG	Watch Hill NY 1550 3187	P-C sand gwk	HS		50543 U				
M14	WHG	Watch Hill NY 1570 3199	VC sand gwk	HS		50544 U				
M15	LWF	Sware Gill NY 1745 2600	M sand gwk with mst rip-ups	HS						
M16	LWF	Sware Gill	fine sand greywacke	HS		50545 U				
M17	LWF	Sware Gill NY 1740 2588	38cm, M-F sand gwk	HS		50546 U				
M17a	LWF	Fisher Wood NY 1830 2940	43cm, G-VC-VF sand gwk with high-matrix content	HS	P	51709 C&U	MA	XRF		
M18	LWF	Fisher Wood NY 1830 2960	high-matrix M sand gwk with horizontal laminae	HS	P	51710 C&U	MA	XRF		
M19	LWF	Fisher Wood	high-matrix gwk	HS						
M20	KST	Whinlatter	bioturbated mst-siltstone	HS						
M21	LWF	Barf NY 2172 2654	mudstone; cone-in-cone struct.	HS						
M23	BBE	Bitter Beck NY 1660 3120	M sand grade laminae in mst	HS	P				REE	
M24	BBE	Bitter Beck NY 1660 3120	M sand grade laminae in mst	HS						
M25	LWF	Low Fell	horizontal burrow	HS						

M26	LWF	Jonah's Gill	calcareous nodule	HS					
M27	LWF	Jonah's Gill	1cm, VF sand, ripple cross lam	HS					
M28	LWF	Jonah's Gill	F sand quartz wacke	HS					
M29a,b,c	LWF	Jonah's Gill	M sand gwk with laminae	HS	P	52363 P	MA	XRF	
M30a,b	LWF	Burnbank Fell NY 1175 2150	F sand gwk, high-matrix	HS		51711 C&U	MA		
M31	LWF	Burnbank Fell NY 1175 2150	F sand gwk, low-matrix	HS					
M32	LWF	Darling Fell	C sand channel-fill gwk	HS					
M33	WHG	Elva Plain	fine sand greywacke	HS		51712 C&U	MA		
M34	WHG	Elva Plain	M sand gwk and mst/siltst	HS					
M35	WHG	Elva Plain NY 1720 3210	medium-coarse sand greywacke	HS		51713 C&U	MA		
M36	WHG	Elva Plain NY 1720 321	mudstone/siltstone/sand-stone laminae above M35	HS	P				REE
M37	LWF	Scawgill Bridge Quarry NY 1770 2560	29cm thick, Tabcde	HS		52364 P	MA		
M38	LWF	Scawgill Bridge Quarry NY 1770 2560	15cm thick, Tabcde	HS		52365 P	MA		
M39	KST	Broom Fell NY 1940 2723	15cm, VF sand gwk with horizontal laminations, Tbc	HS		52366 P	MA		
M40	KST	Broom Fell NY 1940 2723	VF sand gwk with horizontal laminae, Tbc and mst	HS		52367 P	MA		
M41	KST	Thornthwaite Forest	3cm, VF-F sand gwk, Tcd	HS					
M42	KST	Thornthwaite Forest	3cm, VF-F sand gwk	HS					
M43	LWF	Darling Fell NY 1265 2218	F sand grade, top channel	HS	P	52368 P	MA	XRF	
M44	LWF	Darling Fell NY 1265 2218	M sand grade, channel-fill	HS					
M45	LWF	Darling Fell NY 1265 2218	M sand grade, channel-fill	HS	P	52369 P	MA	XRF	
M46	LWF	Darling Fell NY 1265 2218	M sand grade, channel-fill	HS					
M47	LWF	Darling Fell NY 1265 2218	M sand grade, base channel	HS	P	52370 P	MA	XRF	
M48	LWF	Jonah's Gill NY 191342	22cm, F sand gwk, Tb	HS	P	52371 P	MA	XRF	
M49	LWF	Jonah's Gill NY 191342	3cm, F sand gwk, Tc	HS					
M50	LWF	Jonah's Gill NY 191342	5cm, F sand gwk, Tb	HS		52372 P	MA		
M51	LWF	Jonah's Gill NY 191342	6cm, F sand gwk, Tb	HS		52373 P	MA		
M52	LWF	Jonah's Gill NY 191342	4cm FS/VFS gwk, Tc	HS					
M53	LWF	Jonah's Gill NY 191342	2cm siltst/mst/VF sand gwk	HS					
M54b,c	BBE	Trusmadoor NY 278 336	19cm, F sand to siltst/mst, Tbcd	HS		52374 P	MA		
M54m	BBE	Trusmadoor NY 278 336	mudstone	HS	P				REE
M55b,c	BBE	Trusmadoor NY 278 336	17cm, F sand gwk to siltst, Tbc	HS					
M55m	BBE	Trusmadoor NY 278 336	mudstone	HS					
M56c,m	BBE	Trusmadoor NY 278 336	8cm, Tc and mudstone	HS					
M57	LWF	Fisher Wood	high-matrix gwk and mst	HS					
M58	LWF	Fisher Wood NY 1830 2940	12cm, high-matrix gwk	HS	P	51714 C&U	MA	XRF	
M58m	LWF	Fisher Wood NY 1830 2940	mudstone	HS	P				REE
M59	LWF	Fisher Wood NY 1830 2940	17cm, Tbcde	HS					
M60	LWF	Fisher Wood NY 1830 2940	16cm, Tbcd	HS					

M61	LWF	Fisher Wood NY 1836 2948	base of 42cm high-matrix gwk, G-F sand grade	HS	P	52389 P	MA	XRF	
M62	HBE	Swinside	8cm, F-VF sand and mst	HS					
M63	HBE	Swinside NY 1840 2403	M sand gwk of thick M-C bed	HS		52375 P	MA		
M63m	HBE	Swinside NY 1840 2403	mudstone	HS					
M64	HBE	Swinside NY 1840 2403	fine sand greywacke	HS		51715 C&U	MA		
M64m	HBE	Swinside NY 1840 2403	12cm, mudstone	HS					
M90-1	BUF	Causey Pike NY 2195 2075	fine sand greywacke with horizontal laminae, Tb	HS		52874 P	MA		
M90-2	BUF	Causey Pike NY 2190 2075	fine sand greywacke with horizontal laminae, Tb	HS		52875 P	MA		
M90-3	BUF	Causey Pike NY 2185 2075	fine sand greywacke with horizontal laminae, Tb	HS	P	52876 P	MA	XRF	
M90-4	BUF	Goat Gills NY 1910 1825	fine sand greywacke 10cm thick, Ta(b)	HS	P	52877 P	MA	XRF	
M90-5	BUF	Goat Gills NY 1910 1825	FS greywacke, 10cm thick, with horizontal laminae Tb	HS		52878 P	MA		
M90-6	BUF	Robinson NY 2010 1710	FS greywacke with thin horizontal laminae, Tb	HS	P	52879 P	MA	XRF	
M90-7	KST	Beckgrains Bridge NY 190 355	VFS clast from debris flow, strong alteration	HS		52880 P	MA		
M90-8	KST	Beckgrains Bridge NY 190 355	VFS clast from debris flow, strong alteration	HS	P	52881 P	MA	XRF	
M90-9	ING	Ingleton Quarry	VFS-FS greywacke	HS	P	52885 P	MA	XRF	
M90-10	ING	Ingleton Quarry	MS-CS greywacke	HS	P	52886 P	MA	XRF	
M90-11	ING	Ingleton Quarry	Csilt-VFS greywacke	HS	P	52887 P	MA	XRF	
M90-12	ING	Ingleton Quarry	CS greywacke	HS	P	52888 P	MA	XRF	
M90-17	LWF	Tarn Crags, Bowecale Fell NY 334 314	homfelsed greywacke	HS		52882 P	MA		
M90-18	LWF	Raven Crags, Mungrisedale NY 363 307	structureless greywacke, Te	HS		52883 P	MA		
M90-19	LWF	Raven Crags, Mungrisedale NY 363 307	high-matrix greywacke	HS	P	52884 P	MA	XRF	
ING-M	ING	Ingleton Quarry	mudstone	HS	P			XRF	REE
ING-C	ING	Ingleton Quarry	composite greywacke from 5mm crushed pile	HS	P			XRF	
ING-L	ING	Ingleton Quarry	VCS-granule conglomerate			C	L		
IOM1	SMS	Slieau Monagh Slates	slate with 2 cleavage and rare lamination	HS					
IOM2	SMS	Tholt-e-will Glen SC 378 893	slate	HS					
IOM3	SMS	Tholt-e-will Glen SC 378 893	slate	HS					
IOM4	SMS	Tholt-e-will Glen SC 378 893	slate with cordierite	HS					
IOM5	SMS	Sulby River	siltstone below breccia	HS					
IOM6	SSB	Sulby River valley SC 380 904	breccia	HS					
IOM7	NF	Niarbyl SC 212 777	cleaved greywacke	HS	P	52864 P		XRF	
IOM8	NF	Niarbyl SC 212 777	greywacke with lithics	HS					
IOM9	NF	Niarbyl SC 212 777	MS greywacke with lithics	HS	P	52865 P	MA	XRF	

IOM10	LF	Langness SC 278 653	MS quartz-rich greywacke in rare thin-medium beds	HS	P	52866 P	MA	XRF
IOM11	LF	Langness, east shore, south end	FS quartz-rich greywacke in rare thin-medium beds	HS				
IOM12	LF	Langness SC 288 660	FS quartz-rich greywacke in rare thin-medium beds	HS	P	52867 P	MA	XRF
IOM13	LF	Langness SC 280 660	FS quartz-rich greywacke in rare thin-medium beds	HS	P	52868 P	MA	XRF
IOM14	LF	Langness SC 280 660	FS quartz-rich greywacke in rare thin-medium beds	HS		52869 P	MA	
IOM15	NF	Ballanayre Strand	cleaved VFS greywacke	HS				
IOM16	NF	Ballanayre Strand	VFS greywacke	HS				
IOM17	NF	Ballanayre Strand	VFS greywacke	HS				
IOM18	LBG	Gob-y-deigan	cleaved mudstone	HS				
IOM19	LBG	Gob-y-deigan	mudstone clast in breccia	HS				
IOM20	LF	Port Mooar SC 489 908	greywacke	HS		52870 P	MA	
IOM21	LF	Port Mooar SC 489 908	greywacke	HS		52871 P	MA	
IOM22	MBG	Bradda Head, Port Erin SC 184 698	VCS-FS quartz wacke	HS	P	52872 P	MA	XRF
IOM23	MBG	Bradda Head, Port Erin SC 184 698	VCS-FS quartz wacke	HS				
IOM24	MBG	Port Erin beach SC 194 695	top of 4m thick quartz wacke	HS				
IOM25		Port Erin beach SC 194 695	dyke in MBG	HS		52873 P		
M91–1	BRAY	Bray Head	F-M sand grade greywacke	HS		C	MA	
SAMPLES LOANED FROM DR A. H. COOPER (BGS NEWCASTLE)								
CU4A	LWF	sheet NY12SE/NE BGS locality 4, NY 1805 2262	greywacke with ripple cross lamination, Tc			C		
CU4B	LWF	sheet NY12SE/NE BGS locality 4, NY 1805 2262	greywacke with convolute lamination, Tc			C		
CU5A	LWF	BGS locality 5 NY 1807 2258	high-matrix greywacke with mudstone pebble clasts	HS		C ST		
CU5B	LWF	BGS locality 5 NY 1807 2258	high-matrix greywacke with mudstone pebble clasts	HS		C ST	MA by BGS	
CU7	LWF	BGS locality 7 NY 1827 2242	greywacke with thick horizontal laminae and ripple cross laminae			C		
CU8A	LWF	BGS locality 8 NY 1826 2243	1cm thick greywacke			C		
CU9B	LWF	BGS locality 8 NY 1826 2243	greywacke with ripple cross laminae			Cx2	MA by BGS	
CU10A	LWF	BGS locality 8 NY 1826 2243	greywacke with thin horizontal laminae	HS		C ST		
CU10B	LWF	BGS locality 8 NY 1826 2243	high-matrix greywacke with cross laminae	HS		C ST		
CU10C	LWF	BGS locality 8 NY 1826 2243	CS high-matrix greywacke	HS		C ST		
CU10D	LWF	BGS locality 8 NY 1826 2243	CS greywacke, base of bed	HS		C ST P		
CU12	LWF	BGS locality 9 NY 1825 2244	greywacke with ripple cross laminae			C		
CU14	LWF	BGS locality 9 NY 1825 2244	cleaved siltstone/mudstone with thin horizontal laminae			C		

CU15	LWF	BGS locality 9 NY 1824 2245	greywacke with convolute laminae		C	
CU16A	LWF	BGS locality 9-10 NY 1824 2245	greywacke with convolute laminae	HS	C ST	
CU16B	LWF	BGS locality 9-10 NY 1824 2245	structureless greywacke	HS	C ST	MA
CU18A	LWF	BGS locality 10 NY 1820 2249	structureless greywacke	HS	C ST	
CU18B	LWF	BGS locality 10 NY 1820 2249	structureless greywacke with quartz veins	HS	C ST	
CU19	LWF	BGS locality 10 NY 1819 2250	greywacke with thick horiz. & ripple cross laminae & silt		C	
CU20	LWF	BGS locality 11 NY 1818 2251	greywacke with ripple cross laminae	HS	C ST	
CU21	LWF	BGS locality 11 NY 1818 2251	greywacke with thick horizontal laminae, Tb		C	
CU22	LWF	BGS locality 11 NY 1818 2251	greywacke with convolute laminae		C	
CU23A	LWF	BGS locality 12 NY 1816 2252	greywacke massive to ripple cross laminated	HS	C ST	MA
CU23B	LWF	BGS locality 12 NY 1816 2252	F-MS greywacke with thin horizontal laminae (2 of CS), Tb	HS	C ST	
CU24	LWF	BGS locality 12 NY 1816 2252	greywacke with ripple cross laminae		C	
CU25A	LWF	BGS locality 12 NY 1816 2252	greywacke		C	
CU25B	LWF	BGS locality 12 NY 1816 2252	MS greywacke with faint horizontal laminae, Tb		C	
CU26	LWF	BGS locality 13 NY 1814 2253	CS-VCS greywacke	HS	C ST	MA
CU27	LWF	BGS locality 14 NY 1814 2254	FS greywacke in very thin beds		C	
CU28	LWF	BGS locality 14 NY 1812 2255	thick sandstone laminae in siltstone		C	
CU29	LWF	BGS locality 15 NY 1810 2259	MS-CS greywacke with faint thick horizontal laminae, Tb	HS	C ST	
CU29B	LWF	BGS locality 15 NY 1810 2259	CS greywacke with mudstone clasts	HS	C ST	MA
CU30	LWF	BGS locality 15 NY 1810 2259	CS-FS greywacke with thick horizontal laminae of VCS	HS	C ST	L
CU31	LWF	BGS locality 15 NY 1810 2259	greywacke with mudstone fragments up to 2cm long	HS	C ST	
CU32	LWF	BGS locality 15 NY 1810 2259	greywacke	HS	C ST	MA
CU33	LWF	BGS locality 15 NY 1810 2259	CS lithic-rich greywacke with mudstone top	HS	C ST	MA
CU34	LWF	BGS locality 15 NY 1809 2256	VCS greywacke		C	
CU35	LWF	BGS locality 15 NY 1809 2256	VCS greywacke	HS	C ST	MA
CU36	LWF	BGS locality 16 NY 1809 2260	FS greywacke with convolute laminae	HS	C ST	
CU37	LWF	BGS locality 16 NY 1809 2260	greywacke with faint thick horizontal laminae, Tb	HS	C ST	MA
CU38	LWF	BGS locality 16 NY 1809 2260	CS-FS greywacke with thick horizontal laminae	HS	C ST	MA

CU39	LWF	BGS locality 5 NY 1806 2261	FS greywacke with thin horizontal laminae		C	
CU41A	LWF	BGS locality 17 NY 1806 2261	FS greywacke with convolute laminae		C & P	
CU41B	LWF	BGS locality 17 NY 1806 2261	FS greywacke with faint thin horizontal laminae		C & P	
CU41C	LWF	BGS locality 17 NY 1806 2261	structureless greywacke		C & P	
CU41D	LWF	BGS locality 17 NY 1806 2261	CS-MS greywacke, lithic-rich		C & P	
CU42A	LWF	BGS locality 17 NY 1806 2261	MS-CS greywacke, ?high-matrix type	HS	C	
CU42B	LWF	BGS locality 17 NY 1806 2261	CS greywacke, structureless	HS	C	
CU42C	LWF	BGS locality 17 NY 1806 2261	MS greywacke, high-matrix type	HS	C ST	MA
CU70	KST	BGS locality 234 NY 1835 2240	greywacke & mudstone in horizontal laminae with loads		C	
CU71	KST	BGS locality 234 NY 1835 2240	cleaved siltstone		C	
CU72	KST	BGS locality 234 NY 1835 2240	siltstone with 2 cleavages and thin horizontal laminae		C	
CU73	KST	BGS locality 235 NY 1833 2241	FS-MS greywacke with horizontal laminae		C	
CU90	LWF	BGS locality 13 NY 1814 2253	FS greywacke with convolute laminae and siltstone		C	
CU97	HBE	BGS locality 288 NY 1840 2403	pebble and CS clasts in mudstone		C	L
CU98A	HBE	BGS locality 288 NY 1840 2403	pebble and CS clasts in mudstone		C	L
CU100	HBE	BGS locality 288 NY 1840 2403	MS greywacke with quartz veins		C	
CU101	HBE	BGS locality 288 NY 1840 2403	granule conglomerate		C	
CU102	HBE	BGS locality 288 NY 1840 2403	FS-MS greywacke with thin horizontal laminae	HS	C ST	MA
CU103	HBE	BGS locality 288 NY 1840 2403	CS greywacke, structureless	HS	C ST	MA
CU104	HBE	BGS locality 288 NY 1840 2403	MS greywacke with quartz veins		C	
CU177	LWF	NY 1780 2561	greywacke with calcite cement		P	
CU189.7	LWF	Tom Rudd Beck NY 1698 2833	greywacke with calcite cement		P	
CU198	LWF	Tom Rudd Beck NY 1738 2875	greywacke with calcite cement		P	
CU201	LWF	Tom Rudd Beck NY 1678 2864	greywacke with calcite cement		P	
CU203	LWF	Tom Rudd Beck NY 1649 2887	greywacke with calcite cement		P	
CU211	LWF	Tom Rudd Beck NY 1531 2783	greywacke with calcite cement		P	
CU284/1	WHG	NY 1566 3181	MS greywacke with quartz cement		C	MA
CU284/2	WHG	NY 1566 3181	FS greywacke with quartz cement		C	
CU284/3	WHG	NY 1566 3181	FS greywacke with laminae of CS and quartz cement		C	

CU284/4	WHG	NY 1566 3181	FS greywacke with quartz cement and cleavage		C			
CU290	WHG	NY 1557 3146	CS greywacke		C			
CU291	WHG	NY 1557 3146	FS-MS greywacke		C	MA		
CU292	WHG	NY 1557 3146	FS-MS greywacke		C	MA		
CU293	WHG	NY 1560 3156	VFS-FS greywacke/mudstone/ siltstone in thick horizontal laminae		C			
CU294	WHG	NY 1566 3160	FS greywacke, weathered		C			
CU295	WHG	NY 1556 3181	VCS greywacke		C	MA		
CU296	WHG	NY 1640 3166	VFS-FS greywacke/mudstone/ siltstone thick laminae, cleaved		C			
CU298	WHG	NY 1571 3199	MS/FS-VCS greywacke poorly sorted		C	MA		
CU299	WHG	NY 1550 3203	VCS-granule greywacke		C	L		
CU325	WHG	NY 2575 3330	mudstone pebbles and granule conglomerate		C	MA		
CU326	WHG	NY 2575 3330	granule conglomerate		C	MA		
CU327	WHG	NY 259 333	VCS greywacke		C	MA		
CU328	WHG	NY 2745 3305	pebble conglomerate		C	MA		
SAMPLES LOANED FROM DR D. C. COOPER (BGS KEYWORTH)								
KDC601	LWF	Hope Beck NY 1800 2270	FS greywacke with convolute laminae, Tc		C		XRF	
KDC602	LWF	Hope Beck NY 1801 2260	FS greywacke with cross laminae, Tc		C		XRF	
KDC603	LWF	Hope Beck NY 1801 2266	FS greywacke with faint thick horizontal laminae, Tb		C	MA	XRF	
KDC604	LWF	Hope Beck NY 1803 2265	siltstone & VFS greywacke in thin/thick horizontal laminae, Td		C		XRF	
KDC605	LWF	Hope Beck NY 1805 2261	FS-MS greywacke, structureless, Ta		C	MA	XRF	
KDC606	LWF	Hope Beck NY 1805 2261	FS-MS greywacke with faint thick horizontal laminae, Tb		C	MA	XRF	
KDC607	LWF	Hope Beck NY 1805 2261	FS-MS greywacke with faint cross laminae, Tc		C		XRF	
KDC608	LWF	Hope Beck NY 1805 2261	cleaved mudstone/siltstone in thin/thick laminae	P	C		XRF	REE
KDC609	LWF	Hope Beck NY 1807 2258	cleaved mudstone/siltstone in thin/thick laminae with MS		C		XRF	
KDC610	LWF	Hope Beck NY 1807 2258	cleaved siltstone with thin laminae		C		XRF	
KDC611	LWF	Hope Beck NY 1809 2256	CS lithic-rich greywacke, Ta		C	MA	XRF	
KDC612	LWF	Hope Beck NY 1808 2256	VFS/siltstone in thin/thick horizontal laminae with loads		C		XRF	
KDC613	LWF	Hope Beck NY 1808 2256	FS greywacke with ripple cross laminae, Tc		C		XRF	
KDC614	LWF	Hope Beck NY 1808 2256	VCS lithic-rich greywacke with mudstone clasts, Ta		C		XRF	
KDC615	LWF	Hope Beck NY 1808 2256	FS greywacke, structureless		C	MA	XRF	
KDC616	LWF	Hope Beck NY 1812 2255	FS greywacke with thin horizontal laminae, Tb		C	MA	XRF	

KDC617	LWF	Hope Beck	mudstone	P			XRF	
KDC618	LWF	Hope Beck NY 1814 2253	FS greywacke with ripple cross laminae, Tc		C		XRF	
KDC619	LWF	Hope Beck	mudstone	P			XRF	
KDC620	LWF	Hope Beck NY 1816 2251	FS greywacke with faint thin horizontal laminae, Tb		C	MA	XRF	
KDC621	LWF	Hope Beck NY 1816 2251	VFS thick lamina in siltstone & mudstone thin laminae		C		XRF	
KDC622	LWF	Hope Beck NY 1820 2249	cleaved mudstone/siltstone with thin horizontal laminae		C		XRF	
KDC623	LWF	Hope Beck NY 1822 2246	cleaved thick VFS laminae in thin siltstone/mudstone laminae		C		XRF	
KDC624	LWF	Hope Beck NY 1823 2245	FS greywacke with ripple cross laminae, Tc		C		XRF	
KDC625	LWF	Hope Beck NY 1825 2240	mudstone/siltstone thin/thick horizontal laminae, 2 cleavages		C		XRF	
KDC626	KST	Hope Beck NY 1827 2243	FS-MS greywacke with VCS lenses and laminae		C	MA & L	XRF	
KDC627	KST	Hope Beck NY 1827 2243	cleaved VFS/siltstone/mudstone thin/thick horizontal laminae		C		XRF	
KDC628	KST	Hope Beck NY 1830 2241	mudstone/siltstone horizontal laminae	P	C		XRF	
KDC629	KST	Hope Beck NY 1833 2240	FS greywacke with ripple cross laminae, Tc		C		XRF	
KDC630	KST	Hope Beck NY 1833 2240	cleaved siltstone/mudstone thin horizontal laminae	P	C		XRF	REE
KDC631	KST	Hope Beck NY 1833 2240	calcareous mudstone, CS-MS lag, FS with ripple cross laminae		C		XRF	
KDC632	KST	Hope Beck NY 1836 2238	FS greywacke with ripple cross laminae, Tc		C	MA	XRF	
KDC633	KST	Hope Beck NY 1836 2238	cleaved siltstone/mudstone thin/thick laminae	P	C		XRF	
KDC634	KST	Hope Beck NY 1839 2236	siltstone/mudstone in thin horizontal laminae		C		XRF	
KDC635	KST	Hope Beck NY 1842 2234	FS greywacke with ripple cross laminae, Tc, cleaved		C		XRF	
KDC636	KST	Hope Beck NY 1842 2234	siltstone/mudstone in thin horizontal laminae		C		XRF	
KDC637	LWF	Hope Beck NY 1827 2243	FS greywacke with ripple cross laminae, Tc, thin siltstone laminae		C		XRF	
KDC638	LWF	Hope Beck NY 1801 2266	FS greywacke thick lamina with mudstone & siltstone		C		XRF	
KDC639	LWF	Hope Beck NY 1809 2256	MS greywacke, structureless Ta		C	MA		
KDC640	LWF	Hope Beck NY 1809 2258	MS-CS greywacke with mudstone rip-up clasts, Ta		C			
KDC641	LWF	Hope Beck NY 1684 2385	FS greywacke with ripple cross laminae, Tc		C		XRF	
KDC642	LWF	Hope Beck NY 1684 2385	cleaved siltstone/mudstone with thin horizontal laminae	P	C		XRF	
KDC643	LWF	Hope Beck NY 1693 2379	cleaved siltstone/mudstone with thin horizontal laminae		C		XRF	
KDC644	LWF	Hope Beck NY 1693 2379	MS greywacke, structureless		C	MA	XRF	
KDC645	LWF	Hope Beck NY 1693 2379	FS-MS greywacke with faint thin horizontal laminae,Tb		C	MA	XRF	
KDC646	LWF	Hope Beck NY 1696 2373	siltstone in thin/thick laminae in mudstone		C		XRF	

KDC847	LWF	Hope Beck NY 1696 2373	FS greywacke with convolute laminae		C		XRF	
KDC848	LWF	Hope Beck NY 1704 2370	siltstone/VFS thin/thick laminae in mudstone with 2 cleavages	P	C		XRF	
KDC849	LWF	Hope Beck NY 1704 2370	FS-MS greywacke		C	MA	XRF	
KDC850	LWF	Hope Beck NY 1724 2352	siltstone laminae in mudstone, with cleavage		C		XRF	
KDC851	LWF	Hope Beck NY 1727 2350	siltstone laminae in mudstone, with cleavage		C		XRF	
KDC852	LWF	Hope Beck	mudstone				XRF	
KDC853	LWF	Hope Beck	mudstone				XRF	
KDC854	LWF	Hope Beck	mudstone				XRF	
KDC855	LWF	Hope Beck NY 1737 2332	siltstone/VFS thin/thick laminae in mudstone	P	C		XRF	REE
KDC856	LWF	Hope Beck NY 1739 2328	FS-MS greywacke		C	MA	XRF	
KDC479	WHG	Watch Hill NY 1487 3174	10cm thick sandstone				XRF	
KDC480	WHG	Watch Hill NY 1490 3174	20cm thick sandstone				XRF	
KDC481	WHG	Watch Hill NY 1519 3180	thinly bedded sandstone				XRF	
KDC482	WHG	Watch Hill, forest road NY 1487 3174	30cm thick sandstone, massive to graded				XRF	HM
KDC483	WHG	Watch Hill, small quarry NY 1487 3174	20cm thick sandstone				XRF	HM
KDC484	WHG	Watch Hill, in forest NY 1585 3187	30cm thick sandstone				XRF	HM
KDC485	WHG	Watch Hill, in forest NY 1487 3174	thinly bedded sandstone/ siltstone above KDC484	P			XRF	
KDC486	WHG	Watch Hill, forest road NY 1575 3190	10cm sandstone in sandstone/ siltstone thin beds	P			XRF	
KDC444	LWF	Scawgill Bridge Quarry	Tb				XRF	
KDC445	LWF	Scawgill Bridge Quarry	Td above KDC444				XRF	
KDC446	LWF	Scawgill Bridge Quarry	Tc				XRF	
KDC447	LWF	Scawgill Bridge Quarry	Td				XRF	
KDC448	LWF	Scawgill Bridge Quarry	massive sandstone				XRF	
KDC449	LWF	Scawgill Bridge Quarry	silty mudstone				XRF	
KDC450	LWF	quarry by path to Spout Force	silty mudstone	P			XRF	

SAMPLES LOANED FROM BGS KEYWORTH

E50441	ING	Beckermonds Scar borehole SE 8635 8016	coarse to very coarse sand grade greywacke; 298.80m	E50441 C	MA & L	
E50449	ING	Beckermonds Scar borehole SE 8635 8016	fine to medium sand grade greywacke; 489.25m	E50449 C	MA	
E50445	ING	Beckermonds Scar borehole SE 8635 8016	fine to medium sand grade greywacke; 413.25m	E50445 C	MA	
E50448	ING	Beckermonds Scar borehole SE 8635 8016	medium sand grade greywacke; 483.17m	E50448 C	MA	
E50442	ING	Beckermonds Scar borehole SE 8635 8016	very coarse sand grade greywacke; 300.90m	E50442 C	MA	

Appendix 2

RESULTS OF PETROGRAPHICAL MODAL ANALYSIS

KEY

phases in modal analysis		code (e.g. 1234)
MONOQP	strained monocrystalline quartz	**position 1, group**
MONOQV	unstrained monocrystalline quartz	S Skiddaw Group
POLYQ	polycrystalline quartz	**position 2, formation**
PLAG	plagioclase feldspar	B Bitter Beck Fm
KSPAR	potassium and untwinned feldspar	W Watch Hill Fm
LV	volcanic lithic fragments	H Hope Beck Fm
LMV	metavolcanic lithic fragments	L Loweswater Fm
LS	sedimentary lithic fragments	K Kirk Stile Fm
LMS	metasedimentary lithic fragments	**position 3, location**
MICA	detrital mica	T Trusmadoor
PYRITE	pyrite	W Watch Hill
CALCITE	carbonate cement	C Gt. Cockup
CLAY	clay matrix	H Hope Gill
CHLOR	chlorite	N Swinside
HM	heavy minerals	Q Scawgill Br Qy
Q	total quartz	D Darling Fell
F	total feldspar	J Jonah's Gill
L	lithic fragments	M high-matrix
QM	monocrystalline quartz	T Tarn Crags
LT	lithics plus polycrystalline quartz	U Mungrisdale
LITHV	volcanic and metavolcanic lithics	B Broom Fell
LITHS	sedimentary and metasedimentary lithics	S Beckgrains Br
MATRIX	sum of non-QFL framework grains	P Causey Pike
MI	mineralogical maturity index	G Goat Gills
		position 1, group
		M Manx Group
		position 2, formation
		M Maughold banded gp
		L Lonan Flags
		P " " at Port Mooar
		N Niarbyl Flags
		position 1, group
		I Ingleton Group
		position 3, location
		I *Ingleton Qy*
		H Beckermonds *Scar borehole*
		position 1, group
		B Bray Group, Bray Head

Sample	M54B	CU291	CU2841	CU295	CU292	CU298	M33	M35	CU327	CU326	CU328	CU325	KDC644	KDC645	KDC649	KDC656
Code	SBT3	SWW2	SWW2	SWW2	SWW1	SWW1	SWW2	SWW2	SWC2	SWC2	SWC2	SWC2	SHH2	SHH2	SHH2	SHH1
points	300	200	200	200	100	100	300	300	200	200	200	200	200	200	200	100
MONOQP	38.33	48.00	53.00	48.00	45.00	38.00	49.67	38.67	26.00	26.50	23.00	23.50	29.00	45.50	37.50	44.00
MONOQV	0.00	2.50	3.50	0.50	2.00	10.00	1.67	1.33	6.50	2.50	4.00	3.50	1.00	0.50	0.00	8.00
POLYQ	0.33	7.00	12.00	8.00	9.00	5.00	3.00	8.00	8.00	13.50	18.50	8.00	7.50	5.50	2.50	0.00
PLAG	2.00	5.00	3.50	5.50	3.00	3.00	1.33	0.67	1.50	0.50	1.00	2.50	0.50	0.00	0.00	0.00
KSPAR	4.67	15.50	10.00	12.00	10.00	6.00	9.33	7.67	7.00	2.00	4.00	4.00	5.50	4.00	3.50	0.00
LV	0.00	0.00	1.50	1.50	1.00	9.00	0.00	1.00	3.50	7.00	5.50	2.50	2.50	1.00	0.00	0.00
LMV	0.00	0.00	0.00	5.50	0.00	1.00	0.67	1.00	5.50	1.50	2.50	0.50	1.00	1.50	1.50	0.00
LS	0.00	10.50	10.00	10.00	10.00	12.00	1.67	11.33	12.00	23.50	21.00	27.50	3.50	7.50	2.50	0.00
LMS	1.33	0.50	1.00	3.50	7.00	2.00	4.00	2.67	0.50	0.00	0.00	0.50	0.50	0.00	0.50	2.00
MICA	2.00	0.50	0.50	0.00	0.00	0.00	0.00	0.00	0.50	1.00	0.50	0.50	3.00	0.50	0.00	0.00
PYRITE	1.67	1.50	0.50	0.50	3.00	2.00	1.33	1.67	0.50	0.00	0.00	0.00	1.00	1.50	0.00	0.00
CALCITE	0.00	0.00	0.00	0.00	0.00	0.00	0.00	0.00	0.00	0.00	0.00	0.00	3.00	0.50	0.00	0.00
CLAY	48.33	8.50	4.50	4.00	10.00	12.00	26.00	25.67	27.50	22.00	19.00	26.00	39.50	31.50	52.00	44.00
CHLOR	0.33	0.50	0.00	0.50	0.00	0.00	1.33	0.33	0.50	0.00	0.00	0.00	2.00	0.00	0.00	2.00
HM	1.00	0.00	0.00	0.50	0.00	0.00	0.00	0.00	0.50	0.00	1.00	1.00	0.50	0.50	0.00	0.00
TOTAL	100.00	100.00	100.00	100.00	100.00	100.00	100.00	100.00	100.00	100.00	100.00	100.00	100.00	100.00	100.00	100.00
Q	38.67	57.50	68.50	56.50	56.00	53.00	54.30	48.00	40.50	42.50	45.50	35.00	37.50	51.50	40.00	52.00
F	7.67	20.50	13.50	17.50	13.00	9.00	10.67	8.33	8.50	2.50	5.00	6.50	6.00	4.00	3.50	0.00
L	1.67	12.00	12.50	21.00	18.00	27.00	10.67	18.00	28.00	32.00	31.00	33.00	13.50	13.00	7.50	2.00
QM	38.33	50.50	56.50	48.50	47.00	48.00	51.33	40.00	32.50	29.00	27.00	27.00	30.00	46.00	37.50	52.00
LT	2.00	19.00	24.50	29.00	27.00	32.00	13.67	26.00	36.00	45.50	49.50	41.00	19.50	18.50	10.00	2.00
LITHV	0.00	0.00	1.50	7.50	1.00	10.00	0.67	2.00	9.00	8.50	8.00	3.00	3.50	2.50	1.50	0.00
LITHS	1.33	11.00	11.00	13.50	17.00	14.00	5.67	14.00	12.50	23.50	21.00	28.00	4.00	7.50	3.00	2.00
MATRIX1	53.33	11.00	5.50	5.50	13.00	14.00	28.67	27.67	29.50	23.00	20.50	27.50	49.00	34.50	52.00	46.00
MI	80.55	63.89	72.45	59.47	64.37	59.55	71.79	64.58	52.60	55.19	55.83	46.98	65.79	75.18	78.43	96.30

Sample	CU103	CU102	M64	M63	CU26	CU29B	CU37	CU32	CU16b	CU35	CU38	CU33	CU23A	CU42	KDC603	KDC605
Code	SHN1	SHN1	SHN2	SHN3	SLH2	SLH2	SLH2	SLH2	SLH1	SLH1	SLH1	SLH1	SLH1	SLH1	SLH2	SLH2
points	100	100	300	300	200	200	200	200	200	200	100	100	100	100	200	200
MONOQP	56.00	53.00	37.00	55.67	36.00	45.00	37.50	48.00	39.00	41.00	28.00	50.00	56.00	24.00	44.50	27.00
MONOQV	3.00	2.00	3.00	0.33	9.50	9.00	4.00	3.00	7.00	3.50	2.00	2.00	0.00	4.00	0.50	2.50
POLYQ	5.00	2.00	5.00	2.67	10.50	9.50	4.00	5.00	4.00	10.00	2.00	4.00	5.00	10.00	6.00	10.00
PLAG	1.00	2.00	0.67	0.00	4.00	3.00	4.50	5.50	3.00	4.00	6.00	4.00	2.00	3.00	1.50	1.50
KSPAR	7.00	2.00	3.00	2.33	3.50	6.50	7.50	6.00	7.50	11.00	4.00	5.00	0.00	4.00	8.50	10.50
LV	0.00	0.00	0.67	0.00	0.50	0.00	0.00	0.00	2.50	2.00	0.00	1.00	2.00	0.00	1.00	0.00
LMV	0.00	0.00	0.00	0.00	1.00	0.00	0.00	0.00	2.00	0.00	0.00	0.00	0.00	0.00	2.00	0.00
LS	8.00	2.00	0.67	0.33	2.00	4.50	3.50	2.00	2.00	5.00	4.00	5.00	0.00	1.00	2.00	1.00
LMS	0.00	2.00	1.00	4.00	2.50	0.50	0.50	0.00	2.00	0.00	0.00	2.00	0.00	2.00	2.00	2.50
MICA	0.00	1.00	1.00	0.67	1.00	0.00	4.50	0.50	2.00	0.50	5.00	0.00	3.00	7.00	0.00	0.50
PYRITE	1.00	2.00	0.33	0.67	0.50	1.50	1.00	1.00	2.50	0.50	0.00	1.00	0.00	0.00	0.50	0.00
CALCITE	0.00	0.00	0.00	0.00	0.00	0.00	1.00	0.00	0.00	1.50	24.00	0.00	0.00	0.00	7.50	32.50
CLAY	19.00	32.00	46.67	33.33	28.00	20.50	31.00	29.00	26.00	18.00	24.00	24.00	32.00	45.00	21.50	11.50
CHLOR	0.00	0.00	0.67	0.00	0.50	0.00	0.00	0.00	0.50	3.00	1.00	2.00	0.00	0.00	2.50	0.00
HM	0.00	0.00	0.33	0.00	0.50	0.00	1.00	0.00	0.00	0.00	0.00	0.00	0.00	0.00	0.00	0.50
TOTAL	100.00	100.00	100.00	100.00	100.00	100.00	100.00	100.00	100.00	100.00	100.00	100.00	100.00	100.00	100.00	100.00
Q	64.00	57.00	45.00	58.67	56.00	63.50	45.50	56.00	50.00	54.50	32.00	56.00	61.00	38.00	51.00	39.50
F	8.00	4.00	4.33	3.00	7.50	9.50	12.00	16.50	10.50	15.00	10.00	9.00	2.00	7.00	10.00	12.00
L	8.00	4.00	5.67	5.67	6.50	7.00	4.50	2.00	9.00	7.00	4.00	8.00	2.00	3.00	11.50	4.00
QM	59.00	55.00	40.00	56.00	45.50	54.00	41.50	51.00	46.00	44.50	30.00	52.00	56.00	28.00	45.00	29.50
LT	13.00	5.00	10.67	8.33	17.00	16.50	8.50	7.00	13.00	17.00	6.00	12.00	7.00	13.00	17.50	14.00
LITHV	0.00	0.00	0.67	0.00	1.50	0.00	0.00	0.00	4.50	2.00	0.00	1.00	2.00	0.00	3.50	0.00
LITHS	8.00	4.00	1.67	4.33	4.50	5.00	4.00	2.00	4.00	5.00	4.00	7.00	0.00	3.00	4.00	3.50
MATRIX1	20.00	35.00	49.00	34.67	30.50	22.00	38.50	30.50	30.50	23.50	54.00	27.00	35.00	52.00	32.00	45.00
MI	80.00	87.69	81.82	87.12	80.00	79.37	73.39	75.17	71.94	71.24	76.09	76.71	93.85	79.17	70.34	71.17

Sample	KDC606	KDC611	KDC615	KDC616	KDC620	KDC639	M37	M38	M30A	M45	M43	M47	M29C	M48	M50	M51
Code	SLH2	SLH2	SLH2	SLH2	SLH2	SLH2	SLQ3	SLQ3	SLD2	SLD3	SLD3	SLD3	SLJ3	SLJ3	SLJ3	SLJ3
points	200	200	200	200	200	200	300	300	300	300	300	300	300	300	300	300
MONOQP	43.00	41.50	33.00	33.50	48.50	42.00	39.33	31.33	36.67	31.33	24.67	32.00	44.33	48.00	48.33	40.67
MONOQV	0.00	1.00	0.00	0.00	0.00	1.00	0.33	0.33	6.00	3.00	0.00	8.00	5.00	5.00	1.67	4.33
POLYQ	5.00	7.50	2.50	2.00	5.00	8.50	4.33	3.67	3.67	3.33	4.33	5.00	8.33	3.33	1.67	1.33
PLAG	1.00	1.50	3.50	2.00	0.50	1.00	4.33	1.67	0.00	5.33	2.67	3.33	1.33	1.00	0.33	0.33
KSPAR	12.00	6.00	10.00	7.50	5.50	4.50	8.33	10.00	2.33	8.67	7.33	9.00	7.33	3.33	2.67	2.00
LV	0.00	2.50	0.00	0.00	0.00	0.50	0.00	0.00	0.33	0.00	0.00	0.00	0.00	0.00	0.00	0.00
LMV	1.50	4.50	0.00	0.50	0.00	2.50	0.00	0.00	2.00	0.00	0.33	0.00	0.00	0.00	0.00	0.00
LS	2.50	4.00	1.50	3.00	1.50	5.00	0.33	0.33	0.67	1.67	2.33	3.33	0.00	1.00	0.67	1.00
LMS	1.00	2.50	2.00	1.50	1.00	0.00	2.67	1.00	2.00	2.33	3.33	3.67	1.33	0.33	0.00	1.00
MICA	0.50	0.50	1.00	1.00	0.50	1.00	0.00	0.33	0.00	1.33	1.00	0.67	0.33	0.33	1.33	0.33
PYRITE	0.00	1.00	3.50	0.00	0.00	1.00	0.33	1.33	0.67	0.00	0.00	0.33	1.67	0.33	0.00	0.00
CALCITE	7.00	0.50	0.50	0.00	0.00	0.00	0.00	0.00	0.00	0.33	0.00	0.00	19.33	23.33	4.33	10.67
CLAY	25.50	24.50	41.00	49.00	37.00	33.00	38.00	49.33	36.67	41.00	53.67	34.00	10.33	13.67	38.33	36.67
CHLOR	0.50	2.50	0.50	0.00	0.50	0.00	1.33	0.33	8.00	0.67	0.33	0.00	0.00	0.33	0.67	0.67
HM	0.50	0.00	1.00	0.00	0.00	0.00	0.67	0.33	1.00	1.00	0.00	0.67	0.67	0.00	0.00	1.00
TOTAL	100.00	100.00	100.00	100.00	100.00	100.00	100.00	100.00	100.00	100.00	100.00	100.00	100.00	100.00	100.00	100.00
Q	48.00	50.00	35.50	35.50	53.50	51.50	44.00	35.33	46.33	37.67	29.00	45.00	58.00	56.33	51.67	46.33
F	13.00	7.50	13.50	9.50	6.00	5.50	12.67	12.00	2.33	14.00	10.33	12.33	9.33	4.33	3.00	2.33
L	9.00	16.00	5.00	9.50	6.00	14.00	4.00	3.67	9.67	5.33	6.33	8.33	1.33	1.33	0.67	2.67
QM	43.00	42.50	33.00	33.50	48.50	43.00	39.67	31.67	42.67	34.33	24.67	40.00	49.33	53.00	50.00	45.00
LT	14.00	23.50	7.50	11.50	11.00	22.50	8.33	7.33	13.33	8.67	10.67	12.33	10.00	4.67	2.33	4.00
LITHV	1.50	7.00	0.00	0.50	0.00	3.00	0.00	0.00	2.33	0.33	0.33	0.00	0.00	0.00	0.00	0.00
LITHS	4.00	6.50	3.50	4.50	2.50	5.00	3.00	1.33	2.67	4.00	5.67	7.00	1.33	1.33	0.67	2.00
MATRIX1	34.00	29.00	47.50	50.00	38.00	35.00	40.33	51.67	46.33	44.00	55.00	35.67	32.33	38.00	44.67	49.33
MI	68.57	68.03	65.74	65.14	81.68	72.53	72.52	69.27	79.43	66.09	63.50	68.52	84.46	90.58	93.37	90.26

Sample	M58	M18	M17A	M61	M9019	M9017	M9018	KDC626	KDC632	M39	M40	M907	M908	M901	M902	M903
Code	SLM2	SLM2	SLM2	SLM3	SLM4	SLT4	SLU4	SKH2	SKH2	SKB3	SKB4	SRS4	SRS4	SRP4	SRP4	SRP4
points	300	300	300	300	300	200	200	200	200	300	200	200	200	200	200	200
MONOQP	20.33	19.33	20.33	29.33	18.00	23.50	24.50	22.00	36.50	42.00	20.00	32.00	20.50	24.00	47.50	52.50
MONOQV	7.33	5.33	4.33	1.67	4.00	5.50	5.00	0.00	0.50	0.00	4.00	0.00	4.00	9.50	2.00	1.50
POLYQ	6.00	6.33	5.00	3.33	7.00	3.50	7.50	6.00	2.50	1.00	2.50	0.00	4.00	1.00	1.00	2.50
PLAG	2.33	2.00	3.00	2.67	1.00	3.50	6.50	0.00	0.00	2.00	4.00	0.00	2.50	0.50	0.00	3.50
KSPAR	3.33	6.33	9.67	7.33	10.67	14.50	11.00	0.50	2.50	3.00	6.00	3.00	11.50	8.00	2.50	5.50
LV	0.33	2.33	0.33	0.33	1.00	1.00	2.50	0.00	1.50	0.00	0.00	0.00	0.50	0.00	1.00	0.00
LMV	1.00	3.00	1.00	0.67	1.33	1.00	1.50	2.00	0.50	0.00	0.50	0.00	0.50	0.50	0.50	2.00
LS	1.33	1.00	4.67	1.33	3.33	0.00	1.50	8.50	2.00	0.00	2.00	1.50	5.00	2.50	3.50	4.00
LMS	1.33	1.00	1.33	2.67	1.00	0.00	0.50	0.00	1.00	1.00	7.00	1.00	0.00	0.00	0.00	0.50
MICA	2.67	3.00	1.67	2.00	1.33	5.00	1.50	0.00	3.50	1.33	1.00	0.50	0.50	0.00	0.00	0.00
PYRITE	1.00	0.67	1.00	2.00	0.00	0.00	4.00	0.50	2.50	0.00	0.00	4.00	11.00	0.00	0.00	1.50
CALCITE	0.00	0.00	4.00	0.00	0.00	0.00	0.00	47.00	0.00	0.00	0.00	0.50	2.00	12.50	0.00	0.00
CLAY	50.33	46.00	42.00	44.67	48.00	41.00	29.00	13.50	33.00	48.67	47.50	55.00	27.50	53.50	38.50	26.00
CHLOR	2.67	3.00	0.33	1.33	1.67	0.00	3.50	0.00	13.00	0.00	2.50	0.00	0.00	0.00	2.50	0.00
HM	0.00	0.67	1.33	0.67	1.67	1.50	1.50	0.00	1.00	1.00	2.50	1.00	0.00	0.50	1.00	0.50
TOTAL	100.00	100.00	100.00	100.00	100.00	100.00	100.00	100.00	100.00	100.00	100.00	100.00	100.00	100.00	100.00	100.00
Q	33.67	31.00	29.67	34.33	29.00	32.50	37.00	28.00	39.50	43.33	26.50	32.00	28.50	34.50	50.50	56.50
F	5.67	8.33	12.67	10.33	11.67	17.50	17.50	0.50	2.50	5.67	10.00	3.00	14.00	8.50	2.50	9.00
L	7.00	12.00	9.33	6.00	8.67	4.50	6.50	11.00	14.00	2.00	12.00	2.50	9.00	3.00	12.50	7.00
QM	27.67	24.67	24.67	31.00	22.00	29.00	29.50	22.00	37.00	42.00	24.00	32.00	24.50	33.50	49.50	54.00
LT	13.00	18.33	14.33	9.33	15.67	8.00	14.00	17.00	16.50	3.00	14.50	2.50	13.00	4.00	13.50	9.50
LITHV	1.33	5.33	1.33	1.00	2.33	2.00	4.00	2.00	9.00	0.00	0.50	0.00	1.00	0.50	1.50	2.00
LITHS	2.67	2.00	6.00	4.00	4.33	0.00	2.00	8.50	5.00	1.00	9.00	2.50	5.00	2.50	3.50	4.50
MATRIX1	56.67	53.33	50.33	50.67	52.67	47.50	39.50	61.00	53.00	51.00	54.00	62.50	51.50	54.00	42.00	28.00
MI	72.66	60.39	57.42	67.76	58.77	59.63	60.66	70.89	70.54	84.96	54.64	85.33	55.34	75.00	77.69	77.93

Sample	M906	M904	M905	IOM22	IOM10	IOM12	IOM14	IOM20	IOM13	IOM21	IOM9	M909	M9010	M9011	M9012	M9101
Code	SRP4	SRG4	SRG4	MM22	ML10	ML12	ML14	MP20	ML13	MP21	MN09	III4	III4	III4	III4	BAB5
points	200	200	200	200	200	200	200	200	200	200	200	200	200	200	200	200
MONOQP	57.50	37.00	49.50	64.50	47.00	47.50	42.50	46.50	53.00	32.50	27.50	9.50	11.00	11.50	11.50	39.50
MONOQV	1.00	1.00	0.50	12.00	0.50	1.00	0.00	0.00	0.50	0.00	2.50	1.00	4.50	0.00	0.50	5.50
POLYQ	1.50	1.00	1.00	0.50	3.50	4.00	0.50	0.00	4.00	0.00	2.50	2.50	8.00	1.50	2.50	1.00
PLAG	0.00	0.50	1.50	0.00	1.50	2.00	2.50	0.00	2.50	0.00	3.50	2.50	5.00	1.00	2.00	1.00
KSPAR	2.00	1.50	3.00	0.00	2.50	7.50	6.50	0.50	8.50	1.00	10.50	16.00	17.00	8.00	14.00	7.00
LV	0.00	1.00	1.00	0.00	1.50	0.50	0.50	0.00	0.50	0.00	0.00	0.00	7.00	0.00	1.00	0.50
LMV	1.50	0.50	0.50	0.00	1.00	0.50	2.50	0.00	1.00	0.00	1.00	0.50	3.00	0.00	0.00	1.00
LS	1.00	0.00	0.00	3.00	6.00	4.50	2.50	1.00	7.00	0.00	0.00	0.50	0.50	0.00	1.00	0.00
LMS	0.00	0.50	1.00	0.00	1.50	0.50	2.00	0.00	0.50	0.00	2.00	1.50	2.50	1.50	2.00	0.00
MICA	0.50	0.00	0.00	0.00	0.50	0.50	0.00	0.00	0.00	0.50	1.00	2.00	1.50	3.50	2.50	6.00
PYRITE	0.00	3.00	0.00	0.00	0.00	0.00	0.00	0.00	0.00	0.00	0.00	0.00	0.00	0.00	0.00	0.00
CALCITE	0.00	2.00	2.00	0.00	1.50	0.50	0.00	0.00	0.50	0.00	20.50	0.00	1.00	0.00	0.50	0.00
CLAY	33.00	50.50	37.50	3.00	32.00	30.00	38.00	49.00	22.00	60.50	29.00	61.00	37.00	70.00	60.00	37.00
CHLOR	0.00	1.00	0.50	15.00	0.50	0.00	2.00	0.00	0.00	0.00	0.00	2.50	0.00	1.00	2.50	0.50
HM	2.00	0.50	2.00	2.00	0.50	1.00	0.50	3.00	0.00	5.50	0.00	0.50	2.00	2.00	0.00	1.00
TOTAL	100.00	100.00	100.00	100.00	100.00	100.00	100.00	100.00	100.00	100.00	100.00	100.00	100.00	100.00	100.00	100.00
Q	60.00	39.00	51.00	77.00	51.00	52.50	43.00	46.50	57.50	32.50	32.50	13.00	23.50	13.00	14.50	46.00
F	2.00	2.00	4.50	0.00	4.00	9.50	9.00	0.50	11.00	1.00	14.00	18.50	22.00	9.00	16.00	8.00
L	4.00	2.50	4.50	3.00	11.50	6.50	8.50	1.00	11.00	0.00	4.00	6.50	16.00	5.50	9.00	1.50
QM	58.50	38.00	50.00	76.50	47.50	48.50	42.50	46.50	53.50	32.50	30.00	10.50	15.50	11.50	10.00	45.00
LT	5.50	3.50	5.50	3.50	15.00	10.50	9.00	1.00	15.00	0.00	6.50	9.00	24.00	7.00	11.50	2.50
LITHV	1.50	1.50	1.50	2.50	2.50	1.00	3.00	0.00	1.50	0.00	1.00	0.50	10.00	0.00	1.00	1.50
LITHS	1.00	0.50	1.00	0.50	6.00	5.00	4.50	1.00	7.50	0.00	2.00	2.00	3.00	1.50	3.00	0.00
MATRIX1	35.50	57.00	42.00	20.00	35.00	32.00	40.50	52.00	22.50	66.50	50.50	66.00	41.50	76.50	65.50	44.50
MI	90.91	89.65	85.00	96.25	76.69	76.64	71.07	96.87	72.33	97.00	64.36	34.21	38.21	47.27	36.71	82.88

Sample	E50441	E50449	E50445	E50448	E50442
Code	IIH1	IIH2	IIH3	IIH4	IIH5
points	200	200	200	200	200
MONOQP	24.50	18.50	21.50	20.50	30.00
MONOQV	9.50	11.50	7.00	6.00	2.00
POLYQ	14.00	4.50	7.50	4.00	11.00
PLAG	10.00	9.50	7.50	6.00	6.00
KSPAR	13.50	16.00	17.50	27.50	28.50
LV	7.00	1.00	3.00	3.00	4.00
LMV	2.00	1.50	1.00	0.00	1.50
LS	0.00	0.50	1.00	1.00	3.00
LMS	0.00	2.50	0.50	2.00	0.50
MICA	0.00	0.00	0.00	0.00	0.50
PYRITE	0.00	0.00	0.00	0.00	0.00
CALCITE	0.00	0.00	2.00	1.50	0.00
CLAY	16.50	30.00	27.50	27.50	10.00
CHLOR	1.00	0.50	3.50	0.00	1.50
HM	2.00	4.00	0.50	1.00	1.50
TOTAL	100.00	100.00	100.00	100.00	100.00
Q	48.00	34.50	36.00	30.50	43.00
F	23.50	25.50	25.00	34.00	34.50
L	9.00	6.00	5.50	6.50	9.00
QM	34.00	30.00	28.50	26.50	32.00
LT	23.00	10.50	13.00	10.50	20.00
LITHV	9.00	2.50	4.00	3.00	5.50
LITHS	0.00	3.00	1.50	3.00	3.50
MATRIX1	19.50	34.00	33.50	29.00	13.50
MI	59.63	52.27	54.13	42.96	49.71

Appendix 3

ANALYTICAL DETAILS

(a) X-ray fluorescence spectrometry

Sample preparation

In the following text, temperatures are within 5% of stated values. Weighing tolerance is to the nearest milligram for major elements and loss on ignition (LOI), or +/-0.5g for trace element pellets.

Representative splits of finely ground sample are dried at 105°C for three to four hours prior to sample preparation for major elements and loss on ignition determination.

1. Major and minor elements are analysed by XRF on 40mm diameter glass discs which are manufactured as below.

- 0.4g of sample fused with 4g of flux (Johnson Matthey Spectroflux 110 - lithium borate) in a Pt+5% Au crucible for 30 minutes at 1000°C in a muffle furnace.
- Any weight loss from the melt made good with flux after cooling.
- Sample remelted over amal burners, and homogenised by swirling the molten glass.
- Sample cast into a 40mm diameter copper wire ring, held at 180°C on a stainless steel hot plate.
- Disc trimmed of surplus glass after cooling and stored in sealable plastic bag to avoid hydration of the surface before analysis.

2. Loss on ignition measured by roasting known weights (approximately 1g) of sample in porcelain crucibles at 1000°C for 1 hour in a muffle furnace. Samples reweighed when cool, calculated loss expressed as weight %.

3. Trace elements analysed by XRF on 40mm diameter pellets, manufactured as below.

- 15g sample mixed with 1ml glue (made by dissolving 40g PVA in 250ml distilled de-ionised water), then pressed at 10 tons/sq. in. in a 40mm die by means of a hydraulic press. The pressure is held for a few seconds before releasing and extracting the resultant pellet.
- Pellet dried at 105°C for 3-4 hours then stored in a resealable bag to prevent absorption of atmospheric water.

Calibration

The spectrometer is calibrated for each element by measuring X-ray intensity at optimized conditions for a series of both international and synthetic standards. Intensity/concentration curves are established by regression and relevant interelement corrections are applied to refine the curves. The standards used in the calibration stage are listed below:

United States Geological Survey: G-2, GSP-1, AGV-1, BCR-1, PCC-1;

Canadian Certified Reference Materials Project: SY-2, MRG-1;

British Chemical Standards: BCS269, BCS309, BCS315, BCS367, BCS375, BCS376;

National Institute for Metallurgy (S. Africa): MIM-G, NIM-S, NIM-N, NIM-D.

A variety of synthetic standards are manufactured for major element calibration, using weighed amounts of AnalaR and pure compounds, as SiO_2, TiO_2, Al_2O_3, Fe_2O_3, $KMnO_4$, MgO, $CaCO_3$, K_2CO_3 and Na_2HPO_4.

A Philips PW1400 X-ray spectrometer was used, with a PW1730 generator and PW2182 Rh anode tube.

(b) Rare earth element analysis

The rare earth elements (REE) were separated via cation exchange following dissolution in acids (procedure kindly performed by Mr F. Buckley). Acids used in ion exchange (1.75M and 4.0M HCl) were standardised against ConvoL NaOH. The REE elements were analysed by inductively coupled plasma (ICP) spectrometry at Royal Holloway and Bedford New College, following the method of Thompson and Walsh (1989).

Appendix 4

XRF ANALYSES

(a) Data of this study

LOI = loss on ignition

Code, first letter = unit: L = Loweswater Formation (or equivalent); I = Ingleton Group; MX = Manx Group;
second letter = location: H = Hope Beck; J = Jonah's Gill; C = channel fill; R = sandstone raft

XRF ANALYSES (THIS STUDY)

Sample	M17	M18	M29	M43	M45	M47	M48	M58	M61	9019	M903	M904	M906	M908	M909	9010
Code	LH	LH	LJ	LC	LC	LC	LJ	LH	LH	LH	LR	LR	LR	LR	I	I
SIO2	72.84	66.22	77.06	64.19	76.00	78.73	76.39	67.21	70.51	66.76	80.60	77.45	81.58	64.82	59.22	66.13
TIO2	0.60	0.75	0.30	0.89	0.65	0.62	0.43	0.75	0.67	0.81	0.47	0.65	0.47	0.35	0.96	0.75
AL2O3	11.90	14.36	5.10	16.62	11.61	10.07	6.68	12.89	12.59	14.52	7.61	8.10	6.95	7.84	19.70	15.13
FE2O3	5.78	8.08	6.59	7.24	5.07	4.67	8.07	9.21	6.09	6.63	6.51	7.53	7.58	4.92	6.92	6.42
MNO	0.29	0.52	0.68	0.25	0.24	0.18	0.91	0.48	0.38	0.30	0.29	1.15	0.30	1.11	0.10	0.10
MGO	1.25	1.83	1.14	1.82	1.17	1.05	1.21	2.00	1.34	1.63	0.93	1.23	0.79	0.93	2.35	2.13
CAO	0.61	0.32	1.98	0.24	0.18	0.19	0.58	0.51	0.79	1.11	0.17	0.56	0.18	7.99	1.30	1.76
NA2O	2.05	1.80	1.03	2.00	1.85	1.63	0.79	1.29	2.05	2.03	1.13	0.13	0.11	2.07	2.96	3.69
K2O	1.53	2.02	0.53	2.65	1.62	1.40	0.72	1.63	1.76	2.34	0.61	0.95	0.72	0.63	3.43	1.68
P2O5	0.18	0.19	0.28	0.19	0.14	0.16	0.17	0.19	0.15	0.19	0.16	0.10	0.15	0.08	0.14	0.12
LOI	2.93	3.98	5.08	3.38	2.34	2.19	4.68	3.82	3.50	3.94	1.90	2.38	1.80	8.96	3.19	2.60
TOTAL	99.96	100.07	99.77	99.47	100.87	100.89	100.63	99.98	99.83	100.26	100.38	100.23	100.63	99.70	100.27	100.51
SC	13.00	15.00	5.00	14.00	14.00	9.00	8.00	13.00	11.00	15.00	7.00	11.00	6.00	9.00	27.00	12.00
V	76.00	102.00	38.00	118.00	86.00	84.00	46.00	102.00	87.00	97.00	59.00	62.00	52.00	38.00	203.00	139.00
CR	44.00	70.00	64.00	86.00	66.00	56.00	46.00	79.00	56.00	68.00	43.00	51.00	41.00	25.00	71.00	53.00
CO	25.00	42.00	19.00	26.00	21.00	19.00	29.00	42.00	26.00	24.00	25.00	32.00	32.00	25.00	30.00	27.00
NI	22.00	42.00	16.00	38.00	22.00	19.00	25.00	47.00	25.00	22.00	20.00	26.00	18.00	21.00	25.00	21.00
CU	14.00	20.00	8.00	21.00	14.00	10.00	12.00	21.00	16.00	16.00	7.00	13.00	9.00	14.00	49.00	15.00
ZN	59.00	83.00	26.00	77.00	53.00	41.00	33.00	83.00	52.00	71.00	44.00	127.00	47.00	151.00	79.00	76.00
RB	68.00	91.00	22.00	118.00	72.00	61.00	32.00	75.00	78.00	102.00	28.00	52.00	35.00	28.00	117.00	59.00
SR	76.00	78.00	50.00	78.00	62.00	52.00	39.00	58.00	82.00	96.00	24.00	13.00	11.00	105.00	245.00	294.00
Y	24.00	23.00	21.00	27.00	22.00	19.00	22.00	24.00	21.00	30.00	20.00	21.00	23.00	25.00	32.00	25.00
ZR	161.00	170.00	120.00	177.00	165.00	189.00	127.00	187.00	162.00	206.00	162.00	274.00	140.00	116.00	182.00	150.00
NB	10.00	13.00	5.00	17.00	11.00	10.00	8.00	13.00	12.00	14.00	9.00	12.00	9.00	6.00	12.00	9.00
BA	260.00	372.00	97.00	507.00	304.00	248.00	131.00	311.00	302.00	427.00	113.00	154.00	171.00	173.00	530.00	279.00
PB	8.00	18.00	6.00	4.00	5.00	5.00	6.00	11.00	6.00	14.00	7.00	4.00	8.00	48.00	8.00	13.00
TH	12.00	13.00	9.00	15.00	12.00	12.00	10.00	14.00	13.00	14.00	10.00	13.00	11.00	9.00	12.00	10.00
U	2.00	3.00	3.00	2.00	2.00	3.00	2.00	3.00	2.00	4.00	3.00	4.00	3.00	1.00	3.00	2.00

XRF ANALYSES (THIS STUDY)

XRF ANALYSES (THIS STUDY)

Sample Code	9011 I	9012 I	INGM I	INGC I	IOM7 MX7	IOM9 MX9	IM10 MX10	IM12 MX12	IM13 MX13	IM22 MX22
SIO2	61.89	60.48	55.08	61.79	58.72	65.17	80.54	83.44	82.84	92.17
TIO2	0.92	0.85	1.09	0.85	0.85	0.61	0.95	0.35	0.36	0.10
AL2O3	17.36	18.52	21.37	17.54	15.26	10.47	8.78	7.67	6.18	2.69
FE2O3	7.56	6.72	7.10	6.98	6.25	4.06	4.82	4.28	4.23	2.44
MNO	0.11	0.09	0.08	0.10	0.08	0.09	0.03	0.04	0.05	0.06
MGO	2.35	2.21	2.29	2.36	3.42	2.15	1.02	0.92	0.97	0.40
CAO	1.28	1.45	1.66	1.85	3.33	5.25	0.21	0.12	1.21	0.27
NA2O	2.46	2.95	2.13	2.82	2.00	2.03	1.10	1.40	1.15	0.43
K2O	2.90	3.24	4.72	2.69	3.42	1.99	1.00	0.78	0.45	0.34
P2O5	0.11	0.14	0.13	0.16	0.14	0.15	0.09	0.06	0.06	0.21
LOI	3.07	2.80	3.57	3.43	6.61	8.08	1.99	1.47	2.19	0.90
TOTAL	100.01	99.45	99.22	100.57	100.08	100.05	100.53	100.53	99.69	100.01
SC	18.00	15.00	22.00	18.00	16.00	12.00	5.00	6.00	5.00	1.00
V	186.00	156.00	189.00	155.00	124.00	77.00	94.00	55.00	58.00	24.00
CR	71.00	63.00	72.00	62.00	146.00	186.00	85.00	29.00	32.00	14.00
CO	36.00	27.00	26.00	29.00	32.00	17.00	23.00	17.00	16.00	9.00
NI	28.00	26.00	26.00	20.00	84.00	35.00	19.00	16.00	14.00	5.00
CU	40.00	41.00	44.00	29.00	22.00	9.00	5.00	7.00	4.00	5.00
ZN	88.00	84.00	82.00	81.00	56.00	43.00	54.00	50.00	49.00	24.00
RB	98.00	113.00	163.00	94.00	132.00	73.00	42.00	33.00	19.00	15.00
SR	185.00	290.00	234.00	220.00	85.00	119.00	76.00	46.00	59.00	9.00
Y	29.00	29.00	36.00	27.00	35.00	23.00	19.00	10.00	11.00	12.00
ZR	176.00	162.00	211.00	173.00	264.00	248.00	353.00	85.00	123.00	38.00
NB	12.00	10.00	15.00	11.00	17.00	9.00	11.00	6.00	5.00	1.00
BA	494.00	533.00	727.00	447.00	557.00	304.00	147.00	131.00	77.00	47.00
PB	11.00	9.00	11.00	10.00	25.00	7.00	4.00	6.00	19.00	5.00
TH	13.00	12.00	13.00	12.00	16.00	11.00	12.00	10.00	9.00	6.00
U	2.00	2.00	3.00	3.00	4.00	3.00	3.00	2.00	1.00	1.00

(b) Data supplied by the British Geological Survey

LOI = loss on ignition

Code. first letter = formation: K = Kirk Stile Fm; L = Loweswater Fm; H = Hope Beck Fm; W = Watch Hill Fm;
second and third letters = sample number;
fourth letter = depositional unit: A = Ta Bouma division; B = Tb; C = Tc; S, L = silty Tc; T = Td; E = Te; M = mudstone (Te).

XRF ANALYSES (BGS)

Sample Code	KDC601 L01C	KDC602 L02C	KDC603 L03B	KDC604 L04D	KDC605 L05A	KDC606 L06B	KDC607 L07C	KDC608 L08M	KDC609 L09T	KDC610 L10L	KDC611 L11A	KDC612 L12E	KDC613 L13C	KDC614 L14A	KDC615 L15B	KDC616 L16B
SIO2	65.44	65.97	74.22	55.80	56.23	72.66	70.28	55.89	55.55	63.13	76.49	54.62	65.70	62.14	68.14	70.24
TIO2	0.84	0.94	0.58	1.11	0.47	0.68	0.83	1.33	1.06	0.94	0.35	1.25	0.82	0.93	0.69	0.68
AL2O3	15.52	16.00	10.18	21.88	7.84	11.05	14.17	23.96	20.38	16.96	8.15	23.49	14.36	17.61	11.59	11.92
FE2O3	7.92	6.85	4.84	8.17	3.66	5.86	6.09	5.78	10.38	8.00	7.80	7.01	9.23	7.29	6.69	8.52
MNO	0.26	0.19	0.30	0.15	0.70	0.25	0.18	0.13	0.51	0.31	0.43	0.23	0.30	0.24	0.57	0.34
MGO	1.74	1.61	1.14	2.23	1.64	1.61	1.43	1.63	2.39	2.00	1.66	1.86	1.99	1.59	1.51	1.84
CAO	0.29	2.03	0.10	14.38	1.36	1.83	0.27	0.09	0.23	0.31	1.01	0.20	0.34	0.68	2.85	0.39
NA2O	2.09	2.17	1.86	0.61	1.29	1.30	2.11	0.75	0.35	1.45	0.42	0.81	1.59	1.15	1.76	1.56
K2O	2.19	2.44	1.20	4.48	1.14	1.94	1.94	5.39	3.71	2.67	0.73	5.06	1.86	3.39	1.41	1.24
P2O5	0.21	0.18	0.14	0.14	0.08	0.14	0.14	0.12	0.22	0.23	0.48	0.19	0.20	0.41	0.17	0.13
LOI	2.93	2.87	3.15	4.61	14.04	3.31	2.47	4.30	4.63	3.43	2.81	4.41	3.19	3.99	4.44	2.95
TOTAL	99.43	99.49	99.64	99.28	101.47	100.05	99.91	99.37	99.41	99.43	100.33	99.13	99.58	99.42	99.82	99.81
AS	14.00	12.00	10.00	14.00	6.00	9.00	8.00	9.00	28.00	18.00	23.00	23.00	20.00	33.00	16.00	19.00
BA	558.00	526.00	254.00	885.00	177.00	278.00	434.00	924.00	737.00	585.00	154.00	943.00	417.00	643.00	302.00	285.00
CE	64.00	62.00	43.00	93.00	34.00	37.00	47.00	156.00	106.00	80.00	45.00	103.00	52.00	90.00	61.00	42.00
CO	17.00	17.00	12.00	14.00	20.00	17.00	11.00	11.00	32.00	12.00	22.00	11.00	26.00	27.00	17.00	24.00
CR	70.00	73.00	43.00	120.00	36.00	50.00	60.00	143.00	115.00	90.00	30.00	137.00	71.00	95.00	51.00	53.00
CU	23.00	24.00	11.00	21.00	12.00	19.00	24.00	18.00	46.00	31.00	17.00	25.00	30.00	37.00	21.00	22.00
GA	18.00	19.00	10.00	27.00	7.00	12.00	14.00	29.00	24.00	23.00	10.00	30.00	17.00	23.00	10.00	13.00
LA	29.00	40.00	21.00	43.00	30.00	21.00	18.00	76.00	52.00	43.00	19.00	56.00	18.00	52.00	18.00	27.00
NI	43.00	34.00	19.00	56.00	10.00	24.00	35.00	37.00	61.00	47.00	33.00	50.00	49.00	48.00	25.00	40.00
NB	15.00	18.00	10.00	19.00	9.00	12.00	15.00	25.00	18.00	16.00	5.00	20.00	14.00	16.00	12.00	13.00
PB	18.00	28.00	40.00	27.00	18.00	18.00	16.00	21.00	23.00	18.00	16.00	20.00	19.00	28.00	20.00	17.00
RB	92.00	102.00	54.00	185.00	52.00	60.00	86.00	227.00	151.00	113.00	34.00	216.00	78.00	143.00	63.00	69.00
SR	95.00	88.00	92.00	71.00	95.00	78.00	95.00	117.00	91.00	97.00	45.00	101.00	76.00	99.00	106.00	65.00
S	1725.00	728.00	464.00	0.00	236.00	1339.00	172.00	0.00	27.00	0.00	1702.00	0.00	2284.00	3046.00	1603.00	1732.00
TH	16.00	11.00	9.00	18.00	9.00	8.00	13.00	19.00	13.00	12.00	0.00	17.00	8.00	10.00	6.00	11.00
U	4.00	3.00	3.00	3.00	3.00	4.00	3.00	3.00	3.00	1.00	2.00	8.00	2.00	3.00	2.00	3.00
V	93.00	103.00	57.00	140.00	55.00	68.00	92.00	169.00	138.00	111.00	41.00	164.00	97.00	118.00	79.00	78.00
Y	33.00	33.00	34.00	37.00	29.00	22.00	26.00	39.00	36.00	35.00	26.00	39.00	27.00	59.00	27.00	21.00
ZN	78.00	70.00	123.00	97.00	131.00	82.00	68.00	57.00	128.00	81.00	69.00	75.00	116.00	97.00	89.00	94.00
ZR	201.00	256.00	194.00	166.00	157.00	248.00	268.00	202.00	173.00	190.00	108.00	187.00	215.00	188.00	207.00	195.00
MO	0.00	0.00	0.00	0.00	0.00	1.00	0.00	0.00	0.00	0.00	0.00	0.00	0.00	0.00	0.00	0.00

XRF ANALYSES (BGS)

Sample Code	KDC617 L17M	KDC618 L18C	KDC619 L19M	KDC620 L20B	KDC621 L21C	KDC622 L22D	KDC623 L23D	KDC624 L24C	KDC625 L25D	KDC637 L37C	KDC638 L38T	KDC639 L39A	KDC640 L40A	KDC444 L44B	KDC445 L45D	KDC446 L46C
SIO2	55.38	66.62	54.65	73.58	58.73	57.36	54.42	63.76	55.40	65.58	59.18	74.35	65.49	57.39	55.88	66.66
TIO2	1.14	0.86	1.17	0.69	0.91	1.15	1.17	0.95	1.18	0.74	1.09	0.63	0.88	1.00	1.13	0.86
AL2O3	22.10	15.22	23.40	10.92	17.34	22.42	23.47	16.35	22.94	13.10	19.03	10.51	14.96	19.92	22.21	15.35
FE2O3	8.12	7.48	8.20	7.46	11.17	7.50	8.13	8.48	7.96	11.10	8.48	7.52	8.58	10.34	7.73	7.62
MNO	0.25	0.19	0.21	0.21	0.33	0.15	0.20	0.28	0.17	0.36	0.23	0.35	0.32	0.20	0.23	0.18
MGO	1.91	1.73	1.82	1.44	2.38	1.69	1.72	1.77	1.89	1.98	2.15	1.50	2.01	1.84	2.04	1.78
CAO	0.27	0.34	0.24	0.42	0.29	0.36	0.14	0.28	0.27	0.29	0.35	0.34	0.30	0.16	0.23	0.25
NA2O	0.45	1.90	0.75	1.39	1.36	0.74	0.98	1.03	0.63	1.42	1.63	1.25	1.14	0.93	1.32	1.82
K2O	4.57	2.10	4.33	1.11	2.25	3.74	3.70	2.37	4.02	1.35	3.35	1.12	2.22	3.54	4.66	2.32
P2O5	0.23	0.17	0.24	0.11	0.23	0.33	0.17	0.25	0.27	0.25	0.31	0.17	0.20	0.11	0.14	0.17
LOI	4.25	2.85	4.56	2.75	4.16	4.35	4.62	3.50	4.54	3.80	3.66	2.29	3.26	3.93	4.22	2.65
TOTAL	98.67	99.46	99.57	100.08	99.15	99.79	98.72	99.02	99.27	99.97	99.46	100.03	99.36	99.36	99.79	99.66
AS	21.00	14.00	18.00	14.00	24.00	10.00	17.00	20.00	14.00	36.00	21.00	17.00	18.00	4.00	17.00	5.00
BA	845.00	458.00	805.00	257.00	451.00	743.00	772.00	474.00	793.00	326.00	701.00	272.00	543.00	273.00	902.00	491.00
CE	113.00	47.00	102.00	36.00	70.00	104.00	94.00	77.00	92.00	55.00	120.00	46.00	83.00	15.00	83.00	67.00
CO	18.00	15.00	21.00	19.00	18.00	27.00	31.00	26.00	19.00	23.00	17.00	19.00	25.00	18.00	30.00	18.00
CR	126.00	74.00	129.00	60.00	89.00	117.00	125.00	99.00	126.00	69.00	104.00	61.00	93.00	49.00	116.00	71.00
CU	31.00	28.00	30.00	24.00	34.00	25.00	30.00	23.00	19.00	58.00	27.00	27.00	41.00	34.00	47.00	33.00
GA	28.00	20.00	30.00	12.00	20.00	27.00	30.00	21.00	29.00	16.00	24.00	14.00	18.00	11.00	28.00	17.00
LA	69.00	29.00	56.00	18.00	34.00	62.00	57.00	52.00	52.00	24.00	38.00	12.00	20.00	24.00	46.00	26.00
NI	51.00	47.00	52.00	37.00	61.00	48.00	55.00	42.00	50.00	61.00	49.00	38.00	55.00	34.00	62.00	33.00
NB	22.00	14.00	18.00	12.00	16.00	20.00	20.00	16.00	20.00	13.00	19.00	12.00	16.00	12.00	20.00	17.00
PB	22.00	10.00	20.00	20.00	18.00	20.00	44.00	16.00	20.00	30.00	32.00	18.00	24.00	37.00	11.00	18.00
RB	195.00	93.00	184.00	68.00	95.00	170.00	168.00	112.00	186.00	65.00	139.00	49.00	97.00	50.00	188.00	95.00
SR	98.00	93.00	170.00	61.00	89.00	184.00	206.00	73.00	150.00	54.00	88.00	56.00	80.00	91.00	109.00	100.00
S	0.00	0.00	0.00	2036.00	1279.00	0.00	0.00	1853.00	0.00	6457.00	289.00	1277.00	695.00	2031.00	316.00	1838.00
TH	14.00	7.00	14.00	9.00	8.00	16.00	17.00	8.00	21.00	7.00	12.00	7.00	9.00	8.00	12.00	7.00
U	4.00	4.00	4.00	2.00	4.00	2.00	6.00	5.00	4.00	6.00	2.00	0.00	0.00	0.00	2.00	4.00
V	160.00	100.00	143.00	75.00	112.00	144.00	152.00	116.00	149.00	83.00	127.00	76.00	102.00	68.00	141.00	96.00
Y	51.00	26.00	41.00	15.00	36.00	49.00	42.00	41.00	41.00	33.00	63.00	21.00	31.00	22.00	34.00	26.00
ZN	78.00	87.00	90.00	83.00	112.00	84.00	86.00	75.00	73.00	95.00	89.00	75.00	91.00	156.00	101.00	84.00
ZR	196.00	256.00	210.00	272.00	166.00	212.00	175.00	238.00	179.00	175.00	199.00	181.00	208.00	191.00	197.00	242.00
MO	0.00	0.00	0.00	0.00	1.00	0.00	0.00	0.00	0.00	1.00	0.00	0.00	0.00	0.00	0.00	0.00

XRF ANALYSES (BGS)

XRF ANALYSES (BGS)

Sample Code	KDC447 L47D	KDC448 L48B	KDC449 L49E	KDC450 L50M	KDC626 K26A	KDC627 K27M	KDC628 K28E	KDC629 K29C	KDC630 K30E	KDC631 K31L	KDC632 K32C	KDC633 K33M	KDC634 K34M	KDC635 K35C	KDC636 K36M	KDC641 H41S
SIO2	55.33	72.61	53.04	53.56	45.56	53.98	54.22	68.38	53.90	70.88	62.73	57.47	55.93	71.34	55.21	76.06
TIO2	1.07	0.57	1.05	1.11	0.43	1.17	1.22	0.66	1.23	0.39	0.67	1.19	1.24	0.56	1.18	0.61
AL2O3	21.96	10.33	21.42	22.17	7.09	23.67	23.30	11.04	23.54	6.96	11.64	23.70	22.41	9.07	22.19	9.43
FE2O3	9.40	7.82	12.01	10.40	9.29	8.60	8.73	11.92	9.03	11.31	15.23	5.94	8.80	12.52	9.06	7.22
MNO	0.20	0.52	0.75	0.34	2.26	0.48	0.33	0.85	0.35	0.35	0.60	0.24	0.26	0.44	0.40	0.25
MGO	2.13	1.70	2.23	2.17	1.68	1.90	1.80	1.87	1.76	1.32	2.58	1.22	1.71	1.77	1.71	1.36
CAO	0.28	1.31	0.33	0.26	17.16	0.12	0.22	0.26	0.20	2.46	0.60	0.08	0.11	0.36	0.26	0.29
NA2O	1.00	0.94	0.80	1.13	0.06	0.64	0.76	0.00	0.72	0.00	0.00	1.12	1.03	0.00	0.95	0.28
K2O	3.42	1.04	2.92	3.12	0.41	4.28	4.01	0.87	3.71	0.59	0.79	3.94	3.18	0.58	3.15	1.15
P2O5	0.22	0.31	0.24	0.17	0.75	0.15	0.20	0.24	0.20	1.72	0.47	0.10	0.11	0.34	0.24	0.15
LOI	4.41	3.19	4.74	4.37	14.77	4.69	4.49	3.56	4.77	4.13	3.83	4.32	4.56	3.39	4.75	2.77
TOTAL	99.42	100.34	99.53	98.80	99.46	99.68	99.28	99.65	99.41	100.11	99.14	99.32	99.34	100.37	99.10	99.57
AS	23.00	4.00	17.00	25.00	21.00	31.00	38.00	77.00	23.00	117.00	37.00	15.00	14.00	43.00	23.00	21.00
BA	718.00	246.00	655.00	695.00	75.00	827.00	773.00	201.00	650.00	141.00	217.00	752.00	614.00	181.00	678.00	261.00
CE	90.00	32.00	109.00	88.00	82.00	98.00	81.00	65.00	110.00	82.00	83.00	86.00	91.00	70.00	135.00	67.00
CO	16.00	19.00	34.00	27.00	38.00	23.00	13.00	35.00	15.00	61.00	17.00	15.00	15.00	24.00	18.00	30.00
CR	111.00	56.00	118.00	128.00	43.00	136.00	132.00	55.00	140.00	42.00	63.00	133.00	130.00	53.00	124.00	51.00
CU	23.00	23.00	50.00	41.00	24.00	22.00	22.00	45.00	25.00	45.00	50.00	32.00	24.00	66.00	27.00	25.00
GA	27.00	12.00	25.00	27.00	8.00	29.00	28.00	18.00	30.00	10.00	19.00	2.00	24.00	13.00	26.00	12.00
LA	47.00	23.00	57.00	47.00	20.00	55.00	51.00	25.00	49.00	27.00	32.00	45.00	35.00	34.00	47.00	31.00
NI	52.00	28.00	71.00	55.00	30.00	58.00	61.00	53.00	51.00	31.00	72.00	34.00	58.00	60.00	57.00	26.00
NB	20.00	12.00	18.00	20.00	8.00	19.00	19.00	11.00	21.00	8.00	11.00	22.00	22.00	11.00	21.00	11.00
PB	15.00	18.00	23.00	19.00	27.00	17.00	12.00	109.00	42.00	89.00	37.00	22.00	26.00	63.00	20.00	54.00
RB	143.00	47.00	125.00	137.00	22.00	198.00	189.00	44.00	169.00	34.00	38.00	184.00	145.00	31.00	145.00	55.00
SR	166.00	48.00	153.00	154.00	132.00	143.00	150.00	28.00	167.00	58.00	26.00	180.00	146.00	23.00	134.00	36.00
S	17.00	792.00	0.00	144.00	2559.00	0.00	0.00	5154.00	0.0020	123.00	4417.00	12.00	13.00	7260.00	0.00	2362.00
TH	8.00	8.00	10.00	12.00	8.00	13.00	8.00	8.00	13.00	7.00	10.00	17.00	14.00	0.00	12.00	6.00
U	2.00	4.00	3.00	3.00	3.00	5.00	4.00	3.00	3.00	3.00	3.00	4.00	3.00	5.00	4.00	2.00
V	128.00	70.00	149.00	150.00	52.00	151.00	165.00	72.00	154.00	48.00	82.00	141.00	160.00	64.00	143.00	62.00
Y	35.00	21.00	35.00	39.00	40.00	36.00	40.00	27.00	47.00	72.00	43.00	43.00	37.00	26.00	44.00	29.00
ZN	94.00	64.00	118.00	106.00	86.00	75.00	79.00	77.00	83.00	72.00	110.00	61.00	71.00	84.00	84.00	84.00
ZR	177.00	161.00	146.00	160.00	131.00	160.00	167.00	185.00	179.00	92.00	184.00	174.00	189.00	179.00	190.00	188.00
MO	0.00	0.00	0.00	0.00	0.00	0.00	0.00	0.00	0.00	7.00	0.00	0.00	0.00	0.00	0.00	4.00

XRF ANALYSES (BGS)

XRF ANALYSES (BGS)

Sample Code	KDC642 H42M	KDC643 H43T	KDC644 H44A	KDC645 H45B	KDC646 H46T	KDC647 H47S	KDC648 H48M	KDC649 H49S	KDC650 H50M	KDC651 H51M	KDC652 H52M	KDC653 H53M	KDC654 H54M	KDC655 H55M	KDC656 H56S	KDC479 W79A
SIO2	54.94	53.02	77.04	81.66	53.52	78.01	54.13	77.65	53.96	53.10	54.23	53.01	53.12	53.40	79.21	78.99
TIO2	1.13	1.13	0.62	0.51	1.15	0.61	1.13	0.56	1.15	1.17	1.09	1.13	1.17	1.20	0.53	0.40
AL2O3	22.32	22.47	10.24	7.11	23.41	9.17	21.60	8.61	21.97	21.67	22.17	22.68	21.82	22.74	6.65	8.69
FE2O3	9.10	11.19	4.74	5.86	9.37	6.02	10.17	7.72	10.90	10.71	9.89	10.70	10.42	9.85	8.37	5.85
MNO	0.28	0.63	0.29	0.30	0.51	0.36	0.31	0.38	0.23	0.25	0.78	0.62	0.27	0.25	0.31	0.08
MGO	1.99	2.24	1.26	1.16	1.89	1.25	2.09	1.34	2.22	2.25	1.92	2.04	2.13	2.04	1.32	1.02
CAO	0.17	0.22	0.81	0.25	0.23	0.32	0.48	0.19	0.29	0.28	0.18	0.17	0.32	0.15	0.12	0.18
NA2O	1.01	0.71	0.22	0.11	0.96	0.08	0.96	0.47	0.93	1.05	0.70	0.70	1.01	0.97	0.00	1.27
K2O	3.33	3.11	1.68	0.77	3.54	1.24	2.95	0.80	2.95	2.94	3.43	3.30	2.93	3.26	0.52	0.89
P2O5	0.15	0.19	0.16	0.08	0.21	0.11	0.36	0.13	0.21	0.21	0.18	0.19	0.25	0.15	0.12	0.10
LOI	4.44	4.58	3.17	2.14	4.17	2.48	4.34	2.33	4.77	5.45	4.78	5.04	4.99	4.78	2.44	1.85
TOTAL	98.86	99.49	100.23	99.95	98.96	99.65	98.52	100.18	99.58	99.08	99.35	99.58	98.43	98.79	99.59	99.32
AS	35.00	52.00	17.00	12.00	34.00	21.00	36.00	23.00	31.00	28.00	47.00	35.00	38.00	41.00	31.00	0.00
BA	701.00	709.00	411.00	202.00	773.00	282.00	682.00	227.00	882.00	785.00	922.00	901.00	812.00	739.00	142.00	211.00
CE	101.00	89.00	77.00	46.00	122.00	45.00	110.00	30.00	121.00	94.00	92.00	106.00	101.00	86.00	51.00	30.00
CO	10.00	21.00	19.00	15.00	14.00	20.00	12.00	26.00	25.00	16.00	8.00	17.00	17.00	14.00	9.00	15.00
CR	128.00	132.00	59.00	42.00	136.00	49.00	142.00	48.00	143.00	140.00	135.00	136.00	137.00	141.00	46.00	36.00
CU	22.00	49.00	7.00	10.00	17.00	6.00	32.00	47.00	38.00	44.00	35.00	41.00	45.00	47.00	18.00	21.00
GA	28.00	29.00	14.00	7.00	27.00	9.00	26.00	11.00	29.00	32.00	27.00	28.00	26.00	29.00	10.00	9.00
LA	47.00	52.00	36.00	18.00	49.00	29.00	49.00	22.00	42.00	54.00	40.00	50.00	43.00	44.00	18.00	10.00
NI	48.00	59.00	18.00	21.00	50.00	24.00	58.00	26.00	62.00	72.00	57.00	69.00	66.00	62.00	21.00	23.00
NB	20.00	19.00	10.00	10.00	20.00	12.00	19.00	10.00	20.00	20.00	19.00	19.00	20.00	20.00	9.00	8.00
PB	31.00	24.00	41.00	28.00	19.00	11.00	31.00	80.00	15.00	12.00	9.00	16.00	14.00	27.00	192.00	14.00
RB	151.00	136.00	81.00	39.00	156.00	61.00	137.00	43.00	141.00	133.00	155.00	147.00	135.00	146.00	28.00	31.00
SR	175.00	172.00	58.00	25.00	187.00	44.00	166.00	32.00	171.00	150.00	144.00	157.00	162.00	174.00	15.00	28.00
S	0.00	39.00	709.00	1451.00	0.00	762.00	5.00	3642.00	0.00	0.00	19.00	4.00	0.00	0.00	3155.00	0.00
TH	12.00	8.00	4.00	2.00	17.00	3.00	11.00	7.00	6.00	12.00	9.00	9.00	10.00	8.00	10.00	3.00
U	3.00	8.00	3.00	3.00	4.00	0.00	2.00	0.00	0.00	4.00	3.00	3.00	3.00	4.00	0.00	0.00
V	138.00	132.00	75.00	53.00	135.00	68.00	148.00	59.00	145.00	151.00	139.00	132.00	155.00	149.00	57.00	59.00
Y	39.00	37.00	28.00	23.00	39.00	32.00	47.00	22.00	33.00	40.00	35.00	36.00	40.00	38.00	16.00	12.00
ZN	78.00	106.00	87.00	100.00	83.00	92.00	98.00	167.00	218.00	119.00	166.00	130.00	115.00	104.00	64.00	53.00
ZR	162.00	155.00	143.00	210.00	145.00	184.00	157.00	187.00	150.00	157.00	132.00	152.00	160.00	169.00	312.00	121.00
MO	0.00	0.00	0.00	0.00	0.00	0.00	0.00	0.00	0.00	0.00	0.00	1.00	0.00	0.00	0.00	0.00

XRF ANALYSES (BGS)

XRF ANALYSES (BGS)

Sample Code	KDC480 W80A	KDC481 W81A	KDC482 W82A	KDC483 W83A	KDC484 W84A	KDC485 W85S	KDC486 W86S
SIO2	80.18	80.73	83.89	81.69	78.38	64.89	64.66
TIO2	0.40	0.54	0.30	0.31	0.44	0.92	0.94
AL2O3	8.32	8.31	6.07	6.81	8.09	17.57	17.85
FE2O3	5.67	5.24	4.57	5.35	6.14	7.07	7.09
MNO	0.08	0.11	0.16	0.13	0.16	0.14	0.14
MGO	1.04	0.94	0.79	0.93	1.13	1.47	1.38
CAO	0.40	0.15	0.37	0.38	0.61	0.12	0.12
NA2O	1.23	1.41	1.20	1.25	1.40	1.48	1.17
K2O	0.89	0.85	0.52	0.62	0.72	2.99	3.01
P2O5	0.12	0.08	0.09	0.13	0.16	0.10	0.11
LOI	1.86	1.53	1.66	1.83	2.39	3.65	3.59
TOTAL	100.19	99.89	99.62	99.43	99.62	100.40	100.06
AS	0.00	0.00	0.00	0.00	3.00	16.00	16.00
BA	208.00	170.00	112.00	152.00	188.00	604.00	595.00
CE	41.00	27.00	45.00	49.00	42.00	104.00	84.00
CO	17.00	15.00	10.00	15.00	14.00	35.00	29.00
CR	34.00	46.00	25.00	27.00	34.00	96.00	99.00
CU	13.00	18.00	9.00	13.00	9.00	31.00	28.00
GA	8.00	8.00	6.00	6.00	8.00	21.00	20.00
LA	15.00	19.00	12.00	10.00	18.00	31.00	49.00
NI	21.00	18.00	12.00	17.00	17.00	46.00	44.00
NB	8.00	11.00	7.00	8.00	9.00	17.00	18.00
PB	14.00	8.00	9.00	9.00	7.00	17.00	16.00
RB	32.00	28.00	17.00	23.00	28.00	117.00	121.00
SR	29.00	26.00	25.00	32.00	44.00	83.00	84.00
S	0.00	0.00	0.00	0.00	236.00	15.00	9.00
TH	6.00	7.00	5.00	4.00	4.00	21.00	17.00
U	0.00	0.00	0.00	0.00	0.00	5.00	3.00
V	57.00	59.00	33.00	41.00	51.00	120.00	122.00
Y	16.00	14.00	11.00	14.00	15.00	24.00	23.00
ZN	49.00	42.00	26.00	35.00	35.00	52.00	52.00
ZR	138.00	270.00	79.00	87.00	117.00	205.00	211.00
MO	0.00	0.00	0.00	0.00	0.00	3.00	4.00

(c) Skiddaw Group data recalculated to 100% free of LOI

L = Loweswater Fm; K = Kirk Stile Fm; H = Hope Beck Fm; W = Watch Hill Fm

sample	unit	SiO2	TiO2	Al2O3	Fe2O3	MnO	MgO	CaO	Na2O	K2O	P2O5
KDC601	L	67.81	0.87	16.08	8.21	0.27	1.80	0.30	2.17	2.27	0.22
KDC602	L	68.28	0.97	16.56	7.09	0.20	1.67	0.28	2.25	2.53	0.19
KDC603	L	76.92	0.60	10.55	5.02	0.31	1.18	2.10	1.93	1.24	0.15
KDC606	L	75.11	0.70	11.42	6.06	0.26	1.66	1.41	1.89	1.34	0.14
KDC607	L	72.13	0.85	14.54	6.25	0.18	1.47	0.28	2.17	1.99	0.14
KDC610	L	65.76	0.98	17.67	8.33	0.32	2.08	0.32	1.51	2.78	0.24
KDC611	L	78.44	0.36	8.36	8.00	0.44	1.70	1.04	0.43	0.75	0.49
KDC613	L	68.16	0.85	14.90	9.58	0.31	2.06	0.35	1.65	1.93	0.21
KDC614	L	65.12	0.97	18.45	7.64	0.25	1.67	0.71	1.21	3.55	0.43
KDC615	L	71.44	0.72	12.15	7.01	0.60	1.58	2.99	1.85	1.48	0.18
KDC616	L	72.52	0.70	12.31	8.80	0.35	1.90	0.40	1.61	1.28	0.13
KDC618	L	68.96	0.89	15.75	7.74	0.20	1.79	0.35	1.97	2.17	0.18
KDC620	L	75.60	0.71	11.22	7.66	0.22	1.48	0.43	1.43	1.14	0.11
KDC621	L	61.83	0.96	18.25	11.76	0.35	2.51	0.31	1.43	2.37	0.24
KDC624	L	66.75	0.99	17.12	8.88	0.29	1.85	0.29	1.08	2.48	0.26
KDC637	L	68.19	0.77	13.62	11.54	0.37	2.06	0.30	1.48	1.40	0.26
KDC639	L	76.07	0.64	10.75	7.69	0.36	1.53	0.35	1.28	1.15	0.17
KDC640	L	68.21	0.91	15.53	8.91	0.33	2.09	0.31	1.18	2.31	0.21
KDC444	L	73.74	0.65	11.69	8.26	0.28	1.87	0.49	1.75	1.12	0.14
KDC446	L	68.71	0.89	15.82	7.85	0.19	1.83	0.26	1.88	2.39	0.18
KDC448	L	74.74	0.59	10.63	8.05	0.54	1.75	1.35	0.97	1.07	0.32
KDC629	K	71.16	0.69	11.49	12.41	0.88	1.95	0.27	0.00	0.91	0.25
KDC631	K	73.85	0.41	7.25	11.78	0.36	1.38	2.56	0.00	0.61	1.79
KDC632	K	65.82	0.70	12.21	15.98	0.63	2.71	0.63	0.00	0.83	0.49
KDC635	K	73.56	0.58	9.35	12.91	0.45	1.83	0.37	0.00	0.60	0.35
KDC641	H	78.57	0.63	9.74	7.46	0.26	1.40	0.30	0.29	1.19	0.15
KDC644	H	79.37	0.64	10.55	4.88	0.30	1.30	0.83	0.23	1.73	0.16
KDC645	H	83.49	0.52	7.27	5.99	0.31	1.19	0.26	0.11	0.79	0.08
KDC647	H	80.28	0.63	9.44	6.20	0.37	1.29	0.33	0.08	1.28	0.11
KDC649	H	79.36	0.57	8.80	7.89	0.39	1.37	0.19	0.48	0.82	0.13
KDC656	H	81.53	0.55	6.85	8.62	0.32	1.36	0.12	0.00	0.54	0.12
KDC479	W	81.04	0.41	8.92	6.00	0.08	1.05	0.18	1.30	0.91	0.10
KDC480	W	81.54	0.41	8.46	5.77	0.08	1.06	0.41	1.25	0.91	0.12
KDC481	W	82.08	0.55	8.45	5.33	0.11	0.96	0.15	1.43	0.86	0.08
KDC482	W	85.64	0.31	6.20	4.67	0.16	0.81	0.38	1.22	0.53	0 09
KDC483	W	83.70	0.32	6.98	5.48	0.13	0.95	0.39	1.28	0.64	0.13
KDC484	W	80.61	0.45	8.32	6.31	0.16	1.16	*0.63*	*1.44*	*0.74*	*0.16*
KDC485	W	67.07	0.95	18.16	7.31	0.14	1.52	0.12	1.53	3.09	0.10
KDC486	W	67.03	0.97	18.50	7.35	0.15	1.43	0.12	1.21	3.12	0.11

(d) Major element compositions of Phanerozoic greywackes

Greywacke samples of fine and medium sand grainsize, with total Fe expressed as Fe_2O_3, recalculated to 100% free of volatiles and loss-on-ignition.

Code describes type of provenance terrain:

O = oceanic island arc
C = continental island arc
A = active continental margin
P = passive margin

Sources of data:

number	source
1	Bhatia (1983)
2	Chappel (1968)
3	Edwards (1950)
4	Coombs (1954)
5-19	Dickinson (1962)
20	Ricci and Sabatini (1976)
21-23	Connelly (1978)
24	Bhatia (1983)
25-40	Reed (1957)
41-60	Coleman (1972)
61	Bailey et al (1964)
62-65	Huckenholz (1963)
66	Bhatia (1983)
67-100	Van de Kamp et al (1976)
101	Webb and Potter (1969)
102-103	Bhatia (1983)
104	Crook (1974)
105	Nathan (1977)
106-115	Middleton (1972)

Sample Code	O	O	O	O	O	O	O	O
Number	1	2	3	4	5	6	7	8
SIO2	59.36	57.06	59.66	57.81	58.07	56.71	56.78	56.04
TIO2	0.86	1.16	0.94	1.39	0.90	0.85	0.87	0.98
AL2O3	16.35	16.39	20.52	16.76	17.88	17.89	17.95	18.33
FE2O3	7.24	10.19	5.62	9.76	7.15	7.53	7.52	8.46
MNO	0.23	0.17	0.09	0.12	0.12	0.12	0.13	0.13
MGO	2.73	3.87	2.93	4.01	2.98	3.35	3.24	3.37
CAO	7.08	5.23	5.57	3.63	5.65	6.17	6.26	6.21
NA2O	4.78	5.01	2.44	4.55	3.29	4.19	4.18	3.79
K2O	1.17	0.69	1.92	1.65	3.70	2.93	2.82	2.42
P2O5	0.19	0.24	0.31	0.31	0.25	0.26	0.26	0.27
TOTAL	99.99	100.01	100.00	99.99	99.99	100.00	100.01	100.00

Sample Code	O	O	O	O	O	O	O	O
Number	9	10	11	12	13	14	15	16
SIO2	58.50	57.44	58.19	58.00	56.94	57.45	61.39	58.41
TIO2	0.84	0.83	0.95	1.04	0.89	0.83	0.85	0.90
AL2O3	18.14	18.31	18.70	17.50	17.91	18.08	17.53	17.77
FE2O3	6.40	6.38	7.71	7.78	8.39	7.94	6.50	7.99
MNO	0.10	0.10	0.09	0.09	0.10	0.10	0.09	0.09
MGO	2.41	2.39	3.24	3.94	3.83	4.05	2.18	3.64
CAO	5.66	6.14	4.91	6.01	5.59	6.34	5.39	4.99
NA2O	3.98	4.16	4.28	3.21	4.35	3.53	4.04	4.47
K2O	3.67	3.95	1.78	2.28	1.86	1.56	1.87	1.56
P2O5	0.29	0.28	0.15	0.16	0.13	0.14	0.17	0.17
TOTAL	99.99	99.98	100.00	100.01	99.99	100.02	100.01	99.99

Sample Code	O	O	O	O	O	O	O	C
Number	17	18	19	20	21	22	23	24
SIO2	58.01	59.21	58.68	57.32	59.01	66.63	63.29	74.19
TIO2	0.86	0.68	0.85	1.06	0.77	0.66	0.93	0.65
AL2O3	18.37	18.42	17.21	16.49	19.42	15.15	16.39	12.22
FE2O3	7.46	6.77	7.47	8.82	6.59	5.92	7.26	4.30
MNO	0.08	0.09	0.09	0.14	0.17	0.11	0.16	0.08
MGO	3.42	2.91	3.73	4.87	2.32	2.87	3.43	1.48
CAO	6.23	5.93	5.49	5.14	5.86	3.79	3.04	2.63
NA2O	3.84	3.75	4.04	4.13	3.79	3.91	4.12	2.52
K2O	1.56	2.08	2.28	1.75	1.85	0.84	1.20	1.81
P2O5	0.18	0.16	0.15	0.29	0.21	*0.11*	*0.18*	*0.12*
TOTAL	100.01	100.00	99.99	100.01	99.99	99.99	100.00	100.00

Sample Code	C	C	C	C	C	C	C	C
Number	25	26	27	28	29	30	31	32
SIO2	72.74	71.88	69.28	71.15	67.58	72.58	69.80	66.88
TIO2	0.51	0.63	1.57	0.51	0.72	0.51	0.32	0.62
AL2O3	14.22	12.50	15.25	14.51	15.44	14.67	17.02	15.91
FE2O3	3.07	5.85	5.31	3.76	4.88	3.13	3.61	4.66
MNO	0.05	0.06	0.26	0.06	0.07	0.06	0.31	0.08
MGO	1.33	1.24	0.31	1.68	1.92	1.14	1.33	1.95
CAO	1.84	1.93	3.09	1.61	3.43	1.34	2.51	2.90
NA2O	3.79	3.23	3.41	3.72	3.40	3.64	2.49	4.12
K2O	2.35	2.52	1.12	2.86	2.31	2.79	2.38	2.65
P2O5	0.10	0.16	0.39	0.13	0.24	0.12	0.24	0.23
TOTAL	100.00	100.00	99.99	99.99	99.99	99.98	100.01	100.00

Sample Code	C	C	C	C	C	C	C	C
Number	33	34	35	36	37	38	39	40
SIO2	68.45	77.04	78.13	78.41	70.91	78.19	69.10	62.64
TIO2	0.49	0.90	0.64	0.72	0.72	0.68	0.79	0.86
AL2O3	15.86	10.45	10.99	10.64	13.98	9.48	15.19	16.35
FE2O3	3.73	5.37	4.06	4.31	6.15	3.97	6.03	7.66
MNO	0.11	0.05	0.04	0.04	0.05	0.06	0.04	0.12
MGO	1.77	1.42	1.98	1.64	2.75	1.79	2.98	2.88
CAO	2.60	0.85	0.61	0.44	0.53	2.14	0.47	2.75
NA2O	3.88	1.42	1.16	1.52	1.79	1.64	1.89	4.75
K2O	2.94	2.30	2.16	2.06	2.86	1.84	3.30	1.85
P2O5	0.17	0.20	0.23	0.21	0.27	0.21	0.22	0.15
TOTAL	100.00	100.00	100.00	99.99	100.01	100.00	100.01	100.01

Sample Code	C	C	C	C	C	C	C	C
Number	41	42	43	44	45	46	47	48
SIO2	67.54	68.94	67.74	68.36	68.08	66.22	71.55	73.17
TIO2	0.71	0.71	0.54	0.65	0.51	0.81	0.61	0.52
AL2O3	13.47	14.50	14.78	13.59	13.32	14.27	14.33	13.24
FE2O3	6.57	5.73	4.60	6.15	5.14	5.93	5.56	4.97
MNO	0.08	0.04	0.09	0.08	0.08	0.08	0.00	0.04
MGO	3.13	2.84	2.13	2.30	3.75	2.52	2.08	1.64
CAO	3.13	2.42	4.68	3.97	3.43	4.20	1.14	1.23
NA2O	4.07	3.36	3.83	3.55	4.58	4.41	3.12	4.41
K2O	1.15	1.26	1.49	1.15	0.94	1.36	1.45	0.62
P2O5	0.16	0.20	0.13	0.20	0.17	0.20	0.16	0.15
TOTAL	100.01	100.00	100.01	100.00	100.00	100.00	100.00	99.99

Sample Code	C	C	C	C	C	C	C	C
Number	49	50	51	52	53	54	55	56
SIO2	67.54	69.28	67.73	67.87	69.44	71.04	66.90	65.45
TIO2	0.70	0.67	0.69	0.62	0.64	0.59	0.70	0.82
AL2O3	14.36	15.32	15.72	16.20	14.56	14.89	13.75	14.03
FE2O3	6.08	5.36	6.05	5.53	5.50	5.39	5.87	6.88
MNO	0.08	0.07	0.08	0.09	0.07	0.07	0.08	0.08
MGO	3.10	2.06	2.57	2.26	2.36	2.17	4.27	4.99
CAO	2.79	2.26	1.75	1.95	2.67	1.65	4.06	2.70
NA2O	4.54	3.60	3.70	3.90	3.28	2.59	2.81	3.95
K2O	0.62	1.23	1.54	1.44	1.33	1.45	1.35	0.87
P2O5	0.19	0.16	0.16	0.16	0.15	0.16	0.20	0.23
TOTAL	100.00	100.01	99.99	100.02	100.00	100.00	99.99	100.00

Sample Code	C	C	C	C	C	C	C	C
Number	57	58	59	60	61	62	63	64
SIO2	67.94	69.53	68.97	73.12	70.31	74.38	73.18	71.82
TIO2	0.61	0.64	0.63	0.55	0.50	0.52	0.73	0.31
AL2O3	14.23	13.37	13.54	10.75	14.04	13.51	13.99	16.10
FE2O3	5.86	5.55	5.48	4.85	4.61	5.09	4.13	4.86
MNO	0.11	0.07	0.07	0.07	0.10	0.10	0.10	0.10
MGO	3.30	4.14	3.65	3.58	2.31	1.34	1.66	2.27
CAO	2.27	1.66	2.71	3.06	2.51	1.24	1.35	0.83
NA2O	4.54	3.63	3.44	2.74	3.71	2.68	3.01	2.06
K2O	1.03	1.24	1.35	1.16	1.81	1.03	1.66	1.44
P2O5	0.12	0.17	0.17	0.13	0.10	0.10	0.21	0.21
TOTAL	100.01	100.00	100.01	100.01	100.00	99.99	100.02	100.00

Sample Code Number	C 65	A 66	A 67	A 68	A 69	A 70	A 71	A 72
SIO2	72.82	78.32	62.43	73.67	72.15	70.11	69.36	75.89
TIO2	0.74	0.45	0.53	0.41	0.72	0.47	0.51	0.47
AL2O3	16.23	11.04	14.95	12.95	13.58	13.11	15.25	11.80
FE2O3	5.05	2.86	10.67	2.67	4.63	3.77	4.17	4.03
MNO	0.21	0.05	0.11	0.06	0.04	0.10	0.06	0.04
MGO	0.84	1.01	3.29	0.93	1.52	1.13	1.89	1.92
CAO	0.42	1.18	2.83	3.77	0.98	5.87	1.92	1.07
NA2O	2.11	2.32	1.93	4.09	2.80	2.60	3.41	2.89
K2O	1.48	2.70	2.26	1.37	3.47	2.81	3.33	1.79
P2O5	0.11	0.08	1.01	0.09	0.11	0.02	0.09	0.09
TOTAL	100.01	100.01	100.01	100.01	100.00	99.99	99.99	99.99

Sample Code Number	A 73	A 74	A 75	A 76	A 77	A 78	A 79	A 80
SIO2	78.17	70.74	69.83	70.20	76.62	70.16	71.98	72.99
TIO2	0.60	0.66	0.49	0.38	0.28	0.47	0.48	0.22
AL2O3	10.25	14.41	11.68	14.44	9.76	14.65	13.12	15.33
FE2O3	3.94	5.34	4.49	4.09	2.83	4.22	3.19	1.24
MNO	0.06	0.06	0.05	0.06	0.05	0.05	0.06	0.03
MGO	1.11	2.12	1.42	1.79	3.02	1.77	1.83	0.96
CAO	1.82	1.43	7.29	1.78	2.66	1.48	2.38	2.38
NA2O	2.76	3.52	2.51	3.94	3.10	3.49	3.36	3.54
K2O	1.22	1.61	2.10	3.24	1.57	3.52	3.54	3.31
P2O5	0.07	0.10	0.13	0.08	0.10	0.18	0.06	0.00
TOTAL	100.00	99.99	99.99	100.00	99.99	99.99	100.00	100.00

Sample Code Number	A 81	A 82	A 83	A 84	A 85	A 86	A 87	A 88
SIO2	68.11	72.58	70.75	73.94	72.32	71.48	69.74	74.47
TIO2	0.59	0.39	0.53	0.34	0.45	0.47	0.41	0.31
AL2O3	14.64	13.08	13.58	13.69	13.26	13.79	12.57	13.36
FE2O3	5.39	2.61	5.10	2.62	2.51	3.40	4.92	1.87
MNO	0.07	0.05	0.07	0.03	0.04	0.05	0.07	0.02
MGO	1.95	1.56	1.92	1.11	1.56	1.79	1.95	1.96
CAO	2.26	2.09	1.80	1.13	3.30	2.20	4.96	1.17
NA2O	3.68	3.75	2.90	3.60	3.14	3.48	2.68	3.33
K2O	3.07	3.81	3.21	3.46	3.40	3.18	2.48	3.39
P2O5	0.24	0.07	0.12	0.09	0.03	0.15	0.21	0.10
TOTAL	100.00	99.99	99.98	100.01	100.01	99.99	99.99	99.98

Sample Code Number	A 89	A 90	A 91	A 92	A 93	A 94	A 95	A 96
SIO2	72.84	73.84	74.17	75.18	67.87	70.81	70.93	72.42
TIO2	0.41	0.39	0.35	0.30	0.68	0.41	0.36	0.34
AL2O3	13.61	13.93	14.06	11.73	14.85	14.27	14.84	14.15
FE2O3	2.72	1.29	2.25	2.61	4.50	3.47	2.82	2.83
MNO	0.04	0.03	0.03	0.04	0.07	0.06	0.05	0.05
MGO	2.35	0.58	0.92	0.97	1.73	1.36	1.17	1.32
CAO	1.44	2.44	1.24	2.89	4.55	2.88	3.07	2.88
NA2O	3.48	3.67	3.22	2.77	2.93	3.33	3.12	2.84
K2O	2.95	3.57	3.63	3.45	2.63	3.35	3.60	3.12
P2O5	0.14	0.26	0.12	0.06	0.18	0.05	0.03	0.04
TOTAL	99.98	100.00	99.99	100.00	99.99	99.99	99.99	99.99

Sample Code	A	A	A	A	A	P	P	P
Number	97	98	99	100	101	102	103	104
SIO2	72.47	86.34	77.33	66.15	72.82	86.65	87.78	88.66
TIO2	0.25	0.28	0.35	2.00	0.50	0.51	0.28	0.39
AL2O3	14.78	5.98	10.02	12.84	14.73	7.61	8.05	5.87
FE2O3	2.07	1.07	3.18	7.70	3.31	2.40	1.09	1.89
MNO	0.04	0.02	0.05	0.10	0.05	0.01	0.01	0.02
MGO	0.87	0.68	1.39	2.19	0.69	0.40	0.40	0.83
CAO	2.75	2.59	2.96	3.73	1.59	0.10	0.10	0.39
NA2O	3.24	1.22	3.26	2.84	2.62	0.92	0.91	0.69
K2O	3.49	1.81	1.37	1.92	3.67	1.31	1.30	1.18
P2O5	0.02	0.01	0.09	0.54	0.03	0.08	0.08	0.09
TOTAL	99.98	100.00	100.00	100.01	100.01	99.99	100.00	100.01

Sample Code	P	P	P	P	P	P	P	P
Number	105	106	107	108	109	110	111	112
SIO2	73.93	74.83	71.36	68.49	73.02	70.55	78.60	72.86
TIO2	0.69	1.24	1.26	1.44	1.20	1.77	1.39	1.11
AL2O3	12.50	12.78	13.90	16.31	13.02	14.60	11.37	14.00
FE2O3	5.10	5.02	5.48	6.71	5.41	6.51	3.33	5.91
MNO	0.06	0.11	0.14	0.10	0.15	0.11	0.07	0.03
MGO	2.38	0.93	1.34	1.31	1.03	1.12	0.64	0.67
CAO	0.90	0.83	1.85	0.56	1.85	0.44	0.53	0.60
NA2O	1.50	3.00	2.73	2.36	3.17	2.81	2.86	1.80
K2O	2.75	1.20	1.80	2.55	1.06	1.90	1.02	2.91
P2O5	0.20	0.06	0.14	0.16	0.09	0.19	0.18	0.12
TOTAL	100.01	100.00	100.00	99.99	100.00	100.00	99.99	100.01

Sample Code	P	P	P
Number	113	114	115
SIO2	65.92	72.99	68.44
TIO2	1.26	1.28	1.19
AL2O3	16.79	14.41	16.22
FE2O3	8.36	4.89	7.23
MNO	0.04	0.03	0.05
MGO	0.98	0.60	1.12
CAO	0.68	0.82	0.47
NA2O	2.26	2.45	2.19
K2O	3.55	2.39	2.93
P2O5	0.16	0.14	0.15
TOTAL	100.00	100.00	99.99

Appendix 5

RESULTS OF ICP ANALYSIS

Results of rare earth element determinations by ICP, using the Natural Environment Research Council facility at Royal Holloway and Bedford New College, Egham, Surrey.

element	sample (REE content in ppm)			
	M23 Bitter Beck Fm	M54m Bitter Beck Fm	M36 Watch Hill Fm	KDC655 Hope Beck Fm
La	58.6	87.7	87.0	56.8
Ce	95.9	177.9	171.7	117.4
Pr	10.36	19.37	19.13	12.82
Nd	39.2	72.0	71.0	48.8
Sm	7.00	12.42	12.06	9.30
Eu	1.44	2.42	2.22	1.95
Gd	5.60	9.16	7.07	8.21
Dy	5.41	8.96	6.58	7.30
Ho	0.99	1.66	1.30	1.31
Er	3.28	2.42	4.57	4.13

	KDC630 Kirk Stile Fm	KDC608 Loweswater Fm	M58m Loweswater Fm	ING-M Ingleton Group
La	62.8	82.3	69.1	36.3
Ce	129.4	175.1	147.7	77.7
Pr	14.17	19.35	15.62	8.93
Nd	53.8	71.6	58.9	34.8
Sm	10.03	10.99	9.90	7.33
Eu	2.11	2.20	2.03	1.89
Gd	8.43	7.84	7.19	7.25
Dy	8.12	7.21	7.11	7.38
Ho	1.49	1.36	1.31	1.36
Er	4.76	4.48	4.32	4.44

Appendix 6

GEOCHEMICAL STANDARDS

(a) Chemical composition of the upper continental crust

major element oxide	weight %
SiO2	66.0
TiO2	0.5
Al2O3	15.2
*Fe2O3	4.5
MgO	2.2
CaO	4.2
Na2O	3.9
K2O	3.4
P2O5	0.16

*Fe2O3 is total iron as Fe2O3.

trace element	ppm	trace element	ppm
As	1.5	Sc	11
Ba	550	Th	10.7
Ce	64	U	2.8
Co	10	V	60
Cr	35	Y	22
Cu	25	Zn	71
Ga	17	Zr	190
La	30		
Mo	1.5		
Ni	20		
Nb	25		
Pb	20		
Rb	112		
Sr	350		

From Taylor and McLennan (1985)

(b) Rare earth element normalising factors of type I carbonaceous chondrites.

From Taylor and McLennan (1985)

element	chondritic REE normalising factor
La	0.367
Ce	0.957
Pr	0.137
Nd	0.711
Sm	0.231
Eu	0.087
Gd	0.306
Tb	0.058
Dy	0.381
Ho	0.0851
Er	0.249
Tm	0.0356
Yb	0.248
Lu	0.0381
Y	2.1

(c) Rare earth element content of average post-Archaean Australian shale

From Taylor and McLennan (1985)

	REEcontent (ppm) of PAAS
La	38
Ce	80
Pr	8.9
Nd	32
Sm	5.6
Eu	1.1
Gd	4.7
Tb	0.77
Dy	4.4
Ho	1.0
Er	2.9
Tm	0.40
Yb	2.8
Lu	0.43

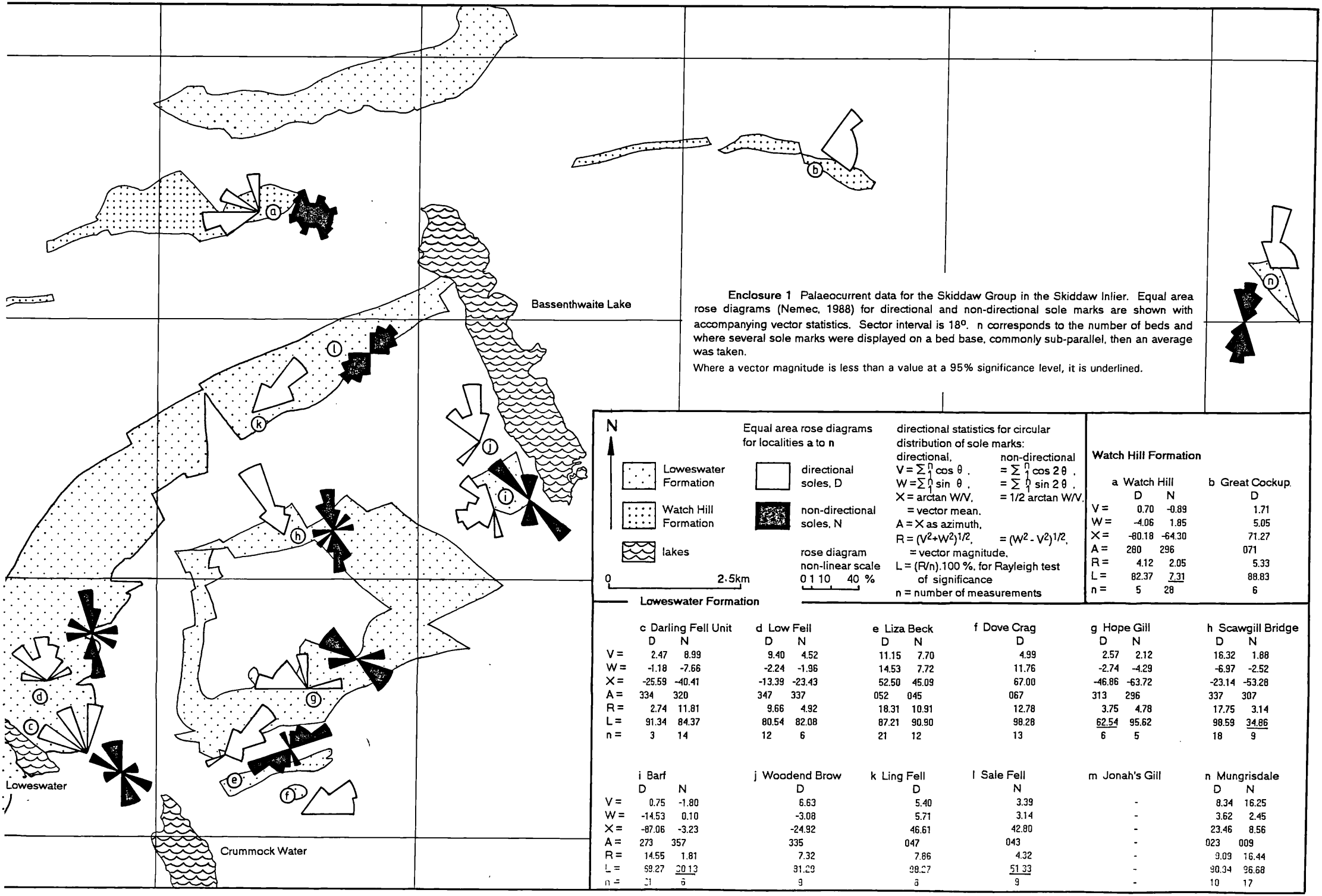

Enclosure 1 Palaeocurrent data for the Skiddaw Group in the Skiddaw Inlier. Equal area rose diagrams (Nemec, 1988) for directional and non-directional sole marks are shown with accompanying vector statistics. Sector interval is 18°. n corresponds to the number of beds and where several sole marks were displayed on a bed base, commonly sub-parallel, then an average was taken.

Where a vector magnitude is less than a value at a 95% significance level, it is underlined.

N

Loweswater Formation

Watch Hill Formation

lakes

0 2·5km

Equal area rose diagrams for localities a to n

directional soles, D

non-directional soles, N

rose diagram non-linear scale 0 1 10 40 %

directional statistics for circular distribution of sole marks:

directional, $V = \sum_1^n \cos\theta$, $W = \sum_1^n \sin\theta$, X = arctan W/V, = vector mean, $A = X$ as azimuth, $R = (V^2+W^2)^{1/2}$, = vector magnitude,

non-directional $= \sum_1^n \cos 2\theta$, $= \sum_1^n \sin 2\theta$, = 1/2 arctan W/V, $= (W^2 - V^2)^{1/2}$,

$L = (R/n).100$ %, for Rayleigh test of significance

n = number of measurements

Watch Hill Formation

	a Watch Hill D	a Watch Hill N	b Great Cockup D
V =	0.70	-0.89	1.71
W =	-4.06	1.85	5.05
X =	-80.18	-64.30	71.27
A =	280	296	071
R =	4.12	2.05	5.33
L =	82.37	7.31	88.83
n =	5	28	6

Loweswater Formation

	c Darling Fell Unit D	c Darling Fell Unit N	d Low Fell D	d Low Fell N	e Liza Beck D	e Liza Beck N	f Dove Crag D	g Hope Gill D	g Hope Gill N	h Scawgill Bridge D	h Scawgill Bridge N
V =	2.47	8.99	9.40	4.52	11.15	7.70	4.99	2.57	2.12	16.32	1.88
W =	-1.18	-7.66	-2.24	-1.96	14.53	7.72	11.76	-2.74	-4.29	-6.97	-2.52
X =	-25.59	-40.41	-13.39	-23.43	52.50	45.09	67.00	-46.86	-63.72	-23.14	-53.28
A =	334	320	347	337	052	045	067	313	296	337	307
R =	2.74	11.81	9.66	4.92	18.31	10.91	12.78	3.75	4.78	17.75	3.14
L =	91.34	84.37	80.54	82.08	87.21	90.90	98.28	62.54	95.62	98.59	34.86
n =	3	14	12	6	21	12	13	6	5	18	9

	i Barf D	i Barf N	j Woodend Brow D	k Ling Fell D	l Sale Fell N	m Jonah's Gill	n Mungrisdale D	n Mungrisdale N
V =	0.75	-1.80	6.63	5.40	3.39	-	8.34	16.25
W =	-14.53	0.10	-3.08	5.71	3.14	-	3.62	2.45
X =	-87.06	-3.23	-24.92	46.61	42.80	-	23.46	8.56
A =	273	357	335	047	043	-	023	009
R =	14.55	1.81	7.32	7.86	4.32	-	9.09	16.44
L =	99.27	30.13	81.29	98.27	51.33	-	90.34	96.68
n =	21	6	9	8	9	-	10	17

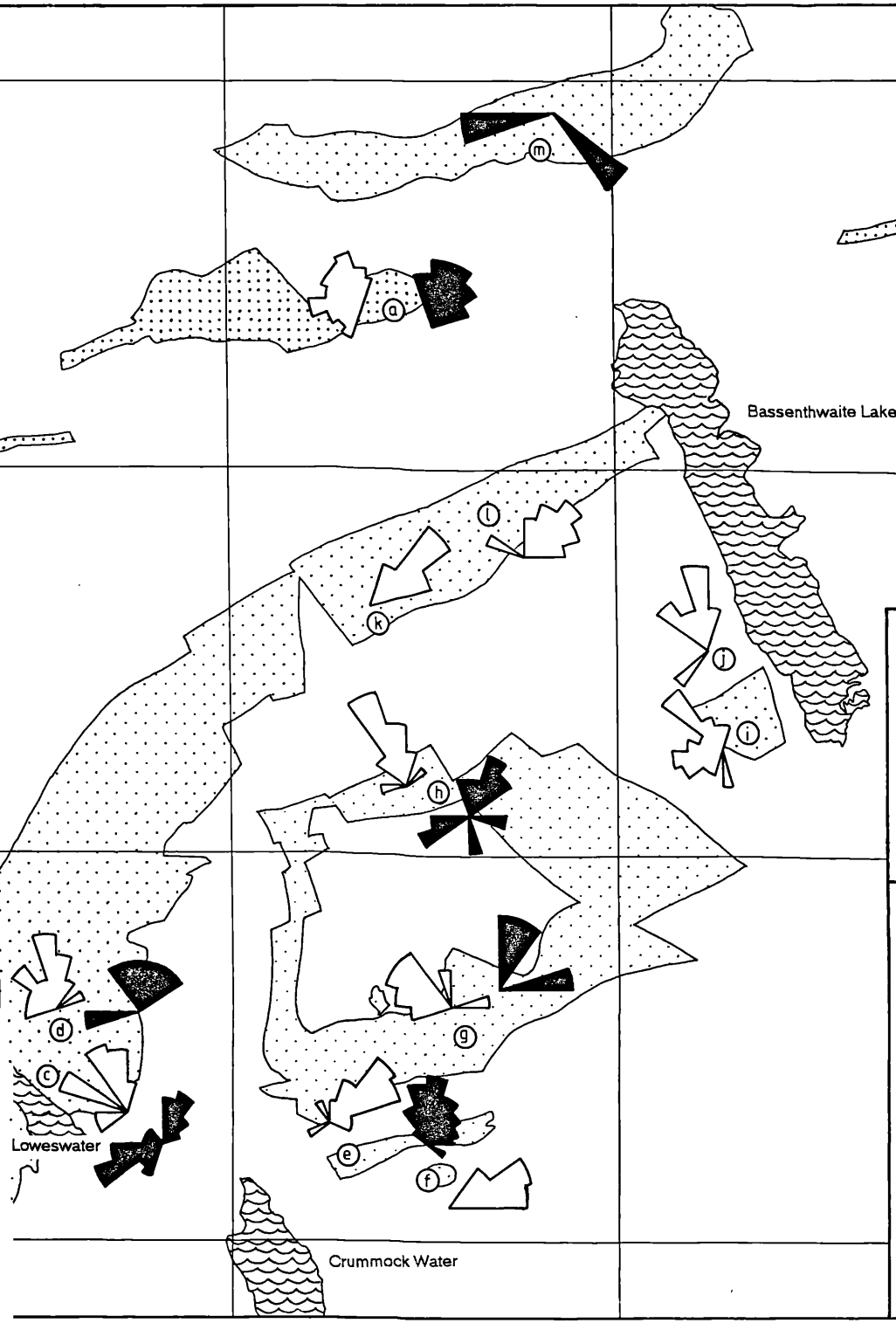

Enclosure 2 Palaeocurrent data for the Skiddaw Group in the Skiddaw Inlier. Equal area rose diagrams (Nemec, 1988) for sole mark directions and ripple current directions are shown with accompanying vector statistics. Sector interval is 18°. For ripple current directions, n corresponds to the number of ripple sets measured. Where ripple directions show a bimodal distribution then vector statistics are calculated for each mode, as recommended by Graham (1988). For sole directions n corresponds to the number of beds. Sole directions are a combination of directional sole marks (flutes and prods) and non-directioonal sole marks (grooves) (see enclosure 1) with an interpretation of flow direction. This was considered valid as directional sole marks usually show a narrow unimodal distribution.
Where a vector magnitude is less than a value at a 95% significance level, it is underlined.

N

Loweswater Formation

Watch Hill Formation

lakes

0 2.5km

Equal area rose diagrams for localities a to n

ripple directions, r (r1, r2 if bimodal)

sole directions, s

rose diagram non-linear scale
0 1 10 40 %

directional statistics of circular distribution
$V = \sum_1^n \cos\theta$
$W = \sum_1^n \sin\theta$
X = arctan W/V = vector mean
A = X as azimuth
$R = (V^2+W^2)^{1/2}$ = vector magnitude
L = (R/n).100 %, for Rayleigh test of significance

Watch Hill Formation

	a Watch Hill r	a Watch Hill s	b Great Cockup s
V =	9.36	6.33	1.71
W =	3.89	-23.30	5.05
X =	22.60	-74.79	71.27
A =	023	285	071
R =	10.13	24.14	5.33
L =	92.12	73.16	88.83
n =	11	33	6

Loweswater Formation

	c Darling Fell Unit r1	c Darling Fell Unit r2	c Darling Fell Unit s	d Low Fell r1	d Low Fell r2	d Low Fell s	e Liza Beck r	e Liza Beck s	f Dove Crag s	g Hope Gill r	g Hope Gill s	h Scawgill Bridge r1	h Scawgill Bridge r2	h Scawgill Bridge s
V =	-9.31	15.36	11.47	-	4.28	13.29	41.94	18.85	4.99	1.91	4.68	-1.87	5.80	23.56
W =	-25.23	7.86	-8.84	-	0.87	-4.20	10.69	22.25	11.76	1.65	-7.02	-2.67	3.59	-9.08
X =	69.74	27.10	-37.63	-	11.54	-16.78	14.29	49.73	67.00	40.87	-56.31	55.03	31.78	-21.08
A =	250	027	322	262	012	343	014	050	067	041	304	235	032	339
R =	26.90	17.25	14.48	-	4.36	14.54	43.28	29.17	12.78	2.52	8.44	3.26	6.82	25.25
L =	92.74	95.85	85.17	-	87.28	80.77	86.56	88.38	98.28	84.08	76.75	81.49	85.27	93.53
n =	29	18	17	1	5	18	50	33	13	3	11	4	8	27

	i Barf s	j Woodend Brow s	k Ling Fell s	l Sale Fell s	m Jonah's Gill r1	m Jonah's Gill r2	n Mungrisdale r	n Mungrisdale s
V =	5.70	6.63	5.40	6.12	-	-	14.42	24.60
W =	-17.09	-3.08	5.71	5.65	-	-	14.11	6.07
X =	-71.55	-24.92	46.61	42.71	-	-	44.37	13.86
A =	288	335	047	043	269	135	044	014
R =	18.02	7.32	7.96	8.32	-	-	20.18	25.33
L =	66.72	81.29	98.27	83.23	-	-	87.73	93.82
n =	27	9	9	10	1	1	23	27

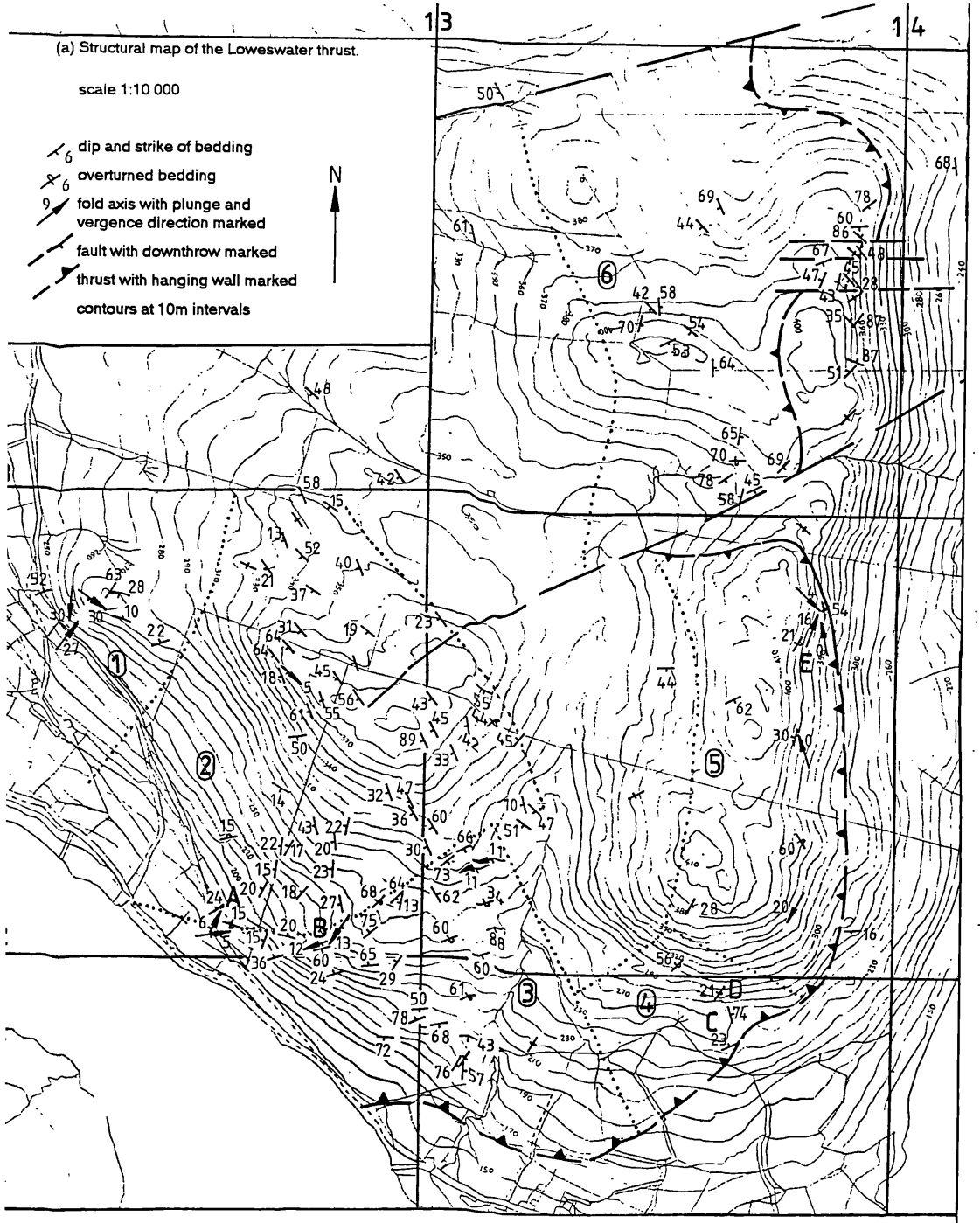

Lower hemisphere, equal area stereonet plots showing:

(b) lineations (slickensides, slickencrysts and lineations unrelated to cleavage) for localites A to E and total.

(c) poles to bedding, with mean fold axis, for sub-areas 1 to 6 anc total.

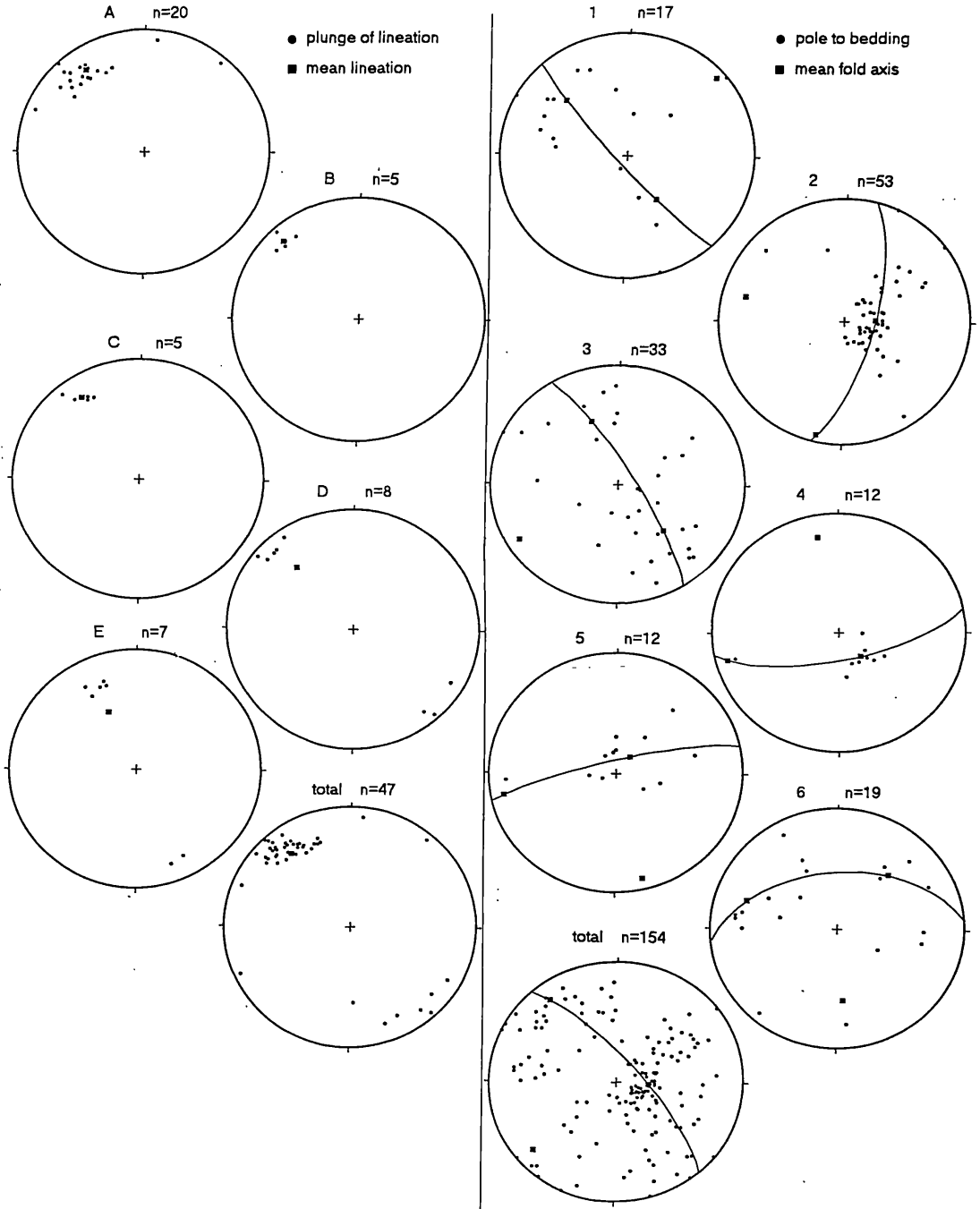

Enclosure 3 Geological structure of the Loweswater Fells; structural map of the Loweswater thrust (a), and lower hemisphere, equal area stereonet plots showing lineations (slickensides, slickencrysts and lineations unrelated to cleavage) for localites A to E and total (b), and for poles to bedding, with mean fold axis, for sub-areas 1 to 6 and total (c).

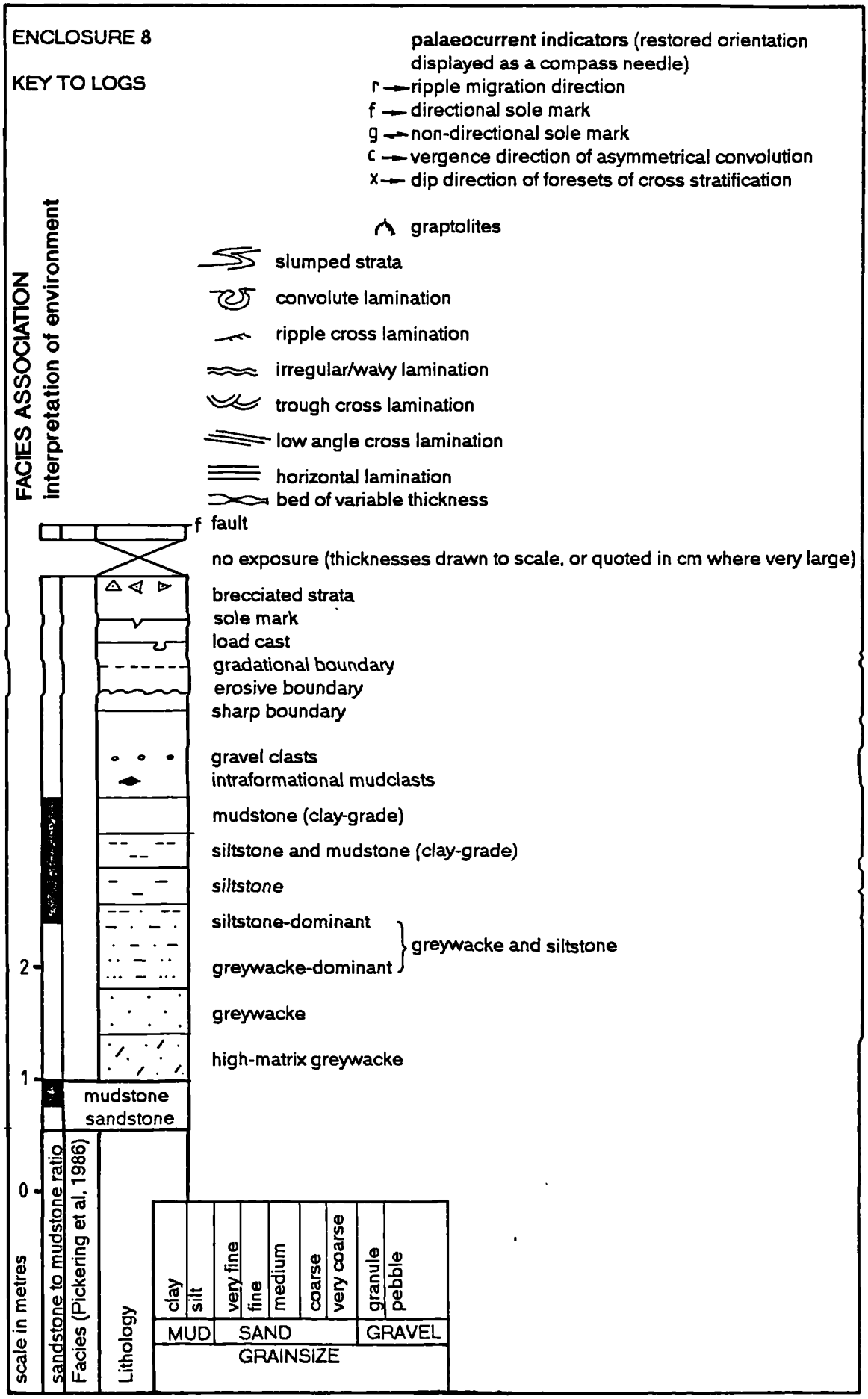
ENCLOSURE 8
KEY TO LOGS
palaeocurrent indicators (restored orientation displayed as a compass needle)
r ripple migration direction
f directional sole mark
g non-directional sole mark
c vergence direction of asymmetrical convolution
x dip direction of foresets of cross stratification
graptolites
slumped strata
convolute lamination
ripple cross lamination
irregular/wavy lamination
trough cross lamination
low angle cross lamination
horizontal lamination
bed of variable thickness
f fault
no exposure (thicknesses drawn to scale, or quoted in cm where very large)
brecciated strata
sole mark
load cast
gradational boundary
erosive boundary
sharp boundary
gravel clasts
intraformational mudclasts
mudstone (clay-grade)
siltstone and mudstone (clay-grade)
siltstone
siltstone-dominant
greywacke and siltstone
greywacke-dominant
greywacke
high-matrix greywacke
mudstone
sandstone
FACIES ASSOCIATION
Interpretation of environment
scale in metres
sandstone to mudstone ratio
Facies (Pickering et al, 1986)
Lithology
2
1
0
clay
silt
very fine
fine
medium
coarse
very coarse
granule
pebble
MUD
SAND
GRAVEL
GRAINSIZE